ISSN 2307-8960 (online)

World Journal of *Clinical Cases*

World J Clin Cases 2024 May 26; 12(15): 2466-2685

Published by Baishideng Publishing Group Inc

World Journal of Clinical Cases

Contents

Thrice Monthly Volume 12 Number 15 May 26, 2024

EDITORIAL

MINIREVIEWS

ORIGINAL ARTICLE

Retrospective Study

Clinical Trials Study

Observational Study

World Journal of Clinical Cases

Thrice Monthly Volume 12 Number 15 May 26, 2024

Contents

World Journal of Clinical Cases

Thrice Monthly Volume 12 Number 15 May 26, 2024

Contents

World Journal of Clinical Cases

Thrice Monthly Volume 12 Number 15 May 26, 2024

Contents

ABOUT COVER

Peer Reviewer of *World Journal of Clinical Cases*, Luca Pio, MD, Surgeon, Pediatric Surgery Department, Giannina Gaslini Institute, Genoa 16147, Italy. lucakeats@hotmail.it

AIMS AND SCOPE

The primary aim of *World Journal of Clinical Cases* (*WJCC*, *World J Clin Cases*) is to provide scholars and readers from various fields of clinical medicine with a platform to publish high-quality clinical research articles and communicate their research findings online.

WJCC mainly publishes articles reporting research results and findings obtained in the field of clinical medicine and covering a wide range of topics, including case control studies, retrospective cohort studies, retrospective studies, clinical trials studies, observational studies, prospective studies, randomized controlled trials, randomized clinical trials, systematic reviews, meta-analysis, and case reports.

INDEXING/ABSTRACTING

The *WJCC* is now abstracted and indexed in Science Citation Index Expanded (SCIE, also known as SciSearch®), Journal Citation Reports/Science Edition, Current Contents®/Clinical Medicine, PubMed, PubMed Central, Reference Citation Analysis, China Science and Technology Journal Database, and Superstar Journals Database. The 2023 Edition of Journal Citation Reports® cites the 2022 impact factor (IF) for *WJCC* as 1.1; IF without journal self cites: 1.1; 5-year IF: 1.3; Journal Citation Indicator: 0.26; Ranking: 133 among 167 journals in medicine, general and internal; and Quartile category: Q4.

RESPONSIBLE EDITORS FOR THIS ISSUE

NAME OF JOURNAL

World Journal of Clinical Cases

ISSN

ISSN 2307-8960 (online)

LAUNCH DATE

April 16, 2013

FREQUENCY

Thrice Monthly

PUBLICATION DATE

May 26, 2024

World Journal of Clinical Cases

Submit a Manuscript: https://www.f6publishing.com

World J Clin Cases 2024 May 26; 12(15): 2466-2474

DOI: 10.12998/wjcc.v12.i15.2466

ISSN 2307-8960 (online)

EDITORIAL

Focal incidental colorectal fluorodeoxyglucose uptake: Should it be spotlighted?

Haejun Lee, Kyung-Hoon Hwang

Specialty type: Radiology, nuclear medicine & medical imaging

Provenance and peer review: Invited article; Externally peer reviewed.

Peer-review model: Single blind

Peer-review report's classification
Scientific Quality: Grade C
Novelty: Grade B
Creativity or Innovation: Grade B
Scientific Significance: Grade B

P-Reviewer: Sun XG, China

Received: December 28, 2023
Revised: March 17, 2024
Accepted: April 12, 2024
Published online: May 26, 2024

Haejun Lee, Kyung-Hoon Hwang, Department of Nuclear Medicine, Gachon University College of Medicine, Gil Medical Center, Incheon 21565, South Korea

Corresponding author: Kyung-Hoon Hwang, MD, PhD, Professor, Department of Nuclear Medicine, Gachon University College of Medicine, Gil Medical Center, No. 21 Namdong-daero 774 beon-gil, Namdong-gu, Incheon 21565, South Korea. forrest88@hanmail.net

Abstract

Fluorine-18 fluorodeoxyglucose (F-18 FDG) positron emission tomography/computed tomography (PET/CT) has emerged as a cornerstone in cancer evaluation imaging, with a well-established history spanning several years. This imaging modality, encompassing the examination of the body from the base of the skull to the upper thighs, comprehensively covers the chest and abdominopelvic regions in a singular scan, allowing for a holistic assessment of nearly the entire body, including areas of marginal interest. The inherent advantage of this expansive scan range lies in its potential to unveil unexpected incidental abnormal hypermetabolic areas. The identification of incidental focal FDG uptake within colorectal regions during PET/CT scans is not an uncommon occurrence, albeit fraught with challenges associated with non-specific FDG uptake. The presence of benign colorectal lesions or physiological uptake poses a particular obstacle, as these may manifest with FDG uptake levels that mimic malignancy. Consequently, physicians are confronted with a diagnostic dilemma when encountering abnormal FDG uptake in unexpected colorectal areas. Existing studies have presented divergent results concerning these uptakes. Standardized uptake value and its derivatives have served as pivotal metrics in quantifying FDG uptake in PET images. In this article, we aim to succinctly explore the distinctive characteristics of FDG, delve into imaging findings, and elucidate the clinical significance of incidental focal colorectal uptake. This discussion aims to contribute valuable insights into the nuanced interpretation of such findings, fostering a comprehensive understanding.

Key Words: Focal; Incidental; Colorectal; Fluorodeoxyglucose; Positron emission tomography; Hypermetabolism

Core Tip: The discovery of incidental focal colorectal fluorine-18 fluorodeoxyglucose uptake on positron emission tomography/computed tomography is not uncommon in clinical settings. This phenomenon presents a unique opportunity to delve into its nuanced implications and clinical relevance. In the forthcoming discourse, we aim to explore the intricate details of these unexpected findings, shedding light on the diagnostic challenges they pose and their potential impact on patient outcomes.

Citation: Lee H, Hwang KH. Focal incidental colorectal fluorodeoxyglucose uptake: Should it be spotlighted? *World J Clin Cases* 2024; 12(15): 2466-2474
URL: https://www.wjgnet.com/2307-8960/full/v12/i15/2466.htm
DOI: https://dx.doi.org/10.12998/wjcc.v12.i15.2466

INTRODUCTION

Since the introduction of fluorine-18 fluorodeoxyglucose (F-18 FDG) for clinical imaging, it has emerged as a pivotal oncologic imaging radiopharmaceutical in the domain of nuclear medicine. F-18 FDG serves as a prominent radioactive tracer for utilization in positron emission tomography (PET) or PET/computed tomography (PET/CT). While PET alone provides functional images with limited anatomical detail, the integration of simultaneous anatomical imaging within the same machine in hybrid PET/CT enables precise localization of FDG metabolism. Given that biochemical alterations precede physical manifestations, the molecular-level insights offered by PET/CT play a crucial role in the early detection of disease states[1,2].

The initial impediment to widespread F-18 FDG use was the necessity for a cyclotron and a radiochemical laboratory for production. However, advancements over time have led to the deployment of this equipment in various regions, significantly enhancing its availability. Currently, F-18 FDG scans are globally employed for purposes ranging from diagnosis to treatment planning, evaluation, and follow-up. The practicality of F-18 FDG for everyday clinical use in hospitals is underscored by its approximate half-life of 110 min.

In contrast to other imaging modalities like CT or magnetic resonance imaging, the F-18 FDG PET/CT scan encompasses a broad range, spanning from the skull base to the upper thigh (torso), or in some instances, the entire body. This extensive scan range may encompass areas of lesser interest, potentially leading to the observation of increased FDG metabolism (hypermetabolism) at unexpected sites. This article delves into the distinctive characteristics of FDG, presenting imaging findings and exploring the clinical significance of incidental focal colorectal hypermetabolism.

CHARACTERISTICS OF F-18 FDG

The initial synthesis of FDG, credited to Pacák *et al*[3] in 1968, marked a significant milestone in medical imaging. F-18 FDG, developed by Ido *et al* in 1978, revolutionized PET imaging and found widespread application in oncology, neurology, and cardiology[3-6]. Structurally based on glucose, FDG substitutes the hydroxyl group on the 2-carbon of a glucose molecule with the fluorine-18 radionuclide[7,8]. Cellular uptake of this glucose analogue occurs primarily through glucose transporters 1 and 3, mirroring the uptake of natural glucose molecules into cells[7-9]. However, due to structural differences, FDG cannot complete the glucose metabolic pathway and becomes trapped within cells[10]. Despite this, the common initial metabolic behavior between FDG and glucose allows FDG to effectively evaluate and represent glucose metabolism in cells.

Living cells need glucose as energy source. The phenomenon known as the Warburg effect elucidates the heightened glucose uptake by cancer cells compared to normal cells for energy production[11]. Cancer cells prefer glycolysis over oxidative phosphorylation for energy production, despite its lower efficiency, as the rapid process aligns with the energy demands of cancer cells[12-15]. The increased glycolytic rate facilitates FDG uptake in cancer cells, enabling visualization through PET[16]. However, it is crucial to note that FDG is not exclusive to cancer cells. Organs with naturally high glucose metabolism, such as the brain or liver, exhibit increased FDG uptake. Moreover, benign conditions with elevated glycolysis also accumulate FDG in cells[17-21]. In essence, FDG demonstrates no discriminatory ability between malignant and benign cells.

The assessment of accumulated FDG involves both visual interpretation and quantitative measurement. The semi-quantitative index known as the standardized uptake value (SUV) serves as a representative dimensionless ratio indicating relative concentration in a region of interest[22]. SUV is calculated as follows: SUV = [tissue radioactivity concentration (decay-corrected) (mCi/mL)]/[injected tracer dose (mCi)/body weight (g)].

The widespread application of SUV is evident in its utility for distinguishing malignant from benign lesions. This is particularly crucial in oncological diagnostics, where determining a cutoff specific to a particular cancer facilitates reference value comparisons. Moreover, SUV plays a pivotal role in the assessment of treatment efficacy, enabling the comparison of pre- and post-therapy imaging data. Various metrics can express SUV, including the maximum SUV (SUVmax) representing the highest value in a single pixel, the mean SUV (SUVmean) derived from the average value in a freely drawn region, and the peak SUV (SUVpeak) determined as the average SUV in a small fixed-sized region centered on a high uptake portion. While SUVmax maintains consistency across different measurements, it is susceptible to noise

[23,24]. SUVmean, on the other hand, is sensitive to variations induced by the delineated area[25,26]. SUVpeak, encompassing a relatively large volume, exhibits resilience against noise interference but may pose challenges in the analysis of small or tiny lesions[27-29]. Additionally, alternative SUV-related parameters such as SUV corrected for lean body mass, metabolic tumor volume, and total lesion glycolysis find application in diverse clinical scenarios. Regrettably, no singular parameter emerges as flawless in addressing all aspects of SUV assessment.

F-18 FDG AVIDITY TO CANCER CELLS

The degree of FDG uptake is subject to variation, influenced by factors such as cellularity, cell activity, tumor size, and the local microenvironment[30-33]. It is important to recognize that not all cancer cells experience glucose deprivation, and FDG accumulation may not always be pronounced within them. In colorectal cancer, SUVmax values exhibited variability based on lesion length, clinical stage, pathological tissue type, and tumor differentiation[34]. For non/low-FDG-avid cancer cells, alternative radiopharmaceuticals like radiolabeled amino acids, choline, and analogues are viable options in PET imaging for cancer detection and management[35-38].

Given the shared plasma membrane protein transport for both glucose and FDG, blood glucose concentration plays a role in FDG transport. Early studies in the 1990s highlighted that elevated blood sugar levels adversely affected image quality, as FDG competed with blood glucose for cellular membrane transport[39-42]. Current guidelines from the European Association of Nuclear Medicine and the Society of Nuclear Medicine and Molecular Imaging recommend conducting F-18 FDG PET/CT when blood glucose is controlled, ideally below 11 mmol/L (approximately 200 mg/dL) [16,43]. While recent literature suggests limited impact of blood glucose levels on imaging outcomes[44-48], adherence to published guidelines remains widespread.

The heightened glycolytic activity of cancer cells contributes to increased FDG uptake, resulting in prominently intense PET imaging[49-51]. SUV is a widely used metric in clinical settings, although its utility is not without limitations. An SUV of 2.5 or higher generally indicates potential malignancy, with an SUVmax of 3.5 to 4 suggested for colon lesions [52]. However, it is crucial to note that both malignant and non-malignant cells can exhibit elevated SUV due to the non-specific uptake mechanism of FDG[53-57]. It is well known that active infectious/inflammatory lesions or benign polyps may present high FDG uptake mimicking malignant lesions[58-62]. Additionally, physiological gastrointestinal FDG uptake is also common and intense colonic FDG uptake with metformin is well known[63-67]. Thus, interpreting high FDG uptake alone does not provide a definitive distinction between malignant and non-malignant lesions. FDG remains impartial in its diagnostic specificity.

F-18 FDG UPTAKE PATTERN, FOCAL *VS* DIFFUSE

When the criteria for heightened FDG uptake are satisfied, resulting in a conspicuous elevation in FDG metabolism within the image, the manifestation of uptake can assume a focal and/or diffuse nature. While not universally applicable, diffuse uptake in certain organs is more likely to be benign or physiological in origin than malignant[54,56,68-71]. In contrast, focal uptake holds greater clinical significance, necessitating careful consideration to avoid overlooking the potential presence of a malignant lesion[72-75]. The uptake pattern is of importance.

Figure 1 illustrates two cases of heightened FDG uptake in the gastrointestinal tract. In panel A, we observe diffuse intestinal FDG uptake in a 58-year-old male patient recently diagnosed with B-cell lymphoblastic lymphoma. Meanwhile, panel B presents hypermetabolism localized to the hepatic flexure area and descending colon of a 51-year-old woman with a previous history of gastric cancer. Despite the high metabolic activity, colonoscopic examinations in both cases revealed no pathological findings such as tumors or inflammation. This absence of detectable abnormalities underscores the physiological nature of the observed bowel uptake, suggesting the complexities and subtleties of interpreting such imaging findings. Figure 2 illustrates the distinct patterns of FDG uptake within the intestinal tract of an 87-year-old male patient diagnosed with non-small cell lung cancer. The image depicts both focal and diffuse FDG uptakes, which are crucial indicators in oncological imaging. Diffuse FDG uptake along the intestinal tract is commonly observed and often attributed to physiological processes. However, it is still imperative to discern between physiological and pathological uptake to guide clinical decision-making effectively. Of particular interest is the focal hypermetabolism detected in the proximal transverse colon. Such localized hypermetabolic activity raises concerns regarding the presence of a potential pathological lesion. In this case, subsequent colonoscopy was performed to elucidate the nature of the observed focal hypermetabolism. Despite the heightened suspicion, no significant abnormal lesions were identified during the procedure. These instances underscore the importance of discerning between physiological and pathological causes of increased FDG uptake in the gastrointestinal tract, particularly in the context of oncological surveillance.

COLORECTAL INCIDENTAL FOCAL F-18 FDG UPTAKE

F-18 FDG PET/CT, an integral component in the assessment of malignant diseases, often reveals suspicious focal colorectal FDG uptake. It is imperative to recognize that the technique has limitations, particularly in detecting non-FDG-avid or small malignant lesions. The likelihood of malignancy or advanced disease correlates with higher FDG uptake, underscoring the significance of diligent examination and interpretation of observed uptake.

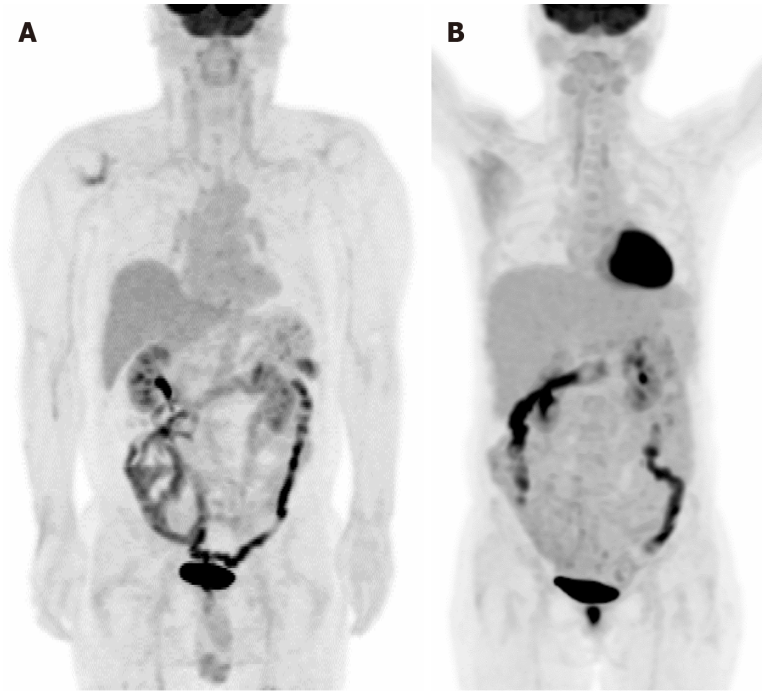

Figure 1 Diffuse physiological bowel fluorine-18 fluorodeoxyglucose uptake. Images depicting fluorine-18 fluorodeoxyglucose uptake in the bowel. A: Diffuse intestinal uptake observed in a 58-year-old male patient diagnosed with B-cell lymphoblastic lymphoma; B: Regions of hypermetabolism are highlighted in the hepatic flexure area and descending colon of a 51-year-old woman with a history of gastric cancer. Colonoscopy examination yielded no evidence of abnormalities such as tumors or inflammation, confirming the physiological nature of the observed bowel uptake.

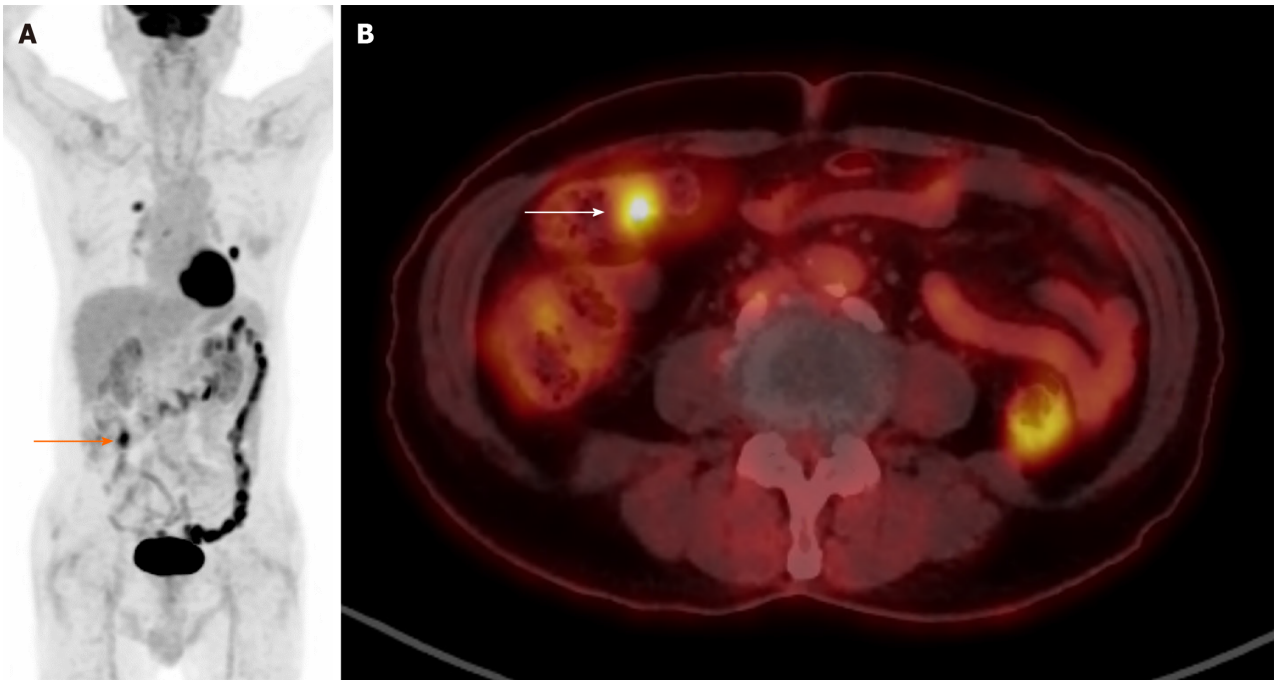

Figure 2 Focal and diffuse intestinal fluorine-18 fluorodeoxyglucose uptake. A 87-year-old man diagnosed with non-small cell lung cancer (squamous cell carcinoma) is depicted. A: Focal (arrow) and diffuse intestinal uptakes are evident. While diffuse uptake may represent physiological activity, a focal hypermetabolic area raises suspicion for a potential pathological lesion; B: Focal uptake is specifically noted in the proximal transverse colon. Subsequent colonoscopy was performed, revealing no significant abnormal lesions.

Incidental colorectal FDG uptake occurs in approximately 5% of cases[76-78], with focal uptake presenting a higher likelihood of malignancy compared to diffuse patterns[71]. Diffuse and segmental uptake may stem from inflammation, physiological processes, or FDG excretion[79,80], generally associated with a lower risk of malignancy. Focal uptake prevalence reaches up to 16%[81], with malignant and premalignant lesions constituting around 70% of focal uptake with SUVmax exceeding approximately 5[72,81-85]. Colonoscopy is often recommended for further investigation in such cases

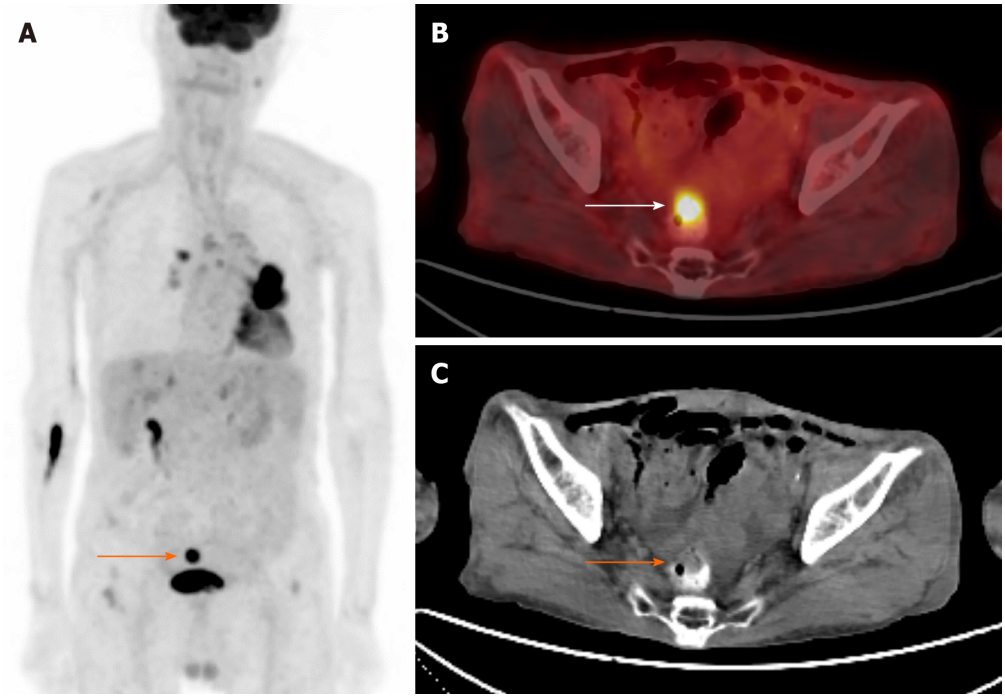

Figure 3 Focal intestinal fluorine-18 fluorodeoxyglucose uptake. A: Maximum intensity projection depicting focal hypermetabolism superior to the urinary bladder (arrow) in an 88-year-old man diagnosed with non-small cell lung cancer; B: Axial view revealing focal hypermetabolism localized in the rectum; C: Non-contrast-enhanced computed tomography obtained from positron emission tomography/computed tomography, highlighting a space-occupying lesion within the rectum. Notably, a discernible posterior radioopaque area suggests the presence of residual contrast material from a prior contrast-enhanced examination. Subsequent colonoscopy and pathological analysis definitively identified the lesion as adenocarcinoma originating from the rectum.

[72,80,81,84-87], although ongoing debates surround the optimal PET parameters for distinguishing premalignant/malignant lesions from benign ones, with varying studies utilizing SUVmax[72,81,83,88,89].

Premalignant lesions are not yet malignant; however, they have more chance to develop into malignant lesions. Adenomas (tubular adenomas, villous adenomas, tubulovillous adenomas) are the most frequent premalignant lesions and others include chronic inflammatory bowel diseases, hereditary syndromes (familial adenomatous polyposis, Peutz-Jeghers syndrome, and juvenile polyposis). Colorectal adenomatous polyps are known to develop in up to 40% of people over the age of 60[90]. While debates persist regarding the role of SUV in differentiating malignant/premalignant from benign lesions[76,91-95], the significance of more than 50% malignancy in focal FDG colorectal uptake is noteworthy. In terms of cancer development by the location (distal or proximal), different genetic mechanisms are suggested[96-98], however, no significant difference was observed in SUVmax depending on location[34]. Notably, the observation of mixed single/multiple focal and diffuse uptake in the colorectal region underscores the complexity of interpretation. In such cases, diffuse uptake does not conclusively exclude the need for further evaluation, including colonoscopy and histopathological confirmation.

Figure 3 illustrates focal hypermetabolism incidentally detected in the rectum of an 88-year-old man previously diagnosed with non-small cell lung cancer in his left lung. Subsequent colonoscopy and pathological analysis confirmed the presence of adenocarcinoma originating from the rectum, establishing a secondary malignancy. This case highlights the importance of vigilant surveillance in cancer patients, as the detection of secondary malignancies or metastases can significantly impact treatment strategies, overall survival rates, and quality of life for patients.

CONCLUSION

The detection of unexpected focal colorectal F-18 FDG uptake is a frequent occurrence, with significant implications for clinical practice. Given the distinctive characteristics of FDG, notably its increased uptake in premalignant and malignant lesions, particularly when indicated by high SUV values, such findings warrant careful consideration. Studies have shown that a substantial proportion, approximately 70%, of focal colorectal FDG uptake corresponds to malignancies or premalignant lesions, especially when the SUVmax exceeds a threshold of approximately 5. While acknowledging the inherent limitations of F-18 FDG PET/CT, which may introduce uncertainty and hesitancy in interpretation, it is crucial to emphasize the diagnostic utility of observed FDG uptake patterns. Clinicians should be guided by these findings to pursue further proactive evaluation, thereby enhancing diagnostic precision and facilitating timely interventions. By leveraging the observed rates of malignancy and the degree of FDG uptake, clinicians can make informed decisions that optimize patient care and outcomes.

FOOTNOTES

Author contributions: Lee H and Hwang KH designed the editorial, searched the articles, analyzed the data and wrote the manuscript; Lee H contributed analytic tools. All authors have read and approved the final manuscript.

Conflict-of-interest statement: The authors declare that they have no conflicting interests.

Country/Territory of origin: South Korea

ORCID number: Haejun Lee 0000-0002-6284-2903; Kyung-Hoon Hwang 0000-0002-9988-1906.

S-Editor: Zheng XM
L-Editor: A
P-Editor: Zheng XM

REFERENCES

1 **Zhu A**, Lee D, Shim H. Metabolic positron emission tomography imaging in cancer detection and therapy response. *Semin Oncol* 2011; **38**: 55-69 [PMID: 21362516 DOI: 10.1053/j.seminoncol.2010.11.012]
2 **Wong CY**, Salem R, Raman S, Gates VL, Dworkin HJ. Evaluating 90Y-glass microsphere treatment response of unresectable colorectal liver metastases by [18F]FDG PET: a comparison with CT or MRI. *Eur J Nucl Med Mol Imaging* 2002; **29**: 815-820 [PMID: 12029557 DOI: 10.1007/s00259-002-0787-4]
3 **Pacák J**, Točík Z, Černý M. Synthesis of 2-deoxy-2-fluoro-D-glucose. *J Chem Soc Chem Commun* 1969; 77 [DOI: 10.1039/C29690000077]
4 **Ido T**, Wan CN, Casella V, Fowler JS, Wolf AP, Reivich M, Kuhl DE. Labeled 2-deoxy-D-glucose analogs. 18F-labeled 2-deoxy-2-fluoro-D-glucose, 2-deoxy-2-fluoro-D-mannose and 14C-2-deoxy-2-fluoro-D-glucose. *J Labelled Comp Radiopharm* 1978; **14**: 175-183 [DOI: 10.1002/jlcr.2580140204]
5 **Guerrero TM**, Hoffman EJ, Dahlbom M, Cutler PD, Hawkins RA, Phelps ME. Characterization of a Whole-Body Imaging Technique for Pet. *IEEE Trans Nucl Sci* 1990; **37**: 676-680 [DOI: 10.1109/23.106697]
6 **Cherry SR**. Fundamentals of positron emission tomography and applications in preclinical drug development. *J Clin Pharmacol* 2001; **41**: 482-491 [PMID: 11361044 DOI: 10.1177/00912700122010357]
7 **Yu S**. Review of F-FDG Synthesis and Quality Control. *Biomed Imaging Interv J* 2006; **2**: e57 [PMID: 21614337 DOI: 10.2349/biij.2.4.e57]
8 **Kelloff GJ**, Hoffman JM, Johnson B, Scher HI, Siegel BA, Cheng EY, Cheson BD, O'Shaughnessy J, Guyton KZ, Mankoff DA, Shankar L, Larson SM, Sigman CC, Schilsky RL, Sullivan DC. Progress and promise of FDG-PET imaging for cancer patient management and oncologic drug development. *Clin Cancer Res* 2005; **11**: 2785-2808 [DOI: 10.1158/1078-0432.CCR-04-2626]
9 **Smith TA**. Facilitative glucose transporter expression in human cancer tissue. *Br J Biomed Sci* 1999; **56**: 285-292 [PMID: 10795374]
10 **Gallagher BM**, Fowler JS, Gutterson NI, MacGregor RR, Wan CN, Wolf AP. Metabolic trapping as a principle of oradiopharmaceutical design: some factors resposible for the biodistribution of [18F] 2-deoxy-2-fluoro-D-glucose. *J Nucl Med* 1978; **19**: 1154-1161 [PMID: 214528]
11 **Warburg O**. Über den Stoffwechsel der Carcinomzelle. *Naturwissenschaften* 1924; **12**: 1131-1137 [DOI: 10.1007/BF01504608]
12 **Rajendran JG**, Mankoff DA, O'Sullivan F, Peterson LM, Schwartz DL, Conrad EU, Spence AM, Muzi M, Farwell DG, Krohn KA. Hypoxia and glucose metabolism in malignant tumors: evaluation by [18F]fluoromisonidazole and [18F]fluorodeoxyglucose positron emission tomography imaging. *Clin Cancer Res* 2004; **10**: 2245-2252 [PMID: 15073099 DOI: 10.1158/1078-0432.ccr-0688-3]
13 **Coleman CN**, Mitchell JB, Camphausen K. Tumor hypoxia: chicken, egg, or a piece of the farm? *J Clin Oncol* 2002; **20**: 610-615 [PMID: 11821437 DOI: 10.1200/JCO.2002.20.3.610]
14 **Annibaldi A**, Widmann C. Glucose metabolism in cancer cells. *Curr Opin Clin Nutr Metab Care* 2010; **13**: 466-470 [PMID: 20473153 DOI: 10.1097/MCO.0b013e32833a5577]
15 **Smith TA**. FDG uptake, tumour characteristics and response to therapy: a review. *Nucl Med Commun* 1998; **19**: 97-105 [PMID: 9548192 DOI: 10.1097/00006231-199802000-00002]
16 **Boellaard R**, Delgado-Bolton R, Oyen WJ, Giammarile F, Tatsch K, Eschner W, Verzijlbergen FJ, Barrington SF, Pike LC, Weber WA, Stroobants S, Delbeke D, Donohoe KJ, Holbrook S, Graham MM, Testanera G, Hoekstra OS, Zijlstra J, Visser E, Hoekstra CJ, Pruim J, Willemsen A, Arends B, Kotzerke J, Bockisch A, Beyer T, Chiti A, Krause BJ; European Association of Nuclear Medicine (EANM). FDG PET/CT: EANM procedure guidelines for tumour imaging: version 2.0. *Eur J Nucl Med Mol Imaging* 2015; **42**: 328-354 [PMID: 25452219 DOI: 10.1007/s00259-014-2961-x]
17 **Vangu MDT**, Momodu JI. F-18 FDG PET/CT Imaging in Normal Variants, Pitfalls and Artifacts in the Abdomen and Pelvis. *Front Nucl Med* 2022; **1** [DOI: 10.3389/fnume.2021.826109]
18 **Li Y**, Behr S. Acute Findings on FDG PET/CT: Key Imaging Features and How to Differentiate Them from Malignancy. *Curr Radiol Rep* 2020; **8**: 22 [PMID: 32953250 DOI: 10.1007/s40134-020-00367-x]
19 **Buyukdereli G**, Kara E, Guler M, Kanat N. Evaluation of Visible Physiological F-18 FDG Uptake Patterns in Spinal Cord on PET/CT. *Neurosurg Quart* 2015; **25**: 403-406 [DOI: 10.1097/wnq.0000000000000073]
20 **Purohit BS**, Ailianou A, Dulguerov N, Becker CD, Ratib O, Becker M. FDG-PET/CT pitfalls in oncological head and neck imaging. *Insights Imaging* 2014; **5**: 585-602 [PMID: 25154759 DOI: 10.1007/s13244-014-0349-x]
21 **Kostakoglu L**, Hardoff R, Mirtcheva R, Goldsmith SJ. PET-CT fusion imaging in differentiating physiologic from pathologic FDG uptake.

Radiographics 2004; **24**: 1411-1431 [PMID: 15371617 DOI: 10.1148/rg.245035725]
22 **Zasadny KR**, Wahl RL. Standardized uptake values of normal tissues at PET with 2-[fluorine-18]-fluoro-2-deoxy-D-glucose: variations with body weight and a method for correction. *Radiology* 1993; **189**: 847-850 [PMID: 8234714 DOI: 10.1148/radiology.189.3.8234714]
23 **Boellaard R**, Krak NC, Hoekstra OS, Lammertsma AA. Effects of noise, image resolution, and ROI definition on the accuracy of standard uptake values: a simulation study. *J Nucl Med* 2004; **45**: 1519-1527 [PMID: 15347719]
24 **Nakamoto Y**, Zasadny KR, Minn H, Wahl RL. Reproducibility of common semi-quantitative parameters for evaluating lung cancer glucose metabolism with positron emission tomography using 2-deoxy-2-[18F]fluoro-D-glucose. *Mol Imaging Biol* 2002; **4**: 171-178 [PMID: 14537140 DOI: 10.1016/s1536-1632(01)00004-x]
25 **Nahmias C**, Wahl LM. Reproducibility of standardized uptake value measurements determined by 18F-FDG PET in malignant tumors. *J Nucl Med* 2008; **49**: 1804-1808 [PMID: 18927325 DOI: 10.2967/jnumed.108.054239]
26 **Krak NC**, Boellaard R, Hoekstra OS, Twisk JW, Hoekstra CJ, Lammertsma AA. Effects of ROI definition and reconstruction method on quantitative outcome and applicability in a response monitoring trial. *Eur J Nucl Med Mol Imaging* 2005; **32**: 294-301 [PMID: 15791438 DOI: 10.1007/s00259-004-1566-1]
27 **Vanderhoek M**, Perlman SB, Jeraj R. Impact of the definition of peak standardized uptake value on quantification of treatment response. *J Nucl Med* 2012; **53**: 4-11 [PMID: 22213818 DOI: 10.2967/jnumed.111.093443]
28 **Oh HH**, Lee SE, Choi IS, Choi WJ, Yoon DS, Min HS, Ra YM, Moon JI, Kang YH. The peak-standardized uptake value (P-SUV) by preoperative positron emission tomography-computed tomography (PET-CT) is a useful indicator of lymph node metastasis in gastric cancer. *J Surg Oncol* 2011; **104**: 530-533 [PMID: 21618250 DOI: 10.1002/jso.21985]
29 **Westerterp M**, Pruim J, Oyen W, Hoekstra O, Paans A, Visser E, van Lanschot J, Sloof G, Boellaard R. Quantification of FDG PET studies using standardised uptake values in multi-centre trials: effects of image reconstruction, resolution and ROI definition parameters. *Eur J Nucl Med Mol Imaging* 2007; **34**: 392-404 [PMID: 17033848 DOI: 10.1007/s00259-006-0224-1]
30 **Sung Y**, Tetrault MA, Takahashi K, Ouyang J, Pratx G, Fakhri GE, Normandin MD. Dependence of fluorodeoxyglucose (FDG) uptake on cell cycle and dry mass: a single-cell study using a multi-modal radiography platform. *Sci Rep* 2020; **10**: 4280 [PMID: 32152343 DOI: 10.1038/s41598-020-59515-0]
31 **Roppongi M**, Izumisawa M, Terasaki K, Muraki Y, Shozushima M. (18)F-FDG and (11)C-choline uptake in proliferating tumor cells is dependent on the cell cycle in vitro. *Ann Nucl Med* 2019; **33**: 237-243 [PMID: 30588580 DOI: 10.1007/s12149-018-01325-6]
32 **Türkcan S**, Kiru L, Naczynski DJ, Sasportas LS, Pratx G. Lactic Acid Accumulation in the Tumor Microenvironment Suppresses (18)F-FDG Uptake. *Cancer Res* 2019; **79**: 410-419 [PMID: 30510121 DOI: 10.1158/0008-5472.CAN-17-0492]
33 **Longo DL**, Bartoli A, Consolino L, Bardini P, Arena F, Schwaiger M, Aime S. In Vivo Imaging of Tumor Metabolism and Acidosis by Combining PET and MRI-CEST pH Imaging. *Cancer Res* 2016; **76**: 6463-6470 [PMID: 27651313 DOI: 10.1158/0008-5472.CAN-16-0825]
34 **Li D**, Wang Y, Liu W, Chen Q, Cai L, Xing X, Gao S. The Correlation between (18)F-FDG PET/CT Imaging SUVmax of Preoperative Colon Cancer Primary Lesions and Clinicopathological Factors. *J Oncol* 2021; **2021**: 4312296 [PMID: 34567115 DOI: 10.1155/2021/4312296]
35 **Verger A**, Imbert L, Zaragori T. Dynamic amino-acid PET in neuro-oncology: a prognostic tool becomes essential. *Eur J Nucl Med Mol Imaging* 2021; **48**: 4129-4132 [PMID: 34518904 DOI: 10.1007/s00259-021-05530-w]
36 **Najjar AM**, Johnson JM, Schellingerhout D. The Emerging Role of Amino Acid PET in Neuro-Oncology. *Bioengineering (Basel)* 2018; **5** [PMID: 30487391 DOI: 10.3390/bioengineering5040104]
37 **Goldstein J**, Even-Sapir E, Ben-Haim S, Saad A, Spieler B, Davidson T, Berger R, Weiss I, Appel S, Lawrence YR, Symon Z. Does Choline PET/CT Change the Management of Prostate Cancer Patients With Biochemical Failure? *Am J Clin Oncol* 2017; **40**: 256-259 [PMID: 25319322 DOI: 10.1097/COC.0000000000000139]
38 **Urso L**, Rocca GC, Borgia F, Lancia F, Malorgio A, Gagliano M, Zanetto M, Uccelli L, Cittanti C, Ippolito C, Evangelista L, Bartolomei M. The Role of [(18)F]F-Choline PET/CT in the Initial Management and Outcome Prediction of Prostate Cancer: A Real-World Experience from a Multidisciplinary Approach. *Biomedicines* 2022; **10** [PMID: 36289724 DOI: 10.3390/biomedicines10102463]
39 **Wahl RL**, Henry CA, Ethier SP. Serum glucose: effects on tumor and normal tissue accumulation of 2-[F-18]-fluoro-2-deoxy-D-glucose in rodents with mammary carcinoma. *Radiology* 1992; **183**: 643-647 [PMID: 1584912 DOI: 10.1148/radiology.183.3.1584912]
40 **Lindholm P**, Minn H, Leskinen-Kallio S, Bergman J, Ruotsalainen U, Joensuu H. Influence of the blood glucose concentration on FDG uptake in cancer--a PET study. *J Nucl Med* 1993; **34**: 1-6 [PMID: 8418248]
41 **Minn H**, Leskinen-Kallio S, Lindholm P, Bergman J, Ruotsalainen U, Teräs M, Haaparanta M. [18F]fluorodeoxyglucose uptake in tumors: kinetic vs. steady-state methods with reference to plasma insulin. *J Comput Assist Tomogr* 1993; **17**: 115-123 [PMID: 8419418]
42 **Langen KJ**, Braun U, Rota Kops E, Herzog H, Kuwert T, Nebeling B, Feinendegen LE. The influence of plasma glucose levels on fluorine-18-fluorodeoxyglucose uptake in bronchial carcinomas. *J Nucl Med* 1993; **34**: 355-359 [PMID: 8441023]
43 **Delbeke D**, Coleman RE, Guiberteau MJ, Brown ML, Royal HD, Siegel BA, Townsend DW, Berland LL, Parker JA, Hubner K, Stabin MG, Zubal G, Kachelriess M, Cronin V, Holbrook S. Procedure guideline for tumor imaging with 18F-FDG PET/CT 1.0. *J Nucl Med* 2006; **47**: 885-895 [PMID: 16644760]
44 **Hara T**, Higashi T, Nakamoto Y, Suga T, Saga T, Ishimori T, Ishizu K, Kawashima H, Kawase S, Matsumoto K, Togashi K. Significance of chronic marked hyperglycemia on FDG-PET: is it really problematic for clinical oncologic imaging? *Ann Nucl Med* 2009; **23**: 657-669 [PMID: 19662347 DOI: 10.1007/s12149-009-0288-7]
45 **Lindholm H**, Brolin F, Jonsson C, Jacobsson H. The relation between the blood glucose level and the FDG uptake of tissues at normal PET examinations. *EJNMMI Res* 2013; **3**: 50 [PMID: 23829959 DOI: 10.1186/2191-219X-3-50]
46 **Sprinz C**, Altmayer S, Zanon M, Watte G, Irion K, Marchiori E, Hochhegger B. Effects of blood glucose level on 18F-FDG uptake for PET/CT in normal organs: A systematic review. *PLoS One* 2018; **13**: e0193140 [PMID: 29486008 DOI: 10.1371/journal.pone.0193140]
47 **Eskian M**, Alavi A, Khorasanizadeh M, Viglianti BL, Jacobsson H, Barwick TD, Meysamie A, Yi SK, Iwano S, Bybel B, Caobelli F, Lococo F, Gea J, Sancho-Muñoz A, Schildt J, Tatcı E, Lapa C, Keramida G, Peters M, Boktor RR, John J, Pitman AG, Mazurek T, Rezaei N. Effect of blood glucose level on standardized uptake value (SUV) in (18)F- FDG PET-scan: a systematic review and meta-analysis of 20,807 individual SUV measurements. *Eur J Nucl Med Mol Imaging* 2019; **46**: 224-237 [PMID: 30350009 DOI: 10.1007/s00259-018-4194-x]
48 **Cengİz A**. The Relation Between the Blood Glucose Level and the FDG Uptake of Tissues at Normal or Near-Normal PET/CT Imaging. *Akd Med J* 2019; **5**: 365-369 [DOI: 10.17954/amj.2019.1709]
49 **Rohren EM**, Turkington TG, Coleman RE. Clinical applications of PET in oncology. *Radiology* 2004; **231**: 305-332 [PMID: 15044750 DOI: 10.1148/radiol.2312021185]

50 **Czernin J**. Clinical applications of FDG-PET in oncology. *Acta Med Austriaca* 2002; **29**: 162-170 [PMID: 12506767 DOI: 10.1046/j.1563-2571.2002.02042.x]

51 **Pinilla I**, Rodríguez-Vigil B, Gómez-León N. Integrated FDG PET/CT: Utility and Applications in Clinical Oncology. *Clin Med Oncol* 2008; **2**: 181-198 [PMID: 21892279 DOI: 10.4137/cmo.s504]

52 **Liu T**, Behr S, Khan S, Osterhoff R, Aparici CM. Focal Colonic FDG Activity with PET/CT: Guidelines for Recommendation of Colonoscopy. *World J Nucl Med* 2015; **14**: 25-30 [PMID: 25709541 DOI: 10.4103/1450-1147.150524]

53 **Cook GJ**, Maisey MN, Fogelman I. Normal variants, artefacts and interpretative pitfalls in PET imaging with 18-fluoro-2-deoxyglucose and carbon-11 methionine. *Eur J Nucl Med* 1999; **26**: 1363-1378 [PMID: 10541839 DOI: 10.1007/s002590050597]

54 **Shreve PD**, Anzai Y, Wahl RL. Pitfalls in oncologic diagnosis with FDG PET imaging: physiologic and benign variants. *Radiographics* 1999; **19**: 61-77; quiz 150 [PMID: 9925392 DOI: 10.1148/radiographics.19.1.g99ja0761]

55 **Cook GJ**, Fogelman I, Maisey MN. Normal physiological and benign pathological variants of 18-fluoro-2-deoxyglucose positron-emission tomography scanning: potential for error in interpretation. *Semin Nucl Med* 1996; **26**: 308-314 [PMID: 8916319 DOI: 10.1016/s0001-2998(96)80006-7]

56 **Ahmad Sarji S**. Physiological uptake in FDG PET simulating disease. *Biomed Imaging Interv J* 2006; **2**: e59 [PMID: 21614339 DOI: 10.2349/biij.2.4.e59]

57 **Adejolu M**, Huo L, Rohren E, Santiago L, Yang WT. False-positive lesions mimicking breast cancer on FDG PET and PET/CT. *AJR Am J Roentgenol* 2012; **198**: W304-W314 [PMID: 22358030 DOI: 10.2214/AJR.11.7130]

58 **Kubota R**, Yamada S, Kubota K, Ishiwata K, Tamahashi N, Ido T. Intratumoral distribution of fluorine-18-fluorodeoxyglucose in vivo: high accumulation in macrophages and granulation tissues studied by microautoradiography. *J Nucl Med* 1992; **33**: 1972-1980 [PMID: 1432158]

59 **Mochizuki T**, Tsukamoto E, Kuge Y, Kanegae K, Zhao S, Hikosaka K, Hosokawa M, Kohanawa M, Tamaki N. FDG uptake and glucose transporter subtype expressions in experimental tumor and inflammation models. *J Nucl Med* 2001; **42**: 1551-1555 [PMID: 11585872]

60 **Love C**, Tomas MB, Tronco GG, Palestro CJ. FDG PET of infection and inflammation. *Radiographics* 2005; **25**: 1357-1368 [PMID: 16160116 DOI: 10.1148/rg.255045122]

61 **Safaie E**, Matthews R, Bergamaschi R. PET scan findings can be false positive. *Tech Coloproctol* 2015; **19**: 329-330 [PMID: 25939996 DOI: 10.1007/s10151-015-1308-3]

62 **Vaidyanathan S**, Patel CN, Scarsbrook AF, Chowdhury FU. FDG PET/CT in infection and inflammation--current and emerging clinical applications. *Clin Radiol* 2015; **70**: 787-800 [PMID: 25917543 DOI: 10.1016/j.crad.2015.03.010]

63 **Gontier E**, Fourme E, Wartski M, Blondet C, Bonardel G, Le Stanc E, Mantzarides M, Foehrenbach H, Pecking AP, Alberini JL. High and typical 18F-FDG bowel uptake in patients treated with metformin. *Eur J Nucl Med Mol Imaging* 2008; **35**: 95-99 [PMID: 17786437 DOI: 10.1007/s00259-007-0563-6]

64 **Oh JR**, Song HC, Chong A, Ha JM, Jeong SY, Min JJ, Bom HS. Impact of medication discontinuation on increased intestinal FDG accumulation in diabetic patients treated with metformin. *AJR Am J Roentgenol* 2010; **195**: 1404-1410 [PMID: 21098202 DOI: 10.2214/AJR.10.4663]

65 **Ozülker T**, Ozülker F, Mert M, Ozpaçaci T. Clearance of the high intestinal (18)F-FDG uptake associated with metformin after stopping the drug. *Eur J Nucl Med Mol Imaging* 2010; **37**: 1011-1017 [PMID: 20107796 DOI: 10.1007/s00259-009-1330-7]

66 **Bybel B**, Greenberg ID, Paterson J, Ducharme J, Leslie WD. Increased F-18 FDG intestinal uptake in diabetic patients on metformin: a matched case-control analysis. *Clin Nucl Med* 2011; **36**: 452-456 [PMID: 21552023 DOI: 10.1097/RLU.0b013e318217399e]

67 **Steenkamp DW**, McDonnell ME, Meibom S. Metformin may be associated with false-negative cancer detection in the gastrointestinal tract on PET/CT. *Endocr Pract* 2014; **20**: 1079-1083 [PMID: 25100379 DOI: 10.4158/EP14127.RA]

68 **Prabhakar HB**, Sahani DV, Fischman AJ, Mueller PR, Blake MA. Bowel hot spots at PET-CT. *Radiographics* 2007; **27**: 145-159 [PMID: 17235004 DOI: 10.1148/rg.271065080]

69 **Tatlidil R**, Jadvar H, Bading JR, Conti PS. Incidental colonic fluorodeoxyglucose uptake: correlation with colonoscopic and histopathologic findings. *Radiology* 2002; **224**: 783-787 [PMID: 12202714 DOI: 10.1148/radiol.2243011214]

70 **Kresnik E**, Mikosch P, Gallowitsch HJ, Heinisch M, Lind P. F-18 fluorodeoxyglucose positron emission tomography in the diagnosis of inflammatory bowel disease. *Clin Nucl Med* 2001; **26**: 867 [PMID: 11564929 DOI: 10.1097/00003072-200110000-00015]

71 **Shmidt E**, Nehra V, Lowe V, Oxentenko AS. Clinical significance of incidental [18 F]FDG uptake in the gastrointestinal tract on PET/CT imaging: a retrospective cohort study. *BMC Gastroenterol* 2016; **16**: 125 [PMID: 27716085 DOI: 10.1186/s12876-016-0545-x]

72 **Gökden Y**, Özülker F, Özülker T. Prevalence and Clinical Significance of Incidental Focal (18)F-FDG Uptake in Colon on PET/CT Imaging. *Mol Imaging Radionucl Ther* 2022; **31**: 96-103 [PMID: 35770960 DOI: 10.4274/mirt.galenos.2022.38247]

73 **de Leijer JF**, Metman MJH, van der Hoorn A, Brouwers AH, Kruijff S, van Hemel BM, Links TP, Westerlaan HE. Focal Thyroid Incidentalomas on (18)F-FDG PET/CT: A Systematic Review and Meta-Analysis on Prevalence, Risk of Malignancy and Inconclusive Fine Needle Aspiration. *Front Endocrinol (Lausanne)* 2021; **12**: 723394 [PMID: 34744999 DOI: 10.3389/fendo.2021.723394]

74 **Aarstad EM**, Nordhaug P, Naghavi-Behzad M, Larsen LB, Gerke O, Hildebrandt MG. Prevalence of focal incidental breast uptake on FDG-PET/CT and risk of malignancy: a systematic review and meta-analysis. *Eur J Hybrid Imaging* 2019; **3**: 16 [PMID: 34191158 DOI: 10.1186/s41824-019-0063-5]

75 **Brown AM**, Lindenberg ML, Sankineni S, Shih JH, Johnson LM, Pruthy S, Kurdziel KA, Merino MJ, Wood BJ, Pinto PA, Choyke PL, Turkbey B. Does focal incidental 18F-FDG PET/CT uptake in the prostate have significance? *Abdom Imaging* 2015; **40**: 3222-3229 [PMID: 26239399 DOI: 10.1007/s00261-015-0520-y]

76 **van Hoeij FB**, Keijsers RG, Loffeld BC, Dun G, Stadhouders PH, Weusten BL. Incidental colonic focal FDG uptake on PET/CT: can the maximum standardized uptake value (SUVmax) guide us in the timing of colonoscopy? *Eur J Nucl Med Mol Imaging* 2015; **42**: 66-71 [PMID: 25139518 DOI: 10.1007/s00259-014-2887-3]

77 **Keyzer C**, Dhaene B, Blocklet D, De Maertelaer V, Goldman S, Gevenois PA. Colonoscopic Findings in Patients With Incidental Colonic Focal FDG Uptake. *AJR Am J Roentgenol* 2015; **204**: W586-W591 [PMID: 25905966 DOI: 10.2214/AJR.14.12817]

78 **Hui YH**, Kung BT, Yong TKA. Incidental Focal Colonic Uptake of 18F-fluorodeoxyglucose on Positron Emission Tomography/Computed Tomography: Its Incidence and Clinical Significance. *Hong Kong J Radiol* 2020; **23**: 275-280 [DOI: 10.12809/hkjr2017040]

79 **Şimşek FS**, İspiroğlu M, Taşdemir B, Köroğlu R, Ünal K, Özercan IH, Entok E, Kuşlu D, Karabulut K. What approach should we take for the incidental finding of increased 18F-FDG uptake foci in the colon on PET/CT? *Nucl Med Commun* 2015; **36**: 1195-1201 [PMID: 26426964 DOI: 10.1097/MNM.0000000000000388]

80 **Salazar Andía G**, Prieto Soriano A, Ortega Candil A, Cabrera Martín MN, González Roiz C, Ortiz Zapata JJ, Cardona Arboniés J, Lapeña

Gutiérrez L, Carreras Delgado JL. Clinical relevance of incidental finding of focal uptakes in the colon during 18F-FDG PET/CT studies in oncology patients without known colorectal carcinoma and evaluation of the impact on management. *Rev Esp Med Nucl Imagen Mol* 2012; **31**: 15-21 [PMID: 21640441 DOI: 10.1016/j.remn.2011.03.014]

81 **Treglia G**, Taralli S, Salsano M, Muoio B, Sadeghi R, Giovanella L. Prevalence and malignancy risk of focal colorectal incidental uptake detected by (18)F-FDG-PET or PET/CT: a meta-analysis. *Radiol Oncol* 2014; **48**: 99-104 [PMID: 24991198 DOI: 10.2478/raon-2013-0035]

82 **Albertsen LN**, Jaensch C, Tornbjerg SM, Teil J, Madsen AH. Correlation between incidental focal colorectal FDG uptake on PET/CT and colonoscopic and histopathological results. *Scand J Gastroenterol* 2022; **57**: 246-252 [PMID: 34735311 DOI: 10.1080/00365521.2021.1998602]

83 **Xu W**, Li H, Guo Z, Zhang L, Zhang R. Combined SUVmax and localized colonic wall thickening parameters to identify high-risk lesions from incidental focal colorectal (18)F-FDG uptake foci. *Front Oncol* 2022; **12**: 972096 [PMID: 36033516 DOI: 10.3389/fonc.2022.972096]

84 **Kousgaard SJ**, Gade M, Petersen LJ, Thorlacius-Ussing O. Incidental detection of colorectal lesions on (18) F-FDG-PET/CT is associated with high proportion of malignancy: A study in 549 patients. *Endosc Int Open* 2020; **8**: E1725-E1731 [PMID: 33269303 DOI: 10.1055/a-1266-3308]

85 **Fuertes J**, Montagut C, Bullich S, Coma MI, Mestre-Fusco A, Suárez-Piñera M, Trampal C, Bellmunt J. Incidental focal uptake in colorectal location on oncologic ^{18}FDG PET and PET/CT studies: histopathological findings and clinical significances. *Rev Esp Med Nucl Imagen Mol* 2015; **34**: 95-101 [PMID: 25263718 DOI: 10.1016/j.remn.2014.07.008]

86 **Rigault E**, Lenoir L, Bouguen G, Pagenault M, Lièvre A, Garin E, Siproudhis L, Bretagne JF. Incidental colorectal focal (18) F-FDG uptake: a novel indication for colonoscopy. *Endosc Int Open* 2017; **5**: E924-E930 [PMID: 28924601 DOI: 10.1055/s-0043-116384]

87 **Lee C**, Koh SJ, Kim JW, Lee KL, Im JP, Kim SG, Kim JS, Jung HC, Kim BG. Incidental colonic 18F-fluorodeoxyglucose uptake: do we need colonoscopy for patients with focal uptake confined to the left-sided colon? *Dig Dis Sci* 2013; **58**: 229-235 [PMID: 22886593 DOI: 10.1007/s10620-012-2333-y]

88 **Cho SH**, Kim SW, Kim WC, Park JM, Yoo IeR, Kim SH, Oh ST. Incidental focal colorectal ^{18}F-fluorodeoxyglucose uptake on positron emission tomography/computed tomography. *World J Gastroenterol* 2013; **19**: 3453-3458 [PMID: 23801838 DOI: 10.3748/wjg.v19.i22.3453]

89 **Wu GZ**, Sun D, Chen JY, Qiu JM, Kong Y. [Clinical diagnostic value of (18)F-FDG PET-CT in incidental finding of focal hypermetabolism focus in the colon and rectum]. *Zhonghua Wei Chang Wai Ke Za Zhi* 2013; **16**: 555-560 [PMID: 23801210]

90 **Levine JS**, Ahnen DJ. Clinical practice. Adenomatous polyps of the colon. *N Engl J Med* 2006; **355**: 2551-2557 [PMID: 17167138 DOI: 10.1056/NEJMcp063038]

91 **Servente L**, Gigirey V, García Fontes M, Alonso O. Incidental focal colonic uptake in studies (18)F-FDG PET/CT. *Rev Esp Med Nucl Imagen Mol (Engl Ed)* 2018; **37**: 15-19 [PMID: 28750749 DOI: 10.1016/j.remn.2017.03.012]

92 **Soltau SR**, Hess S, Nguyen T, Gerke O, Petersen H, Alavi A, Høilund-Carlsen PF. Clinical significance of incidental focal bowel uptake on (18)F-FDG PET/CT as related to colorectal cancer. *Hell J Nucl Med* 2016; **19**: 245-249 [PMID: 27824964]

93 **Purandare NC**, Gawade SK, Puranik AD, Agrawal A, Shah S, Rangarajan V. Etiology and significance of incidentally detected focal colonic uptake on FDG PET/CT. *Indian J Radiol Imaging* 2012; **22**: 260-266 [PMID: 23833416 DOI: 10.4103/0971-3026.111476]

94 **Kei PL**, Vikram R, Yeung HW, Stroehlein JR, Macapinlac HA. Incidental finding of focal FDG uptake in the bowel during PET/CT: CT features and correlation with histopathologic results. *AJR Am J Roentgenol* 2010; **194**: W401-W406 [PMID: 20410385 DOI: 10.2214/AJR.09.3703]

95 **Weston BR**, Iyer RB, Qiao W, Lee JH, Bresalier RS, Ross WA. Ability of integrated positron emission and computed tomography to detect significant colonic pathology: the experience of a tertiary cancer center. *Cancer* 2010; **116**: 1454-1461 [PMID: 20143447 DOI: 10.1002/cncr.24885]

96 **Bufill JA**. Colorectal cancer: evidence for distinct genetic categories based on proximal or distal tumor location. *Ann Intern Med* 1990; **113**: 779-788 [PMID: 2240880 DOI: 10.7326/0003-4819-113-10-779]

97 **Fearon ER**, Vogelstein B. A genetic model for colorectal tumorigenesis. *Cell* 1990; **61**: 759-767 [PMID: 2188735 DOI: 10.1016/0092-8674(90)90186-i]

98 **Beart RW**, Melton LJ 3rd, Maruta M, Dockerty MB, Frydenberg HB, O'Fallon WM. Trends in right and left-sided colon cancer. *Dis Colon Rectum* 1983; **26**: 393-398 [PMID: 6851801 DOI: 10.1007/BF02553382]

World Journal of Clinical Cases

Submit a Manuscript: https://www.f6publishing.com

World J Clin Cases 2024 May 26; 12(15): 2475-2478

DOI: 10.12998/wjcc.v12.i15.2475

ISSN 2307-8960 (online)

EDITORIAL

Optimizing pain management in elderly patients post-knee surgery: A novel collaborative strategy

Abdulqadir J Nashwan

Specialty type: Medicine, research and experimental

Provenance and peer review: Invited article; Externally peer reviewed.

Peer-review model: Single blind

Peer-review report's classification
Scientific Quality: Grade C
Novelty: Grade B
Creativity or Innovation: Grade C
Scientific Significance: Grade C

P-Reviewer: Yang RS, Taiwan

Received: January 14, 2024
Revised: April 5, 2024
Accepted: April 23, 2024
Published online: May 26, 2024

Abdulqadir J Nashwan, Department of Nursing, Hamad Medical Corporation, Doha 3050, Qatar

Corresponding author: Abdulqadir J Nashwan, MSc, Research Scientist, Department of Nursing, Hamad Medical Corporation, Al Rayyan Road, Al Sadd, 3050 Doha, Qatar. anashwan@hamad.qa

Abstract

Total knee replacement, a common surgery among the elderly primarily necessitated by osteoarthritis, replaces the damaged knee joint with an artificial one. Given the aging population and the increasing prevalence of such surgeries, the article highlights the critical need for effective postoperative care strategies. This editorial provides an overview of rehabilitation care for pain in elderly knee replacement patients, emphasizing the importance of a multimodal approach to postoperative recovery. Furthermore, the article advocates for a patient-centered, comprehensive rehabilitation regimen that enhances recovery and quality of life in elderly patients undergoing knee replacement surgery.

Key Words: Elderly; Postoperative pain management; Rehabilitation care; Multimodal pain strategy; Total knee arthroplasty; Enhanced recovery after surgery

Core Tip: The multimodal rehabilitation approach for elderly patients undergoing knee replacement surgery integrates various facets of postoperative care, including tailored physical therapy, advanced pain management techniques, and lifestyle adjustments. Emphasizing the need for personalized treatment plans, the article sheds light on the importance of exercises for reducing inflammation and enhancing mobility, alongside innovative pain management strategies like nerve block devices and non-narcotic medications. It underscores the necessity of continuous monitoring and adaptation of the rehabilitation plan, highlighting its impact on accelerating recovery and improving the quality of life for elderly knee replacement patients.

Citation: Nashwan AJ. Optimizing pain management in elderly patients post-knee surgery: A novel collaborative strategy. *World J Clin Cases* 2024; 12(15): 2475-2478
URL: https://www.wjgnet.com/2307-8960/full/v12/i15/2475.htm
DOI: https://dx.doi.org/10.12998/wjcc.v12.i15.2475

INTRODUCTION

Rehabilitation care for pain in elderly knee replacement patients is a critical aspect of postoperative care that aims to improve the quality of life and expedite recovery. Total knee replacement, often necessitated by conditions like osteoarthritis, involves replacing the damaged knee joint with an artificial one[1]. This surgery is increasingly common among the elderly, with over 600000 procedures performed annually, and these artificial joints typically last for at least 15 years[2].

Postoperative rehabilitation is crucial for successful recovery. In the initial weeks after surgery, outpatient physical therapy is recommended[3]. Exercises are designed to reduce inflammation, increase mobility, and strengthen supporting leg muscles, facilitating improved knee bending[4]. Typical exercises include quadriceps sets, straight leg lifts, ankle pumps, and seated knee bends[4]. Patients are generally encouraged to walk as much as comfortably possible, often starting with the aid of a walker or cane and progressing to independent walking around 3 wk post-surgery[5].

Pain management is another essential component of postoperative care. Knee surgery can be pretty painful, and managing this pain effectively is vital for a successful recovery[6]. While narcotics are often used, they are not considered the most effective for pain relief[7]. A more multimodal approach to pain management is often employed, including using nerve block devices that reduce the need for medication in the first week after surgery[7].

The recovery timeline for elderly patients undergoing knee replacement is typically around 12 wk[8]. This period includes significant improvement in swelling reduction and movement ability within the first four to 6 wk[8]. The following weeks focus on increasing the range of motion and building muscles around the new joint[8]. Adherence to physical therapist and doctor recommendations is crucial for effective recovery without overexerting the patient, which could otherwise delay healing.

Interestingly, the field of Enhanced Recovery After Surgery (ERAS) has witnessed significant advances in recent years, focusing on minimizing surgical stress, optimizing physiological function, and facilitating a faster recovery for patients [9]. One of the notable developments is the integration of digital health technologies, such as telehealth and mobile health applications, which enable real-time monitoring of patient progress and symptoms, thus allowing for personalized adjustments to care plans[10]. Additionally, there's a growing emphasis on multimodal pain management strategies that incorporate regional anesthesia and non-opioid medications, reducing the reliance on opioids and their associated risks [11]. Research into the gut microbiome's role in recovery and the impact of prehabilitation-physical and nutritional preparation before surgery—promises to further refine ERAS protocols[12]. These advancements, combined with a multidisciplinary approach that includes patients in decision-making, signify a shift towards a more holistic, patient-centered care model in surgical recovery (Figure 1). Liu *et al*[13] present a retrospective study evaluating the effectiveness of programmed pain nursing combined with collaborative nursing in elderly patients undergoing knee replacement surgery[13]. It includes an analysis of 116 patients divided into two groups: A control group receiving standard nursing care and an observation group receiving both programmed and collaborative nursing. The study finds that the observation group demonstrated better functional outcomes, including higher activities of daily living (ADL) scores and better knee joint function scores at 2 and 3 months post-discharge, compared to the control group. The study concludes that programmed pain nursing and collaborative nursing can significantly improve patient outcomes regarding pain reduction and enhanced rehabilitation post-knee replacement surgery.

The study's retrospective design is a crucial element to consider. In retrospective studies, researchers analyze existing data to find correlations and patterns. However, this design inherently limits the ability to establish causality firmly. The lack of randomization and control groups means that other variables could influence the outcomes, making it challenging to attribute improvements to specific nursing interventions directly. A randomized controlled trial (RCT), where patients are randomly assigned to different treatment groups, would provide more robust evidence. RCTs are considered the gold standard in clinical research because they minimize bias and allow for a more straightforward interpretation of the effectiveness of an intervention.

The study's sample size, comprising 116 patients, is adequate for initial explorations but might not capture the diversity and complexity of the broader population undergoing knee replacement surgery. Elderly patients can have varying health statuses, comorbidities, and personal circumstances, all of which can influence their recovery. A more extensive and more diverse sample would provide a more representative picture of the population and strengthen the reliability of the findings.

Another consideration is the study's reliance on subjective measures, such as ADL and Visual Analog Scale scores. While valuable for capturing patients' self-reported experiences, these measures are influenced by individual perceptions and biases. Objective measures, alongside these subjective assessments, could provide a more comprehensive understanding of the effectiveness of nursing interventions.

The follow-up duration of three months post-discharge is relatively short. Knee replacement is a major surgery, and its long-term effects can be significant. A more extended follow-up period would allow researchers to observe the sustained impacts of the nursing interventions on patients' recovery, functionality, and overall quality of life. This could be particularly relevant for understanding chronic pain management and long-term mobility.

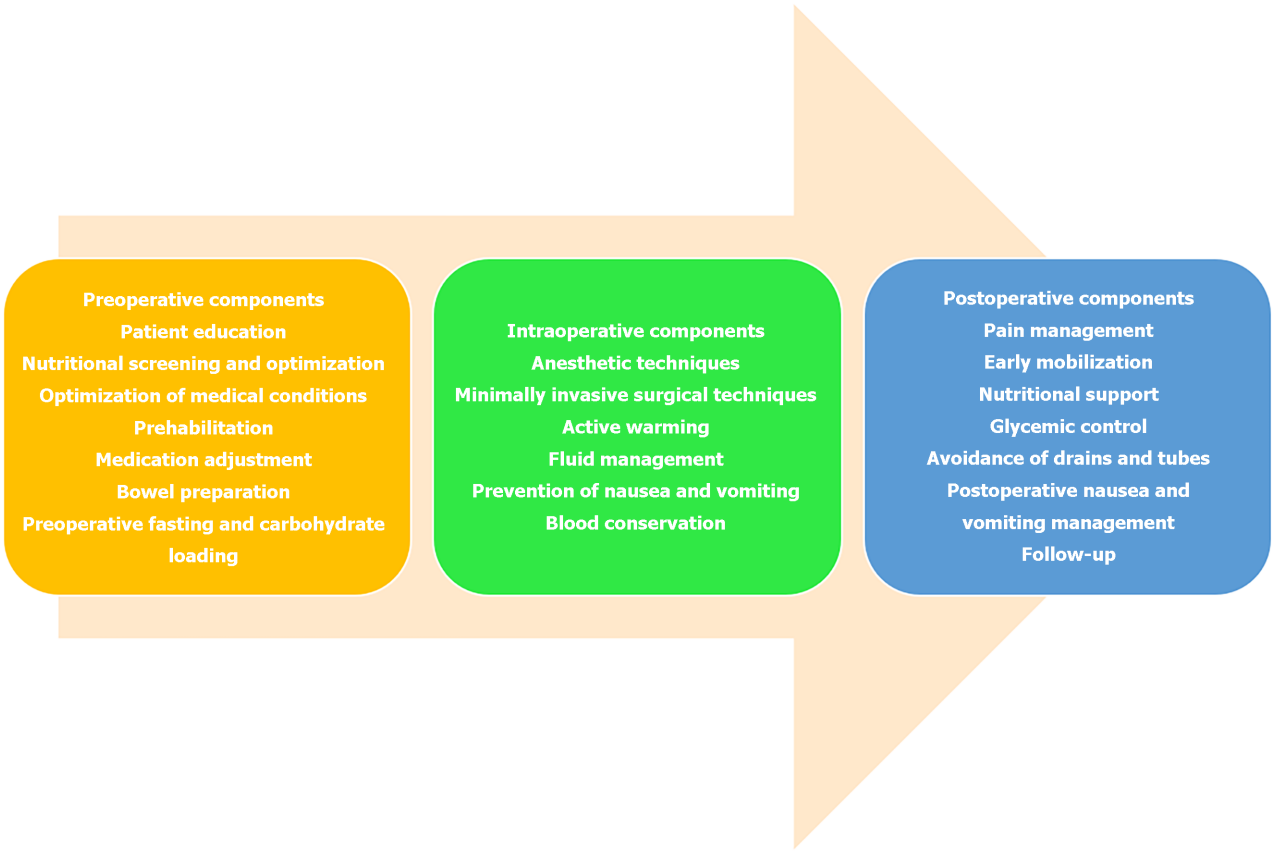

Figure 1 Simplified enhanced recovery after surgery protocol diagram[16].

Furthermore, nutrition plays a critical role in patient recovery, especially after major surgeries like knee replacement [14]. A well-structured nutritional plan can aid in faster wound healing, reduce the risk of infections, and support the overall recovery process[15]. Discussing nutritional strategies within the context of perioperative care could provide insights into optimizing patient outcomes.

Finally, the generalizability of the study's findings is a crucial concern. Since the survey is conducted within a specific patient population and healthcare setting, its results may not be applicable to other settings or populations. Factors like healthcare infrastructure, patient demographics, and cultural differences can influence the outcomes of such interventions. Thus, caution should be exercised in extrapolating these findings to other groups without further research [16].

CONCLUSION

The study offers valuable insights into postoperative care for elderly knee replacement patients, highlighting the potential benefits of integrating programmed pain nursing with collaborative nursing. While the findings suggest positive outcomes, the study's limitations, such as its retrospective design and limited follow-up duration, necessitate further research. Nonetheless, it contributes meaningfully to the field of geriatric orthopedic nursing, proposing a novel approach to pain management and rehabilitation in this vulnerable patient group.

FOOTNOTES

Author contributions: Nashwan AJ contributed to the manuscript's writing, editing, and literature review.

Conflict-of-interest statement: All the authors report no relevant conflicts of interest for this article.

Country of origin: Qatar

ORCID number: Abdulqadir J Nashwan 0000-0003-4845-4119.

S-Editor: Liu H
L-Editor: A
P-Editor: Li X

REFERENCES

1 **Primorac D**, Molnar V, Rod E, Jeleč Ž, Čukelj F, Matišić V, Vrdoljak T, Hudetz D, Hajsok H, Borić I. Knee Osteoarthritis: A Review of Pathogenesis and State-Of-The-Art Non-Operative Therapeutic Considerations. *Genes (Basel)* 2020; **11** [PMID: 32722615 DOI: 10.3390/genes11080854]
2 **Arshi A**, Hughes AJ, Robin JX, Parvizi J, Fillingham YA. Return to Sport After Hip and Knee Arthroplasty: Counseling the Patient on Resuming an Active Lifestyle. *Curr Rev Musculoskelet Med* 2023; **16**: 329-337 [PMID: 37160556 DOI: 10.1007/s12178-023-09839-x]
3 **Wainwright TW**, Burgess L. Early Ambulation and Physiotherapy After Surgery. *Enhanced Recovery After Surgery*2020. [DOI: 10.1007/978-3-030-33443-7_23]
4 **Raposo F**, Ramos M, Lúcia Cruz A. Effects of exercise on knee osteoarthritis: A systematic review. *Musculoskeletal Care* 2021; **19**: 399-435 [PMID: 33666347 DOI: 10.1002/msc.1538]
5 **Matranga E**. Acute care physical therapy for a patient following left total hip arthroplasty. 2021, California State University, Sacramento. Available from: https://hdl.handle.net/10211.3/218623
6 **Keast M**, Hutchinson AF, Khaw D, McDonall J. Impact of Pain on Postoperative Recovery and Participation in Care Following Knee Arthroplasty Surgery: A Qualitative Descriptive Study. *Pain Manag Nurs* 2022; **23**: 541-547 [PMID: 34972657 DOI: 10.1016/j.pmn.2021.11.011]
7 **Laigaard J**, Pedersen C, Rønsbo TN, Mathiesen O, Karlsen APH. Minimal clinically important differences in randomised clinical trials on pain management after total hip and knee arthroplasty: a systematic review. *Br J Anaesth* 2021; **126**: 1029-1037 [PMID: 33678402 DOI: 10.1016/j.bja.2021.01.021]
8 **Wainwright TW**, Gill M, McDonald DA, Middleton RG, Reed M, Sahota O, Yates P, Ljungqvist O. Consensus statement for perioperative care in total hip replacement and total knee replacement surgery: Enhanced Recovery After Surgery (ERAS(®)) Society recommendations. *Acta Orthop* 2020; **91**: 3-19 [PMID: 31663402 DOI: 10.1080/17453674.2019.1683790]
9 **Carli F**. Physiologic considerations of Enhanced Recovery After Surgery (ERAS) programs: implications of the stress response. *Can J Anaesth* 2015; **62**: 110-119 [PMID: 25501695 DOI: 10.1007/s12630-014-0264-0]
10 **Gillis C**, Ljungqvist O, Carli F. Prehabilitation, enhanced recovery after surgery, or both? A narrative review. *Br J Anaesth* 2022; **128**: 434-448 [PMID: 35012741 DOI: 10.1016/j.bja.2021.12.007]
11 **Wardhan R**, Chelly J. Recent advances in acute pain management: understanding the mechanisms of acute pain, the prescription of opioids, and the role of multimodal pain therapy. *F1000Res* 2017; **6**: 2065 [PMID: 29225793 DOI: 10.12688/f1000research.12286.1]
12 **Sibley D**, Chen M, West MA, Matthew AG, Santa Mina D, Randall I. Potential mechanisms of multimodal prehabilitation effects on surgical complications: a narrative review. *Appl Physiol Nutr Metab* 2023; **48**: 639-656 [PMID: 37224570 DOI: 10.1139/apnm-2022-0272]
13 **Liu L**, Guan QZ, Wang LF. Rehabilitation care for pain in elderly knee replacement patients. *World J Clin Cases* 2024; **12**: 721-728 [PMID: 38322695 DOI: 10.12998/wjcc.v12.i4.721]
14 **Smith-Ryan AE**, Hirsch KR, Saylor HE, Gould LM, Blue MNM. Nutritional Considerations and Strategies to Facilitate Injury Recovery and Rehabilitation. *J Athl Train* 2020; **55**: 918-930 [PMID: 32991705 DOI: 10.4085/1062-6050-550-19]
15 **Buckthorpe M**, Gokeler A, Herrington L, Hughes M, Grassi A, Wadey R, Patterson S, Compagnin A, La Rosa G, Della Villa F. Optimising the Early-Stage Rehabilitation Process Post-ACL Reconstruction. *Sports Med* 2024; **54**: 49-72 [PMID: 37787846 DOI: 10.1007/s40279-023-01934-w]
16 **Soffin EM**, YaDeau JT. Enhanced recovery after surgery for primary hip and knee arthroplasty: a review of the evidence. *Br J Anaesth* 2016; **117**: iii62-iii72 [PMID: 27940457 DOI: 10.1093/bja/aew362]

World Journal of Clinical Cases

Submit a Manuscript: https://www.f6publishing.com

World J Clin Cases 2024 May 26; 12(15): 2479-2481

DOI: 10.12998/wjcc.v12.i15.2479

ISSN 2307-8960 (online)

EDITORIAL

Mediastinal emphysema in the context of perforated gastric ulcer

Debkumar Chowdhury

Specialty type: Medicine, research and experimental

Provenance and peer review: Invited article; Externally peer reviewed.

Peer-review model: Single blind

Peer-review report's classification

Scientific Quality: Grade D
Novelty: Grade C
Creativity or Innovation: Grade C
Scientific Significance: Grade C

P-Reviewer: Stepanyan SA, Armenia

Received: February 21, 2024
Revised: April 9, 2024
Accepted: April 11, 2024
Published online: May 26, 2024

Debkumar Chowdhury, Department of Emergency Medicine, Wythenshawe Hospital, Manchester M23 9LT, United Kingdom

Corresponding author: Debkumar Chowdhury, MBChB, MSc, Academic Editor, Academic Fellow, Attending Doctor, Department of Emergency Medicine, Wythenshawe Hospital, Wythenshawe, Manchester M23 9LT, United Kingdom. dc7740@my.bristol.ac.uk

Abstract

In the context of mediastinal emphysema/pneumomediastinum, the main aetiologies are associated with oesophageal perforation, lung pathology or post head and neck surgery related. The main way to differentiate the pathologies would be through Computed Tomographic Imaging of the Thorax and abdomen with oral and intravenous contrast in the context of triple phase imaging. The causes of pneumomediastinum should be differentiated between traumatic and non-traumatic. Oesophageal perforation (Boerhaave syndrome) is associated with Mackler's triad in upto 50% of patients (severe retrosternal chest pain, pneumomediastinum, mediastinitis). Whereas in cases of lung pathology this can be associated with pneumothorax and pleural effusion.

Key Words: Pneumomediastinum; Duodenal ulcer; Computed tomography; Visceral perforation; Diagnostic imaging; Emergency care

Core Tip: It is critically important that the cause of pneumomediastinum is investigated in a timely fashion to ensure that the ensuing comorbidity and mortality is reduced. This editorial highlights the need for early dedicated imaging to ascertain the underlying cause.

Citation: Chowdhury D. Mediastinal emphysema in the context of perforated gastric ulcer. *World J Clin Cases* 2024; 12(15): 2479-2481
URL: https://www.wjgnet.com/2307-8960/full/v12/i15/2479.htm
DOI: https://dx.doi.org/10.12998/wjcc.v12.i15.2479

INTRODUCTION

With much interest the article by Dai *et al*[1] was read with a greater understanding of mediastinal emphysema in the context of perforated gastric ulcer. In the context of mediastinal emphysema/pneumomediastinum, the main aetiologies are associated with oesophageal perforation, lung pathology or post head and neck surgery related. The main way to differentiate the pathologies would be through Computed Tomographic Imaging of the Thorax and abdomen with oral and intravenous contrast in the context of triple phase imaging[2]. The causes of pneumomediastinum should be differentiated between traumatic and non-traumatic. Oesophageal perforation (Boerhaave syndrome) is associated with Mackler's triad in upto 50% of patients (severe retrosternal chest pain, pneumomediastinum, mediastinitis)[3]. Whereas in cases of lung pathology this can be associated with pneumothorax and pleural effusion[4].

In this case the context is that of non-traumatic cause, the main aetiology associated with perforation is due to increased intra-oesophageal pressure associated with a closed oesophageal sphincter[5]. The two main concerning features on clinical examination was that of rebound tenderness with abdominal rigidity and that of a low oxygen saturation on pulse oximetry. In the case following a definitive diagnosis of gastric perforation, the patient underwent open repair of the perforation which led to resolution of symptoms.

Pneumomediastinum has also been documented in cases post head and neck surgery usually in association with intermittent positive pressure ventilation. In these cases, patients would likely have marked subcutaneous emphysema as air tracks across the tissue planes and across the compartments. One of the theories that have been postulated to cause this is laryngeal or tracheal tear during placement of endotracheal tubes and subsequently application high positive end expiratory pressure[6,7].

Oesophagogastroduodenoscopy although would potentially allow direct visualisation of the site of perforation, this diagnostic modality is best avoided to limit any further damage from iatrogenic injuries[8]. This would be typically avoided until the perforation has sealed.

From an emergency department perspective- the diagnosis of pneumomediastinum and its likely source are the pertinent factors. Oesophageal perforation if delayed to diagnosis is associated with increased morbidities and increased mortality. Thereby it is pertinent that appropriate investigations are carried out in an expedited manner. The areas of natural weakness in the gastrointestinal tract need to be evaluated for sites of possible perforation. The commonest site for oesophageal perforation is the left postero-lateral aspect of below the diaphragm, however the young it is noted to that the perforation occurs into the right pleural cavity[9]. As reported in previous cases the incidence of both pneumomediastinum and pneumothorax is rare is context of visceral perforation. One of the main theories to explain this mechanism is that intra-peritoneal air diffuses through the peritoneal membrane reaching the pleural cavity other theories include passage of air through the diaphragmatic fenestrations and the final mechanism is the passage of retroperitoneal air that passes into mediastinal cavity[10,11].

In terms of diagnosis of perforated gastric ulcer, the main imaging modality would a standard porto-venous computed tomography (CT) imaging of the abdomen and pelvis. The standard protocol would include the part of the lung bases, thereby would still be able to detect the presence of bilateral pleural effusion, pneumomediastinum and pneumothorax. If this would be detected then a follow up CT imaging of the thorax and abdomen with oral contrast would be able to differentiate the cause of the pneumomediastinum. In terms of surgical management perforated peptic ulcer would be operated by the general oncall surgical team with the commonest procedure being either laparoscopic with laparotomy (if gross contamination is present) with omental patch repair[12]. However. If the diagnosis is Boerhaave's syndrome then the input of the upper gastrointestinal surgeons would be needed. This can be logistical challenge especially when not all surgical sub-specialities are at the same facility.

CONCLUSION

As highlighted in this editorial, the attending clinician needs a high index of suspicion when considering the various causes of pneumomediastinum in the context of a surgical abdomen.

ACKNOWLEDGEMENTS

I would like to congratulate the authors in the publication of their article.

FOOTNOTES

Author contributions: Chowdhury D wrote and revised the manuscript.

Conflict-of-interest statement: There is no associated conflict of interest in the production of the article.

Country of origin: United Kingdom

ORCID number: Debkumar Chowdhury 0000-0002-4064-2257.

S-Editor: Zheng XM
L-Editor: A
P-Editor: Zheng XM

REFERENCES

1 **Dai ZC**, Gui XW, Yang FH, Zhang HY, Zhang WF. Perforated gastric ulcer causing mediastinal emphysema: A case report. *World J Clin Cases* 2024; **12**: 859-864 [PMID: 38322697 DOI: 10.12998/wjcc.v12.i4.859]
2 **Marini T**, Desai A, Kaproth-Joslin K, Wandtke J, Hobbs SK. Imaging of the oesophagus: beyond cancer. *Insights Imaging* 2017; **8**: 365-376 [PMID: 28303554 DOI: 10.1007/s13244-017-0548-3]
3 **Loftus IA**, Umana EE, Scholtz IP, McElwee D. Mackler's Triad: An Evolving Case of Boerhaave Syndrome in the Emergency Department. *Cureus* 2023; **15**: e37978 [PMID: 37223188 DOI: 10.7759/cureus.37978]
4 **Sathiyaseelan SL**, Senthil N, Varadaraj P. Case of pneumomediastinum due to alveolar rupture following endotracheal intubation. *BMJ Case Rep* 2018; **2018**: bcr2018227027 [PMID: 30279264 DOI: 10.1136/bcr-2018-227027]
5 **Kouritas VK**, Papagiannopoulos K, Lazaridis G, Baka S, Mpoukovinas I, Karavasilis V, Lampaki S, Kioumis I, Pitsiou G, Papaiwannou A, Karavergou A, Kipourou M, Lada M, Organtzis J, Katsikogiannis N, Tsakiridis K, Zarogoulidis K, Zarogoulidis P. Pneumomediastinum. *J Thorac Dis* 2015; **7**: S44-S49 [PMID: 25774307 DOI: 10.3978/j.issn.2072-1439.2015.01.11]
6 **Hung MH**, Shih PY, Yang YM, Lan JY, Fan SZ, Jeng CS. Cervicofacial subcutaneous emphysema following tonsillectomy: implications for anesthesiologists. *Acta Anaesthesiol Taiwan* 2009; **47**: 134-137 [PMID: 19762304 DOI: 10.1016/S1875-4597(09)60040-0]
7 **Saravakos P**, Taxeidis M, Kastanioudakis I, Reichel O. Subcutaneous Emphysema as a Complication of Tonsillectomy: A Systematic Literature Review and Case Report. *Iran J Otorhinolaryngol* 2018; **30**: 3-10 [PMID: 29387658]
8 **Pooyan P**, Puruckherr M, Summers JA, Byrd RP Jr, Roy TM. Pneumomediastinum, pneumopericardium, and epidural pneumatosis in DKA. *J Diabetes Complications* 2004; **18**: 242-247 [PMID: 15207845 DOI: 10.1016/S1056-8727(03)00059-X]
9 **9 Turner AR**, Collier SA, Turner SD. Boerhaave Syndrome. 2023 Dec 4. In: StatPearls [Internet]. Treasure Island (FL): StatPearls Publishing; 2024 Jan- [PMID: 28613559]
10 **Utzig MJ**, Foitzik T, Buhr HJ, Schneider P. [Duodenal ulcer presenting as pneumomediastinum and pneumothorax -- case report]. *Zentralbl Chir* 2002; **127**: 1091-1093 [PMID: 12529827 DOI: 10.1055/s-2002-36471]
11 **Marwan K**, Farmer KC, Varley C, Chapple KS. Pneumothorax, pneumomediastinum, pneumoperitoneum, pneumoretroperitoneum and subcutaneous emphysema following diagnostic colonoscopy. *Ann R Coll Surg Engl* 2007; **89**: W20-W21 [PMID: 17688713 DOI: 10.1308/147870807X188506]
12 **Yamamoto M**, Imamura K. Perforated Ulcer Treatment. In: Lomanto D, Chen WTL, Fuentes MB, editors. Mastering Endo-Laparoscopic and Thoracoscopic Surgery. Singapore: Springer, 2023 [DOI: 10.1007/978-981-19-3755-2_16]

World Journal of Clinical Cases

Submit a Manuscript: https://www.f6publishing.com

World J Clin Cases 2024 May 26; 12(15): 2482-2486

DOI: 10.12998/wjcc.v12.i15.2482

ISSN 2307-8960 (online)

EDITORIAL

Management of lymphedema is really a matter in patients with breast cancer

Jung Eun Choi, Min Cheol Chang

Specialty type: Medicine, research and experimental

Provenance and peer review: Invited article; Externally peer reviewed.

Peer-review model: Single blind

Peer-review report's classification

Scientific Quality: Grade B, Grade B, Grade C

Novelty: Grade B, Grade B, Grade C

Creativity or Innovation: Grade B, Grade B, Grade C

Scientific Significance: Grade A, Grade B, Grade B

P-Reviewer: Ma C, China; Tari DU, Italy

Received: February 24, 2024

Revised: April 8, 2024

Accepted: April 19, 2024

Published online: May 26, 2024

Jung Eun Choi, Department of Surgery, College of Medicine, Yeungnam University, Daegu 705-717, South Korea

Min Cheol Chang, Department of Physical Medicine and Rehabilitation, College of Medicine, Yeungnam University, Daegu 705-717, South Korea

Corresponding author: Min Cheol Chang, MD, Department of Physical Medicine and Rehabilitation, College of Medicine, Yeungnam University, 317-1, Daemyungdong, Namku, Daegu 705-717, South Korea. wheel633@gmail.com

Abstract

Lymphedema is a prevalent complication affecting patients with breast cancer, greatly impacting their quality of life. This editorial describes diagnostic methods and therapeutic interventions for managing lymphedema in patients with breast cancer. Diagnosis relies on clinical evaluation and objective measures, including arm circumference and volumetric assessments, along with lymphoscintigraphy and ultrasonic measurements. Treatment primarily involves complex decongestive physical therapy, comprising manual lymphatic drainage, compression therapy, exercise, and meticulous skin care. These interventions aim to reduce swelling, alleviate discomfort, and prevent further complications. Additionally, lifestyle modifications such as avoiding extreme temperatures and maintaining proper hygiene are essential. Flavonoids can be used for drug therapy. Despite its prevalence, lymphedema often receives inadequate attention in clinical practice, emphasizing the importance of raising awareness and enhancing medical services for affected individuals. Clinicians play a pivotal role in educating patients about preventive measures and ensuring timely intervention. Overall, a comprehensive approach encompassing early diagnosis, multidisciplinary management, and patient education is essential to mitigate the burden of lymphedema in patients with breast cancer and improve their overall well-being.

Key Words: Lymphedema; Breast cancer; Complex decongestive physical therapy; Diagnosis; Treatment

Core Tip: This editorial describes the diagnosis and management of lymphedema in patients with breast cancer. Lymphedema, a common complication of breast cancer treatment, greatly impacts patients' quality of life and psychological well-being. Diagnosis relies on clinical evaluation and objective measures, including arm circumference and volumetric assessments, as well as lymphoscintigraphy and ultrasonic measurements. Treatment involves complex decongestive physical therapy comprising manual lymphatic drainage, compression therapy, exercise, and skin care. Early diagnosis and proper treatment are essential for effective management of lymphedema in patients with breast cancer.

Citation: Choi JE, Chang MC. Management of lymphedema is really a matter in patients with breast cancer. *World J Clin Cases* 2024; 12(15): 2482-2486
URL: https://www.wjgnet.com/2307-8960/full/v12/i15/2482.htm
DOI: https://dx.doi.org/10.12998/wjcc.v12.i15.2482

INTRODUCTION

Lymphedema is an abnormal accumulation of protein-rich fluid in interstitial spaces due to a compromised lymphatic system[1]. In patients with breast cancer, lymphedema commonly occurs in the arm on the operated side because of regional lymph node involvement of the tumor, surgical removal of the lymph nodes for tumor treatment, and radiation therapy[2]. The incidence of this condition following breast cancer treatment has been reported at 5%-60%; such differences in incidence may be attributed to differences in diagnostic criteria, measurement methods, and follow-up periods[3]. The condition is considered as incurable and is a major factor decreasing the quality of life of patients with breast cancer[4]. In addition to cosmetic problems, physical discomfort, and functional impairment, lymphedema causes various psychological problems, such as depression, anxiety, and social avoidance[4]. Moreover, patients often experience inflammation from lymphangitis or cellulitis[5,6]. Stagnant proteins in tissues affected by lymphedema serve as a good medium for bacterial growth, increasing the likelihood of an infection[6]. Therefore, prevention, early diagnosis, and proper treatment of lymphedema are crucial.

In this editorial, we comment on a paper by Mubarak *et al*[7] published in a recent issue of *World Journal of Clinical Cases*. The authors described that the presence of tumor deposits in patients with breast cancer indicates a poor prognosis and recommended that clinicians should carefully investigate the presence of tumor deposits. We describe the diagnosis and management of lymphedema, another important issue in patients with breast cancer.

DIAGNOSIS

Although there is no gold standard test for diagnosing lymphedema, common complaints from patients include feeling heavy, tightness, and/or pain. The objective method most commonly used in clinical practice is measurement of both the left and right arm circumferences at the same position, where a difference of > 2 cm between arms is used to diagnose moderate lymphedema[2,8]. A difference of ≤ 2 cm is considered to indicate mild lymphedema[2]. Volumetric methods can also be used, including the water replacement method, which defines lymphedema as a difference of ≥ 200 mL in volume between the two arms[9]. These assessments should be performed preoperatively and within 1 mo postoperatively; once lymphedema has been identified, weekly assessment should be considered[10]. Upon the completion of treatment, follow-up should be performed every 2-3 mo for 1-2 years[10]. Although medical history assessment and clinical examinations may be sufficient for diagnosis, lymphoscintigraphy can be performed to examine the functional status of the lymphatic system and predict treatment outcomes and prognosis[11]. Moreover, ultrasonic measurement of the thickness of the skin and subcutaneous fat layers as well as changes in echogenicity may also help in diagnosis and severity determination[12].

TREATMENT

Complex decongestive physical therapy, which is primarily used to treat lymphedema, consists of four components: Manual lymphatic drainage, compression therapy, exercise therapy, and skin care[13,14]. This therapy typically involves 2-6 wk of intensive therapy followed by several months of management[13,14]. The effects of properly administered complex decongestive physical therapy and appropriate management of lymphedema can last from several months to as long as 2 years or more[13,14]. In addition, prophylactic administration of this therapy after breast cancer surgery has been reported to reduce the incidence of lymphedema[15].

Herein, we discuss individual therapies comprising complex decongestive physical therapy. Manual lymphatic drainage is a highly specialized massage technique designed to increase the movement of lymphatic fluid (Figure 1)[16]. Slow and rhythmical massage is used to drain congested lymphatic fluid from the non-functioning lymphotome to areas that remain functional; the lymphatic fluid is then removed through the remaining lymph nodes. This massage technique is performed in a proximal-to-distal direction[17] with very superficial and light pressure of approximately 30-45 mmHg

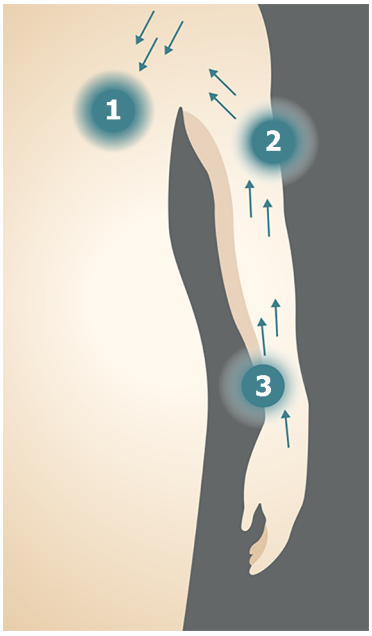

Figure 1 Manual lymphatic drainage. The entire palm is used to gently massage towards the direction of the heart. Massage is subsequently performed from the (1) axilla to (2) the upper arm and then to (3) the forearm.

[18].

Compression therapy involves application of external force, which increases the tissue pressure and facilitates lymphatic and venous circulation to promote lymphatic duct functions[19]. Moreover, it can facilitate the distribution of protein components in fibrotic arm tissues. As compression therapy, a compression bandage (Figure 2A) or compression stocking (Figure 2B) can be applied and should be worn during exercise and activities of daily living[20]. When applying the compression bandage method, a short-stretch, non-elastic bandage is used to increase the working pressure[21]. The patient is also instructed to wear a compression stocking to reduce swelling and maintain an appropriate arm shape and protect the skin, while applying compensatory pressure on the skin that has been stretched and lacks elasticity after the swelling has been reduced[22]. In addition, wearing a compression stocking can enhance the flow of lymphatic fluid, which reduces protein buildup and improves venous circulation[22].

Exercises include upper extremity range of motion exercises, stretching, and resistive exercises for muscle strengthening aimed at preventing and reducing lymphedema[23,24]. Moreover, aerobic exercise can increase sympathetic nervous system activity to enhance the flow of lymphatic fluid[23,24]. These exercises should be performed while wearing a compression bandage or compression stocking to prevent increased lymphatic fluid from pooling on the skin surface[25].

Finally, thorough skin care should be administered to patients with lymphedema[26]. Measures should be taken to prevent and maintain proper hygiene to minimize bacterial infection and lymphedema.

Patients should avoid saunas and tub baths, as they can increase the risk of lymphedema, and should avoid exposure to extreme cold or heat[27]. As dieting can help reduce lymphedema volume, a reduced dietary calorie intake and low-fat diet are recommended to some patients[28].

As drug therapy, flavonoids can be used[29] to enhance lymphangiomotion and reduce capillary permeability. If there are findings of secondary infection, appropriate antibiotics should be administered immediately[30]. Diuretics are not effective in the long term, as they can exacerbate edema by increasing protein accumulation in the interstitial space.

Surgical treatment is another option for patients with lymphedema that is not controlled by conservative treatment. Microsurgical lymphovenous anastomoses, debulking, and liposuction can be performed to remove excess fluid or tissue and relieve symptoms[31]. However, surgical procedures can lead to complications such as delayed wound healing, infection, and recurrence, and, therefore, should be carefully selected.

CONCLUSION

Lymphedema commonly occurs in patients with breast cancer, which can affect not only the quality of life but also physical function and has a negative psychological impact. Therefore, lymphedema should be actively controlled through early diagnosis and proper treatment. Despite the high need for treatment, effective treatments for lymphedema are lacking for patients with breast cancer. Clinicians should acquire sufficient knowledge on the diagnostic and treatment methods and actively provide appropriate medical services to these patients.

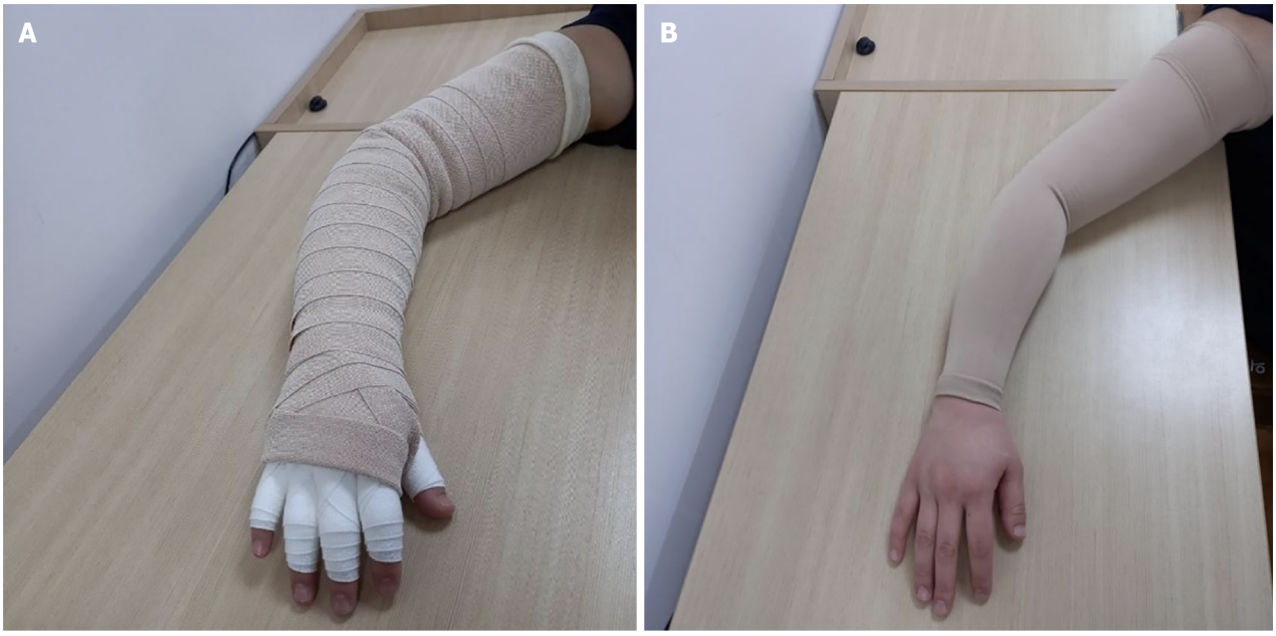

Figure 2 Compression therapy. A: Application of a compression bandage; B: Compression stocking.

FOOTNOTES

Author contributions: Choi JE and Chang MC designed and performed the study, analyzed the data, and wrote the manuscript; both authors have read and approved the final manuscript.

Supported by The National Research Foundation of Korea Grant funded by the Korea Government, No. 00219725.

Conflict-of-interest statement: Both authors report no relevant conflicts of interest for this article.

Country of origin: South Korea

ORCID number: Min Cheol Chang 0000-0002-7629-7213.

S-Editor: Che XX
L-Editor: Wang TQ
P-Editor: Li X

REFERENCES

1 **Manrique OJ**, Bustos SS, Ciudad P, Adabi K, Chen WF, Forte AJ, Cheville AL, Jakub JW, McLaughlin SA, Chen HC. Overview of Lymphedema for Physicians and Other Clinicians: A Review of Fundamental Concepts. *Mayo Clin Proc* 2022; **97**: 1920-1935 [PMID: 32829905 DOI: 10.1016/j.mayocp.2020.01.006]
2 **Tsai RJ**, Dennis LK, Lynch CF, Snetselaar LG, Zamba GKD, Scott-Conner C. Lymphedema following breast cancer: The importance of surgical methods and obesity. *Front Womens Health* 2018; **3** [PMID: 30555923 DOI: 10.15761/FWH.1000144]
3 **Rebegea L**, Firescu D, Dumitru M, Anghel R. The incidence and risk factors for occurrence of arm lymphedema after treatment of breast cancer. *Chirurgia (Bucur)* 2015; **110**: 33-37 [PMID: 25800313]
4 **Taghian NR**, Miller CL, Jammallo LS, O'Toole J, Skolny MN. Lymphedema following breast cancer treatment and impact on quality of life: a review. *Crit Rev Oncol Hematol* 2014; **92**: 227-234 [PMID: 25085806 DOI: 10.1016/j.critrevonc.2014.06.004]
5 **Hosseinzadeh A**, Ebrahimi K, Shahriarirad R, Dalfardi F. Lower limb lymphedema and cellulitis as a complication of COVID-19 vaccine: A case report. *Clin Case Rep* 2022; **10**: e6317 [PMID: 36540881 DOI: 10.1002/ccr3.6317]
6 **Park SI**, Yang EJ, Kim DK, Jeong HJ, Kim GC, Sim YJ. Prevalence and Epidemiological Factors Involved in Cellulitis in Korean Patients With Lymphedema. *Ann Rehabil Med* 2016; **40**: 326-333 [PMID: 27152284 DOI: 10.5535/arm.2016.40.2.326]
7 **Mubarak M**, Rashid R, Shakeel S. Tumor deposits in axillary adipose tissue in patients with breast cancer: Do they matter? *World J Clin Cases* 2024; **12**: 1045-1049 [PMID: 38464926 DOI: 10.12998/wjcc.v12.i6.1045]
8 **Sleigh BC**, Manna B. Lymphedema. 2023 Apr 19. In: StatPearls [Internet]. Treasure Island (FL): StatPearls Publishing; 2024 Jan- [PMID:

30725924]
9 **Armer JM**. The problem of post-breast cancer lymphedema: impact and measurement issues. *Cancer Invest* 2005; **23**: 76-83 [PMID: 15779870]
10 **Cornish BH**, Chapman M, Hirst C, Mirolo B, Bunce IH, Ward LC, Thomas BJ. Early diagnosis of lymphedema using multiple frequency bioimpedance. *Lymphology* 2001; **34**: 2-11 [PMID: 11307661]
11 **Forte AJ**, Boczar D, Huayllani MT, Lu X, Ciudad P. Lymphoscintigraphy for Evaluation of Lymphedema Treatment: A Systematic Review. *Cureus* 2019; **11**: e6363 [PMID: 31886094 DOI: 10.7759/cureus.6363]
12 **de Rezende LF**, Piloni JPM, Kempa VL, Silva JFR, Vilas Boas VF, Carvalho RL, Marx ÂG. Ultrasonography as an instrument to evaluate lymphedema secondary to breast cancer: systematic review. *J Vasc Bras* 2023; **22**: e20220144 [PMID: 38162983 DOI: 10.1590/1677-5449.202201441]
13 **Bergmann A**, Baiocchi JMT, de Andrade MFC. Conservative treatment of lymphedema: the state of the art. *J Vasc Bras* 2021; **20**: e20200091 [PMID: 34777487 DOI: 10.1590/1677-5449.200091]
14 **Tatar KK**, Turhan B. The effects of complex decongestive therapy on pain and functionality in individuals with breast cancer who developed adhesive capsulitis due to lymphedema: an evaluation by an isokinetic computerized system. *Korean J Pain* 2022; **35**: 280-290 [PMID: 35768983 DOI: 10.3344/kjp.2022.35.3.280]
15 **Torres Lacomba M**, Yuste Sánchez MJ, Zapico Goñi A, Prieto Merino D, Mayoral del Moral O, Cerezo Téllez E, Minayo Mogollón E. Effectiveness of early physiotherapy to prevent lymphoedema after surgery for breast cancer: randomised, single blinded, clinical trial. *BMJ* 2010; **340**: b5396 [PMID: 20068255 DOI: 10.1136/bmj.b5396]
16 **Liang M**, Chen Q, Peng K, Deng L, He L, Hou Y, Zhang Y, Guo J, Mei Z, Li L. Manual lymphatic drainage for lymphedema in patients after breast cancer surgery: A systematic review and meta-analysis of randomized controlled trials. *Medicine (Baltimore)* 2020; **99**: e23192 [PMID: 33285693 DOI: 10.1097/MD.0000000000023192]
17 **Liu J**, Chen D, Yin X. Effect of manual lymphatic drainage combined with vacuum sealing drainage on axillary web syndrome caused by breast cancer surgery. *Int Wound J* 2023; **20**: 183-190 [PMID: 35778796 DOI: 10.1111/iwj.13862]
18 **Sanal-Toprak C**, Ozsoy-Unubol T, Bahar-Ozdemir Y, Akyuz G. The efficacy of intermittent pneumatic compression as a substitute for manual lymphatic drainage in complete decongestive therapy in the treatment of breast cancer related lymphedema. *Lymphology* 2019; **52**: 82-91 [PMID: 31525829]
19 **Hobday A**. Use of compression therapy in patients with lymphoedema. *Nurs Stand* 2016; **30**: 50-58; quiz 60 [PMID: 26932650 DOI: 10.7748/ns.30.27.50.s46]
20 **Rabe E**, Földi E, Gerlach H, Jünger M, Lulay G, Miller A, Protz K, Reich-Schupke S, Schwarz T, Stücker M, Valesky E, Pannier F. Medical compression therapy of the extremities with medical compression stockings (MCS), phlebological compression bandages (PCB), and medical adaptive compression systems (MAC) : S2k guideline of the German Phlebology Society (DGP) in cooperation with the following professional associations: DDG, DGA, DGG, GDL, DGL, BVP. *Hautarzt* 2021; **72**: 37-50 [PMID: 33386416 DOI: 10.1007/s00105-020-04706-z]
21 **Rucigaj TP**, Huljev D. [The role of short-stretch bandage in therapy of lymphedema]. *Acta Med Croatica* 2012; **66** Suppl 1: 49-51 [PMID: 23193821]
22 **de Godoy JM**, de Godoy LMP, de Godoy HJP, Guerreiro Godoy MF. Nonelastic Compression Stockings for the Reduction of Lymphedema and the Maintenance of the Results for 2-3 years. *Indian J Community Med* 2021; **46**: 329-330 [PMID: 34321756 DOI: 10.4103/ijcm.IJCM_230_20]
23 **Baklaci M**, Eyigör S, Tanıgör G, Özgür İnbat M, Çalışkan Kabayel S. Assessment of Muscle Strength and Volume Changes in Patients with Breast Cancer-Related Lymphedema. *Oncol Res Treat* 2020; **43**: 584-591 [PMID: 32932259 DOI: 10.1159/000509672]
24 **Kilbreath SL**, Refshauge KM, Beith JM, Ward LC, Lee M, Simpson JM, Hansen R. Upper limb progressive resistance training and stretching exercises following surgery for early breast cancer: a randomized controlled trial. *Breast Cancer Res Treat* 2012; **133**: 667-676 [PMID: 22286332 DOI: 10.1007/s10549-012-1964-1]
25 **Barufi S**, Pereira de Godoy HJ, Pereira de Godoy JM, Guerreiro Godoy MF. Exercising and Compression Mechanism in the Treatment of Lymphedema. *Cureus* 2021; **13**: e16121 [PMID: 34285855 DOI: 10.7759/cureus.16121]
26 **Fife CE**, Farrow W, Hebert AA, Armer NC, Stewart BR, Cormier JN, Armer JM. Skin and Wound Care in Lymphedema Patients: A Taxonomy, Primer, and Literature Review. *Adv Skin Wound Care* 2017; **30**: 305-318 [PMID: 28617750 DOI: 10.1097/01.ASW.0000520501.23702.82]
27 **Cemal Y**, Pusic A, Mehrara BJ. Preventative measures for lymphedema: separating fact from fiction. *J Am Coll Surg* 2011; **213**: 543-551 [PMID: 21802319 DOI: 10.1016/j.jamcollsurg.2011.07.001]
28 **Bonetti G**, Dhuli K, Michelini S, Ricci M, Cestari M, Bertelli M. Dietary supplements in lymphedema. *J Prev Med Hyg* 2022; **63**: E200-E205 [PMID: 36479479 DOI: 10.15167/2421-4248/jpmh2022.63.2S3.2761]
29 **Pecking AP**, Février B, Wargon C, Pillion G. Efficacy of Daflon 500 mg in the treatment of lymphedema (secondary to conventional therapy of breast cancer). *Angiology* 1997; **48**: 93-98 [PMID: 8995350 DOI: 10.1177/000331979704800115]
30 **Senger JB**, Kadle RL, Skoracki RJ. Current Concepts in the Management of Primary Lymphedema. *Medicina (Kaunas)* 2023; **59**: 894 [PMID: 37241126 DOI: 10.3390/medicina59050894]
31 **Schaverien MV**, Coroneos CJ. Surgical Treatment of Lymphedema. *Plast Reconstr Surg* 2019; **144**: 738-758 [PMID: 31461041 DOI: 10.1097/PRS.0000000000005993]

World Journal of Clinical Cases

Submit a Manuscript: https://www.f6publishing.com

World J Clin Cases 2024 May 26; 12(15): 2487-2498

DOI: 10.12998/wjcc.v12.i15.2487

ISSN 2307-8960 (online)

MINIREVIEWS

Management and classification of the fracture of lateral process of talus: An overview and literature update

Chao-Qun Wang, Ulrich Stöckle, Sheng-Nan Dong, Xu-Gui Li, Ze-Xi Ling

Specialty type: Medicine, research and experimental

Provenance and peer review: Unsolicited article; Externally peer reviewed.

Peer-review model: Single blind

Peer-review report's classification

Scientific Quality: Grade B

Novelty: Grade B

Creativity or Innovation: Grade B

Scientific Significance: Grade B

P-Reviewer: Schmidt EJ, United States

Received: December 15, 2023

Revised: March 14, 2024

Accepted: April 9, 2024

Published online: May 26, 2024

Chao-Qun Wang, Sheng-Nan Dong, Xu-Gui Li, Ze-Xi Ling, Department of Traumatic Orthopedics, The Affiliated Hospital of Wuhan Sports University, Wuhan 430079, Hubei Province, China

Ulrich Stöckle, Center of Musculoskeletal Surgery, Berlin Charité Medical University Hospital, Berlin 13353, Germany

Corresponding author: Chao-Qun Wang, MMed, Doctoral Candidate, Attending Orthopaedic Surgeon, Department of Traumatic Orthopedics, The Affiliated Hospital of Wuhan Sports University, No. 279 Luoyu Road, Hongshan District, Wuhan 430079, Hubei Province, China. 2454431220@qq.com

Abstract

Fracture of the lateral process of the talus (FLPT) is uncommon in clinical practice and can be easily missed or misdiagnosed. In recent years, as researchers from all over the world have further deepened their research on FLPT, there has been a breakthrough in the classification, and the methods and principles of clinical management have changed accordingly; however, there is still no standardized guideline for the diagnosis and management of FLPT, and there have been few relevant literature review articles related to this kind of fracture in the past at least 5 years. In this article, we review the clinical classification, classification-based therapeutic recommendations, and prognosis of FLPT, with the aim of providing a reference for the clinical diagnosis and management of this infrequent fracture.

Key Words: Fracture of the lateral process of the talus; Fracture of the talus; Hindfoot injuries; Intraarticular fracture; Subtalar joint

Core Tip: To our knowledge, there are no standardized guidelines for the diagnosis and management of fracture of the lateral process of the talus (FLPT). Furthermore, no relevant review articles have been published in the past 5 years. Recently, there is some new progress in classification and management recommendations of FLPT; consequently, in this article, we mainly reviewed the clinical classification, classification-based therapeutic recommendations and prognosis of FLPT, aiming at providing a much needed reference for clinical diagnosis and management of FLPT.

Citation: Wang CQ, Stöckle U, Dong SN, Li XG, Ling ZX. Management and classification of the fracture of lateral process of talus: An overview and literature update. *World J Clin Cases* 2024; 12(15): 2487-2498
URL: https://www.wjgnet.com/2307-8960/full/v12/i15/2487.htm
DOI: https://dx.doi.org/10.12998/wjcc.v12.i15.2487

INTRODUCTION

Fracture of the lateral process of the talus (FLPT) accounts for less than 0.1% of all fractures and less than 10% of foot fractures[1]. It constitutes 10%-25% of all talar fractures[2] and ranks second only to talar neck fractures. The mechanisms underlying FLPT injury remain inconclusive. However, current literature suggests that forced dorsiflexion, inversion, eversion, and potential external rotation of the foot are all contributing factors[3-5]. Notably, during snowboarding, the motion and stress status of the foot becomes more complicated, increasing the risk of FLPT by approximately 17-fold[2,6-8], with FLPT accounting for 15% of all snowboarding-related ankle injuries and 34% of all snowboarding-related ankle fractures[2], also known as "snowboarders ankle" or "snowboarders fracture", respectively. Although FLPT is the second most common type of talar fracture, clinical cases are rare, especially for isolated FLPT[9-11]. The first description of FLPT was published by Marotolli in 1943[12]; however, until now, the relevant research literature remains limited, mostly comprising case reports and lacking clinical research with a large sample size; therefore, there is still no consensus on the standardized management of FLPT. Herein, we conducted a literature review on the clinical classification, management, and prognosis of FLPT to provide a credible reference for the clinical diagnosis and management of FLPT.

ANATOMY

The talus is the most superior bone of the foot and sits on top of and is supported by the calcaneus[13]. It articulates with the calcaneus and three separate subtalar articular surfaces, making it the second largest tarsal bone. Serving as an osseous link between the leg and foot, approximately two-thirds of the talar surface is covered by articular cartilage, with few muscle or tendon origins or insertions, and it plays an important role in ankle motion[14]. The talus can be divided into three main parts as follows (Figure 1 and Video): The talar head, neck, and body, resembling a snail in the lateral view. The body of the talus has two projections-the posterior and lateral talar processes. The lateral process of the talus extends from the lateral surface of the talar body and is a wedge-shaped protuberance formed by the posterior part of the posterior subtalar articular surface toward the lateral side. It has two main articular cartilage surfaces, forming an articulation with the distal fibula at its lateral superior part and constitutes the outermost part of the posterior subtalar articulation at the underside. The lateral talocalcanean ligament originates at the tip of the lateral talar process. Therefore, FLPT is usually accompanied by damage to the articular cartilage or ligaments related to the subtalar and talofibular joints. Consequently, if missed, delayed, or improperly treated, FLPT may result in malunion or nonunion, which may subsequently lead to posttraumatic arthritis and instability of the subtalar joint. Therefore, one must pay close attention to any suspected FLPT, as well as ensure timely and accurate diagnosis and formulate appropriate treatment plans.

MECHANISM OF INJURY

The definitive mechanism of injury in the FLPT is currently inconclusive, and according to existing research results, dorsiflexion, inversion, eversion, external rotation, and axial impaction are all causative factors[3-5]. Hawkins[15] and Fjeldborg[16] suggested that FLPT is caused by forced dorsiflexion combined with foot inversion; this mechanism of injury has been confirmed in several subsequent studies[17]. Some epidemiological studies on snowboarding injuries have suggested that the occurrence of foot and ankle injuries in this sport is associated with the complexity of specialized movements and the use of old soft-shell boots by athletes[18-20]. Although the mechanism of FLPT has not been clearly stated in these epidemiological studies, the athletes diagnosed with FLPT engaged in jumping and performing various difficult maneuvers in the air, leading to forced dorsiflexion and inversion upon landing, possibly contributing to the development of FLPT[21]. Cadaveric biomechanical experiments by Tinner and Sommer[1] showed that dorsiflexion of the foot, combined with eversion or external rotation, can also lead to FLPT. Jin *et al*[22] reported two cases of FLPT combined with rupture of the medial malleolar deltoid ligament, indirectly proving that eversion or external rotation violence encountered by the foot may also be a causative factor for FLPT. Other clinical studies and vitro biomechanical experiments have shown that FLPT is associated with dorsiflexion, axial impaction, eversion, and external rotation of the foot[5,22]. The authors believe that the causative factors of FLPT are diverse and that different types and intensities of injury violence may lead to significant differences in the fracture site, fragment size, degree of comminution, and displacement. For instance, according to the McCrory-Bladin classification, the mechanism of injury for type 2 and type 3 fractures is concomitant axial impaction violence associated with dorsiflexion and inversion of the foot during landing from a height, whereas type 1 fractures are due to dorsiflexion and inversion violence only. However, attention should be paid to establishing a timely and accurate diagnosis to avoid delays in management due to missed diagnoses, rather than on the correspondence between the mechanism of injury and fracture characteristics.

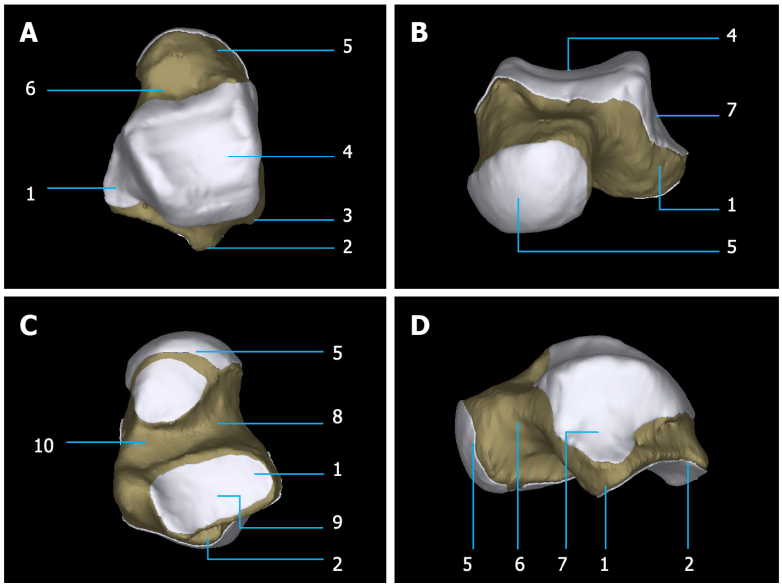

Figure 1 Basic anatomy of the talus. A: Superior view; B: Front view; C: Inferior view; D: Lateral view. 1: Lateral process of the talus; 2: Lateral tubercle of posterior process of the talus; 3: Medial tubercle ot posterior process of the talus; 4: Articular surface with distal end of tibia; 5: Head of talus; 6: Neck of talus; 7: Articular surface with fibula (talofibular joint); 8: Tarsal sinus; 9: Posterior part of subtalar joint; 10: Sulcus tali.

CLASSIFICATION AND CLASSIFICATION-BASED THERAPEUTIC RECOMMENDATION

Hawkins classification

In 1965, Hawkins[15] summarized three main fracture patterns by analyzing the radiographic features of 13 FLPT cases (Figure 2).

Hawkins type 1: A simple fracture of the lateral talar process, with the fracture line extending downward from the talofibular joint surface to the posterior talofibular joint surface; this type of fracture is easily diagnosed on radiographs.

Hawkins type 2: Comminuted fracture of the entire lateral talar process with fracture lines involving both the talofibular and posterior subtalar joint surfaces.

Hawkins type 3: Chip fracture of the anterior-inferior portion of the posterior half of the lateral talar process, which can be visualized only on lateral radiographs. The fracture is located in the region of the tarsal sinus and involves only a small portion of the posterior subtalar joint, without any damage to the talofibular articular surface.

Hawkins[15] recommended that, regardless of the classification, closed reduction should be attempted first by placing the foot in a neutral or everted position and then palpating and manipulating the lateral talus process into an acceptable position under radiography. For Hawkins type 2 and type 3 fractures, as well as type 1 fractures with satisfactory closed reduction, conservative treatment is recommended by immobilizing the foot in a short-leg plaster cast in a neutral position without weight-bearing for 4 wk, and weight-bearing with the maintenance of the plaster cast is allowed in the next 2 wk. For Hawkins type 1 fractures in which displacement of the fractured fragment remains unsatisfactory after attempted closed reduction, both Hawkins[15] and Dimon[23] recommended surgical treatment with open reduction and internal fixation (ORIF). Subsequently, fragment resection or subtalar joint fusion could be considered if complications such as nonunion, malunion, and overgrowth were confirmed after ORIF. From our perspective, Hawkins' management recommendations, which are limited by the relatively backward medical level and conditions at the time, have limited reference value for the current clinical management of FLPT.

McCrory-Bladin classification

In 1996, in order to better reflect the relationship between fracture characteristics and mechanism of injury and subsequently to guide further managements, McCrory and Bladin[21] proposed a new classification of FLPT, also known as McCrory-Bladin classification (Figure 3).

McCrory-Bladin type 1: Chip fracture of the anterior-inferior portion of the lateral talar process, without any damage to the talofibular articular surface. This type corresponds to Hawkins type 3 fracture, which is also considered as the avulsion fracture of the anterior talofibular ligament.

McCrory-Bladin type 2: Simple fracture of the lateral talar process causing some damages to both the talofibular and subtalar articular surfaces. This type corresponds to Hawkins type 1 fracture; however, McCrory and Bladin[21] made some modifications by dividing it into two subtypes based on the displacement of the large fragment, defining an undisplaced fracture as type 2A and a displaced fracture as type 2B.

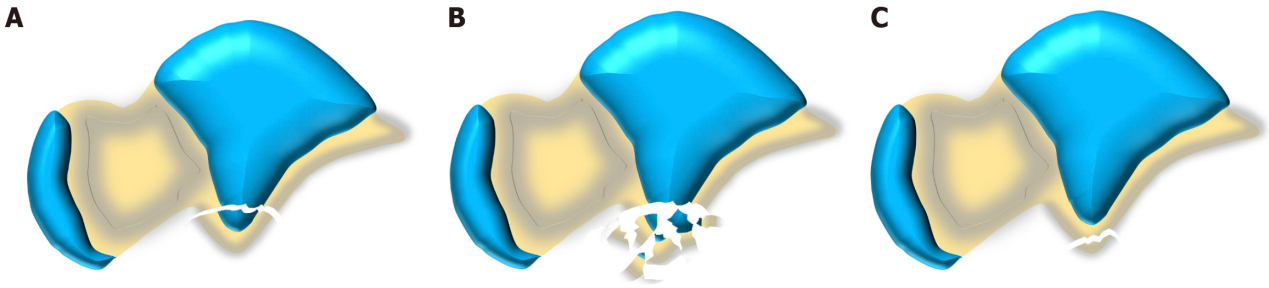

Figure 2 Hawkins classification of the fracture of the lateral process of the talus. A: Hawkins type 1, simple fracture with involvement of both the talofibular and posterior subtalar articular surfaces; B: Hawkins type 2, comminuted fracture; C: Hawkins type 3, the so-called chip fracture, no articular surface injured.

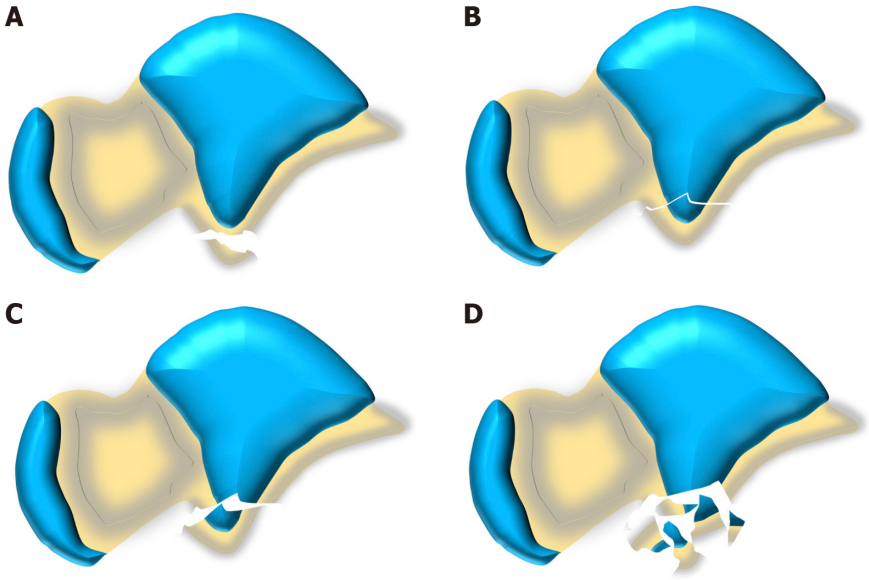

Figure 3 McCrory-Bladin classification of the fracture of the lateral process of the talus. A: McCrory-Bladin type 1, chip fracture; B: McCrory-Bladin type 2A, undisplaced simple intraarticular fracture; C: McCrory-Bladin type 2B, displaced simple intraarticular fracture; D: McCrory-Bladin type 3, comminuted fracture with involvement of both the talofibular and posterior subtalar articular surfaces.

McCrory-Bladin type 3: Comminuted fracture of the entire lateral process with the involvement of both the talofibular and posterior subtalar articular surfaces. This corresponds to Hawkins type 2 fracture.

McCrory and Bladin[21] summarized some of the case reports and provided the following treatment recommendations. For flake fractures (Chip fracture, McCrory-Bladin type 1) and simple fractures with no or minimal displacement (< 2 mm, McCrory-Bladin type 2), satisfactory results can be achieved with a 6-wk short leg plaster cast immobilization, and partial weight bearing were also recommended during this period. For simple fractures with severe displacement (≥ 2 mm, McCrory-Bladin type 2), an ORIF should be used to reconstruct the integrality of articular surfaces. For comminuted FLPT (McCrory-Bladin type 3), surgical treatment becomes unavoidable, and the fracture should be anatomically reduced and solidly fixed if possible; if anatomical reduction cannot be achieved or the fracture is too comminuted to be fixed, resection of all comminuted fragments is recommended to prevent the development of posttraumatic subtalar osteoarthritis. McCrory and Bladin's recommendations for treatment, although summarized in only a few case reports available at the time, are still applicable nowadays. The McCrory-Bladin classification is the most widely used classification method for FLPT in clinical practice.

Boack's classification

In 2004, Boack and Manegold[24] described a different classification that can be applied to fractures of both the lateral and posterior talar processes. The classification consists of four fracture types, each of which is divided into subtypes based on the severity of bone injury, degree of articular cartilage damage, and stability of the ligaments (Figure 4).

Boack's type 1: Chip fracture or avulsion fracture (< 0.5 cm). (1) 1a: An extra-articular fracture of the lateral talar process; (2) 1b: An isolated fracture of the medial tubercle of the posterior talar process; and (3) 1c: An intraarticular fracture of the lateral talar process;

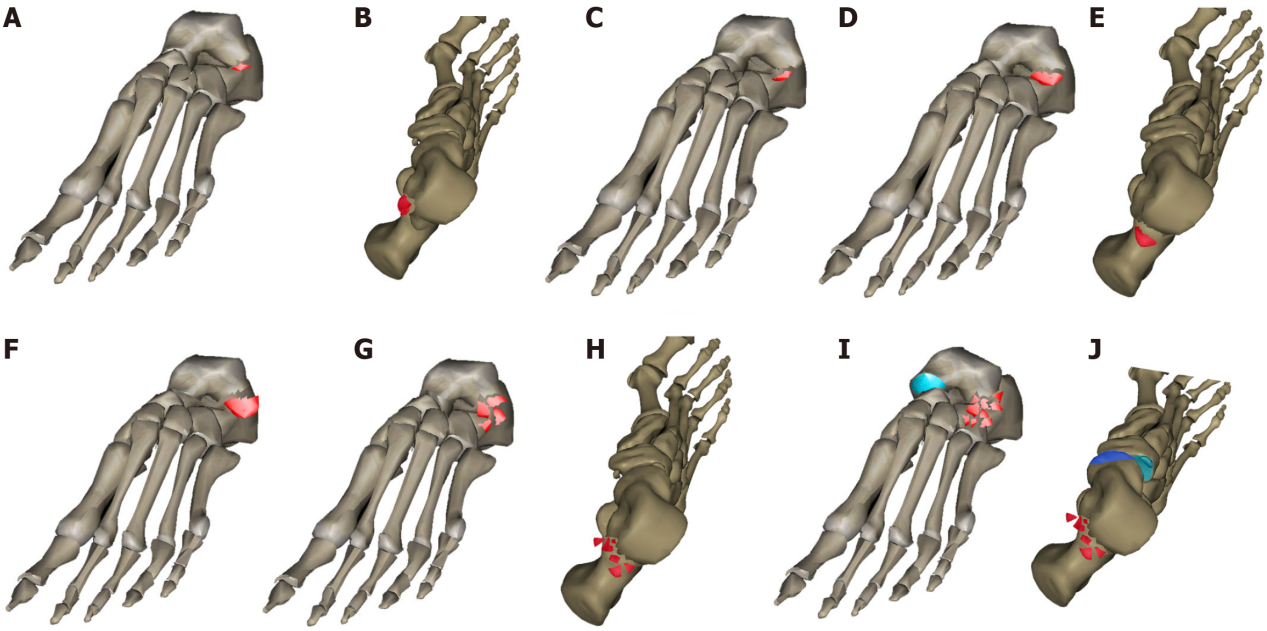

Figure 4 Boack's classification of the fracture of talar process. A: Boack's type 1a, extra-articular fracture of lateral process; B: Boack's type 1b, isolated fracture of the medial tubercle of the posterior talar process; C: Boack's type 1c, intra-articular fracture of the lateral process; D: Boack's type 2a, fracture of the lateral process of talus involving only the subtalar joint but not the talofibular joint; E: Boack's type 2b, fracture of the lateral tuberosity of the posterior talar process; F: Boack's type 3a, a simple fracture of the lateral talar process with involvement of both the talofibular and posterior subtalar articular surfaces; G: Boack's type 3b, comminuted fracture of the lateral talar process; H: Boack's type 3c, comminuted fracture of the posterior talar process with involvement of both lateral and medial tuberosity; I: Boack's type 4, comminuted fracture of the lateral talar process combined with luxation of the subtalar joint; J: Boack's type 4, comminuted fracture of the posterior talar process with luxation of the subtalar joint.

Boack's type 2: Medium-sized fragment (0.5-1.0 cm) with varying degrees of displacement. (1) 2a: FLPT involving only the subtalar joint but not the talofibular joint; and (2) 2b: An isolated fracture of the lateral tuberosity of the posterior talar process.

Boack's type 3: A large fracture fragment (> 1.0 cm) with varying degrees of damage to both the ankle and subtalar joints. (1) 3a: A simple fracture of the lateral talar process, extending from the talofibular joint to the posterior surface of subtalar articulation; (2) 3b: Comminuted fracture of the entire lateral talar process; and (3) 3c: Comminuted fracture of the entire posterior talar process.

Boack's type 4: A severe fracture of either the lateral or posterior talar process combined with instability or luxation of the subtalar joint.

Boack and Manegold[24] recommended that conservative treatment is only indicated for Boack's type 1a FLPT with external immobilization in a short leg cast for 6 wk, during which time weight-bearing walking is allowed, whereas all FLPT involving damage to articular surfaces or with displacements should be treated surgically to reduce the risk of degenerative lesions in the subtalar joints. Type 1c FLPT can be treated arthroscopically with resection of the bony fragments, because even a small intraarticular fragment can damage the articular surface severely, leading to serious adverse outcomes. Although secondary subtalar osteoarthritis or instability after total resection of the lateral talar process has been reported[10], there have been no reports of these lesions occurring secondary to resection of free fragments of the lateral talar process. Arthroscopic evaluation of the extent of articular cartilage damage and fracture comminution is recommended for all Boack's type 2 FLPT, and the decision to perform arthroscopic resection of fragments or arthroscopic internal fixation is based on the results of the arthroscopic evaluation. Boack's type 3a FLPT is recommended to be managed by open or arthroscopic reduction because of the large size of the fracture fragments and their good integrity and subsequently fixed with one or two headless cannulated compression screws, which can avoid articular cartilage damage caused by the head of conventional screws and provide optimal results. The management of Boack's type 3b FLPT depends on the degree of comminution and the size of the fragments, and it is recommended to remove all the fracture fragments if the attempted ORIF fails. In Boack's type 4 FLPT with subtalar joint dislocation, approximately 50% of patients have severe concomitant articular cartilage damage. To manage these cases, Boack and Manegold[24] recommended that subtalar joint repositioning should be completed as soon as possible, along with the arthroscopic evaluation of cartilage damage and arthroscopic resection of fragments to minimize the possibility of sequelae.

Tinner-Sommer's classification

In 2018, Tinner and Sommer[1] as part of their study on FLPT, found that McCrory-Bladin type 1 FLPT cases are extremely rare, accounting for less than 5% of all FLPT cases. Moreover, McCrory-Bladin type 2 FLPT were considered to represent an ideal state because most of the large fragment fractures of the lateral talar process are usually not isolated;

instead, they are often combined with at least one medium-sized fragment from the posterior subtalar articular facet, which was not severely comminuted, and therefore cannot be classified as McCrory-Bladin type 3 FLPT either. Consequently, they modified the McCrory-Bladin classification, with Tinner-Sommer types 1 and 2 FLPT remaining consistent with McCrory-Bladin types 1 and 2, whereas Tinner-Sommer type 3 was divided into three subtypes (Figure 5).

Type 3a: Simple fracture of the lateral talar process, with a medium-sized fragment originating from the posterior subtalar articular surface.

Type 3b: Comminution of the cranial metaphyseal bone of the lateral talar process based on the characteristics of type 3a fractures.

Type 3c: Nonreconstructable comminuted FLPT, corresponding to McCrory-Bladin type 3 fracture.

Although the Tinner-Sommer classification did not consider the displacement of fragments, it suggested that to better combine classification with management recommendations, the displacement of FLPT fragments should be evaluated before providing therapy. As a complement to the classification, they proposed their own criteria for evaluating the displacement of the fragments in FLPT as follows[1]: FLPT with an articular step of < 1 mm and a separation displacement of < 2 mm is defined as nondisplaced (or minimally displaced) fractures, whereas those with an articular surface step of ≥ 1 mm or a gap of ≥ 2 mm are defined as displaced FLPT.

According to the Tinner-Sommer classification[1], all FLPTs with no displacement or minimal displacement should be treated conservatively with cast or splint immobilization for at least 6 wk, during which partial weight bearing (< 10 kg) is allowed. For most Tinner-Sommer type 1 fractures, conservative management is recommended regardless of fracture displacement, whereas a small percentage of type 1 fractures combined with other injuries requiring surgical treatment, such as peroneal tendon slippage, can be managed surgically in conjunction with the surgical treatment of combined injuries, with either internal screw fixation or fragment resection, depending on the size of the fragments. Most of types 2 and 3 FLPT exhibit significant displacement and must be treated surgically. For type 2 and most type 3a FLPT, adequate bony connections can be formed between the major fragment and talar body after reduction, and fixation can be performed with one or two screws. In contrast, due to the presence of metaphyseal comminution in type 3b FLPT and a small percentage of type 3a fractures, the fragment did not have sufficient bone to hold screws; therefore, supportive fixation with a T-shaped osteoplate is recommended in such cases. Type 3c fractures are extremely comminuted, with no possibility of internal fixation, and resection of all fragments is recommended. In addition, compared with conservative treatment, surgical treatment offers the advantage of earlier postoperative articular function training. Therefore, the functional impairment of both the joint and muscle is significantly less than that of cast immobilization, which is especially important for young athletes who need to return to the arena as early as possible.

Wijers's classification

Wijers *et al*[25] noticed that a few FLPTs are combined with injuries to the sustentaculum tali, which could be considered a prestage of a full-blown subtalar or peritalar dislocation. Accordingly, by analyzing coronal computed tomography (CT) scans, Wijers *et al*[25] modified Boack's classification based on the severity, intraarticular or extraarticular location of the fracture, and possible joint dislocations ranging from types 1A to 4B (Figure 6). Type 1A: Small fragment, extraarticular; Type 1B: Small fragment, intraarticular; Type 2: Intermediate fragment, intraarticular; Type 3: Comminuted or severe fracture, intraarticular; Type 4A: FLPT combined with a sustentaculum tali fracture of the calcaneus without joint dislocation; Type 4B: FLPT combined with subtalar or peritalar dislocation.

From Wijers' viewpoint[25], type 1A FLPT as well as nondisplaced type 1B and type 2 FLPTs can be treated conservatively, whereas surgical treatment is recommended for all other fracture types. In addition, he emphasized that type 4B FLPTs require closed reduction of the talus in the emergency department due to concomitant total subtalar or peritalar luxation.

Zhang's classification

In 2023, the research team led by Wang *et al*[26] conducted a retrospective study of 43 FLPT cases and established a new classification system for FLPT based on CT features (Figure 7). This classification method broadly categorized FLPT into two major groups based on whether FLPT was combined with fractures of the ipsilateral talus; each major group was further divided into subtypes based on the fracture characteristics observed on CT scans.

Zhang's type 1: An isolated FLPT, further divided into three subtypes. (1) 1a: Chip fracture of the lateral talar process without involvement of the talofibular joint; (2) 1b: Simple fracture of the lateral talar process with the involvement of both the talofibular and subtalar joints; and (3) 1c: Comminuted fracture of the lateral talar process involving the articular surfaces.

Zhang's type 2: FLPT combined with fractures of other parts of the ipsilateral talus, with or without the involvement of the articular surfaces, was further divided into five subtypes. (1) 2a: FLPT combined with a fracture of the talar head; (2) 2b: FLPT combined with a fracture of the talar neck; (3) 2c: FLPT combined with a fracture of some other parts of the talar body (except for the lateral talar process, which has already been fractured); (4) 2d: FLPT combined with a fracture of the posterior talar process; and (5) 2e: FLPT combined with two or more fractures in other parts of the ipsilateral talus (except for the lateral talar process, which has already been fractured).

By analyzing the existing literatures and combining their own clinical experience, Wang *et al*[26] proposed a new classification for FLPT in 2023 and provided the corresponding treatment recommendations as follows: ORIF is best used for type 1a FLPT; type 1b FLPT should be better treated with fragments resection; type 1c FLPT should be treated conser-

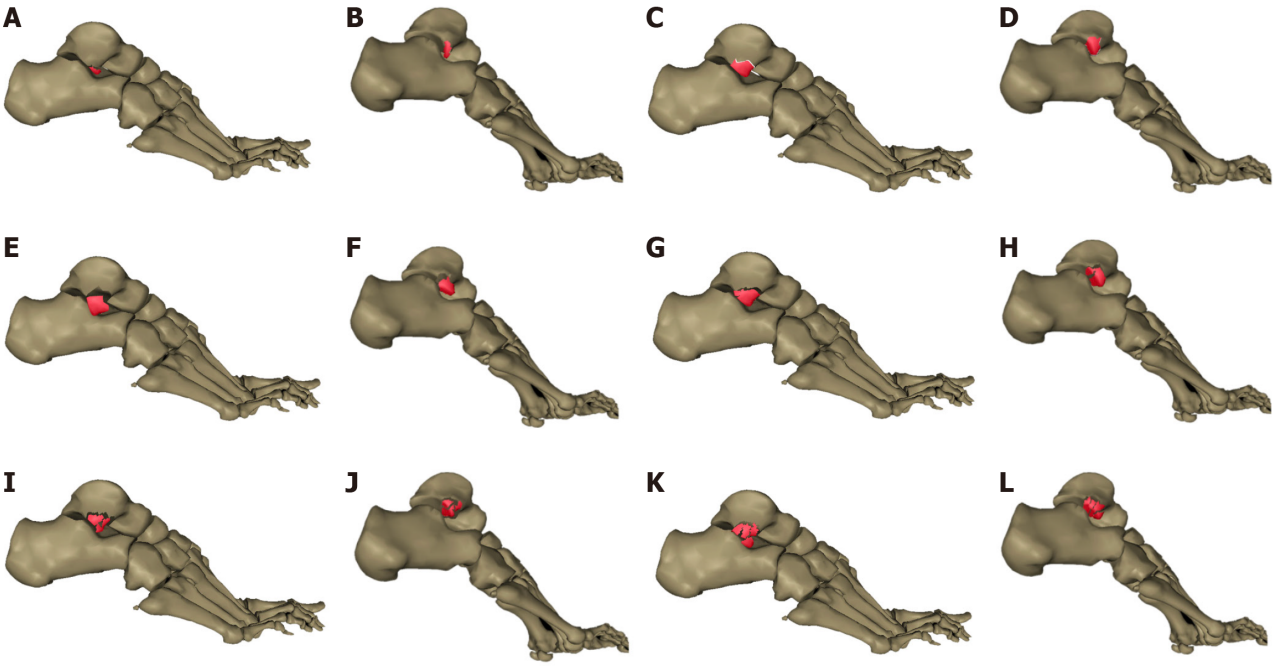

Figure 5 Tinner-Sommer's classification of the fracture of the lateral process of the talus. A: Tinner-Sommer type 1, chip fracture; B: Tinner-Sommer type 1, a posterolateral view; C: Tinner-Sommer type 2a, undisplaced simple intraarticular fracture; D: Tinner-Sommer type 2a, a posterolateral view; E: Tinner-Sommer type 2b, displaced simple intraarticular fracture; F: Tinner-Sommer type 2b, a posterolateral view; G: Tinner-Sommer type 3a, simple fracture of the lateral talar process combined with 1 medium-sized fragment originating from the posterior subtalar articular surface; H: Tinner-Sommer type 3a, a posterolateral view; I: Tinner-Sommer type 3b, comminuted fracture of the lateral talar process on the basis of type 3a; J: Tinner-Sommer type 3b, a posterolateral view; K: Tinner-Sommer type 3c, severely comminuted fracture without chance of full reconstruction; L: Tinner-Sommer type 3c, a posterolateral view.

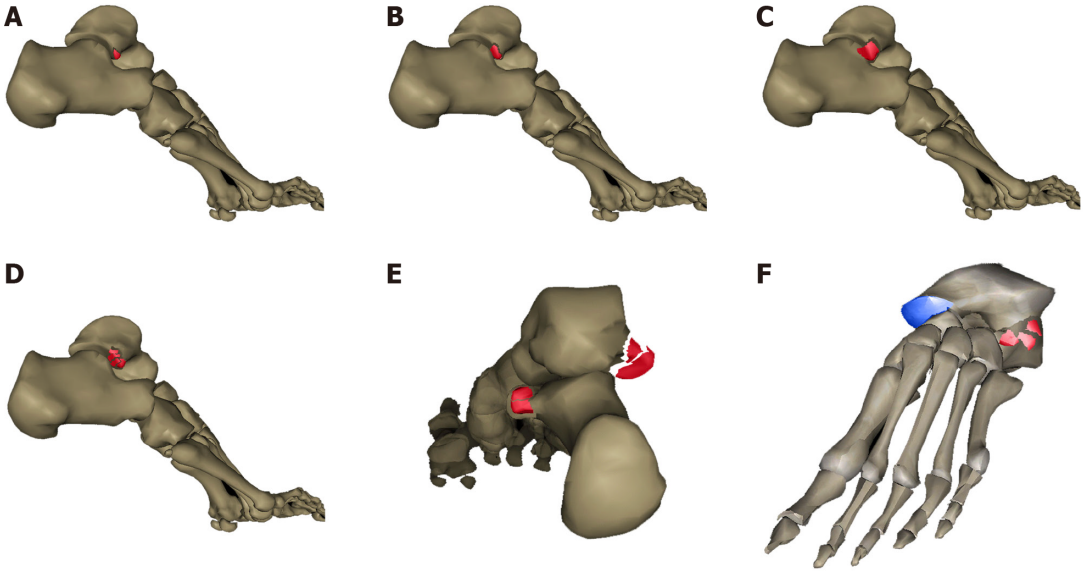

Figure 6 Wijers's classification of the fracture of the lateral process of the talus. A: Wijers type 1A fracture of the lateral process of the talus (FLPT), extra-articular fracture with a small fragment; B: Wijers type 1B FLPT, intra-articular fracture with a small fragment; C: Wijers type 2 FLPT, intra-articular fracture with an intermediate fragment; D: Wijers type 3 FLPT, comminuted intra-articular fracture; E: Wijers type 4A, FLPT combined with a sustentaculum tali fracture of the calcaneus but without joint dislocation; F: Wijers type 4B, FLPT combined with subtalar or peritalar dislocation.

vatively with a plaster cast, and if fracture turned to be nonunion later, the fragments of a smaller size are resected surgically while the larger fracture fragments can be internally fixed with screws; finally, all type 2 FLPTs are recommended to be treated surgically with ORIF.

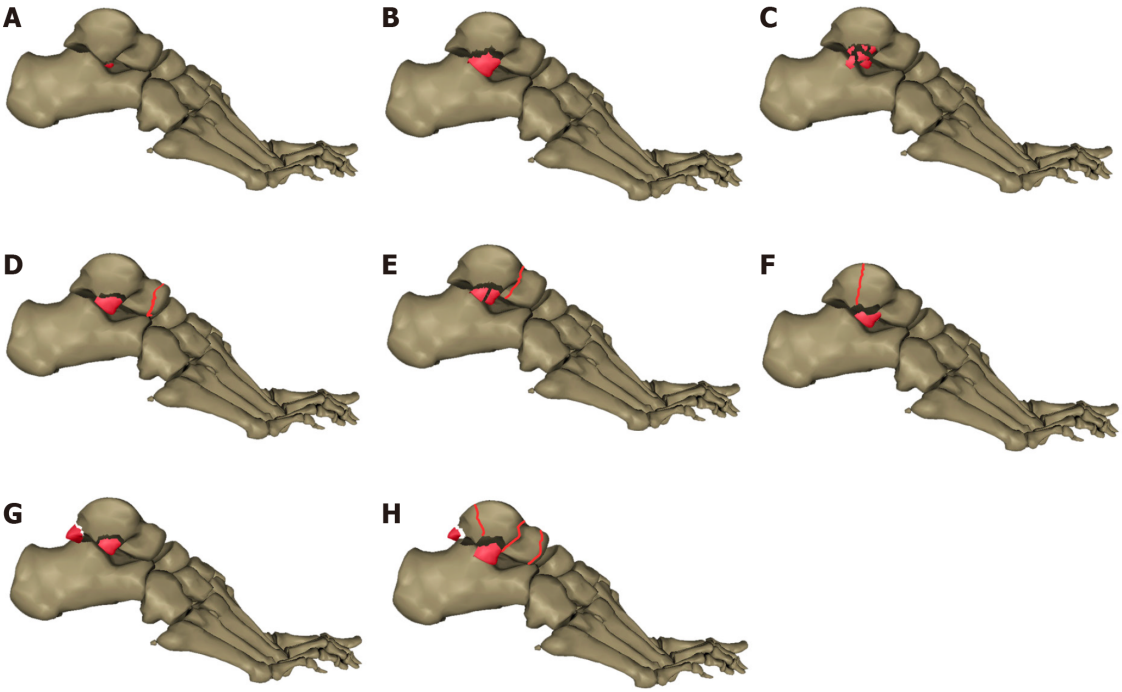

Figure 7 Zhang's classification of the fracture of the lateral process of the talus. A: Zhang's type 1a fracture of the lateral process of the talus (FLPT), chip fracture without involvement of the talofibular joint; B: Zhang's type 1b FLPT, simple fracture with involvement of both the talofibular and subtalar joints; C: Zhang's type 1c FLPT, comminuted fracture; D: Zhang's type 2a, FLPT combined with a fracture of talar head; E: Zhang's type 2b, FLPT combined with a fracture of talar neck; F: Zhang's type 2c, FLPT combined with a fracture of talar body; G: Zhang's type 2d, FLPT combined with a fracture of the posterior talar process; H: Zhang's type 2e, two or more fractures of other part of the ipsilateral talus besides FLPT.

PROGNOSIS REVIEW

The prognosis of FLPT is related to many factors, including age, injury mechanism, fracture classification, management techniques, severity of articular cartilage damage, and presence of concomitant injuries. However, based on our literature review[25-29], we believe that the overall prognosis of FLPT is optimistic (Table 1).

In Hawkins's research[15], seven patients achieved satisfactory results without pain or limitation of motion after immobilization with a plaster cast for 8 wk, whereas six patients experienced temporary disability lasting for approximately half a year after the fracture, of which five patients experienced persistent pain on standing or walking and one patient suffered malunion. Additionally, among the five patients with persistent pain, three patients suffered nonunion and two suffered overgrowth that led to pain or limited dorsiflexion of the foot. Consequently, second surgeries, either fragment resection or subtalar fusion depending on the size of the fragments and secondary changes of the subtalar joint, were performed for all the six patients in whom conservative management failed.

von Winning *et al*[30] reported the midterm results of eight displaced McCrory-Bladin type 2 FLPT cases by conducting an average of 7-year follow-up after ORIF with cannulated screws. In the study, all fractures healed completely. In addition, one patient developed traumatic arthritis of the ankle (Bargon's grade I), and one patient with an associated calcaneus fracture developed subtalar arthritis (Bargon's grade III) and received subsequent subtalar joint arthrodesis. The study revealed good clinical results, with a mean American Orthopedic Foot and Ankle Society (AOFAS) score of 81.4, mean Foot Function Index (FFI) of 19.4, mean physical component summary score of 48.9, and mean mental component summary score of 51.9. However, unlike most other studies, von Winning *et al*[30] compared the prognosis between patients treated surgically within 14 d of the fracture and those who underwent surgical treatment after 14 d of the fracture. The results showed no statistically significant difference between the two groups, suggesting that delayed surgical management does not always lead to poor prognosis.

Hörterer *et al*[6] conducted a study involving 22 patients with FLPT, including 16 patients with Hawkins type 1 fractures, 5 with Hawkins type 2 fractures, and 1 case with Hawkins type 3 fracture. He performed ORIF for Hawkins type 1 fractures and fragment resection for types 2 and 3 fractures. The results showed that 9% of patients suffered minor surgical side infections, and 55% developed symptomatic subtalar osteoarthritis. Moreover, the patient-rated outcomes revealed only moderate-to-good score more than 3 years after surgery.

Ross *et al*[10] followed all patients with FLPT at a level I trauma center over a 10-year period, with a mean follow-up of 6.5 years. This is the most recent and comprehensive study on the prognosis of FLPT. This study finally collected data from 53 patients, among whom 21 (39.6%) underwent initial conservative treatment, whereas 32 (60.4%) received initial surgical treatment. They noted that the failure of conservative treatment was closely related to the displacement rather than the size of the fracture fragments, and that FLPT with displacement had a higher rate of failure when treated conservatively, whereas FLPT without displacement usually did not require additional surgical treatments. Nevertheless, the prognosis of patients who underwent subsequent surgery due to the failure of conservative treatment was comparable to

Table 1 Summary table of prognoses of the included studies

Ref.	Sample size	Classification	Treatments	Prognoses	Remarks regarding prognoses
Hawkins [15], 1965	13	Hawkins type 1: 6; Hawkins type 2: 5; Hawkins type 3: 2	All patients were treated conservatively as the initial treatment	7 patients returned to normal motion without pain or limp. The remaining 6 had residual pain and/or limited motion and underwent subsequent fragments resection or joint fusion surgery, and ultimately 3 still had residual localized pain and mild limitation of movement	In Hawkins' day, the prognosis for conservatively treated patients was not that bad
von Winning *et al*[30], 2020[30]	8	All classified as McCrory-Bladin type 2	ORIF with cannulated screws	All fractures healed completely; Mean AOFAS score was 81.4, mean FFI was 19.4, mean physical component summary score was 48.9, and mean mental component summary score was 51.9	Delayed surgical managements did not significantly lead to a poor prognosis
Hörterer *et al*[6], 2019	22	Hawkins type 1: 16; Hawkins type 2: 5; Hawkins type 3: 1	ORIF: type 1; Fragments resection: type 2 and type 3	2 patients suffered minor surgical side infections. 12 patients developed symptomatic subtalar osteoarthritis, with no significant difference between types 1 and 2 fractures. Only 50% of the patients returned to the previous level of sports	The occurrence of secondary subtalar arthritis after ORIF and fragments resection was the same
Wijers *et al*[25], 2020	36	Wijers type 1A: 1; Wijers type 1B: 6; Wijers type 2: 10; Wijers type 3: 11; Wijers type 4A: 6; Wijers type 4B: 2	Conservative: 8; ORIF: 26; Subtalar joint fusion: 2	18 people were effectively followed up. The median AOFAS hindfoot score was 75 (range: 12-100) points. The median FFI score was 2 (range: 0-9) points. 3 (17%) patients had an excellent result, 8 (44%) patients had a good result, 5 (28%) patients had a fair result, and only 2 (11%) patients had a poor outcome	Patients who received timely and accurate managements were more likely to obtain a satisfactory prognosis
Ross *et al* [10], 2021	53	McCrory-Bladin type 1: 7; McCrory-Bladin type 2: 23; McCrory-Bladin type 3: 23	Conservative treatment was performed for 21 patients as the initial treatment to, of whom 14 underwent second surgery of fragments resection or subtalar joint fusion; ORIF was performed for 32 patients as the initial treatment.	For those whose initial treatments were conservative, PROMIS PF score was 53, FAAM-ADL was 88, FAAM-S was 75. There was no difference in the above indicators between patients who had or had not undergone second surgery. For those whose initial treatments were ORIF, PROMIS PF score was 56, FAAM-ADL was 90; FAAM-S was 77	Long-term prognoses were closely related to fracture displacement, but less so to fragment size, subtalar joint compression injury, and treatment method. However, the rate of subsequent talar arthrodesis was higher in initial conservative treatment group
Wang *et al*[26], 2023	43	Zhang's type 1a: 2; Zhang's type 1b: 1; Zhang's type 1c: 2; Zhang's type 2a: 1; Zhang's type 2b: 6; Zhang's type 2c: 18; Zhang's type 2d: 3; Zhang's type 2e: 10	Conservative: 3; ORIF: 39; Fragments resection: 1	AOFAS score: Zhang's type 1a: 91.5; Zhang's type 1b: 86.0; Zhang's type 1c: 90.5; Zhang's type 2a: 89.0; Zhang's type 2b: 76.7; Zhang's type 2c: 76.6; Zhang's type 2d: 91.3; Zhang's type 2e: 83.5. Complications including nonunion and arthritis were observed in only 7 (16.3%) cases	Prognoses of FLPT were related to simultaneous injuries of other parts of ipsilateral talus
Feng *et al* [28], 2023	42	All fractures were classified as McCrory-Bladin type 3	Arthroscopic internal fixation was performed for 24 cases by using a Double-pully technique combined with Kirschner wire. Open reduction and Kirschner wire fixation were performed for 18 patients	Among the patients treated arthroscopically, only 2 (8.3%) developed subtalar arthritis, with the primary symptoms being local pain and discomfort after exercising that was relieved by taking rest. After 12 months of surgery, the mean PROMIS PF score was 71.6, mean AOFAS score was 94.0, mean FAAM-ADL was 92.5, and mean FAAM-S was 94.4. Among those who underwent open reduction and Kirschner wire fixation, 6 (33.3%) patients developed subtalar arthritis. Consequently, 3 of them underwent a second surgery of subtalar joint fusion. After 12 months of surgery, the mean PROMIS PF score was 62.9, mean AOFAS score was 77.9, mean FAAM-ADL score was 72.1, and mean FAAM-S score was 78.6	Arthroscopic-assisted surgery can help improve the prognoses of FLPT
Feng *et al* [29], 2023	33	All fractures were classified as McCrory-Bladin type 2	21 patients were treated with double-tunnel subtalar arthroscopy combined with hollow compression screw internal fixation. The other 12 patients were treated with ORIF with hollow compression screw	For patients treated arthroscopically, no obvious complication was found. At the final follow-up, the mean AOFAS score was 95.8, mean FFI score was 12.3, mean FAAM-ADL score was 92.7, and mean FAAM-S score was 95.6. Among those who underwent ORIF with hollow compression screw, 2 (16.7%) patients developed local skin numbness associated with nerve injury. At the last follow-up, the mean AOFAS score was 94.8, mean FFI score was 14.4, mean FAAM-ADL score was 89.8, and mean FAAM-S score was 93.6	For McCrory-Bladin type 2 FLPT, the use of compression screw internal fixation could achieve reliable results. However, compared to open surgery, arthroscopy procedure obtained mini trauma and better functions
Mui *et al* [31], 2020	1 delayed	Not mentioned	ORIF with 2 headless compression screw,	An overgrowth of the tip of the lateral talar process led to pain while snowboarding. After 1 yr of the	Delayed FLPT cases can also lead to good long-

	case		followed by an iliac autologous bone graft procedure and anterior talofibular ligament reconstruction with 2 suture anchors	second surgery of the enlarged part excision, the patient returned to his previous level of motion without pain	term prognosis
Killen *et al*[32], 2018	2 delayed cases	Not mentioned	ORIF with a headless compression screw and anterior talofibular ligament reconstruction with a suture anchor	At 12 months after surgery, the mean AOFAS score was 90. Both patients regained recovery of full, activity without any residual pain or symptoms of instability	Delayed FLPT cases can also lead to good long-term prognosis

ORIF: Open reduction and internal fixation; AOFAS: American Orthopedic Foot and Ankle Society; FFI: Foot Function Index; FLPT: Fracture of the lateral process of the talus; PROMIS PF: Patient-reported outcomes measurement information system physical function; FAAM-ADL: Foot and ankle ability measure-activities of daily living; FAAM-S: Foot and ankle ability measure-sports.

that of patients who had satisfactory results after conservative treatment. On the contrary, they concluded that whether FLPT was combined with compression injury of the subtalar joint did not affect the long-term prognosis, and there was no statistically significant difference in the prognosis between patients who were successfully treated with conservative treatment and those who received surgical therapies (whether initial or not); however, the rate of subsequent talar arthrodesis was higher in the conservatively treated group.

In a study of 36 FLPT cases, Wijers *et al*[25] found that excellent and good prognoses accounted for 61%, whereas poor prognosis accounted for only 11% of the cases, regardless of management methods. In addition, concomitant injuries and delayed clinical visits contribute to poor prognosis, indicating that the majority of patients who received timely and accurate management are more likely to obtain a satisfactory prognosis.

An optimistic result was also presented by Wang *et al*[26]. He followed 43 FLPT cases for an average of 35.9 months and used the AOFAS score to evaluate the clinical prognosis. The results showed that AOFAS score was 91.5 ± 1.5 in type 1a, 86.0 ± 0 in type 1b, 90.5 ± 9.5 in type 1c, 89.0 ± 0 in type 2a, 76.7 ± 15.6 in type 2b, 76.6 ± 24.4 in type 2c, 91.3 ± 6.6 in type 2d, and 83.5 ± 11.0 in type 2e of fractures of Zhang's classification. Additionally, complications such as nonunion and arthritis were observed in only seven cases (16.3%).

We also reviewed the prognoses of patients with FLPT treated with different surgical techniques. Feng *et al*[28] performed arthroscopic internal fixation for 24 patients with McCrory-Bladin type 3 FLPT using a Double-pully technique combined with a Kirschner wire. The results showed that only two patients (8.3%) developed subtalar arthritis, with local pain and discomfort after exercising as primary symptoms relieved by taking rest. In another retrospective cohort study, Feng *et al*[29] compared the clinical outcomes between ORIF and arthroscopic-assisted fracture reduction and internal fixation in 33 patients with McCrory-Bladin type 2 FLPT, including 21 and 12 patients in the arthroscopy and ORIF groups, respectively. After a mean follow-up of 19.5 months, the author reported no significant difference in the AOFAS scores between the arthroscopy and ORIF groups at the final follow-up (95.8 ± 3.3 and 94.8 ± 3.7, respectively). However, the FFI was significantly lower in the arthroscopy group than in the ORIF group at the last follow-up (12.3 ± 5.3 and 14.4 ± 6.0, respectively). Additionally, no nerve or tendon complications were observed in the arthroscopy group, whereas two patients developed postoperative numbness in the dorsal region of the foot in the ORIF group. Finally, the author summarized that patients with McCrory-Bladin type 2 FLPT can obtain a good prognosis after internal fixation with compression screws; however, arthroscopic-assisted internal fixation is less invasive and more likely to lead to a better prognosis than ORIF.

Nevertheless, a good prognosis is also observed in delayed cases. Mui *et al*[31] presented a case of a 40-year-old male snowboard instructor with FLPT due to snowboarding. Unfortunately, the patient was initially misdiagnosed with an ankle sprain, and it was not until 6 months later that he was definitively diagnosed with FLPT. Subsequently, he underwent ORIF and an iliac autologous bone graft procedure, which resulted in a complete union of the fracture 3 months after surgery. In addition, the patient resumed his previous level of activity 5 months after surgery. However, at 18 months postoperatively, the patient complained of pain while snowboarding. A subsequent CT scan revealed complete fracture union and an enlarged lateral process forming an accessory anterolateral talar facet, which was confirmed as the cause of the pain. Finally, an additional surgery was performed to resect the enlarged part of the lateral process. A year after the second surgery, the patient was free from pain in the local region and had resumed normal sports activities. Similarly, Killen *et al*[32] reported cases of two patients who underwent reoperation due to nonunion after conservative treatment. Initially, they performed an open reduction of the fracture and used one or two headless cannulated screws for fixation. Subsequently, intraoperative examination showed a positive anterior drawer test; therefore, a suture anchor was placed in the distal fibula to repair the lateral ligament, and the extensor retinaculum and periosteum were used to reinforce the repair. The follow-up results at 12 months after surgery showed complete union and full range of motion in both patients, with no persistent discomfort and an average AOFAS score of 90.

CONCLUSION

In summary, FLPT is rare in clinical practice. Considering that the main symptoms are similar to lateral malleolar soft tissue injuries without specificity, it can be easily missed or misdiagnosed as an ankle sprain, resulting in delayed

diagnosis and treatment, which may eventually lead to subtalar osteoarthritis and instability. Therefore, FLPT must always be considered when diagnosing a dorsiflexed inverted ankle injury, especially resulting from snowboarding.

Imaging examinations for FLPT are essential for establishing accurate diagnosis and classification. Ultrasonography, the use of which to diagnose FLPT has only been shown in one case report[33], is noninvasive, nonradiative, convenient, and targeted. However, with gradually increasing studies on the ultrasonographic features of fractures in the past few years, ultrasonography is expected to become a preliminary screening method for FLPT in the future. Although radiography is currently the preferred examination, small fragments may overlap with other tissues or structures and be difficult to detect on plain radiographs, resulting in a missed diagnosis. Therefore, CT is necessary for patients with a suspicious medical history and symptoms but the fractures cannot be diagnosed certainly on plain radiographs, or for those who have localized accessory ossicles or osteophytes that are difficult to be distinguished from fractures[9,34,35].

The management principle for FLPT is currently controversial, and the selection of conservative treatment, fragment resection, and ORIF for a certain type of fracture is inconclusive, and lacks support from the results of clinical randomized controlled trials, as well as reliable consensus and guidelines. However, ongoing research worldwide has led to a more comprehensive understanding of the pathological and anatomical characteristics of FLPT. New classification systems have emerged constantly and guided the clinical treatment of FLPT more scientifically. However, more data from clinical studies are needed to summarize the pathological characteristics of FLPT to formulate more detailed and reliable treatment principles.

The prognosis of FLPT is related to several factors and cannot be simply generalized. However, based on the current literature, we believe that the overall prognosis of FLPT is good, even in delayed cases. To evaluate the prognosis of FLPT more scientifically, multicenter prospective randomized controlled clinical studies with large sample sizes are urgently required.

ACKNOWLEDGEMENTS

We would like to thank the foot and ankle surgical team of Center of Musculoskeletal Surgery, Berlin Charité Medical University Hospital, for the support and guidance.

FOOTNOTES

Author contributions: Wang CQ and Stöckle U conceptualized the idea; Wang CQ, Stöckle U, Dong SN and Li XG contributed to literatures searching and reviewing; Wang CQ, Dong SN and Ling ZX contributed to manuscript writing and editing; Wang CQ, Li XG and Dong SN contributed to creating figures and tables; Wang CQ, Stöckle U and Ling ZX contributed to manuscript revision. All authors have read and approved the final manuscript.

Supported by The China Scholarship Council, No. 202308420035.

Conflict-of-interest statement: The authors declare that there are no conflicts of interest to report.

Country/Territory of origin: China

ORCID number: Chao-Qun Wang 0009-0005-2254-2614; Ulrich Stöckle 0000-0002-6419-2203; Ze-Xi Ling 0009-0004-8925-9365.

S-Editor: Zheng XM
L-Editor: A
P-Editor: Zhang XD

REFERENCES

1 **Tinner C**, Sommer C. Fractures of the Lateral Process of the Talus. *Foot Ankle Clin* 2018; **23**: 375-395 [PMID: 30097080 DOI: 10.1016/j.fcl.2018.04.009]
2 **Kirkpatrick DP**, Hunter RE, Janes PC, Mastrangelo J, Nicholas RA. The snowboarder's foot and ankle. *Am J Sports Med* 1998; **26**: 271-277 [PMID: 9548123 DOI: 10.1177/03635465980260021901]
3 **Berkowitz MJ**, Kim DH. Process and tubercle fractures of the hindfoot. *J Am Acad Orthop Surg* 2005; **13**: 492-502 [PMID: 16330511 DOI: 10.5435/00124635-200512000-00002]
4 **Funk JR**, Srinivasan SC, Crandall JR. Snowboarder's talus fractures experimentally produced by eversion and dorsiflexion. *Am J Sports Med* 2003; **31**: 921-928 [PMID: 14623658 DOI: 10.1177/03635465030310063001]
5 **Boon AJ**, Smith J, Zobitz ME, Amrami KM. Snowboarder's talus fracture. Mechanism of injury. *Am J Sports Med* 2001; **29**: 333-338 [PMID:

11394605 DOI: 10.1177/03635465010290031401]
6 **Hörterer H**, Baumbach SF, Lemperle S, Altenberger S, Gottschalk O, Mehlhorn AT, Röser A, Walther M. Clinical outcome and concomitant injuries in operatively treated fractures of the lateral process of the talus. *BMC Musculoskelet Disord* 2019; **20**: 219 [PMID: 31092241 DOI: 10.1186/s12891-019-2603-3]
7 **Chan GM**, Yoshida D. Fracture of the lateral process of the talus associated with snowboarding. *Ann Emerg Med* 2003; **41**: 854-858 [PMID: 12764342 DOI: 10.1067/mem.2003.213]
8 **Valderrabano V**, Perren T, Ryf C, Rillmann P, Hintermann B. Snowboarder's talus fracture: treatment outcome of 20 cases after 3.5 years. *Am J Sports Med* 2005; **33**: 871-880 [PMID: 15827363 DOI: 10.1177/0363546504271001]
9 **Perera A**, Baker JF, Lui DF, Stephens MM. The management and outcome of lateral process fracture of the talus. *Foot Ankle Surg* 2010; **16**: 15-20 [PMID: 20152749 DOI: 10.1016/j.fas.2009.03.004]
10 **Ross H**, Marchand L, Cardon J, Beals T, Barg A, Nickisch F, Haller JM. Patient-Reported Outcomes After Lateral Process Talus Fracture. *J Orthop Trauma* 2021; **35**: e470-e474 [PMID: 34091571 DOI: 10.1097/BOT.0000000000002099]
11 **Dale JD**, Ha AS, Chew FS. Update on talar fracture patterns: a large level I trauma center study. *AJR Am J Roentgenol* 2013; **201**: 1087-1092 [PMID: 24147480 DOI: 10.2214/AJR.12.9918]
12 **Ali MKM**, Mbah C, Alwadiya A, Milner S. How a minor trauma can cause long term disability! A misdiagnosed fracture of the lateral process of the talus-A case report and review of literature. *EC Orthop* 2015; **1**: 21-26
13 **Drake R**, Vogl AW, Mitchell AWM. Gray's Anatomy for Students. 5th ed. Amsterdam: Elsevier Pub, 2023: 627-628
14 **Russell TG**, Byerly DW. Talus Fracture. 2023 May 23. In: StatPearls [Internet]. Treasure Island (FL): StatPearls Publishing; 2024 Jan- [PMID: 30969509]
15 **Hawkins LG**. Fracture of the lateral process of the talus. *J Bone Joint Surg Am* 1965; **47**: 1170-1175 [PMID: 14337775]
16 **Fjeldborg O**. Fracture of the lateral process of the talus. Supination-dorsal flexion fracture. *Acta Orthop Scand* 1968; **39**: 407-412 [PMID: 5730318 DOI: 10.3109/17453676808989476]
17 **Mukherjee SK**, Pringle RM, Baxter AD. Fracture of the lateral process of the talus. A report of thirteen cases. *J Bone Joint Surg Br* 1974; **56**: 263-273 [PMID: 4852086]
18 **Bladin C**, Giddings P, Robinson M. Australian snowboard injury data base study. A four-year prospective study. *Am J Sports Med* 1993; **21**: 701-704 [PMID: 8238711 DOI: 10.1177/036354659302100511]
19 **Bladin C**, McCrory P. Snowboarding injuries. An overview. *Sports Med* 1995; **19**: 358-364 [PMID: 7618012 DOI: 10.2165/00007256-199519050-00005]
20 **Pino EC**, Colville MR. Snowboard injuries. *Am J Sports Med* 1989; **17**: 778-781 [PMID: 2624290 DOI: 10.1177/036354658901700610]
21 **McCrory P**, Bladin C. Fractures of the lateral process of the talus: a clinical review. "Snowboarder's ankle". *Clin J Sport Med* 1996; **6**: 124-128 [PMID: 8673570 DOI: 10.1097/00042752-199604000-00011]
22 **Jin XY**, Xiao WY, He T, Dong YQ, Zhang C. Fracture of the lateral process of the talus with associated deltoid ligament injury: a report of 2 cases. *BMC Surg* 2022; **22**: 356 [PMID: 36195942 DOI: 10.1186/s12893-022-01781-y]
23 **Dimon JH 3rd**. Isolated displaced fracture of the posterior facet of the talus. *J Bone Joint Surg Am* 1961; **43-A**: 275-281 [PMID: 13722947]
24 **Boack DH**, Manegold S. Peripheral talar fractures. *Injury* 2004; **35** Suppl 2: SB23-SB35 [PMID: 15315876 DOI: 10.1016/j.injury.2004.07.019]
25 **Wijers O**, Posthuma JJ, De Haas MBJ, Halm JA, Schepers T. Lateral Process Fracture of the Talus: A Case Series and Review of the Literature. *J Foot Ankle Surg* 2020; **59**: 136-141 [PMID: 31668959 DOI: 10.1053/j.jfas.2019.02.003]
26 **Wang Y**, Wang Z, Zhu Y, Fu L, Deng X, Chen W, Zhang Y. New Classification Based on CT and Its Value Evaluation for Fractures of the Lateral Process of the Talus. *J Foot Ankle Surg* 2023; **62**: 644-650 [PMID: 36813634 DOI: 10.1053/j.jfas.2023.01.010]
27 **Sariali E**, Lelièvre JF, Catonné Y. Fractures of the lateral process of the talus. Retrospective study of 44 cases. *Rev Chir Orthop Reparatrice Appar Mot* 2008; **94**: e1-e7 [PMID: 19070708 DOI: 10.1016/j.rco.2008.04.009]
28 **Feng SM**, Xue C, Qi LE, Luo X, Jiang XW, Wang ML, Ma C. Internal fixation of McCrory-Bladin type III fracture of the lateral process of the talus with Kirschner wire Double-pully technique under subtalar arthroscopy. Zhonghua Chuangshang Zazhi 2023; 39: 899-905 [DOI: 10.3760/cma.j.cn501098-20230625-00364]
29 **Feng SM**, Luo X, Xue C, Chen J, Wang K, Shao CQ, Ma C. [Effect of hollow compression screw internal fixation in treating McCrory-Bladin type II lateral process fracture of the talus: open versus arthroscopy surgery]. *Zhonghua Yi Xue Za Zhi* 2023; **103**: 2808-2812 [PMID: 37723056 DOI: 10.3760/cma.j.cn112137-20230403-00541]
30 **von Winning D**, Lippisch R, Pliske G, Adolf D, Walcher F, Piatek S. Surgical treatment of lateral and posterior process fractures of the talus: Mid-term results of 15 cases after 7 years. *Foot Ankle Surg* 2020; **26**: 71-77 [PMID: 30554933 DOI: 10.1016/j.fas.2018.11.013]
31 **Mui T**, Sugimoto K, Sugioka S, Yamasaki T, Tanaka K, Isomoto S, Tanaka Y. Accessory Anterolateral Talar Facet Syndrome After Treatment of Neglected Fracture of the Lateral Process of the Talus: A Case Report. *J Foot Ankle Surg* 2020; **59**: 826-828 [PMID: 31982304 DOI: 10.1053/j.jfas.2019.12.006]
32 **Killen MC**, Karpe P, Limaye R. Fractures of the Lateral Process of the Talus With Associated Ankle Instability: A Report of 2 Cases. *Foot Ankle Spec* 2018; **11**: 378-381 [PMID: 29577747 DOI: 10.1177/1938640018766634]
33 **Copercini M**, Bonvin F, Martinoli C, Bianchi S. Sonographic diagnosis of talar lateral process fracture. *J Ultrasound Med* 2003; **22**: 635-640 [PMID: 12795560 DOI: 10.7863/jum.2003.22.6.635]
34 **Noble J**, Royle SG. Fracture of the lateral process of the talus: computed tomographic scan diagnosis. *Br J Sports Med* 1992; **26**: 245-246 [PMID: 1490216 DOI: 10.1136/bjsm.26.4.245]
35 **Whitby EH**, Barrington NA. Fractures of the lateral process of the talus--the value of lateral tomography. *Br J Radiol* 1995; **68**: 583-586 [PMID: 7627477 DOI: 10.1259/0007-1285-68-810-583]

World Journal of Clinical Cases

Submit a Manuscript: https://www.f6publishing.com

World J Clin Cases 2024 May 26; 12(15): 2499-2505

DOI: 10.12998/wjcc.v12.i15.2499

ISSN 2307-8960 (online)

ORIGINAL ARTICLE

Retrospective Study

Recent trends in bone metastasis treatments: A historical comparison using the new Katagiri score system

Kenji Matsuda, Kazuhiro Shimazu, Hanae Shinozaki, Koji Fukuda, Taichi Yoshida, Daiki Taguchi, Kyoko Nomura, Hiroyuki Shibata

Specialty type: Medicine, research and experimental

Provenance and peer review: Unsolicited article; Externally peer reviewed.

Peer-review model: Single blind

Peer-review report's classification

Scientific Quality: Grade C

Novelty: Grade B

Creativity or Innovation: Grade B

Scientific Significance: Grade B

P-Reviewer: Liu J, China

Received: December 10, 2023

Revised: April 6, 2024

Accepted: April 15, 2024

Published online: May 26, 2024

Kenji Matsuda, Kazuhiro Shimazu, Hanae Shinozaki, Koji Fukuda, Taichi Yoshida, Daiki Taguchi, Hiroyuki Shibata, Department of Clinical Oncology, Akita University Graduate School of Medicine, Akita 010-8543, Japan

Kyoko Nomura, Department of Environmental Health Science and Public Health, Akita University Graduate School of Medicine, Akita 010-8543, Japan

Hiroyuki Shibata, Department of Comprehensive Cancer Control, Akita University Graduate School of Medicine, Akita 010-8543, Japan

Co-first authors: Kenji Matsuda and Kazuhiro Shimazu.

Corresponding author: Hiroyuki Shibata, MD, PhD, Professor, Department of Clinical Oncology, Akita University Graduate School of Medicine, Hondo 1-1-1, Akita 010-8543, Japan. hiroyuki@med.akita-u.ac.jp

Abstract

BACKGROUND

Bone metastasis has various negative impacts. Activities of daily living (ADL) and quality of life (QOL) can be significantly decreased, survival may be impacted, and medical expenses may increase. It is estimated that at least 5% cancer patients might be suffering from bone metastases. In 2016, we published the Comprehensive Guidelines for the Diagnosis and Treatment of Bone Metastasis. Since then, the therapeutic outcomes for patients have gradually improved. As life expectancy is a major determinant of surgical intervention, the strategy should be modified if the prolongation of survival is to be achieved.

AIM

To monitor how bone metastasis treatment has changed before and after launch of our guidelines for bone metastasis.

METHODS

For advanced cancer patients with bone metastasis who visited the Department of Clinical Oncology at Akita University hospital between 2012 and 2023, parameters including the site and number of bone metastases, laboratory data, and survival time, were extracted from electronic medical records and the Katagiri score was calculated. The association with survival was determined for each factor.

RESULTS
Data from 136 patients were obtained. The 1-year survival rate for the poor prognosis group with a higher Katagiri score was 20.0% in this study, which was 6% and an apparent improvement from 2014 when the scoring system was developed. Other factors significantly affecting survival included five or more bone metastases than less (P = 0.0080), and treatment with chemotherapy (P < 0.001), bone modifying agents (P = 0.0175) and immune checkpoint inhibitors (P = 0.0128). In recent years, advances in various treatment methods have extended the survival period for patients with advanced cancer. It is necessary not only to simply extend survival time, but also to maintain ADL and improve QOL.

CONCLUSION
Various therapeutic interventions including surgical approach for bone metastasis, which is a disorder of locomotor organs, are increasingly required. Guidelines and scoring system for prognosis need to be revised promptly.

Key Words: Bone metastasis; New Katagiri scoring system; Prognosis; Immune check point inhibitors; Survival

Core Tip: We investigated bone metastasis patients from 2012 to 2023 at Department of Clinical Oncology, Akita University Hospital to learn about recent trends in treatment methods and outcomes for patients with bone metastases. The prognosis of patients with bone metastases has improved recently. Now, there is a room for surgical interventions to the patients with bone metastases, which have been avoided due to their limited prognosis. These are expected to improve activities of daily living and quality of life and will benefit patients. Accordingly, guidelines and scoring system for prognosis need to be revised.

Citation: Matsuda K, Shimazu K, Shinozaki H, Fukuda K, Yoshida T, Taguchi D, Nomura K, Shibata H. Recent trends in bone metastasis treatments: A historical comparison using the new Katagiri score system. *World J Clin Cases* 2024; 12(15): 2499-2505
URL: https://www.wjgnet.com/2307-8960/full/v12/i15/2499.htm
DOI: https://dx.doi.org/10.12998/wjcc.v12.i15.2499

INTRODUCTION

Bone metastasis has various negative impacts. Activities of daily living (ADL) and quality of life (QOL) may be significantly decreased, survival may be impacted, and medical expenses may increase. Based on the SEER database, 113317 of 2470634 cancer patients in the United States from 2010 to 2016 experienced bone metastases[1].

Treatment of bone metastasis includes orthopedic surgery, radiotherapy, drug treatment including bone modifying agents (BMAs) and palliative care[2]. BMAs can suppress skeletal related events (SREs) composed of pathologic fracture, spinal cord compression, radiation or surgery to bone, and hypercalcemia of malignancy[2]. In recent years, the adjunctive treatments such as radiofrequency ablation are considered. Additionally, carrier-mediated drug delivery, bone substitutes to repair bone defects, and multifunctional scaffolds with bone tissue regeneration and antitumor properties are investigated[3]. In recent years, immune check point inhibitors (ICIs) have been used to treat various cancers[4]. There is a remarkable efficacy of ICIs in the treatment of tumors.

A large number of clinical trials reveal that ICIs have promising therapeutic effects, including overall survival (OS), objective effective rate and progression-free survival[4]. Despite the potential to improve cancer outcomes with use of ICIs, bone metastases remain may have different responses to ICIs than other disease sites[5]. The effects of ICI on bone metastasis should be understood, including elucidation of the bone microenvironment. Palliative care is given not only to relieve pain, but to provide holistic support, so that the QOL of patients can be improved[2].

Various scoring systems that determine the choice of intervention have also been developed[2]. The new Katagiri scoring system (NKSS), which was developed in 2014, is very good tool to predict the life expectancy of bone metastatic patients[6]. The NKSS consists of six items, including: (1) The characteristics of primary cancers; (2) The existence of visceral, brain, and peritoneal dissemination; (3) Laboratory data; (4) Eastern Cooperative Oncology Group performance status (PS); (5) History of chemotherapy; and (6) The existence of multiple bone metastasis. Scores range from 0 to 10[6]. In the NKSS, the survival rate was 27% at 6 months, and 6% at 1 year with an overall prognostic score of ≥ 7[6]. Based on the Japanese comprehensive guidelines for diagnosis and treatment of bone metastasis, published in 2016, surgery is not recommended when prognosis is predicted within 6 months. The prognosis is gradually improving, for example, the 5-year survival rate improved by 2% each year from 2015 to 2019 in the United States[7]. It is also necessary to consider the impact on the scoring system from changes in treatment regimens, such as approval of the ICIs. Therefore, we examined the factors impacting cancer patients with bone metastases from 2012 to 2023.

MATERIALS AND METHODS

Patients

We retrospectively examined the clinical status of patients with bone metastases who underwent treatment at the Department of Clinical Oncology at Akita University hospital from December 2010 to March 2023.

Methods

Patient data included gender, age, site and number of bone metastases, site of primary tumor, metastasis other than bone, symptoms, opportunity for diagnosis, treatment history including radiotherapy, anticancer drugs, opioids, BMA and ICIs was extracted from their electronic medical records. Laboratory data at their visit included serum levels of C-reactive protein, lactate dehydrogenase, total bilirubin, calcium, and the number of platelets. Information regarding PS and ADL were also extracted from the medical records. Furthermore, the patient's life and death were examined as well as their survival time from the day visiting our department, and a score was calculated by the NKSS.

Statistical analyses were performed using BellCureve for Excel Ver 4.04 (Social Survey Research Information Co., Ltd., Japan).

All procedures were conducted according to the Declaration of Helsinki.

RESULTS

Patient characteristics

For 12 years and 4 months, 136 patients were enrolled in this study (Table 1). This number includes 13% of the patients presenting to the Department of Clinical Oncology. Of these, 86 were male (63.2%). Ages ranged from 24 to 84 years, with a median age of 64 years. The primary sites of bone metastases are listed in Table 1. Cancer of unknown primary (CUP) [n = 31 (22.8%)] was the most common, followed by gastric cancer [n = 24 (17.6%)], colorectal cancer, [n = 21 (15.4%)] sarcoma [n = 10 (7.4%)], and pancreatic cancer [n = 9 (6.6%)]. The MST for all cancer patients with bone metastases was 8.6 months [95% confidence interval (95%CI): 6-10 months]. MSTs by primary sites were as follows: CUP (8.6 months, 95%CI: 1-16 months), gastric cancer (6.0 months, 95%CI: 5-7 months), colorectal cancer (8.5 months, 95%CI: 6-11 months), sarcoma (9.2 months, 95%CI: 0-24 months), and pancreatic cancer (9.3 months, 95%CI: 3-16 months). The relatively short survival period may reflect the nature of the Department of Clinical Oncology, which treats very advanced cancers.

Characteristics of bone metastases

The frequency of bone metastases was as follows: single (n = 33, 24.3%), 2 or more and 4 or less (n = 44, 32.4%), and 5 or more (n = 58, 42.6%). The frequency of bone metastasis by site is shown in Supplementary Table 1. Metastases to the spine were the most frequent (n = 97, 71%) and the frequencies were as follows: cervical spine (n = 28, 21%), thoracic spine (n = 71, 52%), and lumbar spine (n = 64, 47%). Metastases to the pelvic bones, including the sacrum, ilium, and pubis were the next most frequent (n = 72, 53%). Metastases to other bones including ribs, scapula, and long bones, such as the femur, were third (n = 67, 49%).

Opportunity for diagnosing bone metastases

Metastases were found in 96 cases by diagnostic imaging (70.5%) (Supplementary Table 2). Of the 136 patients, 16.9% had pain, and 5.1% had neurological symptoms, whereas 2.9% had bone symptoms, such as a fracture and 2.9% had elevated serum alkaline phosphatase levels (Supplementary Table 2). Of 136 cases, 70% were asymptomatic.

Classification by NKSS classification

Calculation by NKSS calculations were conducted on the visiting day. Of the 136 patients, only 3 patients (2.2%) scored 0-3 (lower score), 62 patients (45.6%) scored 4-6 (middle score), and 71 patients (52.2%) scored 7-10 (higher score) (Figure 1A). The survival of the middle-score group (MSG) and the higher-score group (HSG) was examined. The 1-year survival rate was 56% for the MSG (Figure 1A and Table 2). This was similar to that of the original paper, which reported 49.3%. The 1-year survival rate was 20.0% in the HSG (Figure 1A and Table 2). This was greater than three times in the original paper, which was 6.0% (Figure 1A and Table 2). In this study, the MST of the MSG (461 d) was significantly longer compared with that of the HSG (124 d, $P < 0.001$).

Other factors affecting patient survival

Survival with and without symptoms of bone metastasis were compared. The MST was 192 d with symptoms and 254 d without (Supplementary Figure 1). There was no significant difference ($P = 0.4794$). Bone metastases symptoms may not affect the survival of patients.

Next, we examined the effect of the number of bone metastases on survival. The MSTs for patients with ≤ 4 oligo-metastases were 288 d (Figure 1B). However, the MST of patients with at least 5 bone metastases was 180 d (Figure 1B). There was a significant survival difference between ≥ 5 multiple metastases and ≤ 4 oligo-metastases ($P = 0.0080$) (Figure 1B). This indicates that ≥ 5 bone metastases may negatively impact survival.

Table 1 Characteristics of the participants

Primary site	*n*	Median survival time (95%CI, month)
CUP	31	8.6 (1-16)
Gastric cancer	24	6.0 (5-7)
Colorectal cancer	21	8.5 (6-11)
Sarcoma	10	9.2 (0-24)
Pancreatic cancer	9	9.3 (3-16)
NET	7	4.0 (2-7)
Esophageal cancer	6	2.9 (1-4)
Skin cancer	4	34.7 (4-66)
Thymic cancer	3	14.0 (14-14)
Hematologic malignancy	3	Not reached
Urological cancer	3	8.1 (0-17)
Others	6	6.4 (3-10)
Overall	136	8.1 (6-10)

CUP: Cancer of unknown primary; NET: Neuroendocrine tumor; CI: Confidence interval.

Table 2 Historical comparison of survival outcomes between the periods ranging from 2005 to 2008 and 2020 to 2023

NKSS	*n*	1-yr-survival rate in this study (2010-2023) (95%CI)	1-yr-survival rate in the original study (2005-2008) (95%CI)
0-3	3	-	91.4 (85.9–96.9)
4-6	62	56 (43-70)	49.3 (44.0-54.6)
7-10	71	20 (10-31)	6.0 (3.5–8.5)

NKSS: New Katagiri scoring system; CI: Confidence interval.

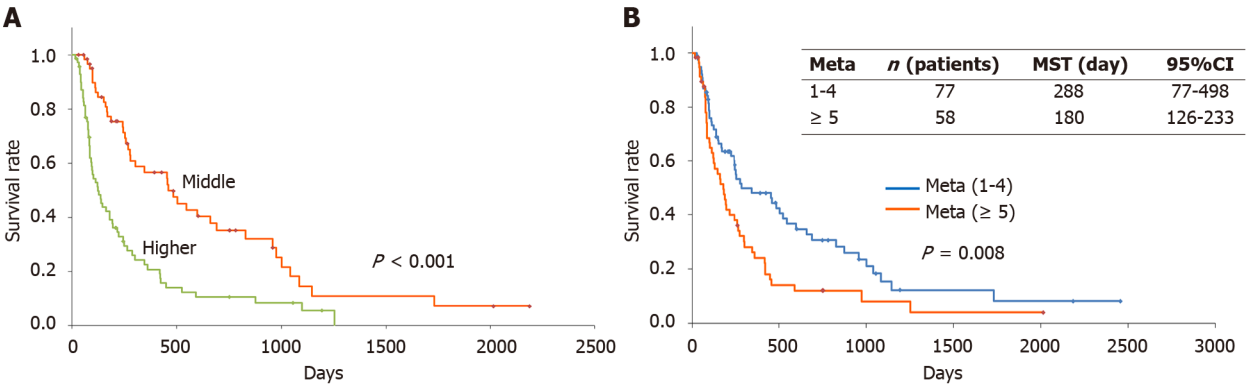

Figure 1 Overall survival of patients with bone metastasis. A: Overall survival by the new Katagiri score. The survival by the new Katagiri score: Middle (4-6), and higher (7-10) is indicated; B: Overall survival of patients with bone metastasis by the number of metastases. Meta: Number of metastases, *n*: Number of patients, MST: Median survival time; CI: Confidence interval.

Survival impact of bone metastases treatments

Of the 136 patients with bone metastases, 72.1% received radiotherapy. The MST was 263 d with radiotherapy and 168 d without (Figure 2A). There was no significant difference between the two groups (P = 0.145) (Figure 2A). The main purpose of radiotherapy is to relief pain, not necessarily to prolong survival. Of the 137 patients, 92.6% received chemotherapy. The MST was 263 d with chemotherapy and 82 d without (P < 0.001) (Figure 2B). Chemotherapy for advanced cancer, if the patient was acceptable, may represent longer survival. Of the 136 patients, 73.5% received BMA. The MST was 276 d with BMA and 99 d without (P = 0.0175) (Figure 2C). The purpose of using BMAs is to prevent the

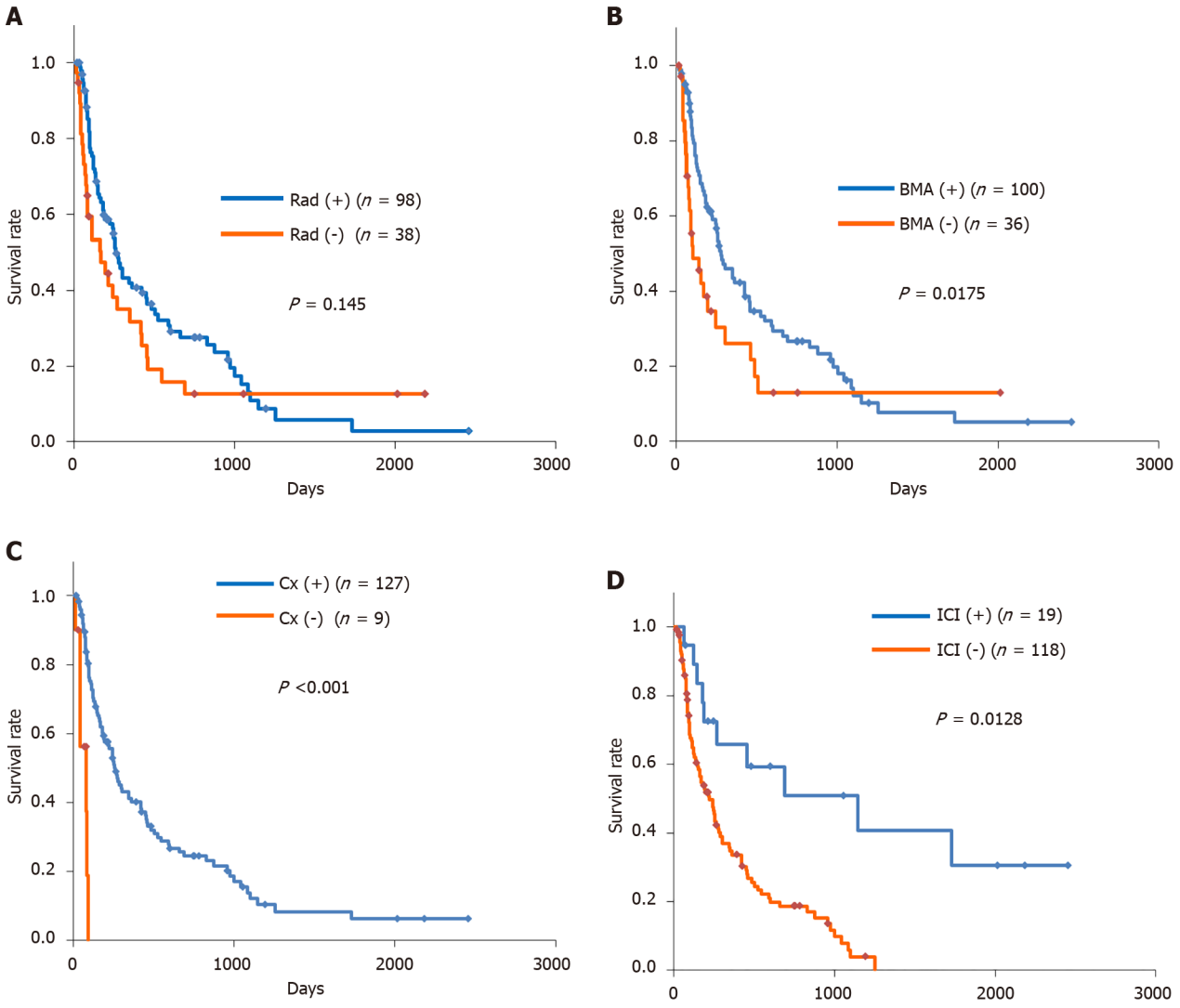

Figure 2 Overall survival of patients with bone metastasis by the type of treatment. A: Radiation; B: Chemotherapy; C: Bone modifying agent; D: Immune check point inhibitors. *n*: Number of patients; Rad: Radiation; Cx: Chemotherapy; BMA: Bone modifying agent; ICI: Immune check point inhibitors.

onset of SREs[2], and as a result, it is expected that the QOL and ADL of the patients with bone metastases will be maintained. Improvements in the QOL and ADL of patients may indirectly contribute to prolonging survival. Of the 136 patients, 14.0% received ICIs. The MST was 1146 d with ICIs and 222 d without (P = 0.0128) (Figure 2D). ICIs may have some survival benefits on the patients with bone metastases.

DISCUSSION

The 1-year survival rate for the MSG was almost the same as the original data, but it was not the same in the HSG, which was 6.0% and 20.0% in the original study and this study, respectively[6]. It is important to identify patients with bone metastasis and predict their survival rate. This information can guide the subsequent treatment and management. The predictive systems should be updated promptly. This study indicates the necessity of updating. Scoring system such as NKSS is used the most commonly, but in the future, machine learning might be preferred because of its innovation and accuracy[8]. It was suggested that chemotherapy, BMA and ICIs may contribute to prolonging survival. In this study, ICI was used in 8 cases (42.1%) of gastric cancer with bone metastases and 6 cases (31.6%) of lung cancer. Generally, patients with bone metastasis have a poor prognosis, so it is difficult to suggest the effectiveness of ICI. Combination therapy of nivolumab and ipilimumab for non-small cell lung cancer (NSCLC) has been shown to be more effective than platinum combination chemotherapy, regardless of the presence or absence of bone metastases[9]. The hazard ratio was higher for patients with bone metastases than those without bone metastases in spite the 95% confidential interval was slightly greater than 1.0[9]. On the other hand, the patients with NSCLC and bone metastases who received ICIs had a higher hazard of death[10]. In the pivotal trial of ICIs for gastric cancer, there is no description of bone metastasis[11]. The ICIs prolong survival in malignant tumors with bone metastasis in CheckMate 025, a randomized phase 3 trial of nivolumab *vs* everolimus in previously treated advanced renal cell carcinoma, in which a subgroup analysis revealed that median OS in patients with bone metastases was 18.5 months with nivolumab *vs* 13.8 months with everolimus[12]. Thus, ICIs might

prolong the survival time of patients with bone metastasis, although it was not significant[12]. The effect on bone metastasis with ICIs is still debatable. The generalizability of our study might be limited as this study is retrospective from a single institute.

Currently, orthopedic interventions are largely inappropriate if the expected survival time is 6 months or less[2]. In this study, the 6-month survival rate of the HSG was 75.3% (Figure 1A). Much more patients in the HSG may have a chance of benefiting from orthopedic treatment. Recently, patient surveillance studies indicated that many patients desire survival with preserved ADL rather than simply prolonging survival[13]. It is very important to keep patients' ADL with bone metastases by various interventions. This study is a retrospective survey at one facility and there were some limitations. It is necessary to expand the scale of such kinds of surveillance to verify the results in the future.

CONCLUSION

In recent years, advances in various treatment methods have extended the survival period for patients with advanced cancer. It is necessary not only to simply extend survival time, but also to maintain ADL and improve QOL. For this purpose, various therapeutic interventions including surgical approach for bone metastasis, which is a disorder of locomotor organs, are increasingly required. Scoring system for the individual patient prognosis should be updated promptly because this system is the starting point for the treatment of bone metastasis.

FOOTNOTES

Author contributions: Matsuda K and Shimazu K contributed equally to this work as co-first authors; Matsuda K, Shimazu K, Shinozaki H, Fukuda K, Yoshida T, Taguchi D and Shibata H treated the patients; Matsuda K and Shimazu K collected and analyzed the data; Nomura K confirmed the statistical analyses; Shibata H overviewed this study and prepared the manuscript.

Institutional review board statement: This study was certified and approved by the Ethics Committees of Akita University (No. 2814).

Informed consent statement: Written informed Consent for Publication of case could not be obtained from all participants. Instead, notification about the purpose and the implementation of the research was made public and an "opt-out" system was implemented to guarantee the opportunity to refuse as much as possible.

Conflict-of-interest statement: No author has any conflict of interest concerning this publication.

Data sharing statement: No additional data are available.

Country/Territory of origin: Japan

ORCID number: Kazuhiro Shimazu 0000-0001-7725-9107; Koji Fukuda 0000-0001-6101-6282; Taichi Yoshida 0000-0002-6912-3223; Hiroyuki Shibata 0000-0003-3581-3506.

S-Editor: Zheng XM
L-Editor: A
P-Editor: Li X

REFERENCES

1 **Huang JF**, Shen J, Li X, Rengan R, Silvestris N, Wang M, Derosa L, Zheng X, Belli A, Zhang XL, Li YM, Wu A. Incidence of patients with bone metastases at diagnosis of solid tumors in adults: a large population-based study. *Ann Transl Med* 2020; **8**: 482 [PMID: 32395526 DOI: 10.21037/atm.2020.03.55]

2 **Shibata H**, Kato S, Sekine I, Abe K, Araki N, Iguchi H, Izumi T, Inaba Y, Osaka I, Kawai A, Kinuya S, Kodaira M, Kobayashi E, Kobayashi T, Sato J, Shinohara N, Takahashi S, Takamatsu Y, Takayama K, Tateishi U, Nagakura H, Hosaka M, Morioka H, Moriya T, Yuasa T, Yurikusa T, Yomiya K, Yoshida M. Diagnosis and treatment of bone metastasis: comprehensive guideline of the Japanese Society of Medical Oncology, Japanese Orthopedic Association, Japanese Urological Association, and Japanese Society for Radiation Oncology. *ESMO Open* 2016; **1**: e000037 [PMID: 27843593 DOI: 10.1136/esmoopen-2016-000037]

3 **Bădilă AE**, Rădulescu DM, Niculescu AG, Grumezescu AM, Rădulescu M, Rădulescu AR. Recent Advances in the Treatment of Bone Metastases and Primary Bone Tumors: An Up-to-Date Review. *Cancers (Basel)* 2021; **13**: 4229 [PMID: 34439383 DOI: 10.3390/cancers13164229]

4 **Tang Q**, Chen Y, Li X, Long S, Shi Y, Yu Y, Wu W, Han L, Wang S. The role of PD-1/PD-L1 and application of immune-checkpoint inhibitors in human cancers. *Front Immunol* 2022; **13**: 964442 [PMID: 36177034 DOI: 10.3389/fimmu.2022.964442]

5 **Wytiaz V**, Van Poznak C. Checkpoint Inhibitors in Bone Metastatic Disease in Solid Tumors. *Curr Osteoporos Rep* 2023; **21**: 323-329 [PMID: 37294479 DOI: 10.1007/s11914-023-00798-3]

6 **Katagiri H**, Okada R, Takagi T, Takahashi M, Murata H, Harada H, Nishimura T, Asakura H, Ogawa H. New prognostic factors and scoring system for patients with skeletal metastasis. *Cancer Med* 2014; **3**: 1359-1367 [PMID: 25044999 DOI: 10.1002/cam4.292]

7 **Siegel RL**, Miller KD, Fuchs HE, Jemal A. Cancer statistics, 2022. *CA Cancer J Clin* 2022; **72**: 7-33 [PMID: 35020204 DOI: 10.3322/caac.21708]

8 **Zhong X**, Lin Y, Zhang W, Bi Q. Predicting diagnosis and survival of bone metastasis in breast cancer using machine learning. *Sci Rep* 2023; **13**: 18301 [PMID: 37880320 DOI: 10.1038/s41598-023-45438-z]

9 **Hellmann MD**, Paz-Ares L, Bernabe Caro R, Zurawski B, Kim SW, Carcereny Costa E, Park K, Alexandru A, Lupinacci L, de la Mora Jimenez E, Sakai H, Albert I, Vergnenegre A, Peters S, Syrigos K, Barlesi F, Reck M, Borghaei H, Brahmer JR, O'Byrne KJ, Geese WJ, Bhagavatheeswaran P, Rabindran SK, Kasinathan RS, Nathan FE, Ramalingam SS. Nivolumab plus Ipilimumab in Advanced Non-Small-Cell Lung Cancer. *N Engl J Med* 2019; **381**: 2020-2031 [PMID: 31562796 DOI: 10.1056/NEJMoa1910231]

10 **Qin A**, Zhao S, Miah A, Wei L, Patel S, Johns A, Grogan M, Bertino EM, He K, Shields PG, Kalemkerian GP, Gadgeel SM, Ramnath N, Schneider BJ, Hassan KA, Szerlip N, Chopra Z, Journey S, Waninger J, Spakowicz D, Carbone DP, Presley CJ, Otterson GA, Green MD, Owen DH. Bone Metastases, Skeletal-Related Events, and Survival in Patients With Metastatic Non-Small Cell Lung Cancer Treated With Immune Checkpoint Inhibitors. *J Natl Compr Canc Netw* 2021; **19**: 915-921 [PMID: 33878726 DOI: 10.6004/jnccn.2020.7668]

11 **Kang YK**, Boku N, Satoh T, Ryu MH, Chao Y, Kato K, Chung HC, Chen JS, Muro K, Kang WK, Yeh KH, Yoshikawa T, Oh SC, Bai LY, Tamura T, Lee KW, Hamamoto Y, Kim JG, Chin K, Oh DY, Minashi K, Cho JY, Tsuda M, Chen LT. Nivolumab in patients with advanced gastric or gastro-oesophageal junction cancer refractory to, or intolerant of, at least two previous chemotherapy regimens (ONO-4538-12, ATTRACTION-2): a randomised, double-blind, placebo-controlled, phase 3 trial. *Lancet* 2017; **390**: 2461-2471 [PMID: 28993052 DOI: 10.1016/S0140-6736(17)31827-5]

12 **Escudier B**, Sharma P, McDermott DF, George S, Hammers HJ, Srinivas S, Tykodi SS, Sosman JA, Procopio G, Plimack ER, Castellano D, Gurney H, Donskov F, Peltola K, Wagstaff J, Gauler TC, Ueda T, Zhao H, Waxman IM, Motzer RJ; CheckMate 025 investigators. CheckMate 025 Randomized Phase 3 Study: Outcomes by Key Baseline Factors and Prior Therapy for Nivolumab Versus Everolimus in Advanced Renal Cell Carcinoma. *Eur Urol* 2017; **72**: 962-971 [PMID: 28262413 DOI: 10.1016/j.eururo.2017.02.010]

13 **Hamano J**, Hiratsuka Y, Morita T, Kizawa Y, Maeda I, Mori M. Preference of Japanese cancer patients for being informed about their prognosis. *Ann Palliat Med* 2022; **11**: 3426-3435 [PMID: 36366893 DOI: 10.21037/apm-22-772]

World Journal of Clinical Cases

Submit a Manuscript: https://www.f6publishing.com

World J Clin Cases 2024 May 26; 12(15): 2506-2521

DOI: 10.12998/wjcc.v12.i15.2506

ISSN 2307-8960 (online)

ORIGINAL ARTICLE

Retrospective Study

Machine learning-based comparison of factors influencing estimated glomerular filtration rate in Chinese women with or without non-alcoholic fatty liver

I-Chien Chen, Lin-Ju Chou, Shih-Chen Huang, Ta-Wei Chu, Shang-Sen Lee

Specialty type: Health care sciences & services

Provenance and peer review: Unsolicited article; Externally peer reviewed.

Peer-review model: Single blind

Peer-review report's classification

Scientific Quality: Grade C, Grade C

Novelty: Grade B, Grade B

Creativity or Innovation: Grade B, Grade B

Scientific Significance: Grade B, Grade C

P-Reviewer: Wang TJ, China

Received: January 2, 2024

Revised: February 13, 2024

Accepted: April 9, 2024

Published online: May 26, 2024

I-Chien Chen, Lin-Ju Chou, Shih-Chen Huang, Department of Nursing, Kaohsiung Armed Forces General Hospital, Kaohsiung 802, Taiwan

Ta-Wei Chu, Department of Obstetrics and Gynecology, Tri-Service General Hospital, National Defense Medical Center, Taipei 114, Taiwan

Ta-Wei Chu, Chief Executive Officer's Office, MJ Health Research Foundation, Taipei 114, Taiwan

Shang-Sen Lee, Department of Urology, Taichung Tzu Chi Hospital, Buddhist Tzu Chi Medical Foundation, Taichung 427, Taiwan

Shang-Sen Lee, School of Medicine, Tzu Chi University, Hualian 970, Taiwan

Shang-Sen Lee, Department of Urology, Tri-Service General Hospital, National Defense Medical Center, Taipei 114, Taiwan

Corresponding author: Shang-Sen Lee, PhD, Chief Physician, Department of Urology, Taichung Tzu Chi Hospital, Buddhist Tzu Chi Medical Foundation, No. 88 Section 1, Fengxing Road, Tanzi Dist., Taichung 427, Taiwan. j520037@yahoo.com.tw

Abstract

BACKGROUND

The prevalence of non-alcoholic fatty liver (NAFLD) has increased recently. Subjects with NAFLD are known to have higher chance for renal function impairment. Many past studies used traditional multiple linear regression (MLR) to identify risk factors for decreased estimated glomerular filtration rate (eGFR). However, medical research is increasingly relying on emerging machine learning (Mach-L) methods. The present study enrolled healthy women to identify factors affecting eGFR in subjects with and without NAFLD (NAFLD+, NAFLD-) and to rank their importance.

AIM

To uses three different Mach-L methods to identify key impact factors for eGFR in healthy women with and without NAFLD.

METHODS
A total of 65535 healthy female study participants were enrolled from the Taiwan MJ cohort, accounting for 32 independent variables including demographic, biochemistry and lifestyle parameters (independent variables), while eGFR was used as the dependent variable. Aside from MLR, three Mach-L methods were applied, including stochastic gradient boosting, eXtreme gradient boosting and elastic net. Errors of estimation were used to define method accuracy, where smaller degree of error indicated better model performance.

RESULTS
Income, albumin, eGFR, High density lipoprotein-Cholesterol, phosphorus, forced expiratory volume in one second (FEV1), and sleep time were all lower in the NAFLD+ group, while other factors were all significantly higher except for smoking area. Mach-L had lower estimation errors, thus outperforming MLR. In Model 1, age, uric acid (UA), FEV1, plasma calcium level (Ca), plasma albumin level (Alb) and T-bilirubin were the most important factors in the NAFLD+ group, as opposed to age, UA, FEV1, Alb, lactic dehydrogenase (LDH) and Ca for the NAFLD- group. Given the importance percentage was much higher than the 2nd important factor, we built Model 2 by removing age.

CONCLUSION
The eGFR were lower in the NAFLD+ group compared to the NAFLD- group, with age being was the most important impact factor in both groups of healthy Chinese women, followed by LDH, UA, FEV1 and Alb. However, for the NAFLD- group, TSH and SBP were the 5th and 6th most important factors, as opposed to Ca and BF in the NAFLD+ group.

Key Words: Non-alcoholic fatty liver; Estimated glomerular filtration rate; Machine learning; Chinese women

Core Tip: We examined influential factors affecting the estimated glomerular filtration rate in healthy women with and without non-alcoholic fatty liver disease (NAFLD) by multiple linear regression and machine learning methods, with machine learning methods providing better performance and showing that age was the most important determining factor in both groups, followed by lactic dehydrogenase, uric acid, forced expiratory volume in one second, and albumin. However, for the NAFLD- group, the 5th and 6th most important impact factors were thyroid-stimulating hormone and systolic blood pressure, as compared to plasma calcium and body fat for the NAFLD+ group.

Citation: Chen IC, Chou LJ, Huang SC, Chu TW, Lee SS. Machine learning-based comparison of factors influencing estimated glomerular filtration rate in Chinese women with or without non-alcoholic fatty liver. *World J Clin Cases* 2024; 12(15): 2506-2521
URL: https://www.wjgnet.com/2307-8960/full/v12/i15/2506.htm
DOI: https://dx.doi.org/10.12998/wjcc.v12.i15.2506

INTRODUCTION

The increased Westernization of lifestyles in Taiwan has driven the prevalence of obesity and obesity-related diseases such as diabetes and metabolic syndrome[1]. Total caloric intake exceeding total energy expenditure results in the accumulation of fat in the liver, leading to nonalcoholic fatty liver disease (NAFLD)[2]. The prevalence of NAFLD has increased recently, ranging from 8%-45% in various countries[3]. Around one-fourth of NAFLD cases eventually progresses to nonalcoholic steatohepatitis, with another 20%-35% further progressing to fibrosis and even hepatocellular carcinoma[4]. Thus, NAFLD is a critical issue for both the community and health providers.

NAFLD has also been shown to be associated with chronic renal disease (CKD)[5], with insulin resistance, obesity, dyslipidemia, and hypertension found to contribute to impaired renal function[5-8]. However, most of these studies relied on traditional statistical analysis methods, with machine learning approaches use in only one study to identify four NAFLD-related genes[9].

Medical research is increasingly applying machine learning (Mach-L) methods to improve prediction accuracy by repeated analysis of large data sets. Some of these studies focused in this area began to use Mach-L[10]. The present study uses three different Mach-L methods to identify key impact factors for estimated glomerular filtration rate (eGFR) in healthy women with and without NAFLD.

MATERIALS AND METHODS

Participant and study design

Data for this study were sourced from the Taiwan MJ Cohort, an ongoing prospective cohort of health examinations conducted by the MJ Health Screening Centers (MJ) a group of three private clinics in Taiwan that provide regular health examinations to their members[11]. These examinations cover more than 100 important biological indicators, including anthropometric measurements, blood tests, imaging tests, *etc*. Each participant completed a self-administered questionnaire covering personal and family medical history, current health status, lifestyle, physical exercise, sleep habits, and dietary habits[12]. The MJ Health Database only includes participants who have provided informed consent. All or part of the data used in this research were authorized by and received from the MJ Health Research Foundation (Authorization Code: MJHRF2023008A). Any interpretations or conclusions described in this paper are those of the authors alone, and do not represent the views of the MJ Health Research Foundation. The study protocol was approved by the Institutional Review Board of the Kaohsiung Armed Forces General Hospital (IRB No.: KAFGHIRB 112-007). As a secondary study which does not collect samples from study participants, a short review was applied and no further informed consent was needed.

A total of 102 847 healthy women were initially enrolled. After excluding subjects with different causes, 65535 women remained for analysis, as shown in Figure 1. The inclusion criteria were as follows: (1) Age between 18 to 65 years old; (2) No known significant disease such as coronary heart disease, stroke, or chronic renal disease; (3) Not taking medications for hypertension, hyperlipidemia, or hyperglycemia; and (4) No regular alcohol consumption; In Model 1, the participants were divided into groups with or without NAFLD (NAFLD+, NAFLD-, respectively). Preliminary Mach-L analysis found that age was the most important factor in both groups (mean = 71.69%), followed by uric acid (respectively 37.17% and 41.99% in the NAFLD+ and NAFLD- groups). We made the second models (Model 2) by removing age from the data set.

The following methods were published in our previous study[13]. On the day of the study, senior nursing staff recorded the subject's medical history, including information on any current medications, and a physical examination was performed. The waist circumference was measured horizontally at the level of the natural waist. The body mass index (BMI) was calculated as the participant's body weight (kg) divided by the square of the participant's height (m). Systolic blood pressure (SBP) and diastolic blood pressure were measured using standard mercury sphygmomanometers on the right arm of each subject while seated.

After fasting for 10 h, blood samples were collected for biochemical analyses. Plasma was separated from the blood within 1 h of collection and stored at 30 °C until analysis for fasting plasma glucose (FPG) and lipid profiling. FPG was measured using the glucose oxidase method (YSI 203 glucose analyzer; Yellow Springs Instruments, Yellow Springs, OH, United States). The triglyceride (TG) levels were measured using the dry multilayer analytical slide method with a Fuji Dri-Chem 3000 analyzer (Fuji Film, Tokyo, Japan). The serum high-density lipoprotein cholesterol (HDL-C) and low-density lipoprotein cholesterol (LDL-C) concentrations were analyzed using an enzymatic cholesterol assay, following dextran sulfate precipitation. The BMD was measured by dual-energy X-ray absorptiometry (Lunar, General Electric, United States). Fatty liver was diagnosed based on the following ultrasound parameters: Parenchymal brightness, liver-to-kidney contrast, deep beam attenuation, bright vessel walls, and gallbladder wall definition. Qualitative grades are conveniently labeled mild (3), moderate (2), severe (1) or normal (0). In the present study, grades 1 to 3 were all defined as fatty liver (FA).

Table 1 shows the 32 variables which were used in the present study. These included participants' body fat (BF), complete blood cell count, biochemistries, thyroid stimulating hormone, C-reactive protein (CRP), education level, marital status, and income level. Drinking area was defined as the product of total drinking duration, frequency of drinking and alcohol percentage. Similarly, smoking area was the product of the duration, frequency of smoking and number of cigarettes. The sport area was the product of duration, frequency, and type of exercise. All the aforementioned parameters were the independent variables and eGFR was the dependent variable.

Traditional statistical method

The data were tested for normal distribution by using the Kolmogorov–Smirnov test and for the homogeneity of variances using Levene's test. Continuous variables were expressed as mean ± SD. One way analysis of variance was applied to compare differences between groups (> 2 groups). The Bonferroni test was for post-hoc evaluation. Pearson's correlation was used to examine the relationships between age and other continuous variables.

Machine learning method

Predictive models for NAFLD with factor ranking were constructed using three different Mach-L methods and part of the following information was published by our group previously[13].

Stochastic gradient boosting (SGB) is a tree-based gradient boosting learning algorithm that combines both bagging and boosting techniques to minimize the loss function to solve the overfitting problem of traditional decision trees[14]. In SGB, many stochastic weak learners of trees are sequentially generated through multiple iterations, where each tree concentrates on correcting or explaining errors in the tree generated in the previous iteration. That is, the residual of the previous iteration tree is used as the input for the newly generated tree. This iterative process is repeated until the convergence condition or a stopping criterion is reached for the maximum number of iterations. Finally, the cumulative results of many trees are used to determine the final robust model.

The second method used in this study is eXtreme gradient boosting (XGBoost), which is based on an optimized extension of SGB[15]. It sequentially trains multiple weak models and assembles them using the gradient boosting output

Table 1 Participant descriptive statistics and risk factors, percentage and mean (± SD)

Characteristics	None	Fatty liver	*P* value
N number	34, 335	31, 200	
Age (yr)	36.75 ± 12.33	47.52 ± 12.8	< 0.001
Income	2.04 ± 1.47	1.61 ± 1.57	< 0.001
Body fat (%)	26.66 ± 5.55	35.96 ± 6.83	< 0.001
Systolic blood pressure (mmHg)	111.83 ± 16.07	124.52 ± 19.68	< 0.001
Diastolic blood pressure (mmHg)	66.81 ± 10.21	73.8 ± 11.69	< 0.001
Leukocyte (× 10^3/μL)	5.93 ± 1.73	6.45 ± 1.73	< 0.001
Hemoglobin (× 10^6/μL)	13.09 ± 1.14	13.36 ± 1.18	< 0.001
Platelets (× 10^3/μL)	248.96 ± 57.74	264.39 ± 63.31	< 0.001
Fasting plasma glucose (mg/dL)	92.75 ± 10.64	103.7 ± 25.6	< 0.001
Total bilirubin (mg/dL)	0.77 ± 0.32	0.73 ± 0.33	< 0.001
Albumin (mg/dL)	4.5 ± 0.26	4.45 ± 0.24	< 0.001
Globulin (mg/dL)	3.08 ± 0.36	3.15 ± 0.36	< 0.001
Alkaline Phosphatase (IU/L)	101.86 ± 49.29	110.72 ± 59.94	< 0.001
Serum glutamic oxaloacetic transaminase (mg/dL)	19.88 ± 11.71	24.61 ± 17.56	< 0.001
Serum glutamic pyruvic transaminase (IU/L)	17.68 ± 18.62	28.72 ± 27.22	< 0.001
Serum γ-glutamyl transpeptidase (IU/L)	14.22 ± 13.94	25.3 ± 30.09	< 0.001
Lactate dehydrogenase (IU/L)	241.42 ± 84.03	246.65 ± 92.63	< 0.001
Estimated glomerular filtration rate (mL/min/1.73 m^2)	89.6 ± 76.89	84.33 ± 72.4	< 0.001
Uric acid (mg/dL)	4.88 ± 1.09	5.67 ± 1.34	< 0.001
Triglyceride (mg/dL)	78.81 ± 42.95	139.02 ± 101.03	< 0.001
High density lipoprotein cholesterol (mg/dL)	61.73 ± 14.8	54.17 ± 13.47	< 0.001
Low density lipoprotein cholesterol (mg/dL)	107.97 ± 30.48	125.76 ± 34.09	< 0.001
Calcium (mg/dL)	9.2 ± 0.39	9.29 ± 0.41	< 0.001
Phosphorus (mg/dL)	3.72 ± 0.44	3.7 ± 0.46	< 0.001
Thyroid stimulating hormone (IU/mL)	1.75 ± 3.25	1.94 ± 3.64	< 0.001
C-reactive protein (mg/dL)	0.19 ± 0.45	0.3 ± 0.51	< 0.001
Forced expiratory volume in one second (L)	2.2 ± 0.46	1.96 ± 0.53	< 0.001
Drink area	0.97 ± 6.5	1.38 ± 8.72	< 0.001
Smoke area	1.5 ± 7.15	1.57 ± 7.89	< 0.001
Betel nut area	0 ± 0	0.02 ± 1.2	< 0.001
Sport area	3.32 ± 5.99	3.96 ± 6.19	< 0.001
Sleep time	2.91 ± 0.59	2.87 ± 0.72	0.25
Marriage, *n* (%)			
Unmarried	13 (458)	8 (438)	< 0.001
Married	19 (939)	2 (1545)	

method, thus improving prediction performance. XGBoost uses Taylor's binomial expansion to approximate the objective function and arbitrary differentiable loss functions to accelerate the model construction convergence process[16]. XGBoost also applies regularized boosting techniques to penalize model complexity and correct overfitting, thereby increasing model's accuracy[15].

Finally, elastic net (EN) can be regarded as a hybrid version of L1 regularization and L2 regularization. The elastic network uses both L1 and L2 regularization, thus integrating the penalty terms of L1 and L2. The advantage of the EN model is that it combines the Ridge penalty item to achieve effective regularization and the Lasso penalty item to select

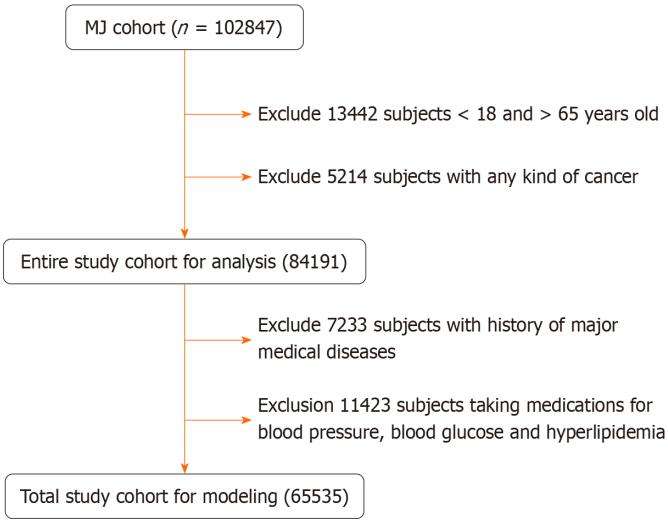

Figure 1 Flowchart of sample selection from the MJ Health Screening Centers Study Cohort.

variables, allowing it to learn models with only a small number of arguments that are non-zero sparse, just like Lasso, but it still maintains some of Ridge's regular properties. EN provides several advantages as follows: It encourages group effects in the case of highly correlated variables, rather than setting some of them to 0 Like Lasso; EN is useful when multiple features are mutually correlated; and Lasso tends to choose one of them at random, while EN tends to choose two[17].

Figure 2 presents the proposed prediction and important variable identification scheme that combines the three Mach-L methods. First, patient data were collected to prepare the dataset. The dataset was then randomly divided into an 80% training dataset for model building and a 20% testing dataset for model testing. In the training process, the hyperparameters of each Mach-L method must be tuned to ensure model effectiveness. In this study, a 10-fold cross-validation technique was used for hyperparameter tuning.

To this end, the training dataset was further randomly divided into a training dataset to build the model with different sets of hyperparameters, and a validation dataset for model validation. All possible combinations of hyperparameters were investigated by grid search. The model with the lowest root mean square error on the validation dataset was viewed as the best model of each Mach-L method. The best models for SGB, XGBoost and EN were generated, and the corresponding variable importance ranking information obtained.

During the testing phase, the performance of the best machine learning models was evaluated using the testing dataset. Since the target variable in this study is a numerical variable, model performance was compared using different metrics, including mean absolute percentage error (MAPE), symmetric mean absolute percentage error (SMAPE), relative absolute error (RAE), root relative squared error (RRSE), and root mean squared error (RMSE). The values for these metrics are listed in Figure 3.

To maximize comparison reliability and stability, the training and testing processes were repeated 10 times. The performance metrics of the three machine learning models were then averaged to compare with the performance of the benchmark multiple linear regression (MLR) model. The same training and testing datasets were used for three the machine learning methods and the MLR model. A model with an average metric lower than that of the MLR model was considered a more convincing model.

The Mach-L methods used in this study may produce percentage of importance of variables due to their unique modeling characteristics. In the final stage of our proposed scheme, we summarize and discuss our significant findings based on the results of Mach-L methods.

All methods were performed using R software version 4.0.5 and RStudio version 1.1.453 with the required packages installed (http://www.R-project.org, accessed on; https://www.rstudio.com/products/rstudio/).

RESULTS

The present study enrolled a total of 65535 participants. Table 1 compares all the variables in the NAFLD+ and NAFLD- groups. In the NAFLD+ group, the following variables were all significantly higher: Age, BF, blood pressure, leukocyte, hemoglobin, platelets, FPG, globulin, alkaline phosphatase, serum glutamic oxaloacetic transaminase, serum glutamic pyruvic transaminase, serum γ-glutamyl transpeptidase, lactic dehydrogenase (LDH), uric acid (UA), Total bilirubin (T-bili), TG, LDL-C, Calcium (Ca), Thyroid stimulating hormone (TSH), CRP, drinking area, betel nut area, and sport area. In the NAFLD+ group, the following variables were significantly lower: Income, albumin (Alb), eGFR, HDL-C, Phosphorus, forced expiratory volume in one second (FEV1), and sleep time. The χ^2 test results showed married participants were more likely to have NAFLD.

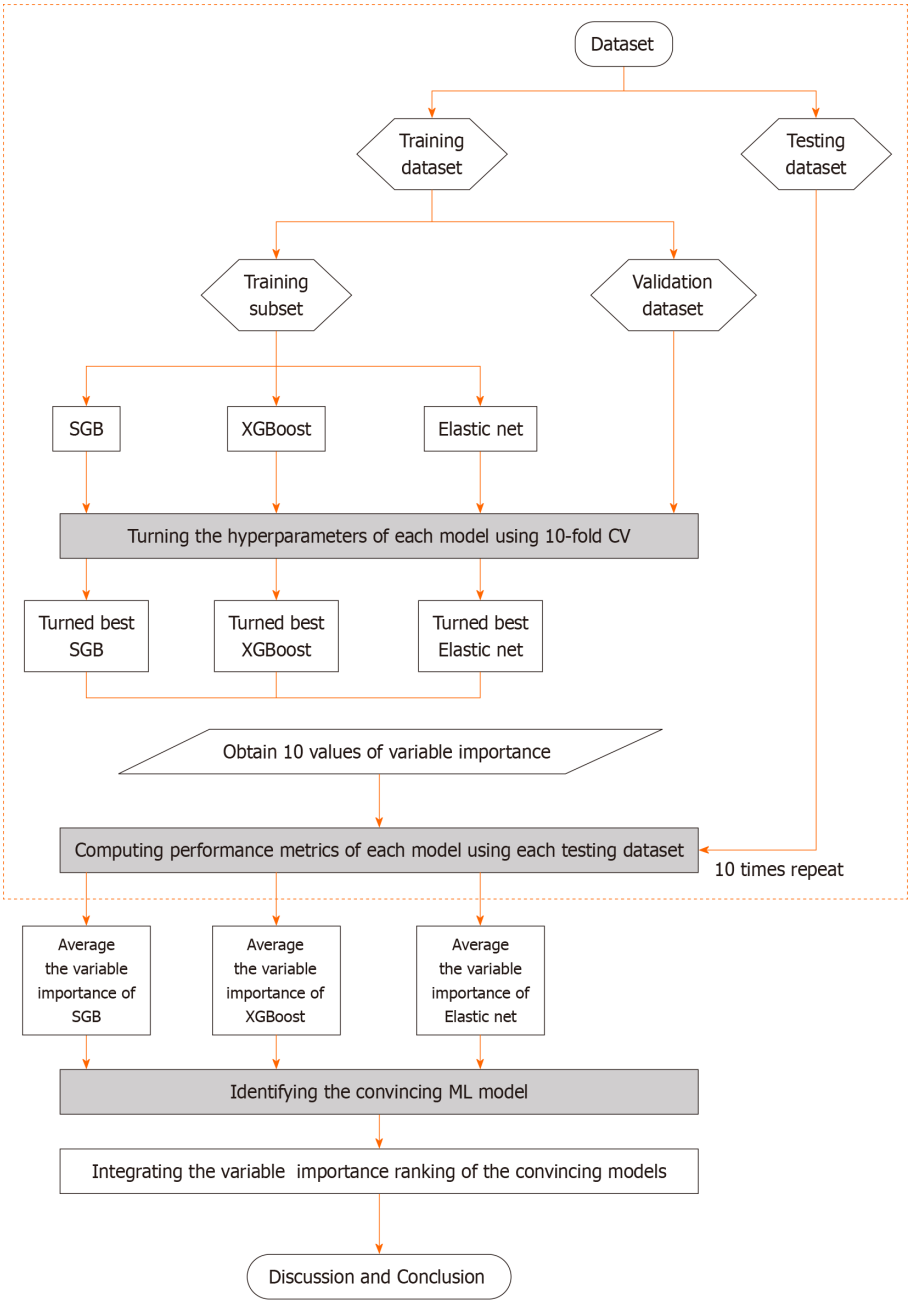

Figure 2 Flowchart of the proposed machine learning methods. XGBoost: eXtreme gradient boosting.

Table 2 compares the performance of LR and other Mach-L methods. Both in Model 1 (with age) and Model 2 (without age), most of the SMAPE, RAE, RRSE and RMSE values were lower in the three Mach-L methods, indicating that the Mach-L methods outperformed MLR. Tables 3-6 show the he importance percentages of the three Mach-L methods, with the averages of these three methods presented in the right column, showing that the most important factors predicting eGFR were age, UA FEV1, Ca, Alb and T-bili in the NAFLD+ group and age, UA, FEV1, Alb, LDH and Ca in the NAFLD- group. The importance percentage of age (71.73% and 71.69%, respectively, for the NAFLD- and NAFLD+ groups) is much higher than that of the following factor, UA (41.99% and 37.17%, respectively for the NAFLD- and NAFLD+ groups). Model 2 was built by removing the age variable, with results shown in Tables 5 and 6. Similar to Model 1, the most important factors were LDH, UA, FEV1, Alb TSH, and SBP for NAFLD- and LDH, UA, FEV1, Alb, Ca and BF for NAFLD+. In Tables 3-6, it should be noted that we used grayscale to show the importance of these factors, the darker the shade of gray, the more important that particular variable was. Figure 4 are the graphic illustrations for Tables 3-6. In Figure 4A, the percentage of importance percentage of the risk factors in participants with NAFLD are shown (Model 1: with age). In the same time, Figure 4B shows the results of without NAFLD in Model 1. Respectively, Figure 4C are results of Model 2 with NAFLD and 3-4 without NAFLD. All the orders of the ranks of percentage importance were the same as the results in the tables. These figures could give a direct concept of these risk factors.

Table 2 Comparison with SMAPE, RAE, RRSE, and RMSE between multiple linear regression and machine learning methods

NAFLD+ group with age	MAPE	SMAPE	RAE	RRSE	RMSE
Linear	0.139	0.132	0.845	0.842	13.959
SGB	0.138	0.131	0.841	0.834	13.825
XGBoost	0.139	0.132	0.845	0.842	13.946
Elasticnet	0.139	0.132	0.845	0.842	13.954
NAFLD- group with age					
Linear	0.133	0.128	0.868	0.862	14.671
SGB	0.132	0.126	0.855	0.857	14.59
XGboost	0.132	0.126	0.853	0.857	14.58
Elasticnet	0.134	0.128	0.868	0.862	14.673
NAFLD+ group without age					
Linear	0.154	0.14	0.872	0.897	15.606
SGB	0.153	0.139	0.865	0.888	15.444
XGboost	0.153	0.14	0.869	0.891	15.49
Elasticnet	0.154	0.14	0.872	0.897	15.596
NAFLD- group without age					
Linear	0.134	0.13	0.905	0.906	15.149
SGB	0.133	0.129	0.895	0.892	14.915
XGboost	0.133	0.129	0.895	0.893	14.916
Elasticnet	0.134	0.13	0.904	0.905	15.119

Data showed as mean; SGB: stochastic gradient boosting, XGBoost: eXtreme gradient boosting; RAE: Relative Absolute Error; RRSE: Root Relative Squared Error; RMSE: Root Mean Squared Error; NAFLD: Non-alcoholic fatty liver.

Metrics	Description	Calculation
SMAPE	Symmetric Mean Absolute Percentage Error	$SMAPE = \frac{1}{n}\sum_{i=1}^{n}\frac{\lvert y_i - \hat{y}_i\rvert}{(\lvert y_i\rvert + \lvert\hat{y}_i\rvert)/2} \times 100$
MAPE	Mean Absolute Percentage Error	$MAPE = \frac{1}{n}\sum_{i=1}^{n}\left\lvert\frac{y_i - \hat{y}_i}{y_i}\right\rvert \times 100$
RAE	Relative Absolute Error	$RAE = \sqrt{\frac{\sum_{i=1}^{n}(y_i - \hat{y}_i)^2}{\sum_{i=1}^{n}(y_i)^2}}$
RRSE	Root Relative Squared Error	$RRSE = \sqrt{\frac{\sum_{i=1}^{n}(y_i - \hat{y}_i)^2}{\sum_{i=1}^{n}(y_i - \hat{y}_i)^2}}$
RMSE	Root Mean Squared Error	$RMSE = \sqrt{\frac{1}{n}\sum_{i=1}^{n}(y_i - \hat{y}_i)^2}$

Figure 3 Equation of performance evaluation metrics. $\hat{y}_i$ and y_i respectively represent predicted and actual values; *n* is the number of instances. SMAPE: Symmetric Mean Absolute Percentage Error; MAPE: Mean Absolute Percentage Error; RAE: Relative Absolute Error; RRSE: Root Relative Squared Error; RMSE: Root Mean Squared Error.

DISCUSSION

We first demonstrated that the eGFR was lower in NAFLD+ group, and identified the six most important factors for NAFLD- and NAFLD+ in Model 1. Model 2 was then built by removing age. Consistent with Model 1, in Model 2 the first four factors were LDH, UA, FEV1 and Alb, but the 5th and 6th most important factors were respectively TSH and SBP in NAFLD- and Alb, BF in NAFLD+.

Table 3 The average of the importance of risk factors derived from stochastic gradient boosting, random forest and extreme gradient boost, in NAFLD+ (Model 1, including age)

Variables	SGB	XGBoost	Elasticnet	Average	Rank
Age	100	100	15.08	71.69	1
Income	0.14	0	0	0.05	
Body fat	3.94	1.9	3.27	3.04	
Systolic blood pressure	1.37	0.67	1.01	1.02	
Diastolic blood pressure	2.67	0.67	1.8	1.71	
Leukocyte	0.72	0.33	4.32	1.79	
Hemoglobin	1	0	0	0.33	
Platelets	3.64	1.62	0.31	1.86	
Fasting plasma glucose	2.92	1.18	0.66	1.59	
Total bilirubin	6.86	2.29	40.24	16.46	6
Albumin	1.84	0.54	49.85	17.41	5
Globulin	0.28	0.29	17.83	6.13	
Alkaline Phosphatase	0.99	0.15	0	0.38	
Serum glutamic oxaloacetic transaminase	1.63	0.36	0	0.66	
Serum glutamic pyruvic transaminase	3.83	1.94	0.82	2.20	
Serum γ-glutamyl transpeptidase	1.89	1.33	0.48	1.23	
Lactate dehydrogenase	23.21	23.25	0.86	15.77	
Uric acid	27.03	24.05	60.42	37.17	2
Triglyceride	0.84	0	0.02	0.29	
High density lipoprotein cholesterol	1.99	0.8	1.16	1.32	
Low density lipoprotein cholesterol	1.78	0.14	0.1	0.67	
Calcium	3.97	2.87	65	23.95	4
Phosphorus	0.79	0.36	0	0.38	
Thyroid stimulating hormone	6.92	3.99	4.91	5.27	
C-reactive protein	0.61	0.22	6.99	2.61	
Forced expiratory volume in one second	6.63	3.41	100	36.68	3
Drink area	0.11	0	0.07	0.06	
Smoke area	0.25	0	0	0.08	
Betel nut area	0	0	0	0.00	
Sport area	0.45	0.2	0.28	0.31	
Sleep time	0.14	0	0	0.05	
Marriage	0	0	1.99	0.66	

SGB: Stochastic gradient boosting; XGBoost: eXtreme gradient boosting; NAFLD: Non-alcoholic fatty liver.

Age was found to be the most important impact factor for eGFR. This is not surprising since renal function progress decreases with aging due to the reduction in the glomerular capillary plasma flow rate and its ultrafiltration coefficient. At the same time, decreased afferent arteriolar resistance directly increases capillary hydraulic pressure. These derangements will induce loss of renal mass, hyalinization, sclerotic glomeruli, and tubulointerstitial fibrosis[18].

Interestingly, Model 2 shows that the order of first four factors (LDH, UA, FEV1 and Alb) were identical in participants with or without NAFLD. The implications of this are detailed as follows.

LDH: LDH is an enzyme in cells which converts glucose to pyruvate under aerobic conditions and is then oxidized to acetyl-CoA. It enters the tricarboxylic acid cycle in mitochondria to generate energy. The lactate signaling axis (LDH-lactate-lactation) has been shown to have many physiological roles related to diseases[19,20]. LDH is determined in

Table 4 The average of the importance of risk factors derived from stochastic gradient boosting, random forest and extreme gradient boost, in NAFLD- (Model 1, including age)

Variables	SGB	XGBoost	Elasticnet	Average	Rank
Age	100	100	15.19	71.73	1
Income	0	0	1.41	0.47	
Body fat	3.69	1.05	4.15	2.96	
Systolic blood pressure	0.46	0.09	0.75	0.43	
Diastolic blood pressure	4.19	3.09	2.96	3.41	
Leukocyte	1.21	0.34	4.52	2.02	
Hemoglobin	4.81	1	11.57	5.79	
Platelets	2.61	1.06	0.2	1.29	
Fasting plasma glucose	0.42	0.21	0.17	0.27	
Total bilirubin	3.11	1.84	19.24	8.06	
Albumin	2.28	1.34	69.53	24.38	4
Globulin	0.42	0.12	3.03	1.19	
Alkaline Phosphatase	1.84	0.22	0.04	0.70	
Serum glutamic oxaloacetic transaminase	0.52	0	0	0.17	
Serum glutamic pyruvic transaminase	3.79	1.94	1.12	2.28	
Serum γ-glutamyl transpeptidase	1.16	0	0.38	0.51	
Lactate dehydrogenase	21.99	18.24	0.97	13.73	5
Uric acid	26.62	22.99	76.35	41.99	2
Triglyceride	1.59	0.31	0	0.63	
High density lipoprotein cholesterol	1.4	0.25	0.65	0.77	
Low density lipoprotein cholesterol	2.37	0.26	0.18	0.94	
Calcium	1.66	0.64	29.96	10.75	6
Phosphorus	2.05	2.07	10.98	5.03	
Thyroid stimulating hormone	11.86	8.69	5.02	8.52	
C-reactive protein	0.42	0	2.73	1.05	
Forced expiratory volume in one second	5.06	3.01	100	36.02	3
Drink area	0	0.25	0	0.08	
Smoke area	0.37	0.17	0.79	0.44	
Betel nut area	0	0	0	0.00	
Sport area	1.13	0.65	1.55	1.11	
Sleep time	0	0	0	0.00	
Marriage	0.13	0	5.51	1.88	

SGB: Stochastic gradient boosting; XGBoost: eXtreme gradient boosting; NAFLD: Non-alcoholic fatty liver.

different zones of normal kidneys and patients with impaired renal function. In 1968, Nielsen *et al*[21] reported higher LDH levels in patients with chronic renal failure, due to by changes of LDH synthesis in response to different types of kidney injury. The results of the present study indicate that, after removing age, LDH was the most important factor related to eGFR.

UA: UA is an end-product of purine metabolism in humans and is mostly excreted *via* the kidneys. Elevated UA is related to many diseases such as gout, diabetes, and metabolic syndrome[22-24]. It could also impair renal function and eventually lead to chronic renal disease *via* various mechanisms such as endothelial dysfunction, activation of renin-angiotensin system, inflammation, and oxidation stress[25-29]. In the present study, it is the second-most important impact factor in Model 2.

Table 5 The average of the importance of risk factors derived from stochastic gradient boosting, random forest and extreme gradient boost, in NAFLD+ (Model 2, excluding age)

Variables	SGB	XGBoost	Elasticnet	Average	Rank
Income	12.88	15.99	8.06	12.31	
Body fat	22.25	16.83	3.85	14.31	5
Systolic blood pressure	11.29	9.24	0.41	6.98	
Diastolic blood pressure	9.17	6.85	1.19	5.74	
Leukocyte	1.73	0.58	1.9	1.40	
Hemoglobin	2.57	0.31	4.27	2.38	
Platelets	17.83	14.87	0.32	11.01	
Fasting plasma glucose	9.72	6.71	0.2	5.54	
Total bilirubin	9.6	3.56	28.65	13.94	
Albumin	12.05	9.81	100	40.62	3
Globulin	1.85	1.25	10.62	4.57	
Alkaline Phosphatase	4.28	0.99	0.06	1.78	
Serum glutamic oxaloacetic transaminase	3.45	3.05	1.45	2.65	
Serum glutamic pyruvic transaminase	16.27	11.92	1.57	9.92	
Serum γ-glutamyl transpeptidase	1.14	0.65	0.28	0.69	
Lactate dehydrogenase	100	100	0.6	66.87	1
Uric acid	50.16	45.66	30.15	41.99	2
Triglyceride	6.23	3.56	0.14	3.31	
High density lipoprotein cholesterol	0.86	0.82	0.05	0.58	
Low density lipoprotein cholesterol	9.6	6.73	0.46	5.60	
Calcium	12.48	9.07	53.48	25.01	4
Phosphorus	0.79	1.87	1.48	1.38	
Thyroid stimulating hormone	16.42	11.23	2.23	9.96	
C-reactive protein	0	0	2.11	0.70	
Forced expiratory volume in one second	39.39	44.32	38.15	40.62	3
Drink area	0	0	0.26	0.09	
Smoke area	0	0	0	0.00	
Betel nut area	0	0	0	0.00	
Sport area	3.95	3.83	1.49	3.09	
Sleep time	0.86	0.5	4.04	1.80	
Marriage	0	0	2.38	0.79	

SGB: Stochastic gradient boosting; XGBoost: eXtreme gradient boosting; NAFLD: Non-alcoholic fatty liver.

FEV1: FEV1 is one of the key parameters for evaluating pulmonary function[30] and is the third-most important impact factor in the present study. The relationship between pulmonary function and renal function is well-established. For example, by using data from National Health and Nutrition Examination Survey between 2007 to 2012, Navaneethan *et al* showed that an estimated glomerular filtration rate (eGFR) < 60 mL/min/1.73 m^2 was associated with higher odds of obstructive lung function[31]. Yu *et al*[32] found that in both Australian and Chinese populations, subjects with lower FEV1 Levels generally had normal renal function. Our results are consistent with these findings.

Alb: Alb is one kind of protein in humans. It consists about half of total protein in the serum, and is used as a biomarker for many diseases. Decreased Alb levels are associated with cardiovascular disease, hear failure, and higher mortality rate[33-35]. Similar to pulmonary function, many studies have found that Alb levels are associated with renal function. For example, Lang *et al*[36] found that lower Alb levels were independently and significantly related to impaired renal function (0.11 mL/min/1.73 m^2 per year for each standard deviation fall in Alb) in the elderly Americans,

Table 6 The average of the importance of risk factors derived from stochastic gradient boosting, random forest and extreme gradient boost, in NAFLD- (Model 2, excluding age)

Variables	SGB	XGBoost	Elasticnet	Average	Rank
Income	2.49	1.95	1.61	2.02	
Body fat	7.57	2.68	1.48	3.91	
Systolic blood pressure	28.66	30.68	0.59	19.98	6
Diastolic blood pressure	18.44	21.96	1.73	14.04	
Leukocyte	9.07	5.26	6.63	6.99	
Hemoglobin	12.51	1.95	3.14	5.87	
Platelets	12.13	8.68	0.23	7.01	
Fasting plasma glucose	6.67	4.96	0.7	4.11	
Total bilirubin	9.07	5.16	3.37	5.87	
Albumin	21.95	20.16	100	47.37	4
Globulin	1.32	0	0	0.44	
Alkaline Phosphatase	2.75	0	0.02	0.92	
Serum glutamic oxaloacetic transaminase	4.06	3.15	1.59	2.93	
Serum glutamic pyruvic transaminase	9.09	6.48	1.74	5.77	
Serum γ-glutamyl transpeptidase	1.11	0	0.11	0.41	
Lactate dehydrogenase	100	100	0.63	66.88	1
Uric acid	66.92	63.24	36.68	55.61	2
Triglyceride	12.39	8	0.34	6.91	
High density lipoprotein cholesterol	2.64	0.67	0.17	1.16	
Low density lipoprotein cholesterol	14.18	10.11	0.51	8.27	
Calcium	3.82	2.4	21.04	9.09	
Phosphorus	5.65	6.52	0.1	4.09	
Thyroid stimulating hormone	34.32	24.16	2.56	20.35	5
C-reactive protein	2.68	0	0	0.89	
Forced expiratory volume in one second	61.02	64.4	26.93	50.78	3
Drink area	1.01	1.21	0	0.74	
Smoke area	2.24	1.22	0.85	1.44	
Betel nut area	0	0	0	0.00	
Sport area	13.32	11.44	2.46	9.07	
Sleep time	0.79	0.47	10.69	3.98	
Marriage	8.88	7.85	30.55	15.76	

SGB: Stochastic gradient boosting; XGBoost: eXtreme gradient boosting; NAFLD: Non-alcoholic fatty liver.

and a similar finding was made for Japanese[37]. Again, our results are consistent with these findings.

In our study, we classified our participants into groups of individuals with and without NAFLD. For both groups, Model 2 showed the same order of the four most important impact factors, diverging thereafter, with TSH and SBP the 5th and 6th ranked factors for NAFLD- as opposed to Ca and BF for NAFLD+. Obesity is one of the most important contributors to NAFLD[38], and thus it is reasonable that body fat levels are a key factor in determining such differences.

Thyroid function influences renal function either systemically, hemodynamically, or directly[39]. Impaired renal function could be noted in both hyper- and hypothyroidism. SBP is negatively related to eGFR[40]. Thus, for the NAFLD- group, our findings are consistent with previous results.

In the NAFLD+ group, both TSH and SBP became less important than Ca and BF. Subjects with lower plasma Ca levels have been found to be more susceptible to renal failure[41]. BF has been proposed as a more precise predictor than BMI for predicting cardiovascular diseases[42]. Increased BF has been shown to be significantly related to inflammation and

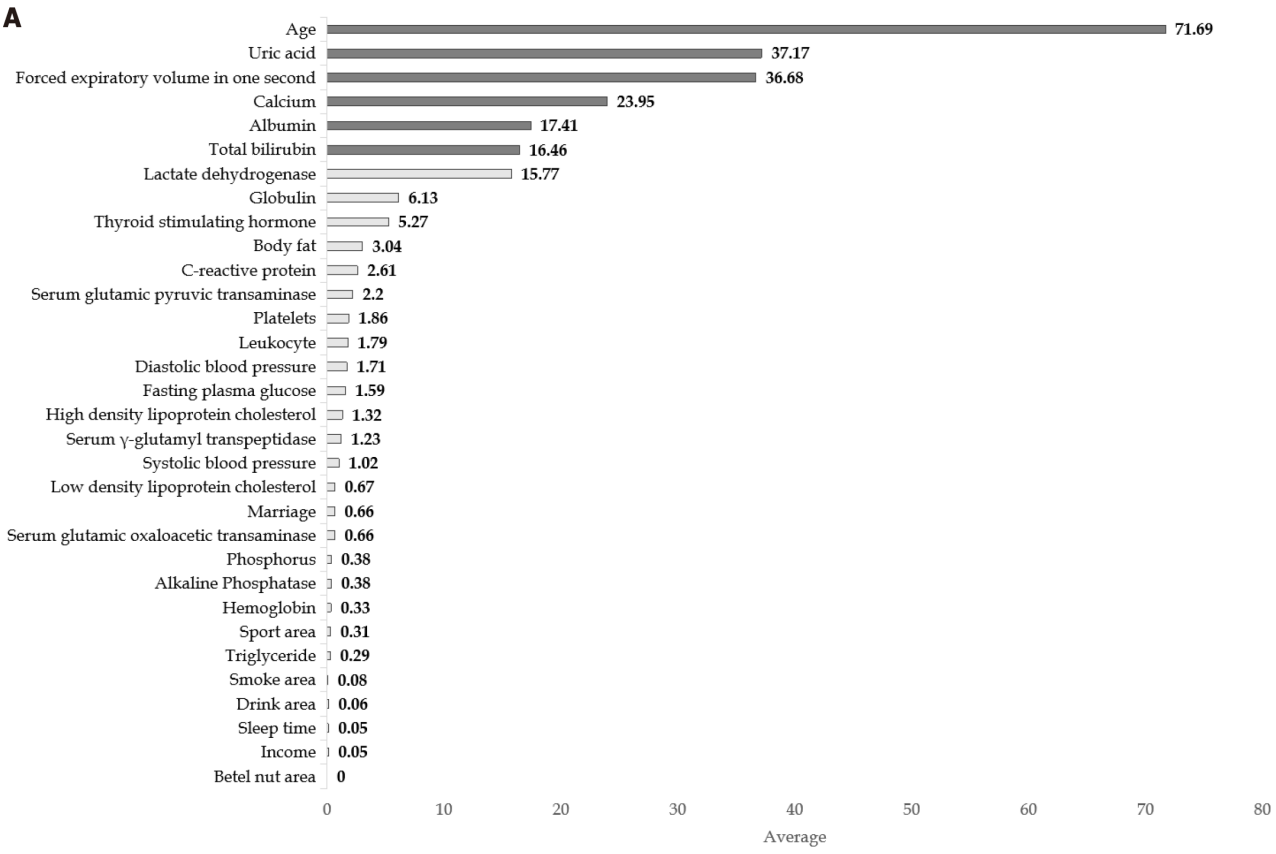
A
Age 71.69
Uric acid 37.17
Forced expiratory volume in one second 36.68
Calcium 23.95
Albumin 17.41
Total bilirubin 16.46
Lactate dehydrogenase 15.77
Globulin 6.13
Thyroid stimulating hormone 5.27
Body fat 3.04
C-reactive protein 2.61
Serum glutamic pyruvic transaminase 2.2
Platelets 1.86
Leukocyte 1.79
Diastolic blood pressure 1.71
Fasting plasma glucose 1.59
High density lipoprotein cholesterol 1.32
Serum γ-glutamyl transpeptidase 1.23
Systolic blood pressure 1.02
Low density lipoprotein cholesterol 0.67
Marriage 0.66
Serum glutamic oxaloacetic transaminase 0.66
Phosphorus 0.38
Alkaline Phosphatase 0.38
Hemoglobin 0.33
Sport area 0.31
Triglyceride 0.29
Smoke area 0.08
Drink area 0.06
Sleep time 0.05
Income 0.05
Betel nut area 0
0 10 20 30 40 50 60 70 80
Average

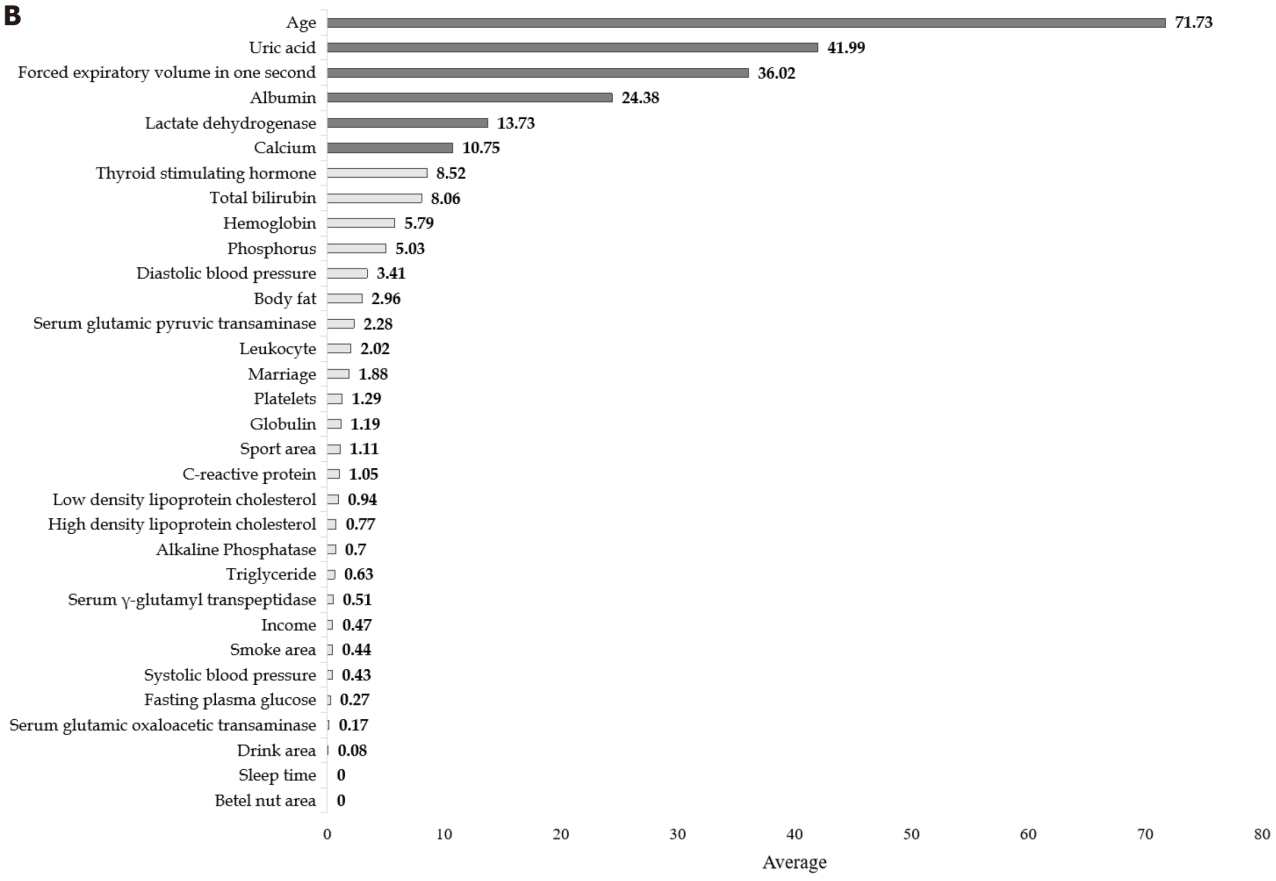
B
Age 71.73
Uric acid 41.99
Forced expiratory volume in one second 36.02
Albumin 24.38
Lactate dehydrogenase 13.73
Calcium 10.75
Thyroid stimulating hormone 8.52
Total bilirubin 8.06
Hemoglobin 5.79
Phosphorus 5.03
Diastolic blood pressure 3.41
Body fat 2.96
Serum glutamic pyruvic transaminase 2.28
Leukocyte 2.02
Marriage 1.88
Platelets 1.29
Globulin 1.19
Sport area 1.11
C-reactive protein 1.05
Low density lipoprotein cholesterol 0.94
High density lipoprotein cholesterol 0.77
Alkaline Phosphatase 0.7
Triglyceride 0.63
Serum γ-glutamyl transpeptidase 0.51
Income 0.47
Smoke area 0.44
Systolic blood pressure 0.43
Fasting plasma glucose 0.27
Serum glutamic oxaloacetic transaminase 0.17
Drink area 0.08
Sleep time 0
Betel nut area 0
0 10 20 30 40 50 60 70 80
Average

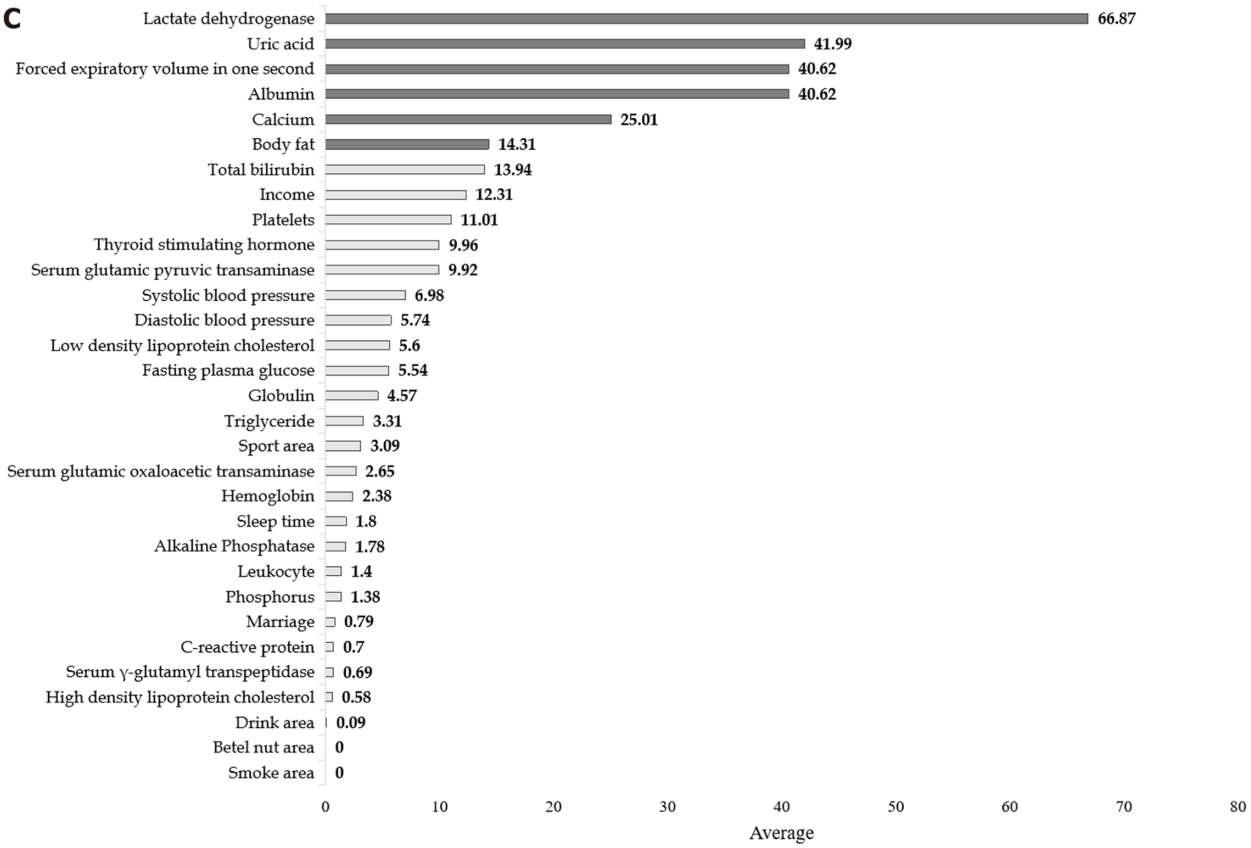

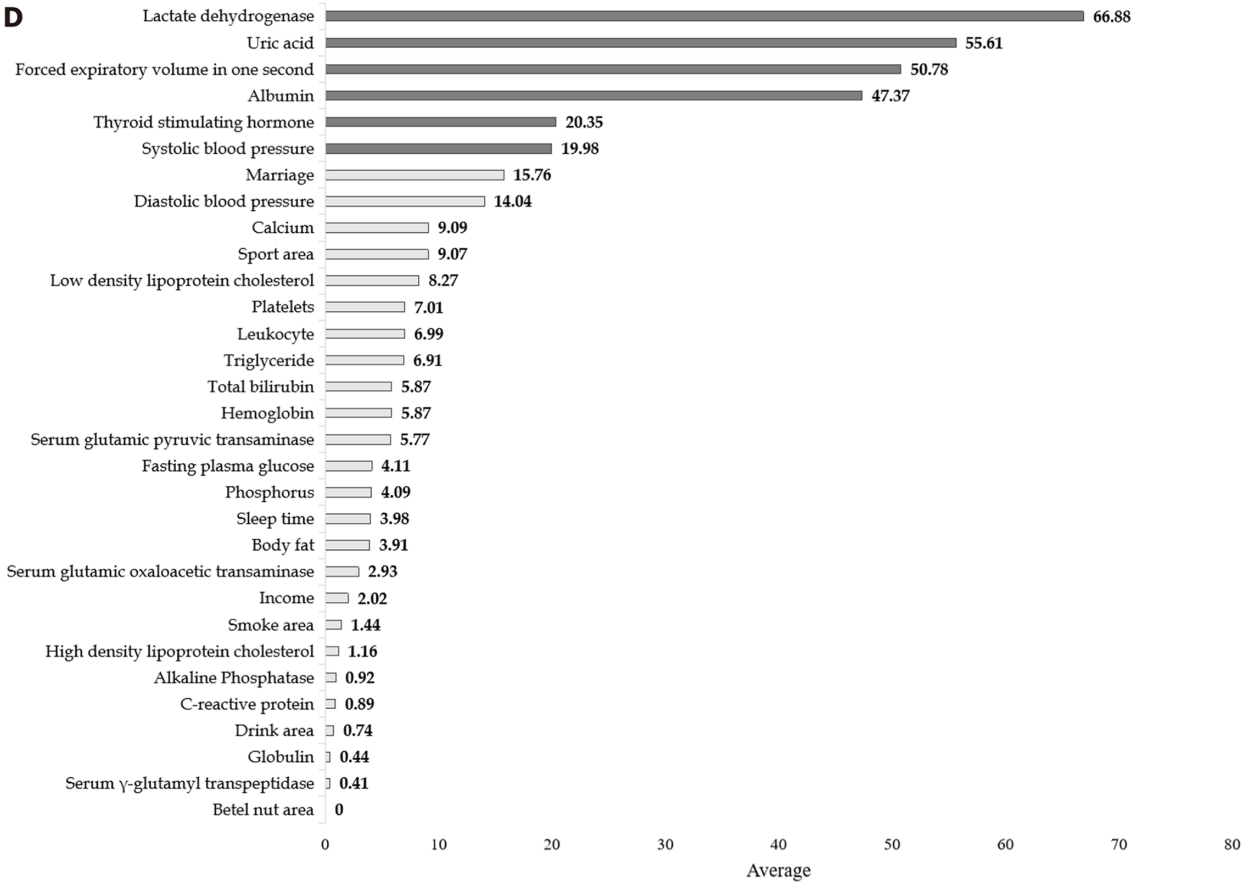

Figure 4 All the orders of the ranks of percentage importance were the same as the results in the tables. A: The average of the risk factors derived from three different machine learning methods (Model 1, NAFLD+ with age); B: The ranks of the risk factors derived from three different machine learning methods (Model 1, NAFLD- with age); C: The ranks of the risk factors derived from three different machine learning methods (Model 2, NAFLD+ without age); D: The ranks of the risk factors derived from three different machine learning methods (Model 2, NAFLD- without age). NAFLD: Non-alcoholic fatty liver.

deterioration of renal function[43]. The increased importance of both Ca and BF indicate that fat levels in the human body impact the relative impact of these factors on renal function. In subjects with higher BF levels, Ca and BF become more important and should be considered differently in terms of their relative influence on renal function.

The present study is subject to certain limitations. First, its cross-sectional nature restricts understanding of causality. A longitudinal design study would provide greater insight into causes and consequences. Second, study participants were restricted to women due to their distinct pathophysiology characteristics. Future work will replicate the study with a male cohort. Finally, the present study only considers ethnic Chinese participants, thus caution should be taken in extrapolating the findings to other ethnic groups.

CONCLUSION

In conclusion, eGFR levels were lower in the NAFLD+ group compared to the NAFLD- group. Age was found to be the most important single factor affecting eGFR. After removing age, LDH, UA, FEV1 and Alb were four leading impact factors in both groups, followed by TSH and SBP for the NAFLD- group, and Ca and BF for the NAFLD+ group.

FOOTNOTES

Author contributions: Chen IC participated in study design and oversight; Chou LJ participated in study design and data collection; Huang SC participated in data collection and data analysis; Lee SS and Chu TW both participated in data analysis and drafted the manuscript. All authors read and approved the final manuscript.

Supported by the Kaohsiung Armed Forces General Hospital.

Institutional review board statement: Ethics approval and participant consent: The research plan was reviewed and approved by the Institutional Review Board of Kaohsiung Armed Forces General Hospital on July 1, 2023 prior to the start of the study.

Informed consent statement: All the authors consent to the publication.

Conflict-of-interest statement: All authors have no conflicts of interest.

Data sharing statement: Availability of data and materials: Data available on request due to privacy/ethical restrictions.

Country/Territory of origin: Taiwan

ORCID number: Ta-Wei Chu 0000-0002-7629-7854; Shang-Sen Lee 0000-0003-4103-113X.

S-Editor: Liu JH
L-Editor: A
P-Editor: Zheng XM

REFERENCES

1 **Ansari S**, Haboubi H, Haboubi N. Adult obesity complications: challenges and clinical impact. *Ther Adv Endocrinol Metab* 2020; **11**: 2042018820934955 [PMID: 32612803 DOI: 10.1177/2042018820934955]
2 **Liu Q**, Bengmark S, Qu S. The role of hepatic fat accumulation in pathogenesis of non-alcoholic fatty liver disease (NAFLD). *Lipids Health Dis* 2010; **9**: 42 [PMID: 20426802 DOI: 10.1186/1476-511X-9-42]
3 **Fazel Y**, Koenig AB, Sayiner M, Goodman ZD, Younossi ZM. Epidemiology and natural history of non-alcoholic fatty liver disease. *Metabolism* 2016; **65**: 1017-1025 [PMID: 26997539 DOI: 10.1016/j.metabol.2016.01.012]
4 **Loomba R**, Friedman SL, Shulman GI. Mechanisms and disease consequences of nonalcoholic fatty liver disease. *Cell* 2021; **184**: 2537-2564 [PMID: 33989548 DOI: 10.1016/j.cell.2021.04.015]
5 **Targher G**, Chonchol MB, Byrne CD. CKD and nonalcoholic fatty liver disease. *Am J Kidney Dis* 2014; **64**: 638-652 [PMID: 25085644 DOI: 10.1053/j.ajkd.2014.05.019]
6 **Kiapidou S**, Liava C, Kalogirou M, Akriviadis E, Sinakos E. Chronic kidney disease in patients with non-alcoholic fatty liver disease: What the Hepatologist should know? *Ann Hepatol* 2020; **19**: 134-144 [PMID: 31606352 DOI: 10.1016/j.aohep.2019.07.013]
7 **Yasui K**, Sumida Y, Mori Y, Mitsuyoshi H, Minami M, Itoh Y, Kanemasa K, Matsubara H, Okanoue T, Yoshikawa T. Nonalcoholic steatohepatitis and increased risk of chronic kidney disease. *Metabolism* 2011; **60**: 735-739 [PMID: 20817213 DOI: 10.1016/j.metabol.2010.07.022]
8 **Chalasani N**, Younossi Z, Lavine JE, Diehl AM, Brunt EM, Cusi K, Charlton M, Sanyal AJ; American Gastroenterological Association;

American Association for the Study of Liver Diseases; American College of Gastroenterologyh. The diagnosis and management of non-alcoholic fatty liver disease: practice guideline by the American Gastroenterological Association, American Association for the Study of Liver Diseases, and American College of Gastroenterology. *Gastroenterology* 2012; **142**: 1592-1609 [PMID: 22656328 DOI: 10.1053/j.gastro.2012.04.001]

9 **Cao Y**, Du Y, Jia W, Ding J, Yuan J, Zhang H, Zhang X, Tao K, Yang Z. Identification of biomarkers for the diagnosis of chronic kidney disease (CKD) with non-alcoholic fatty liver disease (NAFLD) by bioinformatics analysis and machine learning. *Front Endocrinol (Lausanne)* 2023; **14**: 1125829 [PMID: 36923221 DOI: 10.3389/fendo.2023.1125829]

10 **Yuk H**, Gim J, Min JK, Yun J, Heo TY. Artificial Intelligence-based Prediction of Diabetes and Prediabetes Using Health Checkup Data in Korea. *Appl Artif Intell* 2022; **36** [DOI: 10.1080/08839514.2022.2145644]

11 **Wu X**, Tsai SP, Tsao CK, Chiu ML, Tsai MK, Lu PJ, Lee JH, Chen CH, Wen C, Chang SS, Hsu CY, Wen CP. Cohort Profile: The Taiwan MJ Cohort: half a million Chinese with repeated health surveillance data. *Int J Epidemiol* 2017; **46**: 1744-1744g [PMID: 28204597 DOI: 10.1093/ije/dyw282]

12 **Foundation MHR**. The introduction of MJ health database. MJ Health Research Foundation Technical Report, MJHRF-TR-01. 2016

13 **Wu CZ**, Huang LY, Chen FY, Kuo CH, Yeih DF. Using Machine Learning to Predict Abnormal Carotid Intima-Media Thickness in Type 2 Diabetes. *Diagnostics (Basel)* 2023; **13** [PMID: 37296685 DOI: 10.3390/diagnostics13111834]

14 **Friedman JH**. Greedy function approximation: A gradient boosting machine. *Ann Stat* 2001; **29**: 1189-1232 [DOI: 10.1214/aos/1013203451]

15 **Chen T**, Guestrin C. XGBoost: A Scalable Tree Boosting System. Proceedings of the 22nd ACM SIGKDD International Conference on Knowledge Discovery and Data Mining; San Francisco, California, USA: Association for Computing Machinery; 2016; 785-794 [DOI: 10.1145/2939672.2939785]

16 **Torlay L**, Perrone-Bertolotti M, Thomas E, Baciu M. Machine learning-XGBoost analysis of language networks to classify patients with epilepsy. *Brain Inform* 2017; **4**: 159-169 [PMID: 28434153 DOI: 10.1007/s40708-017-0065-7]

17 **Tay JK**, Narasimhan B, Hastie T. Elastic Net Regularization Paths for All Generalized Linear Models. *J Stat Softw* 2023; **106** [PMID: 37138589 DOI: 10.18637/jss.v106.i01]

18 **Weinstein JR**, Anderson S. The aging kidney: physiological changes. *Adv Chronic Kidney Dis* 2010; **17**: 302-307 [PMID: 20610357 DOI: 10.1053/j.ackd.2010.05.002]

19 **Certo M**, Tsai CH, Pucino V, Ho PC, Mauro C. Lactate modulation of immune responses in inflammatory versus tumour microenvironments. *Nat Rev Immunol* 2021; **21**: 151-161 [PMID: 32839570 DOI: 10.1038/s41577-020-0406-2]

20 **Rabinowitz JD**, Enerbäck S. Lactate: the ugly duckling of energy metabolism. *Nat Metab* 2020; **2**: 566-571 [PMID: 32694798 DOI: 10.1038/s42255-020-0243-4]

21 **Nielsen VK**, Kemp E, Laursen T. Lactic dehydrogenase in kidney tissue and renal disease. Adaptive change of the synthesis in acute failure. *Acta Med Scand* 1968; **184**: 109-119 [PMID: 5703958 DOI: 10.1111/j.0954-6820.1968.tb02430.x]

22 **Delacour JL**, Floriot C, Wagschal G, Daoudal P, Chambers R, Xuan PB. Non-cardiac pulmonary edema following intravenous contrast injection. *Intensive Care Med* 1988; **15**: 49-50 [PMID: 3230202 DOI: 10.1007/BF00255637]

23 **Cirillo P**, Sato W, Reungjui S, Heinig M, Gersch M, Sautin Y, Nakagawa T, Johnson RJ. Uric acid, the metabolic syndrome, and renal disease. *J Am Soc Nephrol* 2006; **17**: S165-S168 [PMID: 17130256 DOI: 10.1681/ASN.2006080909]

24 **Nakanishi N**, Okamoto M, Yoshida H, Matsuo Y, Suzuki K, Tatara K. Serum uric acid and risk for development of hypertension and impaired fasting glucose or Type II diabetes in Japanese male office workers. *Eur J Epidemiol* 2003; **18**: 523-530 [PMID: 12908717 DOI: 10.1023/A:1024600905574]

25 **Mazzali M**, Hughes J, Kim YG, Jefferson JA, Kang DH, Gordon KL, Lan HY, Kivlighn S, Johnson RJ. Elevated uric acid increases blood pressure in the rat by a novel crystal-independent mechanism. *Hypertension* 2001; **38**: 1101-1106 [PMID: 11711505 DOI: 10.1161/hy1101.092839]

26 **Sánchez-Lozada LG**, Lanaspa MA, Cristóbal-García M, García-Arroyo F, Soto V, Cruz-Robles D, Nakagawa T, Yu MA, Kang DH, Johnson RJ. Uric acid-induced endothelial dysfunction is associated with mitochondrial alterations and decreased intracellular ATP concentrations. *Nephron Exp Nephrol* 2012; **121**: e71-e78 [PMID: 23235493 DOI: 10.1159/000345509]

27 **Rabadi MM**, Kuo MC, Ghaly T, Rabadi SM, Weber M, Goligorsky MS, Ratliff BB. Interaction between uric acid and HMGB1 translocation and release from endothelial cells. *Am J Physiol Renal Physiol* 2012; **302**: F730-F741 [PMID: 22189943 DOI: 10.1152/ajprenal.00520.2011]

28 **Kurts C**. A crystal-clear mechanism of chronic kidney disease. *Kidney Int* 2013; **84**: 859-861 [PMID: 24172728 DOI: 10.1038/ki.2013.251]

29 **Corry DB**, Eslami P, Yamamoto K, Nyby MD, Makino H, Tuck ML. Uric acid stimulates vascular smooth muscle cell proliferation and oxidative stress *via* the vascular renin-angiotensin system. *J Hypertens* 2008; **26**: 269-275 [PMID: 18192841 DOI: 10.1097/HJH.0b013e3282f240bf]

30 **David S**, Edwards CW. Forced Expiratory Volume. [Updated 2022 Aug 8]. In: StatPearls [Internet]. Treasure Island (FL): StatPearls Publishing; 2023 Jan-. Available from: https://www.ncbi.nlm.nih.gov/books/NBK540970/

31 **Navaneethan SD**, Mandayam S, Arrigain S, Rahman M, Winkelmayer WC, Schold JD. Obstructive and Restrictive Lung Function Measures and CKD: National Health and Nutrition Examination Survey (NHANES) 2007-2012. *Am J Kidney Dis* 2016; **68**: 414-421 [PMID: 27130720 DOI: 10.1053/j.ajkd.2016.03.415]

32 **Yu D**, Chen T, Cai Y, Zhao Z, Simmons D. Association between pulmonary function and renal function: findings from China and Australia. *BMC Nephrol* 2017; **18**: 143 [PMID: 28460631 DOI: 10.1186/s12882-017-0565-y]

33 **Lang J**, Scherzer R, Weekley CC, Tien PC, Grunfeld C, Shlipak MG. Serum albumin and short-term risk for mortality and cardiovascular disease among HIV-infected veterans. *AIDS* 2013; **27**: 1339-1343 [PMID: 23343914 DOI: 10.1097/QAD.0b013e32835f1dd6]

34 **Goldwasser P**, Feldman J. Association of serum albumin and mortality risk. *J Clin Epidemiol* 1997; **50**: 693-703 [PMID: 9250267 DOI: 10.1016/S0895-4356(97)00015-2]

35 **Feldman JG**, Gange SJ, Bacchetti P, Cohen M, Young M, Squires KE, Williams C, Goldwasser P, Anastos K. Serum albumin is a powerful predictor of survival among HIV-1-infected women. *J Acquir Immune Defic Syndr* 2003; **33**: 66-73 [PMID: 12792357 DOI: 10.1097/00126334-200305010-00010]

36 **Lang J**, Katz R, Ix JH, Gutierrez OM, Peralta CA, Parikh CR, Satterfield S, Petrovic S, Devarajan P, Bennett M, Fried LF, Cummings SR, Sarnak MJ, Shlipak MG. Association of serum albumin levels with kidney function decline and incident chronic kidney disease in elders. *Nephrol Dial Transplant* 2018; **33**: 986-992 [PMID: 28992097 DOI: 10.1093/ndt/gfx229]

37 **Cheng T**, Wang X, Han Y, Hao J, Hu H, Hao L. The level of serum albumin is associated with renal prognosis and renal function decline in patients with chronic kidney disease. *BMC Nephrol* 2023; **24**: 57 [PMID: 36922779 DOI: 10.1186/s12882-023-03110-8]

38 National Guideline C. National Institute for Health and Care Excellence: Guidelines. Non-Alcoholic Fatty Liver Disease: Assessment and Management. London: National Institute for Health and Care Excellence (NICE) Copyright © National Institute for Health and Care Excellence, 2016

39 **Iglesias P**, Bajo MA, Selgas R, Díez JJ. Thyroid dysfunction and kidney disease: An update. *Rev Endocr Metab Disord* 2017; **18**: 131-144 [PMID: 27864708 DOI: 10.1007/s11154-016-9395-7]

40 **Peralta CA**, Whooley MA, Ix JH, Shlipak MG. Kidney function and systolic blood pressure new insights from cystatin C: data from the Heart and Soul Study. *Am J Hypertens* 2006; **19**: 939-946 [PMID: 16942937 DOI: 10.1016/j.amjhyper.2006.02.007]

41 Kidney Failure Risk Factor: Serum Calcium. Available from: https://www.kidney.org/content/kidney-failure-risk-factor-serum-calcium.

42 **Zeng Q**, Dong SY, Sun XN, Xie J, Cui Y. Percent body fat is a better predictor of cardiovascular risk factors than body mass index. *Braz J Med Biol Res* 2012; **45**: 591-600 [PMID: 22510779 DOI: 10.1590/S0100-879X2012007500059]

43 **Chen YY**, Fang WH, Wang CC, Kao TW, Chang YW, Yang HF, Wu CJ, Sun YS, Chen WL. Changes of Percent Body Fat as a Useful Surrogate for Risk of Declined Renal Function. *Sci Rep* 2018; **8**: 17289 [PMID: 30470784 DOI: 10.1038/s41598-018-35601-2]

World Journal of Clinical Cases

Submit a Manuscript: https://www.f6publishing.com

World J Clin Cases 2024 May 26; 12(15): 2522-2528

DOI: 10.12998/wjcc.v12.i15.2522

ISSN 2307-8960 (online)

ORIGINAL ARTICLE

Retrospective Study

Effect of three-volt moxibustion with helium-neon laser irradiation on quality of care in patients with lumbar radiculopathy spondylosis

Xiu-Kun Ji, Jian Li

Specialty type: Medicine, research and experimental

Provenance and peer review: Unsolicited article; Externally peer reviewed.

Peer-review model: Single blind

Peer-review report's classification

Scientific Quality: Grade B
Novelty: Grade B
Creativity or Innovation: Grade B
Scientific Significance: Grade B

P-Reviewer: Ampollini L, Italy

Received: February 20, 2024
Revised: March 14, 2024
Accepted: April 7, 2024
Published online: May 26, 2024

Xiu-Kun Ji, Department of Traditional Chinese Medicine, The Second Hospital of Heilongjiang Province, Harbin 150028, Heilongjiang Province, China

Jian Li, Departments of Four Neurology, The Second Hospital of Heilongjiang Province, Harbin 150028, Heilongjiang Province, China

Corresponding author: Jian Li, MNurs, Nurse, Departments of Four Neurology, The Second Hospital of Heilongjiang Province, No. 209 Jiangdu Street, Songbei District, Harbin 150028, Heilongjiang Province, China. man55184141700730@163.com

Abstract

BACKGROUND

Lumbar radiculopathy spondylosis is a relatively common orthopedic disease with a high incidence rate. It most commonly occurs in the lumbar 4-5 and lumbar 5-sacral 1 vertebrae, which account for approximately 95% of cases. It mostly occurs in people aged 30-50 years old and greatly affects their quality of life.

AIM

To determine the effect of triple-voltage acupuncture combined with helium-neon laser irradiation on the quality of care and improvement of symptoms in patients with lumbar radiculopathy spondylolisthesis.

METHODS

In this study, we selected 120 patients with lumbar radiculopathy spondylosis who were treated at our hospital between June 2019 to June 2020. The patients were divided into control and observation groups according to the random number table method, with 60 patients in each group. Patients in the observation group were treated with three-volt moxibustion combined with helium-neon laser irradiation, and those in the control group were treated with lumbar traction. After 1 month of treatment, the lumbar pain scores, lumbar spine motor functions, clinical treatment effects, and nursing satisfaction of the two groups were compared.

RESULTS

The results showed that acupuncture combined with laser irradiation significantly improved the patients' clinical symptoms, *i.e.*, reduced their low back pain, significantly lower numerical rating scale pain scores in the observation group than in the control group, and better lumbar spine motility than in the control

group, compared to lumbar traction. In addition, they were cared for. The treatment effectiveness rate of the observation group was 95.5%, which was significantly higher than that of the control group (81.67%). Satisfaction with care was higher than 90 points in both groups, but the difference was not statistically significant.

CONCLUSION
Our study provides a clinical rationale for the future treatment of patients with lumbar spine disease. However, further extensive research is needed for validation.

Key Words: Moxibustion; Laser irradiation; Clinical rationale; Lumbar spine; Three-volt moxibustion

Core tip: This study investigated the effects of three-volt moxibustion combined with helium-neon laser irradiation on the quality of care and symptom improvement in patients with lumbar radiculopathy-type cervical spondylosis. The results showed that this therapy can effectively improve the quality of care and significantly relieve patients' symptoms, providing a new effective means for the treatment of cervical spondylosis.

Citation: Ji XK, Li J. Effect of three-volt moxibustion with helium-neon laser irradiation on quality of care in patients with lumbar radiculopathy spondylosis. *World J Clin Cases* 2024; 12(15): 2522-2528
URL: https://www.wjgnet.com/2307-8960/full/v12/i15/2522.htm
DOI: https://dx.doi.org/10.12998/wjcc.v12.i15.2522

INTRODUCTION

Lumbar radiculopathy spondylosis is a prevalent spinal disorder that significantly affects patients' quality of life and their physical and mental well-being[1]. The primary symptoms of this condition include lower back pain and sciatica, which, in extreme cases, can lead to restrictions in patient activity[2]. Although the exact prevalence of lumbar radiculopathy spondylosis is unknown, it is often associated with conditions such as herniated lumbar discs, lumbar spinal stenosis, and sciatica[3]. This disease also has a profound impact on the patients' quality of life and physical and mental health. Currently, a range of treatment methods is available for lumbar radiculopathy spondylosis, including medication, physiotherapy, traction, and acupuncture. However, these conventional treatments may not be effective for some patients, necessitating the exploration of new treatment options to improve overall treatment outcomes[3].

In recent years, three-volt moxibustion (TCM) and helium-neon laser irradiation have received increasing attention from the medical community as traditional Chinese medicine and physiotherapy methods[4]. TCM can relieve pain and improve symptoms by stimulating acupuncture points and adjusting the flow of qi and blood[5]. Helium-neon laser irradiation, with its anti-inflammatory, analgesic, and tissue repair-promoting effects, has been widely used to treat various pain and inflammatory diseases[6]. The combined application of these two methods allows for fully utilizing their respective therapeutic advantages, and further improving the therapeutic effects in nerve root-type lumbar spondylosis. However, there is a lack of clinical applications using these two combined approaches in patients with lumbar radiculopathy spondylosis at this stage of research. Several studies have shown that Chinese medicine has achieved remarkable results in the treatment of lumbar radiculopathy spondylosis[7]. TCM care methods such as acupuncture, tuina, Chinese herbs, and rehabilitation training can effectively relieve pain, improve cervical spine mobility, and enhance quality of life. For example, a randomized controlled trial showed that acupuncture can effectively relieve pain and numbness in patients with lumbar radiculopathy spondylosis and is more effective than conventional drug treatment[8].

This study aimed to investigate the effects of TCM combined with helium-neon laser irradiation on the quality of care and symptom improvement in patients with lumbar radiculopathy and spondylosis. In this randomized controlled study, we analyzed and compared the effects of three-voxel moxibustion combined with helium-neon laser irradiation in the treatment of lumbar radiculopathy spondylolisthesis and its effect on patients' quality of life. The results of this study will provide clinicians with new therapeutic options that will help improve the therapeutic effects and quality of life of patients with lumbar radiculopathy and spondylosis.

MATERIALS AND METHODS

Research participants

In this study, we enrolled 120 patients with lumbar radiculopathy spondylosis who received treatment at our hospital between June 2019 and June 2020. The patients were divided into control and experimental groups according to the random number table method, with 60 patients in each group. The study subjects had lumbar radiculopathy spondylosis,

and the inclusion criteria for the study subjects were as follows: (1) Presence of symptoms such as low back pain and lower limb numbness; (2) Herniated lumbar intervertebral discs, degeneration of the intervertebral joints, and other factors leading to nerve root compression; and (3) The patient was conscious and could answer the medical staff's questions independently. The exclusion criteria were as follows: (1) Non-nerve root lumbar spondylosis, such as spinal cord lumbar spondylosis; (2) Severe lumbar spine lesions that cannot be treated with lumbar traction or other treatments; and (3) Combination of other diseases such as stroke and diabetes. The diagnostic criteria for lumbar radiculopathy spondylosis are as follows: (1) Lumbar pain and leg pain radiating along the distribution area of the nerve root aggravated by increasing abdominal pressure; (2) Leg numbness and weakness; (3) Sensory disturbances (widespread or limited), a positive straight leg raising test, limited forward flexion and backward extension, lumbar pain due to lumbar scoliosis, paraspinal tenderness, decreased muscle strength, and decreased or absent Achilles tendon reflexes; and (4) Imaging as a diagnostic tool for lumbar nerve root cervical spondylosis. Magnetic resonance imaging (MRI) can be regarded as the most suitable noninvasive means of examination for lumbar disc herniation at this stage, with a positive rate higher than that of computed tomography. MRI can accurately show spinal cord and nerve root compression and edema or degeneration, and has a good display of spatial microstructure.

In the control group, there were 32 males and 28 females, aged 45-70 years (mean 58.3 ± 6.7 years old), and in the observation group, there were 34 males and 26 females, aged 44-72 years (mean 59.1 ± 7.3 years old). There were no statistically significant differences between the two groups in terms of sex, age, or illness ($P > 0.05$) (Table 1).

Research design

This was a randomized controlled study in which 120 subjects were equally divided into an observation group and a control group. The observation group were treated with TCM combined with a helium-neon laser irradiation care mode, whereas the control group were treated with lumbar traction care.

Observation group nursing mode: TCM combined with helium-neon laser irradiation The TCM position tonifies Yang and drives away cold and overall regulation. One Qihuang moxibustion point was placed on the Da vertebrae, life gate, kidney Yu, Changqiang, danzhong, Guanyuan, foot Sanli, Sanyinjiao, Yongquan for 25 min once a day for 20 d. An interval of 3-5 d was established before performing another course of treatment. A JH30C laser therapeutic instrument was used with a wavelength of 632.8 mm, output power of 40mV, and spot diameter of 2 cm for the irradiation of pressure pain points. In addition, the end of the He-Ne laser fiber was close to the patients' Huanjiao, Lumbar Yangguan, Kidney Yu, Vital Gate, Huizhong, Chengshan, and the key points for acupoint irradiation, and each acupoint was irradiated for 5 min once a day for 20 d. Another course of treatment was administered every to 3-5 d.

Control group: Lumbar traction nursing mode. Lumbar traction is commonly non-surgical treatment used to treat patients with lumbar disc herniation as a form of rehabilitation treatment, as well as lumbar spinal stenosis. This finding is of great significance for the care of patients with lumbar traction. This study focuses on patient care using traction beds. In patients undergoing lumbar traction, are usually placed in the supine or prone position, with the upper half of the body for the corresponding fixed, fixed in the lower limbs of the affected limbs to perform the corresponding skin traction, such as the application of a skin traction fixed band, fixed in the fixed band at the end of the fixed band, that is, the corner of the bed position, placed in the corresponding weight.

Measure indicators

Assessment of the level of lower back pain: This study focused on the assessment of low back pain in patients using the numerical rating scale (NRS), a commonly used pain rating scale that uses numbers from to 0-10 to represent different levels of pain, with 0 indicating no pain and 10 indicating the most severe pain. Patients can choose an appropriate number to represent their level of pain.

Functional assessment of lumbar movement: The assessment of lumbar range of motion mainly refers to the range of motion of the lumbar region when performing movements such as forward flexion, backward extension, lateral bending, and rotation. In this study, lumbar spine function was mainly assessed using the Japanese Orthopedic Association scores (JOA) scoring standard[9]. The highest JOA score was 29, and the lowest was 0. A higher score indicated a better functional status of the lumbar spine, and a lower score indicated more obvious dysfunction. The JOA is divided into 4 grades, with 25-29 as excellent, 16-24 as good, 10-15 as moderate; and < 10 as poor.

Clinical improvement in the patients: In a comparison of treatment efficiency between the two groups, based on the disappearance of pain and recovery of motor function. Cases wherein pain completely disappeared, motor function completely recovered as significantly effective, pain basically disappeared, or motor function basically recovered was considered "effective". Whereas, cases where pain had not disappeared or was aggravated, motor function had not been restored, or motor limitation was aggravated were considered "ineffective". The total effective rate of the treatment = (significantly effective + effective)/total number of cases × 100%.

Satisfaction with care: In this study, nursing care satisfaction was formulated based on the content of daily nursing care for lumbar diseases, and each question was rated using a 5-level scale, such as "very satisfied", "satisfied", "average", "dissatisfied", and "very dissatisfied", with a total of 20 questions and a total score of 100, with the higher score representing a higher satisfaction of the patients and their families with the nursing care model.

Table 1 Basic information about the study population

		Control	Observation	t/χ^2	*P* value
Gender	Male	32	34	1.53	0.097
	Female	28	26		
Aged		58.3 ± 6.7	59.1 ± 7.3	1.64	0.061
Duration of illness (month)		6.5 ± 3.3	7.0 ± 2.5	1.21	0.075
Take care of oneself	Yes	49	47	1.79	0.057
	No	11	13	-	-

Statistical analysis

A database was set up, and the data were entered using Epidata after double-checking. SPSS software (version 26.0) was used to analyze the data. Count data were analyzed using the χ^2 test. Measurement data were expressed as mean ± SD. The two groups before and after the intervention were compared using repeated-measures ANOVA, the two groups were compared using the two independent samples *t*-test, and the two groups within the groups were compared using the least significant difference procedure. Statistical significance was set at $P < 0.05$.

RESULTS

Differences in patients' low back pain scores before and after treatment

Comparing and analyzing the pain levels of the two groups of patients before and after treatment, the results showed that after clinical treatment and care, the NRS pain scores of the patients in the observation and control groups decreased, and there was a significant difference in the pain scores between the observation and control groups (Table 2).

Assessment of lumbar spine motor function before and after patient treatment

Comparing and analyzing the lumbar spine motor function of the two groups of patients before and after treatment, the results showed that after clinical treatment and care, the lumbar spine function of the patients in the observation and control groups improved, and there was a significant difference in the lumbar spine motor ability between the observation and control groups (Table 3).

Comparison of clinical outcomes after treatment between the two groups of patients

The clinical treatment efficiency of the two groups was analyzed and compared, and it was found that the clinical treatment efficiency of the observation group was 95.5% and that of the control group was 81.67%, with a significant difference between the two groups ($P < 0.05$) (Table 4).

Patient care satisfaction scores in both groups

The satisfaction scores of the two groups of patients for the nursing care model were collected, and the results showed that the nursing care satisfaction scores of the two groups were above 90, and there was no significant difference between the scores. Therefore, it was concluded that the nursing care model of three-voxel moxibustion combined with helium-neon laser irradiation was better accepted by patients with lumbar radiculopathy spondylolisthesis (Table 5).

DISCUSSION

This study to explore the TCM combination of helium neon laser irradiation of nerve root lumbar disease nursing quality and the impact of the improvement of clinical symptoms, using randomized controlled study analysis, the results showed that compared to waist traction nursing, acupuncture combined laser irradiation significantly improved the clinical symptoms of patients. Moreover, they also received satisfactory care. The treatment effectiveness rate in the observation group was 95.5%, which was significantly higher than that in the control group (81.67%). Patient satisfaction with nursing in both groups was higher than 90 points; however, the difference was not statistically significant.

Pain is a common symptom of a wide range of diseases and conditions, and has a significant impact on the quality of life and health of patients. Therefore, selecting effective treatments to relieve pain is necessary[10]. The results of this study showed that acupuncture and laser irradiation were effective in relieving pain and were superior to lumbar traction. Acupuncture and laser irradiation may relieve pain by regulating the circulation of qi and blood in the body[11, 12], unblocking the meridians, and promoting inflammation. In addition, acupuncture and laser irradiation have the advantages of ease of operation, safety, reliability, and few adverse effects. In a previous study of patients with low back pain, acupuncture was found to be effective in reducing musculoskeletal pain and improving patients' quality of life. In the present study, laser irradiation may have significantly enhanced the effects of acupuncture, and the combination of

Table 2 Differences in low back pain scores before and after patient treatment

	NRS		*H/t*	*P* value
	Before	After		
Observation group	7.83 ± 0.55	1.74 ± 0.48a	19.891	0
Control group	7.65 ± 0.44	3.14 ± 0.52a	14.214	0
H/t	-0.134	3.066	-	-
P value	0.893	0.002	-	-

[a]*P* < 0.05.
H: Kruskal-Wallis *H* test; NRS: Numerical rating scale.

Table 3 Differences in low back Japanese Orthopedic Association scores before and after patient treatment

	Japanese Orthopedic Association scores		*H/t*	*P* value
	Before	After		
Observation group	6.73 ± 0.63	18.26 ± 0.61a	12.768	0
Control group	5.94 ± 0.23	14.23 ± 0.42a	11.356	0
H/t	0.789	7.875	-	-
P value	453	0	-	-

[a]*P* < 0.05.
H: Kruskal-Wallis *H* test.

Table 4 Comparative analysis of the clinical outcomes of the two groups of patients, *n* (%)

Group	*n*	Significantly effective	Effective	Ineffective	Effective rate
Control group)	60	32 (53.3)	25 (41.67)	3 (0.05)	57 (95.5)
Observation group	60	23 (38.33)	26 (43.33)	11 (18.33)	49 (81.67)
χ^2 value	-	-	-	-	45.759
P value	-	-	-	-	0.000

Table 5 Satisfaction scores in two groups

Group	Satisfaction scores
Observation	93.20 ± 3.5
Control	91.90 ± 2.5
t	4.421
P value	0.061

acupuncture and laser irradiation was more effective in clinically improving lumbar radiculopathy spondylolisthesis than lumbar traction therapy.

In addition to the effective improvement of pain, in this study it was also found that the observation group showed significant results in improving the lumbar spine function of the patients[13]. Compared to the control group, the observation group showed significantly improved JOA scores within the same treatment period. Previous studies have shown that acupuncture improves lumbar spine function, and laser irradiation has been widely used to treat muscle and joint injuries. For example, Boyraz *et al*[14] applied laser acupuncture to treat patients with osteoarthritis; the results showed that this treatment method significantly reduced the patients' pain scores, and its therapeutic effect achieved significant results after 2 wk of treatment. Based on previous studies, it is believed that three-volt acupuncture combined with helium-neon laser irradiation has fewer side effects and a shorter onset of action in the clinical treatment of radiculopathy.

Our study is the first to use a combination of triple-voltage acupuncture and helium-neon laser irradiation for the treatment of radiculopathy and to achieve better clinical results. Our study has the following limitations. First, our study used a randomized controlled study, but due to the strict selection criteria for the study population, we were unable to include a large sample of cases, thus leading to impoverishment of the robustness of the results of our study; we need to further include more study subjects in the future to carry out the study. The second limitation is that the laser irradiation method we used was helium-neon laser irradiation, ignoring the effectiveness of other laser irradiation methods; therefore, future comparisons with other laser irradiation treatments are needed to obtain the best therapeutic effect on patients.

CONCLUSION

Lumbar radiculopathy spondylosis can significantly reduce the quality of life of patients and has a significant impact on their lives and work. In this study, through the use of TCM combined with helium-neon laser irradiation, the pain scores of the patients and function of their lumbar vertebrae improved significantly after treatment, and the study found that the patients' clinical therapeutic efficacy and satisfaction with the nursing care were higher after receiving the treatment. Our study provides a clinical rationale for the future treatment of patients with lumbar spine disease. However, further extensive research is needed for validation.

FOOTNOTES

Author contributions: Ji XK and Li J contributed equally to this work; Ji XK and Li J designed the study, conducted the experiments, analyzed the data and wrote the manuscript. All authors have read and approved the final manuscript.

Institutional review board statement: The study was reviewed and approved by The Second Hospital of Heilongjiang Province Institutional Review Board.

Informed consent statement: All study participants or their legal guardian provided informed written consent about personal and medical data collection prior to study enrolment.

Conflict-of-interest statement: All the authors report no relevant conflicts of interest for this article.

Data sharing statement: No additional data are available.

Country/Territory of origin: China

ORCID number: Xiu-Kun Ji 0009-0004-2286-005X; Jian Li 0009-0007-3899-3262.

S-Editor: Zheng XM
L-Editor: A
P-Editor: Yu HG

REFERENCES

1 **Danazumi MS**, Bello B, Yakasai AM, Kaka B. Two manual therapy techniques for management of lumbar radiculopathy: a randomized clinical trial. *J Osteopath Med* 2021; **121**: 391-400 [PMID: 33705612 DOI: 10.1515/jom-2020-0261]
2 **Satpute K**, Hall T, Bisen R, Lokhande P. The Effect of Spinal Mobilization With Leg Movement in Patients With Lumbar Radiculopathy-A Double-Blind Randomized Controlled Trial. *Arch Phys Med Rehabil* 2019; **100**: 828-836 [PMID: 30521781 DOI: 10.1016/j.apmr.2018.11.004]
3 **Kuligowski T**, Skrzek A, Cieślik B. Manual Therapy in Cervical and Lumbar Radiculopathy: A Systematic Review of the Literature. *Int J Environ Res Public Health* 2021; **18**: 6176 [PMID: 34200510 DOI: 10.3390/ijerph18116176]
4 **Zai FL**, Wu RL, Zheng MF, Guo LY. [Warming Needle Moxibustion Relieves Symptoms of Lumbar Disc Herniation Patients and Upregulates Plasma β-endorphin]. *Zhen Ci Yan Jiu* 2018; **43**: 512-515 [PMID: 30232855 DOI: 10.13702/j.1000-0607.170736]
5 **Wang X**, Wu P, Luo Y, Tao SY, Li Y, Tang J, Jiang NN, Wang J, Zhao Y, Wang ZY. [Moxibustion for rheumatoid arthritis and its effect on related negative emotions]. *Zhongguo Zhen Jiu* 2022; **42**: 1221-1225 [PMID: 36397218 DOI: 10.13703/j.0255-2930.20211110-k0004]
6 **Snyder-Mackler L**, Bork CE. Effect of helium-neon laser irradiation on peripheral sensory nerve latency. *Phys Ther* 1988; **68**: 223-225 [PMID: 3340661 DOI: 10.1093/ptj/68.2.223]
7 **Chen W**, Wang J, Zhou Z, Ren Y, Hua Z, Yan Z, Zhang Y, Chen W. Therapeutic efficacy of traditional Chinese exercises and massage treatment on lumbar instability: a randomized controlled trial. *J Tradit Chin Med* 2020; **40**: 1026-1032 [PMID: 33258355 DOI:

10.19852/j.cnki.jtcm.2020.06.014]

8 **Chen M**, Chen R, Xiong J, Yi F, Chi Z, Zhang B. Effectiveness of heat-sensitive moxibustion in the treatment of lumbar disc herniation: study protocol for a randomized controlled trial. *Trials* 2011; **12**: 226 [PMID: 21995679 DOI: 10.1186/1745-6215-12-226]

9 **Ma Z**, Yu P, Jiang H, Li X, Qian X, Yu Z, Zhu Y, Liu J. Conservative Treatment for Giant Lumbar Disc Herniation: Clinical Study in 409 Cases. *Pain Physician* 2021; **24**: E639-E648 [PMID: 34323452]

10 **Khodadad B**, Letafatkar A, Hadadnezhad M, Shojaedin S. Comparing the Effectiveness of Cognitive Functional Treatment and Lumbar Stabilization Treatment on Pain and Movement Control in Patients With Low Back Pain. *Sports Health* 2020; **12**: 289-295 [PMID: 31841078 DOI: 10.1177/1941738119886854]

11 **Lin R**, Zhu N, Liu J, Li X, Wang Y, Zhang J, Xi C. Acupuncture-movement therapy for acute lumbar sprain: a randomized controlled clinical trial. *J Tradit Chin Med* 2016; **36**: 19-25 [PMID: 26946614 DOI: 10.1016/s0254-6272(16)30003-6]

12 **Goo B**, Kim JH, Kim EJ, Lee HJ, Kim JS, Nam D, Park YC, Kim TH, Baek YH, Nam SS, Seo BK. Thread embedding acupuncture for herniated intervertebral disc of the lumbar spine: A multicenter, randomized, patient-assessor-blinded, controlled, parallel, clinical trial. *Complement Ther Clin Pract* 2022; **46**: 101538 [PMID: 35101704 DOI: 10.1016/j.ctcp.2022.101538]

13 **Plaza-Manzano G**, Cancela-Cilleruelo I, Fernández-de-Las-Peñas C, Cleland JA, Arias-Buría JL, Thoomes-de-Graaf M, Ortega-Santiago R. Effects of Adding a Neurodynamic Mobilization to Motor Control Training in Patients With Lumbar Radiculopathy Due to Disc Herniation: A Randomized Clinical Trial. *Am J Phys Med Rehabil* 2020; **99**: 124-132 [PMID: 31464753 DOI: 10.1097/PHM.0000000000001295]

14 **Boyraz I**, Yildiz A, Koc B, Sarman H. Comparison of high-intensity laser therapy and ultrasound treatment in the patients with lumbar discopathy. *Biomed Res Int* 2015; **2015**: 304328 [PMID: 25883952 DOI: 10.1155/2015/304328]

World Journal of Clinical Cases

Submit a Manuscript: https://www.f6publishing.com

World J Clin Cases 2024 May 26; 12(15): 2529-2541

DOI: 10.12998/wjcc.v12.i15.2529

ISSN 2307-8960 (online)

ORIGINAL ARTICLE

Clinical Trials Study

Endovascular treatment of ruptured lobulated anterior communicating artery aneurysms: A retrospective study of 24 patients

Sheng-Xuan Huang, Xun-Ping Ai, Ze-Hui Kang, Zhi-Yong Chen, Ren-Man Li, Zu-Chao Wu, Feng Zhu

Specialty type: Neuroimaging

Provenance and peer review: Unsolicited article; Externally peer reviewed.

Peer-review model: Single blind

Peer-review report's classification

Scientific Quality: Grade B, Grade C

Novelty: Grade B, Grade C

Creativity or Innovation: Grade B, Grade C

Scientific Significance: Grade B, Grade B,

P-Reviewer: Arboix A, Spain

Received: November 20, 2023

Revised: February 21, 2024

Accepted: April 8, 2024

Published online: May 26, 2024

Sheng-Xuan Huang, Xun-Ping Ai, Ze-Hui Kang, Zhi-Yong Chen, Ren-Man Li, Zu-Chao Wu, Feng Zhu, Department of Neurosurgery, Sanming First Hospital Affiliated to Fujian Medical University, Sanming 365000, Fujian Province, China

Corresponding author: Zu-Chao Wu, PhD, Research Scientist, Department of Neurosurgery, Sanming First Hospital Affiliated to Fujian Medical University, No. 29 Liedongjie, Meilie District, Sanming 365000, Fujian Province, China. 282161043@qq.com

Abstract

BACKGROUND

Lobulated intracranial aneurysm is a special type of aneurysm with at least one additional cyst in the neck or body of the aneurysm. Lobulated intracranial aneurysm is a complex aneurysm with complex morphology and structure and weak tumor wall, which is an independent risk factor for rupture and hemorrhage. Lobular aneurysms located in the anterior communicating artery complex account for 36.9% of all intracranial lobular aneurysms. Due to its special anatomical structure, both craniotomy and endovascular treatment are more difficult. Compared with single-capsule aneurysms, craniotomy for lobular intracranial aneurysms has a higher risk and complication rate.

AIM

To investigate the efficacy and safety of endovascular treatment for ruptured lobulated anterior communicating artery aneurysm (ACoAA).

METHODS

Patients with ruptured lobulated ACoAA received endovascular treatment in Sanming First Hospital Affiliated to Fujian Medical University from June 2020 to June 2022 were retrospectively included. Their demographic, clinical and imaging characteristics, endovascular treatment methods and follow-up results were collected.

RESULTS

A total of 24 patients with ruptured lobulated ACoAA were included, including 9 males (37.5%) and 15 females (62.5%). Their age was 56.2 ± 8.9 years old (range 39-74). The time from rupture to endovascular treatment was 10.9 ± 12.5 h. The maximum diameter of the aneurysms was 5.1 ± 1.0 mm and neck width were 3.0 ±

0.7 mm. Nineteen patients (79.2%) were double-lobed and 5 (20.8%) were multilobed. Fisher's grade: Grade 2 in 16 cases (66.7%), grade 3 in 6 cases (25%), and grade 4 in 2 cases (8.3%). Hunt-Hess grade: Grade 0-2 in 5 cases (20.8%), grade 3-5 in 19 cases (79.2%). Glasgow Coma Scale score: 9-12 in 14 cases (58.3%), 13-15 in 10 cases (41.7%). Immediately postprocedural Raymond-Roy grade: grade 1 in 23 cases (95. 8%), grade 2 in 1 case (4.2%). Raymond-Roy grade in imaging follow-up for 2 wk to 3 months: grade 1 in 23 cases (95.8%), grade 2 in 1 case (4.2%). Follow-up for 2 to 12 months showed that 21 patients (87.5%) had good functional outcomes (modified Rankin Scale score ≤ 2), and there were no deaths.

CONCLUSION
Endovascular treatment is a safe and effective treatment for ruptured lobulated AcoAA.

Key Words: Intracranial aneurysm; Anterior cerebral artery; Endovascular surgery; Embolism; Treatment outcome

Core Tip: For ruptured lobulated anterior communicating artery aneurysm, preoperative angiography was used to fully evaluate the lobulated aneurysm, neck of the tumor and segment A and 1 vessels, to grasp reasonable operation timing, and to minimize the use of multiple or simplified systems for endovascular treatment during the operation, which was conducive to surgical safety and to reduce postoperative complications.

Citation: Huang SX, Ai XP, Kang ZH, Chen ZY, Li RM, Wu ZC, Zhu F. Endovascular treatment of ruptured lobulated anterior communicating artery aneurysms: A retrospective study of 24 patients. *World J Clin Cases* 2024; 12(15): 2529-2541
URL: https://www.wjgnet.com/2307-8960/full/v12/i15/2529.htm
DOI: https://dx.doi.org/10.12998/wjcc.v12.i15.2529

INTRODUCTION

Lobulated intracranial aneurysm is a special type of aneurysm with at least one additional cyst in the neck or body of the aneurysm[1]. Lobulated intracranial aneurysm is a complex aneurysm with complex morphology and structure and weak tumor wall, which is an independent risk factor for rupture and hemorrhage[2]. Lobular aneurysms located in the anterior communicating artery complex account for 36.9% of all intracranial lobular aneurysms[3]. Due to its special anatomical structure, both craniotomy and endovascular treatment are more difficult[4,5]. Compared with single-capsule aneurysms, craniotomy for lobular intracranial aneurysms has a higher risk and complication rate[2]. This is because it is difficult to ensure the complete occlusion of lobular aneurysms and the patency of the carrying artery, and more operations on the surrounding brain tissue are required to expose aneurysms, and the placement of aneurysm clips is more complicated. The prolonged use of fluorescein angiography and brain retractor during repeated operations will prolong the operative time and increase the probability of intraoperative brain injury. In view of the above reasons, the treatment of intracranial complex aneurysms has gradually shifted to intravascular therapy[6,7]. Cerebral infarction in the anterior cerebral artery region secondary to vasospasm after anterior communicating aneurysm rupture is a potentially significant adverse outcome[8]. We analyzed the safety and efficacy of ruptured anterior communicating artery aneurysm (ACoAA) treated intravascular at the Department of Neurosurgery, Sanming First Hospital Affiliated to Fujian Medical University.

MATERIALS AND METHODS

Patients with ruptured lobulated ACoAA who received endovascular therapy at the First Affiliated Sanming Hospital of Fujian Medical University from June 2020 to June 2022 were retrospectively included. Inclusion criteria: (1) Subarachnoid hemorrhage was confirmed by computed tomography (CT) examination; and (2) Lobed ACoAA was indicated by conventional 320-slice CT angiography (CTA), which was confirmed by whole brain digital subtraction angiography (DSA). The evaluation criteria were as follows: Aneurysms located in the anterior communicating artery complex of the brain had ≥ 1 additional aneurysm sac from the common aneurysm neck or tumor body. When the diameter of the additional aneurysm sac was ≥ 63% of the diameter of the largest aneurysm sac, it was lobed; otherwise, it was ascus[1,9-10]; (3) Receive endovascular therapy; (4) Postoperative clinical follow-up time > 3 months. Exclusion criteria: (1) Multiple intracranial aneurysms; (2) Recurrence after previous intravascular therapy; (3) Other intracranial vascular diseases, such as arteriovenous malformation, moyamoya disease, arteriovenous fistula, *etc.*; (4) No interventional treatment was performed due to critical illness or combined with serious underlying diseases; and (5) Incomplete information. This study was approved by the Ethics Committee of the First Affiliated Sanming Hospital of Fujian Medical University (Ming Yilun[2020] 37).

Data collection

Patients' age, sex, duration of rupture (*i.e.*, onset of subarachnoid hemorrhage) to intravascular treatment, disease assessment (Fisher scale, Hunt-Hess scale, Glasgow Coma Scale, GCS score, hydrocephalus), basic aneurysm characteristics (maximum diameter, neck width, number of ascus), endovascular treatment (including extra- vascular drainage), and follow-up results.

Endovascular therapy

Under general anesthesia, the right femoral artery was punctured by Seldinger technique, the 6F vascular sheath was inserted, and the whole body was heparinized. The intracranial blood vessels were investigated in detail for spasticity, arteriosclerosis, stenosis and collateral circulation compensation, and the location of the aneurysm and the carrier artery were determined. The direction of ACoAA, the angulation of the neck and the carrier artery, the shape of the true and lobulated tumors, and the vascular movement of the proximal aneurysms were mainly observed. The size of the neck and the tumor were measured, and the appropriate working Angle was selected based on the criterion that the overall shape of the aneurysm, the neck and the relationship between the neck and the carrier artery could be fully revealed. A long sheath plus an intermediate catheter was routinely used to establish access, and an 8 F long sheath was inserted through the 8 F artery sheath, and then an intermediate catheter was inserted through the long sheath to the C1 segment of the internal carotid artery. For small lobulated aneurysms (maximum diameter < 1 mm), a single microcatheter is guided into the mother tumor under the guidance of a micro-guide wire, and the spring coil is simply used to embolize the mother tumor according to the size of the tumor. In the process of embolization, when the spring ring overflows the bearing artery or is combined with the absolute wide neck, the stent can be used to assist embolization. For large lobular aneurysms, two microcatheters were guided by micro guides into each lobule, embolized with spring rings according to the size of the lobule, and then closed the common neck. If a relatively wide neck or an absolutely wide neck is expected to require stent-assisted treatment, the stent catheter is prepositioned to the distal end of the target vessel under the guidance of a micro-guide wire, and then the embolized microcatheter is placed in the lobules with high probability of rupture or the lobules with difficult placement through the stent mesh, and the aneurysm lobules are embolized one by one by adjusting the embolized microcatheter when the stent is half-released. Or the stent is completely released, and the pre-positioned embolization microcatheter embolizes one of the lobules, and then reshapes, perforates the stent mesh and embolizes the remaining lobules. Simplify multiple system operations as much as possible. For patients who were expected to require stent-assisted treatment during the operation, load dose dual therapy (aspirin 300 mg+ clopidogrel 300 mg) was administered 30 min before surgery. If emergency surgery was performed immediately after admission and stent assistance was required, Tirofiban was injected intravenously (10 μg/kg load) + intravenous [(0.1 μg/(kg min)] for 24 h, followed by dual antiplatelet therapy (aspirin 100 mg+ clopidogrel 75 mg), overlapping for 6 h. If acute thrombosis occurs during the operation, Tirofiban arterial injection plus postoperative intravenous pumping should be given immediately. In case of vasospasm, nimodipine 2 mg is administered slowly. All patients were treated with double antiplatelet agents for 3 months after stent placement, and then adjusted according to the results of angiography review. After the operation, conventional lumbar cisterna continuous drainage or lumbar puncture released bloody cerebrospinal fluid, anti-cerebrovascular spasm, water and electrolyte balance maintenance, dehydration to reduce cranial pressure and nutritional nerve and other symptomatic treatment.

Postoperative evaluation and imaging follow-up

The imaging results immediately after operation and during follow-up were evaluated according to Raymond-Roy occlusion classification[11] to evaluate the degree of embolism: Grade 1, complete occlusion; Grade 2, residual neck; Grade 3, residual tumor. The modified Rankin Scale (mRS) was used to evaluate the clinical outcome, and ≤ 2 was defined as good outcome.

Statistical analysis

SPSS 21.0 software was used for data processing. To conform to the normal distribution of measurement data to ± SD, comparison between the two groups use independent sample *t*-test; Measurement data with non-normal distribution were presented as median and interquartile range, and comparison between the two groups was analyzed using the Mann-Whitney *U* test. Count data were expressed as frequency and percentage, and comparison between groups was analyzed using the chi-square test or Fisher's exact test. Two-sided $P < 0.05$ was considered statistically significant.

RESULTS

Basic data

A total of 30 patients with ruptured lobulated ACoAA were treated during the study period. After excluding 3 patients who gave up treatment, 1 patient who chose craniotomy and 2 patients who were lost to follow-up, 24 patients were finally included in the analysis. There were 9 males (37.5%) and 15 females (62.5%). The average age was 56.2 ± 8.9 years (range 39-74 years). 19 cases (79.2%) were bilobed and 5 cases (20.8%) were poly lobulated. The clinical data of all patients are summarized in Tables 1 and 2.

Treatment outcome

Endovascular treatment was successfully performed in all patients. In 1 patient, the parent artery thrombosis was found

Table 1 Characteristics of patient with ruptured lobulated anterior communicating artery aneurysm

Case Number	Age	Sex	Time from rupture to endovascular treatment (h)	Maximum diameter of the aneurysms (mm)	Neck width (mm)	Lobed number	Fisher's grade	Hunt-Hess grade	Glasgow Coma Scale score	Hydrocephalus	Methods of Treatment	Immediately postprocedural Raymond-Roy grade	Complication	Imaging follow-up method	Follow-up Raymond-Roy grade
1	39	Female	3	4.2	3	2	2	2	13	No	Single microcatheter embolization	1	No	CT angiography	1
2	42	Female	11	5.1	2.8	2	2	3	11	No	Single microcatheter embolization	1	No	CT angiography	1
3	63	Female	6	3.1	2.2	3	2	3	12	No	Auxiliary support coil embolization	1	No	Digital subtraction angiography	1
4	52	Male	7	5.8	4.1	2	2	3	12	No	Auxiliary support coil embolization	1	No	Digital subtraction angiography	1
5	43	Female	4	3.6	3.1	3	3	3	12	No	Auxiliary support coil embolization	1	No	Digital subtraction angiography	1
6	56	Female	6	3.7	2.7	2	3	4	11	No	External ventricular drainage; Double microcatheter embolization	1	No	CT angiography	1
7	71	Female	48	3.6	3	2	2	1	14	No	Single microcatheter embolization	1	No	CT angiography	1
8	48	Male	7	5.5	3	3	2	2	13	No	Double microcatheter embolization	1	No	CT angiography	1
9	61	Female	5	5.1	2.9	2	2	2	15	No	Double microcatheter embolization	1	No	CT angiography	1
10	55	Female	7	5	2.6	2	2	3	13	No	Double microcatheter embolization	1	No	CT angiography	1
11	65	Female	7	8.1	5.3	3	4	4	9	Yes	External ventricular	2	Arterial thrombosis	Digital subtraction	2

										drainage; Auxiliary support coil embolization			angiography	
12	58	Male	5	5.3	3	2	3	3	13	No	Auxiliary support coil embolization	1	No	Digital subtraction angiography	1
13	50	Female	10	4.6	2	2	2	3	13	No	Double microcatheter embolization	1	No	CT angiography	1
14	63	Female	26	5.1	2.1	2	2	3	13	No	Double microcatheter embolization	1	No	CT angiography	1
15	66	Male	6	5	3.2	2	4	4	9	Yes	Double microcatheter embolization	1	Communicating hydrocephalus	CT angiography	1
16	53	Male	8	6.1	3.9	2	3	3	12	No	Auxiliary support coil embolization	1	No	Digital subtraction angiography	1
17	74	Female	50	5.4	3.4	2	2	2	13	No	Double microcatheter embolization	1	No	CT angiography	1
18	61	Male	4	4.3	2.3	2	2	3	12	No	Auxiliary support coil embolization	1	No	Digital subtraction angiography	1
19	55	Male	5	5.7	3	2	3	3	12	No	Double microcatheter embolization	1	No	CT angiography	1
20	60	Female	5	5.7	3.8	3	2	3	12	No	Double microcatheter embolization	1	No	CT angiography	1
21	48	Female	8	5.4	2.5	2	2	3	13	No	Auxiliary support coil embolization	1	No	Digital subtraction angiography	1
22	53	Female	12	4.9	2.3	2	2	4	12	No	Double microcatheter embolization	1	No	CT angiography	1
23	63	Male	7	6.1	2.9	2	3	4	11	No	Auxiliary support coil embolization	1	No	Digital subtraction angiography	1
24	50	Male	6	5.5	2.8	2	2	4	11	No	Auxiliary support coil embolization	1	No	Digital subtraction	1

by angiography after embolization of the aneurysm, and the blood flow was improved after intravenous infusion of tirofiban, but there was still significant neurological deficit (mRS Score 4) after the operation. One patient developed communicating hydrocephalus at 6 months follow-up, and the symptoms were improved after ventriculoperitoneal shunt (mRS Score 3). Immediate postoperative Raymond-Roy classification: 23 cases (95.8%) were grade 1 and 1 case (4.2%) was grade 2. Radiographic follow-up from 2 wk to 3 months showed that 23 cases (95.8%) were grade 1 and 1 case (4.2%) was grade 2. At 2-12 months follow-up, 21 patients (87.5%) had good outcome (mRS Score ≤ 2), 3 patients (12.5%) had poor outcome (mRS Score > 2), and there was no death.

Typical case

Case 9, a 61-year-old female, was admitted to hospital with "sudden severe headache for 5 h". Physical examination: lethargy, GCS score 15, bilateral pupil diameter 2.5 mm, sensitive light reflex, neck resistance, normal muscle strength and muscle tone in extremities, bilateral Babinski sign negative, Hunt-Hess grade 2. Emergency CT showed subarachnoid hemorrhage (Fisher grade 2), and CTA showed ACoAA. In the emergency department, endovascular treatment was performed under general anesthesia. DSA showed that A1 on the left side was divided into A2 on both sides, and ACoAA was bilobed, with sizes of 5.1 mm × 5.0 mm and 4.2 mm × 4.0 mm, respectively, and tumor neck 2.9 mm. Aneurysmal embolization was performed using dual microcatheter technique. Immediate postoperative angiography showed that the aneurysm was completely embolized and both sides were smooth. No aneurysm recurrence was observed in CTA reexamination 2 wk after surgery, and the patient recovered well and was completely asymptomatic at 3 months follow-up (Figure 1).

Case 5, a 43-year-old female, was admitted to hospital with "sudden severe headache for 4 h". Physical examination: Drowsiness, GCS score 12 points, bilateral pupil diameter 2.5 mm, sensitive light reflex, obvious neck resistance, normal muscle strength and muscle tone of extremities, bilateral Barbinsky sign negative, HuntHess grade 3. Subarachnoid hematoma was found on emergency CT (Fisher grade 3) and ACoAA was found on CTA. In the emergency department, endovascular treatment under general anesthesia was performed. DSA showed that A1 on the left side was separated from A2 on both sides, and ACoAA was tri-lobed, with sizes of 3.6 mm × 2.8 mm, 1.1 mm × 1.2 mm and 3.2 mm × 2.5 mm, respectively, and neck 3.1 mm. The stent assisted spring coil technique was used to embolize the aneurysm. Immediately after surgery, the angiography showed that the aneurysm was completely embolized and the bilateral A2 was smooth. Intraoperative Tirofiban arterial injection + continuous intravenous pump injection for 24 h, followed by dual antiplatelet therapy, overlapping for 6 h. Postoperative dual antiplatelet therapy lasted for 3 months. DSA review 3 months later did not show aneurysm recurrence, continue to take aspirin orally. At 12 months follow-up, the patient recovered well with some dizziness (Figure 2).

DISCUSSION

In this research, we fully evaluate the lobulated aneurysm, neck and A1 segment blood vessels, to grasp the reasonable operation time, and to minimize the use of multiple or simplified systems for endovascular treatment during the operation in order to ensure surgical safety and reduce postoperative complications.

Table 2 Average information of patients, *n* (%)

	Double-lobed patients	Multilobed patients
Age	56.3 ± 9.0	55.8 ± 9.7
Sex	8 (42.1)	1 (20)
Time from rupture to endovascular treatment (h)	12.9 ± 13.8	5.8 ± 1.3
Maximum diameter of the aneurysms (mm)	5.0 ± 0.7	5.2 ± 2.0
Neck width (mm)	2.9 ± 0.5	3.5 ± 1.2
Fisher's grade		
Grade 2	13 (68.4)	3 (60)
Grade 3	5 (26.3)	1 (20)
Grade 4	1 (5.2)	1 (20)
Hunt-Hess grade		
Grade 0-2	4 (21.1)	1 (20)
Grade 3-5	15 (78.9)	4 (80)
Glasgow Coma Scale score	12.2 ± 1.3	11.6 ± 1.5
Hydrocephalus	1 (5.2)	1 (20)
Methods of treatment		
Single microcatheter embolization	3 (15.8)	0 (0)
Double microcatheter embolization	8 (42.1)	2 (40)
Auxiliary support coil embolization	7 (36.8)	2 (40)
External ventricular drainage; Double microcatheter embolization	1 (5.3)	0 (0)
External ventricular drainage; Auxiliary support coil embolization	0 (0)	1 (20)
Immediately postprocedural Raymond-Roy grade		
Grade 1	19 (100)	4 (80)
Grade 2	0 (0)	1 (20)
Complication		
Arterial thrombosis	0 (0)	1 (20)
Communicating hydrocephalus	1 (5.2)	0 (0)
Follow-up Raymond-Roy grade		
Grade 1	19 (100)	4 (80)
Grade 2	0 (0)	1 (20)

As for the formation mechanism of lobulated intracranial aneurysms, the vascular self-protective response hypothesis suggests that in the weak part of the vascular wall of an aneurysm on the verge of rupture, it will bulge out like a balloon to reduce the local stress and achieve temporary equilibrium, thus leading to the formation of daughter tumors[12]. When the tumor continues to grow and exceeds a certain shape limit, this balance is disrupted, causing the aneurysm to rupture. The rationality of this hypothesis was confirmed by the numerical simulation of hemodynamics of intracranial lobular aneurysms conducted by researchers[13]. It can be seen that lobular aneurysms are formed on the basis of expansion of the tumor wall, which is originally weaker than the normal blood vessel wall, and are therefore more prone to rupture. Previous studies have shown that aneurysms located in anterior communicating artery, ruptured aneurysms, small aneurysms and irregular aneurysms combined with daughter tumors are independent risk factors for rupture during embolization of intracranial aneurysms[14-16]. Therefore, the endovascular treatment of ruptured lobulated ACoAA is more difficult.

In terms of surgical timing, lobular rupture of AcoAA is an irregular aneurysm with thinner wall, which is prone to re-rupture and bleeding. Therefore, etiological treatment should be carried out as soon as possible after medical treatment such as blood pressure control, sedation and anti-vasospasm. All patients were given intravascular therapy within 3 d. According to literature reports, the probability of rebleeding within the first 3 d after intracranial aneurysm rupture and hemorrhage is 14%, and cerebral vasospasm may occur after 3 d. Therefore, "3H" therapy can be started as soon as possible after endovascular treatment of aneurysms, which has a positive effect on the prevention and treatment of

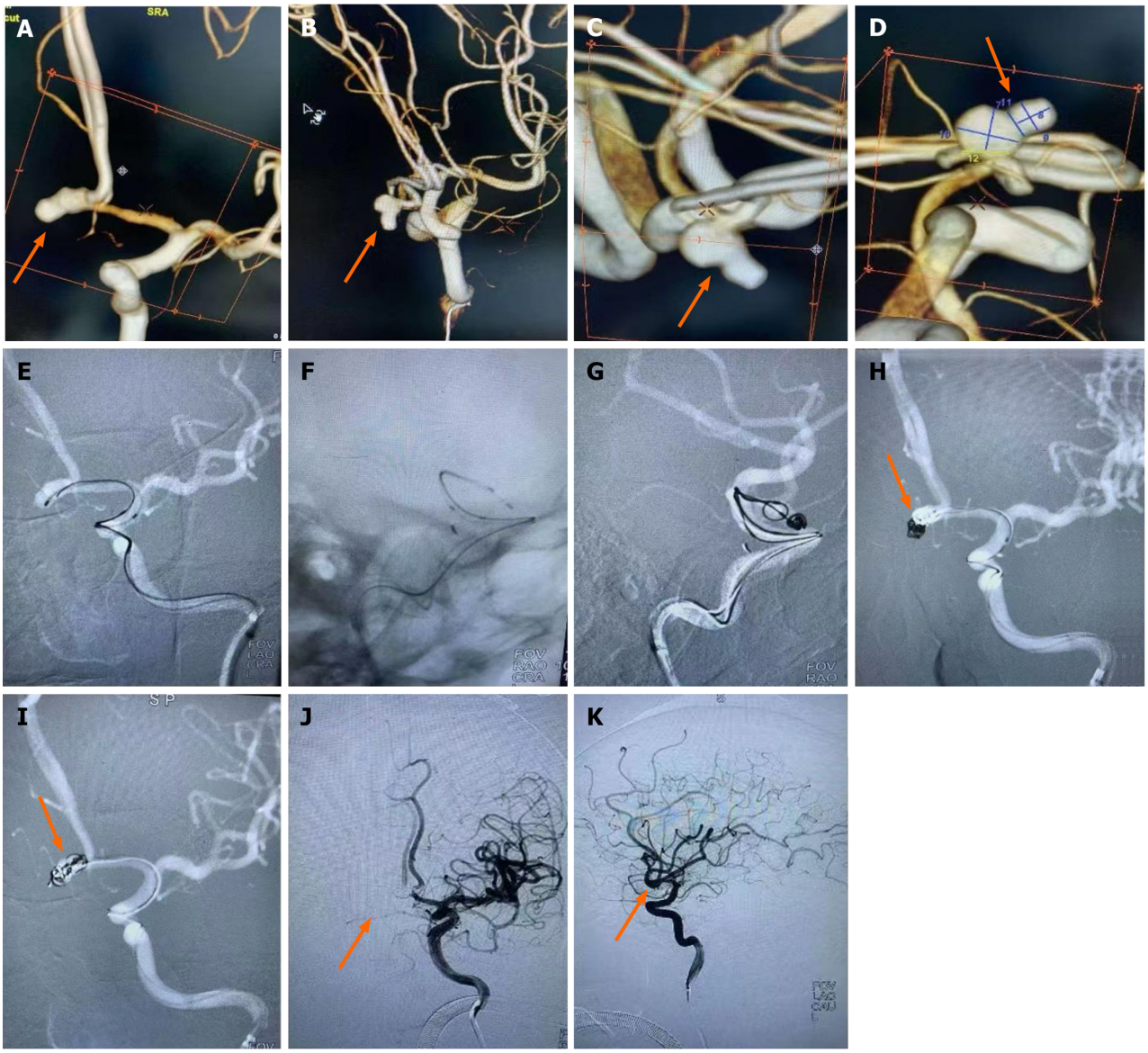

Figure 1 Imaging data of endovascular treatment of typical double-lobed anterior communicating artery aneurysms. A-D: Double-lobed anterior communicating artery aneurysms, the lobes were similar in size to the mother aneurysm and were not on the same long axis (arrows); E-I: Double microcatheters were placed at different working angles to different lobes, and each lobe was embolized alternately in the double microtubes (arrows); J and K: After embolization, the aneurysm was not visualized and bilateral A2 was unobstructed (arrows).

cerebral vasospasm[17]. In this group of cases, there was no adverse outcome caused by aneurysm re-rupture and hemorrhage and severe cerebral vasospasm.

In the interventional treatment of ruptured lobulated AcoAA, the embolization system often requires better support in path establishment because the aneurysm is located at a distant part of the anterior circulation, and some cases are complicated with aortic arch variation, arteriosclerosis or stenosis and tortuosity, resulting in difficulties in the placement of the access catheter. In this group of patients, all use long sheath + intermediate catheter to establish access. Long sheath can provide reliable support, and the distal end of the intermediate catheter is soft, which can reach a further position. The geometric shape and many anatomic variations of anterior cerebral artery A1 will affect the therapeutic effect of interventional surgery, and the dysplasia of segment A1 is an independent predictor of poor functional outcome after ACoAA endovascular therapy[18-20]. In this group, 22 cases were missing anterior cerebral artery A 1 segment on one side, and anterior cerebral artery A 1 segment on the other side was separated from bilateral A 2. Bilateral A1 was present in only 2 cases, but the bilateral A2 was asymmetrical, with one side being thinner. Once vasospasm was combined (4 cases in this group were combined with vasospasm of stage A 1, of which 1 did not improve after continuous nimodipine pumping treatment), multiple systems often could not be successfully put in place, or even could not accommodate multiple systems. In addition, when multiple systems are used, on the one hand, blood vessels may be stimulated and spasm may be aggravated, and prolonged surgical operation may affect distal blood flow; On the other hand, the interference of multiple systems can increase the difficulty and risk of surgery. Therefore, according to the number, size, shape, tip orientation and neck width of aneurysm lobes, this group of patients did not use multiple systems or simplified systems to perform operations, and the postoperative functional outcome rate was as high as 87.5%.

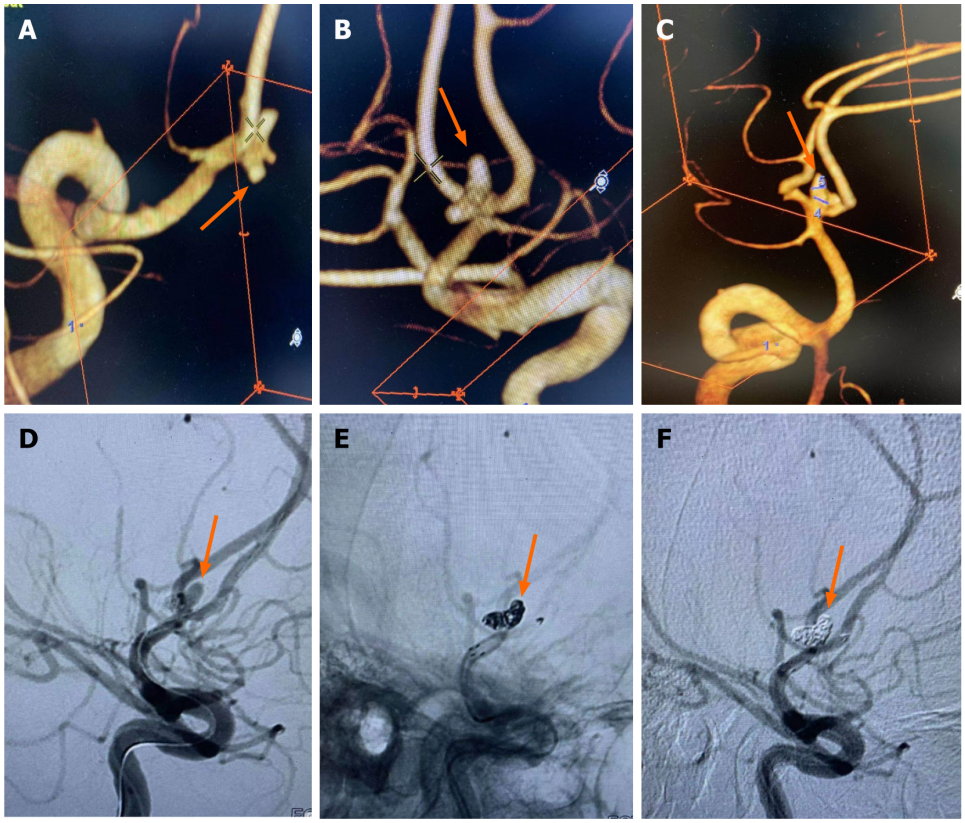

Figure 2 Imaging data of endovascular treatment of typical anterior communicating artery trilobular aneurysms. A-C: Anterior communicating artery trilobular aneurysms (arrows); D: First embolization of the posterior lobe, completely release the stent, embolization of the microcatheter through the stent mesh to the forward lobe, and continue to embolization of the aneurysm (arrow); E-F: Complete embolization of the aneurysm, bilateral A2 patency (arrows).

In this group of cases, when the ACoAA was accompanied by a daughter tumor on the top of the same long axis as the mother tumor, such as the daughter tumor < 1 mm (Figure 3), a single microcatheter was used to place in the mother tumor under the guidance of the guide wire, and the tension should be released at all times during the operation. The daughter tumor was generally the location of the aneurysm rupture, and the guide wire should not be touched. It is not necessary to deliberately plug the tumor during the filling process. If one or two spring rings are attached to the tumor, it is best, but the mother tumor and tumor neck must be packed tightly, and the tumor should not be visible during angiography. If the daughter tumor is larger than 1 mm (Figure 4), the embolization is performed using a single or double embolized microcatheter, but the microcatheter must reach the neck of the daughter tumor or enter the daughter tumor body under the guidance of a guide wire. A spring coil adapted to the size of the daughter tumor is selected for embolization. When the microcatheter placed in the daughter tumor retreated to the mother tumor due to "kicking tube", the mother tumor was further filled with dense.

Although researchers[21] have reported the feasibility and safety of embolizing a variety of intracranial complex lobular ruptured aneurysms with a single microcatheter partition basket technique, the shaping of the microcatheter head is required to be accurate, and the switching position between each lobular aneurysm must be in place. Failure to meet the above requirements is likely to lead to surgical failure. Other researchers[22] have used double microcatheter technology to treat lobular aneurysms and achieved reliable efficacy. By reducing the utilization rate of stents, the use of postoperative dual antiplatelet drugs has been reduced, thus reducing the risk of rebleeding. In this group of cases, when the lobule and the mother tumor were similar in size and not in the same long axis (Figure 1), since the direction of each lobule could not complete the operation at the same working Angle, the double microcatheter was placed in place in different lobules under different working angles, and each lobule was alternately embolized in the double microtubule, and the embolization sequence was flexibly applied. When the embolization reached the common neck of the tumor between lobules, Due to the mutual winding and lateral extrusion between the spring rings, the stability of the spring rings can be achieved even in the relatively wide neck, and the use of the support is reduced. When the double-lobular (Figure 5) and triple-lobular (Figure 2) aneurysms needed stent assistance for embolization due to their wide neck, the stent catheter was placed at a distance of A2 under the guidance of the micro-guide wire. The embolized microcatheter was shaped according to the aneurysm loaves, guided by the micro-guide wire to one of the loaves, and the spring coil was released several times under the semi-release state of the stent. Then the stent is released completely, another embolization microcatheter is inserted through the stent mesh, and the lobules pointing forward are further filled, and finally the aneurysm is completely embolized. When using this technique, it is necessary to consider which lobe of the microcatheter is placed first. Progressive neurological impairment and limb weakness at stroke onset are independent predictors of very early death in patients with nontraumatic subarachnoid hemorrhage. These results further emphasize the need to establish early etiological diagnosis and active management of these patients, including early surgery in

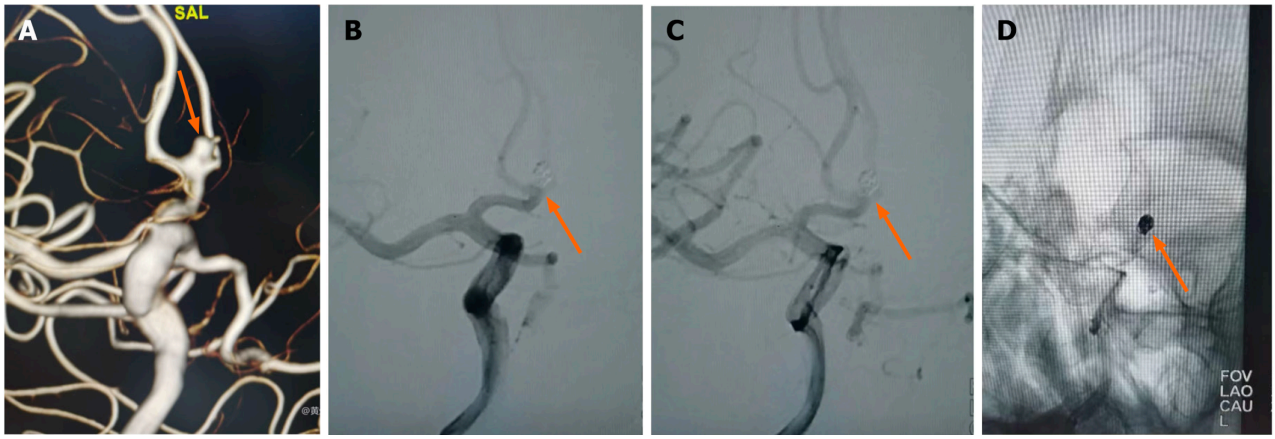

Figure 3 Imaging data of single microcatheter embolization of anterior communicating aneurysm. A: The top of the anterior communicating aneurysm was accompanied by a subaneurysm (less than 1mm), which was on the same long axis as the mother aneurysm (arrow); B-D: Single microcatheter embolization of the aneurysm, without deliberately treating the subaneurysm, after dense embolization, the aneurysm did not develop, and bilateral A2 was unobstructed (arrows).

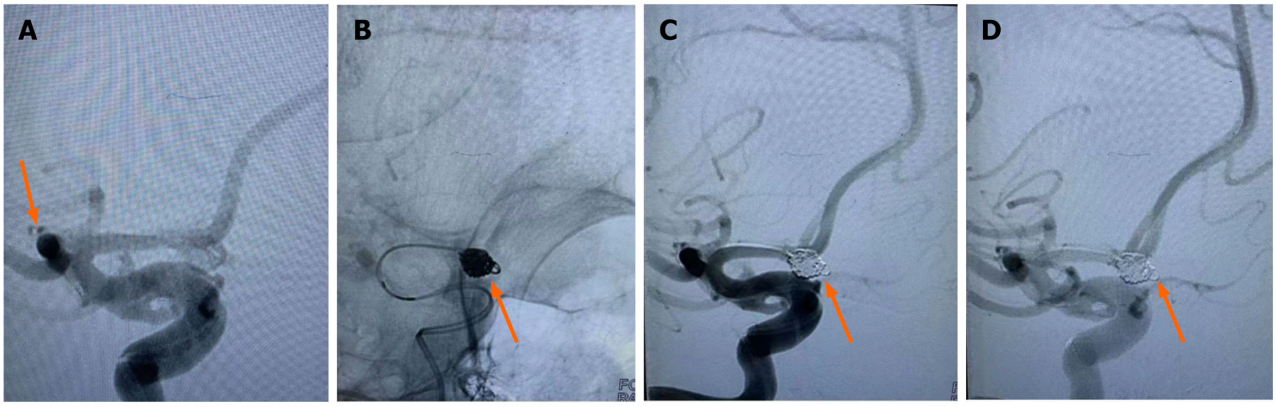

Figure 4 Imaging data of communicating artery aneurysms before embolization with double microcatheter. A: The top of anterior communicating aneurysm is accompanied by A daughter tumor (larger than 1 mm), and the daughter tumor and the mother tumor are on the same long axis (arrow); B: Double microcatheter embolization of aneurysm, alternate filling of daughter tumor and mother tumor (arrow); C and D: Dense embolization, the aneurysm did not develop, and bilateral A2 was patency (arrows).

selected cases[23]. Our experience has been to put in place lobules with a high probability of rupture, such as special morphologic or combined daughter tumors; if it is difficult to determine which lobe is more likely to rupture, select a lobe that is not easy to get through the stent mesh in place.

Limitations of this study

The main limitation of this study is that the sample size is small and the retrospective analysis is difficult to avoid selection bias. In particular, there were no large aneurysms (diameter > 10 mm but ≤ 25 mm) or large aneurysms (diameter > 25 mm) in this group of patients, so whether this concept is safe and effective for intravascular therapy needs further study.

Prospect

In our further experiments, we would include more patient cases and large aneurysms patients in our experiments to verify our present results. And more experiment on the onset mechanism and basic theories would contributes to the understanding of ACoAA.

CONCLUSION

In summary, for ruptured lobulated ACoAA, preoperative angiography was used to fully evaluate the lobulated aneurysm, neck of the tumor and segment A and 1 vessel, to grasp reasonable operation timing, and to minimize the use of multiple or simplified systems for endovascular treatment during the operation, which was conducive to surgical safety and to reduce postoperative complications.

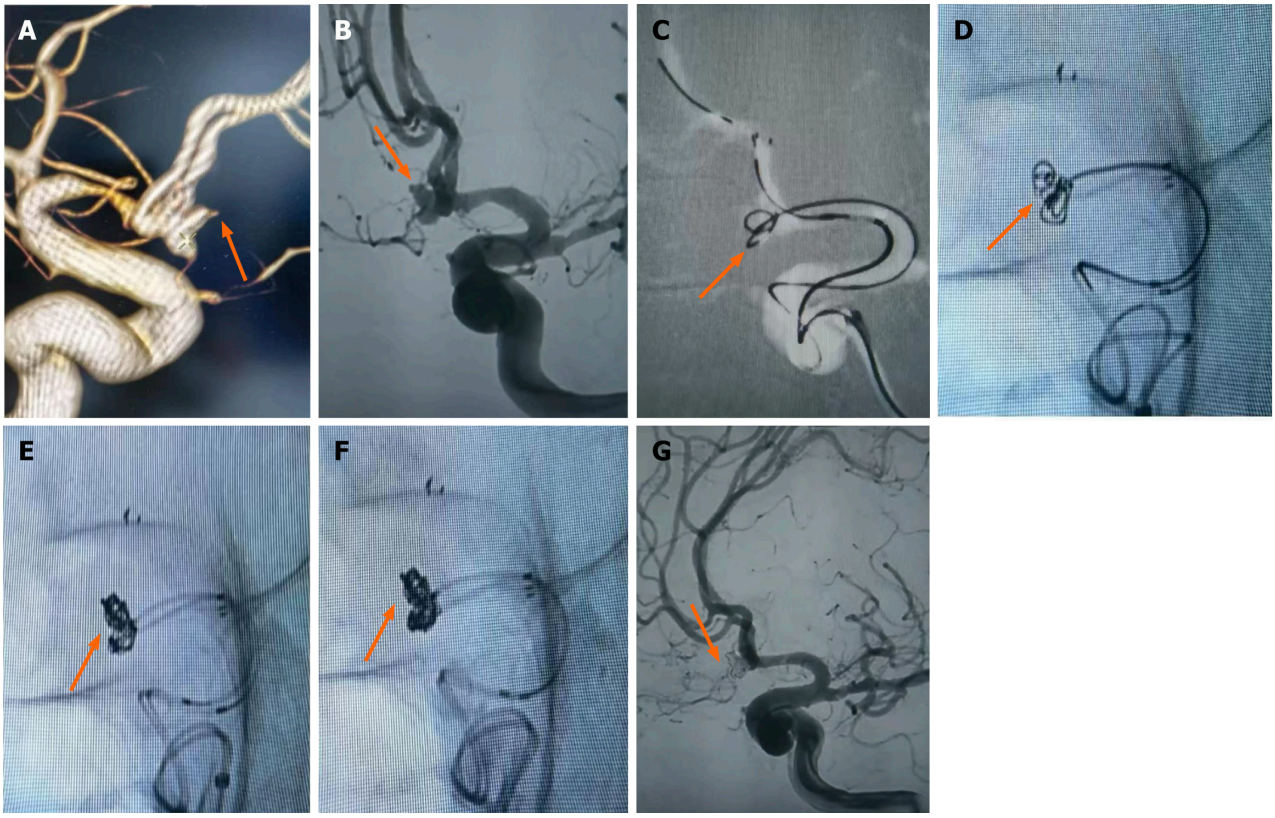

Figure 5 Imaging data of communicating artery aneurysm before stent assisted embolization. A: Anterior communicating double-lobular aneurysm with A1 segment spasm (arrow); B: Segment A1 spasm improved after continuous nimodipine pumping treatment (arrow); C: In the semi-release state of the support, release the spring ring several times in the pointing down lobe (arrow); D-F: Completely released the stent, embolized the microcatheter through the stent mesh into the other lobe, the double microcatheter alternately into the spring coil (arrows); G: After the completion of embolization, the aneurysm did not develop and bilateral A2 was unobstructed (arrow).

FOOTNOTES

Author contributions: Huang SX and Ai XQ performed the expriment, wrote the original manuscript; Kang ZH, Chen ZY, and Li RM contributes to the data collection and analysis; Wu ZC and Zhu F designed the experiment and revised the manuscript.

Supported by Fujian Province Health Young and Middle-aged Backbone Personnel Training Project, No. 2021GGB022; and Fujian Medical University Sailing Fund, No. 2019QH1262.

Institutional review board statement: The study was reviewed and approved by the Sanming First Hospital Affiliated to Fujian Medical University Institutional Review Board (No. SFH23051).

Clinical trial registration statement: This study was registered by ClinicalTrials. The registered number is No. 04371253.

Informed consent statement: All study participants, or their legal guardian, provided informed written consent prior to study enrollment.

Conflict-of-interest statement: All authors have no conflicts of interest to disclose.

Data sharing statement: The data is available from the corresponding author based on reasonable request.

CONSORT 2010 statement: The authors have read the CONSORT 2010 statement, and the manuscript was prepared and revised according to the CONSORT 2010 statement.

Country/Territory of origin: China

ORCID number: Sheng-Xuan Huang 0009-0005-1111-5668.

S-Editor: Liu JH
L-Editor: A
P-Editor: Zhang XD

REFERENCES

1 **Forbes G**, Fox AJ, Huston J 3rd, Wiebers DO, Torner J. Interobserver variability in angiographic measurement and morphologic characterization of intracranial aneurysms: a report from the International Study of Unruptured Intracranial Aneurysms. *AJNR Am J Neuroradiol* 1996; **17**: 1407-1415 [PMID: 8883634]
2 **Goertz L**, Kasuya H, Hamisch C, Kabbasch C, von Spreckelsen N, Ludyga D, Timmer M, Stavrinou P, Goldbrunner R, Brinker G, Krischek B. Impact of aneurysm shape on morbidity after clipping of unruptured intracranial aneurysms. *Acta Neurochir (Wien)* 2018; **160**: 2169-2176 [PMID: 30225810 DOI: 10.1007/s00701-018-3675-9]
3 **Goertz L**, Hamisch C, Pflaeging M, Kabbasch C, Borggrefe J, Timmer M, Stavrinou P, Goldbrunner R, Brinker G, Mpotsaris A, Krischek B. Angiographic Characteristics of Lobulated Intracranial Aneurysms. *World Neurosurg* 2019; **131**: e353-e361 [PMID: 31362105 DOI: 10.1016/j.wneu.2019.07.163]
4 **Borggrefe J**, Behme D, Mpotsaris A, Weber W. Complications Associated with Cerebral Aneurysm Morphology in Balloon-Assisted Coil Embolization of Ruptured and Unruptured Aneurysms-a Single-Center Analysis of 116 Consecutive Cases. *World Neurosurg* 2016; **91**: 483-489 [PMID: 27150653 DOI: 10.1016/j.wneu.2016.04.091]
5 **Matsukawa H**, Kamiyama H, Miyazaki T, Kinoshita Y, Noda K, Ota N, Saito N, Takeda R, Tokuda S, Tanikawa R. Impacts of a Size Ratio on Outcome in Patients with Surgically Treated Unruptured Nondissecting Anterior Cerebral Artery Aneurysms. *World Neurosurg* 2018; **111**: e250-e260 [PMID: 29258945 DOI: 10.1016/j.wneu.2017.12.031]
6 **Bender MT**, Wendt H, Monarch T, Lin LM, Jiang B, Huang J, Coon AL, Tamargo RJ, Colby GP. Shifting Treatment Paradigms for Ruptured Aneurysms from Open Surgery to Endovascular Therapy Over 25 Years. *World Neurosurg* 2017; **106**: 919-924 [PMID: 28736346 DOI: 10.1016/j.wneu.2017.07.074]
7 **Chiaradio JC**, Guzman L, Padilla L, Chiaradio MP. Intravascular graft stent treatment of a ruptured fusiform dissecting aneurysm of the intracranial vertebral artery: technical case report. *Neurosurgery* 2002; **50**: 213-6; discussion 216 [PMID: 11844254 DOI: 10.1097/00006123-200201000-00034]
8 **Arboix A**, García-Eroles L, Sellarés N, Raga A, Oliveres M, Massons J. Infarction in the territory of the anterior cerebral artery: clinical study of 51 patients. *BMC Neurol* 2009; **9**: 30 [PMID: 19589132 DOI: 10.1186/1471-2377-9-30]
9 **Abboud T**, Rustom J, Bester M, Czorlich P, Vittorazzi E, Pinnschmidt HO, Westphal M, Regelsberger J. Morphology of Ruptured and Unruptured Intracranial Aneurysms. *World Neurosurg* 2017; **99**: 610-617 [PMID: 28017741 DOI: 10.1016/j.wneu.2016.12.053]
10 **Mayer TE**. The unruptured intracranial aneurysm treatment score: A multidisciplinary consensus. *Neurology* 2016; **86**: 792-793 [PMID: 26903491 DOI: 10.1212/01.wnl.0000481228.68055.71]
11 **Raymond J**, Guilbert F, Weill A, Georganos SA, Juravsky L, Lambert A, Lamoureux J, Chagnon M, Roy D. Long-term angiographic recurrences after selective endovascular treatment of aneurysms with detachable coils. *Stroke* 2003; **34**: 1398-1403 [PMID: 12775880 DOI: 10.1161/01.STR.0000073841.88563.E9]
12 **Meng H**, Feng Y, Woodward SH, Bendok BR, Hanel RA, Guterman LR, Hopkins LN. Mathematical model of the rupture mechanism of intracranial saccular aneurysms through daughter aneurysm formation and growth. *Neurol Res* 2005; **27**: 459-465 [PMID: 15978170 DOI: 10.1179/016164105X25171]
13 **Oliveira IL**, Santos GB, Gasche JL, Militzer J, Baccin CE. Non-Newtonian Blood Modeling in Intracranial Aneurysm Hemodynamics: Impact on the Wall Shear Stress and Oscillatory Shear Index Metrics for Ruptured and Unruptured Cases. *J Biomech Eng* 2021; **143** [PMID: 33729441 DOI: 10.1115/1.4050539]
14 **Liu P**, Lv X, Li Y, Lv M. Stent-assisted coiling of ruptured wide-necked intracranial aneurysms: A single-center experience of 218 consecutive patients. *Neurol India* 2016; **64** Suppl: S70-S77 [PMID: 26954972 DOI: 10.4103/0028-3886.178045]
15 **Li L**, Zhang X, Feng Z, Zhao R, Hong B, Xu Y, Huang Q, Liu J. Risk Factors for Intraprocedural Rupture in the Endovascular Treatment of Unruptured Intracranial Aneurysms: A Single-Center Experience with 1232 Procedures. *World Neurosurg* 2019; **123**: e9-e14 [PMID: 30278291 DOI: 10.1016/j.wneu.2018.09.164]
16 **Park YK**, Yi HJ, Choi KS, Lee YJ, Chun HJ. Intraprocedural Rupture During Endovascular Treatment of Intracranial Aneurysm: Clinical Results and Literature Review. *World Neurosurg* 2018; **114**: e605-e615 [PMID: 29548958 DOI: 10.1016/j.wneu.2018.03.040]
17 **Egashira Y**, Yoshimura S, Enomoto Y, Ishiguro M, Asano T, Iwama T. Ultra-early endovascular embolization of ruptured cerebral aneurysm and the increased risk of hematoma growth unrelated to aneurysmal rebleeding. *J Neurosurg* 2013; **118**: 1003-1008 [PMID: 23240702 DOI: 10.3171/2012.11.JNS12610]
18 **Ye J**, Zheng P, Hassan M, Jiang S, Zheng J. Relationship of the angle between the A1 and A2 segments of the anterior cerebral artery with formation and rupture of anterior communicating artery aneurysm. *J Neurol Sci* 2017; **375**: 170-174 [PMID: 28320123 DOI: 10.1016/j.jns.2017.01.062]
19 **Jabbarli R**, Reinhard M, Roelz R, Kaier K, Weyerbrock A, Taschner C, Scheiwe C, Shah M. Clinical relevance of anterior cerebral artery asymmetry in aneurysmal subarachnoid hemorrhage. *J Neurosurg* 2017; **127**: 1070-1076 [PMID: 28009232 DOI: 10.3171/2016.9.JNS161706]
20 **Yang F**, Li H, Wu J, Li M, Chen X, Jiang P, Li Z, Cao Y, Wang S. Relationship of A1 Segment Hypoplasia with the Radiologic and Clinical Outcomes of Surgical Clipping of Anterior Communicating Artery Aneurysms. *World Neurosurg* 2017; **106**: 806-812 [PMID: 28765030 DOI: 10.1016/j.wneu.2017.07.122]
21 **Feng X**, Peng F, Miao Z, Tong X, Niu H, Zhang B, Wang L, Guo E, Qi P, Lu J, Mo D, Wu Z, Wang D, Liu A. Procedural Complications and Factors Influencing Immediate Angiographic Results after Endovascular Treatment of Small (<5 mm) Ruptured Intracranial Aneurysms. *J Stroke Cerebrovasc Dis* 2020; **29**: 104624 [PMID: 32222417 DOI: 10.1016/j.jstrokecerebrovasdis.2019.104624]
22 **Uchikawa Y**, Mori K, Shiigai M, Konishi T, Hoshiai S, Ishigro T, Hiyama T, Nakai Y, Minami M. Double Coaxial Microcatheter Technique for Glue Embolization of Renal Arteriovenous Malformations. *Cardiovasc Intervent Radiol* 2015; **38**: 1277-1283 [PMID: 26253779 DOI: 10.1007/s00270-015-1188-y]

23 **Arboix A**, Martí-Vilalta JL. Predictive clinical factors of very early in-hospital mortality in subarachnoid hemorrhage. *Clin Neurol Neurosurg* 1999; **101**: 100-105 [PMID: 10467904 DOI: 10.1016/s0303-8467(99)00026-8]

World Journal of Clinical Cases

Submit a Manuscript: https://www.f6publishing.com

World J Clin Cases 2024 May 26; 12(15): 2542-2550

DOI: 10.12998/wjcc.v12.i15.2542

ISSN 2307-8960 (online)

ORIGINAL ARTICLE

Observational Study

Efficacy and safety of carrimycin in ten patients with severe pneumonia following solid organ transplantation

Xian-Quan Cui, Lu-Wei Zhang, Peng Zhao, Jing-Jing Feng

Specialty type: Medicine, research and experimental

Provenance and peer review: Unsolicited article; Externally peer reviewed.

Peer-review model: Single blind

Peer-review report's scientific quality classification

Grade A (Excellent): 0
Grade B (Very good): 0
Grade C (Good): C
Grade D (Fair): 0
Grade E (Poor): 0

P-Reviewer: Koerkamp BG, Netherlands

Received: January 25, 2024
Peer-review started: January 25, 2024
First decision: February 8, 2024
Revised: February 24, 2024
Accepted: March 28, 2024
Article in press: March 28, 2024
Published online: May 26, 2024

Xian-Quan Cui, Peng Zhao, Department of Organ Transplantation, Qilu Hospital of Shandong University, Jinan 250012, Shandong Province, China

Lu-Wei Zhang, Jing-Jing Feng, Department of Blood Purification, Qilu Hospital of Shandong University, Jinan 250012, Shandong Province, China

Corresponding author: Jing-Jing Feng, MBBS, Doctor, Department of Blood Purification, Qilu Hospital of Shandong University, No. 107 Wenhua West Road, Jinan 250012, Shandong Province, China. feng.jing.jing@126.com

Abstract

BACKGROUND

The number of patients undergoing solid organ transplantation has increased annually. However, infections in solid organ transplant recipients can have a severe effect on patient survival owing to the continued use of immunosuppressants. Carrimycin is a novel macrolide antibiotic produced by genetically engineered streptomyces spiramyceticus harboring a 4''-O-isovaleryltransferase gene (ist) from streptomyces thermotoleran. Carrimycin has good antibacterial and antiviral effects. However, no relevant studies have been conducted on the efficacy and safety of carrimycin in patients with severe pneumonia (SP) after solid organ transplantation.

AIM

To explore the efficacy and safety of carrimycin in patients with SP after solid organ transplantation to provide a medication reference for clinical treatment.

METHODS

In March 2022, ten patients with SP following solid-organ transplantation were treated at our hospital between January 2021 and March 2022. When the condition was critical and difficult to control with other drugs, carrimycin was administered. These ten patients' clinical features and treatment protocols were retrospectively analyzed, and the efficacy and safety of carrimycin for treating SP following solid organ transplantation were evaluated.

RESULTS

All ten patients were included in the analysis. Regarding etiological agent detection, there were three cases of fungal pneumonia, two cases of bacterial pneumonia, two cases of Pneumocystis pneumonia, and three cases of mixed

infections. After treatment with carrimycin, the disease in seven patients significantly improved, the course of the disease was significantly shortened, fever was quickly controlled, chest computed tomography was significantly improved, and oxygenation was significantly improved. Finally, the patients were discharged after curing. One patient died of acute respiratory distress syndrome, and two patients discontinued treatment.

CONCLUSION
Carrimycin is a safe and effective treatment modality for SP following solid organ transplantation. Carrimycin may have antibacterial and antiviral effects in patients with SP following solid organ transplantation.

Key Words: Carrimycin; Organ transplantation; Severe pneumonia; Immunosuppressant; Infection; Antiviral drugs

Core Tip: In this study, the clinical features and treatment projects of 10 cases of severe pneumonia (SP) after solid organ transplantation were retrospectively analyzed. It was conformed that carrimycin is a safe and effective modality in the treatment of SP after solid organ transplantation.

Citation: Cui XQ, Zhang LW, Zhao P, Feng JJ. Efficacy and safety of carrimycin in ten patients with severe pneumonia following solid organ transplantation. *World J Clin Cases* 2024; 12(15): 2542-2550
URL: https://www.wjgnet.com/2307-8960/full/v12/i15/2542.htm
DOI: https://dx.doi.org/10.12998/wjcc.v12.i15.2542

INTRODUCTION

The number of patients undergoing solid-organ transplantation (SOT) is increasing. Post-operative complications can severely affect patient survival[1]. Among these, pneumonia is a frequent infectious complication of SOT. It is considered the chief cause of morbidity and mortality in renal allograft recipients due to the continued use of immunosuppressants [2,3]. Pneumonia can lead to acute respiratory distress syndrome (ARDS)[4], with an occurrence rate ranging from 0.2% to 4.3%[5,6] and a mortality rate of 22.5%–67%[7-11]. The mortality rate has been reported to be nearly 100% in patients on ventilation[12]. However, the curative effect of conventional drugs is often poor and seriously puzzling for clinicians.

Carrimycin is a novel macrolide antibiotic produced by genetically engineered streptomyces spiramyceticus harboring a 4''-O-isovaleryltransferase gene (ist) from streptomyces thermotolerans. Carrimycin is a broad-spectrum antibacterial agent and is effective against Gram-positive cocci, β-lactamase-producing bacteria, *Mycoplasma*, and *Chlamydia*, as well as some Gram-negative bacilli and fungi. Additionally, it has been reported that carrimycin can be used to treat Coronavirus disease 2019 (COVID-19) with good therapeutic effect[13]. Previous studies have verified the antitumor effects of carrimycin *in vitro* and *in vivo*[14].

However, no relevant studies have been conducted on the efficacy of carrimycin in patients with post-SOT infections. In this study, we investigated the efficacy and safety of carrimycin in SOT recipients *in vitro* and *in vivo* for the first time between January 2021 and March 2022; 10 patients with severe pneumonia (SP) following SOT were treated at our hospital. When the condition was critical and difficult to control with other drugs, carrimycin was administered. Through a retrospective analysis and summary of the clinical data of these patients, this study preliminarily discusses the efficacy and safety of carrimycin for treating SP following SOT to provide a medication reference for clinical treatment.

MATERIALS AND METHODS

Clinical characteristics

Among the ten patients, there were six males and four females, aged 27-63 years, all of whom underwent transplantation for the first time, including nine renal transplant recipients and one liver transplant recipient (Table 1).

Diagnostic criteria of SP after SOT

In this study, the diagnostic criteria of SP following SOT were based on the American Thoracic Society criteria and slightly adjusted in combination with the characteristics of SOT[15]: (1) Long-term application of immunosuppressants after SOT; (2) clinical symptoms of persistent fever, cough and progressive dyspnea; (3) an aspiratory rate > 30 *per* min; (4) an arterial oxygen partial pressure/oxygen inspiratory fraction (PaO_2/FiO_2) ratio < 250; and (5) chest film pneumonia showed and rapidly expanded by more than 50% in a short time. Diagnostic criteria of ARDS[16]: (1) Timing: Acute onset; (2) oxygenation: $PaO_2/FiO_2 \leq 200$ mmHg regardless of positive end-expiratory pressure; (3) chest radiograph: Bilateral infiltrates seen on frontal chest radiograph; and (4) airway pressure: ≤ 18 mm Hg when measured or no clinical evidence of left atrial hypertension.

Table 1 Clinical characteristics of 10 patients with severe pneumonia after solid organ transplantation

Recipient	Gender	Age	Type of transplanted organ	Transplant time
1	Male	46	Renal transplantation	27 d
2	Male	63	Renal transplantation	5 months
3	Female	34	Renal transplantation	13 months
4	Male	55	Liver transplantation	7 d
5	Male	56	Renal transplantation	4 months
6	Female	27	Renal transplantation	5 months
7	Female	55	Renal transplantation	3 months
8	Male	60	Renal transplantation	16 yr
9	Male	27	Renal transplantation	4 months
10	Female	40	Renal transplantation	7 yr

Immunosuppressive regimens

Eight patients (excluding cases 4 and 8), were treated with basiliximab or anti-thymocyte globulin for immunity induction therapy. Methylprednisolone (1000 mg) was administered intravenously during surgery, and methylprednisolone (500 mg/d) was administered intravenously for two consecutive d after transplantation. Methylprednisolone tablets were administered orally at 0.8 mg/kg·d on the fourth day after transplantation, decreasing by 4 mg *per* d to 16 mg/d and then by 4 mg per wk to 4 mg/d. After transplantation, except in case 8, cyclosporine + mycophenolate mofetil + methylprednisolone was administered; in the other 9 cases, tacrolimus + mycophenolate mofetil + methylprednisolone was administered. The blood tacrolimus and cyclosporine concentrations were maintained at 5-10 ng/mL, and the concentration of cyclosporine was maintained at 100-150 ng/mL. The dosage of mycophenolate mofetil used was 1000-1500 mg/d.

The time and clinical characteristics of infection

According to Rubinl's "infection schedule" stage[17], the time distribution of SP cases in this group is 2 cases (20%, 2/10) in the first month after surgery, 5 cases (50%, 5/10) in 2–6 months, and 3 cases (30%, 3/10) after 6 months. Clinical features: (1) Most patients have a regular temperature, but some present low or high fever. Fever was evident in the morning. The onset of fever is often delayed by 1–2 h daily. After sweating, the fever resolved. A few patients showed massive sweating, but their body temperatures were normal. When they developed a high fever, it was mostly persistent; and (2) there may be no obvious dyspnea symptoms in the early stage, followed by chest tightness, suffocation, accelerated heart rate, and other symptoms that worsen after activity, with or without coughing. No sputum was detected in the early or middle stages, and blood gas analysis indicated severe hypoxemia; (3) this disease progresses rapidly. After the symptoms of dyspnea and hypoxia, the disease progresses rapidly. Although noninvasive or invasive ventilation is used, some patients die from respiratory failure; and (4) it is often accompanied by multiple-organ dysfunction syndrome (MODS).

Treatment protocols

According to our center's experience, we summarized the "five early" scheme for treating pulmonary infection after SOT. (1) Early discontinuation of immunosuppressants. Immunosuppressants were discontinued immediately after the patient experienced symptoms of hypoxia. During this period, rejection generally does not occur due to patients' excessive immunosuppressive state; (2) early use of glucocorticoids. Glucocorticoids have anti-inflammatory and anti-rejection effects. The dose and frequency of methylprednisolone administration were determined based on the patient's body temperature. The dose was 40–80 mg every 12 h in the early stages. After the body temperature normalized for 3 d, methylprednisolone was gradually reduced to 40 mg qd and then changed to oral methylprednisolone tablets for maintenance; (3) early use of human immunoglobulin. The dosage of human immunoglobulin is 0.5 g/(kg/d), which is usually treated for 3-5 d. The course of treatment and dosage should be adjusted according to the patient's situation; (4) early combined use of multiple drugs. It can be seen from the ten patients in this study that before the pathogen is determined, the treatment needs to include gram-positive bacteria, gram-negative bacteria, fungi, viruses, and *Pneumocystis yersiniae*. After identifying the pathogen, select the appropriate anti-infective drugs according to the pathogen (Table 2); and (5) early use of noninvasive ventilation. For patients with hypoxemia on blood gas analysis, the early use of non-invasive ventilation is conducive to reducing respiratory muscle fatigue, improving ventilation function, reducing lung injury, and reducing oxygen consumption. Delayed treatment may aggravate the patient's disease and lead to the use of invasive ventilation, resulting in complications such as ventilator-associated pneumonia. In addition, attention should be paid to increasing the patients' nutrition and treating hypoproteinemia, which is conducive to maintaining blood pressure stability and improving immunity. For those who had used the above measures and were still worsening, carrimycin was used for treatment. The dose of carrimycin was 400 mg orally on the first day and 200 mg orally every d for seven d.

Table 2 Treatment protocols of 10 patients with severe pneumonia after solid organ transplantation

Recipient	Treatment protocols
1	Carrimycin + Vancocin + Levofloxacin
2	Carrimycin + Amphotericin B
3	Carrimycin + Caspofungin + Trimethoprim-sulfamethoxazole
4	Carrimycin + Meropenem + Linezolid + Caspofungin
5	Carrimycin + Ganciclovir + Moxifloxacin + Trimethoprim-sulfamethoxazole + Peramivir
6	Carrimycin + Caspofungin + Piperacillin sodium and tazobactam sodium + Imipenem + Trimethoprim-sulfamethoxazole
7	Carrimycin + Meropenem + Azithromycin + Caspofungin
8	Carrimycin + Moxifloxacin + Ganciclovir + Peramivir + Imipenem + Piperacillin sodium and tazobactam sodium + Tigecycline + Linezolid + Fluconazole
9	Carrimycin + Caspofungin + Trimethoprim-sulfamethoxazole + Imipenem + Moxifloxacin
10	Carrimycin + Imipenem + Ganciclovir + Voriconazole

RESULTS

Pathogens

There were three cases of fungal pneumonia, two cases of bacterial pneumonia, two cases of pneumocystis pneumonia, and three cases with mixed infections (Table 3).

After treatment with carrimycin, the disease in seven patients significantly improved, the course of disease was significantly shortened, fever was quickly controlled, chest computed tomography was significantly improved (Figure 1), and oxygenation was significantly improved. Finally, all anti-infective drugs were gradually discontinued, and the patients were discharged after treatment. One patient died from ARDS, and two patients discontinued treatment (Table 4).

DISCUSSION

After transplantation, patients require immunosuppressants for anti-rejection therapy. Immunosuppressants include cyclosporine, tacrolimus, prednisone, and mycophenolate mofetil, which can prevent rejection by inhibiting cellular and humoral immunity; however, long-term use of immunosuppressants weakens the immunity of patients. Compared to the general population, infections in SOT recipients are far more complicated and prone to opportunistic infections, mixed infections, rare bacterial infections, and severe infections, making diagnosis more difficult. Delayed diagnosis leads to delayed treatment and poor prognosis[18,19].

Pneumonia is a major threat in renal allograft recipients[20]. According to various studies, pneumonia rates range from 4.5% to 20%[21-28], and pneumonia accounts for 8%–70.3% of all infectious complications[29-32] following kidney transplantation. SP can lead to cellular immune disorders and pro- and anti-inflammatory cytokine imbalances[33]. SP is characterized by occult onset, rapid progress, difficulty in identifying pathogens, and poor treatment effects, and can develop into respiratory failure and even systemic failure in a short time. SP easily develops into ARDS, which is the most direct cause of death in patients with pulmonary infection after renal transplantation[34]. Bacteria are the most common pathogens causing infections after SOT, particularly in the early post-transplantation period[35,36]. In addition to bacterial infections, many other pathogens, such as viruses, fungi, *Mycoplasma*, and *Pneumocystis jirovecii*, can also cause pneumonia. With the application of next generation sequencing technology, bronchoalveolar lavage, and other technologies, the technology for identifying pathogens is improving; however, some patients are still unable to identify pathogens in a short time, resulting in disease progression and even death.

In terms of treatment, we generally use high-efficiency broad-spectrum antibiotics after admission, combined with antiviral, anti-*Pneumocystis yersinia*, and antifungal drugs. However, multiple previous hospitalizations, invasive interventions, and prior antibiotic use make SOT recipients susceptible to colonization by nosocomial and antibiotic-resistant pathogens, including Methicillin-resistant *Staphylococcus* aureus, vancomycin-resistant *Enterococcus*, and resistant gram-negative bacilli[37-39]. Patients with SP often exhibit anorexia, and the body is in a highly decomposed state, resulting in malnutrition and a further reduction in immune function. Therefore, conventional drugs typically have poor efficacy. When patients are infected, many inflammatory mediators and cytokines released during the inflammatory reaction cause acute lung injury, which can cause ARDS and even lead to systemic inflammatory response syndrome and MODS[40]. Although various treatment measures have been adopted, the condition of some patients cannot be effectively controlled. Therefore, there is an urgent need to identify drugs with good antibacterial activity and low biotoxicity.

Carrimycin is a new class I drug developed by the Institute of Pharmaceutical Biotechnology of the Chinese Academy of Medical Sciences. Shenyang Tonglian Group Co., Ltd. Carrimycin was approved for listing in June 2019. It is a new drug with independent intellectual property rights in China. Carrimycin is a genetically engineered drug developed

Table 3 Pathogens of 10 patients with severe pneumonia after solid organ

Recipients	Pathogens
1	*Legionnella* + *Corynebacterium striatum*
2	*Mucor*
3	*Pneumocystis jirovecii*
4	*Baumanii* + *Staphylococcus epidermidis*
5	*Pneumocystis jirovecii* + *Cytomegalovirus*
6	*Pneumocystis jirovecii*
7	*Haemophilus parainfluenzae* + *Mycoplasma*
8	*Acinetobacter* + *Coronavirus*
9	*Acinetobacter*
10	*Aspergillus*

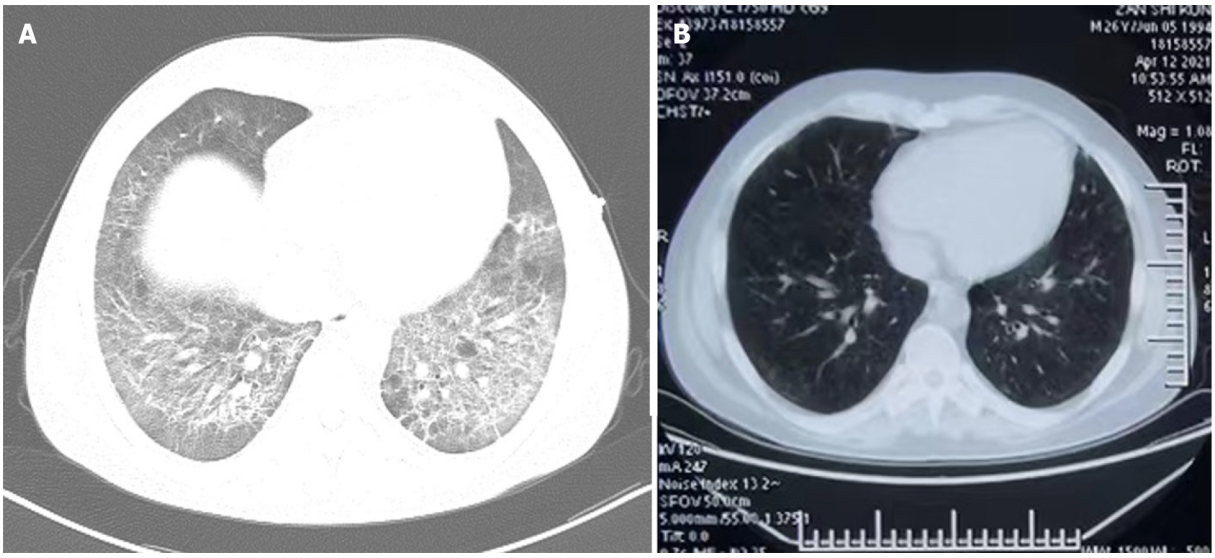

Figure 1 Chest computed tomography images before and after treatment with carrimycin. A: Chest computed tomography (CT) images before treatment with carrimycin; B: Chest CT images after treatment with carrimycin.

using synthetic biological technology and belongs to the macrolide class of antibiotics. The main components of carrimycin were isovalerylspiramycin III, II, and I (Figure 2), with minor components consisting of butyrylspiramycin III, propionylspiramycin III, acetylspiramycin III, butyrylspiramycin II, propionylspiramycin II, acetylspiramycin II[41-44]. Compared with acylspiramycin, the longer alkyl chains at position 4'' render carrimycin increased antibacterial potency, especially *in vivo*, because of its higher lipophilicity[45,46].

The China Food and Drug Administration approved carrimycin for the treatment of acute tracheal bronchitis caused by *Haemophilus influenzae, Streptococcus pneumoniae* and acute sinusitis caused by *Streptococcus pneumoniae, Haemophilus influenzae, Streptococcus pyogenes, Moraxella catarrhalis*, and *Staphylococcus*. Carrimycin can inhibit bacterial protein synthesis by blocking the activity of peptidyl transferase in the 50s ribosome, which can directly inhibit bacterial growth. Carrimycin can combine with peroxide-scavenging enzymes to induce peroxide and destroy biological macromolecules such as DNA to achieve sterilization (Table 5). *In vivo*, carrimycin can promote neutrophils to migrate to inflammatory sites to destroy and phagocytize bacteria and damaged cells and enhance the phagocytosis of macrophages to regulate immunity and enhance resistance. In addition, capreomycin also plays a certain role in inhibiting inflammation and improving inflammation and edema of important organs such as the heart and lungs. A pharmacokinetic study of carrimycin confirmed that its half-life was longer than that of spiramycin, and some metabolites of carrimycin maintained antibacterial activity. The tissue permeability of carrimycin is enhanced, and it has a marked post-antibiotic effect[46]. Carrimycin has broad prospects in clinical applications, but there has been no research on the application of carrimycin in SP following SOT.

Based on our previous observations, we found that the use of carrimycin in patients with low immune function often achieved unexpected results. The specific mechanism is unclear, which may be related to clindamycin improving T lymphocyte function and repairing immune damage. Therefore, we administered carrimycin to patients receiving long-term oral immunosuppressants after organ transplantation. The ten patients in this study were treated with carrimycin

Table 4 Outcomes of 10 patients with severe pneumonia after solid organ transplantation

Recipient	Outcome of transplants	Clinical outcomes
1	Remove	Abandoning treatment
2	Normal	Cure
3	Normal	Death
4	Normal	Cure
5	Normal	Cure
6	Normal	Abandoning treatment
7	Normal	Cure
8	Normal	Cure
9	Normal	Cure
10	Normal	Cure

Table 5 Antibacterial spectrum of carrimycin found so far

Pathogens	Antimicrobial spectrum
Gram-positive bacterium	*Streptococcus pneumoniae, Streptococcus pyogenes, Streptococcus agalactiae, Streptococcus digestae, Other Streptococcus, Staphylococcus aureus, Legionella pneumophila*
Gram-negative bacterium	*Haemophilus influenzae, Moraxella catarrh, Neisseria gonorrhoeae*
Anaerobe	*Digestococcus, Bacteroid, Clostridium, Prevotella, Propionibacterium*
Atypical pathogens	*Mycoplasma pneumoniae, Ureaplasma urealyticum, Chlamydia trachomatis, Chlamydia pneumonia*

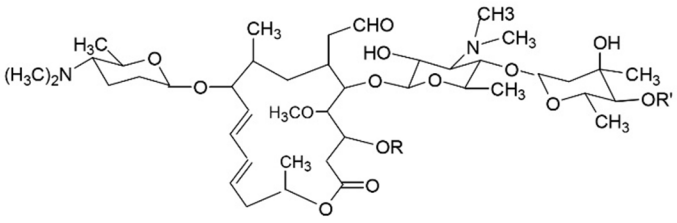

Figure 2 Molecular structure of three main components of carrimycin. Isovaleryl spiramycin I: R = H, molecular formula: C48H82N2O15, molecular weight: 926; Isovaleryl spiramycin II: R = COCH3, molecular formula: C50H84N2O16, molecular weight: 968; Isovaleryl spiramycin III: R = COCH2COCH3, molecular formula: C51H86N2O16, molecular weight: 982.

following poor response to other drugs. Carrimycin treatment was found to be effective. It is speculated that this is related to the direct bactericidal and bacteriostatic effects of carrimycin, which may also be related to the effects of carrimycin in improving immune function and repairing tissue damage. Our center will further study the specific mechanisms of action of carrimycin in improving the immune function of patients.

In addition, among the ten patients treated with carrimycin, case 5 was complicated by cytomegalovirus infection, and case 8 was complicated by coronavirus infection. After treatment with carrimycin, these patients showed positive effects, suggesting that carrimycin may have antiviral effects. Our results are consistent with those of previous studies, which have found that the main active component of carrimycin strongly binds the angiotensin-converting enzyme type 2 receptor protein and can also bind to the 3-chymotrypsin-like protease binding site; therefore, it has great potential value and unique therapeutic advantages in anti-Severe acute respiratory syndrome coronavirus 2 infection[13]. However, further studies are required to confirm the antiviral effects of carrimycin.

This study has some limitations. As our study had only a comparatively small number of samples from a single center, more studies need to verify the general applicability of our research conclusions. In addition, more research is needed on the timing, course of treatment, and antibacterial spectrum of carrimycin for treating pulmonary infections in SOT recipients. Our center will continue to collect clinical data on carrimycin in treating SP in SOT recipients to make a more reliable evidence-based evaluation of its efficacy and safety and provide new medication options for treating SP in SOT recipients.

CONCLUSION

This study found that carrimycin is safe and effective for treating SP in SOT recipients. Because carrimycin is a newly developed drug in China, many current experimental studies are based on basic and animal trials. The efficacy and safety of carrimycin in clinical treatment require further confirmation of clinical data.

FOOTNOTES

Author contributions: Cui XQ and Zhang LW designed this study and wrote the manuscript; Zhao P participated in collection and analysis of data; Feng JJ reviewed and revised the manuscript. All authors read and approved the final manuscript.

Institutional review board statement: The study was reviewed and approved by Qilu Hospital of Shandong University Institutional Review Board (Approval No. KYLL-202306-099).

Informed consent statement: The study was reviewed and approved for exemption from informed consent by the Institutional Review Board of Qilu Hospital, Shandong University.

Conflict-of-interest statement: All the authors declare that they have no conflict of interest.

Data sharing statement: All data are kept by the corresponding author and can be released upon reasonable request.

STROBE statement: The authors have read the STROBE Statement -checklist of items, and the manuscript was prepared and revised according to the STROBE Statement- checklist of items.

Country/Territory of origin: China

ORCID number: Jing-Jing Feng 0000-0001-6746-2865.

S-Editor: Liu H
L-Editor: A
P-Editor: Yu HG

REFERENCES

1 **Wolfe RA**, Roys EC, Merion RM. Trends in organ donation and transplantation in the United States, 1999-2008. *Am J Transplant* 2010; **10**: 961-972 [PMID: 20420646 DOI: 10.1111/j.1600-6143.2010.03021.x]
2 **Dulek DE**, Mueller NJ; AST Infectious Diseases Community of Practice. Pneumonia in solid organ transplantation: Guidelines from the American Society of Transplantation Infectious Diseases Community of Practice. *Clin Transplant* 2019; **33**: e13545 [PMID: 30900275 DOI: 10.1111/ctr.13545]
3 **Wilmes D**, Coche E, Rodriguez-Villalobos H, Kanaan N. Bacterial pneumonia in kidney transplant recipients. *Respir Med* 2018; **137**: 89-94 [PMID: 29605219 DOI: 10.1016/j.rmed.2018.02.022]
4 **Dong B**, Wang Y, Wang G, Wang W, Zhou H, Fu Y. A retrospective study of cytomegalovirus pneumonia in renal transplant patients. *Exp Ther Med* 2014; **7**: 1111-1115 [PMID: 24940395 DOI: 10.3892/etm.2014.1577]
5 **Shih CJ**, Tarng DC, Yang WC, Yang CY. Immunosuppressant dose reduction and long-term rejection risk in renal transplant recipients with severe bacterial pneumonia. *Singapore Med J* 2014; **55**: 372-377 [PMID: 25091886 DOI: 10.11622/smedj.2014089]
6 **Shorr AF**, Abbott KC, Agadoa LY. Acute respiratory distress syndrome after kidney transplantation: epidemiology, risk factors, and outcomes. *Crit Care Med* 2003; **31**: 1325-1330 [PMID: 12771598 DOI: 10.1097/01.CCM.0000053645.38356.A6]
7 **Canet E**, Osman D, Lambert J, Guitton C, Heng AE, Argaud L, Klouche K, Mourad G, Legendre C, Timsit JF, Rondeau E, Hourmant M, Durrbach A, Glotz D, Souweine B, Schlemmer B, Azoulay E. Acute respiratory failure in kidney transplant recipients: a multicenter study. *Crit Care* 2011; **15**: R91 [PMID: 21385434 DOI: 10.1186/cc10091]
8 **Candan S**, Pirat A, Varol G, Torgay A, Zeyneloglu P, Arslan G. Respiratory problems in renal transplant recipients admitted to intensive care during long-term follow-up. *Transplant Proc* 2006; **38**: 1354-1356 [PMID: 16797301 DOI: 10.1016/j.transproceed.2006.02.083]
9 **Kirilov D**, Cohen J, Shapiro M, Grozovski E, Singer P. The course and outcome of renal transplant recipients admitted to a general intensive care unit. *Transplant Proc* 2003; **35**: 606 [PMID: 12644065 DOI: 10.1016/s0041-1345(03)00007-1]
10 **Sun Q**, Liu ZH, Chen J, Ji S, Tang Z, Cheng Z, Ji D, Li LS. An aggressive systematic strategy for acute respiratory distress syndrome caused by severe pneumonia after renal transplantation. *Transpl Int* 2006; **19**: 110-116 [PMID: 16441359 DOI: 10.1111/j.1432-2277.2005.00245.x]
11 **Tu GW**, Ju MJ, Zheng YJ, Zhu DM, Xu M, Rong RM, Zhu TY, Luo Z. An interdisciplinary approach for renal transplant recipients with severe pneumonia: a single ICU experience. *Intensive Care Med* 2014; **40**: 914-915 [PMID: 24777707 DOI: 10.1007/s00134-014-3296-6]
12 **Capulong MG**, Mendoza M, Chavez J. Cytomegalovirus pneumonia in renal transplant patients. *Transplant Proc* 1998; **30**: 3151-3153

[PMID: 9838394 DOI: 10.1016/s0041-1345(98)00973-7]

13 **Yan H**, Sun J, Wang K, Wang H, Wu S, Bao L, He W, Wang D, Zhu A, Zhang T, Gao R, Dong B, Li J, Yang L, Zhong M, Lv Q, Qin F, Zhuang Z, Huang X, Yang X, Li Y, Che Y, Jiang J. Repurposing carrimycin as an antiviral agent against human coronaviruses, including the currently pandemic SARS-CoV-2. *Acta Pharm Sin B* 2021; **11**: 2850-2858 [PMID: 33723501 DOI: 10.1016/j.apsb.2021.02.024]

14 **Liang SY**, Zhao TC, Zhou ZH, Ju WT, Liu Y, Tan YR, Zhu DW, Zhang ZY, Zhong LP. Anti-tumor effect of carrimycin on oral squamous cell carcinoma cells in vitro and in vivo. *Transl Oncol* 2021; **14**: 101074 [PMID: 33744726 DOI: 10.1016/j.tranon.2021.101074]

15 **Mandell LA**, Wunderink RG, Anzueto A, Bartlett JG, Campbell GD, Dean NC, Dowell SF, File TM Jr, Musher DM, Niederman MS, Torres A, Whitney CG; Infectious Diseases Society of America; American Thoracic Society. Infectious Diseases Society of America/American Thoracic Society consensus guidelines on the management of community-acquired pneumonia in adults. *Clin Infect Dis* 2007; **44** Suppl 2: S27-S72 [PMID: 17278083 DOI: 10.1086/511159]

16 **Bernard GR**, Artigas A, Brigham KL, Carlet J, Falke K, Hudson L, Lamy M, LeGall JR, Morris A, Spragg R. Report of the American-European consensus conference on ARDS: definitions, mechanisms, relevant outcomes and clinical trial coordination. The Consensus Committee. *Intensive Care Med* 1994; **20**: 225-232 [PMID: 8014293 DOI: 10.1007/bf01704707]

17 **Rubin RH**, Ikonen T, Gummert JF, Morris RE. The therapeutic prescription for the organ transplant recipient: the linkage of immunosuppression and antimicrobial strategies. *Transpl Infect Dis* 1999; **1**: 29-39 [PMID: 11428969 DOI: 10.1034/j.1399-3062.1999.10104.x]

18 **Xu Y**, Jin T. Manipulating cell motility by Legionella: Speeding up or slowing down? *J Transl Int Med* 2023; **11**: 24-25 [PMID: 37223615 DOI: 10.2478/jtim-2022-0064]

19 **Xu Z**, Mo X, Kong Y, Wen Q, Han T, Lyu M, Xu L, Chang Y, Zhang X, Huang X, Wang Y. Mini-dose methotrexate combined with methylprednisolone as a first-line treatment for acute graft-versus-host disease: A phase 2 trial. *J Transl Int Med* 2023; **11**: 255-264 [PMID: 37662885 DOI: 10.2478/jtim-2023-0111]

20 **Jackson KR**, Motter JD, Bae S, Kernodle A, Long JJ, Werbel W, Avery R, Durand C, Massie AB, Desai N, Garonzik-Wang J, Segev DL. Characterizing the landscape and impact of infections following kidney transplantation. *Am J Transplant* 2021; **21**: 198-207 [PMID: 32506639 DOI: 10.1111/ajt.16106]

21 **Yıldırım F**, Karaman İ, Kaya A. Current situation in ARDS in the light of recent studies: Classification, epidemiology and pharmacotherapeutics. *Tuberk Toraks* 2021; **69**: 535-546 [PMID: 34957747 DOI: 10.5578/tt.20219611]

22 **Shah A**, Shah M. Advancement of deep learning in pneumonia/Covid-19 classification and localization: A systematic review with qualitative and quantitative analysis. *Chronic Dis Transl Med* 2022; **8**: 154-171 [PMID: 35572951 DOI: 10.1002/cdt3.17]

23 **Pourmand G**, Salem S, Mehrsai A, Taherimahmoudi M, Ebrahimi R, Pourmand MR. Infectious complications after kidney transplantation: a single-center experience. *Transpl Infect Dis* 2007; **9**: 302-309 [PMID: 17511823 DOI: 10.1111/j.1399-3062.2007.00229.x]

24 **García-Prado ME**, Cordero E, Cabello V, Pereira P, Torrubia FJ, Ruíz M, Cisneros JM. [Infectious complications in 159 consecutive kidney transplant recipients]. *Enferm Infecc Microbiol Clin* 2009; **27**: 22-27 [PMID: 19217999 DOI: 10.1016/j.eimc.2008.02.004]

25 **Veroux M**, Giuffrida G, Corona D, Gagliano M, Scriffignano V, Vizcarra D, Tallarita T, Zerbo D, Virgilio C, Sciacca A, Cappello D, Stefani S, Veroux P. Infective complications in renal allograft recipients: epidemiology and outcome. *Transplant Proc* 2008; **40**: 1873-1876 [PMID: 18675076 DOI: 10.1016/j.transproceed.2008.05.065]

26 **Charfeddine K**, Zaghden S, Kharrat M, Kamoun K, Jarraya F, Hachicha J. Infectious complications in kidney transplant recipients: a single-center experience. *Transplant Proc* 2005; **37**: 2823-2825 [PMID: 16182820 DOI: 10.1016/j.transproceed.2005.05.009]

27 **Kalra V**, Agarwal SK, Khilnani GC, Kapil A, Dar L, Singh UB, Mirdha BR, Xess I, Gupta S, Bhowmik D, Tiwari SC, Dash SC. Spectrum of pulmonary infections in renal transplant recipients in the tropics: a single center study. *Int Urol Nephrol* 2005; **37**: 551-559 [PMID: 16307341 DOI: 10.1007/s11255-005-4012-9]

28 **Sileri P**, Pursell KJ, Coady NT, Giacomoni A, Berliti S, Tzoracoleftherakis E, Testa G, Benedetti E. A standardized protocol for the treatment of severe pneumonia in kidney transplant recipients. *Clin Transplant* 2002; **16**: 450-454 [PMID: 12437626 DOI: 10.1034/j.1399-0012.2002.02079.x]

29 **de Carvalho MA**, Freitas FG, Silva Junior HT, Bafi AT, Machado FR, Pestana JO. Mortality predictors in renal transplant recipients with severe sepsis and septic shock. *PLoS One* 2014; **9**: e111610 [PMID: 25369197 DOI: 10.1371/journal.pone.0111610]

30 **Bige N**, Zafrani L, Lambert J, Peraldi MN, Snanoudj R, Reuter D, Legendre C, Chevret S, Lemiale V, Schlemmer B, Azoulay E, Canet E. Severe infections requiring intensive care unit admission in kidney transplant recipients: impact on graft outcome. *Transpl Infect Dis* 2014; **16**: 588-596 [PMID: 24966154 DOI: 10.1111/tid.12249]

31 **Alangaden GJ**, Thyagarajan R, Gruber SA, Morawski K, Garnick J, El-Amm JM, West MS, Sillix DH, Chandrasekar PH, Haririan A. Infectious complications after kidney transplantation: current epidemiology and associated risk factors. *Clin Transplant* 2006; **20**: 401-409 [PMID: 16842513 DOI: 10.1111/j.1399-0012.2006.00519.x]

32 **Mouloudi E**, Massa E, Georgiadou E, Iosifidis E, Katsika E, Rembelakos G, Gakis D, Imvrios G, Papanikolaou V, Papadopoulos S, Gritsi-Gerogianni N. Infections related to renal transplantation requiring intensive care admission: a 20-year study. *Transplant Proc* 2012; **44**: 2721-2723 [PMID: 23146504 DOI: 10.1016/j.transproceed.2012.09.023]

33 **Dukhinova M**, Kokinos E, Kuchur P, Komissarov A, Shtro A. Macrophage-derived cytokines in pneumonia: Linking cellular immunology and genetics. *Cytokine Growth Factor Rev* 2021; **59**: 46-61 [PMID: 33342718 DOI: 10.1016/j.cytogfr.2020.11.003]

34 **Lee I**, Barton TD. Viral respiratory tract infections in transplant patients: epidemiology, recognition and management. *Drugs* 2007; **67**: 1411-1427 [PMID: 17600390 DOI: 10.2165/00003495-200767100-00004]

35 **Garzoni C**; AST Infectious Diseases Community of Practice. Multiply resistant gram-positive bacteria methicillin-resistant, vancomycin-intermediate and vancomycin-resistant Staphylococcus aureus (MRSA, VISA, VRSA) in solid organ transplant recipients. *Am J Transplant* 2009; **9** Suppl 4: S41-S49 [PMID: 20070694 DOI: 10.1111/j.1600-6143.2009.02892.x]

36 **Shafiekhani M**, Mirjalili M, Vazin A. Prevalence, Risk Factors And Treatment Of The Most Common Gram-Negative Bacterial Infections In Liver Transplant Recipients: A Review. *Infect Drug Resist* 2019; **12**: 3485-3495 [PMID: 32009806 DOI: 10.2147/IDR.S226217]

37 **van Delden C**, Blumberg EA; AST Infectious Diseases Community of Practice. Multidrug resistant gram-negative bacteria in solid organ transplant recipients. *Am J Transplant* 2009; **9** Suppl 4: S27-S34 [PMID: 20070690 DOI: 10.1111/j.1600-6143.2009.02890.x]

38 **Cervera C**, van Delden C, Gavaldà J, Welte T, Akova M, Carratalà J; ESCMID Study Group for Infections in Compromised Hosts. Multidrug-resistant bacteria in solid organ transplant recipients. *Clin Microbiol Infect* 2014; **20** Suppl 7: 49-73 [PMID: 24861521 DOI: 10.1111/1469-0691.12687]

39 **Shafiekhani M**, Karimzadeh I, Nikeghbalian S, Firoozifar M, Pouladfar G, Vazin A. Comparison of Ceftizoxime Plus Ampicillin-Sulbactam versus Gentamicin Plus Ampicillin-Sulbactam in the Prevention of Post-Transplant Early Bacterial Infections in Liver Transplant Recipients: A Randomized Controlled Trial. *Infect Drug Resist* 2020; **13**: 89-98 [PMID: 32021323 DOI: 10.2147/IDR.S222934]

40 **Cao H**, Huang J, Chang J, Zhu Y, Liang J, Sun C, Lin J. Predictors of progression in idiopathic inflammatory myopathies with interstitial lung disease. *J Transl Int Med* 2023; **11**: 46-56 [PMID: 37533847 DOI: 10.2478/jtim-2022-0029]

41 **Lu Z**, Zhang X, Dai J, Wang Y, He W. Engineering of leucine-responsive regulatory protein improves spiramycin and bitespiramycin biosynthesis. *Microb Cell Fact* 2019; **18**: 38 [PMID: 30782164 DOI: 10.1186/s12934-019-1086-0]

42 **Sano M**, Sunazuka T, Tanaka H, Yamashita K, Okachi R, Omura S. Chemical modification of spiramycins. VI. Synthesis and antibacterial activities of 3,3"-di-O-acyl-4"-O-sulfonyl and 3,3"-di-O-acyl-4"-O-alkyl derivatives of spiramycin I. *J Antibiot (Tokyo)* 1985; **38**: 1350-1358 [PMID: 4066488 DOI: 10.7164/antibiotics.38.1350]

43 **Epp JK**, Huber ML, Turner JR, Goodson T, Schoner BE. Production of a hybrid macrolide antibiotic in Streptomyces ambofaciens and Streptomyces lividans by introduction of a cloned carbomycin biosynthetic gene from Streptomyces thermotolerans. *Gene* 1989; **85**: 293-301 [PMID: 2628170 DOI: 10.1016/0378-1119(89)90421-6]

44 **Guangdong S**, Jianlu D, Yiguang W. Construction and physiological studies on a stable bioengineered strain of shengjimycin. *J Antibiot (Tokyo)* 2001; **54**: 66-73 [PMID: 11269716 DOI: 10.7164/antibiotics.54.66]

45 **Shi XG**, Sun YM, Zhang YF, Zhong DF. Tissue distribution of bitespiramycin and spiramycin in rats. *Acta Pharmacol Sin* 2004; **25**: 1396-1401 [PMID: 15525458]

46 **Shi XG**, Fawcett JP, Chen XY, Zhong DF. Structural identification of bitespiramycin metabolites in rat: a single oral dose study. *Xenobiotica* 2005; **35**: 343-358 [PMID: 16019956 DOI: 10.1080/00498250500087580]

World Journal of Clinical Cases

Submit a Manuscript: https://www.f6publishing.com

World J Clin Cases 2024 May 26; 12(15): 2551-2559

DOI: 10.12998/wjcc.v12.i15.2551

ISSN 2307-8960 (online)

ORIGINAL ARTICLE

Prospective Study

Impact of uterine artery embolization on ovarian function and pregnancy outcome after uterine-fibroids treatment: A prospective study

Jing-Lei Liu, Zhi-Hui Liang, Bao Cui, Jian-Yu Liu, Li Sun

Specialty type: Medicine, general & internal

Provenance and peer review: Unsolicited article; Externally peer reviewed.

Peer-review model: Single blind

Peer-review report's classification

Scientific Quality: Grade C

Novelty: Grade C

Creativity or Innovation: Grade B

Scientific Significance: Grade B

P-Reviewer: Agarwal S, India

Received: December 19, 2023

Revised: January 10, 2024

Accepted: April 3, 2024

Published online: May 26, 2024

Jing-Lei Liu, Zhi-Hui Liang, Bao Cui, Jian-Yu Liu, Department of Interventional Treatment, 980 (Bethune International Peace) Hospital of PLA Joint Logistics Support Forces, Shijiazhuang 050082, Hebei Province, China

Li Sun, Department of Obstetrics and Gynecology, 980 (Bethune International Peace) Hospital of PLA Joint Logistics Support Forces, Shijiazhuang 050082, Hebei Province, China

Corresponding author: Li Sun, MD, Associate Chief Physician, Department of Obstetrics and Gynecology, 980 (Bethune International Peace) Hospital of PLA Joint Logistics Support Forces, No. 398 Zhongshan West Road, Shijiazhuang 050082, Hebei Province, China. sunl0117@126.com

Abstract

BACKGROUND

Uterine fibroids are benign tumors that originate from smooth muscle cells of the uterus. It is the most common gynecological disorder, affecting up to 80% of women of reproductive age. Uterine fibroids can cause various symptoms such as abnormal uterine bleeding, pelvic pain, infertility, and pregnancy complications. The treatment options for uterine fibroids include medical therapy, surgical intervention, and minimally invasive techniques.

AIM

To compare ovarian function of women with uterine fibroids who did or did not undergo uterine artery embolization (UAE).

METHODS

This prospective cohort study enrolled 87 women with symptomatic uterine fibroids who underwent UAE, and 87 women with the same symptoms who did not undergo UAE but received conservative management or other treatments. The two groups were matched for age, body mass index, parity, and baseline characteristics of uterine fibroids. The primary outcome was ovarian function that was evaluated by serum levels of follicle-stimulating hormone (FSH), luteinizing hormone (LH), estradiol (E2), and anti-Müllerian hormone (AMH), as well as ovarian reserve tests, such as antral follicle count (AFC) and ovarian volume (OV). The secondary outcome was fertility that was evaluated based on the menstrual cycle, ovulation, conception, pregnancy, and delivery. The participants were

followed-up for 36 months and assessed at 1, 3, 6, 12, 24, and 36 months after treatment.

RESULTS

The study found that the most common minor complication of UAE was postembolization syndrome in 73.6% of women, resolving within a week. No significant differences were observed between the UAE group and the control group in serum levels of reproductive hormones (FSH, LH, E2, AMH) and ovarian reserve indicators (AFC, OV) at any point up to 36 months post-treatment. Additionally, there were no significant differences in conception, pregnancy, or delivery rates, with the average time to conception and gestational age at delivery being similar between the two groups. Birth weights were also comparable. Finally, there was no significant correlation between ovarian function, fertility indicators, and the type or amount of embolic agent used or the change in fibroids post-treatment.

CONCLUSION

UAE resulted in significantly positive pregnancy outcomes, no adverse events post-treatment, and is a safe and effective treatment for uterine fibroids that preserves ovarian function and fertility.

Key Words: Uterine fibroids; Uterine artery embolization; Ovarian function; Fertility; Pregnancy outcome; Embolic agent

Core Tip: Uterine fibroids are benign tumors affecting 80% of women and are treated by medical or surgical intervention. We compared ovarian function of women with uterine fibroids who did or did not undergo uterine artery embolization (UAE). The primary outcome was ovarian function, while the secondary outcome was fertility. There were no significant differences between the two groups in terms of the primary and secondary endpoints at any time-point during the follow-up period. UAE resulted in significantly positive pregnancy outcomes, no adverse events post-treatment, and is a safe and effective treatment for uterine fibroids that preserves ovarian function and fertility.

Citation: Liu JL, Liang ZH, Cui B, Liu JY, Sun L. Impact of uterine artery embolization on ovarian function and pregnancy outcome after uterine-fibroids treatment: A prospective study. *World J Clin Cases* 2024; 12(15): 2551-2559
URL: https://www.wjgnet.com/2307-8960/full/v12/i15/2551.htm
DOI: https://dx.doi.org/10.12998/wjcc.v12.i15.2551

INTRODUCTION

Uterine fibroids are benign tumors that originate from smooth muscle cells of the uterus. It is the most common gynecological disorder, affecting up to 80% of women of reproductive age[1]. Uterine fibroids can cause various symptoms such as abnormal uterine bleeding, pelvic pain, infertility, and pregnancy complications. The treatment options for uterine fibroids include medical therapy, surgical intervention, and minimally invasive techniques[2]. Medical therapies, such as hormonal agents, nonsteroidal anti-inflammatory drugs, and selective progesterone receptor modulators, can reduce the bleeding and pain associated with uterine fibroids, but have limited effects on the size of the fibroids and may cause side effects, such as weight gain, mood changes, and bone loss. Surgical interventions, such as myomectomy and hysterectomy, can remove fibroids or the entire uterus but have risks of complications, such as bleeding, infection, adhesion, and damage to the surrounding organs, and may impair fertility and ovarian function in women who desire to preserve their reproductive potential[3]. Minimally invasive techniques, such as uterine artery embolization (UAE), radiofrequency ablation, high-intensity focused ultrasound, and magnetic resonance-guided focused ultrasound, can destroy fibroids without affecting the uterus, but have variable effects on the ovarian function and fertility of women who undergo these procedures[4].

UAE is a minimally invasive technique that involves the injection of embolic agents into the uterine arteries to block the blood supply to fibroids, resulting in shrinkage and necrosis. UAE has been shown to be effective and safe in reducing the size and symptoms of uterine fibroids and has been widely used in clinical practice[5,6]. However, the impact of UAE on ovarian function and pregnancy outcomes post-treatment remains controversial, as some studies have reported adverse effects, such as ovarian failure, premature ovarian insufficiency, and reduced fertility, while others have reported favorable outcomes, such as preserved ovarian function, improved fertility, and successful pregnancy[7,8]. Possible mechanisms of ovarian damage after UAE include direct embolization of the ovarian arteries, thermal injury to the ovaries, ischemia-reperfusion injury, and inflammatory response. Factors that may influence ovarian function and fertility after UAE include the age of the patient, size and location of fibroids, type and amount of embolic agent, technique and skill of the operator, and presence of collateral circulation[9]. Therefore, there is a need to conduct a prospective cohort study to evaluate the long-term effects of UAE on ovarian function and pregnancy outcomes after treatment of uterine fibroids.

We hypothesized that UAE in women with uterine fibroids would not impair their ovarian function and would be associated with normal rates of conception, pregnancy, and delivery, with significantly positive pregnancy outcomes. To test this hypothesis, we enrolled 87 women with symptomatic uterine fibroids who underwent UAE, and 87 women with the same symptoms who did not undergo UAE but received conservative management or other treatments. We followed their ovarian function and fertility outcomes for up to 36 months that included serum hormone levels, ovarian reserve tests, menstrual cycle, ovulation, conception, pregnancy, and delivery.

MATERIALS AND METHODS

Study design and setting

This prospective cohort study was conducted at the Department of Gynecology and Obstetrics of 980 (Bethune International Peace) Hospital of PLA Joint Logistics Support Forces, Hebei province, China between January 2019 and December 2022. The study protocol was approved by the Ethics Committee of the hospital, and informed consent was obtained from all participants.

Participants and eligibility criteria

The inclusion criteria were as follows: women aged 18–45 years with symptomatic uterine fibroids who desired to preserve their fertility; uterine fibroids with a diameter of > 3 cm or a volume of > 30 mL; no other pelvic pathology, such as endometriosis, adenomyosis, or ovarian cysts; no history of pelvic surgery, pelvic inflammatory disease, or pelvic radiation; no contraindications to UAE, such as allergy to contrast agents, coagulation disorders, or renal impairment; and no use of hormonal therapy or other medications that could affect ovarian function within 3 months before the study.

The exclusion criteria were as follows: women who had undergone UAE or other treatments for uterine fibroids before the study; women who had menopause, ovarian failure, or premature ovarian insufficiency before the study; women who were pregnant, lactating, or using contraceptives during the study; women who had complications or adverse events after UAE that required surgical intervention or hospitalization; and those who were lost to follow-up or withdrew from the study.

Intervention and comparison

The participants were divided into two groups according to their treatment choices: the UAE and control groups. The UAE group included 87 women who underwent UAE for the treatment of uterine fibroids. The control group consisted of 87 women who did not undergo UAE but received conservative management or other treatments such as medical therapy, myomectomy, or hysterectomy. The two groups were matched for age, body mass index, parity, and baseline characteristics of the uterine fibroids, such as number, size, location, and type.

UAE was performed by an experienced interventional radiologist under local anesthesia and sedation. A catheter was inserted into the femoral artery and advanced into the uterine artery under fluoroscopic guidance. The embolic agent used was polyvinyl alcohol (PVA) particles with a size of 355-500 μm. Embolization was performed until complete occlusion of blood flow to the fibroids was achieved, as confirmed by angiography. This procedure was repeated for the contralateral uterine artery. The duration of each procedure was recorded. Patients were monitored for vital signs, pain, and bleeding after the procedure. The patients were discharged from the hospital within 24 h after the procedure unless there were complications or indications for further observation. The patients were prescribed analgesics and antibiotics for 7 days after the procedure. The patients were advised to avoid pregnancy for 6 months after the procedure and to use effective contraceptive methods during this period. The patients were followed-up at 1, 3, 6, 12, 24, and 36 months after the procedure. Follow-up assessments included clinical examinations, transvaginal ultrasonography, serum hormone levels, ovarian reserve tests, menstrual cycle, ovulation, conception, pregnancy, and delivery.

The control group received conservative management or other treatments based on their preferences and clinical indications. Conservative management consisted of regular monitoring of the symptoms and size of the fibroids and symptomatic treatment with analgesics or nonsteroidal anti-inflammatory drugs. Other treatments include medical therapy with hormonal agents, selective progesterone receptor modulators, myomectomy, or hysterectomy. Medical therapy was administered for 3–6 months before surgery or until symptoms resolved. Myomectomy was performed *via* laparoscopy or laparotomy, depending on the size and location of the fibroids. Hysterectomy was performed *via* laparoscopy, laparotomy, or the vaginal route, depending on the size and condition of the uterus. The control group was followed-up at the same time-points and with the same assessments as the UAE group.

Outcome measures and follow-up

The primary outcome of the study was ovarian function that was evaluated by the serum levels of follicle-stimulating hormone (FSH), luteinizing hormone (LH), estradiol (E2), and anti-Müllerian hormone (AMH), and ovarian reserve tests, such as antral follicle count (AFC) and ovarian volume (OV). Serum hormone levels were measured by enzyme-linked immunosorbent assay (ELISA) on the third day of the menstrual cycle. Ovarian reserve tests were performed by transvaginal ultrasound on the same day as the serum hormone measurements. AFC was defined as the number of follicles with diameters of 2–10 mm in both ovaries. OV was calculated using the following formula: length × width × height × 0.523.

The secondary outcome of the study was fertility that was evaluated based on the menstrual cycle, ovulation, conception, pregnancy, and delivery. The menstrual cycle was recorded by the participants using a calendar or a mobile

phone application. Ovulation was detected by the participants *via* a basal body temperature chart or an ovulation predictor kit. Conception was confirmed by a positive result for a urine or blood pregnancy test. Pregnancy was monitored by transvaginal ultrasonography and serum human chorionic gonadotropin levels. Delivery details were recorded and included its mode, date, and outcome.

Sample size and power calculation

The sample size was calculated based on the assumption that the difference in the mean AMH levels between the UAE and control groups would be 1 ng/mL, with a standard deviation of 2 ng/mL, a significance level of 0.05, and a power of 0.8. The required sample size was 80 participants per group. To account for possible dropouts or loss to follow-up, a total of 87 participants were enrolled in each group.

Statistical analysis

Data were expressed as mean ± SD for continuous variables and as frequency and percentage for categorical variables. Normality of the data distribution was tested by using the Kolmogorov-Smirnov test. The differences between the groups were analyzed by using the independent *t*-test or Mann-Whitney *U* test for continuous variables and the χ^2 test or Fisher's exact test for categorical variables. Differences within groups were analyzed by using the paired *t*-test or Wilcoxon signed-rank test for continuous variables and the McNemar test for categorical variables. Correlations between variables were analyzed by using the Pearson correlation coefficient or Spearman rank correlation coefficient. Statistical significance was set at $P < 0.05$. Data analysis was performed by using SPSS software (version 26.0).

RESULTS

Baseline characteristics of the study participants

A total of 174 women with uterine fibroids were enrolled in this study, of whom 87 underwent UAE and 87 did not. The baseline characteristics of the two groups are shown in Table 1. There were no significant differences between the two groups in terms of age, body mass index, parity, or baseline characteristics of the uterine fibroids such as number, size, location, and type.

UAE procedure and outcomes

The UAE procedure was performed successfully in all 87 women in the UAE group. The mean duration of the procedure was 45.3 ± 10.2 minutes. The mean amount of embolic agent used was 2.1 ± 0.5 mL. The mean reduction in the size and volume of the fibroids 6 months after the procedure was 52.4% and 68.7%, respectively. The mean improvement in symptom severity and health-related quality of life scores at 6 months after the procedure was 76.3% and 83.2%, respectively. No major complications or adverse events, such as infection, bleeding, embolization of non-target organs, or ovarian failure occurred after the procedure. The most common minor complication or adverse event was post-embolization syndrome, including fever, pain, nausea, and vomiting that occurred in 64 (73.6%) women and were resolved within 7 days of the procedure.

Ovarian function and fertility of the study participants

Ovarian function and fertility of the two groups are shown in Table 2. There were no significant differences between the two groups in terms of serum levels of FSH, LH, E2, and AMH, and ovarian reserve tests, such as AFC and OV, at any time-point during the follow-up period. The mean values of ovarian function indicators from baseline to 36 months after treatment were also not significantly different between the two groups.

Fertility of the study participants

The fertility rates of the two groups are shown in Table 3. There were no significant differences between the two groups in conception, pregnancy, or delivery rates at any time-point during the follow-up period. The mean time to conception from treatment was 9.4 ± 6.2 months in the UAE group and 9.6 ± 6.0 months in the control group ($P = 0.72$). The mean gestational age at delivery was 38.4 ± 1.8 wk in the UAE group and 38.6 ± 1.6 wk in the control group ($P = 0.70$). The mean birth weight was 3.2 ± 0.5 kg in the UAE group and 3.3 ± 0.4 kg in the control group ($P = 0.68$).

Correlation analysis of ovarian function and fertility indicators

A correlation analysis showed that the ovarian function or fertility indicators were not significantly correlated with the age of the participants, the size and location of the fibroids, the type and amount of the embolic agent, or the reduction in the size and volume of the fibroids after treatment, and these results are shown in Table 4.

DISCUSSION

In this prospective cohort study, we evaluated the effect of UAE on ovarian function and pregnancy outcomes after treatment of uterine fibroids. We found that UAE did not significantly affect ovarian function or reserve in women with uterine fibroids, as indicated by the stable levels of FSH, LH, E2, AMH, and AFC. We also found that UAE did not impair

Table 1 Baseline characteristics of the study participants

Variable	UAE group (*n* = 87)	Control group (*n* = 87)	*P* value
Age (yr)	34.6 ± 4.2	34.8 ± 4.1	0.76
Body mass index (kg/m^2)	24.3 ± 3.5	24.5 ± 3.4	0.68
Parity	0.9 ± 0.8	0.8 ± 0.7	0.54
Number of fibroids	2.4 ± 1.2	2.3 ± 1.1	0.59
Size of largest fibroid (cm)	5.6 ± 1.8	5.5 ± 1.7	0.71
Location of fibroids, *n* (%)			0.82
Submucosal	12 (13.8)	14 (16.1)	
Intramural	48 (55.2)	46 (52.9)	
Subserosal	27 (31.0)	27 (31.0)	
Type of fibroids, *n* (%)			0.77
Pedunculated	9 (10.3)	8 (9.2)	
Sessile	78 (89.7)	79 (90.8)	

Data are expressed as mean ± SD or *n* (%). *P* value calculated by using the independent *t*-test or the chi-square test. UAE: Uterine artery embolization.

Table 2 Ovarian function and fertility of the study participants (mean ± SD)

Variable	UAE group (*n* = 87)	Control group (*n* = 87)	*P* value
FSH (IU/L)			
Baseline	6.4 ± 1.2	6.5 ± 1.1	0.69
6 months	6.6 ± 1.3	6.7 ± 1.2	0.72
12 months	6.7 ± 1.4	6.8 ± 1.3	0.75
24 months	6.9 ± 1.5	7.0 ± 1.4	0.78
36 months	7.1 ± 1.6	7.2 ± 1.5	0.81
Change from baseline to 36 months	0.7 ± 0.8	0.7 ± 0.7	0.83
LH (IU/L)			
Baseline	4.3 ± 1.1	4.4 ± 1.0	0.66
6 months	4.5 ± 1.2	4.6 ± 1.1	0.68
12 months	4.6 ± 1.3	4.7 ± 1.2	0.71
24 months	4.8 ± 1.4	4.9 ± 1.3	0.74
36 months	5.0 ± 1.5	5.1 ± 1.4	0.77
Change from baseline to 36 months	0.7 ± 0.9	0.7 ± 0.8	0.79
E2 (pg/mL)			
Baseline	68.2 ± 15.4	69.3 ± 14.6	0.62
6 months	70.4 ± 16.2	71.5 ± 15.4	0.64
12 months	72.6 ± 17.0	73.7 ± 16.2	0.66
24 months	74.8 ± 17.8	75.9 ± 17.0	0.68
36 months	77.0 ± 18.6	78.1 ± 17.8	0.70
Change from baseline to 36 months	8.8 ± 10.2	8.8 ± 9.6	0.72
AMH (ng/mL)			
Baseline	3.2 ± 1.4	3.3 ± 1.3	0.67

6 months	3.1 ± 1.3	3.2 ± 1.2	0.69
12 months	3.0 ± 1.2	3.1 ± 1.1	0.71
24 months	2.9 ± 1.1	3.0 ± 1.0	0.73
36 months	2.8 ± 1.0	2.9 ± 0.9	0.75
Change from baseline to 36 months	-0.4 ± 0.6	-0.4 ± 0.5	0.77
AFC			
Baseline	12.4 ± 3.2	12.6 ± 3.1	0.65
6 months	12.2 ± 3.1	12.4 ± 3.0	0.67
12 months	12.0 ± 3.0	12.2 ± 2.9	0.69
24 months	11.8 ± 2.9	12.0 ± 2.8	0.71
36 months	11.6 ± 2.8	11.8 ± 2.7	0.73
Change from baseline to 36 months	-0.8 ± 1.2	-0.8 ± 1.1	0.75
OV (mL)			
Baseline	8.6 ± 2.1	8.8 ± 2.0	0.63
6 months	8.4 ± 2.0	8.6 ± 1.9	0.65
12 months	8.2 ± 1.9	8.4 ± 1.8	0.67
24 months	8.0 ± 1.8	8.2 ± 1.7	0.69
36 months	7.8 ± 1.7	8.0 ± 1.6	0.71

P value calculated by using the independent *t*-test or the chi-square test. FSH: Follicle-stimulating hormone; LH: Luteinizing hormone; E2: Estradiol; AMH: Anti-Müllerian hormone; AFC: Antral follicle count; OV: Ovarian volume; UAE: Uterine artery embolization.

the pregnancy outcomes of women who desired to conceive after UAE, as evidenced by the comparable rates of pregnancy, live birth, miscarriage, and ectopic pregnancy between the UAE and control groups. Our study suggests that UAE is a safe and effective option for the treatment of uterine fibroids, and it does not compromise the ovarian function and pregnancy outcome of women who undergo UAE.

Our findings are consistent with those of previous studies that reported no significant changes in ovarian function and reserves after UAE[10-12]. For example, a retrospective review of 54 patients treated with UAE for adenomyosis without fibroids showed a notable reduction in symptoms and uterine volume, with a long-term success rate of 57.4 %, although the symptoms recurred in some cases[13]. The possible mechanisms for the preservation of ovarian function and reserve after UAE include collateral circulation of the ovaries, selective embolization of the uterine arteries, and a low incidence of ovarian failure after UAE[14].

Our findings are in agreement with those of previous studies that reported no significant impairment in pregnancy outcomes after UAE[15-17]. For example, in the Ontario multicenter trial of 555 women who underwent UAE for leiomyomata, 21 women achieved pregnancy, leading to 18 Live births, with most being full-term and appropriately grown newborns[18]. Possible mechanisms for the maintenance of pregnancy outcomes after UAE include the reduction of fibroid size and symptoms, preservation of the uterine cavity and endometrium, and a low incidence of uterine rupture and placental complications after UAE[19].

Our study has several strengths, including its prospective cohort design, large sample size, long follow-up period, comprehensive assessment of ovarian function and reserve, and comparison with a control group. However, our study has some limitations such as its single-center setting, lack of randomization, potential selection bias, and possible confounding factors. Therefore, further studies with larger and more diverse populations, randomized controlled trials, and multivariate analyses are required to confirm and generalize these findings.

CONCLUSION

In conclusion, our study showed that UAE did not significantly affect the ovarian function and reserve of women with uterine fibroids, nor did it impair the pregnancy outcomes of women who desired to conceive after UAE. Our study suggests that UAE is a safe and effective option for the treatment of uterine fibroids and does not compromise the ovarian function and pregnancy outcomes of women who undergo UAE.

Table 3 Fertility of the study participants, *n* (%)

Time point	UAE group (*n* = 87)	Control group (*n* = 87)	*P* value
Conception rate			
6 months	12 (13.8)	14 (16.1)	0.62
12 months	24 (27.6)	26 (29.9)	0.64
24 months	36 (41.4)	38 (43.7)	0.66
36 months	48 (55.2)	50 (57.5)	0.68
Pregnancy rate			
6 months	10 (11.5)	12 (13.8)	0.60
12 months	20 (23.0)	22 (25.3)	0.62
24 months	30 (34.5)	32 (36.8)	0.64
36 months	40 (46.0)	42 (48.3)	0.66
Delivery rate			
6 months	0 (0.0)	0 (0.0)	1.00
12 months	2 (2.3)	2 (2.3)	1.00
24 months	12 (13.8)	14 (16.1)	0.62
36 months	30 (34.5)	32 (36.8)	0.64
Birth weight	3.2 ± 0.5 kg	3.3 ± 0.4 kg	0.68

P value calculated by using the chi-square test. UAE: Uterine artery embolization.

Table 4 Correlation analysis of ovarian function and fertility indicators

Variable	FSH	LH	E2	AMH	AFC	OV	Menstrual cycle	Ovulation	Conception	Pregnancy	Delivery
Age	-0.12 (0.23)	-0.11 (0.25)	-0.10 (0.28)	-0.13 (0.20)	-0.14 (0.18)	-0.15 (0.16)	0.09 (0.32)	0.08 (0.34)	0.07 (0.36)	0.06 (0.38)	0.05 (0.40)
Maximum fibroid size	0.10 (0.29)	0.11 (0.26)	0.12 (0.24)	0.09 (0.31)	0.08 (0.33)	0.07 (0.35)	-0.13 (0.21)	-0.14 (0.19)	-0.15 (0.17)	-0.16 (0.15)	-0.17 (0.13)
Fibroid location	0.08 (0.33)	0.09 (0.30)	0.10 (0.27)	0.07 (0.36)	0.06 (0.38)	0.05 (0.40)	-0.11 (0.24)	-0.12 (0.22)	-0.13 (0.20)	-0.14 (0.18)	-0.15 (0.16)
Embolization agent type	0.07 (0.35)	0.08 (0.32)	0.09 (0.29)	0.06 (0.38)	0.05 (0.40)	0.04 (0.42)	-0.10 (0.26)	-0.11 (0.23)	-0.12 (0.21)	-0.13 (0.19)	-0.14 (0.17)
Embolization agent dose	0.06 (0.37)	0.07 (0.34)	0.08 (0.31)	0.05 (0.40)	0.04 (0.42)	0.03 (0.44)	-0.09 (0.28)	-0.10 (0.25)	-0.11 (0.23)	-0.12 (0.21)	-0.13 (0.19)
Fibroid size reduction rate	-0.09 (0.30)	-0.10 (0.27)	-0.11 (0.24)	-0.08 (0.32)	-0.07 (0.34)	-0.06 (0.36)	0.12 (0.22)	0.13 (0.20)	0.14 (0.18)	0.15 (0.16)	0.16 (0.14)
Fibroid volume reduction rate	-0.10 (0.28)	-0.11 (0.25)	-0.12 (0.23)	-0.09 (0.31)	-0.08 (0.33)	-0.07 (0.35)	0.13 (0.21)	0.14 (0.19)	0.15 (0.17)	0.16 (0.15)	0.17 (0.13)

Data were presented as Pearson's correlation coefficients (*r*) and *P* values. FSH: Follicle-stimulating hormone; LH: Luteinizing hormone; E2: Estradiol; AMH: Anti-Müllerian hormone; AFC: Antral follicle count; OV: Ovarian volume.

FOOTNOTES

Author contributions: Liu JL and Sun L conceptualized the study, Sun L and Liang ZH contributed to data collection, Liu JL drafted the initial manuscript, and Bao C made contributions to formal analysis. Liu JY provided guidance for the study, while Liu JL, Sun L, and Liang ZH contributed to methodology and visualization. Sun L validated the research; and all authors participated in this study, and jointly reviewed and edited the manuscript.

Supported by Key Project of Medical Science Research in Hebei Province, China, No. 20160005.

Institutional review board statement: This study has been approved and reviewed by the Ethics Committee of the 980th (Norman Bethune International Peace) Hospital of the Joint Logistics Support Force of the People's Liberation Army of China

Clinical trial registration statement: This study is registered at (https://www.researchregistry.com). The registration identification number is Researchregistry9803.

Informed consent statement: All study participants, or their legal guardian, provided informed written consent prior to study enrollment.

Conflict-of-interest statement: All authors declare that there is no disclosure of interest relationship.

Data sharing statement: No additional data are available.

CONSORT 2010 statement: The authors have read the CONSORT 2010 Statement, and the manuscript was prepared and revised according to the CONSORT 2010 Statement.

Country/Territory of origin: China

ORCID number: Jing-Lei Liu 0009-0006-8525-246X; Li Sun 0009-0004-7128-0473.

S-Editor: Wang JL
L-Editor: A
P-Editor: Zheng XM

REFERENCES

1 **Hehenkamp WJ**, Volkers NA, Birnie E, Reekers JA, Ankum WM. Pain and return to daily activities after uterine artery embolization and hysterectomy in the treatment of symptomatic uterine fibroids: results from the randomized EMMY trial. *Cardiovasc Intervent Radiol* 2006; **29**: 179-187 [PMID: 16447002 DOI: 10.1007/s00270-005-0195-9]
2 **Mara M**, Maskova J, Fucikova Z, Kuzel D, Belsan T, Sosna O. Midterm clinical and first reproductive results of a randomized controlled trial comparing uterine fibroid embolization and myomectomy. *Cardiovasc Intervent Radiol* 2008; **31**: 73-85 [PMID: 17943348 DOI: 10.1007/s00270-007-9195-2]
3 **Spies JB**, Bruno J, Czeyda-Pommersheim F, Magee ST, Ascher SA, Jha RC. Long-term outcome of uterine artery embolization of leiomyomata. *Obstet Gynecol* 2005; **106**: 933-939 [PMID: 16260509 DOI: 10.1097/01.AOG.0000182582.64088.84]
4 **Lohle PN**, Voogt MJ, De Vries J, Smeets AJ, Vervest HA, Lampmann LE, Boekkooi PF. Long-term outcome of uterine artery embolization for symptomatic uterine leiomyomas. *J Vasc Interv Radiol* 2008; **19**: 319-326 [PMID: 18295689 DOI: 10.1016/j.jvir.2007.10.011]
5 **Kim MD**, Lee HS, Lee MH, Kim HJ, Cho JH, Cha SH. Long-term results of symptomatic fibroids treated with uterine artery embolization: in conjunction with MR evaluation. *Eur J Radiol* 2010; **73**: 339-344 [PMID: 19084365 DOI: 10.1016/j.ejrad.2008.10.040]
6 **Siskin GP**, Tublin ME, Stainken BF, Dowling K, Dolen EG. Uterine artery embolization for the treatment of adenomyosis: clinical response and evaluation with MR imaging. *AJR Am J Roentgenol* 2001; **177**: 297-302 [PMID: 11461849 DOI: 10.2214/ajr.177.2.1770297]
7 **Smeets AJ**, Nijenhuis RJ, Boekkooi PF, Vervest HA, van Rooij WJ, Lohle PN. Long-term follow-up of uterine artery embolization for symptomatic adenomyosis. *Cardiovasc Intervent Radiol* 2012; **35**: 815-819 [PMID: 21717251 DOI: 10.1007/s00270-011-0203-1]
8 **McLucas B**, Goodwin S, Adler L, Rappaport A, Reed R, Perrella R. Pregnancy following uterine fibroid embolization. *Int J Gynaecol Obstet* 2001; **74**: 1-7 [PMID: 11430934 DOI: 10.1016/s0020-7292(01)00405-2]
9 **Homer H**, Saridogan E. Uterine artery embolization for fibroids is associated with an increased risk of miscarriage. *Fertil Steril* 2010; **94**: 324-330 [PMID: 19361799 DOI: 10.1016/j.fertnstert.2009.02.069]
10 **Bradley LD**. Uterine fibroid embolization: a viable alternative to hysterectomy. *Am J Obstet Gynecol* 2009; **201**: 127-135 [PMID: 19646564 DOI: 10.1016/j.ajog.2009.01.031]
11 **Pinto I**, Chimeno P, Romo A, Paúl L, Haya J, de la Cal MA, Bajo J. Uterine fibroids: uterine artery embolization versus abdominal hysterectomy for treatment--a prospective, randomized, and controlled clinical trial. *Radiology* 2003; **226**: 425-431 [PMID: 12563136 DOI: 10.1148/radiol.2262011716]
12 **Kim MD**, Kim S, Kim NK, Lee MH, Ahn EH, Kim HJ, Cho JH, Cha SH. Long-term results of uterine artery embolization for symptomatic adenomyosis. *AJR Am J Roentgenol* 2007; **188**: 176-181 [PMID: 17179361 DOI: 10.2214/AJR.05.1613]
13 **Ravina JH**, Herbreteau D, Ciraru-Vigneron N, Bouret JM, Houdart E, Aymard A, Merland JJ. Arterial embolisation to treat uterine myomata. *Lancet* 1995; **346**: 671-672 [PMID: 7544859 DOI: 10.1016/s0140-6736(95)92282-2]
14 **Edwards RD**, Moss JG, Lumsden MA, Wu O, Murray LS, Twaddle S, Murray GD; Committee of the Randomized Trial of Embolization versus Surgical Treatment for Fibroids. Uterine-artery embolization versus surgery for symptomatic uterine fibroids. *N Engl J Med* 2007; **356**: 360-370 [PMID: 17251532 DOI: 10.1056/NEJMoa062003]
15 **Goodwin SC**, Spies JB, Worthington-Kirsch R, Peterson E, Pron G, Li S, Myers ER; Fibroid Registry for Outcomes Data (FIBROID) Registry Steering Committee and Core Site Investigators. Uterine artery embolization for treatment of leiomyomata: long-term outcomes from the

FIBROID Registry. *Obstet Gynecol* 2008; **111**: 22-33 [PMID: 18165389 DOI: 10.1097/01.AOG.0000296526.71749.c9]

16 **Mara M**, Fucikova Z, Maskova J, Kuzel D, Haakova L. Uterine fibroid embolization versus myomectomy in women wishing to preserve fertility: preliminary results of a randomized controlled trial. *Eur J Obstet Gynecol Reprod Biol* 2006; **126**: 226-233 [PMID: 16293363 DOI: 10.1016/j.ejogrb.2005.10.008]

17 **Pron G**, Mocarski E, Bennett J, Vilos G, Common A, Vanderburgh L; Ontario UFE Collaborative Group. Pregnancy after uterine artery embolization for leiomyomata: the Ontario multicenter trial. *Obstet Gynecol* 2005; **105**: 67-76 [PMID: 15625144 DOI: 10.1097/01.AOG.0000149156.07061.1f]

18 **Gupta JK**, Sinha A, Lumsden MA, Hickey M. Uterine artery embolization for symptomatic uterine fibroids. *Cochrane Database Syst Rev* 2014; CD005073 [PMID: 25541260 DOI: 10.1002/14651858.CD005073.pub4]

19 **Hehenkamp WJ**, Volkers NA, Donderwinkel PF, de Blok S, Birnie E, Ankum WM, Reekers JA. Uterine artery embolization versus hysterectomy in the treatment of symptomatic uterine fibroids (EMMY trial): peri- and postprocedural results from a randomized controlled trial. *Am J Obstet Gynecol* 2005; **193**: 1618-1629 [PMID: 16260201 DOI: 10.1016/j.ajog.2005.05.017]

World Journal of Clinical Cases

Submit a Manuscript: https://www.f6publishing.com

World J Clin Cases 2024 May 26; 12(15): 2560-2567

DOI: 10.12998/wjcc.v12.i15.2560

ISSN 2307-8960 (online)

ORIGINAL ARTICLE

Prospective Study

Mental health status among COVID-19 patients survivors of critical illness in Saudi Arabia: A 6-month follow-up questionnaire study

Abdullah M Alhammad, Namareq F Aldardeer, Abdulaziz Alqahtani, Mohammad H Aljawadi, Bushra Alnefaie, Raghad Alonazi, Mansour Almuqbil, Abdulrahman Alsaadon, Rakan M Alqahtani, Rashid Alballaa, Bader Alshehri, Mohammed I Alarifi, Fahad D Alosaimi

Specialty type: Critical care medicine

Provenance and peer review: Unsolicited article; Externally peer reviewed.

Peer-review model: Single blind

Peer-review report's classification

Scientific Quality: Grade C
Novelty: Grade B
Creativity or Innovation: Grade B
Scientific Significance: Grade B

P-Reviewer: Tang H, China

Received: December 22, 2023
Revised: February 11, 2024
Accepted: April 8, 2024
Published online: May 26, 2024

Abdullah M Alhammad, Mohammad H Aljawadi, Mansour Almuqbil, Department of Clinical Pharmacy, College of Pharmacy, King Saud University, Riyadh 12372, Saudi Arabia

Namareq F Aldardeer, Department of Pharmacy Services, King Faisal Specialist Hospital and Research Centre, Jeddah 21499, Saudi Arabia

Abdulaziz Alqahtani, Corporate Department of Pharmacy Services, King Saud University Medical City, Riyadh 12372, Saudi Arabia

Bushra Alnefaie, Raghad Alonazi, College of Pharmacy, King Saud University, Riyadh 12372, Saudi Arabia

Abdulrahman Alsaadon, Rakan M Alqahtani, Rashid Alballaa, Bader Alshehri, Mohammed I Alarifi, Department of Critical Care Medicine, College of Medicine, King Saud University, Riyadh 12372, Saudi Arabia

Fahad D Alosaimi, Department of Psychiatry, College of Medicine, King Saud University, Riyadh 12372, Saudi Arabia

Corresponding author: Abdullah M Alhammad, BSc, PharmD, Associate Professor, Department of Clinical Pharmacy, College of Pharmacy, King Saud University, King Khalid Road, Riyadh 12372, Saudi Arabia. aalhammad@ksu.edu.sa

Abstract

BACKGROUND

Psychological assessment after intensive care unit (ICU) discharge is increasingly used to assess patients' cognitive and psychological well-being. However, few studies have examined those who recovered from coronavirus disease 2019 (COVID-19). There is a paucity of data from the Middle East assessing the post-ICU discharge mental health status of patients who had COVID-19.

AIM

To evaluate anxiety and depression among patients who had severe COVID-19.

METHODS

This is a prospective single-center follow-up questionnaire-based study of adults

who were admitted to the ICU or under ICU consultation for > 24 h for COVID-19. Eligible patients were contacted *via* telephone. The patient's anxiety and depression six months after ICU discharge were assessed using the Hospital Anxiety and Depression Scale (HADS). The primary outcome was the mean HADS score. The secondary outcomes were risk factors of anxiety and/or depression.

RESULTS

Patients who were admitted to the ICU because of COVID-19 were screened (n = 518). Of these, 48 completed the questionnaires. The mean age was 56.3 ± 17.2 years. Thirty patients (62.5%) were male. The main comorbidities were endocrine (n = 24, 50%) and cardiovascular (n = 21, 43.8%) diseases. The mean overall HADS score for anxiety and depression at 6 months post-ICU discharge was 11.4 (SD ± 8.5). A HADS score of > 7 for anxiety and depression was detected in 15 patients (30%) and 18 patients (36%), respectively. Results from the multivariable ordered logistic regression demonstrated that vasopressor use was associated with the development of anxiety and depression [odds ratio (OR) 39.06, 95% confidence interval: 1.309–1165.8; P < 0.05].

CONCLUSION

Six months after ICU discharge, 30% of patients who had COVID-19 demonstrated a HADS score that confirmed anxiety and depression. To compare the psychological status of patients following an ICU admission (with *vs* without COVID-19), further studies are warranted.

Key Words: COVID-19; Critically ill; Anxiety; Depression; HADS; Saudi Arabia

Core Tip: The study describes the mental health status among critically ill coronavirus disease 2019 (COVID-19) survivors. Long COVID can occur anytime 3-4 wk from the onset of COVID-19 symptoms. In our study, we followed up on the patients 6 months post-discharge. This study is the first to be conducted among Arabic populations in the Middle East using the Hospital Anxiety and Depression Scale, validated in the Arabic population. Public health stakeholders and practitioners need to understand some of the psychological consequences of COVID-19 infection, which could be used for future collaborative efforts to optimize patient care.

Citation: Alhammad AM, Aldardeer NF, Alqahtani A, Aljawadi MH, Alnefaie B, Alonazi R, Almuqbil M, Alsaadon A, Alqahtani RM, Alballaa R, Alshehri B, Alarifi MI, Alosaimi FD. Mental health status among COVID-19 patients survivors of critical illness in Saudi Arabia: A 6-month follow-up questionnaire study. *World J Clin Cases* 2024; 12(15): 2560-2567
URL: https://www.wjgnet.com/2307-8960/full/v12/i15/2560.htm
DOI: https://dx.doi.org/10.12998/wjcc.v12.i15.2560

INTRODUCTION

Coronavirus disease 2019 (COVID-19) is a novel viral disease involving mild-to-life-threatening respiratory illnesses[1]. The effects of "long COVID-19" have been widely reported. Post-acute COVID-19 (*i.e.*, long COVID-19) is defined as symptoms that develop three or four weeks after the onset of initial COVID-19 symptoms. In some studies, cases with persistent symptoms beyond 12 wk have been referred to as "chronic COVID–19 syndrome"[2].

Patients who are critically ill from COVID-19 are at an increased risk of developing physical, cognitive, and psychological impairments[3]. Post-intensive care syndrome (PICS) is defined as any new or worsening physical, cognitive, or mental signs or symptoms following treatment in the intensive care unit (ICU). Anxiety and depression are two of the three main psychological components of PICS. The development of anxiety and depression three to 12 months after ICU discharge is not uncommon, affecting 46% and 29% of ICU patients, respectively[3]. In a Canadian population-based study of critically ill patients, the prevalence of mental disorders increased over 5 years after ICU discharge, from 41.5% (pre-hospitalization) to 55.6% (post-hospitalization)[4]. In a meta-analysis that included 28 studies, six studies examined the post-ICU psychological status of patients with severe acute respiratory syndrome (SARS) or Middle East Respiratory Syndrome, the authors reported that at least one-third of patients experienced psychological conditions including anxiety (30%) and depression (33%), six months post-recovery[5].

The Hospital Anxiety and Depression Scale (HADS) is a validated tool used to assess anxiety and depression in non-psychiatric hospitals. In calculating the HADS score, somatic symptoms of anxiety or depression, such as dizziness and fatigue, were excluded (to minimize confounding factors from physical diseases). Moreover, symptoms associated with serious psychiatric disorders were also excluded. Such symptoms are uncommon in medically ill populations[6]. The Arabic version of the HADS, validated in Arabic populations[7], is used with critically ill patients[8].

Results from a systematic review of patients with post-COVID-19 syndrome found that the frequency of depressive symptoms +12 wk after severe acute respiratory syndrome coronavirus 2 infection, ranged from 11% to 28%. Moreover, the frequency of clinically significant and/or severe depressive symptoms ranged from 3% to 12%. Furthermore, the

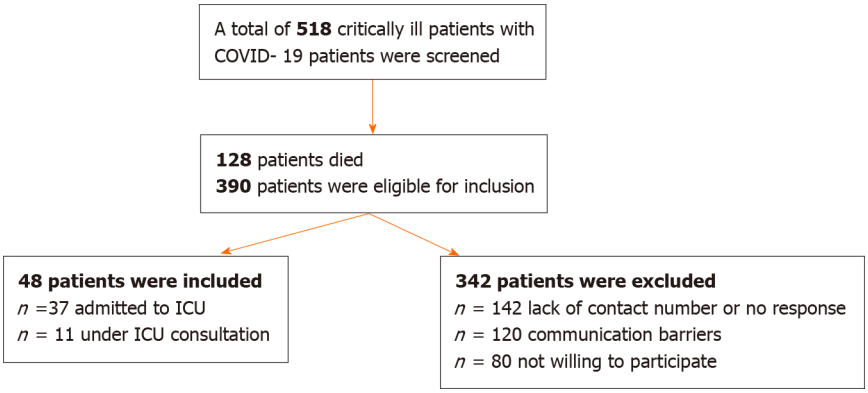

Figure 1 Patient screening process. COVID-19: Coronavirus disease 2019; ICU: Intensive care unit.

review concluded that the severity of acute COVID-19 was not associated with the frequency of depressive symptoms[9]. A recent retrospective matched cohort study evaluated 236739 patients six months after illness. The study found a 46% increase in mood, anxiety, and psychotic disorders among patients with COVID–19 patients compared to a matched cohort of patients with influenza[10]. Data from the Middle East assessing the mental health status of patients with COVID-19 after post-ICU discharge are lacking. Using a validated assessment tool, this study aimed to evaluate anxiety and depression among patients who had COVID-19 and identify the associated risk factors.

MATERIALS AND METHODS

This prospective, single-center study was designed to assess the psychological status of patients with COVID-19, who were critically ill and admitted to the ICU. We screened all patients with laboratory or radiological confirmation of COVID-19, who were either admitted to the ICU or under ICU observation for > 24 h, between April 2020 and November 2020. Adults (≥ 18 years of age) were screened for eligibility. Patients eligible to participate in this study were contacted by telephone 6 months post-ICU discharge between October 2020 to May 2021. Those who consented completed a questionnaire that assessed their psychological status. Patients with language barriers and those who were unwilling to participate were excluded. Our study used the Arabic version of the HADS to evaluate anxiety and depression among patients with COVID-19 who were critically ill. The questionnaire was completed six months after ICU discharge. The HADS consists of 14 questions: Seven for screening anxiety symptoms and seven for signs of depression[11]. Each question was rated on a scale of 0–3 points. A score of 8 or greater on the anxiety or depression subscale represents clinically significant anxiety or depression[12]. Demographic data (age, sex, and weight), Glasgow Coma score, severity score [Acute Physiology and Chronic Health Evaluation II (APACHE II)], ICU and hospital length of stay, comorbidities, and ICU care details including respiratory support and medications, such as corticosteroids, vasopressors, neuromuscular blocking agents, and tocilizumab, were extracted from the hospital system. All methods were performed in accordance with relevant guidelines and regulations.

Study outcomes

The primary outcome was the mean HADS score six months after ICU discharge. Secondary outcomes were risk factors associated with anxiety and/or depression.

Statistical analysis

Continuous variables were presented as means with standard deviations, while categorical variables were presented as frequencies and percentages. We categorized the patients based on the proportion meeting the predefined anxiety or depression threshold six months after ICU discharge. Of note, the authors of HADS suggested a 4-tier system (normal ≤ 7, mild 8-10, moderate 11-14, and severe 15-21) for considering severity[13]. We employed multivariable ordered logistic regression to analyze the factors associated with anxiety and/or depression. The data were analyzed using STATA 14 (StataCorp LP, College Station, TX, United States)[14].

RESULTS

During the study period, 518 patients with COVID-19 admitted to the ICU were screened. Of the 390 patients who met the inclusion criteria, 48 completed the questionnaire (Figure 1). Most of the included patients were male 30 (62.5%). The mean age was 56.3 ± 17.2 years. The mean length of ICU stay was 9.1 ± 7.4 d. The main comorbidities were endocrine (*n* = 24, 50%) and cardiovascular (*n* = 21, 43.8 %) diseases (Table 1). The mean HADS score for anxiety and depression was 11.4 (SD ± 8.5). In this study, anxiety and depression (HADS score > 7) were detected in 15 (31.3%) and 18 (37.5%) of patients, respectively, six months after ICU discharge (Table 2). Importantly, results from the multivariate ordered logistic

Table 1 Participant characteristics

Characteristics	*n* = 48
Age (years), mean ± SD	56.3 ± 17.2
Gender (male), *n* (%)	30 (62.5)
Weight (kg), mean ± SD	79.4 ± 20.4
APACHE II score, mean ± SD	12.4 ± 8.1
ICU LOS, (days) mean ± SD	9.1 ± 7.4
Hospital LOS (days), mean ± SD	23.1 ± 17.7
Glasgow coma score, mean ± SD	13.8 ± 3.3
Comorbidities, *n* (%)	
Endocrine diseases	24 (50)
Cardiovascular diseases	21 (43.8)
Respiratory diseases	5 (10.4)
Autoimmune/Inflammatory diseases	3 (6.3)
Hematological diseases	3 (6.3)
Renal diseases	3 (6.3)
Neurological diseases	2 (4.2)
Preexisting mental health problems	2 (4.2)
Hepatic diseases	1 (2.1)
ICU course *n* (%)	
Oxygen support	23 (47.9)
Non-invasive mechanical ventilation	6 (12.5)
Mechanical ventilation	5 (10.4)
Corticosteroid	27 (56.3)
Vasopressor	7 (14.7)
Neuromuscular blocking agents	2 (4)
Tocilizumab	8 (16.3)

APACHE II: Acute physiology and chronic health evaluation; ICU: Intensive care unit.

regression analysis demonstrated that vasopressor use was associated with the development of anxiety and depression [odds ratio (OR) 39.06, 95%CI: 1.309–1165.8; $P < 0.05$] (Table 3).

DISCUSSION

Our six-month follow-up questionnaire-based study found that at least one-third of patients under ICU care for COVID-19 experienced anxiety or depression following discharge. A recent retrospective study evaluated the six-month psychological outcomes of COVID-19 survivors and found that severe COVID-19 was associated with a higher incidence of mood, anxiety, or psychotic disorders than mild disease [hazard ratio (HR) 1.34, 95%CI: 1.24-1.46; P value < 0.0001][10]. In another recent study of 1617 patients, 23% had anxiety or depression at the 6-month follow-up (based on symptoms, exercise capacity, and quality of life). However, the same study found that only 4% of patients were admitted to the ICU [15]. Another single-center questionnaire study conducted in Saudi Arabia examined persistent symptoms 2 to 6 months post-COVID-19, regardless of severity. The results suggested that approximately half of the participants experienced persistent symptoms. Of these patients, 13% had anxiety and 10% had depression[16].

In this present study, we detected higher prevalences of anxiety and depression. This could be attributed to the increased severity of COVID-19, and the associated medical comorbidities, given the critical setting.

Inadequate brain perfusion and vasopressor-induced enhanced emotional memories may have contributed to the development of anxiety symptoms in our study[17]. One prospective cohort study examined 157 patients from general ICUs to explore the risk factors for psychological morbidity after three months of follow-up. It was shown that 44% of the

Table 2 Hospital Anxiety and Depression Scale scores among the participants (*n* = 48)

HADS cut-off scores, *n* (%)	Anxiety	Depression
Normal (≤ 7)	33 (68.8)	30 (62.5)
Mild (8-10)	4 (8.3)	13 (27)
Moderate (11-14)	7 (14.5)	3 (6.3)
Severe score (15-21)	4 (8.3)	2 (4.1)
Average score, mean ± SD	5.81 ± 5.1	5.6 ± 4
HADS average total score, mean ± SD	11.4 ± 8.5	

HADS: Hospital anxiety and depression scale.

Table 3 Multivariable ordered logistic regression for a factor associated with Hospital Anxiety and Depression Scale (*n* = 48)

Variable	Odds ratio (95%CI)	*P* value
Age	1.007 (0.955–1.061)	NS
Gender	1.294 (0.275–6.098)	NS
APACHEII	0.919 (0.790–1.069)	NS
Cardiovascular diseases	0.963 (0.206–4.496)	NS
Respiratory diseases	0.084 (0.005–1.542)	NS
Endocrine diseases	0.550 (0.123–2.453)	NS
Renal diseases	0.165 (0.001–32.99)	NS
Autoimmune/Inflammatory diseases	0.721 (0.040–12.95)	NS
Hematological diseases	0.067 (0.001–8.979)	NS
Oxygen support	6.119 (0.418–89.63)	NS
Non-invasive mechanical ventilation	1.082 (0.025–46.40)	NS
Mechanical ventilation	0.042 (0.0001–10.47)	NS
Corticosteroid use	0.094 (0.006–1.420)	NS
Vasopressor use	39.06 (1.309–1165.8)	< 0.05
Tocilizumab use	1.783 (0.215–14.81)	NS

HADS: Hospital anxiety and depression scale; NS: Non-significant; APACHE II: Acute physiology and chronic health evaluation.

participants were affected by anxiety, and the highest clinical risk factor for increased anxiety was the use of inotropes and vasopressors. However, no association has been observed between depression and vasopressor use[18]. This is consistent with our findings, which indicated that the need for vasopressors was associated with a higher HADS score.

Moreover, in our study, approximately 50% of patients required oxygen support, and approximately 25% required non-invasive and invasive mechanical ventilation. A prospective cohort study that evaluated patients with COVID-19 four months after discharge found that 26% and 18% of the 51 intubated patients, and 33.6% and 21.7% of the 126 patients who were not intubated, had symptoms of anxiety and depression, respectively[19].

The mean ICU length of stay in our study was 9.1 +/- 7.4 d. A prospective cohort study with a 5-year follow-up compared the physical outcomes between 276 patients with a prolonged ICU stay (≥ 8 d) and 398 patients with a short ICU stay. The study found that patients who required a long stay had significantly higher morbidity than those who had a short stay[20]. Additionally, a prospective cohort study of 46 patients with severe COVID-19 showed that depressive symptoms were more prominent in patients with physical impairment three months after ICU discharge[21].

To compare male and female long-term outcomes after intensive care for COVID-19 in terms of mortality, a prospective cohort study was conducted on 1722 male and 632 female ICU patients with COVID-19. The study found that males had poor long-term outcomes, with a 90–d mortality of 28.2% in males and 23.4% in females [22]. However, in terms of psychological symptoms, a single-center prospective cohort study investigated whether there was an association between the female sex and long-term COVID among 377 patients who were hospitalized due to COVID-19. The HADS was used for the anxiety and depression assessments. Overall, all psychological symptoms were significantly higher in females than males [anxiety symptoms 29.2% *vs* 12.9% (P = 0.001), depression symptoms 16.1% *vs* 7.5% (P = 0.009)][23]. Our

results did not show any sex-related differences in the development of anxiety or depression. However, our finding could be attributed to the small sample size.

Our study has a few limitations. First, this was a single-center study with a small sample size, which may affect the generalizability of our findings. We screened many patients for eligibility, and more than 70% were excluded because of mortality, inability to reach the patient, or communication barriers. Second, a control group was lacking in our study. It would be of interest to compare anxiety and depression between patients with and without COVID-19 in future studies. Third, our study involved a single-point evaluation. We did not take differentiate psychological symptoms. Hence, for some patients, the symptoms may have previously existed, while for others, the symptoms may have been triggered during or after COVID-19. However, only two patients in our cohort had preexisting mental health diagnoses. Finally, using a screening scale to identify anxiety and depression may be less accurate than diagnostic interviews conducted by a specialized clinician. However, the HADS is a recognized validated instrument and is easier to implement in busy ICU settings.

Our study has the advantage of being conducted in the Middle East. We were able to evaluate anxiety and depression in patients who were critically ill with COVID-19. And investigate the associated risk factors. Additionally, the study covered a six-month follow-up period and used a validated questionnaire to evaluate depression and anxiety.

The long-term effects of COVID-19 affect many organ systems. This is a growing area of research as long COVID-19 can substantially affect the quality of life[2]. Ensuring the continuity of care for patients with COVID-19 beyond the acute phase of illness is crucial for addressing the long-term health consequences. To improve current clinical practice, post-acute care clinics or specialized follow-up programs for patients with long COVID-19 should be considered. These clinics would aim to provide comprehensive assessment of ongoing symptoms, monitor potential complications, and offer tailored treatment plans based on the needs of individual patients. Additionally, promoting multidisciplinary care that engages healthcare professionals from various specialties (*e.g.*, pulmonology, cardiology, and psychology) can ensure holistic care for patients with diverse post-COVID-19 manifestations. Patient education is also paramount, as it can empower individuals to actively participate in their care, recognize signs of worsening symptoms through screening questionnaires, and adopt healthy lifestyle behaviors to promote recovery. Telemedicine and remote monitoring technologies can further facilitate continuity of care by enabling healthcare providers to remotely monitor patients' progress, provide timely interventions, and offer ongoing support, while overcoming access barriers[2,24]. Continuity of care for patients with COVID-19 beyond the acute illness, including psychological care, may assist in the early detection of anxiety and depression. Evidence suggests that initial and recurrent psychiatric illnesses occur between 14 and 19 d post-acute COVID-19[10]. Our study highlights the importance of psychological evaluation for patients who were discharged from the ICU following COVID-19 and the benefit of up to 6 months of follow-up to determine appropriate interventions. To verify our findings, further studies comparing the psychological status of patients with and without COVID-19 are warranted.

CONCLUSION

Patients with moderate-to-severe COVID-19 were anxious or depressed up to six months post-ICU discharge. To compare the psychological status of patients with or without COVID-19, further investigations are warranted.

ACKNOWLEDGEMENTS

The authors thank the Researchers Supporting Project number, King Saud University, Riyadh, Saudi Arabia, No. RSPD2024R919.

FOOTNOTES

Author contributions: Alhammad AM contributed to resources, data curation, visualization, supervision, project administration; Alqahtani A contributed to investigation. Aljawadi MH contributed to formal analysis; Alhammad AM, Aldardeer NF, and Alosaimi FD contributed to conceptualization; Alhammad AM and Aldardeer NF contributed to methodology; Alhammad AM and Alosaimi FD contributed to validation; Alhammad AM and Aldardeer NF contributed to writing-original draft; Alhammad AM, Aljawadi MH, Alnefaie B, Alonazi R, Almuqbil M, Alsaadoon A, Alqahtani RM, Alballaa R, Alshehri B, Alarifi MI, and Alosaimi FD contributed to writing-review and editing.

Institutional review board statement: This study was approved by the Institutional Review Board of King Saud University (reference number: E-19-4182). All methods were performed in accordance with relevant guidelines and regulations.

Informed consent statement: All study participants provided verbal informed consent to participate and authorized their de-identified data to be used in this publication.

Conflict-of-interest statement: The author reports no conflicts of interest in this work.

Data sharing statement: The dataset supporting the conclusions of this article is available by request from the corresponding author.

CONSORT 2010 statement: The authors have read the CONSORT 2010 statement, and the manuscript was prepared and revised according to the CONSORT 2010 statement.

Country/Territory of origin: Saudi Arabia

ORCID number: Abdullah M Alhammad 0000-0002-9806-2503; Fahad D Alosaimi 0000-0003-1027-5836.

Corresponding Author's Membership in Professional Societies: Saudi Society of Clinical Pharmacy, 20212715; Saudi Critical Care Society, 202113661.

S-Editor: Liu JH
L-Editor: A
P-Editor: Yu HG

REFERENCES

1 **Wang C**, Zhao H. The Impact of COVID-19 on Anxiety in Chinese University Students. *Front Psychol* 2020; **11**: 1168 [PMID: 32574244 DOI: 10.3389/fpsyg.2020.01168]
2 **Nalbandian A**, Sehgal K, Gupta A, Madhavan MV, McGroder C, Stevens JS, Cook JR, Nordvig AS, Shalev D, Sehrawat TS, Ahluwalia N, Bikdeli B, Dietz D, Der-Nigoghossian C, Liyanage-Don N, Rosner GF, Bernstein EJ, Mohan S, Beckley AA, Seres DS, Choueiri TK, Uriel N, Ausiello JC, Accili D, Freedberg DE, Baldwin M, Schwartz A, Brodie D, Garcia CK, Elkind MSV, Connors JM, Bilezikian JP, Landry DW, Wan EY. Post-acute COVID-19 syndrome. *Nat Med* 2021; **27**: 601-615 [PMID: 33753937 DOI: 10.1038/s41591-021-01283-z]
3 **Hatch R**, Young D, Barber V, Griffiths J, Harrison DA, Watkinson P. Anxiety, Depression and Post Traumatic Stress Disorder after critical illness: a UK-wide prospective cohort study. *Crit Care* 2018; **22**: 310 [PMID: 30466485 DOI: 10.1186/s13054-018-2223-6]
4 **Olafson K**, Marrie RA, Bolton JM, Bernstein CN, Bienvenu OJ, Kredentser MS, Logsetty S, Chateau D, Nie Y, Blouw M, Afifi TO, Stein MB, Leslie WD, Katz LY, Mota N, El-Gabalawy R, Enns MW, Leong C, Sweatman S, Sareen J. The 5-year pre- and post-hospitalization treated prevalence of mental disorders and psychotropic medication use in critically ill patients: a Canadian population-based study. *Intensive Care Med* 2021; **47**: 1450-1461 [PMID: 34495357 DOI: 10.1007/s00134-021-06513-z]
5 **Ahmed H**, Patel K, Greenwood DC, Halpin S, Lewthwaite P, Salawu A, Eyre L, Breen A, O'Connor R, Jones A, Sivan M. Long-term clinical outcomes in survivors of severe acute respiratory syndrome and Middle East respiratory syndrome coronavirus outbreaks after hospitalisation or ICU admission: A systematic review and meta-analysis. *J Rehabil Med* 2020; **52**: jrm00063 [PMID: 32449782 DOI: 10.2340/16501977-2694]
6 **Bjelland I**, Dahl AA, Haug TT, Neckelmann D. The validity of the Hospital Anxiety and Depression Scale. An updated literature review. *J Psychosom Res* 2002; **52**: 69-77 [PMID: 11832252 DOI: 10.1016/s0022-3999(01)00296-3]
7 **Terkawi AS**, Tsang S, AlKahtani GJ, Al-Mousa SH, Al Musaed S, AlZoraigi US, Alasfar EM, Doais KS, Abdulrahman A, Altirkawi KA. Development and validation of Arabic version of the Hospital Anxiety and Depression Scale. *Saudi J Anaesth* 2017; **11**: S11-S18 [PMID: 28616000 DOI: 10.4103/sja.SJA_43_17]
8 **Shdaifat SA**, Al Qadire M. Anxiety and depression among patients admitted to intensive care. *Nurs Crit Care* 2022; **27**: 106-112 [PMID: 32844542 DOI: 10.1111/nicc.12536]
9 **Renaud-Charest O**, Lui LMW, Eskander S, Ceban F, Ho R, Di Vincenzo JD, Rosenblat JD, Lee Y, Subramaniapillai M, McIntyre RS. Onset and frequency of depression in post-COVID-19 syndrome: A systematic review. *J Psychiatr Res* 2021; **144**: 129-137 [PMID: 34619491 DOI: 10.1016/j.jpsychires.2021.09.054]
10 **Taquet M**, Geddes JR, Husain M, Luciano S, Harrison PJ. 6-month neurological and psychiatric outcomes in 236 379 survivors of COVID-19: a retrospective cohort study using electronic health records. *Lancet Psychiatry* 2021; **8**: 416-427 [PMID: 33836148 DOI: 10.1016/S2215-0366(21)00084-5]
11 **Hatch R**, Young D, Barber V, Harrison DA, Watkinson P. The effect of postal questionnaire burden on response rate and answer patterns following admission to intensive care: a randomised controlled trial. *BMC Med Res Methodol* 2017; **17**: 49 [PMID: 28347296 DOI: 10.1186/s12874-017-0319-3]
12 **Mikkelsen ME**, Still M, Anderson BJ, Bienvenu OJ, Brodsky MB, Brummel N, Butcher B, Clay AS, Felt H, Ferrante LE, Haines KJ, Harhay MO, Hope AA, Hopkins RO, Hosey M, Hough CTL, Jackson JC, Johnson A, Khan B, Lone NI, MacTavish P, McPeake J, Montgomery-Yates A, Needham DM, Netzer G, Schorr C, Skidmore B, Stollings JL, Umberger R, Andrews A, Iwashyna TJ, Sevin CM. Society of Critical Care Medicine's International Consensus Conference on Prediction and Identification of Long-Term Impairments After Critical Illness. *Crit Care Med* 2020; **48**: 1670-1679 [PMID: 32947467 DOI: 10.1097/CCM.0000000000004586]
13 **Snaith RP**, Zigmond AS. The hospital Anxiey and depression scale with the irritability-depression-anxiety scale and the Leeds situational anxiety scale: manual. Windsor, UK: NFER-NELSON, 1994
14 **StataCorp**. Stata statistical software. Release 17. TX: StataCorp LP, College Station. StataCrop LLC, 2021
15 **Huang C**, Huang L, Wang Y, Li X, Ren L, Gu X, Kang L, Guo L, Liu M, Zhou X, Luo J, Huang Z, Tu S, Zhao Y, Chen L, Xu D, Li Y, Li C, Peng L, Xie W, Cui D, Shang L, Fan G, Xu J, Wang G, Zhong J, Wang C, Wang J, Zhang D, Cao B. 6-month consequences of COVID-19 in patients discharged from hospital: a cohort study. *Lancet* 2021; **397**: 220-232 [PMID: 33428867 DOI: 10.1016/S0140-6736(20)32656-8]
16 **Garout MA**, Saleh SAK, Adly HM, Abdulkhaliq AA, Khafagy AA, Abdeltawab MR, Rabaan AA, Rodriguez-Morales AJ, Al-Tawfiq JA, Alandiyjany MN. Post-COVID-19 syndrome: assessment of short- and long-term post-recovery symptoms in recovered cases in Saudi Arabia.

Infection 2022; **50**: 1431-1439 [PMID: 35294728 DOI: 10.1007/s15010-022-01788-w]

17 **VanValkinburgh D**, Kerndt CC, Hashmi MF. Inotropes and vasopressors. Signa Vitae 2023 Feb 19 [Cited 2023 Jul 4]; 13: 46-52. Available from: https://www.ncbi.nlm.nih.gov/books/NBK482411/

18 **Wade DM**, Howell DC, Weinman JA, Hardy RJ, Mythen MG, Brewin CR, Borja-Boluda S, Matejowsky CF, Raine RA. Investigating risk factors for psychological morbidity three months after intensive care: a prospective cohort study. *Crit Care* 2012; **16**: R192 [PMID: 23068129 DOI: 10.1186/cc11677]

19 **Writing Committee for the COMEBAC Study Group**, Morin L, Savale L, Pham T, Colle R, Figueiredo S, Harrois A, Gasnier M, Lecoq AL, Meyrignac O, Noel N, Baudry E, Bellin MF, Beurnier A, Choucha W, Corruble E, Dortet L, Hardy-Leger I, Radiguer F, Sportouch S, Verny C, Wyplosz B, Zaidan M, Becquemont L, Montani D, Monnet X. Four-Month Clinical Status of a Cohort of Patients After Hospitalization for COVID-19. *JAMA* 2021; **325**: 1525-1534 [PMID: 33729425 DOI: 10.1001/jama.2021.3331]

20 **Hermans G**, Van Aerde N, Meersseman P, Van Mechelen H, Debaveye Y, Wilmer A, Gunst J, Casaer MP, Dubois J, Wouters P, Gosselink R, Van den Berghe G. Five-year mortality and morbidity impact of prolonged *vs* brief ICU stay: a propensity score matched cohort study. *Thorax* 2019; **74**: 1037-1045 [PMID: 31481633 DOI: 10.1136/thoraxjnl-2018-213020]

21 **van Gassel RJJ**, Bels J, Remij L, van Bussel BCT, Posthuma R, Gietema HA, Verbunt J, van der Horst ICC, Olde Damink SWM, van Santen S, van de Poll MCG. Functional Outcomes and Their Association With Physical Performance in Mechanically Ventilated Coronavirus Disease 2019 Survivors at 3 Months Following Hospital Discharge: A Cohort Study. *Crit Care Med* 2021; **49**: 1726-1738 [PMID: 33967204 DOI: 10.1097/CCM.0000000000005089]

22 **Zettersten E**, Engerström L, Bell M, Jäderling G, Mårtensson J, Block L, Larsson E. Long-term outcome after intensive care for COVID-19: differences between men and women-a nationwide cohort study. *Crit Care* 2021; **25**: 86 [PMID: 33632273 DOI: 10.1186/s13054-021-03511-x]

23 **Bai F**, Tomasoni D, Falcinella C, Barbanotti D, Castoldi R, Mulè G, Augello M, Mondatore D, Allegrini M, Cona A, Tesoro D, Tagliaferri G, Viganò O, Suardi E, Tincati C, Beringheli T, Varisco B, Battistini CL, Piscopo K, Vegni E, Tavelli A, Terzoni S, Marchetti G, Monforte AD. Female gender is associated with long COVID syndrome: a prospective cohort study. *Clin Microbiol Infect* 2022; **28**: 611.e9-611.e16 [PMID: 34763058 DOI: 10.1016/j.cmi.2021.11.002]

24 **Schmidt K**, Gensichen J, Gehrke-Beck S, Kosilek RP, Kühne F, Heintze C, Baldwin LM, Needham DM. Management of COVID-19 ICU-survivors in primary care: - a narrative review. *BMC Fam Pract* 2021; **22**: 160 [PMID: 34303344 DOI: 10.1186/s12875-021-01464-2]

World Journal of Clinical Cases

Submit a Manuscript: https://www.f6publishing.com

World J Clin Cases 2024 May 26; 12(15): 2568-2577

DOI: 10.12998/wjcc.v12.i15.2568

ISSN 2307-8960 (online)

ORIGINAL ARTICLE

Prospective Study

Triceps skinfold thickness trajectories and the risk of all-cause mortality: A prospective cohort study

Na Yang, Li-Yun He, Zi-Yi Li, Yu-Cheng Yang, Fan Ping, Ling-Ling Xu, Wei Li, Hua-Bing Zhang, Yu-Xiu Li

Specialty type: Medicine, research and experimental

Provenance and peer review: Unsolicited article; Externally peer reviewed.

Peer-review model: Single blind

Peer-review report's classification

Scientific Quality: Grade C

Novelty: Grade B

Creativity or Innovation: Grade B

Scientific Significance: Grade B

P-Reviewer: Soriano-Ursúa MA, Mexico

Received: February 5, 2024

Revised: April 2, 2024

Accepted: April 8, 2024

Published online: May 26, 2024

Na Yang, Li-Yun He, Zi-Yi Li, Yu-Cheng Yang, Fan Ping, Ling-Ling Xu, Wei Li, Hua-Bing Zhang, Yu-Xiu Li, Department of Endocrinology, Key Laboratory of Endocrinology of National Health Commission, Peking Union Medical College Hospital, Chinese Academy of Medical Sciences & Peking Union Medical College, Beijing 100730, China

Co-corresponding authors: Hua-Bing Zhang and Yu-Xiu Li.

Corresponding author: Hua-Bing Zhang, MD, Chief Doctor, Department of Endocrinology, Key Laboratory of Endocrinology of National Health Commission, Peking Union Medical College Hospital, Chinese Academy of Medical Sciences & Peking Union Medical College, No. 1 Shuaifuyuan, Wangfujing Street, Beijing 100730, China. huabingzhangchn@163.com

Abstract

BACKGROUND

The measurement of triceps skinfold (TSF) thickness serves as a noninvasive metric for evaluating subcutaneous fat distribution. Despite its clinical utility, the TSF thickness trajectories and their correlation with overall mortality have not been thoroughly investigated.

AIM

To explore TSF thickness trajectories of Chinese adults and to examine their associations with all-cause mortality.

METHODS

This study encompassed a cohort of 14747 adults sourced from the China Health and Nutrition Survey. Latent class trajectory modeling was employed to identify distinct trajectories of TSF thickness. Subjects were classified into subgroups reflective of their respective TSF thickness trajectory. We utilized multivariate Cox regression analyses and mediation examinations to explore the link between TSF thickness trajectory and overall mortality, including contributory factors.

RESULTS

Upon adjustment for multiple confounding factors, we discerned that males in the 'Class 2: Thin–stable' and 'Class 3: Thin–moderate' TSF thickness trajectories exhibited a markedly reduced risk of mortality from all causes in comparison to the 'Class 1: Extremely thin' subgroup. In the mediation analyses, the Geriatric Nutritional Risk Index was found to be a partial intermediary in the relationship between TSF thickness trajectories and mortality. For females, a lower TSF

thickness pattern was significantly predictive of elevated all-cause mortality risk exclusively within the non-elderly cohort.

CONCLUSION
In males and non-elderly females, lower TSF thickness trajectories are significantly predictive of heightened mortality risk, independent of single-point TSF thickness, body mass index, and waist circumference.

Key Words: Triceps skinfold thickness; Trajectory; All-cause mortality; Body mass index; Geriatric Nutritional Risk Index

Core Tip: In this prospective cohort study, 14747 adults from the China Health and Nutrition Survey (1993-2015) were included and lower triceps skinfold (TSF) thickness trajectories in males and non-elderly females were significantly associated with an increased risk of all-cause mortality, independent of the one-point TSF thickness, body mass index, and waist circumference. When the TSF thickness in early adulthood was similar, even if the TSF thickness subsequently increased, there was no significant difference in the risk of all-cause mortality.

Citation: Yang N, He LY, Li ZY, Yang YC, Ping F, Xu LL, Li W, Zhang HB, Li YX. Triceps skinfold thickness trajectories and the risk of all-cause mortality: A prospective cohort study. *World J Clin Cases* 2024; 12(15): 2568-2577
URL: https://www.wjgnet.com/2307-8960/full/v12/i15/2568.htm
DOI: https://dx.doi.org/10.12998/wjcc.v12.i15.2568

INTRODUCTION

The body mass index (BMI) is commonly used in epidemiological studies as a primary anthropometric indicator for mortality risk assessment. Existing literature shows a J-shaped or U-shaped correlation between BMI and the incidence of mortality from all causes within the general population[1,2]. Yet, the utility of BMI as a mortality indicator remains under scrutiny due to its inability to accurately represent the regional distribution of body fat, which may lead to considerable variability among individuals a similar BMI[1-5]. As such, estimations of body composition have gained recognition as potentially significant prognosticators of mortality[6,7].

The triceps skinfold (TSF) thickness is an alternative anthropometric measure that is noninvasive, straightforward, readily accessible, and cost-effective, enabling the assessment of peripheral fat distribution[8]. This measure is increasingly considered a viable proxy for exploring the interplay between subcutaneous adiposity and mortality risk[4,9-14]. Unlike isolated or sporadic TSF measurements, longitudinal trajectory analysis captures the temporal evolution of TSF thickness, potentially elucidating a more comprehensive understanding of its association with mortality. Despite the apparent importance, there seems to be a gap in research endeavors examining the connection between TSF thickness trajectories and all-cause mortality.

Hence, the main objective of this investigation is to identify distinct TSF thickness trajectories within a substantial cohort of Chinese adults and to examine their potential associations with all-cause mortality.

MATERIALS AND METHODS

The China Health and Nutrition Survey

The China Health and Nutrition Survey (CHNS) represents a comprehensive, ongoing prospective study, spanning cross China. Comprising 10 rigorous rounds of data collection, this survey encompasses a representative sample from nine provinces, accounting for nearly half of China's population[15]. Ethical approval was secured from the respective Institutional Review Boards of the University of North Carolina at Chapel Hill and the National Institute for Nutrition and Health, Chinese Center for Disease Control and Prevention, with all participants providing informed consent. The methodology and survey design have been elaborated in prior publications[16].

Study population

Supplementary Figure 1 illustrates the study cohort's selection flowchart. Considering the absence of complete anthropometric data prior to 1993, our analysis included adult participants from eight CHNS waves between 1993 and 2015. Initially, 32963 individuals were deemed eligible; however, exclusions were made for pregnancy, incomplete or anomalous anthropometric data, baseline cardiovascular or oncological diseases, and lack of follow-up data.

Data collection

Mid-arm anthropometric measurements: Standardized procedures were adhered to by skilled health workers to perform mid-arm measurements in triplicate, per individual, to ensure precision, with the mean value used for subsequent analyses. TSF thickness was measured at the posterior mid-point between the olecranon and acromion apex, with accuracy to 0.5 mm, utilizing a skinfold caliper. Mid-upper arm circumference (MUAC) was determined at the midpoint of the extended arm, precise to 0.1 cm. The mid-arm muscle circumference was computed by subtracting π times the TSF thickness from the MUAC[17].

Covariates: Demographics were obtained *via* structured interviews conducted by trained interviewers. Dietary assessments were ascertained based on a thorough three-day food consumption diary and household inventory[16]. Physical activity encompassed both occupational and domestic activity[18]. For participants of the 2009 survey wave, fasting venous blood samples were obtained[19]. The Geriatric Nutritional Risk Index (GNRI)[20] = 1.489 × serum albumin (Alb) (g/L) + 41.7 × present weight/ideal weight (kg). The ideal weight was derived from the Lorentz formula as follows: Ideal weight for females = 0.60 × height (cm) – 40, ideal weight for males = 0.75 × height (cm) – 62.5, and a present weight/ ideal weight ratio is set to 1 if it is no less than 1. Insulin resistance was assessed through the Homeostatic Model Assessment for Insulin Resistance (HOMA-IR) index, based on fasting insulin and glucose levels[21].

Ascertainment of outcome: Mortality data, including the exact date of death, were ascertained from family reports during each survey wave. The baseline was set as the date of first entry with complete mid-arm measurements, with follow-up duration calculated up to death, loss to follow-up, or end of the study period, whichever occurred first.

Statistical analysis

Descriptive analysis: Baseline characteristics were categorized and analyzed, with continuous variables presented as means ± SD and categorical variables as counts (percentages). Comparative analyses across trajectory groups employed analysis of variance (ANOVA), Kruskal-Wallis, or Chi-square tests.

Trajectory modeling: Latent class trajectory models discerned TSF thickness trajectories for both genders, employing the lcmm package in R with a censored normal model[22]. Criteria for model selection included the lowest Bayesian information criterion, internal consistency as reflected by average posterior probability, and adequate trajectory class size (at least 5% of the sample population within each trajectory class) to evaluate mortality risk[15,23-26].

Mortality associations: Kaplan-Meier curves and log-rank tests examined TSF thickness trajectory-mortality associations. Cox models calculated hazard ratios (HRs) and 95% confidence intervals (95%CIs), adjusting multiple variables across four models. Model 1 was adjusted for age, marital status, educational attainment level, household income per capita level, and living in the city. Model 2 included the variables from Model 1 and also adjusted for: smoking status, alcohol consumption, physical activity level, total energy intake, fat intake, protein intake, carbohydrate intake, systolic blood pressure, and diastolic blood pressure. Model 3 included the variables in Model 2 and was adjusted for BMI, waist circumference (WC), TSF thickness, and MUAC. Model 4 was adjusted for the variables in Model 3, as well as the history of diabetes and hypertension.

Subgroup and mediation analyses: Subgroups were analyzed based on blood samples, using trajectory classifications from the total sample. Mediation analysis, conducted with the lavaan package in R, examined biomarkers as mediators between TSF thickness trajectories and mortality risk.

To ascertain the incremental value of trajectory analysis over single-time-point evaluations, we stratified baseline TSF thickness into tertiles for both genders, employing the lowest tertile as a referential baseline. Subsequently, the relationship between baseline TSF thickness and all-cause mortality was examined.

We undertook stratified analyses to investigate the influence of age (< 60 years, ≥ 60 years), BMI (< 24 kg/m^2, ≥ 24 kg/m^2)[27], and central adiposity WC ≥ 90 cm in males or ≥ 80 cm in females)[28]. The potential for effect modification was quantified by calculating interaction terms (P_interaction) within the multivariable framework, multiplying TSF thickness trajectory classifications by stratifying variables.

All statistical analyses were performed with SPSS for Windows (version 20.0; IBM Corporation, Chicago, IL, United States) and R version 4.0.2 (www.r-project.org/), and $P < 0.05$ (two-sided) was considered statistically significant.

RESULTS

From the CHNS dataset, a total of 32963 adults were initially identified. After applying the exclusion criteria, the study cohort was refined to 14745 adults (mean age 42.4 ± 15.1 years; 49.1% males), as shown in Supplementary Figure 1. There were 1019 documented mortalities during the study period.

Trajectories of TSF thickness across adulthood

Figure 1 illustrates the TSF thickness trajectories among male and female participants, respectively. In males, 'Class 1: Extremely thin' denotes consistently extremely low TSF thickness through adulthood, 'Class 2: Thin–stable' represents consistently thin measurements, and 'Class 3: Thin–moderate' reflects an increase from thin to moderate values over time. There were 29.1% males in Class 1, 52.1% in Class 2, and 18.8% in Class 3. For females, 'Class 1: Thin–stable' indicates a steady thin TSF thickness measurement, 'Class 2: Thin–moderate' reflects an increase from thin to moderate, and 'Class 3:

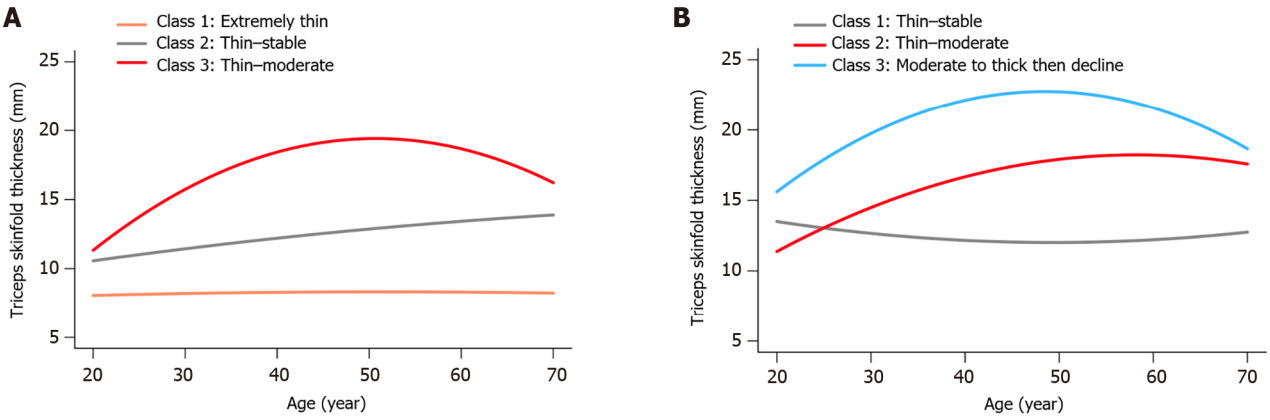

Figure 1 Trajectories of triceps skinfold thickness from the China Health and Nutrition Survey by latent class trajectory model. A: Males; B: Females.

Moderate to thick then decline' describes an initial increase followed by a reduction in older age. There were 26.5% females in Class 1, 65.1% in Class 2, and 8.4% in Class 3.

Correlation between TSF thickness trajectories and all-cause mortality

The baseline characteristics of the participants, stratified by TSF thickness trajectories, are delineated in Supplementary Table 1. Using 'Class 1' as the reference group, Kaplan-Meier survival analysis revealed that individuals classified within 'Class 3' demonstrated superior cumulative survival rates (Supplementary Figure 2, $P < 0.05$) across both genders.

Table 1 elucidates the sex-specific association among TSF thickness trajectories and all-cause mortality, refined through multivariable-adjusted Cox regression models. For the male subset, when compared with 'Class 1,' the other trajectories were inversely correlated with mortality risk, persisting across all analytical models. Notably, 'Class 3' did not exhibit a statistically significant differential in mortality risk relative to 'Class 2' [HR 0.858 (95%CI: 0.582, 1.263)], post comprehensive adjustments. In the female subset, multivariate adjustments revealed no discernable correlation between TSF thickness trajectories and mortality risk.

Trajectories of TSF thickness trajectories and biochemical parameters

Differences in biomarkers across TSF thickness trajectory classes are shown in Supplementary Table 2. Figure 2 shows the mediation effects of GNRI, high-sensitivity C-reactive protein (hs-CRP), and HOMA-IR on the association between trajectories and the risk of all-cause mortality in males. The direct effect of the TSF thickness trajectory was estimated to be 0.142. β1 to β6 were used to calculate the overall indirect effect of these factors (βind = −0.152 for GNRI, $P < 0.05$; −0.015 for hs-CRP, $P = 0.06$; and 0.005 for HOMA-IR, $P = 0.176$). The percentages of the total effects mediated by GNRI were estimated to be 50.0%.

Association of one-point TSF thickness with all-cause mortality

The Kaplan-Meier estimate of the all-cause mortality of males by one-point TSF thickness showed no significant differences among tertiles ($P = 0.297$, Supplementary Figure 3A). Supplementary Table 3 shows that TSF thickness measured at a single time point was not significantly associated with all-cause mortality for males or females.

Subgroup analyses stratified by age, BMI, and abdominal obesity

Subgroup analyses were conducted to evaluate the association between TSF thickness trajectories and all-cause mortality (Figure 3). Although a significant difference was only observed in the age < 60 years group, there was no significant interactive effect of TSF thickness trajectories and age group in males ($P_{interaction} = 0.528$). Notably, for females, only those in the age < 60 years group had a significantly decreased risk of all-cause mortality in Class 2 and Class 3 compared with Class 1 [HR 0.582 (95%CI: 0.404, 0.838) for Class 2; HR 0.237 (95%CI: 0.068, 0.829) for Class 3], indicating that the effect of TSF thickness trajectories for females on all-cause mortality was greater in those with younger age, which was also supported by our finding that there was a significant interactive effect of TSF thickness trajectories and age group on all-cause mortality ($P_{interaction} = 0.014$). There was no significant effect of BMI or WC modification on the association between TSF thickness trajectories and all-cause mortality for males or females ($P_{interaction} > 0.05$).

DISCUSSION

In this longitudinal analysis of the Chinese population over two decades, our findings indicate a significant association between lower TSF thickness trajectories for males and an elevated risk of all-cause mortality. Notably, initial TSF thickness measurements in early adulthood, even when similar among individuals, did not yield significant predictive differences in mortality risk over time. Additionally, GNRI was identified as a partial mediator in the relationship

Table 1 Association between triceps skinfold thickness trajectories and risk of all-cause mortality by sex

Trajectories	No. of participants/death	Model 1	Model 2	Model 3	Model 4
		HR (95%CI)	HR (95%CI)	HR (95%CI)	HR (95%CI)
Male					
Class 1	2132/335	1	1	1	1
Class 2	3818/221	0.674 (0.564, 0.805)	0.685 (0.572, 0.820)	0.654 (0.532, 0.805)	0.651 (0.529, 0.801)
Class 3	1379/40	0.670 (0.476, 0.942)	0.675 (0.478, 0.954)	0.628 (0.415, 0.949)	0.635 (0.420, 0.961)
Female					
Class 1	1968/213	1	1	1	1
Class 2	4828/206	0.827 (0.680, 1.007)	0.844 (0.693, 1.029)	0.982 (0.777, 1.241)	0.984 (0.779, 1.244)
Class 3	620/4	0.335 (0.124, 0.910)	0.341 (0.126, 0.927)	0.441 (0.156, 1.246)	0.447 (0.158, 1.264)

Model 1 was adjusted for age, marriage status (married or not), educational attainment levels (low, medium, or high), household income per capita levels (low, medium, or high), and living in city (yes or no). Model 2 was adjusted for the variables in Model 1 as well as smoking status (ever/current or never smoker), alcohol consumption (yes or no), physical activity levels (low, moderate, or high), total energy intake, fat intake, protein intake, carbohydrate intake. Model 3 included variables in Model 2 and was adjusted for body mass index, waist circumference, triceps skinfold thickness, mid-upper arm circumference, systolic blood pressure, and diastolic blood pressure. Model 4 was adjusted for the variables in Model 3 as well as the history of diabetes and hypertension.

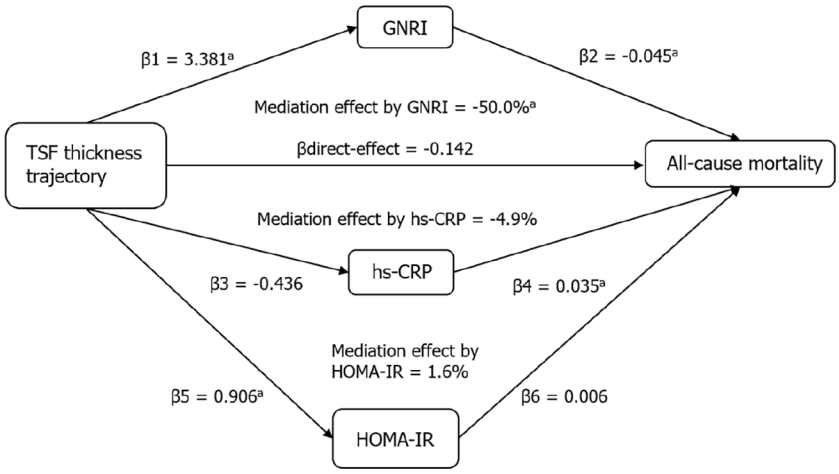

Figure 2 Mediation effects on the association between triceps skinfold thickness trajectories and risk of all-cause mortality. ª*P* < 0.05. GNRI: Geriatric Nutritional Risk Index; hs-CRP: High-sensitivity C-reactive protein; HOMA-IR: Homeostatic Model Assessment of Insulin Resistance; TSF: Triceps skinfold.

between TSF thickness trajectories and mortality outcomes. For females, the association of lower TSF thickness with increased mortality was confined to the non-elderly demographic.

Our analysis revealed a heightened risk of all-cause mortality associated with persistently low TSF thickness trajectories compared to others. This association persisted even controlling for baseline TSF thickness. Moreover, in our cohort, a one-time measurement of TSF thickness did not correlate with mortality in either gender, underscoring that TSF thickness trajectories may be a more indicative measure of mortality risk than a single measurement. Previous literature reports inconsistent findings on the relationship between TSF thickness and mortality[9,12,13,29-32], with many studies being cross-sectional or focused on particular cohorts such as older adults, hemodialysis patients, or those with liver cirrhosis. Our study extends the exploration to a comprehensive adult population, contributing novel insights to the discourse. Notably, the extremely low TSF thickness trajectory was prevalent in 18.8% of the male participants, meriting further investigation. Additionally, we observed that similar TSF thickness levels in early adulthood did not result in mortality risk divergence in later years, regardless of subsequent increases. These findings challenge prior studies that highlighted the significance of TSF thickness predominantly in older populations[4,10], and instead, accentuates the detrimental effects of lower TSF thickness in early adulthood and the necessity of monitoring TSF thickness progression throughout life.

This study unveils an intriguing gender-specific observation: The novel association between TSF thickness and mortality was exclusively noted for males and non-elderly females. This gender disparity may stem from the fact that females typically exhibit higher body fat percentages than males at equivalent BMI levels[33]. Additionally, estrogen is

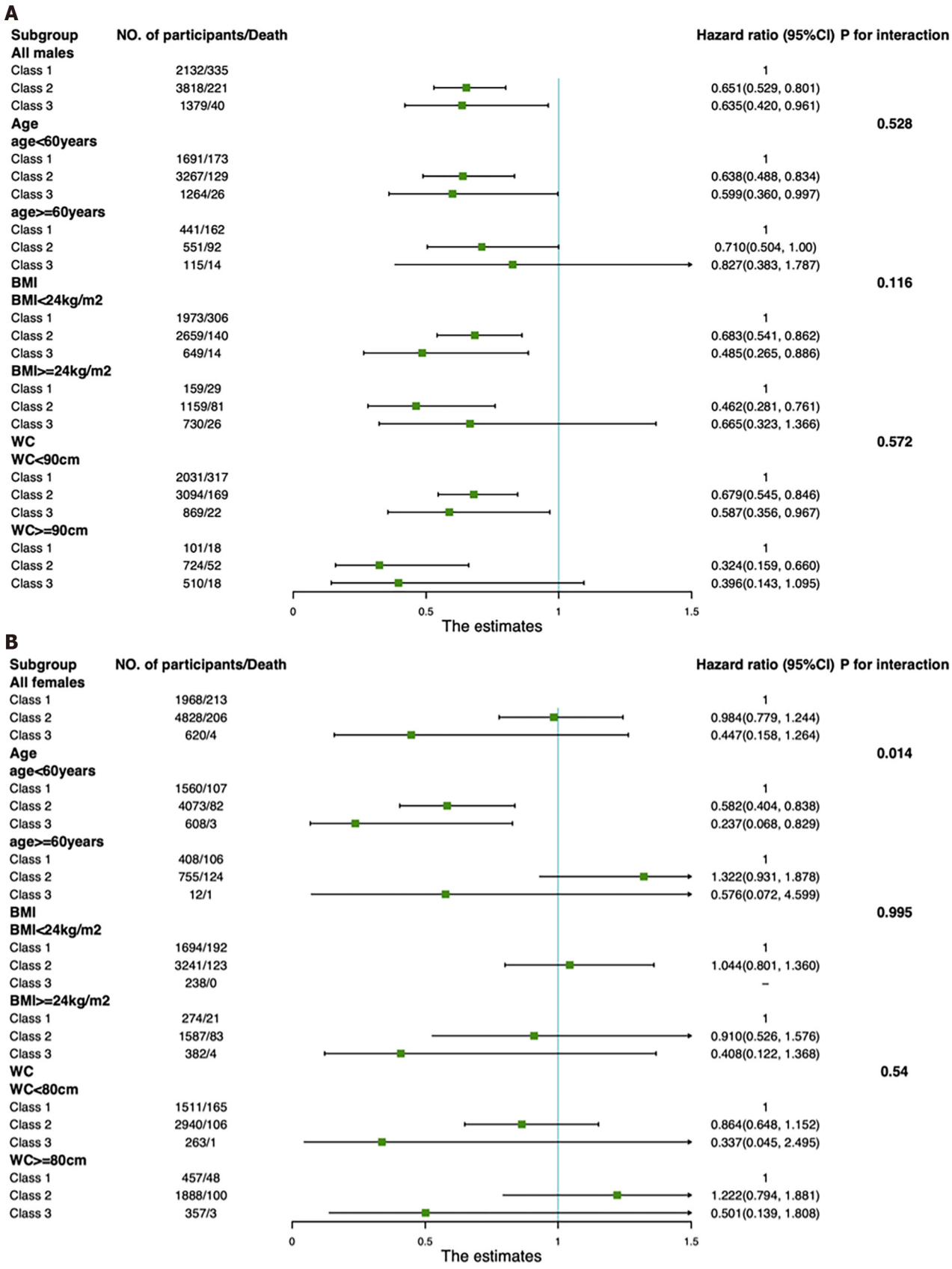

Figure 3 Association of triceps skinfold thickness trajectories with all-cause mortality stratified by age, body mass index, and waist circumference. All models were adjusted for the cofounders in Table 1. A: Males; B: Females. 95%CI: 95% confidence interval; BMI: Body mass index; WC: Waist circumference.

known to modulate fat distribution, preferentially augmenting subcutaneous rather than visceral fat accumulation in females[7,34,35]. This finding diverges from some prior studies which suggested a more pronounced protective role of TSF thickness for females[29]. For instance, a prospective study highlighted that females with colorectal cancer presenting with low TSF thickness faced a 40% increased risk of adverse outcomes compared to those with normal TSF thickness [30], whereas TSF thickness did not emerge as a prognostic determinant for males. Our data also revealed a predominance of extremely low TSF thickness trajectories for males, while for females the trajectory was more frequently characterized by thicker TSF thickness, corroborating earlier assertions of gender-based differences in subcutaneous fat distribution. Moreover, our subgroup analyses suggest a significant association between TSF thickness trajectories and mortality in younger females, hinting that TSF thickness may exert a more substantial impact earlier in life, thereby underscoring the need for vigilant monitoring of TSF thickness from early adulthood. Nonetheless, the physiological underpinnings of regional fat accumulation are intricate and not yet fully elucidated[36], necessitating further investigation in this domain.

Previous studies on TSF thickness and mortality risk have largely focused on elderly populations, indicating an increased risk of all-cause mortality with thinner skinfolds[12], However, our study suggests that the trajectory of TSF thickness may have a greater impact on younger individuals, highlighting the importance of early and continuous monitoring of skinfold thickness changes to potentially influence mortality risk. Our study data lacks specific causes of death, but a review of previous literature indicates that previous studies have explored the role of TSF thickness in predicting mortality risk associated with cancer, cardiovascular and cerebrovascular diseases, and dialysis. Data from NHANES suggest that lower TSF thickness is associated with a higher risk of cardiovascular disease mortality but not with cerebrovascular disease mortality[4]. A multicenter study demonstrated a significant correlation between low skinfold thickness and increased risk of cancer-related mortality[36]. Another study on colorectal cancer mortality risk indicated that lower TSF thickness was associated with increased mortality risk for females but not for males[30]. In dialysis patients, lower TSF thickness was linked to higher mortality risk[37]. However, there is currently a lack of research on the relationship between TSF thickness trajectories and specific disease mortality risks, necessitating further studies.

Our findings reveal that the GNRI serves as a partial mediator in the correlation between TSF thickness trajectories and all-cause mortality, suggesting that the impact of TSF thickness on mortality may predominantly be channeled through nutritional status rather than metabolic factors such as insulin resistance. While Alb is a recognized clinical marker of nutritional status, its circulating level can be influenced by a multitude of factors[38]. Hence, we delved deeper into the relationship between GNRI and various TSF thickness trajectories. Incorporating Alb, weight, and height, GNRI is advocated as an economical yet effective instrument for evaluating nutritional status[39,40]. This study discovered an inverse relationship between TSF thickness trajectories and GNRI, with GNRI exhibiting a significant mediating role in the association between TSF thickness trajectory and mortality. This observation suggests that TSF thickness may act as an indirect indicator of overall nutritional and health status. Aligning with previous studies, our findings suggest that a greater TSF thickness may confer protection against malnutrition and cachexia, potentially mitigating mortality risks associated with chronic and malignant conditions[29,41].

This investigation stands as the first study examining the trajectory of TSF thickness in relation to all-cause mortality, distinguished by its extensive cohort and prolonged observation period. Our research indicates that TSF thickness trajectories offer additional predictive insights on mortality risk, transcending the data provided by single TSF thickness measurements, BMI, and WC. Moreover, our inclusive approach, encompassing adults across a wide age spectrum, has demonstrated that the implications of TSF thickness trajectories extend well beyond geriatric demographics. We also delved into potential underlying mechanisms for our findings, contributing to a deeper understanding of this area. Nevertheless, this study had several limitations. Primarily, it is imperative to acknowledge that our cohort consisted exclusively of individuals from China, which may limit the applicability of our findings across different ethnic groups. We recognize this as a limitation and suggest that future research should aim to include a more ethnically diverse population. As an observational study, it precludes the establishment of causality. The lack of cause-specific mortality data precludes a comprehensive analysis, as deaths due to extraneous causes could introduce an element of bias. This gap in data restricts our ability to dissect and discuss the multifactorial nature of mortality in relation to TSF thickness trajectory. We acknowledge this as a critical area for future studies and aim to explore these aspects further in subsequent studies, provided that relevant data become accessible.

CONCLUSION

In conclusion, trajectories with lower TSF thickness for males and non-elderly females were significantly associated with an increased risk of all-cause mortality, independent of the one-point TSF thickness, BMI, and WC. This study additionally emphasizes the harmful effects of lower TSF thickness in early healthy adulthood and the importance of monitoring TSF thickness over the adult life course. Further studies in different ethnic populations are required to verify this conclusion.

ACKNOWLEDGMENTS

This research uses data from China Health and Nutrition Survey (CHNS). We thank the National Institute of Nutrition and Food Safety, China Center for Disease Control and Prevention, Carolina Population Center, the University of North

Carolina at Chapel Hill, the NIH (R01-HD30880, DK056350, and R01-HD38700) and the Fogarty International Center, NIH for financial support for the CHNS data collection and analysis. We also thank the China-Japan Friendship Hospital and Ministry of Health for their support with the CHNS 2009 survey.

FOOTNOTES

Author contributions: Zhang HB and Yang N conceived and designed the study; Yang N, He LY, and Yang YC conducted fieldwork, experiments, clinical activities, and data collection and compilation; Yang N, Zhang HB, and Li ZY analyzed and interpreted the data; all authors contributed to drafting the manuscript, revising it, and providing critique; Zhang HB and Li YX managed the overall and/or sectional scientific aspects of the study. As co-corresponding authors, Zhang HB and Li YX have equally contributed to all aspects of this manuscript, including conception, data analysis, drafting, and revision. The joint efforts Zhang HB and Li YX have been instrumental in ensuring the integrity and quality of the research presented.

Supported by National High Level Hospital Clinical Research Funding, No. 2022-PUMCH-B-015; CAMS Innovation Fund for Medical Sciences, No. 2021-1-12M-002; CAMS Innovation Fund for Medical Sciences, No. 2023-I2M-C&T-B-043; and Beijing Municipal Natural Science Foundation, No. M22014.

Institutional review board statement: The study was reviewed and approved by the University of North Carolina at Chapel Hill and the National Institute for Nutrition and Health, Chinese Center for Disease Control and Prevention Institutional Review Board.

Informed consent statement: All study participants, or their legal guardian, provided informed written consent prior to study enrollment.

Conflict-of-interest statement: The authors declare no conflicts of interest.

Data sharing statement: All data utilized in this study can be accessed through the official website of the China Health and Nutrition Survey (CHNS) and the website is https://www.cpc.unc.edu/projects/china.

Country/Territory of origin: China

ORCID number: Na Yang 0000-0003-4175-9411; Li-Yun He 0000-0002-2450-791X; Fan Ping 0000-0001-7650-6612; Hua-Bing Zhang 0000-0001-6259-7584; Yu-Xiu Li 0000-0001-7500-0855.

S-Editor: Lin C
L-Editor: A
P-Editor: Yu HG

REFERENCES

1 **Lee DH**, Keum N, Hu FB, Orav EJ, Rimm EB, Willett WC, Giovannucci EL. Predicted lean body mass, fat mass, and all cause and cause specific mortality in men: prospective US cohort study. *BMJ* 2018; **362**: k2575 [PMID: 29970408 DOI: 10.1136/bmj.k2575]

2 **Global BMI Mortality Collaboration**, Di Angelantonio E, Bhupathiraju ShN, Wormser D, Gao P, Kaptoge S, Berrington de Gonzalez A, Cairns BJ, Huxley R, Jackson ChL, Joshy G, Lewington S, Manson JE, Murphy N, Patel AV, Samet JM, Woodward M, Zheng W, Zhou M, Bansal N, Barricarte A, Carter B, Cerhan JR, Smith GD, Fang X, Franco OH, Green J, Halsey J, Hildebrand JS, Jung KJ, Korda RJ, McLerran DF, Moore SC, O'Keeffe LM, Paige E, Ramond A, Reeves GK, Rolland B, Sacerdote C, Sattar N, Sofianopoulou E, Stevens J, Thun M, Ueshima H, Yang L, Yun YD, Willeit P, Banks E, Beral V, Chen Zh, Gapstur SM, Gunter MJ, Hartge P, Jee SH, Lam TH, Peto R, Potter JD, Willett WC, Thompson SG, Danesh J, Hu FB. Body-mass index and all-cause mortality: individual-participant-data meta-analysis of 239 prospective studies in four continents. *Lancet* 2016; **388**: 776-786 [PMID: 27423262 DOI: 10.1016/S0140-6736(16)30175-1]

3 **Jayedi A**, Soltani S, Zargar MS, Khan TA, Shab-Bidar S. Central fatness and risk of all cause mortality: systematic review and dose-response meta-analysis of 72 prospective cohort studies. *BMJ* 2020; **370**: m3324 [PMID: 32967840 DOI: 10.1136/bmj.m3324]

4 **Li W**, Yin H, Chen Y, Liu Q, Wang Y, Qiu D, Ma H, Geng Q. Associations Between Adult Triceps Skinfold Thickness and All-Cause, Cardiovascular and Cerebrovascular Mortality in NHANES 1999-2010: A Retrospective National Study. *Front Cardiovasc Med* 2022; **9**: 858994 [PMID: 35620519 DOI: 10.3389/fcvm.2022.858994]

5 **Neeland IJ**, Poirier P, Després JP. Cardiovascular and Metabolic Heterogeneity of Obesity: Clinical Challenges and Implications for Management. *Circulation* 2018; **137**: 1391-1406 [PMID: 29581366 DOI: 10.1161/CIRCULATIONAHA.117.029617]

6 **Liu XC**, Liu L, Yu YL, Huang JY, Chen CL, Lo K, Huang YQ, Feng YQ. The Association of Subscapular Skinfold with All-Cause, Cardiovascular and Cerebrovascular Mortality. *Risk Manag Healthc Policy* 2020; **13**: 955-963 [PMID: 32801969 DOI: 10.2147/RMHP.S262300]

7 **Stefan N**. Causes, consequences, and treatment of metabolically unhealthy fat distribution. *Lancet Diabetes Endocrinol* 2020; **8**: 616-627 [PMID: 32559477 DOI: 10.1016/S2213-8587(20)30110-8]

8 **Nickerson BS**, Fedewa MV, Cicone Z, Esco MR. The relative accuracy of skinfolds compared to four-compartment estimates of body composition. *Clin Nutr* 2020; **39**: 1112-1116 [PMID: 31036415 DOI: 10.1016/j.clnu.2019.04.018]

9 **Loh WJ**, Johnston DG, Oliver N, Godsland IF. Skinfold thickness measurements and mortality in white males during 27.7 years of follow-up. *Int J Obes (Lond)* 2018; **42**: 1939-1945 [PMID: 29491491 DOI: 10.1038/s41366-018-0034-0]

10 **He L**, Yang N, Wang J, Huang J, Li W, Xu L, Ping F, Li Y, Zhang H. Mid-Arm Muscle and Subcutaneous Fat Associated with All-Cause Mortality Independent of BMI: A Prospective Cohort Study. *Obesity (Silver Spring)* 2021; **29**: 1203-1214 [PMID: 34021531 DOI: 10.1002/oby.23179]

11 **Kim J**, Meade T, Haines A. Skinfold thickness, body mass index, and fatal coronary heart disease: 30 year follow up of the Northwick Park heart study. *J Epidemiol Community Health* 2006; **60**: 275-279 [PMID: 16476761 DOI: 10.1136/jech.2005.042200]

12 **Enoki H**, Kuzuya M, Masuda Y, Hirakawa Y, Iwata M, Hasegawa J, Izawa S, Iguchi A. Anthropometric measurements of mid-upper arm as a mortality predictor for community-dwelling Japanese elderly: the Nagoya Longitudinal Study of Frail Elderly (NLS-FE). *Clin Nutr* 2007; **26**: 597-604 [PMID: 17669559 DOI: 10.1016/j.clnu.2007.06.008]

13 **Huang CX**, Tighiouart H, Beddhu S, Cheung AK, Dwyer JT, Eknoyan G, Beck GJ, Levey AS, Sarnak MJ. Both low muscle mass and low fat are associated with higher all-cause mortality in hemodialysis patients. *Kidney Int* 2010; **77**: 624-629 [PMID: 20072111 DOI: 10.1038/ki.2009.524]

14 **de Almeida Roediger M**, de Fátima Nunes Marucci M, Quintiliano Scarpelli Dourado DA, de Oliveira C, Licio Ferreira Santos J, de Oliveira Duarte YA. Body Composition Changes and 10-Year Mortality Risk in Older Brazilian Adults: Analysis of Prospective Data from the SABE Study. *J Nutr Health Aging* 2019; **23**: 51-59 [PMID: 30569068 DOI: 10.1007/s12603-018-1118-1]

15 **Han T**, Zhang S, Duan W, Ren X, Wei C, Sun C, Li Y. Eighteen-year alcohol consumption trajectories and their association with risk of type 2 diabetes and its related factors: the China Health and Nutrition Survey. *Diabetologia* 2019; **62**: 970-980 [PMID: 30923839 DOI: 10.1007/s00125-019-4851-z]

16 **He J**, Fang A, Yu S, Shen X, Li K. Dietary Nonheme, Heme, and Total Iron Intake and the Risk of Diabetes in Adults: Results From the China Health and Nutrition Survey. *Diabetes Care* 2020; **43**: 776-784 [PMID: 32033991 DOI: 10.2337/dc19-2202]

17 **Barazzoni R**, Jensen GL, Correia MITD, Gonzalez MC, Higashiguchi T, Shi HP, Bischoff SC, Boirie Y, Carrasco F, Cruz-Jentoft A, Fuchs-Tarlovsky V, Fukushima R, Heymsfield S, Mourtzakis M, Muscaritoli M, Norman K, Nyulasi I, Prisprasert V, Prado C, de van der Schuren M, Yoshida S, Yu Y, Cederholm T, Compher C. Guidance for assessment of the muscle mass phenotypic criterion for the Global Leadership Initiative on Malnutrition (GLIM) diagnosis of malnutrition. *Clin Nutr* 2022; **41**: 1425-1433 [PMID: 35450768 DOI: 10.1016/j.clnu.2022.02.001]

18 **Xue Y**, Shen Q, Li C, Dai Z, He T. The Visceral Adipose Index in Relation to Incidence of Hypertension in Chinese Adults: China Health and Nutrition Survey (CHNS). *Nutrients* 2020; **12** [PMID: 32197411 DOI: 10.3390/nu12030805]

19 **Zhu B**, Li Y, Shi Y, Song N, Fang Y, Ding X. Long-term drinking behavior change patterns and its association with hyperuricemia in chinese adults: evidence from China Health and Nutrition Survey. *BMC Public Health* 2022; **22**: 1230 [PMID: 35725435 DOI: 10.1186/s12889-022-13637-4]

20 **Riveros C**, Jazayeri SB, Chalfant V, Ahmed F, Bandyk M, Balaji KC. The Geriatric Nutritional Risk Index Predicts Postoperative Outcomes in Bladder Cancer: A Propensity Score-Matched Analysis. *J Urol* 2022; **207**: 797-804 [PMID: 34854753 DOI: 10.1097/JU.0000000000002342]

21 **Wang T**, Li M, Zeng T, Hu R, Xu Y, Xu M, Zhao Z, Chen Y, Wang S, Lin H, Yu X, Chen G, Su Q, Mu Y, Chen L, Tang X, Yan L, Qin G, Wan Q, Gao Z, Wang G, Shen F, Luo Z, Qin Y, Huo Y, Li Q, Ye Z, Zhang Y, Liu C, Wang Y, Wu S, Yang T, Deng H, Zhao J, Shi L, Ning G, Bi Y, Wang W, Lu J. Association Between Insulin Resistance and Cardiovascular Disease Risk Varies According to Glucose Tolerance Status: A Nationwide Prospective Cohort Study. *Diabetes Care* 2022; **45**: 1863-1872 [PMID: 35700159 DOI: 10.2337/dc22-0202]

22 **Lennon H**, Kelly S, Sperrin M, Buchan I, Cross AJ, Leitzmann M, Cook MB, Renehan AG. Framework to construct and interpret latent class trajectory modelling. *BMJ Open* 2018; **8**: e020683 [PMID: 29982203 DOI: 10.1136/bmjopen-2017-020683]

23 **Wang Y**, Hou W, Siddiqi SM, Sun C, Han T, Yang J. Association of sleep trajectory in adulthood with risk of hypertension and its related risk factors: the China Health and Nutrition Survey. *J Clin Sleep Med* 2020; **16**: 515-521 [PMID: 32003742 DOI: 10.5664/jcsm.8254]

24 **Sanchez-Sanchez JL**, Izquierdo M, Carnicero-Carreño JA, García-García FJ, Rodríguez-Mañas L. Physical activity trajectories, mortality, hospitalization, and disability in the Toledo Study of Healthy Aging. *J Cachexia Sarcopenia Muscle* 2020; **11**: 1007-1017 [PMID: 32163233 DOI: 10.1002/jcsm.12566]

25 **Charles A**, Detilleux J, Buckinx F, Reginster JY, Gruslin B, Bruyère O. Physical performance trajectories and mortality among nursing home residents: results of the SENIOR cohort. *Age Ageing* 2020; **49**: 800-806 [PMID: 32179907 DOI: 10.1093/ageing/afaa034]

26 **Chen Y**, Cai C, Tan J, Lei X, Chen Q, Zhang J, Zhang Y. High-risk Growth Trajectory Related to Childhood Overweight/Obesity and Its Predictive Model at Birth. *J Clin Endocrinol Metab* 2022; **107**: e4015-e4026 [PMID: 35862057 DOI: 10.1210/clinem/dgac441]

27 **Gao M**, Lv J, Yu C, Guo Y, Bian Z, Yang R, Du H, Yang L, Chen Y, Li Z, Zhang X, Chen J, Qi L, Chen Z, Huang T, Li L; China Kadoorie Biobank (CKB) Collaborative Group. Metabolically healthy obesity, transition to unhealthy metabolic status, and vascular disease in Chinese adults: A cohort study. *PLoS Med* 2020; **17**: e1003351 [PMID: 33125374 DOI: 10.1371/journal.pmed.1003351]

28 **Huang G**, Xu J, Zhang Z, Cai L, Liu H, Yu X. Total cholesterol and high density lipoprotein cholesterol ratio is associated with metabolic syndrome in a very elderly Chinese population. *Sci Rep* 2022; **12**: 15212 [PMID: 36075943 DOI: 10.1038/s41598-022-19445-5]

29 **Wu SE**, Chen WL. Not the enemy: potential protective benefits of superficial subcutaneous adipose tissue. *Pol Arch Intern Med* 2022; **132** [PMID: 35420008 DOI: 10.20452/pamw.16237]

30 **Xie H**, Ruan G, Zhang H, Ge Y, Zhang Q, Lin S, Song M, Zhang X, Liu X, Li X, Zhang K, Yang M, Tang M, Deng L, Gan J, Shi H. Sex differences in the association of triceps skinfold thickness and colorectal cancer mortality. *Nutrition* 2022; **103-104**: 111811 [PMID: 36155916 DOI: 10.1016/j.nut.2022.111811]

31 **de Santana FM**, Domiciano DS, Gonçalves MA, Machado LG, Figueiredo CP, Lopes JB, Caparbo VF, Takayama L, Menezes PR, Pereira RM. Association of Appendicular Lean Mass, and Subcutaneous and Visceral Adipose Tissue With Mortality in Older Brazilians: The São Paulo Ageing & Health Study. *J Bone Miner Res* 2019; **34**: 1264-1274 [PMID: 30866105 DOI: 10.1002/jbmr.3710]

32 **Oppert JM**, Charles MA, Thibult N, Guy-Grand B, Eschwège E, Ducimetière P. Anthropometric estimates of muscle and fat mass in relation to cardiac and cancer mortality in men: the Paris Prospective Study. *Am J Clin Nutr* 2002; **75**: 1107-1113 [PMID: 12036820 DOI: 10.1093/ajcn/75.6.1107]

33 **Liu Y**, Sun G, Li Y. A prospective cohort study on the association of lean body mass estimated by mid-upper arm muscle circumference with hypertension risk in Chinese residents. *J Clin Hypertens (Greenwich)* 2022; **24**: 329-338 [PMID: 35174624 DOI: 10.1111/jch.14412]

34 **Tang HK**, Bowe SJ, Nguyen THHD, Dibley MJ. Triceps and subscapular skinfold thickness percentiles of a school-based sample of

adolescents in Ho Chi Minh City, Vietnam. *Eur J Clin Nutr* 2020; **74**: 1483-1487 [PMID: 32249817 DOI: 10.1038/s41430-020-0626-3]

35 **Ebadi M**, Tandon P, Moctezuma-Velazquez C, Ghosh S, Baracos VE, Mazurak VC, Montano-Loza AJ. Low subcutaneous adiposity associates with higher mortality in female patients with cirrhosis. *J Hepatol* 2018; **69**: 608-616 [PMID: 29709682 DOI: 10.1016/j.jhep.2018.04.015]

36 **Yin L**, Zhang L, Li N, Guo J, Liu L, Lin X, Fan Y, Liu J, Zhang M, Chong F, Chen X, Wang C, Wang X, Liang T, Liu X, Deng L, Li W, Yang M, Yu J, Yang S, Zuo Z, Yuan K, Yu M, Song C, Cui J, Li S, Guo Z, Shi H, Xu H. Several anthropometric measurements and cancer mortality: predictor screening, threshold determination, and joint analysis in a multicenter cohort of 12138 adults. *Eur J Clin Nutr* 2022; **76**: 756-764 [PMID: 34584226 DOI: 10.1038/s41430-021-01009-x]

37 **Noori N**, Kopple JD, Kovesdy CP, Feroze U, Sim JJ, Murali SB, Luna A, Gomez M, Luna C, Bross R, Nissenson AR, Kalantar-Zadeh K. Mid-arm muscle circumference and quality of life and survival in maintenance hemodialysis patients. *Clin J Am Soc Nephrol* 2010; **5**: 2258-2268 [PMID: 20947789 DOI: 10.2215/CJN.02080310]

38 **Hayama T**, Hashiguchi Y, Ozawa T, Watanabe M, Fukushima Y, Shimada R, Nozawa K, Matsuda K, Fujii S, Fukagawa T. The preoperative geriatric nutritional risk index (GNRI) is an independent prognostic factor in elderly patients underwent curative resection for colorectal cancer. *Sci Rep* 2022; **12**: 3682 [PMID: 35256659 DOI: 10.1038/s41598-022-07540-6]

39 **Xiang Q**, Li Y, Xia X, Deng C, Wu X, Hou L, Yue J, Dong B. Associations of geriatric nutrition risk index and other nutritional risk-related indexes with sarcopenia presence and their value in sarcopenia diagnosis. *BMC Geriatr* 2022; **22**: 327 [PMID: 35428245 DOI: 10.1186/s12877-022-03036-0]

40 **Güç ZG**, Alacacıoğlu A, Kalender ME, Oflazoğlu U, Ünal S, Yıldız Y, Salman T, Küçükzeybek Y, Tarhan MO. HALP score and GNRI: Simple and easily accessible indexes for predicting prognosis in advanced stage NSCLC patients. The İzmir oncology group (IZOG) study. *Front Nutr* 2022; **9**: 905292 [PMID: 36061883 DOI: 10.3389/fnut.2022.905292]

41 **Pinto AC**, Sousa AS, Amaral TF, Guerra RS. Association Between Anthropometric Indicators of Nutrition Status and Length of Hospital Stay in Hospitalized Patients. *JPEN J Parenter Enteral Nutr* 2021; **45**: 381-393 [PMID: 32618361 DOI: 10.1002/jpen.1844]

World Journal of Clinical Cases

Submit a Manuscript: https://www.f6publishing.com

World J Clin Cases 2024 May 26; 12(15): 2578-2585

DOI: 10.12998/wjcc.v12.i15.2578

ISSN 2307-8960 (online)

ORIGINAL ARTICLE

Randomized Controlled Trial

Evaluation of the effects of health education interventions for hypertensive patients based on the health belief model

Hong-Mei Wang, Ying Chen, Yan-Hua Shen, Xiao-Mei Wang

Specialty type: Medicine, research and experimental

Provenance and peer review: Unsolicited article; Externally peer reviewed.

Peer-review model: Single blind

Peer-review report's classification

Scientific Quality: Grade C

Novelty: Grade B

Creativity or Innovation: Grade B

Scientific Significance: Grade B

P-Reviewer: Wright A, United Kingdom

Received: February 19, 2024

Revised: March 11, 2024

Accepted: April 8, 2024

Published online: May 26, 2024

Hong-Mei Wang, Yan-Hua Shen, Xiao-Mei Wang, Department of Emergency, Lishui Second People's Hospital, Lishui 323000, Zhejiang Province, China

Ying Chen, Department of Pancreatic and Biliary Surgery, The First Affiliated Hospital of China Medical University, Shenyang 110002, Liaoning Province, China

Co-first authors: Hong-Mei Wang and Ying Chen.

Corresponding author: Hong-Mei Wang, Nurse, Department of Emergency, Lishui Second People's Hospital, No. 69 Beihuan Road, Liandu District, Lishui 323000, Zhejiang Province, China. vmxa671@163.com

Abstract

BACKGROUND

Hypertension is a major risk factor for cardiovascular disease and stroke, and its prevalence is increasing worldwide. Health education interventions based on the health belief model (HBM) can improve the knowledge, attitudes, and behaviors of patients with hypertension and help them control their blood pressure.

AIM

To evaluate the effects of health education interventions based on the HBM in patients with hypertension in China.

METHODS

Between 2021 and 2023, 140 patients with hypertension were randomly assigned to either the intervention or control group. The intervention group received health education based on the HBM, including lectures, brochures, videos, and counseling sessions, whereas the control group received routine care. Outcomes were measured at baseline, three months, and six months after the intervention and included blood pressure, medication adherence, self-efficacy, and perceived benefits, barriers, susceptibility, and severity.

RESULTS

The intervention group had significantly lower systolic blood pressure [mean difference (MD): -8.2 mmHg, $P < 0.001$] and diastolic blood pressure (MD: -5.1 mmHg, $P = 0.002$) compared to the control group at six months. The intervention group also had higher medication adherence (MD: 1.8, $P < 0.001$), self-efficacy (MD: 12.4, $P < 0.001$), perceived benefits (MD: 3.2, $P < 0.001$), lower perceived

barriers (MD: -2.6, P = 0.001), higher perceived susceptibility (MD: 2.8, P = 0.002), and higher perceived severity (MD: 3.1, P < 0.001) than the control group at six months.

CONCLUSION

Health education interventions based on the HBM effectively improve blood pressure control and health beliefs in patients with hypertension and should be implemented in clinical practice and community settings.

Key Words: Hypertension; Health education; Health belief model; Blood pressure control; Randomized controlled trial

Core Tip: Health education interventions based on the health belief model (HBM) significantly improve blood pressure control and health beliefs in patients with hypertension. This study, conducted in China from 2021 to 2023, demonstrated that patients who received HBM-based education had lower blood pressure, better medication adherence, and improved self-efficacy than those who received routine care. Implementing such interventions in clinical and community settings can effectively help patients with hypertension manage their condition and enhance their overall health outcomes.

Citation: Wang HM, Chen Y, Shen YH, Wang XM. Evaluation of the effects of health education interventions for hypertensive patients based on the health belief model. *World J Clin Cases* 2024; 12(15): 2578-2585
URL: https://www.wjgnet.com/2307-8960/full/v12/i15/2578.htm
DOI: https://dx.doi.org/10.12998/wjcc.v12.i15.2578

INTRODUCTION

Hypertension, also known as high blood pressure, is a chronic condition that occurs when the blood force acting on the arterial walls is excessively high[1]. Hypertension can damage blood vessels and organs and increase the risk of cardiovascular disease (CVD) and stroke[2]. According to the World Health Organization, hypertension affects approximately 1.13 billion people worldwide and is responsible for 10.4 million deaths annually[3]. In China, hypertension is a major public health problem, with an estimated prevalence of 23.2% among adults, a low awareness rate of 48.2%, a low treatment rate of 40.7%, and a low control rate of 15.3%[4]. Therefore, effective prevention and management of hypertension are essential to reduce the burden of CVD and stroke in China.

Health education is one of the key strategies for preventing and controlling hypertension, as it can improve the knowledge, attitudes, and behaviors of patients with hypertension and help them adopt healthy lifestyles and adhere to medications[5]. The health belief model (HBM) is a widely used theoretical framework for health education interventions that posits that health behaviors are influenced by six constructs: Perceived susceptibility, perceived severity, perceived benefits, perceived barriers, self-efficacy, and cues to action[6]. Perceived susceptibility refers to the belief that one is at risk of developing a disease or experiencing negative consequences; perceived severity refers to the belief that the disease or its consequences are serious or harmful; perceived benefits refer to the belief that taking a certain action will reduce the risk or severity of the disease or its consequences; perceived barriers refer to the belief that there are obstacles or costs associated with taking a certain action; self-efficacy refers to the belief that one has the ability or confidence to perform a certain action; and cues to action refer to the factors that trigger or motivate one to take a certain action[7]. According to the HBM, health behaviors are more likely to occur when individuals perceive a high susceptibility to and severity of a disease, perceive more benefits than barriers to taking action, have high self-efficacy, and receive cues for action[8].

Several studies have applied the HBM to design and evaluate health education interventions for patients with hypertension in different settings and populations[9-15]. The results showed that health education interventions based on the HBM could improve the blood pressure control and health beliefs of patients with hypertension compared with usual care or other interventions. However, most of these studies have been conducted in developed countries or regions, such as the United States, Europe, and Taiwan, and there is a lack of evidence on the effectiveness of health education interventions based on the HBM for patients with hypertension in mainland China. Moreover, most of these studies used a single or limited mode of delivery for health education interventions such as lectures, brochures, or telephone calls. There is a need to explore the use of multiple and diverse modes of delivery for health education interventions based on the HBM, such as videos, counseling sessions, and online platforms.

Therefore, this study aimed to evaluate the effects of health education interventions based on the HBM on patients with hypertension in China from 2021 to 2023.

MATERIALS AND METHODS

Study design and setting

This randomized controlled trial was divided into the intervention and control groups. This study was conducted at two health centers in the Lishui Second People's Hospital from January 2021 to June 2023. The choice of community health centers was based on their willingness to participate and the similarity of population size, socio-economic status, and medical service provision. The research plan was approved by the ethics committee of Lishui Second People's Hospital, and all participants provided written informed consent before enrollment.

Participants and sampling

The participants were patients with hypertension who met the following inclusion criteria: (1) Aged 18 years or above; (2) diagnosed with hypertension according to the 2018 Chinese guidelines for the management of hypertension (systolic blood pressure ≥ 140 mmHg and/or diastolic blood pressure ≥ 90 mmHg, or taking antihypertensive medication)[16]; (3) registered as residents in the catchment area of community health centers; (4) able to communicate in mandarin and read and write Chinese; and (5) willing to participate in and follow the study procedures. The exclusion criteria were as follows: (1) Secondary hypertension or other serious co-morbidities such as heart failure, renal failure, or stroke; (2) cognitive impairment or mental disorders that could affect the understanding and completion of the questionnaires; and (3) participation in other similar health education interventions during the study period.

The sample size was calculated based on the primary outcome of systolic blood pressure. Assuming a mean difference of 10 mmHg between the intervention and control groups, a standard deviation of 15 mmHg, a significance level of 0.05, a power of 0.80, and a dropout rate of 20%, the required sample size was 64 patients *per* group. To achieve this sample size, 140 patients with hypertension were recruited from two community health centers using convenience sampling. The recruitment process was as follows: (1) The staff of the community health centers screened the eligible patients from their electronic medical records and contacted them by phone or home visits; (2) the staff explained the purpose and procedures of the study to the interested patients and obtained their written informed consent; (3) the staff collected the baseline data from the consenting patients using standardized questionnaires and measured their blood pressure using a calibrated electronic sphygmomanometer; (4) the staff randomly assigned the patients to either the intervention group or the control group using a computer-generated random number table; and (5) the staff informed the patients about their group allocation and provided them with relevant instructions.

Intervention

The intervention group received health education interventions based on the HBM, whereas the control group received routine care. The health education interventions consisted of four components: Lectures, brochures, videos, and counseling sessions. The lectures were delivered by trained nurses in a classroom setting at community health centers. The lectures covered topics such as the definition, causes, complications, prevention, and treatment of hypertension; the importance of medication adherence and lifestyle modification; and the application of HBM constructs to enhance self-efficacy and overcome barriers. The interactive lectures used various methods, such as demonstrations, role-plays, games, and quizzes, to engage participants. The lectures lasted approximately one hour each and were held once a month for three months. The brochures were designed based on the HBM constructs and contained information and tips for controlling blood pressure. Brochures were distributed to participants after each lecture and were made available online. The videos were produced by professional media companies and featured stories of patients with hypertension who successfully controlled their blood pressure by following the HBM principles[17]. The videos were shown to the participants during lectures and were made accessible online. The counseling sessions were conducted one-on-one by trained nurses at community health centers or *via* phone. The counseling sessions aimed to provide participants with individualized feedback, guidance, support, and reinforcement based on their blood pressure levels, medication adherence, lifestyle behaviors, and health beliefs. The counseling sessions lasted approximately 15 min each and were held once every two weeks for three months.

The control group received routine care in accordance with the National Guidelines for Hypertension Management in China[16]. Routine care included regular blood pressure monitoring, prescription medication, and general health education regarding the prevention and control of hypertension. The control group did not receive any specific interventions based on the HBM.

Data collection

Data were collected at baseline (before randomization), three months (after the intervention), and six months (follow-up) after the intervention. Data were collected by trained research assistants blinded to the participants' group allocation. The data collection methods included questionnaires and blood pressure measurements.

Questionnaires were self-administered by the participants and contained questions on demographic characteristics, medication adherence, self-efficacy, as well as perceived benefits, barriers, susceptibility, and severity. Medication adherence was measured using the 8-item Morisky Medication Adherence Scale (MMAS-8), which assesses the frequency and reasons for missing or skipping medication doses[18]. The MMAS-8 has a total score ranging from 0 to 8, with higher scores indicating better medication adherence. Self-efficacy was measured using the 10-item Self-Efficacy for Managing Chronic Disease Scale, which assesses confidence in performing various self-management behaviors related to chronic diseases. The total score ranged from 10 to 100, with higher scores indicating higher self-efficacy. Perceived benefits, barriers, susceptibility, and severity were measured using the 16-item Hypertension Health Belief Scale, which assesses beliefs regarding the advantages and disadvantages of taking antihypertensive medications and lifestyle modifications,

the likelihood and seriousness of developing hypertension-related complications, and the cues to action for blood pressure control. This scale has four subscales, each containing four items. Each item uses a 5-point Likert scale ranging from 1 (strongly disagree) to 5 (strongly agree). The subscale scores were calculated by summing the item scores, with higher scores indicating higher levels of the corresponding construct.

Trained research assistants measured the blood pressure using a calibrated electronic sphygmomanometer. The participants were instructed to sit quietly for at least 5 min before the measurement and avoid smoking, drinking caffeinated beverages, or exercising for 30 min before the measurement. Blood pressure was measured three times on the right arm at intervals of at least 1 min, and the average of the three readings was recorded as the blood pressure value. The systolic and diastolic blood pressures were recorded in millimeters of mercury (mmHg).

Data analysis

Data were analyzed using SPSS version 26.0. Descriptive statistics were used to describe the demographic characteristics, blood pressure, medication adherence, self-efficacy, and health beliefs of the participants in both groups at baseline and three and six months after the intervention. Independent *t*-tests or chi-square tests were used to compare the baseline differences between the two groups. Repeated-measures analysis of variance (ANOVA) or generalized estimating equations (GEE) were used to compare changes in blood pressure, medication adherence, self-efficacy, and health beliefs between the two groups over time. The level of significance was set at $P < 0.05$.

RESULTS

A total of 140 patients with hypertension were recruited and randomized into an intervention group ($n = 70$) and a control group ($n = 70$). The baseline characteristics of the study participants are presented in Table 1. There were no significant differences between the two groups in terms of age, sex, education level, marital status, occupation, smoking status, drinking status, body mass index, duration of hypertension, number of antihypertensive drugs, baseline blood pressure, medication adherence, self-efficacy, or health beliefs.

Changes in blood pressure, medication adherence, self-efficacy, and health beliefs between the two groups over time are shown in Table 2. The repeated-measures ANOVA or GEE results showed significant group-by-time interactions for all outcomes, indicating that the intervention group had significantly different outcomes than the control group over time. The intervention group had significantly lower systolic and diastolic blood pressure, higher medication adherence, higher self-efficacy, higher perceived benefits, perceived barriers, perceived susceptibility, and perceived severity than the control group three and six months after the intervention.

DISCUSSION

This study evaluated the effects of health education interventions based on the HBM on patients with hypertension in China from 2021 to 2023. The results showed that the intervention group had significantly lower systolic and diastolic blood pressure, higher medication adherence, higher self-efficacy, higher perceived benefits, lower perceived barriers, higher perceived susceptibility, and higher perceived severity than the control group three and six months after the intervention.

The findings of this study are consistent with those of previous studies that have applied the HBM to design and evaluate health education interventions for patients with hypertension in different settings and populations[19-25]. Health education interventions based on the HBM can improve blood pressure control and health beliefs of patients with hypertension by enhancing their knowledge, attitudes, and behaviors related to hypertension prevention and management. The HBM constructs can explain how patients with hypertension perceive the risk and severity of hypertension and its complications, weigh the benefits and barriers of taking antihypertensive medication and modifying their lifestyle, gain confidence and motivation to perform self-management behaviors, and receive cues and support from healthcare providers and other sources[26,27]. Health education interventions based on the HBM can address these constructs by providing tailored and comprehensive information, feedback, guidance, support, and reinforcement for patients[28-30].

The strengths of this study include the use of a randomized controlled trial design, multiple and diverse modes of delivery of health education interventions based on the HBM, and standardized and validated instruments to measure outcomes. The limitations of this study include the relatively small sample size, short duration of follow-up, lack of blinding of the participants and intervention providers, and the potential influence of confounding factors, such as co-morbidities, socio-economic status, and health service utilization.

The implications of this study are as follows: (1) Health education interventions based on the HBM should be implemented in clinical practice and community settings to prevent and manage hypertension; (2) health education interventions based on the HBM should use multiple and diverse modes of delivery to enhance their effectiveness and accessibility; (3) health education interventions based on the HBM should be evaluated using rigorous methods and long-term follow-up to assess their impact and sustainability; and (4) health education interventions based on the HBM should be tailored to the specific needs and preferences of patients with hypertension in different contexts and cultures.

Table 1 Baseline characteristics of the participants, *n* (%)/mean ± SD

Variable	Intervention group (*n* = 80)	Control group (*n* = 80)	*P* value
Age (yr)	58.6 ± 9.4	59.2 ± 10.2	0.64
Gender			0.87
Male	37 (52.9)	36 (51.4)	
Female	33 (47.1)	34 (48.6)	
Education level			0.76
Primary school or below	15 (21.4)	16 (22.9)	
Middle school	31 (44.3)	30 (42.9)	
High school or above	24 (34.3)	24 (34.3)	
Marital status			0.81
Married or cohabiting	64 (91.4)	63 (90.0)	
Single, divorced, or widowed	6 (8.6)	7 (10.0)	
Occupation			0.69
Employed or self-employed	39 (55.7)	37 (52.9)	
Retired or unemployed	31 (44.3)	33 (47.1)	
Smoking status			0.92
Current smoker	11 (15.7)	10 (14.3)	
Former smoker or never smoker	59 (84.3)	60 (85.7)	
Drinking status			0.77
Current drinker	13 (18.6)	14 (20.0)	
Former drinker or never drinker	57 (81.4)	56 (80.0)	
Body mass index (kg/m^2)	25.4 ± 3.2	25.7 ± 3.6	0.54
Duration of hypertension (yr)	8.3 ± 6.4	8.7 ± 7.2	0.71
Number of antihypertensive drugs			0.83
One	31 (44.3)	29 (41.4)	
Two or more	39 (55.7)	41 (58.6)	
Systolic blood pressure (mmHg)	149 ± 14	150 ± 15	0.67
Diastolic blood pressure (mmHg)	91 ± 9	92 ± 10	0.59
Medication adherence score			
MMAS-8	6.2 ± 1.8	6.3 ± 1.9	0.68
Self-efficacy score			
SEMCDS	68.4 ± 1.7	68.6 ± 1.8	0.51
Perceived benefits score			
HHBS	16.8 ± 2.4	16.9 ± 2.6	0.32
Perceived barriers score			
HHBS	11.2 ± 3.1	11.4 ± 3.3	0.49
Perceived susceptibility score			
HHBS	14.6 ± 2.9	14.7 ± 3.1	0.56
Perceived severity score			
HHBS	15.4 ± 2.7	1 .5 ± 2.8	0.68

P values are based on independent *t*-tests or chi-square tests. MMAS-8: Morisky medication adherence scale; SEMCDS: Self-efficacy for managing chronic

disease scale; HHBS: Hypertension health belief scale.

Table 2 Changes in blood pressure, medication adherence, self-efficacy, and health beliefs between the two groups over time, mean ± SD

Variable	Intervention group (*n* = 70)			Control group (*n* = 80)			Group-by-time interaction
	Baseline	3 months	6 months	Baseline	3 months	6 months	*P* value
Systolic blood pressure (mmHg)	149 ± 14	136 ± 12[a]	133 ± 11[a]	150 ± 14	145 ± 13	143 ± 12	< 0.001
Diastolic blood pressure (mmHg)	91 ± 9	83 ± 8[a]	81 ± 7[a]	92 ± 9	89 ± 8	88 ± 7	< 0.001
Medication adherence score (MMAS-8)	6.2 ± 1.8	7.4 ± 1.1[a]	7.6 ± 1.0[a]	6.1 ± 1.8	6.5 ± 1.7	6.7 ± 1.6	< 0.001
Self-efficacy score (SEMCDS)	68.4 ± 1.7	72.4 ± 1.5[a]	73.2 ± 1.4[a]	68.0 ± 1.7	69.5 ± 1.6	70.0 ± 1.5	< 0.001
Perceived benefits score (HHBS)	16.8 ± 2.4	18.2 ± 2.2[a]	18.5 ± 2.1[a]	16.7 ± 2.4	17.0 ± 2.3	17.2 ± 2.2	< 0.001
Perceived barriers score (HHBS)	11.2 ± 3.1	9.8 ± 2.9[a]	9.5 ± 2.8[a]	11.3 ± 3.1	10.9 ± 3.0	10.7 ± 2.9	< 0.001
Perceived susceptibility score (HHBS)	14.6 ± 2.9	16.0 ± 2.7[a]	16.3 ± 2.6[a]	14.5 ± 2.9	15.0 ± 2.8	15.2 ± 2.7	< 0.001
Perceived severity score (HHBS)	15.4 ± 2.7	16.8 ± 2.5[a]	17.1 ± 2.4[a]	15.3 ± 2.7	15.8 ± 2.6	16.0 ± 2.5	< 0.001

[a]$P < 0.05$ (significant differences between the intervention and control groups at the same time point).
MMAS-8: Morisky medication adherence scale; SEMCDS: Self-efficacy for managing chronic disease scale; HHBS: Hypertension health belief scale.

CONCLUSION

This study demonstrated that health education interventions based on the HBM effectively improved blood pressure control and health beliefs of patients with hypertension in China from 2021 to 2023. This study suggests that health education interventions based on the HBM should be widely adopted and further evaluated for the prevention and management of hypertension.

FOOTNOTES

Author contributions: Wang HM, Wang XM and Chen Y conceptualized the research, contributed to data collection, drafted the initial manuscript, and contributed to formal analysis; Wang HM provided guidance for this study, and together with Sheng YH, they contributed to methodology and visualization; Wang HM and Chen Y validated this study. All authors participated in this study and jointly reviewed and edited the manuscript.

Institutional review board statement: This study was reviewed and approved by the Institutional Review Committee of the Second People's Hospital of Lishui City.

Clinical trial registration statement: This study is registered at: https://www.researchregistry.com. The registration identification number is Researchregistry9847.

Informed consent statement: All study participants, or their legal guardian, provided informed written consent prior to study enrollment.

Conflict-of-interest statement: All the authors report no relevant conflicts of interest for this article.

Data sharing statement: No additional data are available.

CONSORT 2010 statement: The authors have read the CONSORT 2010 statement, and the manuscript was prepared and revised according to the CONSORT 2010 statement.

Country/Territory of origin: China

ORCID number: Hong-Mei Wang 0009-0002-4150-7185.

S-Editor: Liu H
L-Editor: A
P-Editor: Yu HG

REFERENCES

1 **Forrester SJ**, Booz GW, Sigmund CD, Coffman TM, Kawai T, Rizzo V, Scalia R, Eguchi S. Angiotensin II Signal Transduction: An Update on Mechanisms of Physiology and Pathophysiology. *Physiol Rev* 2018; **98**: 1627-1738 [PMID: 29873596 DOI: 10.1152/physrev.00038.2017]
2 **Li Y**, Yang L, Wang L, Zhang M, Huang Z, Deng Q, Zhou M, Chen Z. Burden of hypertension in China: A nationally representative survey of 174,621 adults. *Int J Cardiol* 2017; **227**: 516-523 [PMID: 27856040 DOI: 10.1016/j.ijcard.2016.10.110]
3 **Mills KT**, Bundy JD, Kelly TN, Reed JE, Kearney PM, Reynolds K, Chen J, He J. Global Disparities of Hypertension Prevalence and Control: A Systematic Analysis of Population-Based Studies From 90 Countries. *Circulation* 2016; **134**: 441-450 [PMID: 27502908 DOI: 10.1161/CIRCULATIONAHA.115.018912]
4 **Hu L**, Huang X, You C, Li J, Hong K, Li P, Wu Y, Wu Q, Bao H, Cheng X. Prevalence and Risk Factors of Prehypertension and Hypertension in Southern China. *PLoS One* 2017; **12**: e0170238 [PMID: 28095471 DOI: 10.1371/journal.pone.0170238]
5 **Shen Y**, Wang TT, Gao M, Hu K, Zhu XR, Zhang X, Wang FB, He C, Sun XY. [Effectiveness evaluation of health belief model-based health education intervention for patients with hypertension in community settings]. *Zhonghua Yu Fang Yi Xue Za Zhi* 2020; **54**: 155-159 [PMID: 32074702 DOI: 10.3760/cma.j.issn.0253-9624.2020.02.008]
6 **Chen Y**, Li X, Jing G, Pan B, Ge L, Bing Z, Yang K, Han X. Health education interventions for older adults with hypertension: A systematic review and meta-analysis. *Public Health Nurs* 2020; **37**: 461-469 [PMID: 31943315 DOI: 10.1111/phn.12698]
7 **Khorsandi M**, Fekrizadeh Z, Roozbahani N. Investigation of the effect of education based on the health belief model on the adoption of hypertension-controlling behaviors in the elderly. *Clin Interv Aging* 2017; **12**: 233-240 [PMID: 28184154 DOI: 10.2147/CIA.S117142]
8 **Gharouni K**, Ardalan A, Araban M, Ebrahimzadeh F, Bakhtiar K, Almasian M, Bastami F. Application of Freire's adult education model in modifying the psychological constructs of health belief model in self-medication behaviors of older adults: a randomized controlled trial. *BMC Public Health* 2020; **20**: 1350 [PMID: 32887596 DOI: 10.1186/s12889-020-09425-7]
9 **Lollis CM**, Johnson EH, Antoni MH. The efficacy of the health belief model for predicting condom usage and risky sexual practices in university students. *AIDS Educ Prev* 1997; **9**: 551-563 [PMID: 9451482]
10 **Parsa P**, Mirmohammadi A, Khodakarami B, Roshanaiee G, Soltani F. Effects of Breast Self-Examination Consultation Based on the Health Belief Model on Knowledge and Performance of Iranian Women Aged Over 40 Years. *Asian Pac J Cancer Prev* 2016; **17**: 3849-3854 [PMID: 27644628]
11 **Azadi NA**, Ziapour A, Lebni JY, Irandoost SF, Abbas J, Chaboksavar F. The effect of education based on health belief model on promoting preventive behaviors of hypertensive disease in staff of the Iran University of Medical Sciences. *Arch Public Health* 2021; **79**: 69 [PMID: 33952339 DOI: 10.1186/s13690-021-00594-4]
12 **Tam HL**, Wong EML, Cheung K. Effectiveness of Educational Interventions on Adherence to Lifestyle Modifications Among Hypertensive Patients: An Integrative Review. *Int J Environ Res Public Health* 2020; **17** [PMID: 32272601 DOI: 10.3390/ijerph17072513]
13 **Sadeghi R**, Masoudi MR, Patelarou A, Khanjani N. Predictive Factors for the Care and Control of Hypertension Based on the Health Belief Model Among Hypertensive Patients During the COVID-19 Epidemic in Sirjan, Iran. *Curr Hypertens Rev* 2022; **18**: 78-84 [PMID: 34082684 DOI: 10.2174/1573402117666210603115309]
14 **Ramezankhani A**, Ghaffari M, Etemad K, Fallah F. Effect of the health belief model based education on hypertension reduction among elderly women affiliated with Shahid Beheshti University of Medical Sciences-2018. *J Health Field* 2019; **6**: 6-12 [DOI: 10.22037/jhf.v6i4.23121]
15 **Lu CH**, Tang ST, Lei YX, Zhang MQ, Lin WQ, Ding SH, Wang PX. Community-based interventions in hypertensive patients: a comparison of three health education strategies. *BMC Public Health* 2015; **15**: 33 [PMID: 25631224 DOI: 10.1186/s12889-015-1401-6]
16 **Liu LS**. Writing Group of 2010 Chinese Guidelines for the Management of Hypertension. [2010 Chinese guidelines for the management of hypertension]. *Zhonghua Xin Xue Guan Bing Za Zhi* 2011; **39**: 579-615 [PMID: 22088239]
17 **Panahi R**, Siboni FS, Kheiri M, Ghoozlu KJ, Shafaei M, Dehghankar L. Promoting the adoption of behaviors to prevent osteoporosis using the health belief model integrated with health literacy: quasi-experimental intervention study. *BMC Public Health* 2021; **21**: 2221 [PMID: 34872550 DOI: 10.1186/s12889-021-12300-8]
18 **Schroeder K**, Fahey T, Ebrahim S. How can we improve adherence to blood pressure-lowering medication in ambulatory care? Systematic review of randomized controlled trials. *Arch Intern Med* 2004; **164**: 722-732 [PMID: 15078641 DOI: 10.1001/archinte.164.7.722]
19 **Habibzadeh H**, Bagherzadi A, Didarloo A, Khalkhali H. The effect of patient education based on health belief model on hospital readmission preventive behaviors and readmission rate in patients with a primary diagnosis of acute coronary syndrome: a quasi-experimental study. *BMC Cardiovasc Disord* 2021; **21**: 595 [PMID: 34915850 DOI: 10.1186/s12872-021-02413-8]
20 **Jeihooni AK**, Dindarloo SF, Harsini PA. Effectiveness of Health Belief Model on Oral Cancer Prevention in Smoker Men. *J Cancer Educ* 2019; **34**: 920-927 [PMID: 29992432 DOI: 10.1007/s13187-018-1396-7]
21 **Cheraghi P**, Poorolajal J, Hazavehi SM, Rezapur-Shahkolai F. Effect of educating mothers on injury prevention among children aged <5 years using the Health Belief Model: a randomized controlled trial. *Public Health* 2014; **128**: 825-830 [PMID: 25189328 DOI: 10.1016/j.puhe.2014.06.017]
22 **Khoramabadi M**, Dolatian M, Hajian S, Zamanian M, Taheripanah R, Sheikhan Z, Mahmoodi Z, Seyedi-Moghadam A. Effects of Education Based on Health Belief Model on Dietary Behaviors of Iranian Pregnant Women. *Glob J Health Sci* 2015; **8**: 230-239 [PMID: 26383208 DOI: 10.5539/gjhs.v8n2p230]
23 **Baghianimoghadam MH**, Shogafard G, Sanati HR, Baghianimoghadam B, Mazloomy SS, Askarshahi M. Application of the health belief model in promotion of self-care in heart failure patients. *Acta Med Iran* 2013; **51**: 52-58 [PMID: 23456585]
24 **Khani Jeihooni A**, Hidarnia A, Kaveh MH, Hajizadeh E. The effect of a prevention program based on health belief model on osteoporosis. *J Res Health Sci* 2015; **15**: 47-53 [PMID: 25821026]
25 **Xu LJ**, Meng Q, He SW, Yin XL, Tang ZL, Bo HY, Lan XY. The effects of health education on patients with hypertension in China: A meta-

analysis. *Health Educ J* 2014; **73**: 137-149 [DOI: 10.1177/0017896912471033]

26 **Khanal MK**, Bhandari P, Dhungana RR, Rawal LB, Gurung Y, Paudel KN, Singh A, Devkota S, Courten B. Effectiveness of community-based health education and home support program to reduce blood pressure among patients with uncontrolled hypertension in Nepal: A cluster-randomized trial. *PLoS One* 2021; **16**: e0258406 [PMID: 34637478 DOI: 10.1371/journal.pone.0258406]

27 **Zeng XY**, Zhang M, Li YC, Huang ZJ, Wang LM. [Study on effects of community-based management of hypertension patients aged ≥35 years and influencing factors in urban and rural areas of China, 2010]. *Zhonghua Liu Xing Bing Xue Za Zhi* 2016; **37**: 612-617 [PMID: 27188348 DOI: 10.3760/cma.j.issn.0254-6450.2016.05.005]

28 **Larki A**, Tahmasebi R, Reisi M. Factors Predicting Self-Care Behaviors among Low Health Literacy Hypertensive Patients Based on Health Belief Model in Bushehr District, South of Iran. *Int J Hypertens* 2018; **2018**: 9752736 [PMID: 29780639 DOI: 10.1155/2018/9752736]

29 **Khodaminasab A**, Reisi M, Vahedparast H, Tahmasebi R, Javadzade H. Utilizing a health-promotion model to predict self-care adherence in patients undergoing coronary angioplasty in Bushehr, Iran. *Patient Prefer Adherence* 2019; **13**: 409-417 [PMID: 31040649 DOI: 10.2147/PPA.S181755]

30 **Dehghani-Tafti A**, Mazloomy Mahmoodabad SS, Morowatisharifabad MA, Afkhami Ardakani M, Rezaeipandari H, Lotfi MH. Determinants of Self-Care in Diabetic Patients Based on Health Belief Model. *Glob J Health Sci* 2015; **7**: 33-42 [PMID: 26156902 DOI: 10.5539/gjhs.v7n5p33]

World Journal of Clinical Cases

Submit a Manuscript: https://www.f6publishing.com

World J Clin Cases 2024 May 26; 12(15): 2586-2596

DOI: 10.12998/wjcc.v12.i15.2586

ISSN 2307-8960 (online)

CASE REPORT

Retroperitoneal bronchogenic cyst: A case report and review of literature

Abdul Malik, Qais Ahmad Naseer, Muhammad Asad Iqbal, Shi-Ya Han, Sheng-Chun Dang

Specialty type: Medicine, research and experimental

Provenance and peer review: Unsolicited article; Externally peer reviewed.

Peer-review model: Single blind

Peer-review report's classification

Scientific Quality: Grade A, Grade C

Novelty: Grade A, Grade C

Creativity or Innovation: Grade A, Grade C

Scientific Significance: Grade A, Grade B

P-Reviewer: Gokce E, Türkiye; Sultana N, Bangladesh

Received: November 26, 2023

Revised: February 28, 2024

Accepted: April 7, 2024

Published online: May 26, 2024

Abdul Malik, Qais Ahmad Naseer, Muhammad Asad Iqbal, Sheng-Chun Dang, Department of General Surgery, The Affiliated Hospital of Jiangsu University, Zhenjiang 212001, Jiangsu Province, China

Abdul Malik, Department of Preventive Medicine and Public Health Laboratory Science, School of Medicine, Jiangsu University, Zhenjiang 212013, Jiangsu Province, China

Qais Ahmad Naseer, Department of Laboratory Medicine, School of Medicine, Jiangsu University, Zhenjiang 212013, Jiangsu Province, China

Shi-Ya Han, Department of Clinical Pharmacy, Shenyang Pharmaceutical University, Shenyang 110000, Liaoning Province, China

Sheng-Chun Dang, Department of Surgery, Siyang Hospital, Suqian 223700, Jiangsu Province, China

Co-first authors: Abdul Malik and Qais Ahmad Naseer.

Corresponding author: Sheng-Chun Dang, MD, Chief Doctor, Professor, Surgeon, Department of General Surgery, The Affiliated Hospital of Jiangsu University, No. 438 Jiefang Road, Zhenjiang 212001, Jiangsu Province, China. dscgu@163.com

Abstract

BACKGROUND

Bronchogenic cysts are rare developmental anomalies that belong to the category of congenital enterogenous cysts. They arise from lung buds and are present at birth. The embryonic foregut is their origin. Typically, they are located within the chest cavity, particularly in the cavum mediastinale of the thoracic cavity or lodged in the pulmonary parenchyma, and are considered a type of lung bud malformation.

CASE SUMMARY

A 49-year-old male patient was admitted to the hospital due to the detection of a retroperitoneal mass during a physical examination. Two weeks before admission, the patient underwent a physical examination and routine laboratory tests, which revealed a space-occupying mass in the retroperitoneal region. The patient did not report any symptoms (such as abdominal pain, flatulence, nausea, vomiting, high fever, or chills). The computed tomography (CT) revealed a retroperitoneal space-occupying lesion with minimal enhancement and a CT value of approximately 36

Hounsfield units. The lesion was not delineated from the boundary of the pancreatic body and was closely related to the retroperitoneum locally.

CONCLUSION
Following a series of tests, an abdominal mass was identified, prompting the implementation of a laparoscopic retroperitoneal mass excision procedure. During the investigation, an 8 cm × 7 cm cystic round-shaped mass with a distinct demarcation was identified in the upper posterior region of the pancreas. Subsequently, full resection of the mass was performed. Postoperative pathological examination reveled a cystic mass characterized by a smooth inner wall. The cystic mass was found to contain a white, viscous liquid within its capsule.

Key Words: Bronchogenic cyst; Retroperitoneal space; Excision; Laparoscopic surgery; Case report

Core Tip: A 49-year-old male with no significant medical or family history was diagnosed with a retroperitoneal mass during a routine physical examination, despite showing no typical symptoms. The absence of common diseases such as hypertension or diabetes in his medical history, with normal physical examination and laboratory results, highlighted the unusual nature of this case. The mass, detected incidentally, underscoreds the importance of routine health checks in identifying potentially serious conditions in asymptomatic patients. This case emphasizes the critical role of comprehensive evaluations and the need for surgical intervention in managing unexpected findings, demonstrating the value of caution in routine medical examinations.

Citation: Malik A, Naseer QA, Iqbal MA, Han SY, Dang SC. Retroperitoneal bronchogenic cyst: A case report and review of literature. *World J Clin Cases* 2024; 12(15): 2586-2596
URL: https://www.wjgnet.com/2307-8960/full/v12/i15/2586.htm
DOI: https://dx.doi.org/10.12998/wjcc.v12.i15.2586

INTRODUCTION

Bronchogenic cysts originate from the foregut and are most commonly situated in the mediastinum, as noted previously [1,2]. However, these cystic anomalies have also been identified in less common locations, including the esophagus, as reported by Altieri *et al*[1] and near the diaphragm[3,4]. While often presenting without symptoms, these cysts may lead to clinical concerns through infection or by exerting pressure on adjacent anatomical structures, as described previously [2]. To mitigate such issues and avert further complications, surgical removal of the cysts is frequently advocated[2]. While these cysts are generally asymptomatic, they can become infected or exert compressive effects on adjacent tissues [2]. This case study describes a case involving a subdiaphragmatic retroperitoneal bronchogenic cyst, with a definitive diagnosis established through histopathological examination of the surgically excised specimen.

CASE PRESENTATION

Chief complaints

A retroperitoneal mass was identified during a routine physical examination. The mass was detected two weeks prior to his admission, through physical assessment and standard laboratory tests.

History of present illness

A 49-year-old male who was hospitalized following a routine physical examination unexpectedly revealed a retroperitoneal mass despite the absence of symptoms such as nausea, vomiting, fever, abdominal pain, or distension.

History of past illness

The patient's medical history was devoid of any conditions, including the absence of other diseases such as hypertension (HTN), diabetes mellitus (DM), heart disease, or tuberculosis (TB).

Personal and family history

The patient reported no family history of any disease or cancerous growth.

Physical examination

During the physical examination, the patient's abdominal area exhibited a flat and soft appearance, without any

indications of gastrointestinal problems or peristaltic movements. Moreover, there were no signs of varices in the abdominal wall, tenderness, rebound pain, or muscle guarding. The liver and spleen displayed normal characteristics, and Murphy's sign elicited a negative response. No pain was elicited during percussion in the liver and kidney regions, and no anomalies were detected during digital rectal examination. The vital signs of the patient were recorded as follows: Body temperature of 36.2 ℃, arterial blood pressure of 130/65 mmHg, SpO_2 level of 95%, pulse rate of 105 beats per minute, and respiration rate of 19 breaths per minute. In general, the findings of the physical examination were within normal limits.

Laboratory examinations

Laboratory analyses revealed a C-reactive protein concentration of 24.0 mg/L, a white blood cell (WBC) count of 12.4 × 10^9/L, and a neutrophil proportion of 77.6%. The results of the endocrine assessment conducted to evaluate excessive adrenal secretion revealed no abnormalities, as shown in Table 1. Blood biochemistry results fell within the normal range, and after comprehensive laboratory analyses and a thorough physical examination, there were no evident contraindications for the surgical extraction of the tumor.

Table 1 presents the results of a series of presurgery laboratory tests conducted on the patient. It provides the actual values of various measured parameters, their corresponding normal reference values, and the units of measurement. The first parameter in the table is the leukocyte or WBC count, which measures the total WBCs in the bloodstream. The patient's WBC count was determined to be 6.1 × 10^9/L, and this value falls within the typical reference range of 3.5-9.5 × 10^9/L. Additionally, the table includes various types of WBCs, such as neutrophils, lymphocytes, monocytes, eosinophils, and basophils. The patient's neutrophil count was slightly below the standard range, while the lymphocyte count was within the normal reference range. The counts of the other types of WBCs all fell within their respective normal ranges. Additionally, the table reports the values of four tumor markers: Carbohydrate antigen (CA)19-9, carcinoembryonic antigen (CEA), alpha-fetoprotein (AFP), and CA125. Tumor markers are substances produced either by cancer cells or by normal cells in response to cancer. They serve the purpose of detecting cancer, monitoring its progression, and evaluating treatment efficacy. In this particular case, all four tumor markers were within their normal reference ranges, signifying the absence of evidence for cancer.

Imaging examinations

Further diagnostic evaluations were undertaken through noncontrast computed tomography (CT) scans to characterize the retroperitoneal space-occupying lesion. Imaging revealed that the lesion demonstrated characteristics suggestive of limited enhancement, an observation attributable to the imaging technique employed. The cyst content was noted to have a uniform density, with CT values ranging between 17 and 36 Hounsfield units, which are indicative of the lesion composition. A notable finding was the increased thickness of the cyst wall, a feature that may suggest underlying contamination or inflammation. Figure 1 shows the anatomical location of an oval cystic lesion situated at the posterior lower aspect of the left lateral lobe of the liver, within the retroperitoneal space, adjacent to the right side of the spine, and to the left of the inferior vena cava. However, it is important to clarify that the figure predominantly shows a large cystic mass accompanied by scattered calcifications within the abdominal-pelvic cavity, without distinct demarcation of the specific lesion across the mentioned anatomical landmarks.

Further diagnostic work-up

Upon identifying an unexpected retroperitoneal mass during a standard physical examination, the 49-year-old male was subjected to a noncontrast CT scan, which delineated a lesion with limited enhancement and a uniform density, alongside an increased cyst wall thickness, suggesting possible underlying issues. The decision for surgical intervention was made, leading to the laparoscopic resection of the mass. Intraoperatively, the lesion, located on the dorsal side of the upper pole of the left kidney, was noted for its soft, gray-yellow appearance with a smooth surface. The tumor was characterized as soft and gray-yellow and had a smooth surface, and it was successfully completely excised. Upon opening the mass, a thick, jelly like substance was found within, and the thickness of the capsule wall measured approximately 0.2 cm, as shown in Figure 2A. The resected specimen, measuring 8.8 cm × 7.2 cm × 2.6 cm, underwent histopathological examination, which confirmed the diagnosis of a retroperitoneal bronchogenic cyst (Figure 2B). This examination revealed a cystic mass with a smooth inner wall, containing white viscous fluid, and a capsule wall lined with pseudostratified ciliated columnar epithelium, inclusive of glands, cartilage, and smooth muscle. Immunohistochemical analysis was not detailed in the initial text but would typically be considered for further characterization of the tissue, especially in distinguishing the cyst's benign nature from potential malignancies, by assessing specific markers relevant to bronchogenic cysts.

FINAL DIAGNOSIS

Considering the patient's clinical presentation and subsequent investigative findings, the final diagnosis was determined to be a retroperitoneal bronchogenic cyst.

Table 1 Results obtained from the preoperative laboratory tests

Actual parameter	Amount of concentration	Reference values
Leukocyte (WBC), × 10^9/L	6.1	3.5-9.5
Neutrophils, × 10^9/L	2.6	1.8-6.3
Lymphocytes, × 10^9/L	2.6	1.1-3.2
Monocytes, × 10^9/L	0.7	0.1-0.6
Eosinophils, × 10^9/L	0.12	0.02-0.52
Basophil, × 10^9/L	0.07	0-0.06
CA19-9, U/mL	3.3	< 37.0
CEA, ng/mL	2.3	< 5.0
AFP, ng/mL	1.25	< 8.78
CA125, U/mL	6.1	< 35

WBC: White blood cell; AFP: Alpha-fetoprotein; CA: Carbohydrate antigen; CEA: Carcinoembryonic antigen.

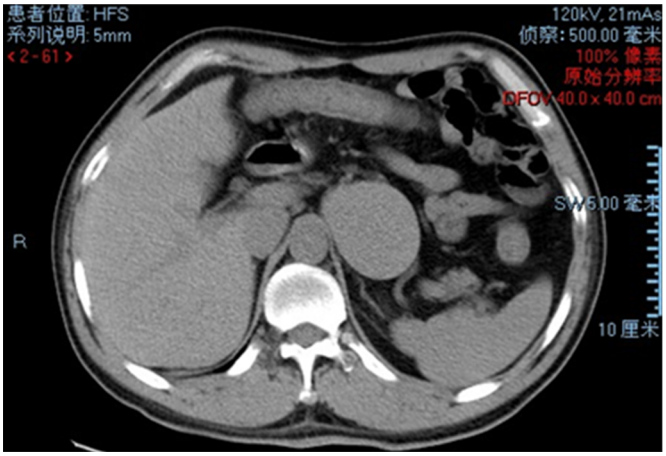

Figure 1 Abdominal noncontrast computed tomography scan depicting a sizable cystic formation. The scan also revealed scattered calcifications throughout the abdominal and pelvic regions.

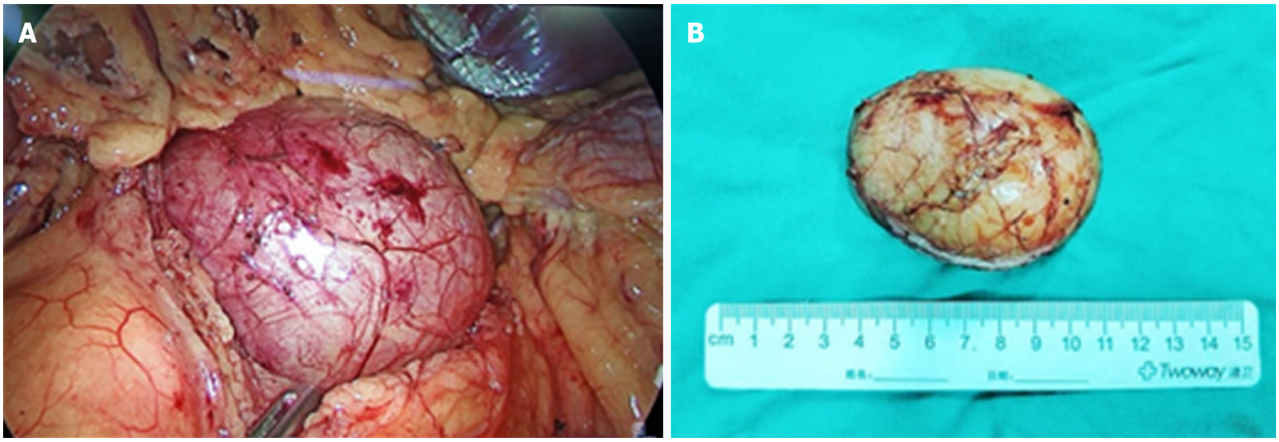

Figure 2 Cystic-solid tumor. A: Relationship of cystic lesions with surrounding structures and their maximum diameter; B: Complete surgical removal of the cystic-solid tumor, measuring 8.8 cm in length, 7.2 cm in width, and 2.6 cm in depth.

TREATMENT

The patient was treated through laparoscopic resection of the retroperitoneal lesion under general anesthesia, successfully excising the cystic lesion. Postoperative recovery was uneventful, leading to discharge five days after the procedure without any complications.

OUTCOME AND FOLLOW-UP

The surgical procedure was carried out successfully, and the patient was safely transferred to the hospital ward without any postoperative complaints. Subsequent laboratory results indicated a reduction in C-reactive protein levels and WBC count, with a recorded value of 6.1-9 mg/L, while the neutrophil percentage remained at 77.6%. The patient's condition remained stable, characterized by normal vital signs, satisfactory overall well-being, restful sleep, and a positive mental state. Examination of the abdomen did not reveal any tenderness, and bowel sounds were within the expected range. After a postoperative recovery period of five days, the patient exhibited excellent progress without any complications, which ultimately led to their discharge from the hospital.

DISCUSSION

Bronchogenic cysts are a type of congenital developmental anomaly that typically occurs in the mediastinum but can also occur in other areas, such as the abdominal cavity, skin, and diaphragm. Retroperitoneal bronchogenic cysts are frequently observed in the left adrenal region and frequently exhibit an absence of symptoms, hence contributing to the potential for misdiagnosis[5]. It is crucial to distinguish these cysts from other conditions, such as adrenal adenomas, renal cysts, and cystic teratomas. As a consequence of the initial findings, the patient was referred to the surgical department for further evaluation and medical intervention. Throughout the illness, the patient did not manifest any distressing symptoms, such as abdominal pain, abdominal distension, diarrhea, hematuria, urinary pain, frequent urination, cold sensitivity, fever, night sweats, cough, or hemoptysis. Both urinary and bowel functions were reported to be normal, and no significant recent weight loss was documented. Furthermore, the patient had no previous medical history of conditions such as HTN, DM, heart disease, or TB. This case report highlights the discovery of a retroperitoneal space-occupying lesion in a patient who exhibited no accompanying symptoms. Imaging findings suggested the presence of additional cystic lesions within the retroperitoneal region, necessitating further inquiries to establish an accurate diagnosis and develop a suitable course of treatment for this individual.

There were no indications of varices, tenderness, rebound pain, or muscle guarding. Both the liver and spleen appeared normal. Percussion in the liver and kidney areas did not elicit any pain, and digital rectal examination revealed no abnormalities. Overall, the physical examination findings were within normal parameters.

Laboratory tests showed a C-reactive protein level of 24.0 mg/L, a WBC count of 12.4 × 10^9/L, and a neutrophil percentage of 77.6%. Endocrine evaluation for excessive adrenal secretion revealed no abnormalities (Table 1). A CT scan revealed a retroperitoneal mass without significant enhancement. While the diagnosis confirmed the presence of an abdominal mass, further pathological assessment was needed for precise characterization. Blood biochemistry results were normal. After thorough laboratory analyses and physical examination, there were no contraindications for surgical tumor removal. Surgery was scheduled following appropriate preoperative assessments.

Bronchogenic cysts can be categorized into three types based on their location: Intrapulmonary, mediastinal, and ectopic. The mediastinal type is the most prevalent and typically manifests as a clearly defined cystic structure in the posterior mediastinum. Ectopic variants, which can appear in locations such as the neck, brain, and spinal dura, are rare and may occasionally be found in the retroperitoneal area. Retroperitoneal bronchogenic cysts are exceedingly rare, with only sixty-two cases reported in the medical literature. Among these cases, approximately thirty were verified as genuine retroperitoneal bronchogenic cysts based on anatomical and pathological criteria[6]. Retroperitoneal bronchogenic cysts are an uncommon, accounting for only 0.03% of the tumor incidence. These cysts are thought to have their origins in the embryonic foregut and arise from a segment of the abnormally developed trachea and bronchial tree that takes shape in the early stages following the detachment and implantation of the plumule in the abdominal cavity[5,7]. The concept posits a potential correlation between the occurrence of retroperitoneal bronchogenic cysts on the left side of the body and the separation of the plumule from the left side after anterior bowel transposition. Retroperitoneal bronchogenic cysts are a rare clinical discovery, and most of these lesions typically cluster around the left adrenal gland. The peripancreatic area is the second most frequently affected site for these cysts and can occasionally be mistaken for adenomas during preoperative imaging[8,9]. We examined a patient with a congenital malformation in the posterior mediastinum, likely attributed to the abnormal development of the foregut. One of the retroperitoneal cysts initially appeared as a left adrenal cyst and was effectively excised using laparoscopic techniques. The cyst was definitively diagnosed as a bronchogenic cyst through pathological analysis, highlighting the need to consider bronchogenic cysts as a possible diagnosis for retroperitoneal cysts.

Retroperitoneal bronchogenic cysts generally remain asymptomatic unless complications such as infection or significant enlargement leading to the compression of neighboring organs arise. The usual indications may involve unexplained abdominal swelling and a sense of fullness before lunchtime. In certain instances, when the adrenal glands are compressed, symptoms resembling those associated with pheochromocytoma have been documented. Early diagnosis and prompt treatment are crucial for preventing potential complications, as elevated levels of hormones may be released

if left untreated[10,11]. Retroperitoneal bronchogenic cysts exhibit a nearly equal distribution between genders, affecting both women and men. Approximately 82% of these cysts are observed to localize on the left side of the abdominal region [12]. Bronchogenic cysts situated in deep anatomical locations, such as the posterior pelvic peritoneum, pose significant challenges in preoperative identification and are commonly subject to misdiagnosis[13]. The patient underwent a laparoscopic resection procedure for the retro-abdominal lesion under general anesthesia. No ascites was detected in the pelvic cavity, and there were no apparent abnormalities in various abdominal organs, including the liver, stomach, lungs, glands, spleen, small intestine, large intestine, and pelvic cavity. During the operation, the tumor was located on the dorsal side of the upper pole of the left kidney, as illustrated in Figure 2A.

Symptoms such as sickness, vomiting, and stomach discomfort may be useful in obtaining a diagnosis through medical assessment if the lesions become substantial enough to compress neighboring organs. While CT and magnetic resonance imaging are valuable diagnostic modalities for retroperitoneal bronchogenic cysts, the process of establishing a definitive diagnosis can be complex due to various aspects, including the protein or calcium composition of the cysts, their dimensions, compaction, or the potential occurrence of infection[8,14,15]. The tumor was characterized as soft and gray-yellow and had a smooth surface, and it was successfully completely excised. Upon opening the mass, a thick, jelly like substance was found within, and the thickness of the capsule wall measured approximately 0.2 cm, as shown in Figure 2B.

The retroperitoneal bronchogenic cyst was established during the postoperative pathological examination. The mass exhibited a rounded shape, measuring approximately 8 cm × 7 cm, and had a soft consistency with an intact capsule. Microscopic examination of the specimen revealed a cystic mass with a smooth inner wall, containing white viscous fluid. The capsule wall was lined with pseudostratified ciliated columnar epithelium and included glands, cartilage, and smooth muscle. The pathological diagnosis confirmed tha the mass was as a bronchogenic cyst, as depicted in Figure 3.

Following a successful surgical procedure, the patient was transferred safely to the hospital ward without experiencing any postoperative issues. Subsequent laboratory results showed decreased C-reactive protein levels and WBC counts, with a recorded range of 6.1-9 mg/L, while the neutrophil percentage remained stable at 77.6%. The patient's condition remained stable, with normal vital signs, satisfactory overall well-being, restful sleep, and a positive mental state. Abdominal examination revealed no tenderness, and bowel sounds were normal. After a 5-d postoperative recovery period, the patient made excellent progress without complications, leading to discharge from the hospital. Surgical removal is typically the treatment of choice, and symptoms of this lesion type often improve following surgical intervention. Fifty percent of all retroperitoneal bronchogenic cysts are discovered incidentally[8].

During sonogram investigation, retroperitoneal cystic lesions typically present as anechoic lesions with or without echo fragmentation. Computerized axial tomography typically indicates a thin-walled, well-defined lesion with low water density and little enhancement, although these lesions may have high density due to protein content, hemorrhagic content, or sticky mucinous tissue. Fluid level and wall calcification may also beobserved[6]. Retroperitoneal cystic lesions have a wide range of possible causes, including adrenal cysts, pancreatic pseudocysts, teratomas, and cystic lymphangiomas. Bronchogenic cysts are treated surgically and have a very good long-term success rate[2,12].

The use of endoscopic ultrasound (EUS) seems to exhibit a higher level of effectiveness compared to CT in the identification and characterization of retroperitoneal cystic masses. This is mostly due to its ability to provide a clear depiction of the mass itself, as well as the surrounding structures within the posterior peritoneal region. EUS-guided fine-needle aspiration is a diagnostic procedure that can be employed to ascertain the malignancy or benign nature of a lesion. There have been recorded instances of retroperitoneal bronchogenic cysts with notably increased levels of serum CA19-9, while the underlying cause for this increase remains unclear and requires additional investigation[16]. The use of serum CA19-9 measurement has the potential to provide valuable diagnostic information for the identification of retroperitoneal bronchogenic cysts[17]. Retroperitoneal bronchogenic cysts were first described by Miller *et al*[18] in 1953 and are considered to be extremely rare. A thorough examination of the PubMed database has shown a total of 88 recorded cases of retroperitoneal bronchogenic cysts in the global English-language literature from 1991 to 2022. In the context of this study, a comprehensive analysis was conducted on a total of 40 publications, each presenting detailed information on 45 cases involving the laparoscopic extraction of red blood cells. The evaluation encompassed the entirety of the texts as well as the pathological findings associated with these cases. Table 2 provides a concise summary of the papers that are included for reference.

Tokuda *et al*[19] reported the first laparoscopic resection of such cysts in 1997, with a focus on cysts up to 3 cm in size. It is worth noting that this particular surgical treatment has been predominantly documented in China, with 17 cases (37.8%). Subsequently, 8 cases were recorded in Japan (17.8%), while 6 cases were reported in the United States (13.3%). The observation of differences based on regional and racial factors is consistent with the findings reported by Liang *et al* [20]. Comprehensive literature reviews were sequentially conducted by Cetinkurşun *et al*[21], Liang *et al*[20], Govaerts *et al*[6], and Yuan *et al*[22] in the years 1997, 2005, 2012, and 2021, respectively. It is noteworthy to emphasize that the aforementioned research included a significant cohort of patients who underwent surgical procedures utilizing the open technique. After successful surgical resection and pathological confirmation of the bronchogenic cyst, comprehensive preoperative assessment, which plays a crucial role in guiding the surgical approach. Table 1 presents the results of a series of presurgery laboratory tests conducted on the patient, providing a detailed account of the patient's clinical status prior to the operation. This includes the actual values of various measured parameters, their corresponding normal reference values, and the units of measurement. Specifically, the leukocyte or WBC count, which measures the total WBCs in the bloodstream, was determined to be within the typical reference range, indicating no infection or inflammation. Additionally, the table reports the values of four tumor markers: CA19-9, CEA, AFP, and CA125, all of which are within their normal reference ranges, indication the absence of evidence for cancer. This comprehensive laboratory analysis, alongside a thorough physical examination, underscored the absence of contraindications for surgical extraction of the tumor, facilitating a well-informed decision to proceed with laparoscopic resection. Furthermore, our study was extended

Table 2 A literature review on laparoscopic and robotic surgery for retroperitoneal bronchogenic cysts

Country	Year	Age (yr)	Sex	Location	Size (cm)	Chief complaint	Surgical technique	First author	Ref.
Japan	1997	24	F	L adrenal gland	3	Asymptomatic	Laparoscopic	Tokuda N	[19]
Japan	1998	49	F	R adrenal gland	3.2 × 2.2	Asymptomatic	Laparoscopic	Yamamoto E	[23]
Australia	2002	15	M	L adrenal gland	5.5 × 3.5 × 1.2	L flank pain	Laparoscopic	McCrystal DJ	[24]
Australia	2002	8	F	L adrenal gland	4 × 3 × 2	Abdominal pain	Laparoscopic	McCrystal DJ	[24]
United States	2003	59	F	L adrenal gland	7 × 5	Asymptomatic	Laparoscopic	Hedayati N	[25]
Japan	2003	41	F	L adrenal gland	9.2	L flank pain	Laparoscopic	Ishikawa T	[26]
Japan	2004	36	M	L adrenal gland	5 × 3	Asymptomatic	Laparoscopic	Ishizuka O	[27]
United States	2007	75	F	L adrenal gland	5	Abdominal pain	Laparoscopic	Terry NE	[28]
China	2007	55	M	L adrenal gland	4 × 3	Asymptomatic	Laparoscopic	Chu PY	[29]
Japan	2007	39	M	L adrenal gland	3.5 × 3	Fever	Laparoscopic	Minei S	[30]
United States	2008	40	M	L adrenal gland	6.2	Asymptomatic	Laparoscopic	Roma A	[31]
Korea	2009	41	F	L adrenal gland	4.8 × 3.5 × 4.2	Asymptomatic	Laparoscopic	Chung JM	[12]
United States	2009	67	M	L upper-quadrant	3.9 × 3.7	Asymptomatic	Laparoscopic	Obando J	[32]
Portland	2010	44	M	L adrenal gland	3	Asymptomatic	Laparoscopic	El Youssef R	[33]
Japan	2010	64	F	Stomach posterior wall	3 × 4 × 2	Asymptomatic	Laparoscopic	Inaba K	[34]
Spain	2010	67	M	Gastro-esophageal junction	6	Low back pain	Laparoscopic	Díaz Nieto R	[35]
United States	2012	23	F	R adrenal gland	4	Asymptomatic	Robotic	Alguraan Z	[36]
United States	2012	23	F	L adrenal gland	5.2 × 4	Abdominal discomfort	Laparoscopic	O'Neal PB	[37]
Germany	2013	50	M	L adrenal gland	4	L flank pain	Laparoscopic	Jannasch O	[38]
China	2013	50	F	Pancreas posterior wall	3	L flank pain	Laparoscopic	Cai Y	[39]
Switzerland	2013	42	F	L adrenal gland	5 × 3.6 × 4	Epigastric pain	Laparoscopic	Runge T	[40]
Portugal	2013	36	F	L upper quadrant	8	Abdominal pain	Laparoscopic	Castro R	[41]
China	2014	30	F	L adrenal gland	1.5 × 2 × 2	Asymptomatic	Laparoscopic	Dong B	[42]
China	2014	51	M	L adrenal gland	4.5	Headache	Laparoscopic	Cao DH	[43]
Japan	2014	27	M	L adrenal gland	5.4 × 3.8	Asymptomatic	Laparoscopic	Terasaka T	[44]
China	2015	8	M	L adrenal gland	4	Asymptomatic	Laparoscopic	Zhang D	[45]
India	2015	34	F	R hypochondrium	10 × 6	R flank heavy	Laparoscopic	Trehan M	[46]
China	2015	52	M	L crus of the diaphragm	2.5 × 2.5 × 0.5	Asymptomatic	Laparoscopic	Jiang X	[47]
Türkiye	2015	25	F	L adrenal gland	4	L flank pain	Laparoscopic	Bulut G	[48]
Korea	2015	57	M	L adrenal gland	4.8 × 2.5	Asymptomatic	Laparoscopic	Yoon YR	[49]
China	2017	48	F	L adrenal gland	8 × 6 × 5.5	Epigastric pain	Laparoscopic	Wang M	[17]
China	2018	78	M	Inferior of the L renal vein, L side of IVC	7	Asymptomatic	Robotic	Liu Q	[50]
China	2018	33	M	L hepatic hilum	4.5	Asymptomatic	Robotic	Liu Q	[50]
Türkiye	2018	38	F	L adrenal gland	NA	L upper abdominal pain	Laparoscopic	Bolton JW	[51]

India	2020	30	M	L adrenal gland	7 × 5	Upper abdominal pain	Laparoscopic	Sinha V	[52]
China	2020	33	M	R adrenal gland	3.1 × 5.9	Asymptomatic	Laparoscopic	Wen Y	[53]
China	2020	27	M	L adrenal gland	2.1 × 4.1	Asymptomatic	Laparoscopic	Wen Y	[53]
China	2021	41	F	L adrenal gland	3.5 × 3	Lumbar back discomfort	Laparoscopic	Qingyu J	[54]
China	2021	17	F	L adrenal gland	2.9 × 1.7 × 2.8	Epigastric pain	Laparoscopic	Wu LD	[55]
China	2021	53	F	L adrenal gland	3.3 × 2.7 × 3.5	Back pain	Laparoscopic	Yuan K	[22]
New Zealand	2021	39	M	L adrenal gland	3	L flank pain	Laparoscopic	Cowan S	[56]
Japan	2022	16	F	Under the L diaphragm	3.8	Upper abdominal pain	Laparoscopic	Tadokoro T	[57]
China	2022	27	M	R adrenal gland	3.6 × 3.5 × 3.4	Asymptomatic	Laparoscopic	Hu BY	[58]
China	2022	18	M	L adrenal gland	7.1 × 3.6 × 7	Asymptomatic	Laparoscopic	Hu BY	[58]
China	2022	6	M	L adrenal gland	4.5 × 2.8 × 8	Abdominal pain	Laparoscopic	Hu BY	[58]

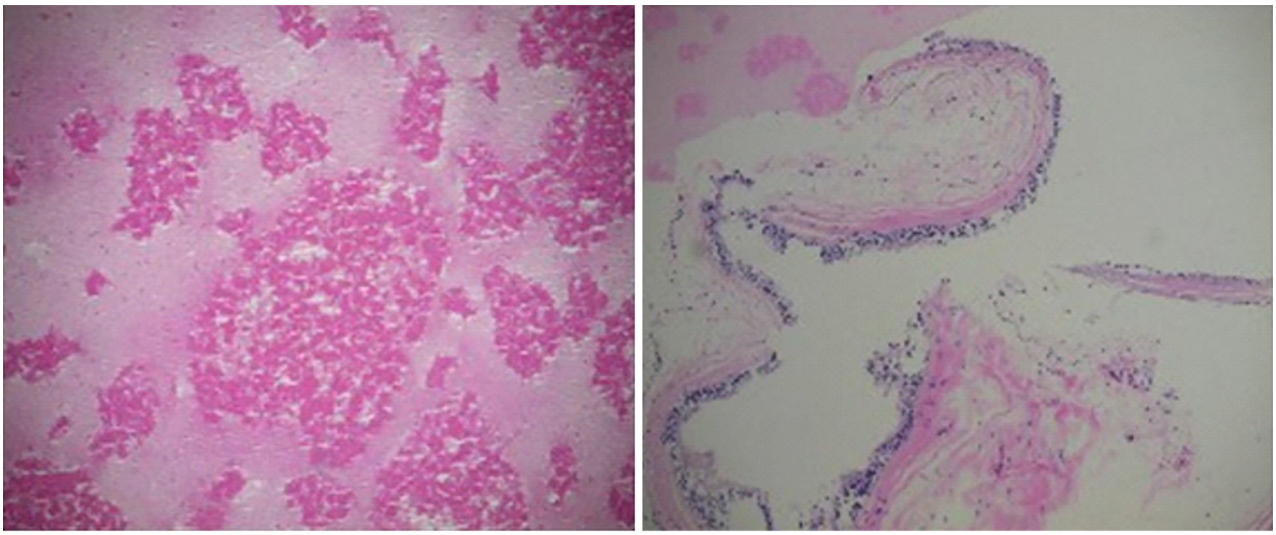

Figure 3 Histopathological analysis showing a retroperitoneal mass identified as an ectopic bronchogenic cyst, featuring nodular tissue in shades of gray-white and yellow. The cystic portion contains a light yellow, soft, gelatinous substance, encased by a smooth, encapsulated surface.

to incorporate the latest findings from the preceding 2 years and address any deficiencies that were not covered in previous enquiries. These collaborative endeavors resulted in consistent discoveries concerning the clinical attributes of the illness, including elements such as the age of the patients, initial symptoms, and prevalent anatomical sites of the cysts.

CONCLUSION

In summary, retroperitoneal bronchogenic cysts, while rare and often asymptomatic, are typically identified incidentally and best managed through surgical removal, with laparoscopic excision being the preferred method. The case discussed illustrates the successful laparoscopic resection of such a cyst, emphasizing the importance of a multidisciplinary approach for optimal diagnosis and management. The challenges in preoperative diagnosis due to the deep anatomical locations of cyst highlight the need for prompt intervention to prevent complications. The current literature supports the effectiveness of laparoscopic surgery, noting a favorable long-term prognosis without recurrence. Future research should focus on enhancing diagnostic techniques and exploring less invasive treatment options, underscoring the necessity of further studies to improve patient care for this condition.

ACKNOWLEDGEMENTS

We would like to express our gratitude to our patient and their family for allowing us to publish this case report.

FOOTNOTES

Author contributions: Malik A and Naseer QA contributed equally to this work as co-first authors; Malik A, Naseer QA, Iqbal MA and Han SY were responsible for the data collection and manuscript composition; Dang SC played a pivotal role in critically revising the manuscript for important intellectual content, ensuring the accuracy and integrity of the work. All authors reviewed and endorsed the final manuscript.

Informed consent statement: All study participants or their legal guardian provided informed written consent about personal and medical data collection prior to study enrolment.

Conflict-of-interest statement: All the authors report no relevant conflicts of interest for this article.

CARE Checklist (2016) statement: The authors have read the CARE Checklist (2016), and the manuscript was prepared and revised according to the CARE Checklist (2016).

Country/Territory of origin: China

ORCID number: Sheng-Chun Dang 0000-0001-8878-9007.

S-Editor: Zheng XM
L-Editor: A
P-Editor: Li X

REFERENCES

1 **Altieri MS**, Zheng R, Pryor AD, Heimann A, Ahn S, Telem DA. Esophageal bronchogenic cyst and review of the literature. *Surg Endosc* 2015; **29**: 3010-3015 [PMID: 25669636 DOI: 10.1007/s00464-015-4082-4]
2 **Coselli MP**, de Ipolyi P, Bloss RS, Diaz RF, Fitzgerald JB. Bronchogenic cysts above and below the diaphragm: report of eight cases. *Ann Thorac Surg* 1987; **44**: 491-494 [PMID: 3675053 DOI: 10.1016/s0003-4975(10)62106-6]
3 **Simonetti S**, Canalís E, Macías L, Carrasco MA. Clinico-pathological features of the intradiaphragmatic bronchogenic cysts: report of a case and review of the literature. *Pathologica* 2018; **110**: 116-120 [PMID: 30546149]
4 **Jiang C**, Wang H, Chen G, Jiang G, Zhang P. Intradiaphragmatic bronchogenic cyst. *Ann Thorac Surg* 2013; **96**: 681-683 [PMID: 23910110 DOI: 10.1016/j.athoracsur.2012.10.031]
5 **McAdams HP**, Kirejczyk WM, Rosado-de-Christenson ML, Matsumoto S. Bronchogenic cyst: imaging features with clinical and histopathologic correlation. *Radiology* 2000; **217**: 441-446 [PMID: 11058643 DOI: 10.1148/radiology.217.2.r00nv19441]
6 **Govaerts K**, Van Eyken P, Verswijvel G, Van der Speeten K. A bronchogenic cyst, presenting as a retroperitoneal cystic mass. *Rare Tumors* 2012; **4**: e13 [PMID: 22532911 DOI: 10.4081/rt.2012.e13]
7 **St-Georges R**, Deslauriers J, Duranceau A, Vaillancourt R, Deschamps C, Beauchamp G, Pagé A, Brisson J. Clinical spectrum of bronchogenic cysts of the mediastinum and lung in the adult. *Ann Thorac Surg* 1991; **52**: 6-13 [PMID: 2069465 DOI: 10.1016/0003-4975(91)91409-o]
8 **Wang SE**, Tsai YF, Su CH, Shyr YM, Lee RC, Tsai WC, Li FY, Chen TH, Wu CW, Lui WY. Retroperitoneal bronchogenic cyst mimicking pancreatic cystic lesion. *J Chin Med Assoc* 2006; **69**: 538-542 [PMID: 17116617 DOI: 10.1016/s1726-4901(09)70325-9]
9 **Carachi R**, Azmy A. Foregut duplications. *Pediatr Surg Int* 2002; **18**: 371-374 [PMID: 12415358 DOI: 10.1007/s00383-002-0835-y]
10 **Anderson MI**, O'Reilly KJ, Costabile RA. Retroperitoneal bronchogenic cyst mimicking a pheochromocytoma. *J Urol* 2001; **166**: 1379-1380 [PMID: 11547079 DOI: 10.1016/s0022-5347(05)65774-6]
11 **Doggett RS**, Carty SE, Clarke MR. Retroperitoneal bronchogenic cyst masquerading clinically and radiologically as a phaeochromocytoma. *Virchows Arch* 1997; **431**: 73-76 [PMID: 9247635 DOI: 10.1007/s004280050071]
12 **Chung JM**, Jung MJ, Lee W, Choi S. Retroperitoneal bronchogenic cyst presenting as adrenal tumor in adult successfully treated with retroperitoneal laparoscopic surgery. *Urology* 2009; **73**: 442.e13-442.e15 [PMID: 18468665 DOI: 10.1016/j.urology.2008.02.056]
13 **Liu HS**, Li SQ, Cao ZL, Zhang ZY, Ren H. Clinical features and treatment of bronchogenic cyst in adults. *Chin Med Sci J* 2009; **24**: 60-63 [PMID: 19382427 DOI: 10.1016/s1001-9294(09)60061-4]
14 **Yang DM**, Jung DH, Kim H, Kang JH, Kim SH, Kim JH, Hwang HY. Retroperitoneal cystic masses: CT, clinical, and pathologic findings and literature review. *Radiographics* 2004; **24**: 1353-1365 [PMID: 15371613 DOI: 10.1148/rg.245045017]
15 **Lim LL**, Ho KY, Goh PM. Preoperative diagnosis of a paraesophageal bronchogenic cyst using endosonography. *Ann Thorac Surg* 2002; **73**: 633-635 [PMID: 11845887 DOI: 10.1016/s0003-4975(01)03119-8]

16 **He WT**, Deng JY, Liang H, Xiao JY, Cao FL. Bronchogenic cyst of the stomach: A case report. *World J Clin Cases* 2020; **8**: 1525-1531 [PMID: 32368546 DOI: 10.12998/wjcc.v8.i8.1525]

17 **Wang M**, He X, Qiu X, Tian C, Li J, Lv M. Retroperitoneal bronchogenic cyst resembling an adrenal tumor with high levels of serum carbohydrate antigen 19-9: A case report. *Medicine (Baltimore)* 2017; **96**: e7678 [PMID: 28767594 DOI: 10.1097/MD.0000000000007678]

18 **Miller RF**, Graub M, Pashuck ET. Bronchogenic cysts; anomalies resulting from maldevelopment of the primitive foregut and midgut. *Am J Roentgenol Radium Ther Nucl Med* 1953; **70**: 771-785 [PMID: 13092330]

19 **Tokuda N**, Naito S, Uozumi J, Shimura H, Takayanagi R, Kumazawa J. A retroperitoneal bronchogenic cyst treated with laparoscopic surgery. *J Urol* 1997; **157**: 619 [PMID: 8996372 DOI: 10.1097/00005392-199702000-00058]

20 **Liang MK**, Yee HT, Song JW, Marks JL. Subdiaphragmatic bronchogenic cysts: a comprehensive review of the literature. *Am Surg* 2005; **71**: 1034-1041 [PMID: 16447475 DOI: 10.1177/000313480507101210]

21 **Cetinkurşun S**, Oztürk H, Celasun B, Sakarya MT, Sürer I. Isolate abdominal bronchogenic cyst: a case report. *Eur J Pediatr Surg* 1997; **7**: 103-105 [PMID: 9165257 DOI: 10.1055/s-2008-1071064]

22 **Yuan K**, Shu M, Ma Y, Feng W, Ye J, Yuan Y. Ectopic bronchogenic cyst in the retroperitoneal region: a case report and literature review of adult patients. *BMC Surg* 2021; **21**: 347 [PMID: 34544401 DOI: 10.1186/s12893-021-01341-w]

23 **Yamamoto E**, Nakayama H, Ozaki N, Kitamura Y, Funatsuka M, Ueda M, Chikugo K, Hirata A, Kurashina A, Kuratsuka H, Nakagawa M, Nagaoka S. Laparoscopically resected foregut cyst adjacent to the right adrenal gland. *Diagn Ther Endosc* 1998; **5**: 53-56 [PMID: 18493480 DOI: 10.1155/DTE.5.53]

24 **McCrystal DJ**, Borzi PA. Retroperitoneoscopic resection of retroperitoneal bronchogenic cysts. *Pediatr Surg Int* 2002; **18**: 375-377 [PMID: 12415359 DOI: 10.1007/s00383-002-0829-9]

25 **Hedayati N**, Cai DX, McHenry CR. Subdiaphragmatic bronchogenic cyst masquerading as an "adrenal incidentaloma". *J Gastrointest Surg* 2003; **7**: 802-804 [PMID: 13129560 DOI: 10.1016/s1091-255x(03)00134-3]

26 **Ishikawa T**, Kawabata G, Okada H, Arakawa S, Kamidono S, Fujisawa M. Retroperitoneal bronchogenic cyst managed with retroperitoneoscopic surgery. *J Urol* 2003; **169**: 1078-1079 [PMID: 12576850 DOI: 10.1097/01.ju.0000049902.69707.12]

27 **Ishizuka O**, Misawa K, Nakazawa M, Nishizawa O. A retroperitoneal bronchogenic cyst: laparoscopic treatment. *Urol Int* 2004; **72**: 269-270 [PMID: 15084776 DOI: 10.1159/000077129]

28 **Terry NE**, Senkowski CK, Check W, Brower ST. Retroperitoneal foregut duplication cyst presenting as an adrenal mass. *Am Surg* 2007; **73**: 89-92 [PMID: 17249466 DOI: 10.1177/000313480707300121]

29 **Chu PY**, Hwang TI, Teng TH, Lee CC. A retroperitoneal bronchogenic cyst successfully treated by laparoscopic surgery. *Ann Saudi Med* 2007; **27**: 199-200 [PMID: 17568163 DOI: 10.5144/0256-4947.2007.199]

30 **Minei S**, Igarashi T, Hirano D. A case of retroperitoneal bronchogenic cyst treated by laparoscopic surgery. *Hinyokika Kiyo* 2007; **53**: 171-174 [PMID: 17447486]

31 **Roma A**, Varsegi M, Magi-Galluzzi C, Ulbright T, Zhou M. The distinction of bronchogenic cyst from metastatic testicular teratoma: a light microscopic and immunohistochemical study. *Am J Clin Pathol* 2008; **130**: 265-273 [PMID: 18628097 DOI: 10.1309/JKJU9VE1P4WXVCPG]

32 **Obando J**, Merkle E, Bean SM. A retroperitoneal bronchogenic cyst. *Clin Gastroenterol Hepatol* 2009; **7**: A24-Ae1 [PMID: 19095083 DOI: 10.1016/j.cgh.2008.11.011]

33 **El Youssef R**, Fleseriu M, Sheppard BC. Adrenal and pancreatic presentation of subdiaphragmatic retroperitoneal bronchogenic cysts. *Arch Surg* 2010; **145**: 302-304 [PMID: 20231633 DOI: 10.1001/archsurg.2010.12]

34 **Inaba K**, Sakurai Y, Umeki Y, Kanaya S, Komori Y, Uyama I. Laparoscopic excision of subdiaphragmatic bronchogenic cyst occurring in the retroperitoneum: report of a case. *Surg Laparosc Endosc Percutan Tech* 2010; **20**: e199-e203 [PMID: 21150402 DOI: 10.1097/SLE.0b013e3181fcbe92]

35 **Díaz Nieto R**, Naranjo Torres A, Gómez Alvarez M, Ruiz Rabelo JF, Pérez Manrique MC, Ciria Bru R, Valverde Martínez A, Roldán de la Rúa J, Alonso Gómez J, Rufián Peña S. Intraabdominal bronchogenic cyst. *J Gastrointest Surg* 2010; **14**: 756-758 [PMID: 19475460 DOI: 10.1007/s11605-009-0932-5]

36 **Alguraan Z**, Agcaoglu O, El-Hayek K, Hamrahian AH, Siperstein A, Berber E. Retroperitoneal masses mimicking adrenal tumors. *Endocr Pract* 2012; **18**: 335-341 [PMID: 22068255 DOI: 10.4158/EP11240.OR]

37 **O'Neal PB**, Moore FD, Gawande A, Cho NL, King EE, Moalem J, Ruan D. Bronchogenic cyst masquerading as an adrenal tumor: a case of mistaken identity. *Endocr Pract* 2012; **18**: e102-e105 [PMID: 22440987 DOI: 10.4158/EP11186.CR]

38 **Jannasch O**, Büschel P, Wodner C, Seidensticker M, Kuhn R, Lippert H, Mroczkowski P. Retroperitoneoscopic and laparoscopic removal of periadrenally located bronchogenic cysts--a systematic review. *Pol Przegl Chir* 2013; **85**: 706-713 [PMID: 24468591 DOI: 10.2478/pjs-2013-0108]

39 **Cai Y**, Guo Z, Cai Q, Dai S, Gao W, Niu Y, Li G, Zhang Y. Bronchogenic cysts in retroperitoneal region. *Abdom Imaging* 2013; **38**: 211-214 [PMID: 22664911 DOI: 10.1007/s00261-012-9909-z]

40 **Runge T**, Blank A, Schäfer SC, Candinas D, Gloor B, Angst E. A retroperitoneal bronchogenic cyst mimicking a pancreatic or adrenal mass. *Case Rep Gastroenterol* 2013; **7**: 428-432 [PMID: 24403880 DOI: 10.1159/000355879]

41 **Castro R**, Oliveira MI, Fernandes T, Madureira AJ. Retroperitoneal bronchogenic cyst: MRI findings. *Case Rep Radiol* 2013; **2013**: 853795 [PMID: 24381777 DOI: 10.1155/2013/853795]

42 **Dong B**, Zhou H, Zhang J, Wang Y, Fu Y. Diagnosis and treatment of retroperitoneal bronchogenic cysts: A case report. *Oncol Lett* 2014; **7**: 2157-2159 [PMID: 24932307 DOI: 10.3892/ol.2014.1974]

43 **Cao DH**, Zheng S, Lv X, Yin R, Liu LR, Yang L, Huang Y, Wei Q. Multilocular bronchogenic cyst of the bilateral adrenal: report of a rare case and review of literature. *Int J Clin Exp Pathol* 2014; **7**: 3418-3422 [PMID: 25031770]

44 **Terasaka T**, Otsuka F, Ogura-Ochi K, Miyoshi T, Inagaki K, Kobayashi Y, Nasu Y, Makino H. Retroperitoneal bronchogenic cyst: a rare incidentaloma discovered in a juvenile hypertensive patient. *Hypertens Res* 2014; **37**: 595-597 [PMID: 24599012 DOI: 10.1038/hr.2014.38]

45 **Zhang D**, Zhang Y, Liu X, Zhu J, Feng C, Yang C, Wu S, Liu J, Hua Y, Liu F, Zhang N, He D, Lin T, Wei G. Challenge in preoperative diagnosis of retroperitoneal mucinous cyst in a pediatric patient. *Int J Clin Exp Med* 2015; **8**: 19540-19547 [PMID: 26770607]

46 **Trehan M**, Singla S, Singh J, Garg N, Mahajan A. A Rare Case of Intra- Abdominal Bronchogenic Cyst- A Case Report. *J Clin Diagn Res* 2015; **9**: PD03-PD04 [PMID: 26675877 DOI: 10.7860/JCDR/2015/12949.6761]

47 **Jiang X**, Zeng H, Gong J, Huang R. Unusual uptake of radioiodine in a retroperitoneal bronchogenic cyst in a patient with thyroid carcinoma.

Clin Nucl Med 2015; **40**: 435-436 [PMID: 25546201 DOI: 10.1097/RLU.0000000000000664]

48 **Bulut G**, Bulut MD, Bahadır I, Kotan Ç. Bronchogenic cyst mimicking an adrenal mass in the retroperitoneal region: report of a rare case. *Indian J Pathol Microbiol* 2015; **58**: 96-98 [PMID: 25673605 DOI: 10.4103/0377-4929.151200]

49 **Yoon YR**, Choi J, Lee SM, Kim YJ, Cho HD, Lee JW, Jeon YS. Retroperitoneal Bronchogenic Cyst Presenting Paraadrenal Tumor Incidentally Detected by (18)F-FDG PET/CT. *Nucl Med Mol Imaging* 2015; **49**: 69-72 [PMID: 25767626 DOI: 10.1007/s13139-014-0306-0]

50 **Liu Q**, Gao Y, Zhao Z, Zhao G, Liu R, Lau WY. Robotic resection of benign nonadrenal retroperitoneal tumors: A consecutive case series. *Int J Surg* 2018; **55**: 188-192 [PMID: 29656130 DOI: 10.1016/j.ijsu.2018.04.013]

51 **Bolton JW**, Shahian DM. Asymptomatic bronchogenic cysts: what is the best management? *Ann Thorac Surg* 1992; **53**: 1134-1137 [PMID: 1596146 DOI: 10.1016/0003-4975(92)90412-w]

52 **Sinha V**, Nandi P, Shankar M, Sardana N. Retroperitoneal Bronchogenic Cyst: A Rare Case Study. *Cureus* 2020; **12**: e10421 [PMID: 33062536 DOI: 10.7759/cureus.10421]

53 **Wen Y**, Chen W, Chen J, He X. Retroperitoneal bronchogenic cyst resembling an adrenal tumor: two case reports and literature review. *J Int Med Res* 2020; **48**: 300060520925673 [PMID: 32436418 DOI: 10.1177/0300060520925673]

54 **Qingyu J**, Xiaolong L, Ruohan Z, Licong M, Zhichao T, Qingwei C, Yuan W, Ying Z. Computed tomography helps pre-operative evaluation before laparoscopic resection of retroperitoneal bronchogenic cyst: A case report. *J Minim Access Surg* 2021; **17**: 95-97 [PMID: 32964892 DOI: 10.4103/jmas.JMAS_72_20]

55 **Wu LD**, Wen K, Cheng ZR, Alwalid O, Han P. Retroperitoneal bronchogenic cyst in suprarenal region treated by laparoscopic resection: A case report. *World J Clin Cases* 2021; **9**: 7245-7250 [PMID: 34540985 DOI: 10.12998/wjcc.v9.i24.7245]

56 **Cowan S**, Gunawardene A, Davenport E. Retroperitoneal bronchogenic cyst mistaken as an adrenal adenoma. *ANZ J Surg* 2021; **91**: E526-E527 [PMID: 33336493 DOI: 10.1111/ans.16515]

57 **Tadokoro T**, Misumi T, Itamoto T, Nakahara H, Matsugu Y, Ikeda S, Oshita A, Hotta R, Miguchi M, Chogahara I, Nishikawa S, Hiroi S, Nishisaka T. Retroperitoneal Bronchogenic Cyst Resected by Single-Incision Laparoscopic Surgery in an Adolescent Female: A Case Report. *Asian J Endosc Surg* 2022; **15**: 206-210 [PMID: 34369650 DOI: 10.1111/ases.12973]

58 **Hu BY**, Yu H, Shen J. A retroperitoneal bronchogenic cyst clinically mimicking an adrenal mass: three case reports and a literature review. *J Int Med Res* 2022; **50**: 3000605211072664 [PMID: 35023387 DOI: 10.1177/03000605211072664]

World Journal of Clinical Cases

Submit a Manuscript: https://www.f6publishing.com

World J Clin Cases 2024 May 26; 12(15): 2597-2605

DOI: 10.12998/wjcc.v12.i15.2597

ISSN 2307-8960 (online)

CASE REPORT

Pituitary metastasis from lung adenocarcinoma: A case report

Qing Wang, Xiao-Wei Liu, Ke-Yu Chen

Specialty type: Medicine, research and experimental

Provenance and peer review: Unsolicited article; Externally peer reviewed.

Peer-review model: Single blind

Peer-review report's classification

Scientific Quality: Grade C
Novelty: Grade B
Creativity or Innovation: Grade B
Scientific Significance: Grade C

P-Reviewer: Chien CR, Taiwan

Received: December 26, 2023
Revised: March 20, 2024
Accepted: April 10, 2024
Published online: May 26, 2024

Qing Wang, Department of Critical Care Medicine, Chengdu First People's Hospital, Chengdu 610000, Sichuan Province, China

Xiao-Wei Liu, Ke-Yu Chen, Department of Neurosurgery, Chengdu Second People's Hospital, Chengdu 610017, Sichuan Province, China

Xiao-Wei Liu, Department of the First Clinical Medical College, Lanzhou University, Lanzhou 730000, Gansu Province, China

Xiao-Wei Liu, Evidence Based Medicine Center, School of Basic Medical Sciences, Lanzhou University, Lanzhou 730000, Gansu Province, China

Corresponding author: Ke-Yu Chen, MD, Doctor, Department of Neurosurgery, Chengdu Second People's Hospital, No.10 Qingyun Road, Jinjiang District, Chengdu 610017, Sichuan Province, China. chenk8@qq.com

Abstract

BACKGROUND

Pituitary gland metastasis is an unusual event, and pituitary metastasis from lung adenocarcinoma is extremely rare and associated with poor prognosis. To date, approximately 15 cases have been reported.

CASE SUMMARY

Here, we present the case of a 64-year-old woman with pituitary metastasis derived from lung adenocarcinoma, which was difficult to distinguish from other sellar tumors. The patient presented to the neurosurgery clinic with blurred vision and intermittent headache. During hospitalization, brain computed tomography (CT) and magnetic resonance imaging revealed a pituitary macroadenoma. Chest CT revealed irregular nodules in the basal segment of the lower lobe of the left lung, which were likely lung cancer. Positron emission tomography-CT revealed a carbohydrate metabolism tumor in the lungs and sellar region, which was considered malignant. Postoperative pathological examination of the sellar tumor revealed lung adenocarcinoma.

CONCLUSION

Excision of pituitary metastases combined with radiotherapy and chemotherapy should be a priority treatment for patients with pituitary metastasis.

Key Words: Pituitary metastasis; Lung adenocarcinoma; Prolactin; Sellar region tumors; Case report

Core Tip: Pituitary metastasis from lung adenocarcinoma is extremely rare, but physicians should consider it if it rapidly develops clinical symptoms or grows quickly, especially in patients with other tumors or those with a history of other systemic malignancies. Radiotherapy and chemotherapy are recommended as initial treatments. The blood supply to pituitary metastases is extremely rich; therefore, neurosurgeons must make adequate surgical preparations and plans.

Citation: Wang Q, Liu XW, Chen KY. Pituitary metastasis from lung adenocarcinoma: A case report. *World J Clin Cases* 2024; 12(15): 2597-2605
URL: https://www.wjgnet.com/2307-8960/full/v12/i15/2597.htm
DOI: https://dx.doi.org/10.12998/wjcc.v12.i15.2597

INTRODUCTION

Pituitary metastasis is a rare condition with poor prognosis. The occurrence rate is approximately 1% for all sellar region tumors, with a median survival of less than 1 year[1]. Patients have non-specific clinical symptoms, such as visual field deficits, cranial nerve palsy, anterior pituitary dysfunction, ophthalmoplegia, and diabetes insipidus. Computed tomography (CT) and magnetic resonance imaging (MRI) reveal non-specific diagnostic characteristics. Lung cancer is the leading cause of death among all cancers worldwide[2]. It transfers to the nervous system, bone, liver, and respiratory system. It is important for clinicians to improve awareness to differentiate pituitary metastases in all sellar region tumors, especially in patients aged > 60 years. Here, we report the case of a 64-year-old woman with pituitary metastasis derived from lung adenocarcinoma.

CASE PRESENTATION

Chief complaints

A 64-year-old Asian woman was hospitalized for blurred vision and intermittent headache of 3 months.

History of present illness

Symptoms started 3 months before presentation with blurred vision and intermittent headache.

History of past illness

The patient had no history of hospitalization.

Personal and family history

The patient had no significant personal or family history.

Physical examination

The patient's vital signs were unremarkable. Ophthalmological examination showed that the naked vision was 0.25 in the right eye and 0.8 in the left eye.

Laboratory examinations

Routine blood and urine analyses showed normal results. The endocrine examination results are presented in Table 1.

Imaging examinations

Brain CT showed that the sellar region tumor was related to the carotid artery and was considered a pituitary macroadenoma. Chest CT showed irregular nodules in the basal segment of the lower lobe of the left lung, measuring 2.0 cm × 1.7 cm, which were likely lung cancer. Brain MRI indicated sellar region tumors with isointense signals on T1- and T2-weighted images and an hourglass sign (Figure 1). The tumor was homogeneously enhanced on contrast MRI. The lesion was approximately 1.6 cm × 0.8 cm × 1.3 cm, which was considered pituitary macroadenoma. Positron emission tomography-CT revealed a carbohydrate metabolism tumor in the lungs and sellar region, which was considered malignant. Fiber bronchoscopy revealed a neoplasm in the left lung and hematoxylin and eosin (H&E) staining suggested lung adenocarcinoma.

Pathological examination

H&E staining of the sellar mass revealed a metastatic adenocarcinoma (Figure 2A). Immunohistochemistry showed positive results for CK7 (Figure 2B), CK18 (Figure 2C), TTF-1 (Figure 2D), Napsin A (+) (Figure 2E), and GATA3 (+)

Table 1 Endocrine examination result

Hormone	Level measured	Normal level
ACTH (pg/mL)	17.20	7.2-63.3
PRL (high) (ng/mL)	> 200	2.18-26.53
GH (ng/mL)	0.32	0.02-4.77
TSH (μIU/mL)	1.987	0.35-4.94
T3 (nmol/L)	1.69	0.89-2.44
TT4 (low) (nmol/L)	61.22	62.70-150.80
FT3 (pmol/L)	4.26	2.43-6.01
FT4 (pmol/L)	9.96	9.00-19.00
Tg (ng/mL)	9.988	0.20-70.00
LH (low) (pmol/L)	0.03	5.16-61.99
FSH (low) (mIU/mL)	1.08	26.72-133.41
E2 (pg/mL)	< 10	< 10-28
P4 (ng/mL)	< 0.1	< 0.1-0.2
CORT (8:00) (μg/dL)	1.0	6.02-18.4
CORT (16:00) (μg/dL)	1.5	2.68-10.5
CORT (24:00) (μg/dL)	1.1	2.68-10.5
TES (pmol/L)	< 12.98	10.83-56.94

ACTH: Adrenocorticotropic hormone; PRL: Prolactin hormone; GH: Growth hormone; TSH: Thyroid stimulating hormone; T3: Triiodothyronine; TT4: Total tetraiodothyronine; FT3: Free triiodothyronine; FT4: Free tetraiodothyronine; Tg: Thyroglobulin; LH: Luteinizing hormone; FSH: Follicle stimulating hormone; E2: Estrogen hormone; P4: Progestational hormone; CORT: Cortisol; TES: Testosterone.

(Figure 2F) and negative results for CK20, CDX-2, GFAP, PAX-8, ER, and HER2. The Ki-67 index was 10%, indicating metastatic lung adenocarcinoma (Figure 2G). Next-generation sequencing confirmed somatic mutations in *TSC2*, *POLD1*, *ARID1A*, *CTNNB1*, *ERBB2*, and expressed *PD-L1* (tumor proportion score = 1%) (Table 2).

FINAL DIAGNOSIS

Based on the patient's clinical symptoms and physical, imaging, and pathological examinations, the final diagnosis was pituitary metastasis.

TREATMENT

The patient was taken to the operating room for resection of the right coronary flap tumor of the sellar mass. During the operation, the tumor was gray, tough, aggressive, and rich in blood supply, infiltrating the sellar turcica, third ventricle of the cerebrum, and frontal lobe. The intraoperative bleeding volume was approximately 500 mL. Postoperatively, the patient recovered well and the vision was improved. The patient was advised to undergo immune and chemical therapies at a cancer hospital. Postoperative MRI revealed no tumor regrowth within 3 months (Figure 3).

OUTCOME AND FOLLOW-UP

The patient is still alive, with no recurrence noted 1 year after surgery.

DISCUSSION

The literature was searched in PubMed till March 14, 2024. The medical subject heading search terms and strategies

Table 2 Somatic gene mutations

Gene	Expressed region	Nucleotide	Amino acid	Mutation abundance (%)
TSC2	Exon 36	c.4585C>T	p.R1529W	5.1
POLD1	Exon19	c.2312C>T	p.A771V	3.8
ARID1A	Exon 1	c.1058C>T	p.A353V	5.1
ARID1A	Exon 1	c.308C>T	p.S103L	7.7
CTNNB1	Exon 4	c.79G>A	p.G27R	13.5
ERBB2	Exon 23	c.2339C>T	p.A800V	5.1

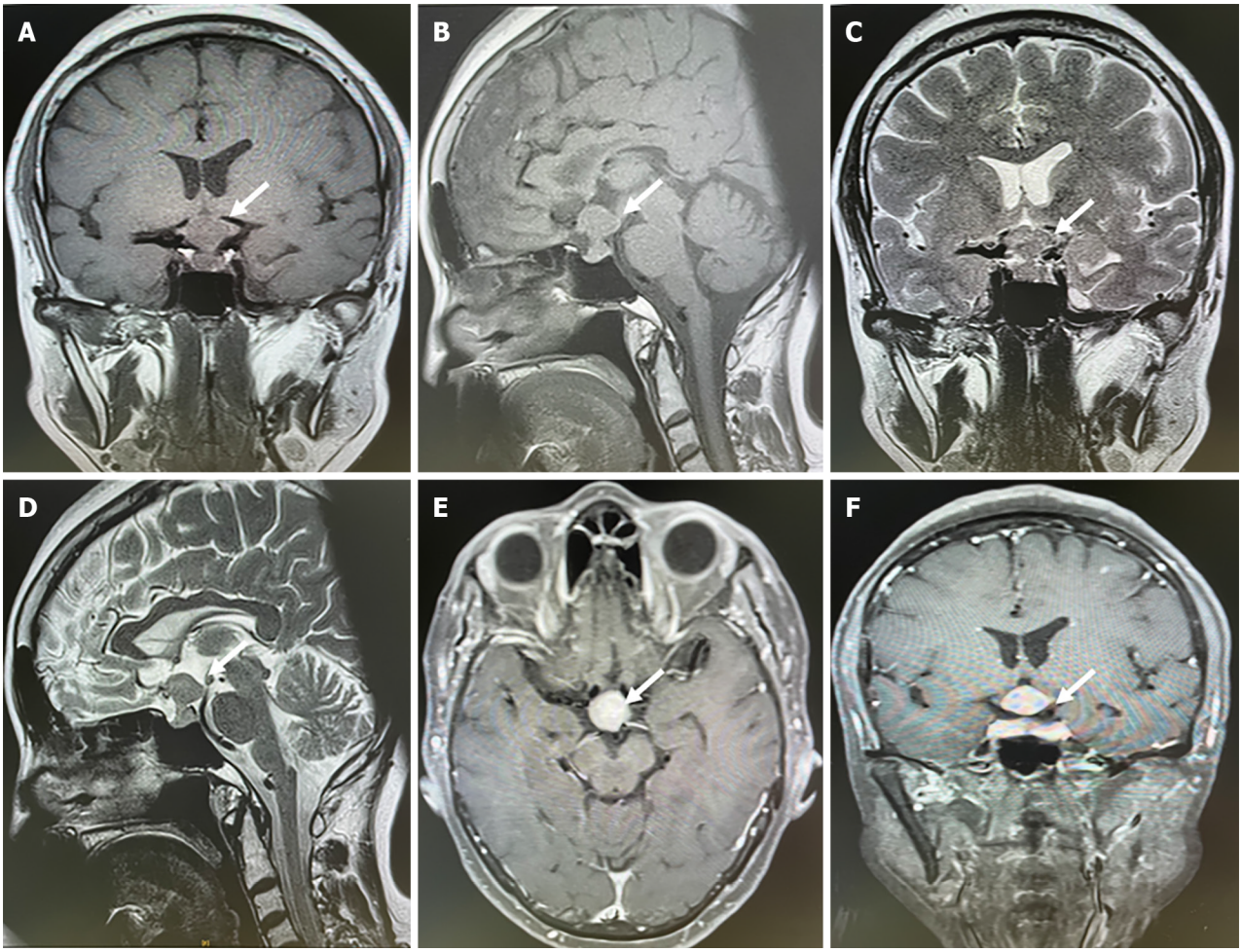

Figure 1 Sellar magnetic resonance imaging showed a sellar lesion related to carotid artery. A-D: The leision located in the sellar region presented with an isointense signal on T1 and T2-weighted images and could see hourglass sign; E and F: The leision was intensified homogenously enhanced after contrast magnetic resonance imaging.

included pituitary metastasis and lung cancer. In total, 352 studies were screened using the PubMed database. The language was restricted to English and only published articles were included. We reviewed 15 articles that reported pituitary metastasis from lung adenocarcinoma. A flowchart of the literature selection process is shown in Figure 4. The characteristics of the included studies are presented in Table 3.

Sellar tumors mostly originate from pituitary adenomas and rarely metastasize to other organs. Autopsies have revealed that pituitary metastases account for nearly 5% of all pituitary metastases in sellar tumors. In surgical sections, less than 1% of all sellar tumors are associated with pituitary metastasis[3]. Pituitary metastases always metastasize from the lungs and breasts, accounting for 39.7% and 23.7% of cases, respectively[4]. Small cell carcinomas are usually transferred to the liver and brain parenchyma, whereas adenocarcinomas often affect the bone and respiratory system[5]. A Swedish study reported that small cell lung cancer was the most frequent type of pituitary metastasis among all lung cancers. In contrast, adenocarcinoma rarely metastasizes to the pituitary gland but rather to the lungs and bones[6]. The present article reports the case of a patient with lung adenocarcinoma metastasizing to the pituitary gland without distant

Table 3 Summary of previously reported cases of pituitary metastasis from lung adenocarcinoma

Ref.	Year	Age (yr)	Sex	Symptom	Hormone	Treatment	Tumor Supply	Survival
Asim and Elashaal [13]	2023	54	F	None	ACTH (low), COTR (low), LH (low), FSH (low), TES (low), TSH (low), FT3 (low), FT4 (low)	RT, ST	ND	Alive, 3 months
Amaral *et al*[14]	2022	43	M	Headache, VFD	ACTH (low), CORT (low), FSH (low), FT4 (low), TES (low), LH (low)	ST, CT, RT, IT	R	Alive, 15 months
Wong *et al*[15]	2022	53	F	VFD	ND	ST, RT, CT	ND	Alive, 24 months
Han *et al*[16]	2022	48	F	Headache, DI	ACTH (low), Cort (low), PRL (high)	ST, CT	ND	Alive, 20 months
Lopes *et al*[17]	2021	62	F	Fatigue, Headache, Nocturia, Polydipsia, BV	FT4 (low), CORT (low), ACTH (low), FSH (low), PRL (high)	ST, CT	R	Alive, 24 months
Tanaka *et al*[9]	2021	80	F	Polyuria, Polydipsia	ADH (low)	RT, CT	ND	Alive, 7 months
Liu *et al*[3]	2021	53	M	BV, DI, VFD, Polyuria, Vomit, Fatigue	CORT (low), TSH (high), T4 (low), FSH (low), LH (low), PRL (high)	ST	R	Dead, 4 months
Watanabe *et al*[18]	2020	70	M	Anorexia	ADH (low), ACTH (low), CORT (low), FSH (low), LH (low), TSH (low)	RT, CT	ND	Dead, 5 months
Rajakumar *et al*[19]	2020	49	F	Headache, VFD	LH (low), FSH (low), CORT (low), TES (low), FT4 (low)	ST, RT, CT	NR	ND
Alhashem *et al*[11]	2020	54	M	Headache, Droop bilateral eyelid	ND	ST	NR	ND
Sheahan *et al*[5]	2020	52	F	MB	ACTH (low), CORT (low), FSH (low), TSH (low), PRL (high)	ST, CT	ND	ND
Yao *et al*[20]	2019	67	M	Headache, Vomit, ptosis	PRL (high), FSH (low), LH (low), ACTH (low), Cort (low)	ST, RT	ND	Dead, 3 months
Sirinvaravong *et al* [21]	2019	72	F	DI	PRL (high), FSH (low), LH (low), TSH (high)	ST	ND	Dead, 4 months
Gulati *et al*[12]	2015	47	F	Headache, DI	TSH (low), FSH (low)	ST	ND	ND
Arai *et al*[22]	2010	61	F	VFD	Normal	ST, RT	NR	Alive, 3 months

F: Female; M: Male; R: Rich; CSI: Cavernous sinus invasion; VFD: Visual field defect; ND: Not described; NR: Not rich; BV: Blurred vision; MB: Monocular blindness; DI: Dizziness; ACTH: Adrenocorticotropic hormone; ADH: Vasopressin; CORT: Cortisol hormone; PRL: Prolactin hormone; TSH: Thyroid stimulating hormone; FT3: Free triiodothyronine; FT4: Free tetraiodothyronine; LH: Luteinizing hormone; FSH: Follicle stimulating hormone; Cort: Cortisol; TES: Testosterone; ST: Surgery treatment; CT: Chemotherapy; IT: Immunotherapy; RT: Radiotherapy.

metastasis.

The clinical symptoms and radiographic findings of pituitary metastases are nonspecific. Patients present with visual field deficits, diabetes insipidus, cranial nerve palsy, or anterior pituitary dysfunction. Pituitary metastasis is a rare disease with poor prognosis. It is difficult to diagnose, especially in patients who are not diagnosed with a primary cancer. Physicians should consider these diseases, especially in older patients presenting with new-onset deficiencies in visual and anterior pituitary hormones. Pituitary adenoma often manifests hypointense on T1-weighted images and hyperintense on T2-weighted images, similar to pituitary metastasis. This is the main reason for misdiagnosis. However, pituitary metastasis often manifests as pituitary stalk thickening, invasion of the cavernous sinus, and coexistence of brain lesions, which have been observed in pituitary adenomas. Furthermore, if patients have other tumors detected on imaging or a history of other systemic malignancies, neurosurgeons should consider pituitary metastasis.

Pituitary metastases mostly located in posterior pituitary alone or combined with anterior pituitary accounting for 84.6%. Only 15.4% of cases have been found in the anterior pituitary alone[7]. It is mainly because the location and blood

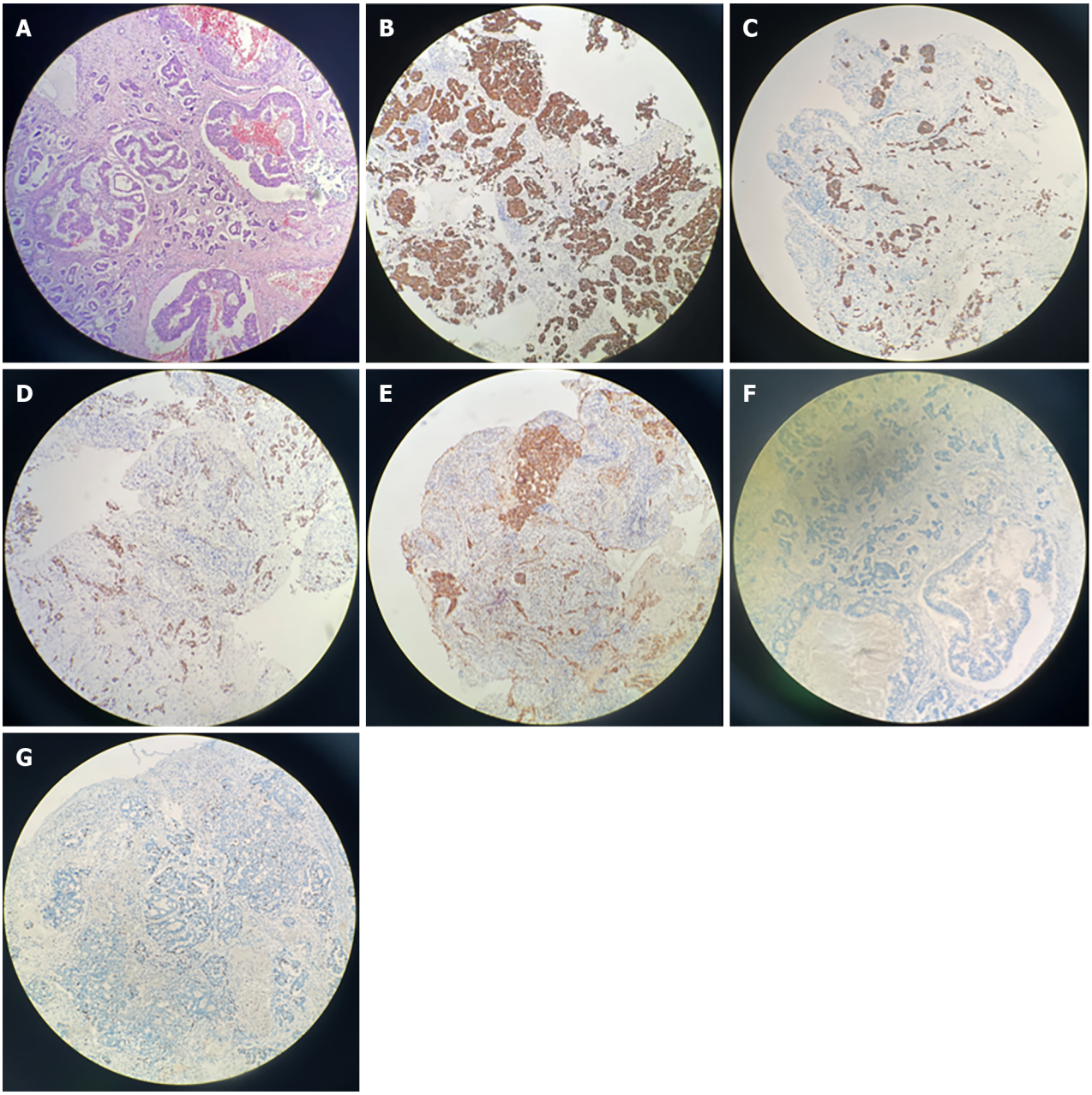

Figure 2 The histological features of the lesions revealed pituitary metastasis from lung adenocarcinoma. A: Hematoxylin and eosin staining found epithelial neoplasm and considered metastatic adenocarcinoma (× 100); B-F: Immunohistochemistry revealed positive for CK7, CK18, TTF-1, NapsinA and GATA3 (× 100); G: Immunohistochemical staining of Ki-67 (× 100).

supply. The posterior pituitary has larger area to contact with the dura mater compared to anterior. The posterior pituitary receives blood supply from hypophyseal artery. on the contrary, the anterior pituitary only receives venous supply through hypophyseal portal system. The patient was admitted to the hospital due to blurred vision and headache accompanied by increased prolactin hormone and decreased cortisol, suggesting that the tumor had damaged both anterior and posterior pituitary glands. During operation, the tumor was tough, aggressive, and rich of blood which was different from the common sellar region tumors, such as pituitary adenoma, craniopharyngiomas and so on. According to the operation features and fiber bronchoscope, we suspected the tumor was likely pituitary metastases from lung. After operation, H&E and immunohistochemistry all confirmed pituitary metastasis from lung adenocarcinoma.

There are currently no standard protocols for the treatment of pituitary metastasis. The treatment for pituitary metastasis includes surgery, chemotherapy, and radiotherapy (RT). The choice of treatment depends on the primary tumor, clinical symptoms, and physical conditions. Surgical eradication includes transsphenoidal surgery and craniotomy. Total resection is difficult to achieve using either surgical method. Moreover, pituitary metastasis is highly aggressive and can destroy the sellar base and diaphragm and can adhere tightly to the pituitary gland. However, pituitary metastasis has a tough texture and abundant blood supply, which increases the difficulty of surgery. Although there is no consensus on whether surgery can extend the overall survival of patients with pituitary metastasis, it can relieve the symptoms and serve as a pathological diagnosis for treatment. RT and chemotherapy are recommended as initial treatments. RT can not only control local diseases with few morbidities but can also provide symptom relief.

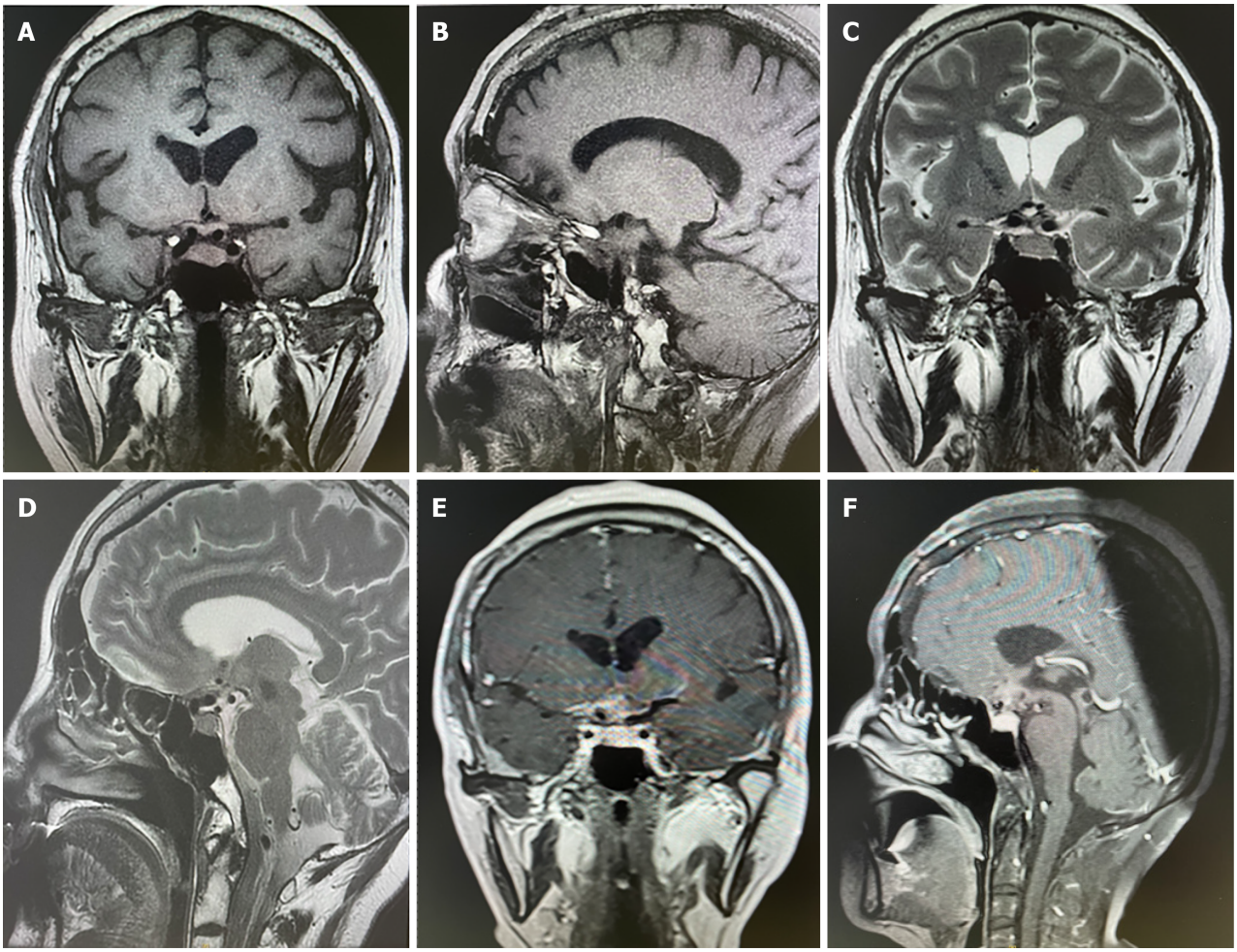

Figure 3 Sellar magnetic resonance imaging showed no neoplasm recurrence in 3 months after surgery. A-D: Postoperative changes of sellar region and there was no leision found in T1 and T2-weighted images; E and F: There was no intensified leision imaging after contrast magnetic resonance imaging.

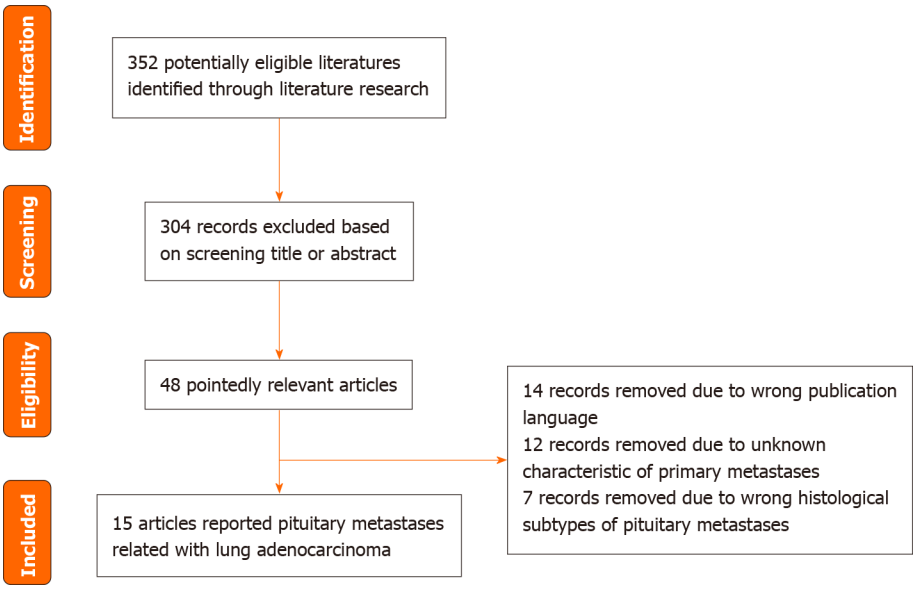

Figure 4 Flowchart of the study selection.

However, the 5-year radiation-associated hypopituitarism rate is 20% and 10-15 years radiation-associated hypopituitarism has been reported in up to 80% of cases[8,9]. Standard chemotherapy or immunotherapy crossing the blood-brain barrier indicates that patients with multiple organ involvement have longer survival advantages, although the evidence is limited to case reports[10]. The prognosis of pituitary metastasis is relatively poor. The median survival of pituitary metastasis was reported 17 months (range 0-240 months) while the longest survival of pituitary metastasis from lung adenocarcinoma was recorded 32 months[11]. It's reported that the younger age, longer interval after pituitary metastasis, smaller pituitary lesion and utilization of RT and chemotherapy all correlated with improved survival[12].

CONCLUSION

Pituitary metastasis from lung adenocarcinoma is extremely rare, but physicians should consider it if rapidly developing clinical symptoms or growing quickly, especially for the patients found other tumors on images or had a history of other system malignancy. RT and chemotherapy are recommended as the initial treatments. The blood supply to pituitary metastases is extremely rich, so it is necessary for neurosurgeons to make adequate operation preparations and surgery plans.

FOOTNOTES

Author contributions: Wang Q and Liu XW contributed equally to this article; Wang Q wrote the manuscript; Liu XW made literature research and data collections; Chen KY revised the article.

Informed consent statement: Informed written consent was obtained from the patient and her families for publication of this report and any accompanying images.

Conflict-of-interest statement: All the authors report no relevant conflicts of interest for this article.

CARE Checklist (2016) statement: The authors have read the CARE Checklist (2016), and the manuscript was prepared and revised according to the CARE Checklist (2016).

Country/Territory of origin: China

ORCID number: Xiao-Wei Liu 0000-0002-1862-9101; Ke-Yu Chen 0009-0007-2026-2082.

S-Editor: Zheng XM
L-Editor: A
P-Editor: Yu HG

REFERENCES

1 **Liu X**, Wang R, Li M, Chen G. Pituitary Metastasis of Lung Neuroendocrine Carcinoma Mimicking Pituitary Adenoma:Case Report and Literature Review. *Front Endocrinol (Lausanne)* 2021; **12**: 678947 [PMID: 34335467 DOI: 10.3389/fendo.2021.678947]
2 **Nooreldeen R**, Bach H. Current and Future Development in Lung Cancer Diagnosis. *Int J Mol Sci* 2021; **22** [PMID: 34445366 DOI: 10.3390/ijms22168661]
3 **Liu CY**, Wang YB, Zhu HQ, You JL, Liu Z, Zhang XF. Hyperprolactinemia due to pituitary metastasis: A case report. *World J Clin Cases* 2021; **9**: 190-196 [PMID: 33511184 DOI: 10.12998/wjcc.v9.i1.190]
4 **Komninos J**, Vlassopoulou V, Protopapa D, Korfias S, Kontogeorgos G, Sakas DE, Thalassinos NC. Tumors metastatic to the pituitary gland: case report and literature review. *J Clin Endocrinol Metab* 2004; **89**: 574-580 [PMID: 14764764 DOI: 10.1210/jc.2003-030395]
5 **Sheahan KH**, Huffman GC, DeWitt JC, Gilbert MP. Metastatic Lung Cancer Presenting as Monocular Blindness and Panhypopituitarism Secondary to a Pituitary Metastasis. *Am J Case Rep* 2020; **21**: e920948 [PMID: 32321907 DOI: 10.12659/AJCR.920948]
6 **Riihimäki M**, Hemminki A, Fallah M, Thomsen H, Sundquist K, Sundquist J, Hemminki K. Metastatic sites and survival in lung cancer. *Lung Cancer* 2014; **86**: 78-84 [PMID: 25130083 DOI: 10.1016/j.lungcan.2014.07.020]
7 **Ng S**, Fomekong F, Delabar V, Jacquesson T, Enachescu C, Raverot G, Manet R, Jouanneau E. Current status and treatment modalities in metastases to the pituitary: a systematic review. *J Neurooncol* 2020; **146**: 219-227 [PMID: 31933258 DOI: 10.1007/s11060-020-03396-w]
8 **Gilard V**, Alexandru C, Proust F, Derrey S, Hannequin P, Langlois O. Pituitary metastasis: is there still a place for neurosurgical treatment? *J Neurooncol* 2016; **126**: 219-224 [PMID: 26514360 DOI: 10.1007/s11060-015-1967-y]
9 **Tanaka S**, Hirabayashi T, Kimoto M, Hama M, Hachiya T, Gomi K. Gefitinib Treatment Was Unsuccessful for Central Diabetes Insipidus Due to Pituitary Metastasis of Lung Adenocarcinoma. *Intern Med* 2021; **60**: 1073-1076 [PMID: 33162476 DOI: 10.2169/internalmedicine.5643-20]

10 **Castle-Kirszbaum M**, Goldschlager T, Ho B, Wang YY, King J. Twelve cases of pituitary metastasis: a case series and review of the literature. *Pituitary* 2018; **21**: 463-473 [PMID: 29974330 DOI: 10.1007/s11102-018-0899-x]

11 **Alhashem A**, Taha M, Almomen A. Pituitary metastasis of lung adenocarcinoma: Case report and literature review. *Int J Surg Case Rep* 2020; **67**: 98-101 [PMID: 32058309 DOI: 10.1016/j.ijscr.2020.01.013]

12 **Gulati S**, Kiefer C, Karim NA. Diabetes Insipidus: An Unusual Presentation of Adenocarcinoma of the Lung in a Patient with no Identifiable Lung Mass. *N Am J Med Sci* 2015; **7**: 476-479 [PMID: 26713294 DOI: 10.4103/1947-2714.168677]

13 **Asim SA**, Elashaal AA. Metastasis of lung adenocarcinoma to the pituitary gland. *Radiol Case Rep* 2023; **18**: 3487-3491 [PMID: 37588239 DOI: 10.1016/j.radcr.2023.07.025]

14 **Amaral S**, Matias A, Bouça B, Manique I, Palha A, Cortez L, Cerqueira L, Forte D, Sagarribay A, Dutra E, Cristóvão M, Pontinha C, Mafra M, Silva-Nunes J. Pituitary metastasis as the first manifestation of lung carcinoma. *Clin Case Rep* 2022; **10**: e6601 [PMID: 36518913 DOI: 10.1002/ccr3.6601]

15 **Wong PS**, Rajoo S, Achmad Sankala H, Long Bidin MB. Unusual presentation of lung carcinoma with pituitary metastasis: a challenging diagnosis and sodium management dilemmas. *Endocr Oncol* 2022; **2**: K15-K20 [PMID: 37435455 DOI: 10.1530/EO-22-0064]

16 **Han D**, Zhao K, Yang Q, Zhang L, Fei S. Secondary mutant ALK-I1171s in pituitary metastases from a patient with ALK fusion-positive advanced lung adenocarcinoma: A case report and literature review. *Front Oncol* 2022; **12**: 1016320 [PMID: 36324562 DOI: 10.3389/fonc.2022.1016320]

17 **Lopes AM**, Pereira J, Ribeiro I, Martins da Silva A, Queiroga H, Amaral C. Pituitary metastasis unveiling a lung adenocarcinoma. *Endocrinol Diabetes Metab Case Rep* 2021; **2021**: 20-0211 [PMID: 33865234 DOI: 10.1530/EDM-20-0211]

18 **Watanabe M**, Yasuda J, Ashida K, Matsuo Y, Nagayama A, Goto Y, Iwata S, Watanabe M, Sasaki J, Hoshino T, Nomura M. Masked Diabetes Insipidus Hidden by Severe Hyponatremia: A Case of Pituitary Metastasis of Lung Adenocarcinoma. *Am J Case Rep* 2020; **21**: e928113 [PMID: 33335085 DOI: 10.12659/AJCR.928113]

19 **Rajakumar R**, Rahmatullah IH, Rahim AA. Case Report of a Pituitary Metastasis from Lung Adenocarcinoma Masquerading as Pituitary Adenoma. *J ASEAN Fed Endocr Soc* 2020; **35**: 133-136 [PMID: 33442183 DOI: 10.15605/jafes.035.01.24]

20 **Yao H**, Rui W, Zhang Y, Liu Y, Lin S, Tang H, Zhao W, Wu Z. Prolactin-Secreting Lung Adenocarcinoma Metastatic to the Pituitary Mimicking a Prolactinoma: A Case Report. *Neurosurgery* 2019; **85**: E773-E778 [PMID: 30137505 DOI: 10.1093/neuros/nyy386]

21 **Sirinvaravong S**, Vibhatavata P, Chunharojrith P, Cheunsuchon P, Sriussadaporn S. Diabetes insipidus and panhypopituitarism as a first presentation of silent adenocarcinoma of lung: a case report and literature review. *BMC Endocr Disord* 2019; **19**: 114 [PMID: 31664980 DOI: 10.1186/s12902-019-0445-5]

22 **Arai A**, Morishita A, Hanada Y, Aihara H. Solitary metastatic tumor within the optic chiasm--case report. *Neurol Med Chir (Tokyo)* 2010; **50**: 158-161 [PMID: 20185885 DOI: 10.2176/nmc.50.158]

World Journal of Clinical Cases

Submit a Manuscript: https://www.f6publishing.com

World J Clin Cases 2024 May 26; 12(15): 2606-2613

DOI: 10.12998/wjcc.v12.i15.2606

ISSN 2307-8960 (online)

CASE REPORT

Primary Ewing sarcoma of the kidney mimicking cystic papillary renal cell carcinoma in an older patient: A case report

Suhong Kim, Jongsoo Park, Young Hwii Ko, Hee Jung Kwon

Specialty type: Medicine, research and experimental

Provenance and peer review: Unsolicited article; Externally peer reviewed.

Peer-review model: Single blind

Peer-review report's classification

Scientific Quality: Grade B

Novelty: Grade B

Creativity or Innovation: Grade B

Scientific Significance: Grade B

P-Reviewer: Wani I, India

Received: January 8, 2024

Revised: March 6, 2024

Accepted: April 7, 2024

Published online: May 26, 2024

Suhong Kim, Jongsoo Park, Department of Radiology, Yeungnam University, Daegu 42415, South Korea

Young Hwii Ko, Department of Urology, Yeungnam University, Daegu 42415, South Korea

Hee Jung Kwon, Department of Pathology, Yeungnam University, Daegu 42415, South Korea

Corresponding author: Hee Jung Kwon, MD, PhD, Assistant Professor, Department of Pathology, Yeungnam University, 170 Hyeonchung-ro, Nam-gu, Daegu 42415, South Korea. hjs336@ynu.ac.kr

Abstract

BACKGROUND

Ewing's sarcoma (ES) is a neuroectodermal tumor that typically occurs in the bones and soft tissues of children and young adults. Primary renal ES is rare; only a few cases and a small case series have been documented, and only four cases involved primary renal ES in older people (> 65 years old).

CASE SUMMARY

Herein, we describe the radiological and pathological features of primary renal ES in an older person. A 76-year-old man complained of poor oral intake and was found to have a large cystic renal mass with indistinct margins on computed tomography. Ultrasound-guided biopsy revealed that the tumor contained small round blue cells. The patient underwent a right radical nephrectomy. The tumor cells showed diffuse membranous CD99, and nuclear friend leukemia integration 1 transcription factor and NK2 Homeobox 2. Fluorescence *in situ* hybridization revealed *EWSR1* translocation. Postoperatively, ^{18}F-fluorodeoxyglucose positron emission tomography revealed no evidence of metastasis. The patient was diagnosed with primary renal ES. Six months following the surgery, local recurrence and distant metastasis were observed. Primary renal ES is rare and often lethal in older individuals. The specific imaging findings are unknown, and treatment protocols have not been standardized.

CONCLUSION

This case report describes the radiological and pathological features of primary renal ES in an older person.

Key Words: Ewing sarcoma; Elder; Renal; Kidney; Neuroectodermal; Case report

Core Tip: Primary renal Ewing's sarcoma (ES) is extremely rare, whereas shown aggressive radiological features and poor outcome. It is important to consider primary renal ES in the differential diagnosis when renal mass shown indistinctive margin and necrosis/hemorrhage in older patients. Primary renal ES undergo surgical resection and receive adjuvant chemotherapy. Moreover, radiation therapy is efficient for local recurrence.

Citation: Kim S, Park J, Ko YH, Kwon HJ. Primary Ewing sarcoma of the kidney mimicking cystic papillary renal cell carcinoma in an older patient: A case report. *World J Clin Cases* 2024; 12(15): 2606-2613
URL: https://www.wjgnet.com/2307-8960/full/v12/i15/2606.htm
DOI: https://dx.doi.org/10.12998/wjcc.v12.i15.2606

INTRODUCTION

Ewing's sarcoma (ES) is an aggressive malignant tumor that typically arises from the bones, and rarely from the retroperitoneum, head and neck, parameningeal, and genitourinary systems. ES mostly affects children and young adults, and is uncommon in older people. ES of the kidney was first described in 1975[1] and has a reported incidence of approximately 100 cases[1-3]. Among them, primary renal ES in older people (> 65 years) has been reported in only four patients in the English literature[4-7]. Primary renal ES typically remain asymptomatic initially, but when the tumor grows large enough, the tumor often manifest symptoms such as flank pain and hematuria.

Owing to its rarity, ES is sometimes misdiagnosed as other more common kidney cancers. ES lacks specific radiological findings; however, common features include large necrotic masses and intratumoral hemorrhage. Contrast-enhanced imaging reveal a mild and progressive enhancement pattern frequently associated with invasion of the perirenal fascia and renal sinuses[8]. Histological characteristics that confirm positive CD99 expression and the existence of a reciprocal translocation between the ES gene on chromosome 22 and members of the ETS family, most commonly friend leukemia integration 1 transcription factor (FLI1) or ERG, are typically used to confirm tissue diagnosis[6]. Primary renal ES has an aggressive clinical course and a poor prognosis. However, there is no consensus on optimal treatment because of its rarity.

This study reports a rare case of primary renal ES in an older man. Additionally, we reviewed the literature on primary renal ES in older patients.

CASE PRESENTATION

Chief complaints

Appetite loss for several months.

History of present illness

A 76-year-old male visited our hospital complaining of appetite loss for several months.

History of past illness

The patient had hypertension.

Personal and family history

The patient had no familial medial history.

Physical examination

Tenderness and percussion pain in the left flank were observed during the physical examination.

Laboratory examinations

The complete blood count, serum electrolyte values, and urine analysis results were all within the normal ranges. The patient showed normal kidney function test with blood urea nitrogen of 15.7 mg/dL, serum creatinin of 0.75 mg/dL, serum uric acid of 5.3 mg/dL and modification of diet in renal disease-estimated glomerular filtration rate of 100.99.

Imaging examinations

On renal ultrasonography, an 11 cm × 10 cm cystic lesion was identified in the right renal lower pole with a 4.4 cm × 1.8 cm solid component on the posterior aspect of the cystic lesion, which showed increased vascularity on color doppler mode (Figure 1A and B). On computed tomography (CT), a pre-contrast phase axial CT shows a cystic lesion with a mass

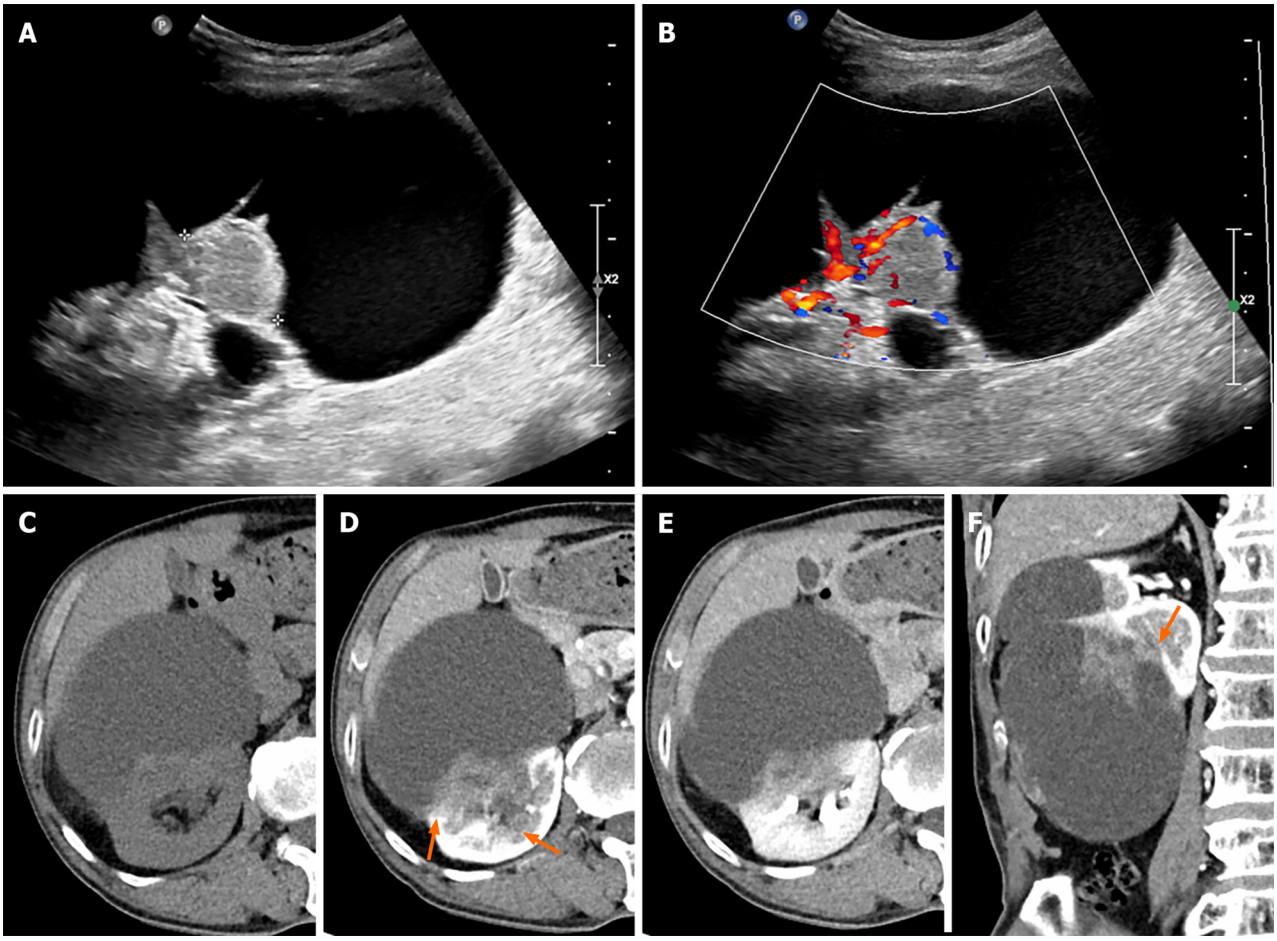

Figure 1 Initial ultrasound and abdominal computed tomography scan of the right kidney. A: An 11 cm × 10 cm cystic lesion is noted in the right kidney with a 3.2 cm solid component on ultrasound B-mode; B: Increased vascularity is seen in the solid component on color doppler mode; C: A pre-contrast phase axial computed tomography (CT) shows a cystic lesion with a mass at the posterior-lateral aspect of the right kidney interpolar region-lower pole. A subtle high-attenuation area is seen in the cystic lesion, suggesting hemorrhage; D and E: Corticomedullary and excretory phase axial CT shows progressive enhancement of the mass (pre-contrast phase: 40 HU, corticomedullary phase: 70 HU, excretory phase: 80 HU) and a suspiciously indistinct margin (orange arrows) and invasion of the sinus; F: Corticomedullary phase coronal CT scan shows an irregular enhancing mass in a lesion with indistinct margins (orange arrow).

at the posterior-lateral aspect of the right kidney interpolar region-lower pole (Figure 1C). A subtle high-attenuation area is seen in the cystic lesion, suggesting hemorrhage. Corticomedullary and excretory phase axial CT shows progressive enhancement of the mass (pre-contrast phase: 40 HU, corticomedullary phase: 70 HU, excretory phase: 80 HU) and a suspiciously indistinct margin and invasion of the sinus (Figure 1D and E). Corticomedullary phase coronal CT scan shows an irregular enhancing mass in a lesion with indistinct margins (Figure 1F).

Further diagnostic work-up

Ultrasound guided, core needle biopsy: Under suspicion of cystic papillary renal cell carcinoma (RCC), an ultrasound-guided core needle biopsy was performed for a targeted intracystic solid mass. Histological evaluation revealed solid sheets of primitive, small, and uniform cells with hyperchromatic nuclei and scant cytoplasm. Immunohistochemical staining was positive for synaptophysin and CD99. Staining for desmin, FLI1, leukocyte common antigen (LCA), pan-cytokeratin, neuron-specific enolase, and S100 were negative. Fluorescence *in situ* hybridization (FISH) using formalin-fixed, paraffin-embedded tissues showed a t(11; 22) Ewing sarcoma region 1 (*EWSR1*) translocation (zytolight SPEC *EWSR1* dual color break-apart probe, ZytoVision GmbH, Fischkai 127572 Bremerhaven, Germany). The mass was suggestive of ES.

Surgical examination: The patient underwent a radical nephrectomy. The tumor was located at the lower pole of the right kidney. The large cystic tumor was well demarcated by the perirenal adipose tissue without rupture. Most tumors were cystic lesions, whereas the solid area showed gross infiltration of the renal parenchyma (Figure 2A). The border of the tumor infiltrating the renal parenchyma was confirmed using hematoxylin-eosin (HE) staining (Figure 2B). The tumor exhibited multifocal necrosis (Figure 2C). The solid part of the tumor in the specimen was composed of small round cells with scanty cytoplasm, similar to that in the biopsy specimen (Figure 2D). Ancillary tests for CD56, chromogranin A, FLI1, LCA, thyroid transcription factor-1, and cytokeratins (AE1/AE3) were negative. The tumor cells exhibited diffuse membranous staining for CD99 (Figure 2E) and NK2 Homeobox 2 (NKX2.2) (Figure 2F). FISH using formalin-fixed, paraffin-embedded tissues showed a t(11; 22) *EWSR1* translocation (Figure 2G) (zytolight SPEC *EWSR1* dual color break-

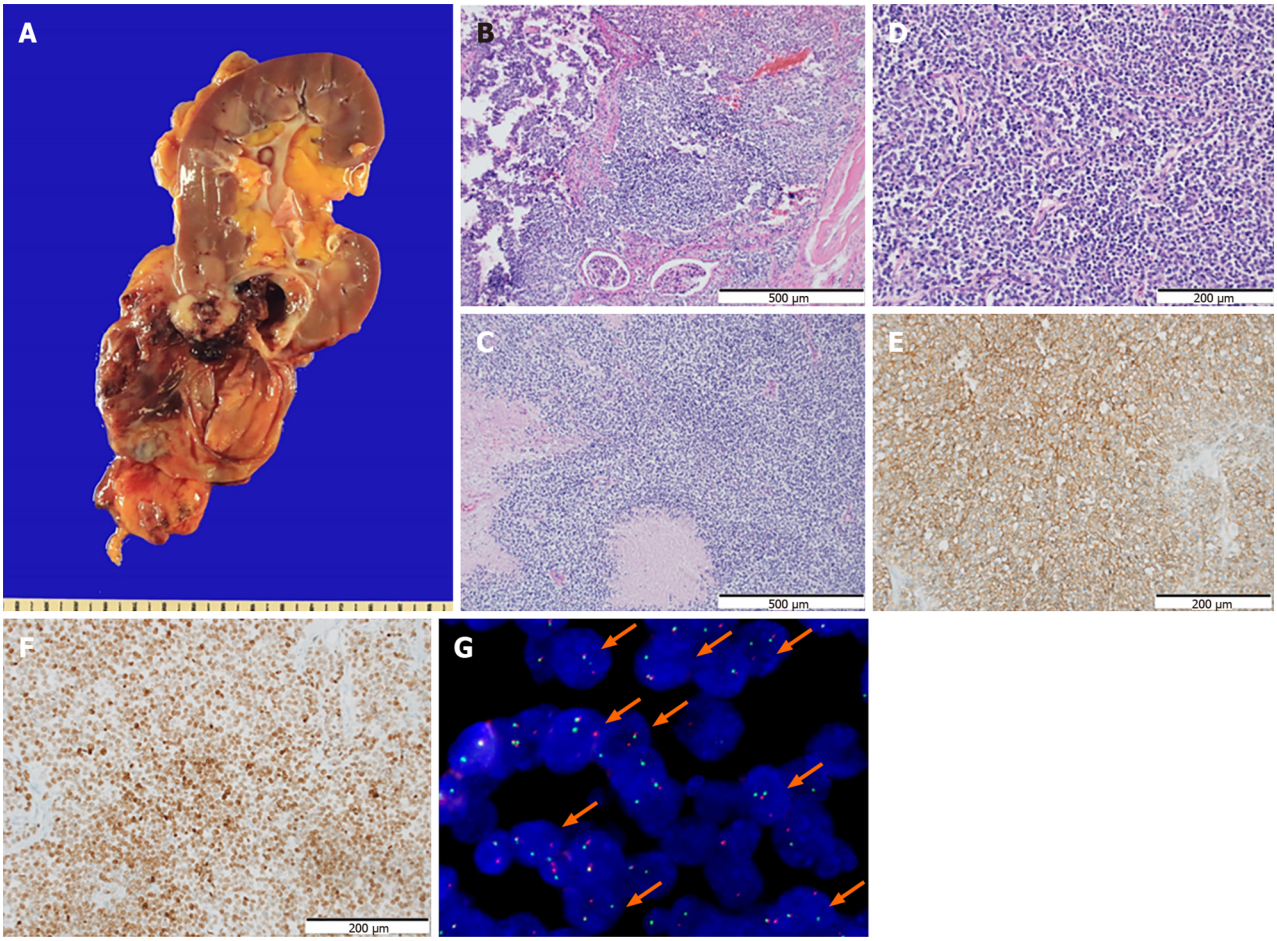

Figure 2 Morphological features and immunostaining results of the tumor. A: A huge cystic mass in the lower pole of the right kidney without rupture. Most parts of the tumor consisted of cystic lesions, while the solid area showed infiltration into the renal parenchyma grossly; B: The border of the tumor infiltrating into the renal parenchyma is also identified on the hematoxylin and eosin (HE) sections (× 100). Staining method: HE staining; C: Frequent necrosis is observed (× 100). Staining method: HE staining; D: The section shows a relatively diffuse sheet pattern composed of small round tumor cells. The tumor cells show no glandular or squamous differentiation and present moderate pleomorphism (× 200). The nuclei are monotonous with inconspicuous nucleoli. The tumor has scanty or clear cytoplasm (× 200). Staining method: HE staining; E and F: The tumor cells exhibit diffuse membranous stain for CD99 (E, × 200) and nuclear stain for NK2 Homeobox 2 (F, × 200). Staining method: Polymer method; G: Fluorescence *in situ* hybridization exhibits the diagnostic t (11; 22) *EWSR1* translocation (orange arrows).

apart probe, ZytoVision GmbH, Fischkai 127572 Bremerhaven, Germany).

FINAL DIAGNOSIS

The diagnosis was primary renal ES.

TREATMENT

The patient underwent right radical nephrectomy. The patient did not undergo chemotherapy.

OUTCOME AND FOLLOW-UP

Postoperatively, torso positron emission tomography revealed no involvement of other organs (Figure 3A), and a whole-body bone scan revealed no abnormal uptake lesions. No recurrence was observed on abdominal or chest CT scans 3 months after surgery; however, CT performed 6 months after surgery showed local recurrence and peritoneal metastasis (Figure 3B-D). Thus, radiotherapy was administered for 10 cycles to control the pain. Eight months after surgery, abdominal CT revealed a locally controlled recurrent mass at the right nephrectomy site; however, multiple, more aggravated metastases were discovered (Figure 3E-G), and the patient died. The follow-up duration was 10 months.

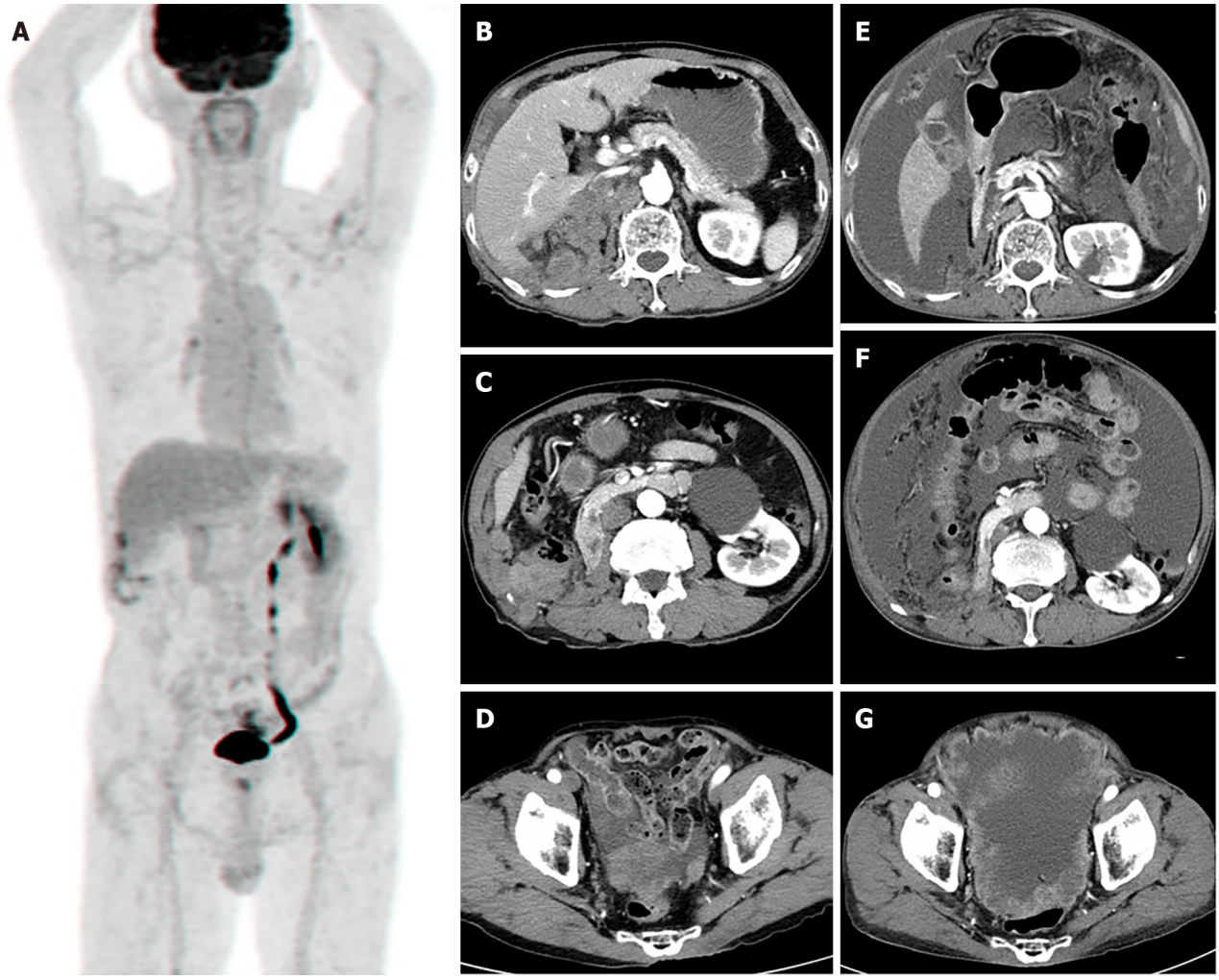

Figure 3 Immediate post-operative ^{18}F-fluorodeoxyglucose torso positron emission tomography scan and follow up abdominal computed tomography. A: ^{18}F-fluorodeoxyglucose (FDG) torso positron emission tomography after right nephrectomy shows mild FDG uptake at operation site, which suggested postoperative changes. No other abnormal FDG uptake was demonstrated; B-D: Abdominal computed tomography (CT), taken 6 months after right nephrectomy, shows local recurrence and peritoneal metastasis; E-G: Abdominal CT scan, taken 8 months after right nephrectomy, shows locally controlled local recurrence result from radiotherapy but more progression of peritoneal metastasis with increased malignant ascites.

DISCUSSION

The ES family of tumors comprises a group of high-grade small round cell tumors, including ES of the bone, extraskeletal ES, peripheral primitive neuroectodermal tumors (PNET), and thoracopulmonary PNET. The pathogenesis of ES is presently understood to involve the EWS/FLI oncoprotein, derived from reciprocal translocation between 11 and 22, t (11, 22) (q24; q12). This can be confirmed through FISH or reverse transcriptase polymerase chain reaction (RT-PCR).

Tumors are common in young children and adolescents. The average age at diagnosis was 30.7 years with a male to female ratio of 6:4[8]. Limited number of cases of primary renal ES with an aggressive clinical course has been reported in the English literature. Moreover, only four cases of ES in older people have been reported in the English literature (Table 1). Among a total of five older patients (aged 60 years or older) with primary renal ES, four died. The mean overall survival (OS) was 18.3 months, and the median OS was 16 months. This was shorter than the median OS of primary renal ES treated with radical nephrectomy of 27.4 months in a previous study[8]. This suggests that primary renal ES in older people has a worse prognosis, and that age is a significant prognostic factor for primary renal ES. Additionally, 60% of patients presented with metastasis at diagnosis. These results are similar to those of a previous study that reported metastasis in 37.5%–60% of the primary renal ES/PNET cases[2,6,9]. The high incidence of metastatic disease may be due to the aggressive nature of primary renal ES or the absence of specific clinical presentations of retroperitoneal tumors.

Renal ES/PNET is not only a significant challenge for imaging diagnosis but also poses diagnostic challenges for pathology. Although there are no specific radiological findings for ES, the following are known: Large masses (60% of tumors > 10 cm) are heterogeneous in the non-contrast phase. Among the tumors, 95.9%, 32.7%, and 11.6% showed necrosis, intratumoral hemorrhage, and parenchymal calcification, respectively. In contrast, mild and progressive enhancement with invasion of the perirenal fascia (47.2%) and renal sinuses (67.9%) has been noted[8]. The radiological findings of PNET are similar to those of ES. PNET presents as a weakly enhanced large mass with multiple septate appearances, peripheral hemorrhage/necrosis, renal vein, or inferior vena cava thrombosis, accompanied by distant

Table 1 Clinical characteristics, treatment, and outcomes of five older patients with primary renal Ewing's sarcoma of kidney

Case	Age	Sex	Size	Side	Presentation	Surgery	Other therapy	Recurrence or metastasis	Follow-up (month)	Status
Current case	76	M	11	R	Incidentally found	Nephrectomy	RTx	Local recurrence, carcinomatosis	10	Dead
1	69	F	5	R	Abdominal pain	Nephrectomy	CTx	Lung, bone	25	Dead
2	70	F	NA	NA	NA	Nephrectomy	CTx + INF	Lung	16	Dead
3	69	F	NA	NA	NA	Nephrectomy	CTx	Lung	22	Dead
4	73	M	NA	R	Incidentally found	Nephrectomy	CTx	No	7	Alive

RTx: Radiation therapy; CTx: Chemotherapy; INF: Interferon-γ.

metastasis or renal vein thrombosis[10].

Our case showed an enhanced portion with extensive necrosis, mimicking cystic papillary RCC. Papillary RCC, a subtype of RCC constituting 10%-15% of RCCs cases, typically shows homogeneous enhancement on CT scans. However, approximately 15% of papillary RCC show heterogeneous enhancement with a large size (> 10 cm) and presence of a cystic portion or necrosis. Moreover, approximately 7% of these tumors may have intratumoral calcifications. The typical dynamic enhancement pattern of papillary RCC is characterized by mild (20 HU-40 HU) and persistent enhancement[11]. Approximately 98% of the tumors had a well-defined boundary that altered kidney contours and displaced adjacent structures; only 2% of papillary RCC showed an infiltrating margin, which commonly represented a high Fuhrman grade and had sarcomatoid features. Compared to the RCC, renal ES shares similar imaging findings with papillary RCC. In particular, ES/PNETs show an indistinctive infiltrative margin, which is a characteristic of ES. In the present case, the mass showed indistinctive margins with infiltration into the normal renal parenchyma. In addition, papillary RCC has lower incidence of renal vein invasion and lymph node metastasis; however, renal ES have highly incidence of renal vein invasion and lymph node metastasis.

Small round cell tumors present a diagnostic challenge for pathologists because of the poorly differentiated features of these high-grade tumors. Furthermore, ES masses often present with extensive hemorrhage and necrosis, and fine-needle biopsy is usually inadequate for diagnosis[12]. In many cases, round cell tumors require large immunohistochemical (IHC) panels and molecular testing. Light microscopy revealed the presence of small round tumor cells arranged in sheets, forming Homer-Wright rosettes. Tumor cells are positive for neuroectodermal IHC markers such as neuron-specific enolase and synaptophysin. The demonstration of reciprocal translocation t (11; 22) (q24; q12) by genetic studies is considered specific to PNET and ES[13].

According to EURO EWING 2012, treatment recommendations exist for primary ES[14]. Most patients undergo surgical resection and receive adjuvant chemotherapy. Effective chemotherapeutic agents include vincristine, doxorubicin, ifosfamide, etoposide, actinomycin D, and cyclophosphamide[15]. Molecular targeted therapies, including insulin-like growth factor 1 receptor antibodies, have shown promise for Ewing sarcoma family of tumours[16]. Our patient did not receive adjuvant chemotherapy; however, chemotherapy has been administered in other cases, leading to better outcomes. Radiotherapy is recommended for skeletal ES if unresectable tumors or unexpected positive margins are recommended for skeletal ES[17]. In the EURO EWING 2012 trial, patients with unresectable tumors, residual tumors, or metastases responded well to radiotherapy. Our patient showed local recurrence on abdominal CT, showing locally controlled recurrent tumors after radiotherapy.

CONCLUSION

ES should always be considered a differential diagnosis for aggressive renal tumors in older patients. While imaging diagnosis for renal ES still has limitations, when large-sized renal masses have necrosis, hemorrhage, and indistinctive margins with mild and persistent enhancement on dynamic contrast enhancement studies, although rare, considering primary ES is necessary, even in older patients, as a differential diagnosis. The final diagnosis is by histopathology with IHC and cytogenetic studies, such as FISH or RT-PCR. Early detection is crucial for the prompt initiation of chemotherapy with or without radiation therapy, and radiology plays an increasingly important role in diagnosis, staging, treatment monitoring, and surveillance.

FOOTNOTES

Author contributions: Kim S and Kwon HJ completed conceptualization; Kwon HJ and Ko YH completed data curation; Kim S, Park J and Kwon HJ wrote the original draft; Kim S reviewed and edited the mauscuript; All authors have read and agreed to the published version of the manuscript.

Supported by Yeungnam University, No. 223A580026.

Informed consent statement: The requirement for informed consent was waived by the board because of the patient's death.

Conflict-of-interest statement: The authors declare no conflicts of interest.

CARE Checklist (2016) statement: The authors have read the CARE Checklist (2016), and the manuscript was prepared and revised according to the CARE Checklist (2016).

Country/Territory of origin: South Korea

ORCID number: Suhong Kim 0000-0003-2128-3524; Hee Jung Kwon 0000-0002-8800-7690.

S-Editor: Che XX
L-Editor: A
P-Editor: Yu HG

REFERENCES

1 **Seemayer TA**, Thelmo WL, Bolande RP, Wiglesworth FW. Peripheral neuroectodermal tumors. *Perspect Pediatr Pathol* 1975; **2**: 151-172 [PMID: 1129029]
2 **Rowe RG**, Thomas DG, Schuetze SM, Hafez KS, Lawlor ER, Chugh R. Ewing sarcoma of the kidney: case series and literature review of an often overlooked entity in the diagnosis of primary renal tumors. *Urology* 2013; **81**: 347-353 [PMID: 23374800 DOI: 10.1016/j.urology.2012.10.016]
3 **Zhang S**, Li Y, Wang R, Song B. Ewing's sarcoma/primitive neuroectodermal tumor of the kidney: a case report and literature review. *Transl Androl Urol* 2019; **8**: 562-566 [PMID: 31807433 DOI: 10.21037/tau.2019.09.46]
4 **Jimenez RE**, Folpe AL, Lapham RL, Ro JY, O'Shea PA, Weiss SW, Amin MB. Primary Ewing's sarcoma/primitive neuroectodermal tumor of the kidney: a clinicopathologic and immunohistochemical analysis of 11 cases. *Am J Surg Pathol* 2002; **26**: 320-327 [PMID: 11859203 DOI: 10.1097/00000478-200203000-00005]
5 **Murugan P**, Rao P, Tamboli P, Czerniak B, Guo CC. Primary Ewing Sarcoma / Primitive Neuroectodermal Tumor of the Kidney: A Clinicopathologic Study of 23 Cases. *Pathol Oncol Res* 2018; **24**: 153-159 [PMID: 28429277 DOI: 10.1007/s12253-017-0228-0]
6 **Tarek N**, Said R, Andersen CR, Suki TS, Foglesong J, Herzog CE, Tannir NM, Patel S, Ratan R, Ludwig JA, Daw NC. Primary Ewing Sarcoma/Primitive Neuroectodermal Tumor of the Kidney: The MD Anderson Cancer Center Experience. *Cancers (Basel)* 2020; **12**: 2927 [PMID: 33050651 DOI: 10.3390/cancers12102927]
7 **Wedde TB**, Lobmaier IV, Brennhovd B, Lohne F, Hall KS. Primary Ewing's Sarcoma of the Kidney in a 73-Year-Old Man. *Sarcoma* 2011; **2011**: 978319 [PMID: 21776194 DOI: 10.1155/2011/978319]
8 **Hu X**, Li D, Cai J. Experience of CT diagnosis and management of primary renal Ewing's sarcoma: A retrospective analysis of 6 cases and a literature review. *Medicine (Baltimore)* 2022; **101**: e32189 [PMID: 36626543 DOI: 10.1097/MD.0000000000032189]
9 **Zöllner S**, Dirksen U, Jürgens H, Ranft A. Renal Ewing tumors. *Ann Oncol* 2013; **24**: 2455-2461 [PMID: 23761687 DOI: 10.1093/annonc/mdt215]
10 **Lee H**, Cho JY, Kim SH, Jung DC, Kim JK, Choi HJ. Imaging findings of primitive neuroectodermal tumors of the kidney. *J Comput Assist Tomogr* 2009; **33**: 882-886 [PMID: 19940655 DOI: 10.1097/RCT.0b013e31819e938b]
11 **Couvidat C**, Eiss D, Verkarre V, Merran S, Corréas JM, Méjean A, Hélénon O. Renal papillary carcinoma: CT and MRI features. *Diagn Interv Imaging* 2014; **95**: 1055-1063 [PMID: 25443332 DOI: 10.1016/j.diii.2014.03.013]
12 **Burchill SA**. Ewing's sarcoma: diagnostic, prognostic, and therapeutic implications of molecular abnormalities. *J Clin Pathol* 2003; **56**: 96-102 [PMID: 12560386 DOI: 10.1136/jcp.56.2.96]
13 **Takeuchi T**, Iwasaki H, Ohjimi Y, Kaneko Y, Ishiguro M, Fujita C, Miura Y, Hiratsuka Y, Sakamoto K, Kikuchi M. Renal primitive neuroectodermal tumor: an immunohistochemical and cytogenetic analysis. *Pathol Int* 1996; **46**: 292-297 [PMID: 8726854 DOI: 10.1111/j.1440-1827.1996.tb03613.x]
14 **Anderton J**, Moroz V, Marec-Bérard P, Gaspar N, Laurence V, Martín-Broto J, Sastre A, Gelderblom H, Owens C, Kaiser S, Fernández-Pinto M, Fenwick N, Evans A, Strauss S, Whelan J, Wheatley K, Brennan B. International randomised controlled trial for the treatment of newly diagnosed EWING sarcoma family of tumours - EURO EWING 2012 Protocol. *Trials* 2020; **21**: 96 [PMID: 31952545 DOI: 10.1186/s13063-019-4026-8]
15 **Grier HE**, Krailo MD, Tarbell NJ, Link MP, Fryer CJ, Pritchard DJ, Gebhardt MC, Dickman PS, Perlman EJ, Meyers PA, Donaldson SS, Moore S, Rausen AR, Vietti TJ, Miser JS. Addition of ifosfamide and etoposide to standard chemotherapy for Ewing's sarcoma and primitive neuroectodermal tumor of bone. *N Engl J Med* 2003; **348**: 694-701 [PMID: 12594313 DOI: 10.1056/NEJMoa020890]
16 **Javery O**, Krajewski K, O'Regan K, Kis B, Giardino A, Jagannathan J, Ramaiya NH. A to Z of extraskeletal Ewing sarcoma family of tumors in adults: imaging features of primary disease, metastatic patterns, and treatment responses. *AJR Am J Roentgenol* 2011; **197**: W1015-1022 [PMID: 22109315 DOI: 10.2214/AJR.11.6667]
17 **DuBois SG**, Krailo MD, Gebhardt MC, Donaldson SS, Marcus KJ, Dormans J, Shamberger RC, Sailer S, Nicholas RW, Healey JH, Tarbell NJ, Randall RL, Devidas M, Meyer JS, Granowetter L, Womer RB, Bernstein M, Marina N, Grier HE. Comparative evaluation of local control

strategies in localized Ewing sarcoma of bone: a report from the Children's Oncology Group. *Cancer* 2015; **121**: 467-475 [PMID: 25251206 DOI: 10.1002/cncr.29065]

World Journal of Clinical Cases

Submit a Manuscript: https://www.f6publishing.com

World J Clin Cases 2024 May 26; 12(15): 2614-2620

DOI: 10.12998/wjcc.v12.i15.2614

ISSN 2307-8960 (online)

CASE REPORT

Transparent cap adjusted the stent placed for stenosis after endoscopic injection of esophageal varices: A case report

Fu-Long Zhang, Jing Xu, Yuan-Dong Zhu, Qian-Neng Wu, Yan Shi, Lei Fang, Dan Zhou, Hai Wang, Chao-Jun Huang, Chun-Hua Zhou, Qun Zhu

Specialty type: Medicine, research and experimental

Provenance and peer review: Unsolicited article; Externally peer reviewed.

Peer-review model: Single blind

Peer-review report's classification

Scientific Quality: Grade C, Grade D

Novelty: Grade B, Grade D

Creativity or Innovation: Grade B, Grade C

Scientific Significance: Grade B, Grade C

P-Reviewer: Takemura N, Japan; Ueda H, Japan

Received: January 21, 2024

Revised: February 8, 2024

Accepted: April 8, 2024

Published online: May 26, 2024

Fu-Long Zhang, Yuan-Dong Zhu, Qian-Neng Wu, Yan Shi, Lei Fang, Dan Zhou, Hai Wang, Chao-Jun Huang, Chun-Hua Zhou, Qun Zhu, Department of Gastroenterology, Hangzhou Xixi hospital, Hangzhou 310023, Zhejiang Province, China

Jing Xu, Department of Hepatopathy, Hangzhou Xixi hospital, Hangzhou 310023, Zhejiang Province, China

Corresponding author: Yuan-Dong Zhu, Doctor, Director, Professor, Department of Gastroenterology, Hangzhou Xixi hospital, No. 2 Henbu Street, Xihu District, Hangzhou 310023, Zhejiang Province, China. zhuyuandong2022@163.com

Abstract

BACKGROUND

The stent embedded in the esophageal mucosa is one of the complications after stenting for esophageal stricture. We present a case of stent adjustment with the aid of a transparent cap after endoscopic injection of an esophageal varices stent.

CASE SUMMARY

A 61-year-old male patient came to the hospital with discomfort of the chest after the stent implanted for the stenosis because of endoscopic injection of esophageal varices. The gastroscopy was performed, and the stent embedded into the esophageal mucosa. At first, we pulled the recycling line for shrinking the stent, however, the mucosa could not be removed from the stent. Then a forceps was performed to remove the mucosa in the stent, nevertheless, the bleeding form the mucosa was obvious. And then, we used a transparent cap to scrape the mucosa along the stent, and the mucosa were removed successfully without bleeding.

CONCLUSION

A transparent cap helps gastroscopy to remove the mucosa embedded in the stent after endoscopic injection of the esophageal varices stent.

Key Words: Stent; Transparent cap; Stenosis; Endoscopic injection; Esophageal varices; Case report

Core Tip: Esophageal stenosis is one of the complications of endoscopic injection for treatment of esophageal varices. The stent embedding into the esophageal mucosa is one of the complications after stenting for esophageal stricture. We present a case of stent adjustment with the aid of a transparent cap after endoscopic injection of an esophageal varices stent.

Citation: Zhang FL, Xu J, Zhu YD, Wu QN, Shi Y, Fang L, Zhou D, Wang H, Huang CJ, Zhou CH, Zhu Q. Transparent cap adjusted the stent placed for stenosis after endoscopic injection of esophageal varices: A case report. *World J Clin Cases* 2024; 12(15): 2614-2620
URL: https://www.wjgnet.com/2307-8960/full/v12/i15/2614.htm
DOI: https://dx.doi.org/10.12998/wjcc.v12.i15.2614

INTRODUCTION

Esophageal stenosis is one of the complications of endoscopic injection for treatment of esophageal varices, and the incidence is between 2%-10%[1]. There was no report on the use of self-expanding metal stents (SEMS) for the treatment of esophageal strictures after endoscopic injection for esophageal varices. The stent embedding in the esophageal mucosa is one of the serious complications of SEMS for the treatment of esophageal strictures. We present in this article a case in which a transparent cap adjusted the stent implanted for the stenosis after endoscopic injection of cyanoacrylate (CYA) and sclerotherapy for esophageal varices.

CASE PRESENTATION

Chief complaints

A 61-year-old male patient presented to the hospital with discomfort of the chest for one month.

History of present illness

One month ago, the stent was implanted for the patient with esophageal stenosis who underwent endoscopic injection of cyanoacrylate and sclerotherapy for esophageal varices.

History of past illness

The patient suffered surgery for hepatocellular carcinoma 3 years ago.

Personal and family history

All other personal and family medical history was normal.

Physical examination

Diseased liver face, no yellowing of the skin or sclera, clear breath sounds on both lungs auscultation, no dry or wet rales, heart rate of 76 beats/min, regular heart rhythm, soft abdomen, no tenderness or rebound pain, the spleen and the ribs were accessible, and there was no edema in either lower limb.

Laboratory examinations

The laboratory result showed prothrombin time, alanine aminotransferase, creatine kinase (CK), CK-MB, creatinine, carbohydrate antigen (CA) 199, carcinoembryonic antigen, glucose, C-reactive protein, cholesterol, triglyceride and lipase were in normal range. White blood cell, Hemoglobin, platelet, dimer, amylase, total bilirubin, alpha-fetoprotein and CA125 were not in normal. HbsAg, hepatitis C antibody, human immunodefciency virus antibody, syphilis antibody, anti-nuclear anti-bodies were all negative (Table 1).

Imaging examinations

The computed tomography of chest and electrocardiogram were normal. We used an endoscope (EG-760R, diameter 9.3 mm, FUJIFILM, Japan) to observe retention in the esophageal cavity (Figure 1A), paying close attention to residual varices (Figure 1A) as we removed the residue. When the esophageal stricture was exposed (Figure 1B), we performed balloon dilatation (18 mm 55 mm, Nanjing Minimally Invasive Medical Technology Co, Ltd, Nanjing, China) to dilate the stricture (Figure 1C) until the body of the endoscope could smoothly pass through the stenosis. We inserted a semi-covered SEMS (20 mm × 60 mm; Nanjing Minimally Invasive Medical Technology Co, Ltd, Nanjing, China) across the stricture *via* hard wire girding (Figure 1D). Additionally, we were careful to be aware of residual varices when inserted the SEMS (Figure 1E). After the SEMS was implanted, the stricture showed obvious improvement and dilation (Figure 1F).

The gastroscopy showed that the anal side of the stent was normal; however, the oral side of the stent was embedded into the esophageal mucosa (Figure 1G). First, we attempted to pull the recycling line to shrink the SEMS to remove the

Table 1 The laboratory result of the patient before treatment

	Laboratory result	Normal
WBC (10^9/L)	2.22	(3.4-9.5)
HB (g/L)	80	(115-150)
Platelet (10^9/L)	31	(125-350)
PT(s)	13.5	(9.7-13.5)
Dimer (mg/L)	4.36	(0-0.55)
ALT (u/L)	23	(9-50)
TB (umol/L)	20.89	(3-20)
CK (u/L)	30	(20-180)
CK-MB (u/L)	20	(0-30)
Cr (umol/L)	67	(40-80)
CA199 (kU/L)	6.20	(0-35)
CEA (ug/L)	1.90	(0-5)
AFP (ug/L)	12.48	(0-9)
CA125 (ug/L)	101.10	(0-35)
CRP (mg/L)	9.50	(0-10)
Triglyceride (mmol/L)	0.60	(0-1.7)
Cholesterol (mmol/L)	2.87	(2.86-5.98)
Amylase (U/L)	201	(35-135)
Lipase (U/L)	106	(0-190)
Glucose (mmol/L)	5.41	3.0-6.1
HbsAg	Negative	Negative
HIV Ab	Negative	Negative
Sp Ab	Negative	Negative
ANA	Negative	Negative
Hc Ab	Negative	Negative

WBC: White blood cell; HB: Hemoglobin; TB: Total bilirubin; CK: Creatine kinase; ALT: Alanine aminotransferase; Cr: Creatinine; CEA: Carcinoembryonic antigen; AFP: Alpha-fetoprotein; CA: Carbohydrate antigen; CRP: C-reactive protein; PT: Prothrombin time; HbsAg: Hepatitis B surface antigen; Hc Ab: Hepatitis C antibody; HIV Ab: Human immunodefciency virus antibody; Sp Ab: Syphilis antibody; ANA: Anti-nuclear anti-bodies.

mucosa embedded in the stent (Figure 1H and I); however, the mucosa could not be removed from the stent (Figure 1J). Then, forceps were used to remove the mucosa in the stent, but the patient experience obvious esophageal bleeding (Figure 1K). We then used a transparent cap to scrape the mucosa embedded in the stent along the SEMS (Figure 1L and M), and the mucosa was removed successfully without further bleeding (Figure 1N).

FINAL DIAGNOSIS

The esophageal mucosa embedded the stent which was implanted for the stenosis after endoscopic injection of esophageal varices.

TREATMENT

We used a transparent cap to scrape the mucosa embedded the stent along the SEMS and the mucosa were removed successfully without bleeding.

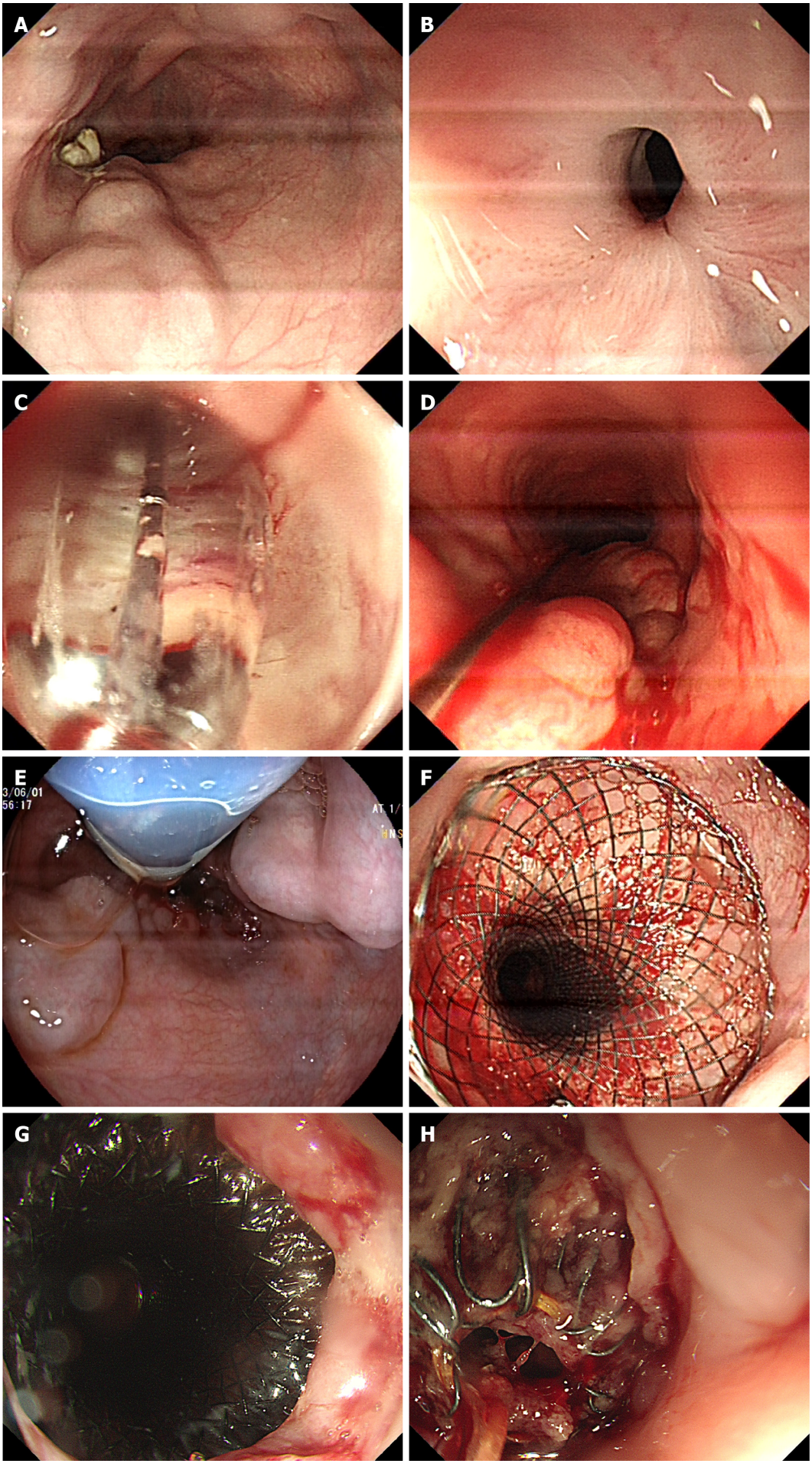
A
B
C
D
E
3/06/01
56:17
F
G
H

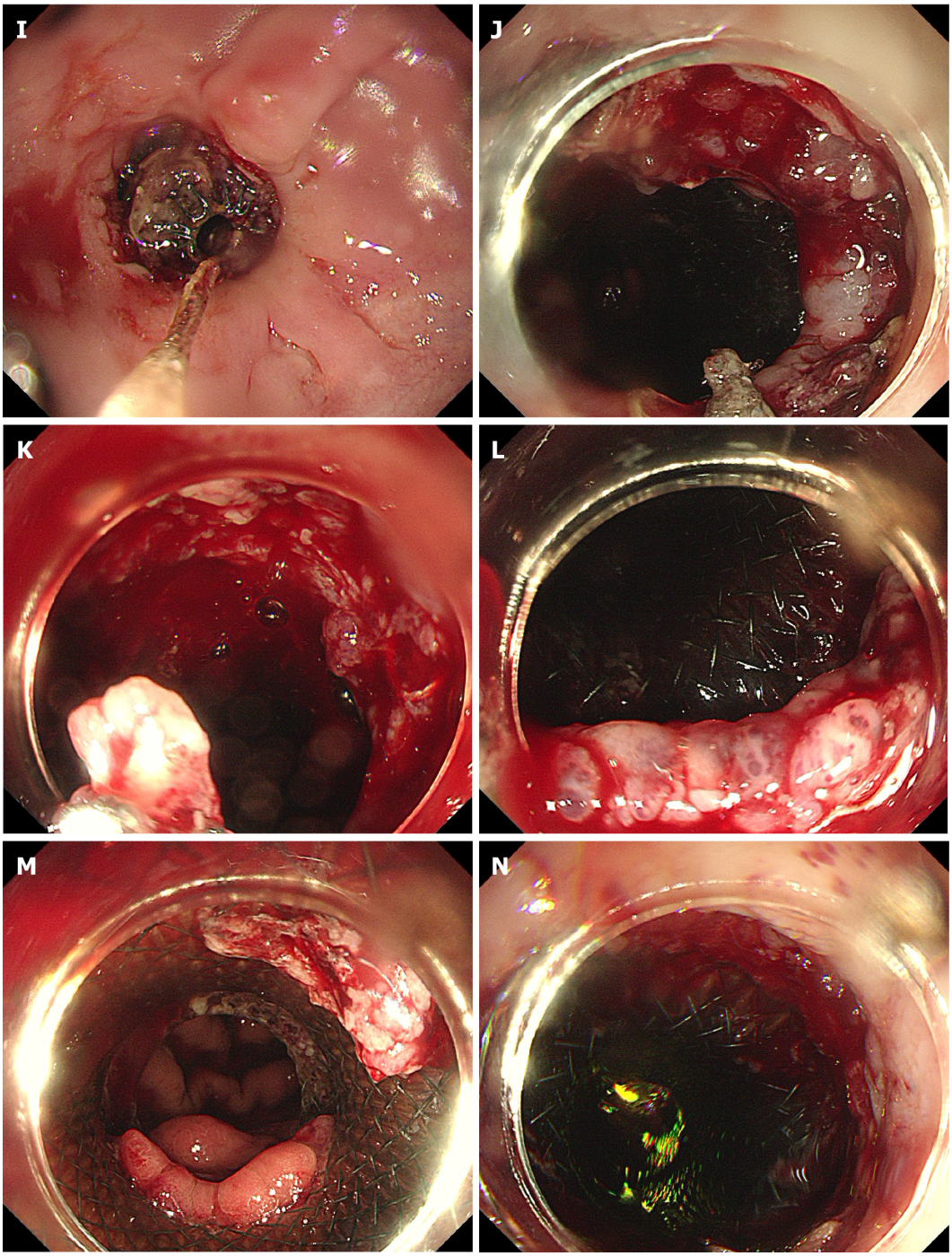

Figure 1 Transparent cap adjusted the stent placed for stenosis after endoscopic injection of esophageal varices. A: Residual varices were observed above the stricture, and we should be alert to residual varices; B: The esophageal stricture exposed entirely; C: We used balloon dilatation to improve the stricture; D: The self-expanding metal stents (SEMS) was passed through the stricture by a hard wire girding; E: We should be alert to the residual varices, when we were placing the SEMS; F: After the implanting the SEMS, the stricture was improved obviously; G: Oral side of the stent embedded into the esophageal mucosa; H: The recycling line was pulled for shrinking the stent; I: We try to pull the recycling line for shrinking the SEMS to remove mucosa embedded the stent; J: Mucosa embedded the stent could not be removed by shrinking the SEMS; K: A forceps was performed to remove mucosa embedded the stent, nevertheless, the bleeding was obvious; L: A transparent cap was used to scrape the mucosa embedded the stent; M: The tissue was scraped and pushed into the stomach along the SEMS with a transparent cap; N: Mucosa embedded the stent were removed successfully without bleeding.

OUTCOME AND FOLLOW-UP

The patient experienced relief from chest pain, and there was no infection, bleeding or perforation after adjusting the SEMS and removing the mucosa embedded in the stent. The patient was discharged from the hospital the next day.

DISCUSSION

Endoscopic sclerotherapy was considered the main treatment for esophageal varices[2]. In recent years cyanoacrylate injection was performed successfully for esophageal varices without any bleeding recurrence[3]. Esophageal stricture is one of the complication after endoscopic injection cyanoacrylate and/or sclerotherapy esophageal varices. Esophageal stricture is related to local inflammation, ulceration, and fibrosis caused by multiple injection[4]. The standard treatment for esophageal stricture after injection for esophageal varices is not mentioned in international guidelines[5]. European society of gastrointestinal endoscopy[6] recommended that the use of esophageal stent for the treatment of benign esophageal strictures had mainly been investigated in the context of refractory or recurrent benign esophageal strictures, and esophageal stent placement had a potential benefit because of its continuous expansion force, which may lead to stricture remodeling. Stent placement will extend the esophageal stricture, however, we should be alert to the complications, such as chest pain, reflux esophagitis, displacement or detachment, and tissue embedded stents[7-9].

Tissue embedded stents and chest pain are the common complications of esophageal stent placement. In this case, we used a transparent cap to assist the gastroscopy to successfully remove mucosa embedded the stent which was implanted for the stenosis after endoscopic injection esophageal varices with CYA and sclerotherapy. The advantages of the transparent cap for adjusting the stent are as follows: (1) The transparent cap is small and allows for a clear field of vision close to the stent; (2) the mucosa embedded in the stent could not be removed by shrinking the SEMS with the recycling line alone, but the transparent cap could easily scrape the tissue; (3) removing the tissue with forceps may lead to bleeding; On the other hand, if forceps are hooked into the SEMS, it is difficult to remove the forceps; (4) if esophageal bleeding occurs, a transparent cap can be used to effectively suppress the bleeding; (5) the tissue could be scraped and pushed into the stomach along the SEMS with a transparent cap, which could reduce the likelihood of complication by aspiration pneumonia; and (6) the front of the transparent cap is soft and flexible, which is safe for interacting with residual varices. However, there are several limitations for using the transparent cap to adjust the stent: (1) Although the transparent cap can assist gastroscopy in successfully removing mucosa embedded in the stent, the stent may become embedded in the tissue again afterwards; and (2) if the patient often suffers from chest pain, gastroscopy may need to be performed regularly to observe the situation of the stent.

CONCLUSION

A transparent cap could assist the gastroscopy to remove the mucosa embedded the stent which was implanted for the stenosis after endoscopic injection of esophageal varices.

FOOTNOTES

Author contributions: Zhang FL and Zhu YD contributed equally to this work; Zhang FL and Zhu YD designed the research study; Wu QN, Shi Y, Zhou D, Fang L, Huang CJ, Wang H, Zhu Q and Zhou CH performed the research; Zhang FL and Xu J analyzed the data and wrote the manuscript. All authors have read and approve the final manuscript.

Supported by Hangzhou Agricultural and Social Development Research Guidance Project, No. 20220919Y037.

Informed consent statement: Written informed consent was obtained from the patient for publication.

Conflict-of-interest statement: The authors declare that they have no competing interests.

CARE Checklist (2016) statement: The authors have read the CARE Checklist (2016), and the manuscript was prepared and revised according to the CARE Checklist (2016).

Country/Territory of origin: China

ORCID number: Jing Xu 0000-0002-0074-1306; Yuan-Dong Zhu 0000-0002-6384-6412; Yan Shi 0000-0002-0778-4579.

S-Editor: Liu H
L-Editor: A
P-Editor: Zhang XD

REFERENCES

1 **de Franchis R**, Primignani M. Endoscopic treatments for portal hypertension. *Semin Liver Dis* 1999; **19**: 439-455 [PMID: 10643628 DOI: 10.1055/s-2007-1007131]

2 **Eisen GM**, Baron TH, Dominitz JA, Faigel DO, Goldstein JL, Johanson JF, Mallery JS, Raddawi HM, Vargo JJ, Waring JP, Fanelli RD, Wheeler-Harbaugh J; Standards Practice Committe, American Society for Gastrointestinal Endoscopy. The role of endoscopic therapy in the management of variceal hemorrhage. *Gastrointest Endosc* 2002; **56**: 618-620 [PMID: 12397264 DOI: 10.1016/s0016-5107(02)70105-3]

3 **Kalista KF**, Hanif SA, Nababan SH, Lesmana CRA, Hasan I, Gani R. The Clinical Role of Endoscopic Ultrasound for Management of Bleeding Esophageal Varices in Liver Cirrhosis. *Case Rep Gastroenterol* 2022; **16**: 295-300 [PMID: 35814797 DOI: 10.1159/000524529]

4 **Linghu EQ**. [Endoscopic diagnosis and treatment of upper gastrointestinal hemorrhage caused by esophagus-gastric varice]. *Zhonghua Xiaohuabing Yu Yingxiang Zazhi* 2012; **2**: 1-3 [DOI: 10.3877/cma.j.issn.2095-2015.2012.01.001]

5 **Sami SS**, Haboubi HN, Ang Y, Boger P, Bhandari P, de Caestecker J, Griffiths H, Haidry R, Laasch HU, Patel P, Paterson S, Ragunath K, Watson P, Siersema PD, Attwood SE. UK guidelines on oesophageal dilatation in clinical practice. *Gut* 2018; **67**: 1000-1023 [PMID: 29478034 DOI: 10.1136/gutjnl-2017-315414]

6 **Spaander MCW**, van der Bogt RD, Baron TH, Albers D, Blero D, de Ceglie A, Conio M, Czakó L, Everett S, Garcia-Pagán JC, Ginès A, Jovani M, Repici A, Rodrigues-Pinto E, Siersema PD, Fuccio L, van Hooft JE. Esophageal stenting for benign and malignant disease: European Society of Gastrointestinal Endoscopy (ESGE) Guideline - Update 2021. *Endoscopy* 2021; **53**: 751-762 [PMID: 33930932 DOI: 10.1055/a-1475-0063]

7 **Fugazza A**, Lamonaca L, Mercante G, Civilini E, Pradella A, Anderloni A, Repici A. The worst adverse event for an endoscopist after esophageal stent placement: an aortoesophageal fistula. *Endoscopy* 2022; **54**: E44-E45 [PMID: 33682894 DOI: 10.1055/a-1368-3677]

8 **Singla V**, Khare S, Arora A, Kumar A, Sharma P, Bansal N, Anikhindi SA. Use of loop and clips to prevent migration of esophageal stent. *Endoscopy* 2021; **53**: E421-E422 [PMID: 33506470 DOI: 10.1055/a-1326-1143]

9 **Ou Y**, Chen L, Li J, Ye Y, Chen Z, Cai L, Liao J. Endoscopic removal of a migrated esophageal covered self-expandable metal stent: the nylon loop pusher-assisted method. *Endoscopy* 2022; **54**: E744-E745 [PMID: 35299269 DOI: 10.1055/a-1738-9465]

World Journal of Clinical Cases

Submit a Manuscript: https://www.f6publishing.com

World J Clin Cases 2024 May 26; 12(15): 2621-2626

DOI: 10.12998/wjcc.v12.i15.2621

ISSN 2307-8960 (online)

CASE REPORT

Acute upper gastrointestinal bleeding due to portal hypertension in a patient with primary myelofibrosis: A case report

Yu Chen, Bing-Bing Kong, He Yin, Hao Liu, Sheng Wu, Ting Xu

Specialty type: Emergency medicine

Provenance and peer review: Unsolicited article; Externally peer reviewed.

Peer-review model: Single blind

Peer-review report's classification

Scientific Quality: Grade C

Novelty: Grade C

Creativity or Innovation: Grade C

Scientific Significance: Grade C

P-Reviewer: Atta H, United States

Received: January 21, 2024

Revised: February 10, 2024

Accepted: April 7, 2024

Published online: May 26, 2024

Yu Chen, Bing-Bing Kong, He Yin, Sheng Wu, Ting Xu, Department of Emergency, Beijing Tsinghua Changgung Hospital, School of Clinical Medicine, Tsinghua University, Beijing 102218, China

Hao Liu, Department of Pathology, Beijing Tsinghua Changgung Hospital, School of Clinical Medicine, Tsinghua University, Beijing 102218, China

Corresponding author: Ting Xu, MD, Doctor, Department of Emergency, Beijing Tsinghua Changgung Hospital, School of Clinical Medicine, Tsinghua University, No. 168 Litang Road, Changping District, Beijing 102218, China. xta01392@btch.edu.cn

Abstract

BACKGROUND

Acute upper gastrointestinal bleeding is a common medical emergency that has a 10% hospital mortality rate. According to the etiology, this disease can be divided into acute varicose veins and nonvaricose veins. Bleeding from esophageal varices is a life-threatening complication of portal hypertension. Portal hypertension is a clinical syndrome defined as a portal venous pressure that exceeds 10 mmHg. Cirrhosis is the most common cause of portal hypertension, and thrombosis of the portal system not associated with liver cirrhosis is the second most common cause of portal hypertension in the Western world. Primary myeloproliferative disorders are the main cause of portal venous thrombosis, and somatic mutations in the *Janus kinase 2* gene (*JAK2 V617F*) can be found in approximately 90% of polycythemia vera, 50% of essential thrombocyrosis and 50% of primary myelofibrosis.

CASE SUMMARY

We present a rare case of primary myelofibrosis with gastrointestinal bleeding as the primary manifestation that presented as portal-superior-splenic mesenteric vein thrombosis. Peripheral blood tests revealed the presence of the *JAK2 V617F* mutation. Bone marrow biopsy ultimately confirmed the diagnosis of myelofibrosis (MF-2 grade).

CONCLUSION

In patients with acute esophageal variceal bleeding due to portal hypertension and vein thrombosis without cirrhosis, the possibility of myeloproliferative neoplasms should be considered, and the *JAK2* mutation test should be performed.

Key Words: Acute esophageal variceal bleeding; Portal hypertension; Myelofibrosis; *JAK2 V617F* mutation; Case report

Core Tip: Emergency physicians often encounter patients with acute esophageal variceal bleeding and portal vein thrombosis. We hope that this case report can increase the awareness that in patients who present with variceal bleeding without liver cirrhosis, myeloproliferative neoplasms such as myelofibrosis with the *JAK2 V617F* mutant, can be identified and treated early to minimize the consequences and avoid bleeding.

Citation: Chen Y, Kong BB, Yin H, Liu H, Wu S, Xu T. Acute upper gastrointestinal bleeding due to portal hypertension in a patient with primary myelofibrosis: A case report. *World J Clin Cases* 2024; 12(15): 2621-2626
URL: https://www.wjgnet.com/2307-8960/full/v12/i15/2621.htm
DOI: https://dx.doi.org/10.12998/wjcc.v12.i15.2621

INTRODUCTION

Acute esophageal variceal bleeding is a common complication in patients with cirrhotic portal hypertension[1]. However, the most common cause of noncirrhotic portal hypertension is portal and splenic vein thrombosis[2]. Myeloproliferative neoplasms (MPNs), such as polycythemia vera, essential thrombocytosis, myelofibrosis or unclassified myeloproliferative diseases, can predispose patients to splanchnic vein thrombosis.

Myelofibrosis, a myeloproliferative neoplasm, is characterized by stem cell-derived clonal myeloproliferation, bone marrow fibrosis, anemia, massive splenomegaly and extramedullary hematopoiesis. Primary myelofibrosis patients have a relevant and life-threatening risk of thrombosis[3]. According to a meta-analysis, the prevalence of MPN in Budd-Chiari syndrome (BCS) and portal vein thrombosis (PVT) patients are approximately 30%-50% and 15%-30%, respectively[4].

The *JAK2 V617F* mutation is a common gain-of-function mutation leading to the development of MPN. This mutation is present in approximately 50% of patients with primary myelofibrosis and essential thrombocythemia and in nearly all patients with polycythemia vera[5,6]. The *JAK2 V617F* mutation may predispose patients to portal vein thrombosis.

CASE PRESENTATION

Chief complaints

A 69-year-old woman presented to the emergency department with complaints of hematemesis (approximately 100-200 mL of blood), accompanied by chills and hematochezia (approximately 100 mL of blood), transient blurred vision, no acid reflux, and no abdominal pain.

History of present illness

On admission, her consciousness was clear. The patient had a massive upper bleeding episode on the first day, accompanied by tachycardia, tachypnea, cool clammy skin, hypotension and confusion. No signs of chronic liver disease or autoimmune liver disease were identified.

History of past illness

She had a history of hypertension and thrombocythemia 4 years prior.

Personal and family history

The patient had no significant prior family history.

Physical examination

She had a blood pressure of 106/53 mmHg and a heart rate of 86 beats/min upon arrival at the emergency room.

Laboratory examinations

Laboratory data were shown in Table 1.

Imaging examinations

Examinations images were shown in Figure 1.

Table 1 Laboratory data

Examination item	Data
Hematology	
WBC	41.5 × 10^9/L
Hb	148 g/L
Plt	1181 × 10^9/L
NEUT%	87.6%
CRP	2.24 mg/L
Serological test	
Hepatitis B	Negative
Hepatitis C	Negative
Blood chemistry	
ALT	22.3 U/L
D-BIL	4.5 umol/L
ALB	33.2 g/L
BUN	13.1 mmol/L
Cre	95 umol/L
K	6.87 mmol/L
LDH	375 U/L
Ammonia	173.1 umol/L
Autoantibodies	
ANA/AMA-M2	Negative
SLA/LKM-1	Negative
LC-1/anti-gp210	Negative
SP100/SMA	Negative
Coagulation	
PT	15.1 s
APTT	35 s
Fbg	2.26 g/L

WBC: White blood cell; Hb: Hemoglobin; Plt: Platelet; NEUT%: neutrophilic granulocyte percentage; CRP: C-reactive protein; ALT: Alanine aminotransferase; D-BIL: Direct bilirubin; ALB: Albumin; BUN: Blood urea nitrogen; Cre: Creatinine; K: Serum potassium; LDH: Lactate dehydrogenase; ANA: Anti-nuclear antibody; AMA: Anti-mitochondrial antibody; SLA: Soluble liver antigen; LKM-1: Liver-kidney microsomal type 1 antibody; LC-1: Liver cytosol antibody type 1; anti-gp210: Anti-glycoprotein 210; SP100: Anti-sp100 antibodies; SMA: Smooth muscle antibody; PT: Prothrombin time; APTT: Activated partial thromboplastin time; Fbg: Fibrinogen.

FINAL DIAGNOSIS

The final diagnosis of the patient in the present study was primary myelofibrosis with acute esophageal variceal bleeding combined with splanchnic vein thrombosis (SVT).

TREATMENT

The first endoscopic variceal ligation with a rubber band and endoscopic injection sclerotherapy with tissue glue were carried out successfully on the first day after admission. After gastrointestinal bleeding stabilized, the patient was discharged on long-term oral ruxolitinib (10 mg, twice a day) for the treatment of myelofibrosis and hydroxyurea platelet-lowering therapy.

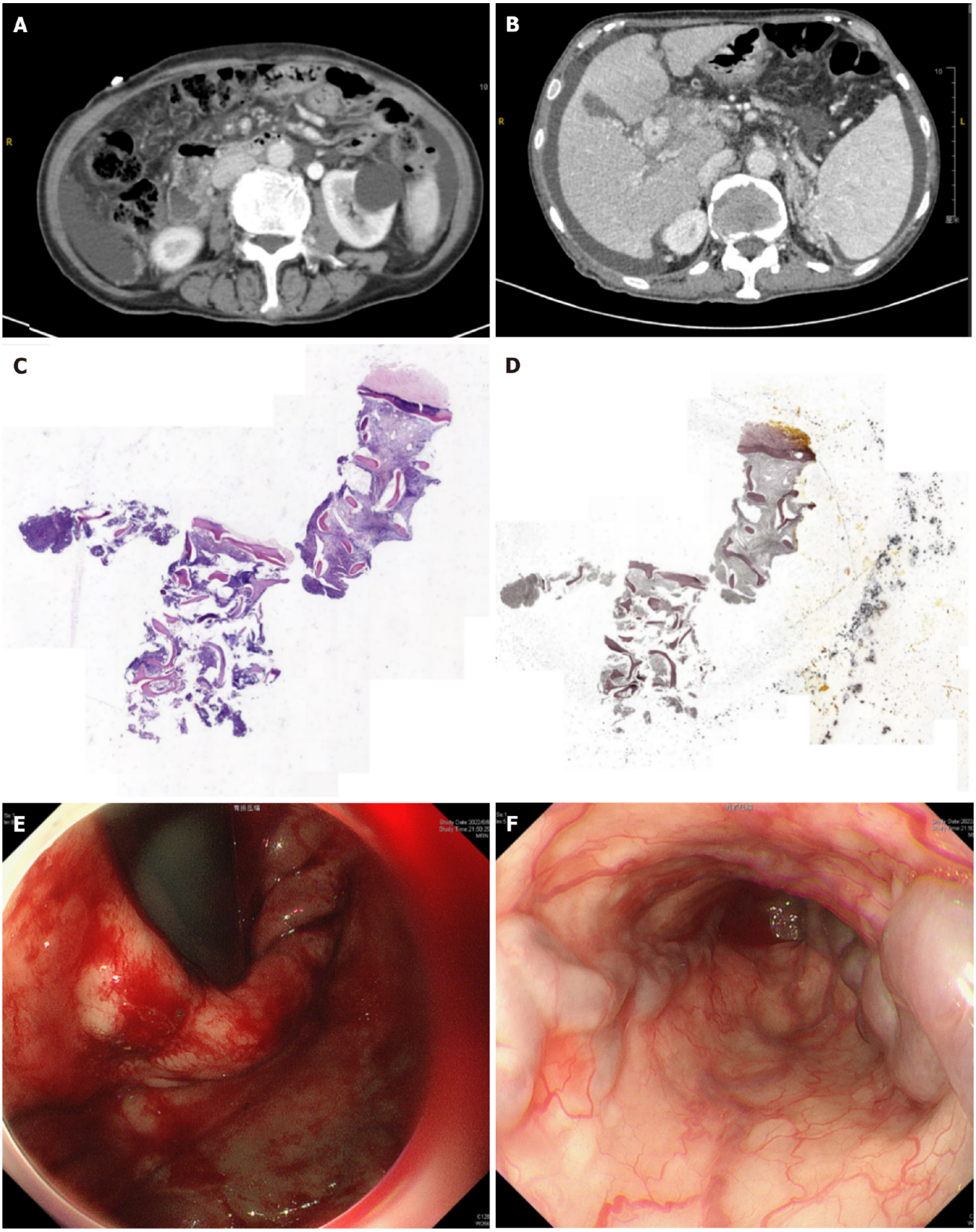

Figure 1 Examinations images. A and B: Contrast-enhanced abdominal computerized tomography image demonstrating extensive splanchnic vein thrombosis involving the portal, splenic, and superior mesenteric veins; C amd D: Bone marrow biopsy revealed that myelofibrosis (MF-2 grade) was accompanied by a significant increase in platelet count; E and F: An emergency endoscopy showed esophagogastric varices (F3CbRc+Les, severe). A white thrombus was detected on the middle of the esophageal varices.

OUTCOME AND FOLLOW-UP

After 4 months, the patient experienced esophageal variceal hemorrhage again, and the emergency endoscopist performed emergency endoscopic esophageal variceal band ligation. At present, the patient has long been a follow-up patient in the Hematology Department of our hospital.

DISCUSSION

Acute esophageal variceal bleeding is a medical emergency associated with high morbidity and mortality and is a serious complication of portal hypertension (PH), usually due to cirrhosis[7]. The most serious complication of portal hypertension is acute variceal bleeding. Endoscopy plays a pivotal role in the diagnosis and risk assessment of bleeding *via* esophageal varices. In adults, cirrhosis accounts for more than 90% of PH patients; nevertheless, the second most common cause is portal vein thrombosis in the Western world[8]. PVT is defined as a partial or complete obstruction of the portal vein by a thrombus resulting in impeded blood flow[9]. PVT is caused by both local (such as malignant tumors, infection, and cirrhosis) and systemic risk factors (myeloproliferative disorders, antiphospholipid syndrome, and paroxysmal nocturnal hemoglobinuria) and is identified in 30% and 70%, respectively[10]. Overall, patients with PVT, which has an incidence of 30% to 40%, are affected by chronic myeloproliferative diseases, usually polycythemia vera, essential thrombocytosis, myelofibrosis or unclassified myeloproliferative diseases[11]. Myelofibrosis is characterized by stem cell-derived clonal myeloproliferation, bone marrow fibrosis, anemia, splenomegaly, and extramedullary hematopoiesis[12,13]. In a retrospective study involving 181 patients, primary myelofibrosis (n = 47), essential thrombocythaemia (n = 67) or polycythaemia vera (n = 67) were identified, and SVT was the primary clinical manifestation. PVT and BCS were found in 60.3% and 17.1%, respectively; correspondingly, thrombosis of the mesenteric or splenic veins was diagnosed in 10% and 13%, respectively[12]. We present a rare case of primary myelofibrosis with gastrointestinal bleeding as the primary manifestation that presented as portal-superior-splenic mesenteric vein thrombosis. Myeloproliferative neoplasms are the most common cause of splanchnic vein thrombosis in the absence of cirrhosis or nearby malignancies. These conditions have a common pathogenesis and are derived from JAK-STAT pathway activation through the presence of the *JAK2* gene calreticulin. *JAK2 V617F*-positive myeloproliferative disorders are a less common etiology of abdominal vein thrombosis. Approximately 90% of polycythemia vera strains are positive for the *V617F* mutant JAK2 protein, and 50% of these patients have primary myelofibrosis and essential thrombocytosis[14]. The presence of the *JAK2 V617F* mutation facilitates the formation of thrombosis. *JAK2 V617F* can increase megakaryocyte ploidy and mobility and platelet aggregation, leading to increased thrombotic formation[15]. Therefore, *JAK2 V617F* can be a prognostic indicator of vein thrombosis in patients with myeloproliferative disorders. Ruxolitinib is a selective inhibitor of Janus kinase (JAK)1/JAK2 approved by the European Medicines Agency for the treatment of intermediate- and high-risk myelofibrosis[16]. JAKs play a critical role in the pathogenesis of inflammatory and hematopoietic cytokines and immune-mediated disorders, such as through the inhibition of interleukin-6 signaling and the proliferation of *JAK2 V617F*-positive Ba/F3 cells[17,18]. According to the results of clinical studies, 59% of patients in the ruxolitinib subgroup had a ≥ 35% reduction in the spleen volume in patients with myelofibrosis-related splenomegaly, and ruxolitinib was effective in patients with and without the *JAK2 V617F* mutation[19,20]. After we added ruxolitinib, extramedullary hematopoiesis was suppressed, and the number of white blood cells decreased gradually.

CONCLUSION

When patients with acute esophageal variceal bleeding and PVT are observed in the Emergency Department, multiple concurrent risk factors for thrombosis, such as *JAK2*-related SVT, should be checked for in all patients without advanced cirrhosis or cancer. Thrombosis of the portal vein, splenic vein and superior mesenteric vein may be the initial manifestation of primary myelofibrosis, even in the early stages of the disease. The presence of the *JAK2* mutation is a crucial prothrombotic risk factor that can contribute to large venous thrombosis.

ACKNOWLEDGEMENTS

We would like to thank the patient. We extend our thanks to the Gastroenterology, Radiology, and Pathology Departments of the Beijing Tsinghua Changgung Hospital for facilitating the acquisition of the relevant materials.

FOOTNOTES

Author contributions: Chen Y and Xu T designed the research; Wu S and Xu T performed the research; Liu H contributed new analytic tools; Kong BB and Yin H analyzed the data; Chen Y and Xu T wrote the paper.

Informed consent statement: All study participants provided informed written consent prior to study enrollment.

Conflict-of-interest statement: We declare that we have no financial and personal relationships with other people ororganizations that can inappropriately influence our work, there is no professional or other personal interest of anynature or kind in any product, service and/or company that could be construed as influencing the position presentedin, or the review of, the manuscript entitled.

CARE Checklist (2016) statement: The authors have read the CARE Checklist (2016), and the manuscript was prepared and revised according to the CARE Checklist (2016).

Country/Territory of origin: China

ORCID number: Yu Chen 0000-0001-6238-6007; Bing-Bing Kong 0009-0007-6762-436X; He Yin 0009-0002-9831-5010; Sheng Wu 0000-0003-0362-9894; Ting Xu 0009-0003-9308-4417.

S-Editor: Che XX
L-Editor: A
P-Editor: Zhang XD

REFERENCES

1 Acute upper gastrointestinal bleeding in over 16s: management. London: National Institute for Health and Care Excellence (NICE); 2016 Aug- [PMID: 32186836]
2 **Valla DC**, Condat B, Lebrec D. Spectrum of portal vein thrombosis in the West. *J Gastroenterol Hepatol* 2002; **17** Suppl 3: S224-S227 [PMID: 12472940 DOI: 10.1046/j.1440-1746.17.s3.4.x]
3 **Barbui T**, Ghirardi A, Carobbio A, Masciulli A, Carioli G, Rambaldi A, Finazzi MC, Bellini M, Rumi E, Vanni D, Borsani O, Passamonti F, Mora B, Brociner M, Guglielmelli P, Paoli C, Alvarez-Larran A, Triguero A, Garrote M, Pettersson H, Andréasson B, Barosi G, Vannucchi AM. Increased risk of thrombosis in JAK2 V617F-positive patients with primary myelofibrosis and interaction of the mutation with the IPSS score. *Blood Cancer J* 2022; **12**: 156 [PMID: 36385103 DOI: 10.1038/s41408-022-00743-0]
4 **Smalberg JH**, Arends LR, Valla DC, Kiladjian JJ, Janssen HL, Leebeek FW. Myeloproliferative neoplasms in Budd-Chiari syndrome and portal vein thrombosis: a meta-analysis. *Blood* 2012; **120**: 4921-4928 [PMID: 23043069 DOI: 10.1182/blood-2011-09-376517]
5 **Spivak JL**. Narrative review: Thrombocytosis, polycythemia vera, and JAK2 mutations: The phenotypic mimicry of chronic myeloproliferation. *Ann Intern Med* 2010; **152**: 300-306 [PMID: 20194236 DOI: 10.7326/0003-4819-152-5-201003020-00008]
6 **Leebeek FW**, Smalberg JH, Janssen HL. Prothrombotic disorders in abdominal vein thrombosis. *Neth J Med* 2012; **70**: 400-405 [PMID: 23123534]
7 **Zuckerman MJ**, Elhanafi S, Mendoza Ladd A. Endoscopic Treatment of Esophageal Varices. *Clin Liver Dis* 2022; **26**: 21-37 [PMID: 34802661 DOI: 10.1016/j.cld.2021.08.003]
8 **Turco L**, Garcia-Tsao G. Portal Hypertension: Pathogenesis and Diagnosis. *Clin Liver Dis* 2019; **23**: 573-587 [PMID: 31563212 DOI: 10.1016/j.cld.2019.07.007]
9 **Margini C**, Berzigotti A. Portal vein thrombosis: The role of imaging in the clinical setting. *Dig Liver Dis* 2017; **49**: 113-120 [PMID: 27965037 DOI: 10.1016/j.dld.2016.11.013]
10 **Basit SA**, Stone CD, Gish R. Portal vein thrombosis. *Clin Liver Dis* 2015; **19**: 199-221 [PMID: 25454305 DOI: 10.1016/j.cld.2014.09.012]
11 **DeLeve LD**, Valla DC, Garcia-Tsao G. Vascular disorders of the liver. *Hepatology* 2009; **49**: 1729-1764 [DOI: 10.1002/hep.22772]
12 **De Stefano V**, Vannucchi AM, Ruggeri M, Cervantes F, Alvarez-Larrán A, Iurlo A, Randi ML, Pieri L, Rossi E, Guglielmelli P, Betti S, Elli E, Finazzi MC, Finazzi G, Zetterberg E, Vianelli N, Gaidano G, Nichele I, Cattaneo D, Palova M, Ellis MH, Cacciola E, Tieghi A, Hernandez-Boluda JC, Pungolino E, Specchia G, Rapezzi D, Forcina A, Musolino C, Carobbio A, Griesshammer M, Barbui T. Splanchnic vein thrombosis in myeloproliferative neoplasms: risk factors for recurrences in a cohort of 181 patients. *Blood Cancer J* 2016; **6**: e493 [PMID: 27813534 DOI: 10.1038/bcj.2016.103]
13 **Tefferi A**. Primary myelofibrosis: 2012 update on diagnosis, risk stratification, and management. *Am J Hematol* 2011; **86**: 1017-1026 [PMID: 22086865 DOI: 10.1002/ajh.22210]
14 **Koschmieder S**. How I Manage Thrombotic/Thromboembolic Complications in Myeloproliferative Neoplasms. *Hamostaseologie* 2020; **40**: 47-53 [PMID: 32050290 DOI: 10.1055/s-0040-1701474]
15 **Fleischman AG**, Tyner JW. Causal role for JAK2 V617F in thrombosis. *Blood* 2013; **122**: 3705-3706 [PMID: 24288407 DOI: 10.1182/blood-2013-10-531665]
16 **Harrison C**, Kiladjian JJ, Al-Ali HK, Gisslinger H, Waltzman R, Stalbovskaya V, McQuitty M, Hunter DS, Levy R, Knoops L, Cervantes F, Vannucchi AM, Barbui T, Barosi G. JAK inhibition with ruxolitinib versus best available therapy for myelofibrosis. *N Engl J Med* 2012; **366**: 787-798 [PMID: 22375970 DOI: 10.1056/NEJMoa1110556]
17 **Arana Yi C**, Tam CS, Verstovsek S. Efficacy and safety of ruxolitinib in the treatment of patients with myelofibrosis. *Future Oncol* 2015; **11**: 719-733 [PMID: 25757677 DOI: 10.2217/fon.14.272]
18 **Quintás-Cardama A**, Kantarjian H, Cortes J, Verstovsek S. Janus kinase inhibitors for the treatment of myeloproliferative neoplasias and beyond. *Nat Rev Drug Discov* 2011; **10**: 127-140 [PMID: 21283107 DOI: 10.1038/nrd3264]
19 **Verstovsek S**, Gotlib J, Mesa RA, Vannucchi AM, Kiladjian JJ, Cervantes F, Harrison CN, Paquette R, Sun W, Naim A, Langmuir P, Dong T, Gopalakrishna P, Gupta V. Long-term survival in patients treated with ruxolitinib for myelofibrosis: COMFORT-I and -II pooled analyses. *J Hematol Oncol* 2017; **10**: 156 [PMID: 28962635 DOI: 10.1186/s13045-017-0527-7]
20 **Verstovsek S**, Mesa RA, Gotlib J, Levy RS, Gupta V, DiPersio JF, Catalano JV, Deininger M, Miller C, Silver RT, Talpaz M, Winton EF, Harvey JH Jr, Arcasoy MO, Hexner E, Lyons RM, Paquette R, Raza A, Vaddi K, Erickson-Viitanen S, Koumenis IL, Sun W, Sandor V, Kantarjian HM. A double-blind, placebo-controlled trial of ruxolitinib for myelofibrosis. *N Engl J Med* 2012; **366**: 799-807 [PMID: 22375971 DOI: 10.1056/NEJMoa1110557]

World Journal of Clinical Cases

Submit a Manuscript: https://www.f6publishing.com

World J Clin Cases 2024 May 26; 12(15): 2627-2635

DOI: 10.12998/wjcc.v12.i15.2627

ISSN 2307-8960 (online)

CASE REPORT

C634Y mutation in *RET*-induced multiple endocrine neoplasia type 2A: A case report

Hui-Fen Zhang, Shu-Ling Huang, Wen-Li Wang, Yu-Qing Zhou, Jun Jiang, Zhuo-Jin Dai

Specialty type: Medicine, research and experimental

Provenance and peer review: Unsolicited article; Externally peer reviewed.

Peer-review model: Single blind

Peer-review report's classification

Scientific Quality: Grade C
Novelty: Grade C
Creativity or Innovation: Grade B
Scientific Significance: Grade C

P-Reviewer: Saberi S, United States

Received: January 25, 2024
Revised: March 10, 2024
Accepted: April 9, 2024
Published online: May 26, 2024

Hui-Fen Zhang, Shu-Ling Huang, Wen-Li Wang, Yu-Qing Zhou, Department of Endocrinology, Dongguan Hospital of Guangzhou University of Chinese Medicine, Dongguan 523003, Guangdong Province, China

Jun Jiang, Department of Science and Technology Services, Beijing Macro and Micro Test Co., Ltd., Beijing 100318, China

Zhuo-Jin Dai, The First Clinical Medical College, Guangdong Medical University, Zhanjiang 524023, Guangdong Province, China

Corresponding author: Yu-Qing Zhou, MMed, Chief, Professor, Department of Endocrinology, Dongguan Hospital of Guangzhou University of Chinese Medicine, No. 3, Dongcheng Section, Songshanhu Avenue, Dongcheng District, Dongguan 523003, Guangdong Province, China. 1411396541@qq.com

Abstract

BACKGROUND

Multiple endocrine neoplasia type 2 (MEN2) is a rare, autosomal dominant endocrine disease. Currently, the *RET* proto-oncogene is the only gene implicated in MEN2A pathogenesis. Once an *RET* carrier is detected, family members should be screened to enable early detection of medullary thyroid carcinoma, pheochromocytoma, and hyperparatitity. Among these, medullary thyroid carcinoma is the main factor responsible for patient mortality. Accordingly, delineating strategies to inform clinical follow-up and treatment plans based on genes is paramount for clinical practitioners.

CASE SUMMARY

Herein, we present *RET* proto-oncogene mutations, clinical characteristics, and treatment strategies in a family with MEN2A. A family study was conducted on patients diagnosed with MEN2A. DNA was extracted from the peripheral blood of family members, and first-generation exon sequencing of the *RET* proto-oncogene was conducted. The *C634Y* mutation was identified in three family members spanning three generations. Two patients were sequentially diagnosed with pheochromocytomas and bilateral medullary thyroid carcinomas. A 9-year-old child harboring the gene mutation was diagnosed with medullary thyroid carcinoma. Surgical resection of the tumors was performed. All family members were advised to undergo complete genetic testing related to the *C634Y* mutation, and the corresponding treatments administered based on test results and associated clinical guidelines.

CONCLUSION
Advancements in MEN2A research are important for familial management, assessment of medullary thyroid cancer invasive risk, and deciding surgical timing.

Key Words: Multiple endocrine neoplasia type 2A; Mutation; *RET* proto-oncogene; Medullary thyroid carcinoma; Pheochromocytoma; Case report

Core Tip: Gene sequencing was performed on an adult Asian female patient with bilateral pheochromocytoma and thyroid carcinoma. A mutation, characterized by a nucleotide (c.T1901A) and amino acid (p.Cys634Tyr) change, was identified, supporting multiple endocrine neoplasia type 2A development. Genetic screening of family members revealed the patient's father and son are carriers of the mutation. Clinical follow-up direction and treatment plan were guided by genetic testing. The patient and her son were diagnosed with orthotopic medullary thyroid carcinoma, facilitating timely and early detection in the early stage of cancer and potentially improving the survival rate of patients.

Citation: Zhang HF, Huang SL, Wang WL, Zhou YQ, Jiang J, Dai ZJ. *C634Y* mutation in *RET*-induced multiple endocrine neoplasia type 2A: A case report. *World J Clin Cases* 2024; 12(15): 2627-2635
URL: https://www.wjgnet.com/2307-8960/full/v12/i15/2627.htm
DOI: https://dx.doi.org/10.12998/wjcc.v12.i15.2627

INTRODUCTION

Multiple endocrine neoplasia type 2 (MEN2) is a rare, autosomal dominant endocrine disease. It has two distinct subtypes, MEN2A (95%) and MEN2B (5%)[1,2], with an incidence rate of MEN2A 13–24 per 1000000[1,2]. Currently, the *RET* proto-oncogene is the only gene implicated in the pathogenesis of MEN2A. With a clear correlation between the genotype and phenotype, the *RET* proto-oncogene serves as an essential diagnostic tool for MEN2A. Managing patients through *RET* proto-oncogene testing and genetic counseling can not only optimize the prognosis associated with the genotype but also improve the quality of life of the patient's family members.

In this study, we retrospectively analyzed the clinical characteristics and gene mutation status of three generations of a Han Chinese family diagnosed with MEN2A to explore the significance of *RET* mutations and their relevance for clinical diagnosis and treatment and determine their pathological characteristics.

CASE PRESENTATION

Chief complaints

A 30-year-old woman presented to the hospital with recurring headaches, palpitations, and hyperhidrosis.

History of present illness

The patient presented with paroxysmal headache, palpitation, hyperhidrosis, and a blood pressure of 180-165/95-105 mmHg, without obvious inducement 3 months ago. While these symptoms were slightly relieved after rest, they recurred.

History of past illness

No known drug allergy history was noted. The patient had no surgical history.

Personal and family history

The patient experienced menstrual cycles lasting approximately 6 d every 28-30 d. No notable medical conditions in her family history existed, and she had no history of sexually transmitted diseases.

Physical examination

The vital signs were as follows: Temperature of 36.2 °C; respiration of 19 breaths/min; pulse rate of 110 beats/min; and blood pressure of 180/105 mmHg. The patient was alert and oriented, and her vital signs were stable.

Laboratory examinations

Mesonephrinephrine substance (MNS) levels were as follows: 3-methoxytyramine (3-MT) 0.12 nmol/L (< 0.18), methoxy-adrenaline (MN) 4.1 nmol/L↑ (≤ 0.50), and methoxynorepinephrine (NMN) 2.36 nmol/L↑ (≤ 0.90). There were no

observed abnormalities in blood and urine routine, ion levels, liver and kidney functions, tumor markers, blood lipid levels, five parameters of thyroid function, circadian cortisol rhythm, 24-h urinary cortisol level, and adrenocorticotropic hormone level.

Imaging examinations

Bilateral adrenal computed tomography (CT): Bilateral adrenal mass occupying lesions (left diameter approximately 29 mm, right diameter approximately 50 mm with a clear boundary, enhanced scan uneven and significantly enhanced, and lower density necrosis within) (Figure 1A).

Patients

Between 2016 and 2022, a Han Chinese family of three generations and five members with MEN2A were clinically monitored at the Department of Endocrinology, Dongguan TCM Hospital. The family comprised 1 female and 4 male members, ranging in age from 3 to 60 years. This study was approved by the Medical Ethics Committee of Dongguan Hospital of Traditional Chinese Medicine (Approval Number: PJ [2022] 41) and conducted in accordance with the tenets of the Declaration of Helsinki [2013]. Written informed consent for the publication of this report and any accompanying images was obtained from all family members, and legal guardians provided signatures for the children.

Family survey results

Proband IIa was a 30-year-old female who was hospitalized in August 2016 because of persistent dizziness for over 3 months, coupled with hypertension. The patient's blood pressure was consistently in the range of 180-165/95-105 mmHg. The MNS tests revealed the following: 3-MT level 0.12 nmol/L (< 0.18); MN level 4.1 nmol/L↑ (≤ 0.50); and NMN 2.36 nmol/L↑ (≤ 0.90). The results of further testing, including routine blood and urine tests, ion levels, liver and kidney functions, tumor markers, lipid levels, thyroid function, cortisol rhythm, 24-h urinary cortisol level, and adrenocorticotropic hormone level, were within normal ranges. CT of the adrenal glands revealed space-occupying lesions in the form of bilateral adrenal masses (Figure 1A). Surgery was performed to excise the masses, and enterolysis was also performed. Postoperative pathological examination identified the masses as pheochromocytomas. A thyroid B-ultrasound performed on 10 January 2017 revealed the presence of bilateral thyroid nodules (Figure 2A). The patient's calcitonin level was elevated to 29.49 pg/mL↑ (0-9.52). The parathyroid hormone (PTH) level was determined to be 1.97 pmol/L (1.6-6.9) and the corresponding blood calcium level was 2.41 mmol/L (2-2.5). Thyroglobulin (Tg) was 13.587 ng/mL (0-30). An *RET* gene test conducted on February 13, 2017 (MM_020975) revealed a clinically significant mutation characterized by a nucleotide (c. T1901A) and amino acid (p.Cys634Tyr) change, supporting MEN2A diagnosis. Considering the results of the patient's gene mutation, the bilateral thyroid masses were diagnosed as medullary thyroid carcinomas. Consequently, a bilateral total thyroidectomy was performed in April 2017. Pathological examination confirmed bilateral medullary thyroid carcinomas. In 2021, uterine fibroids were identified for which hysterectomy was performed. The pathological examination indicated leiomyoma (uterus).

The proband's father, designated Ia, developed the disease at 60 years of age. He had a medical history of hypertension and diabetes for more than a decade. Upon identification of the *RET* proto-oncogene mutation, adrenal CT in 2018 revealed a right adrenal mass (Figure 1B). The MN and NMN levels were elevated to 4.5 and 2.26 nmol/L↑, respectively, whereas the 3-MT level was 0.1 nmol/L. Patient Ia underwent laparoscopic resection of the right adrenal mass, which was pathologically diagnosed as right pheochromocytoma. Three months after the adrenal surgery, additional screening using thyroid ultrasound revealed bilateral solid nodules within the thyroid (Figure 2B). The calcitonin level was drastically elevated to 972.2 pg/mL↑↑. The patient underwent complete bilateral thyroidectomy accompanied by cervical lymph node resection. Pathological results revealed bilateral medullary thyroid carcinoma with lymph node metastasis (Figure 3). Postoperative follow-up indicated that the dynamic review of MNS, MN, NMN, and calcitonin levels returned to normal levels.

Patients IIc and IId were two younger brothers with no history of hypertension. No suspicious mutations were detected in the *RET* proto-oncogene of these patients and their blood calcium, PTH, calcitonin, thyroid, and parathyroid levels, color Doppler ultrasound, and adrenal CT/color Doppler ultrasound results were all within the normal ranges.

The son of the patient, referred to as IIIa, was found to harbor a mutation in the *RET* proto-oncogene at the age of 3 years and 10 months. No noticeable abnormalities were detected on thyroid or parathyroid color Doppler ultrasonography. Prophylactic total thyroidectomy was suggested; however, the patient's family declined. Upon a 5-year follow-up in 2022, an elevated calcitonin level of 18.93 pg/mL↑ was detected, with a Tg level of 19.6 ng/mL, PTH level of 7.22 pg/mL↓, and calcium level of 1.96 mmol/L↓. Therefore, a bilateral thyroidectomy was performed. Postoperative pathology revealed medullary thyroid carcinoma in the left lobe.

The clinical characteristics of the family are presented in Table 1.

RET gene sequencing results

A *c.T1901A* mutation was identified in the 11th exon of *RET*, resulting in an amino acid change (p.Cys634Tyr) in the protein. This mutation was also detected in Ia, IIa, and IIIa at the same position (Figures 4 and 5, Table 2)

FINAL DIAGNOSIS

Three family members were diagnosed with MEN2 and harbored a *c.T1901A* mutation in the 11th exon of *RET*.

Table 1 Clinical characteristics of the family members

Patient	Age at onset/follow-up	*RET* proto-oncogene mutation	3-MT	MN	NMN	Ct	Ca	PTH	Thyroid and parathyroid color Doppler ultrasound	Adrenal gland examination	Pathological diagnosis
Ia	60 years old	Yes[1]	0.10	4.5↑	2.26↑	972.2↑	2.47	4.13	Bilateral thyroid nodules	Adrenal CT: Right adrenal space-occupying mass	Right PHEO, bilateral MTC with lymph node metastasis
IIa	30 years old	Yes[1]	0.12	4.1↑	2.36↑	29.49↑	2.41	1.97	Bilateral thyroid nodules	Adrenal CT: Bilateral adrenal space-occupying mass	Bilateral PHEO, bilateral MTC
IIc	27 years old	No	N	N	N	N	N	N	N	Color Doppler ultrasound: N	-
IId	24 years old	No	N	N	N	N	N	N	N	Color Doppler ultrasound: N	-
IIIa	9 years old	Yes[1]	-	-	-	18.93	1.96	7.22	N	Color Doppler ultrasound: N	Left MTC

[1]Type of genetic mutation: *p.Cys634Tyr*.
3-MT: 3-methoxytyramine (nmol/L), reference value < 0.18 nmol/L; MN: Metanephrine (nmol/L), reference value ≤ 0.50 nmol/L; N: Normal; NMN: Normetanephrine (nmol/L), reference value ≤ 0.90 nmol/L; Ct: Calcitonin (pg/mL), reference value 0-9.52 pg/mL; Ca: blood calcium (mmol/L), reference value 2-2.5 mmol/L; PTH: Parathyroid hormone (pmol/L), reference value 1.6-6.9 pmol/L; CT: Computed tomography; PHEO: Pheochromocytoma; MTC: Medullary thyroid carcinoma.

Table 2 Genetic sequencing of *RET* (NM_020975)-exon11

Mutation position	Change in nucleic acids	Change in amino acids	RS-ID	Hom/Het
EI1/CDS11	*c.G1901A*	*p.Cys634Tyr*	CM941237	Het

Hom: Homozygous mutation; Het: Heterozygous mutation.

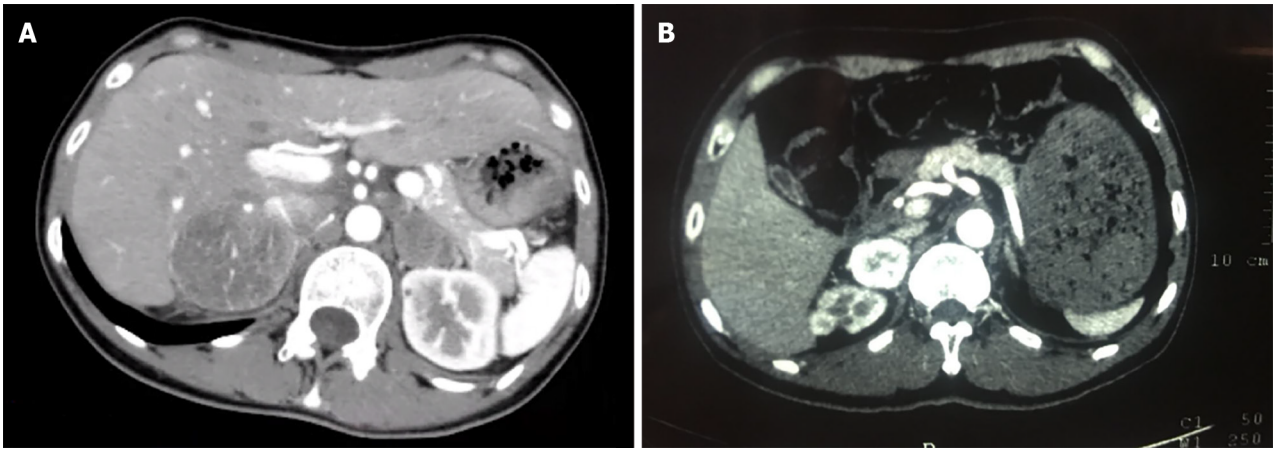

Figure 1 Bilateral adrenal computed tomography scans. A: Contrast-enhanced bilateral adrenal computed tomography scans of proband IIa. Space-occupying lesions of the bilateral adrenal masses were observed; B: Non-contrast enhanced + contrast-enhanced bilateral adrenal computed tomography scans of patient Ib.

TREATMENT

The patient underwent thyroidectomy and was diagnosed with medullary thyroid carcinoma by postoperative pathology.

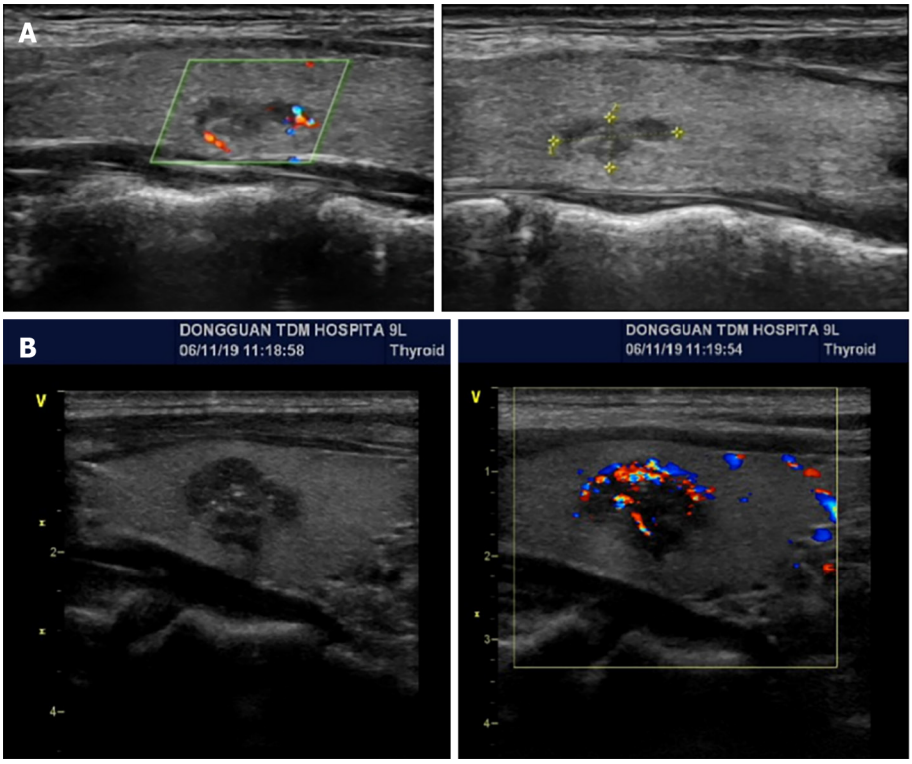

Figure 2 Thyroid B-ultrasound. A: Proband IIa. Bilateral thyroid nodules were observed (10 mm × 4 mm); B: Patient Ib. A hypoechoic nodule (16 mm × 11 mm) was observed in the right thyroid.

OUTCOME AND FOLLOW-UP

The patient's father and his son, who was found to harbor a mutation in the *RET* proto-oncogene, underwent adrenal and thyroid screening. The father was diagnosed with bilateral pheochromocytoma and medullary thyroid carcinoma with metastasis, while the son was diagnosed with medullary thyroid carcinoma.

DISCUSSION

There is a strong correlation between the incidence and prognosis of MEN2A and mutations in the *RET* proto-oncogene. Donis-Keller *et al*[3] were the first to report that mutations in the *RET* proto-oncogene cause MEN2A. Three years later, the International *RET* Mutation Consortium compiled and investigated the clinical and pathological characteristics of *RET* proto-oncogenes in 477 families with MEN2A, MEN2B, and familial medullary thyroid cancer (FMTC) mutations, confirming the pathogenic role of the *RET* proto-oncogene in MEN2 syndrome. Located on 10q11.2, the *RET* proto-oncogene, a tyrosine kinase receptor, comprises 21 exons and approximately 1100 amino acid residues. When *RET* receptors dimerize after binding to the co-receptor (GDNF family receptor alpha), the phosphorylation of intracellular tyrosine residues is triggered, thus playing a role in cell proliferation regulation, cell differentiation, gene expression, and other cellular processes. This cascade can lead to excessive cell proliferation, resulting in carcinogenesis.

To date, over 1000 cases of MEN2A, both sporadic and familial, have been reported globally, with less than 200 cases reported in China, including more than 80 sporadic and 90 familial cases[4-6]. Approximately 95% of patients with classic MEN2A harbor *RET* gene mutations at codons 634, 609, 611, and 618 of exon 11 and codon 620 of exon 10; of these, 85% are located in codon 634 of exon 11[7]. In a comprehensive global review on MEN2-related *RET* pathogenic variants, the pathogenic variants at codon 634 are the most prevalent, found in between 30% and 50% of affected patients; for codon 634 mutations, the relative frequency in China is higher than those found in Brazil, France, Germany, Italy, United Kingdom, Japan, or United States[8].

There are four MEN2A variants: Classic MEN2A, MEN2A with cutaneous lichen amyloidosis, MEN2A with Hirschsprung disease, and MEN2A with FMTC[1,2]. Classic MEN2A is the most common type, manifesting primarily as medullary thyroid cancer (MTC), pheochromocytoma, and hyperparathyroidism[7]. Nearly 100% of patients present with multifocal and bilateral MTC, which is typically the first disorder, usually occurring before 30 years of age[9]. Only 15% of MEN2A cases are symptomatic at the time of diagnosis, and the remaining 85% are identified *via* screening[10].

The occurrence of MEN2A associated with extra-adrenal and malignant pheochromocytomas[11] is rare. Primary hyperparathyroidism may not be prevalent in MEN2A, potentially appearing in as few as 3%-11% of cases[12]. Most cases (56%-88%) are asymptomatic at the time of diagnosis[13], and complications, such as hypercalcemia crisis, are rare. *RET* gene testing is especially crucial for early MEN2A detection, offering predictive diagnosis and treatment for family

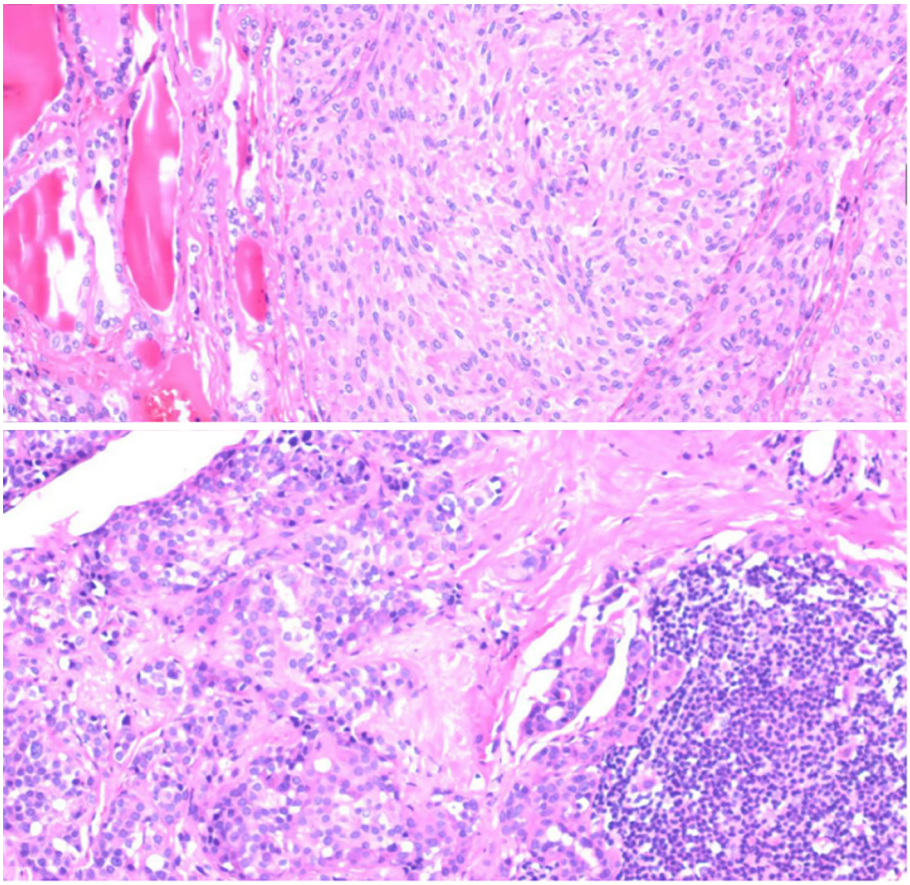

Figure 3 Bilateral thyroid pathology of patient Ib. Medullary thyroid carcinoma was observed.

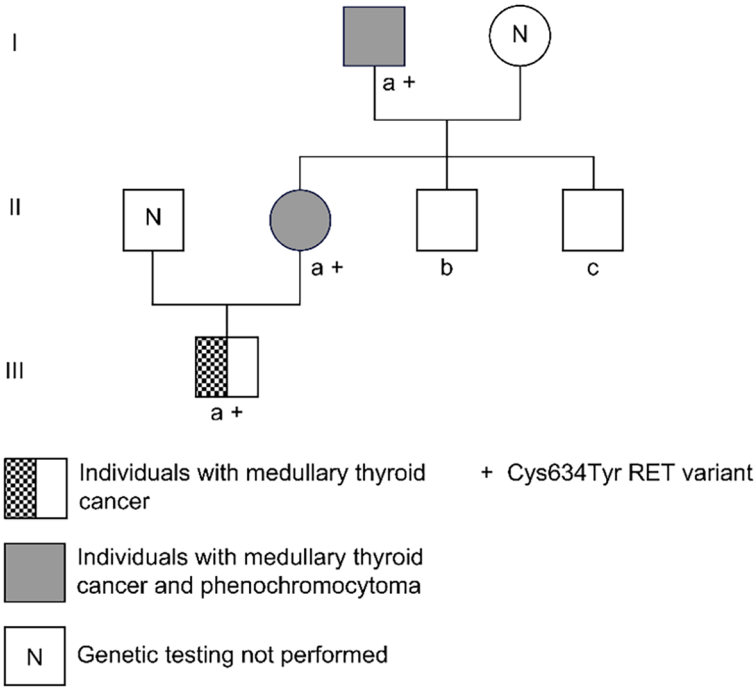

Figure 4 Pedigree chart of the family.

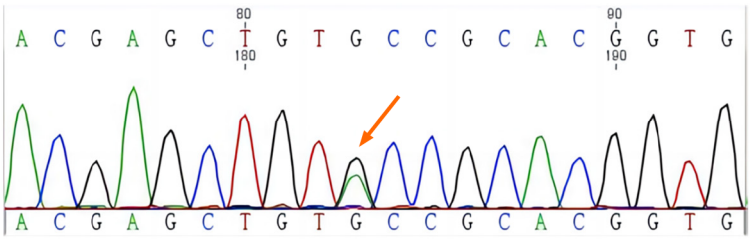

Figure 5 DNA sequencing showing the mutation characterized by a nucleotide (c. T1901A) and an amino acid (p.Cys634Tyr) change in the family members.

members.

Mortality in MEN 2 is primarily attributed to MTC. The 10-year overall survival for patients with MTC has been estimated to be 64%[14]. Guidelines from the American, British, and European Thyroid Associations endorse *RET* analysis for all patients with confirmed MTC. Over 50% of patients with MTC with lymph node involvement experience disease relapse leading to death, which is the primary cause of mortality in patients with MEN2A[15]. A large long-term follow-up study demonstrated that prophylactic thyroidectomy in patients with MEN2A harboring the *C634Y* mutation enables disease cure without inducing any long-term complications[16]. Therefore, the prognosis of MEN2A primarily depends on the status of MTC. Currently, surgery is the only effective treatment for MTC. Prophylactic thyroidectomy in patients with early asymptomatic MEN2A is crucial to prevent carcinogenesis and its complications and improve survival rates.

When considering prophylactic thyroidectomy, the focus is on the *RET* mutation type, age, and calcitonin level. The American Thyroid Association classifies *RET* mutations into three categories based on the invasive risk of MTC: Medium, high, and extremely high. The more invasive the tumor, the earlier the prophylactic thyroidectomy should be performed and the larger the range of the thyroid necessitating surgical removal. Based on this categorization, different surgical indications have been proposed for patient treatment depending on the risk level[7,17]. The classic MEN2A 634 chromosomal mutation is a high-risk mutation; high-risk mutations transition from normal to C-cell hyperplasia within an average of 5 years, and to MTC N0 and MTC N1 within 19 and 31 years, respectively[18]. Prophylactic thyroidectomy is recommended before the age of 5 years. However, clinicians must carefully weigh the risk of surgical complications in children, increased recurrence rates during lymph node dissection, and the probability of cure[19,20]. Monitoring calcitonin level is another crucial evaluation standard. A French study of 170 young patients aged < 21 years confirmed the major role of calcitonin testing in prophylactic thyroidectomies, indicating that all preoperative patients with calcitonin levels < 30 pg/mL, regardless of whether their MTC was classified as extremely high-, high-, or medium-risk, were cured after thyroidectomy[21].

Raue and Frank-Raue[22] suggested a three-point management strategy for patients with MEN2: (1) Confirm the pathogenic *RET* gene mutation type; (2) classify MTC risk groups; and (3) determine preoperative calcitonin levels to ensure that asymptomatic carriers undergo timely MTC removal. Both high- and moderate-risk groups could determine the timing of surgery based on calcitonin level[21-24]. Once the calcitonin levels surpass the upper limit of normal level, surgery can be performed. This approach may postpone thyroidectomy until the patient reaches full growth, thereby reducing surgical complications, such as permanent hypoparathyroidism and recurrent laryngeal nerve injury, and preventing overtreatment.

In the family with MEN2A discussed in this study, three members harbored a heterozygous mutation of nucleotide c.T1901A, which caused the 634th amino acid of the encoded protein to mutate from cysteine to tyrosine. Among the mutations in codon 634, the *C634Y* mutation is uncommon and may present a more indolent clinical course. In this family with the high-risk *C634Y* mutation, proband IIa first presented with pheochromocytoma. Given the patient's age of 30 years, the atypical presentation of calcitonin levels, and color Doppler ultrasound findings, a thyroidectomy was performed. Postoperative pathological examination confirmed the presence of MTC without lymph node metastasis. A 5-year follow-up revealed normal calcitonin levels and thyroid color Doppler ultrasound findings, with no signs of recurrence. Regular follow-ups with abdominal CT and MN levels were also normal, with no pheochromocytoma or pheochromocytic tissue, suggesting a benign pheochromocytoma. The proband's father, who had a history of hypertension and did not participate in regular health examinations, was found to have an *RET* gene *C634Y* mutation through genetic testing. This finding led to surgical intervention for the pheochromocytoma and MTC, both of which were pathologically confirmed. However, owing to the advanced age at which testing was conducted, the MTC had already metastasized to the lymph nodes, necessitating stringent monitoring of calcitonin levels to prevent recurrence. The gene mutation carrier IIIa harbors a high-risk mutation. According to the guidelines, total thyroidectomy can be performed before the age of 5 years; however, given the child's growth and developmental needs, along with relatively higher surgical risks, and in accordance with the family's wishes, we opted to closely monitor calcitonin level and thyroid color Doppler ultrasound. After 5 years of follow-up, an increase in calcitonin level was detected when the child turned 9 years old, necessitating a prophylactic thyroidectomy. Subsequent pathological examination confirmed the presence of MTC.

The thyroid conditions of the three aforementioned patients were managed in accordance with the American Thyroid Association guidelines, considering the genotype–phenotype relationship of MEN2A, which effectively guided clinical diagnosis and treatment. At the time of diagnosis of the disease in the proband, she was diagnosed with bilateral

pheochromocytomas, whereas her father had a unilateral pheochromocytoma. These findings align with previous reports on MEN2A pheochromocytomas, which can be either unilateral or bilateral, with rare malignancies. None of the three patients exhibited signs of hyperparathyroidism, thereby necessitating long-term monitoring of blood calcium and PTH levels and parathyroid color Doppler ultrasonography.

In this report, we highlight that gene detection in three generations of a family can be used for early screening of related diseases, especially for the diagnosis and treatment of early medullary thyroid cancer. However, owing to the limited number of patients, there are certain limitations, and it will be more meaningful to screen the genes and related diseases in Ia parents and siblings.

CONCLUSION

In summary, *RET* proto-oncogene mutations play crucial roles in determining the clinical phenotype and prognosis of patients with MEN2A. In a clinical setting, advancements in genetic research on MEN2A can be leveraged for familial management; assess the invasive risk of MTC based on *RET* gene mutation types, age, and calcitonin levels; and decide the timing of surgery. This study offers considerable guidance regarding the onset, progression, and prognosis of pheochromocytoma and hyperparathyroidism.

ACKNOWLEDGEMENTS

We thank the doctors and nurses at the Department of Endocrinology, Guangzhou University of Chinese Medicine, Dongguan TCM Hospital for their help in this study. We express gratitude to our partner, Beijing Hongwei Testing Co., Ltd, for their excellent cooperation and technical support.

FOOTNOTES

Author contributions: Zhang HF and Huang SL wrote the original draft; Zhang HF, Huang SL, Wang WL, Jiang J, and Dai ZJ reviewed and edited the manuscript; Zhou YQ contributed to the methodology and supervision; All authors read and approved the final manuscript.

Supported by The Finance Bureau of Dongguan City, Guangdong Province.

Informed consent statement: All study participants, or their legal guardians, provided informed written consent prior to study enrollment.

Conflict-of-interest statement: The authors declare that they have no conflict of interest to disclose.

CARE Checklist (2016) statement: The authors have read the CARE Checklist (2016), and the manuscript was prepared and revised according to the CARE Checklist (2016).

Country/Territory of origin: China

ORCID number: Hui-Fen Zhang 0009-0009-9103-4129; Shu-Ling Huang 0000-0002-6082-0014; Wen-Li Wang 0009-0008-5446-2813; Yu-Qing Zhou 0000-0002-2011-6372; Jun Jiang 0000-0002-7119-2682; Zhuo-Jin Dai 0000-0003-1047-2549.

S-Editor: Che XX
L-Editor: A
P-Editor: Yu HG

REFERENCES

1 **Mathiesen JS**, Kroustrup JP, Vestergaard P, Madsen M, Stochholm K, Poulsen PL, Krogh Rasmussen Å, Feldt-Rasmussen U, Schytte S, Pedersen HB, Hahn CH, Bentzen J, Gaustadnes M, Ørntoft TF, Hansen TVO, Nielsen FC, Brixen K, Frederiksen AL, Godballe C. Incidence and prevalence of multiple endocrine neoplasia 2B in Denmark: a nationwide study. *Endocr Relat Cancer* 2017; **24**: L39-L42 [PMID: 28438782 DOI: 10.1530/ERC-17-0122]

2 **Mathiesen JS**, Kroustrup JP, Vestergaard P, Stochholm K, Poulsen PL, Rasmussen ÅK, Feldt-Rasmussen U, Schytte S, Pedersen HB, Hahn CH, Bentzen J, Möller S, Gaustadnes M, Rossing M, Nielsen FC, Brixen K, Frederiksen AL, Godballe C. Incidence and prevalence of multiple

endocrine neoplasia 2A in Denmark 1901-2014: a nationwide study. *Clin Epidemiol* 2018; **10**: 1479-1487 [PMID: 30349395 DOI: 10.2147/CLEP.S174606]

3 **Donis-Keller H**, Dou S, Chi D, Carlson KM, Toshima K, Lairmore TC, Howe JR, Moley JF, Goodfellow P, Wells SA Jr. Mutations in the RET proto-oncogene are associated with MEN 2A and FMTC. *Hum Mol Genet* 1993; **2**: 851-856 [PMID: 8103403 DOI: 10.1093/hmg/2.7.851]

4 **Chen L**, Zhang JX, Liu DG, Liu HG. A Familial Case of Multiple Endocrine Neoplasia 2A: From Morphology to Genetic Alterations Penetration in Three Generations of a Family. *Diagnostics (Basel)* 2023; **13**: 955 [PMID: 36900098 DOI: 10.3390/diagnostics13050955]

5 **Lu F**, Chen X, Bai Y, Feng Y, Wu J. A large Chinese pedigree of multiple endocrine neoplasia type 2A with a novel C634Y/D707E germline mutation in RET exon 11. *Oncol Lett* 2017; **14**: 3552-3558 [PMID: 28943896 DOI: 10.3892/ol.2017.6583]

6 **Du ZF**, Li PF, Zhao JQ, Cao ZL, Li F, Ma JM, Qi XP. Genetic diagnosis of a Chinese multiple endocrine neoplasia type 2A family through whole genome sequencing. *J Biosci* 2017; **42**: 209-218 [PMID: 28569245 DOI: 10.1007/s12038-017-9686-5]

7 **Wells SA Jr**, Asa SL, Dralle H, Elisei R, Evans DB, Gagel RF, Lee N, Machens A, Moley JF, Pacini F, Raue F, Frank-Raue K, Robinson B, Rosenthal MS, Santoro M, Schlumberger M, Shah M, Waguespack SG; American Thyroid Association Guidelines Task Force on Medullary Thyroid Carcinoma. Revised American Thyroid Association guidelines for the management of medullary thyroid carcinoma. *Thyroid* 2015; **25**: 567-610 [PMID: 25810047 DOI: 10.1089/thy.2014.0335]

8 **Maciel RMB**, Maia AL. GLOBAL ENDOCRINOLOGY: Geographical variation in the profile of RET variants in patients with medullary thyroid cancer: a comprehensive review. *Eur J Endocrinol* 2021; **186**: R15-R30 [PMID: 34757920 DOI: 10.1530/EJE-21-0753]

9 **Elisei R**, Romei C. Looking for RET alterations in thyroid cancer: clinical relevance, methodology and timing. *Endocrine* 2023; **81**: 206-215 [PMID: 37195581 DOI: 10.1007/s12020-023-03368-w]

10 **Mathiesen JS**, Kroustrup JP, Vestergaard P, Stochholm K, Poulsen PL, Rasmussen ÅK, Feldt-Rasmussen U, Schytte S, Londero SC, Pedersen HB, Hahn CH, Bentzen J, Möller S, Gaustadnes M, Rossing M, Nielsen FC, Brixen K, Frederiksen AL, Godballe C. Survival and Long-Term Biochemical Cure in Medullary Thyroid Carcinoma in Denmark 1997-2014: A Nationwide Study. *Thyroid* 2019; **29**: 368-377 [PMID: 30618340 DOI: 10.1089/thy.2018.0564]

11 **Mucha L**, Leidig-Bruckner G, Frank-Raue K, Bruckner T, Kroiss M, Raue F; German study group for rare thyroid cancer. Phaeochromocytoma in multiple endocrine neoplasia type 2: RET codon-specific penetrance and changes in management during the last four decades. *Clin Endocrinol (Oxf)* 2017; **87**: 320-326 [PMID: 28605116 DOI: 10.1111/cen.13386]

12 **Machens A**, Elwerr M, Lorenz K, Weber F, Dralle H. 100-Year evolution of precision medicine and surgery for multiple endocrine neoplasia type 2A. *Endocrine* 2020; **68**: 368-376 [PMID: 32100189 DOI: 10.1007/s12020-020-02232-5]

13 **Twigt BA**, Scholten A, Valk GD, Rinkes IH, Vriens MR. Differences between sporadic and MEN related primary hyperparathyroidism; clinical expression, preoperative workup, operative strategy and follow-up. *Orphanet J Rare Dis* 2013; **8**: 50 [PMID: 23547958 DOI: 10.1186/1750-1172-8-50]

14 **Mathiesen JS**, Effraimidis G, Rossing M, Rasmussen ÅK, Hoejberg L, Bastholt L, Godballe C, Oturai P, Feldt-Rasmussen U. Multiple endocrine neoplasia type 2: A review. *Semin Cancer Biol* 2022; **79**: 163-179 [PMID: 33812987 DOI: 10.1016/j.semcancer.2021.03.035]

15 **American Thyroid Association Guidelines Task Force**; Kloos RT, Eng C, Evans DB, Francis GL, Gagel RF, Gharib H, Moley JF, Pacini F, Ringel MD, Schlumberger M, Wells SA Jr. Medullary thyroid cancer: management guidelines of the American Thyroid Association. *Thyroid* 2009; **19**: 565-612 [PMID: 19469690 DOI: 10.1089/thy.2008.0403]

16 **Febrero B**, Rodríguez JM, Ríos A, Segura P, Pérez-Sánchez B, Torregrosa N, Hernández AM, Parrilla P. Prophylactic thyroidectomy in multiple endocrine neoplasia 2 (MEN2) patients with the C634Y mutation: A long-term follow-up in a large single-center cohort. *Eur J Surg Oncol* 2019; **45**: 625-630 [PMID: 30366876 DOI: 10.1016/j.ejso.2018.09.002]

17 **Wells SA Jr**, Pacini F, Robinson BG, Santoro M. Multiple endocrine neoplasia type 2 and familial medullary thyroid carcinoma: an update. *J Clin Endocrinol Metab* 2013; **98**: 3149-3164 [PMID: 23744408 DOI: 10.1210/jc.2013-1204]

18 **Machens A**, Lorenz K, Weber F, Dralle H. Genotype-specific progression of hereditary medullary thyroid cancer. *Hum Mutat* 2018; **39**: 860-869 [PMID: 29656518 DOI: 10.1002/humu.23430]

19 **Kluijfhout WP**, van Beek DJ, Verrijn Stuart AA, Lodewijk L, Valk GD, van der Zee DC, Vriens MR, Borel Rinkes IHM. Postoperative Complications After Prophylactic Thyroidectomy for Very Young Patients With Multiple Endocrine Neoplasia Type 2: Retrospective Cohort Analysis. *Medicine (Baltimore)* 2015; **94**: e1108 [PMID: 26200612 DOI: 10.1097/MD.0000000000001108]

20 **Machens A**, Dralle H. Advances in risk-oriented surgery for multiple endocrine neoplasia type 2. *Endocr Relat Cancer* 2018; **25**: T41-T52 [PMID: 28883084 DOI: 10.1530/ERC-17-0202]

21 **Rohmer V**, Vidal-Trecan G, Bourdelot A, Niccoli P, Murat A, Wemeau JL, Borson-Chazot F, Schvartz C, Tabarin A, Chabre O, Chabrier G, Caron P, Rodien P, Schlumberger M, Baudin E; Groupe Français des Tumeurs Endocrines. Prognostic factors of disease-free survival after thyroidectomy in 170 young patients with a RET germline mutation: a multicenter study of the Groupe Francais d'Etude des Tumeurs Endocrines. *J Clin Endocrinol Metab* 2011; **96**: E509-E518 [PMID: 21190982 DOI: 10.1210/jc.2010-1234]

22 **Raue F**, Frank-Raue K. Update on Multiple Endocrine Neoplasia Type 2: Focus on Medullary Thyroid Carcinoma. *J Endocr Soc* 2018; **2**: 933-943 [PMID: 30087948 DOI: 10.1210/js.2018-00178]

23 **Lifante JC**, Blanchard C, Mirallié E, David A, Peix JL. Role of preoperative basal calcitonin levels in the timing of prophylactic thyroidectomy in patients with germline RET mutations. *World J Surg* 2014; **38**: 576-581 [PMID: 24357249 DOI: 10.1007/s00268-013-2413-y]

24 **Zhang X**, Yan D, Wang J, Wan H, Zhang Y, He Y, Liu W, Zhang B. Is new American Thyroid Association risk classification for hereditary medullary thyroid carcinoma applicable to Chinese patients? A single-center study. *Chin J Cancer Res* 2017; **29**: 223-230 [PMID: 28729773 DOI: 10.21147/j.issn.1000-9604.2017.03.08]

World Journal of Clinical Cases

Submit a Manuscript: https://www.f6publishing.com

World J Clin Cases 2024 May 26; 12(15): 2636-2641

DOI: 10.12998/wjcc.v12.i15.2636

ISSN 2307-8960 (online)

CASE REPORT

Role of savolitinib in advanced gastric adenocarcinoma with meningeal carcinomatosis and cerebellar metastasis: A case report

Zhi-Yun Weng, Wen-Ye Huang, Bin-Kan Shi, Jian-Jia Pan

Specialty type: Medicine, research and experimental

Provenance and peer review: Unsolicited article; Externally peer reviewed.

Peer-review model: Single blind

Peer-review report's classification

Scientific Quality: Grade C, Grade C, Grade C

Novelty: Grade A, Grade B, Grade C

Creativity or Innovation: Grade A, Grade B, Grade C

Scientific Significance: Grade B, Grade B, Grade C

P-Reviewer: Adam CA, Romania; Haddadi S, Algeria

Received: January 30, 2024

Revised: February 14, 2024

Accepted: April 7, 2024

Published online: May 26, 2024

Zhi-Yun Weng, Wen-Ye Huang, Bin-Kan Shi, Jian-Jia Pan, Department of Hematology, The Affiliated Yueqing Hospital of Wenzhou Medical University, Yueqing 325600, Zhejiang Province, China

Co-first authors: Zhi-Yun Weng and Wen-Ye Huang.

Corresponding author: Zhi-Yun Weng, PhD, Chief Doctor, Department of Hematology, The Affiliated Yueqing Hospital of Wenzhou Medical University, No. 338 Qingyuan Road, Yueqing 325600, Zhejiang Province, China. weng_zhi_yun@163.com

Abstract

BACKGROUND

Brain metastases (BM) are very rare in gastric adenocarcinoma (GaC), and patients with BMs have a higher mortality rate due to stronger tumor aggressiveness. However, its pathogenesis remains unclear. Genetic testing revealed cellular-mesenchymal epithelial transition factor receptor (MET) amplification. Therefore, treatment with savolitinib, a small molecule inhibitor of c-Met, was selected.

CASE SUMMARY

A 66-year-old woman was diagnosed with advanced GaC 6 months prior to presentation due to back pain. Cerebellar and meningeal metastases were observed during candonilimab combined with oxaliplatin and capecitabine therapy. The patient experienced frequent generalized seizures and persistent drowsiness in the emergency department. Genetic testing of cerebrospinal fluid and peripheral blood revealed increased MET amplification. After discussing treatment options with the patient, savolitinib tablets were administered. After a month of treatment, the intracranial lesions shrank considerably.

CONCLUSION

BM is very rare in advanced GaC, especially in meningeal cancer, that is characterized by rapid disease deterioration. There are very few effective treatment options available; however, technological breakthroughs in genomics have provided a basis for personalized treatment. Furthermore, MET amplification may be a key driver of BM in gastric cancer; however, this conclusion requires further investigation.

Key Words: Cellular-mesenchymal epithelial transition factor receptor; Savolitinib;

Meningeal carcinomatosis; Gastric adenocarcinoma; Case report

Core Tip: Common metastatic sites for gastric adenocarcinoma (GaC) occur in the lymph nodes, liver, and lungs. Additionally, brain metastases (BM) are rare. Interestingly, mesenchymal epithelial transition factor receptor (MET) amplification in GaC is rare, and its role in tumor metastasis remains unclear. Several previous reports have described the association between MET amplification and BM with GaC. This case highlights the unique phenomenon of rapid BM in advanced GaC after first-line treatment and the rapid short-term reduction of cerebellar metastases after the use of savolitinib. Therefore, it is hypothesized that MET amplification may be a key driver of BMs in GaC.

Citation: Weng ZY, Huang WY, Shi BK, Pan JJ. Role of savolitinib in advanced gastric adenocarcinoma with meningeal carcinomatosis and cerebellar metastasis: A case report. *World J Clin Cases* 2024; 12(15): 2636-2641
URL: https://www.wjgnet.com/2307-8960/full/v12/i15/2636.htm
DOI: https://dx.doi.org/10.12998/wjcc.v12.i15.2636

INTRODUCTION

The 2020 Global Cancer Statistics show that gastric cancer ranks fifth in global cancer incidence, with a prevalence of approximately 5.6%[1]. Advanced gastric adenocarcinoma (GaC) is the most predominant pathological type of gastric cancer, and is a multifactorial and heterogeneous disease. Approximately 1/3 of GaC patients have distant metastasis at the time of diagnosis; these patients have higher mortality rates due to stronger tumor aggressiveness[2]. Common metastatic sites of GaC include the peritoneum, lymph nodes, liver, and lungs. However, only 1%-2% of advanced GaC patients develop intracranial metastases and meningeal carcinomatosis (MC)[3].

A patient with advanced GaC harboring mesenchymal epithelial transition factor receptor (MET) amplification, intracranial metastases, and MC treated with savolitinib tablets is presented in this case study. The patient demonstrated rapid shrinkage of intracranial tumors in the short term.

CASE PRESENTATION

Chief complaints

A 66-year-old female presented to the emergency department due to frequent generalized seizures occurring within a week and persistent drowsiness.

History of present illness

In November 2023, the patient developed dizziness, headache, walking instability, tinnitus, and hearing loss. A head magnetic resonance imaging (MRI) indicated meningeal thickening and occupation of the cerebellum and occipital bone. The patient underwent lumbar puncture, which revealed an increase in cerebrospinal fluid (CSF) pressure of > 400 mm H_2O, indicating a rapid disease progression, seizures developed more gradually.

History of past illness

In November 2022, the patient underwent gastroscopy with no abnormality. In May 2023, the patient was treated at another hospital for lumbar pain, and lumbar MRI was performed. Abnormal vertebral signals were considered for tumor metastasis. After further examination by positron emission tomography/computed tomography and gastroscopy, the patient was diagnosed with advanced GaC with multiple metastases to the abdominal lymph nodes and lumbar vertebrae. In June 2023, the patient was treated with the regimen of Candonilimab + oxaliplatin and capecitabine (CAPEOX). After two courses of treatment, the patient showed elevated troponin and aminotransferase levels. Considering the adverse immune reactions, the above drugs were discontinued and gamma globulin and methylprednisolone were administered to suppress the immune system. In September 2023, the patient was administered another two courses of CAPEOX chemotherapy because of disease progression.

Personal and family history

The patient denied any family history of tumors or other notable medical history.

Physical examination

The patient's vital signs were as follows: Body temperature, 38 °C; blood pressure, 170/94 mmHg; heart rate, 95 beats/min; respiratory rate, 18 breaths/min. When receiving treatment, the patient was in a shallow coma, with left conjunctival

congestion, and she demonstrated signs of mydriasis.

Laboratory examinations

Laboratory investigations revealed normocytic anemia (hemoglobin, 66 g/L), elevated leukocyte (14 × 10^9/L), and elevated C-reactive protein (28.48 mg/L). Tumor markers, including carcinoembryonic antigen (56.2 ng/mL) and carbohydrate antigen 199 (139.4 U/mL), were above the reference range. Genetic testing of CSF and peripheral blood revealed an increased MET copy number and genetic mutations at the TP53p.R213 Locus.

Pathological diagnosis

Gastric mucosal pathology: Less differentiated adenocarcinoma, differentiated grades II–III, and mixed type Lauren classification.

The immunohistochemical results of the Gastric mucosal are as follows: Claudin18.2 (40% +); Her-2 (0); Met (90%); MLH (+); MSH2 (+); MSH6 (+); programmed death 1 (tumor-, interstitial 5% +); programmed death-ligand 1 (PD-L1) (tumor-, interstitial 5% +); PMS (+); TROP2 (100% +++); Ki67 (90% +); EBER (-).

Imaging examinations

MRI revealed thickening of the meninges and abnormal diffuse signals in the skull. A mass on the right cerebellar showed mixed-signal intensity. In December 2023 there was a decrease in the lesions, but the top right nodules increased (Figure 1).

FINAL DIAGNOSIS

The GaC invaded the surrounding tissues and caused pelvic implant metastasis accompanied by multiple metastases to the bone, liver, cerebellum, and meninges. The patient was diagnosed with GaC (cT4NxM1 IV) and was comatose at the time of admission.

TREATMENT

Considering the patient's poor health and comatose state with intracranial metastases and MC, the tumor was rapidly transferred after chemotherapy. After discussion, savolitinib tablets were administered to treat this patient.

OUTCOME AND FOLLOW-UP

After 4 d of oral administration of savolitinib, the patient regained autonomous consciousness and her lower limb muscle strength returned to grade IV after 2 wk. After one month of treatment, with the help of her family, she was able to walk normally. During hospitalization, MRI was used to examine the patient's brain, and the results showed that the cerebellar tumor had shrunk significantly, and the CSF pressure had returned to normal levels. After one month of treatment with savolitinib and a small-molecule MET kinase inhibitor, the patient's brain tumor was rapidly controlled in the short term, extending the patient's survival time.

DISCUSSION

Three major biomarkers, namely, HER2, PD-L1, and deficient mismatch repair/microsatellite instability-high group (dMMR/MSI-H), have been identified in advanced GaC to guide the main pathway of treatment decisions, and anti-angiogenesis large and small molecule targeting drugs can also be considered as second-line and above treatment. The accurate understanding of GaC has improved substantially over time, with considerable advancements made in treatment methods using molecule targeting drugs as compared to the era of chemotherapy. Despite this progress, there is still a gap between current clinical practices and ideal outcomes[4-6]. In reality, the proportion of patients with HER2-positive, PD-L1 CPS ≥ 5%, dMMR/MSI-H targets are small, thus they fall into a "high specific, low coverage" population. Although immune checkpoint inhibitors are used regardless of PD-L1 expression levels, their efficacy is limited with "wide coverage and low specificity". Therefore, the examination of biomarkers to screen for beneficial traits and avoid ineffective treatments is required.

The *MET* gene is a proto-oncogene that encodes epithelial-mesenchymal transformation factor (c-Met), a receptor of hepatocyte growth factor. Under physiological conditions, the MET signaling pathway is involved in embryonic development and tissue regeneration, whereas in tumors, activation of the MET pathway can induce tumor occurrence, invasion, and metastasis[7]. Savolitinib is a selective MET inhibitor that prevents MET activation by disrupting the MET signal transduction pathway in an adenosine triphosphate competitive manner, resulting in the inhibition of tumor cell growth[8]. The proportion of MET amplification is low, constituting 4%–6% of GaC[9]. Furthermore, MET amplification includes two forms: primary amplification, defined as the activated MET signal at the time of tumor diagnosis, and

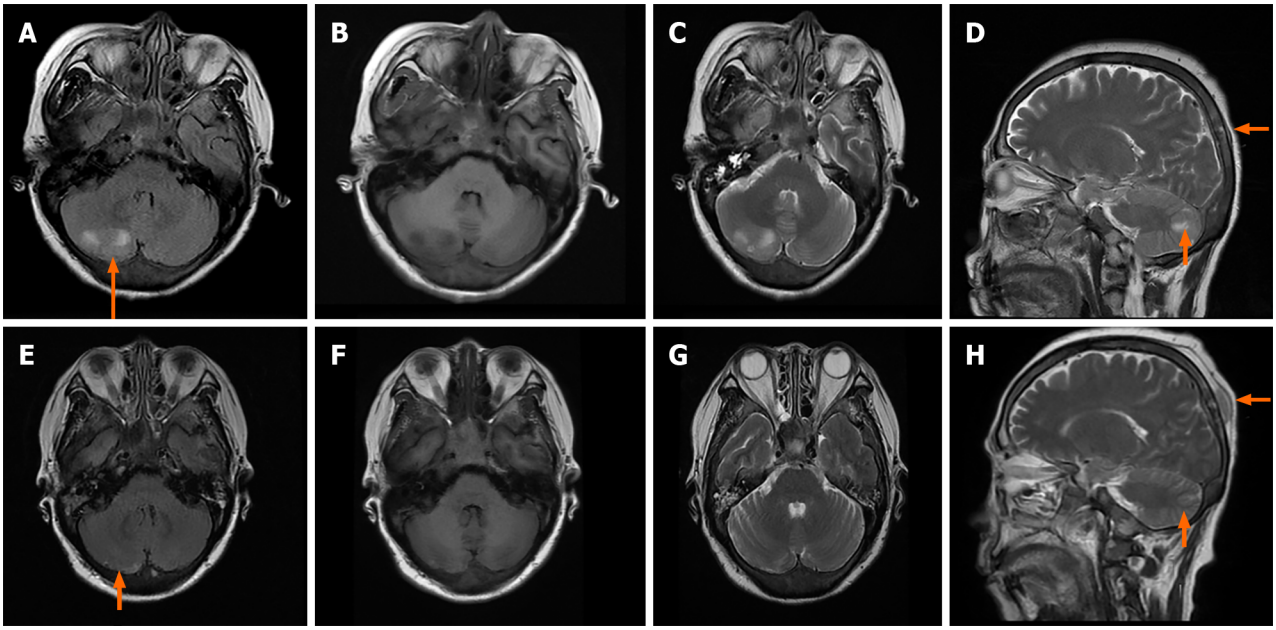

Figure 1 Enhanced magnetic resonance imaging image of a patient with brain metastasis undergoing savolitinib treatment. A: Fluid attenuated inversion recovery image (November 11, 2023); B: T1 image (November 11, 2023); C: T2 image (November 11, 2023); D: Sagittal view of T2 image (November 11, 2023); E: Fluid attenuated inversion recovery image (December 26, 2023); F: T1 image (December 26, 2023); G: T2 image (December 26, 2023); H: Sagittal view of T2 image (December 26, 2023). Orange arrow shows the tumor.

secondary amplification, which refers to MET amplification detected after tumor treatment[10]. Patients with primary amplification have worse prognosis than those with secondary amplification[11]. Notably, GaC with MET amplification often appears more aggressive and advanced in the real world[12,13].

The most interesting aspect of this case was the rare intracranial metastasis and meningeal cancer. Therefore, to determine the factors associated with GaC brain metastases (BM), a comprehensive cohort study was carried out[14]. The results showed that BMs occurred less frequently in patients with antrum/pylorus tumors, and that patients with bone and lung metastases were more likely to develop BMs. However, this phenomenon is rare in liver metastases. In addition, there was a /significant negative correlation between BMs and age. Octogenarians had significantly fewer BMs compared to patients aged 60–69 years. BMs are very rare in GaC, and the clinical data of the 11 patients are summarized in Table 1. A review of these data revealed that the age of these patients was generally higher, mainly related to the target of HER2. Further, 10 of the 11 patients opted for radiation therapy and surgical resection as their treatment choice.

It has been reported that patients with HER2+ GaC may have an increased risk of developing BM; however, the role of MET amplification in BM is unclear[15]. According to the well-known "seed and soil" hypothesis, tumor cells can survive and thrive only after adapting to the brain microenvironment microenvironment[16]. Pericytes, brain microvascular endothelial cells, and astrocytes are the three major components of blood–brain barrier[17]. For cancer cells to grow in the brain, they must acquire two key properties: overcoming the tumor-killing ability of glial cells and altering the brain microenvironment to create a suitable environment for tumor cells to survive. Activation glial cells and altering the brain microenvironment to create a suitable environment for tumor cells to survive. Activation of the c-Met signaling pathway can induce the secretion of interleukin (IL) 8 and CXCL1, which promotes the adhesion of tumor cells to brain endothelial cells and stimulates the formation of micro vessels. In addition, this signaling pathway secretes additional IL1β, causing astrocytes to secrete the ligand hepatocellular growth factor (HGF) of c-MET. This vicious feed-forward c-Met/HGF loop generates a favorable microenvironment for metastatic cells astrocytes to secrete the ligand HGF of c-MET. This vicious feed-forward c-Met/HGF loop generates a favorable microenvironment for metastatic cells[18]. However, this conclusion was reached during a search for breast cancer. In this case, the patient developed BM in the short term and achieved partial remission quickly after administration of savolitinib. Therefore, it is speculated that intracranial tumor subsets may be driven mainly by c-MET amplification.

CONCLUSION

BM are rare in advanced GaC, casing a rapid deterioration in these patients, especially in MC. There are very few effective treatment options available; however, technological breakthroughs in genomics have provided a basis for personalized treatment. Therefore, MET amplification may be a key driver of BMs in gastric cancer; however, this conclusion requires further investigation.

Table 1 Summary of previously published series of cases

Ref.	Case No.	Age/sex	BM	Therapy	Target point	Ending	Survival (month)
Cinar *et al*[19]	1	55/M	+	Gamma-knife; Irinotecan + trastuzumab	HER2	Dead	1
Cinar *et al*[19]	2	60/M	+	Radiotherapy; Trastuzumab + capecitabine + carboplatin; Clinical trial	HER2	Dead	24
Katayanagi *et al*[20]	3	77/M	+	X-knife + surgical resection	Unknown	PR	> 12
Kitayama *et al*[21]	4	76/M	+	Paclitaxel + surgical resection + radiation therapy	Unknown	PR	5
Sakurai *et al*[22]	5	78/F	+	Radiation therapy	Unknown	Dead	4
Rino *et al*[23]	6	63/M	+	Irinotecan + cisplatin + radiation therapy	Unknown	PR	No specified
Rino *et al*[23]	7	78/M	+	Irinotecan + cisplatin + Cyber-knife	Unknown	PR	No specified
Kostoglou *et al*[24]	8	69/F	+	Radiation therapy + surgical resection	HER2	Dead	4
Ahn *et al*[25]	9	38/M	+	Stereotactic radiosurgery + anti-PD-1	Unknown	PR	> 26
Kosco *et al*[26]	10	73/F	+	Radiation therapy + surgical resection + pharmacological intervention	Unknown	CR	> 26
Murakami *et al*[27]	11	65/M	+	Supportive care	Unknown	Dead	1

BM: Brain metastases; PR: Partial response; CR: Complete response; HER2: Human epidermal growth factor receptor 2.

FOOTNOTES

Author contributions: Weng ZY provided direction and guidance throughout the preparation of this manuscript; Huang WY drafted the paper; Shi BK contributed to data analysis; Pan JJ made critical revisions related to important intellectual content of the manuscript; Weng ZY and Huang WY contributed equally to the manuscript; All authors have read and approved the final manuscript.

Informed consent statement: Written consent was obtained from the patient's family to participate in the study.

Conflict-of-interest statement: The authors declare that they have no conflicts of interest to disclose.

CARE Checklist (2016) statement: The authors have read the CARE Checklist (2016), and the manuscript was prepared and revised according to the CARE Checklist (2016).

Country/Territory of origin: China

ORCID number: Zhi-Yun Weng 0000-0002-0914-249X; Wen-Ye Huang 0000-0002-4474-3469; Bin-Kan Shi 0009-0008-4112-8832; Jian-Jia Pan 0009-0006-1937-3597.

S-Editor: Che XX
L-Editor: A
P-Editor: Yu HG

REFERENCES

1 **Sung H**, Ferlay J, Siegel RL, Laversanne M, Soerjomataram I, Jemal A, Bray F. Global Cancer Statistics 2020: GLOBOCAN Estimates of Incidence and Mortality Worldwide for 36 Cancers in 185 Countries. *CA Cancer J Clin* 2021; **71**: 209-249 [PMID: 33538338 DOI: 10.3322/caac.21660]

2 **Huang L**, Jansen L, Balavarca Y, Verhoeven RHA, Ruurda JP, Van Eycken L, De Schutter H, Johansson J, Lindblad M, Johannesen TB, Zadnik V, Žagar T, Mägi M, Bastiaannet E, Lagarde SM, van de Velde CJH, Schrotz-King P, Brenner H. Decreasing resection rates for nonmetastatic gastric cancer in Europe and the United States. *Clin Transl Med* 2020; **10**: e203 [PMID: 33135354 DOI: 10.1002/ctm2.203]

3 **Huang L**, Jansen L, Verhoeven RHA, Ruurda JP, Van Eycken L, De Schutter H, Johansson J, Lindblad M, Johannesen TB, Zadnik V, Žagar T,

Mägi M, Lagarde SM, Bastiaannet E, van de Velde CJH, Schrotz-King P, Brenner H. Largely varying patterns and trends of primary cancer-directed resection for gastric carcinoma with synchronous distant metastasis in Europe and the US: a population-based study calling for further standardization of care. *Ther Adv Med Oncol* 2021; **13**: 17588359211027837 [PMID: 34262618 DOI: 10.1177/17588359211027837]

4 **Muro K**, Chung HC, Shankaran V, Geva R, Catenacci D, Gupta S, Eder JP, Golan T, Le DT, Burtness B, McRee AJ, Lin CC, Pathiraja K, Lunceford J, Emancipator K, Juco J, Koshiji M, Bang YJ. Pembrolizumab for patients with PD-L1-positive advanced gastric cancer (KEYNOTE-012): a multicentre, open-label, phase 1b trial. *Lancet Oncol* 2016; **17**: 717-726 [PMID: 27157491 DOI: 10.1016/S1470-2045(16)00175-3]

5 **Li J**, Qin S, Xu J, Guo W, Xiong J, Bai Y, Sun G, Yang Y, Wang L, Xu N, Cheng Y, Wang Z, Zheng L, Tao M, Zhu X, Ji D, Liu X, Yu H. Apatinib for chemotherapy-refractory advanced metastatic gastric cancer: results from a randomized, placebo-controlled, parallel-arm, phase II trial. *J Clin Oncol* 2013; **31**: 3219-3225 [PMID: 23918952 DOI: 10.1200/JCO.2013.48.8585]

6 **Sampera A**, Sánchez-Martín FJ, Arpí O, Visa L, Iglesias M, Menéndez S, Gaye É, Dalmases A, Clavé S, Gelabert-Baldrich M, Poulsen TT, Kragh M, Bellosillo B, Albanell J, Rovira A, Montagut C. HER-Family Ligands Promote Acquired Resistance to Trastuzumab in Gastric Cancer. *Mol Cancer Ther* 2019; **18**: 2135-2145 [PMID: 31484705 DOI: 10.1158/1535-7163.MCT-19-0455]

7 **de Bono JS**, Yap TA. c-MET: an exciting new target for anticancer therapy. *Ther Adv Med Oncol* 2011; **3**: S3-S5 [PMID: 22128286 DOI: 10.1177/1758834011423402]

8 **Lee TS**, Kim JY, Lee MH, Cho IR, Paik WH, Ryu JK, Kim YT, Lee SH. Savolitinib: A Promising Targeting Agent for Cancer. *Cancers (Basel)* 2023; **15** [PMID: 37835402 DOI: 10.3390/cancers15194708]

9 **Janjigian YY**, Tang LH, Coit DG, Kelsen DP, Francone TD, Weiser MR, Jhanwar SC, Shah MA. MET expression and amplification in patients with localized gastric cancer. *Cancer Epidemiol Biomarkers Prev* 2011; **20**: 1021-1027 [PMID: 21393565 DOI: 10.1158/1055-9965.EPI-10-1080]

10 **Guo R**, Luo J, Chang J, Rekhtman N, Arcila M, Drilon A. MET-dependent solid tumours - molecular diagnosis and targeted therapy. *Nat Rev Clin Oncol* 2020; **17**: 569-587 [PMID: 32514147 DOI: 10.1038/s41571-020-0377-z]

11 **Zhang J**, Guo L, Liu X, Li W, Ying J. MET overexpression, gene amplification and relevant clinicopathological features in gastric adenocarcinoma. *Oncotarget* 2017; **8**: 10264-10273 [PMID: 28052014 DOI: 10.18632/oncotarget.14382]

12 **Peng Z**, Zhu Y, Wang Q, Gao J, Li Y, Ge S, Shen L. Prognostic significance of MET amplification and expression in gastric cancer: a systematic review with meta-analysis. *PLoS One* 2014; **9**: e84502 [PMID: 24416238 DOI: 10.1371/journal.pone.0084502]

13 **Fuse N**, Kuboki Y, Kuwata T, Nishina T, Kadowaki S, Shinozaki E, Machida N, Yuki S, Ooki A, Kajiura S, Kimura T, Yamanaka T, Shitara K, Nagatsuma AK, Yoshino T, Ochiai A, Ohtsu A. Prognostic impact of HER2, EGFR, and c-MET status on overall survival of advanced gastric cancer patients. *Gastric Cancer* 2016; **19**: 183-191 [PMID: 25682441 DOI: 10.1007/s10120-015-0471-6]

14 **Huang L**, Wang L, Shi Y, Zhao Y, Xu C, Zhang J, Hu W. Brain metastasis from gastric adenocarcinoma: A large comprehensive population-based cohort study on risk factors and prognosis. *Front Oncol* 2022; **12**: 897681 [PMID: 36338733 DOI: 10.3389/fonc.2022.897681]

15 **Limon D**, Gal O, Gordon N, Katz L, Perl G, Purim O, Amit L, Stemmer SM, Kundel Y, Ben-Aharon I, Brenner B, Siegal T, Yust-Katz S. Brain metastasis in gastroesophageal adenocarcinoma and HER2 status. *J Neurooncol* 2018; **138**: 315-320 [PMID: 29429124 DOI: 10.1007/s11060-018-2798-4]

16 **Fidler IJ**. The pathogenesis of cancer metastasis: the 'seed and soil' hypothesis revisited. *Nat Rev Cancer* 2003; **3**: 453-458 [PMID: 12778135 DOI: 10.1038/nrc1098]

17 **Abbott NJ**, Rönnbäck L, Hansson E. Astrocyte-endothelial interactions at the blood-brain barrier. *Nat Rev Neurosci* 2006; **7**: 41-53 [PMID: 16371949 DOI: 10.1038/nrn1824]

18 **Xing F**, Liu Y, Sharma S, Wu K, Chan MD, Lo HW, Carpenter RL, Metheny-Barlow LJ, Zhou X, Qasem SA, Pasche B, Watabe K. Activation of the c-Met Pathway Mobilizes an Inflammatory Network in the Brain Microenvironment to Promote Brain Metastasis of Breast Cancer. *Cancer Res* 2016; **76**: 4970-4980 [PMID: 27364556 DOI: 10.1158/0008-5472.CAN-15-3541]

19 **Cinar P**, Calkins SM, Venook AP, Kelley RK. A case series of patients with HER2-overexpressed primary metastatic gastroesophageal adenocarcinoma. *Anticancer Res* 2014; **34**: 7357-7360 [PMID: 25503172]

20 **Katayanagi S**, Arai K, Iwasaki Y, Takahashi K, Yamaguchi T, Matsumoto H, Miyamoto H. [A case of liver metastases from gastric cancer successfully treated with induced hypertensive chemotherapy]. *Gan To Kagaku Ryoho* 2003; **30**: 1722-1725 [PMID: 14619503]

21 **Kitayama Y**, Yoden Y, Okamoto N. [A case of effective paclitaxel therapy for gastric cancer with brain metastasis]. *Gan To Kagaku Ryoho* 2006; **33**: 981-984 [PMID: 16835492]

22 **Sakurai K**, Muguruma K, Murata A, Toyokawa T, Amano R, Kubo N, Tanaka H, Yashiro M, Maeda K, Ohira M, Hirakawa K. Early gastric cancer with suspected brain metastasis arising eight years after curative resection: a case report. *BMC Res Notes* 2014; **7**: 818 [PMID: 25411022 DOI: 10.1186/1756-0500-7-818]

23 **Rino Y**, Sekino Y, Yamada T, Nakayama T, Arai H, Kanari M, Saeki H, Yukawa N, Wada N, Masuda M, Higashida T, Imada T. [Irinotecan+cisplatin and irradiation are effective for brain metastases of gastric cancer--two case reports]. *Gan To Kagaku Ryoho* 2007; **34**: 1095-1098 [PMID: 17637547]

24 **Kostoglou A**, Tzanakis N, Epaggelis I, Vlasis K, Skandalakis P, Filippou D. Solitary cerebellum metastasis from gastric adenocarcinoma. A rare case report. *Int J Surg Case Rep* 2019; **57**: 110-112 [PMID: 30952022 DOI: 10.1016/j.ijscr.2019.02.048]

25 **Ahn MJ**, Lee K, Lee KH, Kim JW, Kim IY, Bae WK. Combination of anti-PD-1 therapy and stereotactic radiosurgery for a gastric cancer patient with brain metastasis: a case report. *BMC Cancer* 2018; **18**: 173 [PMID: 29433469 DOI: 10.1186/s12885-017-3906-0]

26 **Kosco E**, King N, Waack A, Hoyt A, Schroeder J. Gastric Cancer With Brain Metastasis: A Case Report. *Cureus* 2023; **15**: e50040 [PMID: 38186505 DOI: 10.7759/cureus.50040]

27 **Murakami Y**, Kobayashi T, Naruse Y, Watanabe F, Ishino A, Kanai R, Goto T, Saito K. Exclusive Cerebellar and Leptomeningeal Metastases from Early Gastric Cancer 14 Months after Proximal Gastrectomy: An Autopsy Case Report. *NMC Case Rep J* 2019; **6**: 65-70 [PMID: 31016104 DOI: 10.2176/nmccrj.cr.2018-0175]

World Journal of Clinical Cases

Submit a Manuscript: https://www.f6publishing.com

World J Clin Cases 2024 May 26; 12(15): 2642-2648

DOI: 10.12998/wjcc.v12.i15.2642

ISSN 2307-8960 (online)

CASE REPORT

Tuberous sclerosis complex combined with primary lymphedema: A case report

Xing-Peng Li, Xiao-Li Sun, Xin Liu, Zhe Wen, Li-Hua Jiang, Yan Fu, Yun-Long Yue, Ren-Gui Wang

Specialty type: Medicine, research and experimental

Provenance and peer review: Unsolicited article; Externally peer reviewed.

Peer-review model: Single blind

Peer-review report's classification
Scientific Quality: Grade B
Novelty: Grade B
Creativity or Innovation: Grade B
Scientific Significance: Grade C

P-Reviewer: Kumar R, India

Received: February 4, 2024
Revised: March 8, 2024
Accepted: April 9, 2024
Published online: May 26, 2024

Xing-Peng Li, Xiao-Li Sun, Li-Hua Jiang, Yan Fu, Ren-Gui Wang, Department of Radiology, Beijing Shijitan Hospital Affiliated to Capital Medical University, Beijing 100038, China

Xin Liu, Department of Lymph Surgery, Beijing Shijitan Hospital Affiliated to Capital Medical University, Beijing 100038, China

Zhe Wen, Department of Nuclear Medicine, Beijing Shijitan Hospital Affiliated to Capital Medical University, Beijing 100038, China

Yun-Long Yue, Department of MRI, Beijing Shijitan Hospital Affiliated to Capital Medical University, Beijing 100038, China

Corresponding author: Ren-Gui Wang, MD, PhD, Chief Doctor, Chief Physician, Full Professor, Department of Radiology, Beijing Shijitan Hospital Affiliated to Capital Medical University, No. 10 Yangfangdian Tieyi Road, Beijing 100038, China. wangrg@bjsjth.cn

Abstract

BACKGROUND

Tuberous sclerosis complex (TSC) and primary lymphedema (PLE) are both rare diseases, and it is even rarer for both to occur in the same patient. In this work, we have provided a detailed description of a patient's clinical presentation, imaging findings, and treatment. And a retrospective analysis was conducted on 14 published relevant case reports.

CASE SUMMARY

A 16-year-old male came to our hospital for treatment due to right lower limb swelling. This swelling is already present from birth. The patient's memory had been progressively declining. Seizures had occurred 1 year prior at an unknown frequency. The patient was diagnosed with TSC combined with PLE through multimodal imaging examination: Computed tomography, magnetic resonance imaging, and lymphoscintigraphy. The patient underwent liposuction. The swelling of the patient's right lower limb significantly improved after surgery. Epilepsy did not occur.after taking antiepileptic drugs and sirolimus.

CONCLUSION

TSC with PLE is a rare and systemic disease. Imaging can detect lesions of this disease, which are important for diagnosis and treatment.

Key Words: Tuberous sclerosis complex; Lymphedema; Sirolimus; Multimodal imaging

examination; Case report

Core Tip: Tuberous sclerosis complex with primary lymphedema (TSC-PLE) is a rare, congenital and systemic disease closely related to gene mutations. The clinical manifestations of TSC-PLE are diverse. Multiple imaging methods can detect systemic organ and tissue lesions, which are important for clinical diagnosis and treatment. Rapamycin-targeted therapy is the main treatment for this disease and can simultaneously treat the symptoms of both TSC and PLE. Liposuction can effectively improve limb swelling in patients. This case is the 17th patient with TSC-PLE worldwide. And this case has comprehensive clinical, imaging, genetic testing and treatment.

Citation: Li XP, Sun XL, Liu X, Wen Z, Jiang LH, Fu Y, Yue YL, Wang RG. Tuberous sclerosis complex combined with primary lymphedema: A case report. *World J Clin Cases* 2024; 12(15): 2642-2648
URL: https://www.wjgnet.com/2307-8960/full/v12/i15/2642.htm
DOI: https://dx.doi.org/10.12998/wjcc.v12.i15.2642

INTRODUCTION

Tuberous sclerosis complex (TSC) is an autosomal dominant genetic diseases characterized by multiple organ lesions and closely related to the *TSC* gene[1-3]. Lymphedema (LE) is the accumulation of protein rich lymphatic fluid in subcutaneous interstitial tissue, irreversible fibrosis of adipose tissue, and ultimately causing limb swelling. LE can be divided into primary LE (PLE) and secondary LE based on its etiology[4]. TSC and PLE are rare diseases, and it is even rarer for both to occur in the same patient. In this work, we aimed to intended to increase awareness of TSC and PLE by reporting a case and reviewing the relevant literature.

CASE PRESENTATION

Chief complaints

A 16-year-old male came to our hospital for treatment due to right lower limb swelling. This swelling is already present from birth without any obvious cause or reason. It worsened after activity and improved after rest.

History of present illness

Ten years prior, there had been swelling of the right scrotum and fluid accumulation in the right testicular sheath. Seven years prior, the patient had broken out with erysipelas. In recent years, the patient's memory had been progressively declining. Seizures had occurred 1 year prior at an unknown frequency but improved after treatment with antiepileptic medication.

Physical examination

The skin became red and thick and exhibited poor elasticity, high temperature, and visible pigmentation. Restricted movement of joints was observed in the right lower limb.

Laboratory examinations

Genetic testing revealed a mutation in the *TSC2* gene. The heterozygous mutation of nucleotide number 2251 from cytosine C to thymine T (c.2251C>T) resulted in a mutation of amino acid number 751 from arginine to terminator (p.ARG751Ter). The patient's parents did not exhibit any *TSC* gene abnormalities.

Imaging examinations

A computed tomography (CT) scan of the head revealed symmetrically distributed calcified nodules located beneath the ependymal membrane of both lateral ventricles (Figure 1A). An abdominal enhanced CT scan showed multiple, regular and well-defined nodules in both kidneys. The internal density of the nodule was uneven, with visible fat density and soft tissue density (Figure 1B). A chest CT scan showed multiple ground glass opacities in both lungs, mainly distributed under the pleura, with a diameter of 3-10 mm. However, no pulmonary cysts were found in either lung (Figure 1C). In addition, $^{99}Tc^{m}$-DX-lymphoscintigraphy revealed thickening of the right lower limb, but lymphatic vessels in the right lower limb were not visualized. The right inguinal, iliac, and lumbar lymphatic vessels and lymph nodes were not visualized, and the imaging agent was diffusely and unevenly distributed in the right lower limb, waist, buttocks, and external genital area (Figure 2). The short time inversion recovery sequence of the lower limb magnetic resonance imaging (MRI) showed thickening of the skin and swelling of subcutaneous soft tissue in the right lower limb, with

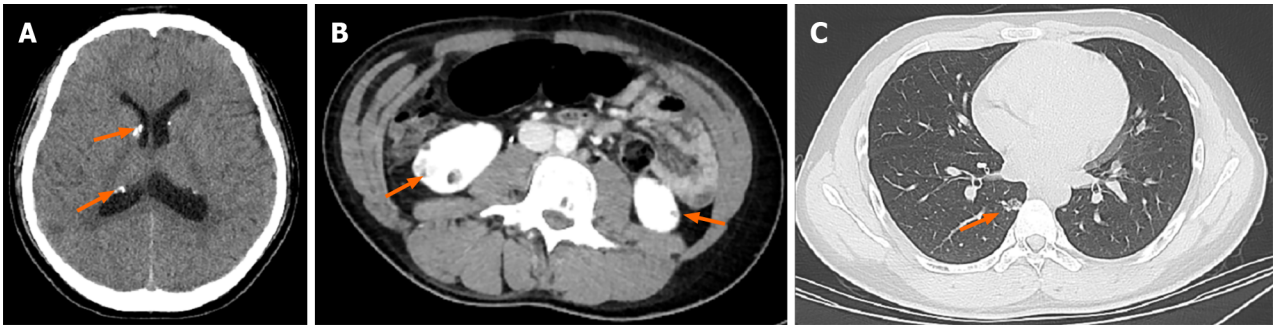

Figure 1 Computed tomography scan. A: Computed tomography (CT) scan of the head. Calcified nodules located beneath the ependymal membrane of both lateral ventricles; symmetrically distributed (orange arrow); B: Abdominal CT enhancement. Multiple regular and well-defined nodules in both kidneys, with visible fat density inside. After enhancement, the solid components are enhanced, but the fat components are not enhanced (orange arrow); C: Chest CT scan. An irregular ground glass opacity nodule in the posterior basal segment of the right lower lobe of the lung (orange arrow).

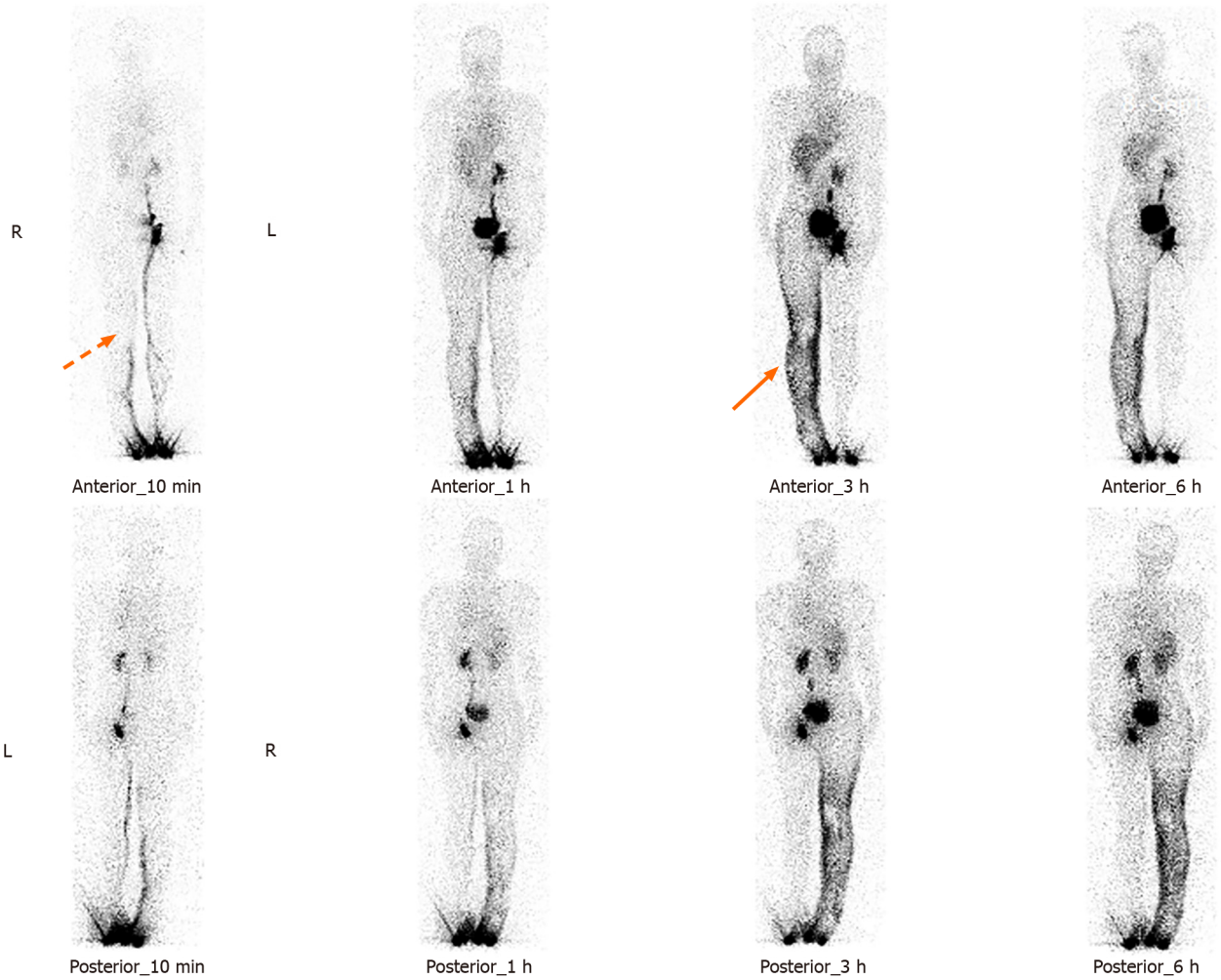

Figure 2 $^{99}Tc^{m}$-DX-lymphoscintigraphy: The imaging agent was diffusely and unevenly distributed in the right lower limb, waist, buttocks, and external genital area (orange arrow). The lymphatic vessels in the right lower limb were not visualized, and the right inguinal, iliac, and lumbar lymphatic vessels and lymph nodes were not visualized (orange dashed arrow).

honeycomb, crescent, and band signs visible inside. Thickened, tortuous, and dilated veins were also observed (Figures 3 and 4).

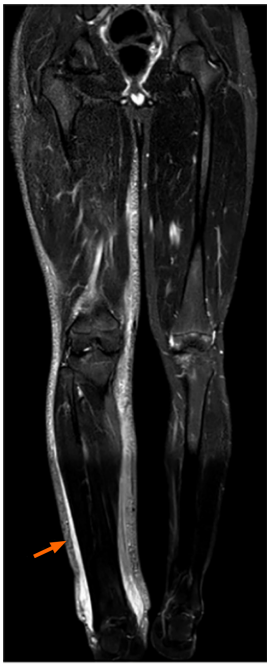

Figure 3 Coronal view of the short time inversion recovery sequence of the entire lower limb. Compared with those on the left, the skin on the right lower limb was thickened, and the subcutaneous soft tissue was swollen, with abnormally high signal shadows visible inside (orange arrows).

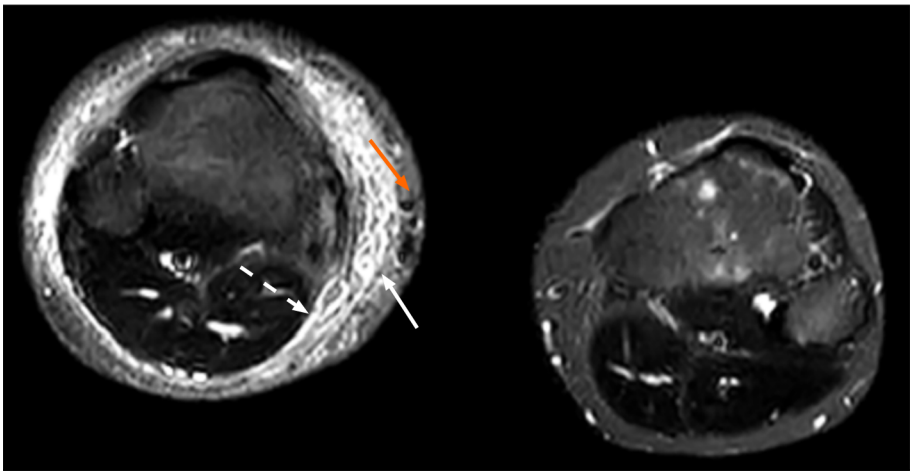

Figure 4 Short time inversion recovery sequence transverse section of lower limb magnetic resonance imaging: Signs of lymphedema in subcutaneous soft tissue, including the honeycomb sign (white arrow) and band sign (white dashed arrow). Thickened, tortuous and dilated veins were observed (orange arrow).

FINAL DIAGNOSIS

Based on comprehensive clinical, imaging, and genetic testing, the male patient was diagnosed with TSC combined with PLE.

TREATMENT

The patient was prescribed oral oxcarbazepine and sodium valproate to suppress seizures and sirolimus to treat the TSC. The patient underwent liposuction and volume reduction surgery to reduce lower limb edema.

OUTCOME AND FOLLOW-UP

Prognosis: The swelling of the patient's right lower limb significantly improved after surgery, and the morphology improved well. Epilepsy did not occur.

DISCUSSION

TSC is an autosomal dominant genetic disorder characterized by lesions in multiple organs. *TSC1* or *TSC2* gene mutations can lead to structural activation of the mechanical target of rapamycin pathway, dysregulation of cell proliferation, and obstruction of lymphangiogenesis. The incidence rate is approximately 1/6000-10000; these tumours can be familial or sporadic and are more likely to occur in young males. The typical clinical manifestations of the Vogt triad are epilepsy, intellectual disability, and facial sebaceous adenoma. Almost all organs in the body can be affected[1-3] (the skin, nervous system, heart, lungs, kidneys, bones, *etc*.). The main treatment method for TSC is the targeted drug rapamycin. The present patient was a male adolescent with clinical manifestations of epilepsy. The imaging findings included subependymal nodules, bilateral renal angiomyolipomas, and multiple ground glass opacity in both lungs on chest CT. Genetic testing revealed *TSC2 gene* mutations, consistent with previous literature reports[3].

PLE of the lower limbs is caused by congenital structural and/or functional deficiencies in the lymphatic system, leading to impaired lymphatic return and the accumulation of protein-rich fluid in the interstitial tissue in the skin and subcutaneous soft tissue of the lower limbs. Prolonged and progressive stimulation of adipose tissue ultimately leads to abnormal proliferation of fibrous connective tissue and irreversible fibrosis of adipose tissue. The most common clinical manifestation is obvious swelling of the skin of the lower limbs, with early onset of collapsible oedema. The skin gradually hardens over time, and there is late onset of abnormal thickening and segmental hypertrophy of the affected limb. In severe cases, this condition can lead to "elephantiasis" of the affected limb, bilateral limb asymmetry, and even limb deformities. The pathogenesis may be related to the following gene mutations[4-6]: Vascular endothelial growth factor receptor-3 (*VEGFR-3*), SRY-related high mobility group Box 18, and forkhead Box C2. The overall incidence rate of PLE is 1-2/100000, and PLE usually occurs in childhood, and there are more women affected than men[4]. The patient was diagnosed with primary lower limb LE through clinical and imaging examinations. The clinical manifestation was swelling of the right lower limb without obvious cause. A typical honeycomb-like pattern (honeycomb sign) was observed in the subcutaneous soft tissue of the right lower limb *via* MRI, and $^{99}Tc^{m}$-DX-lymphoscintigraphy revealed the absence of lymphatic vessels and lymph nodes in the right lower limb accompanied by right lower limb skin lymphatic reflux, which is consistent with the imaging findings of LE reported by Liu *et al*[7] and Wen *et al*[8].

According to the literature, TSC with PLE (TSC-PLE) has only been observed in case reports. A summary of all relevant literature retrieved from PubMed from 1986 to 2023 is presented in Table 1. There were a total of 14 articles and 16 cases. Including this case report, there were a total of 17 patients, including 11 females (64.7%) and 6 males (35.3%). There were more women with TSC-PLE than men, with an age range of 0-28 years and an average age of 6.3 years. LE is more common in adolescents than in adults, and LE often occurs in the lower limbs; there was a total of 15 cases (88.2%), and all 15 cases of oedema occurred in one limb (two cases are unknown). There were 3 patients with *TSC1* gene mutations, 7 patients with *TSC2* gene mutations, and 7 patients with unclear gene mutations. Geffrey *et al*[9] reported that the incidence rate of PLE in TSC patients was 0.70% (2/286). However, the pathological and physiological mechanisms of TSC-PLE are not yet clear. Among the more than 20 genes involved in lymphatic system development, some are closely related to the mTOR pathway. Therefore, several researchers speculate that there may be five possible reasons for the occurrence of TSC-PLE: (1) The phosphoinositol 3-kinase signalling pathway plays an important role in the formation and remodelling of the lymphatic system. Due to *TSC* gene mutations, mTOR is activated, thereby inhibiting lymphatic vessel growth. Eventually, the affected limb's lymphatic system develops poorly[10]; (2) *VEGFR-3* and *VEGF-C* are important regulatory factors that promote lymphatic vessel proliferation and cell migration. Studies have shown that *VEGF-C* can activate downstream mTOR/S6 kinase signalling pathways and that activated mTOR acts through *p70S6 kinase*[11]; (3) mTOR directly participates in the generation of lymphatic vessels: Studies have shown that the expression of mTOR in lymphatic endothelial cells is significantly increased and that mTOR is abnormally activated in lymphatic malformations [11]; (4) The reason why the incidence rate of female patients with TSC-PLE increases significantly may be related to oestrogen[9]; and (5) Smooth cell hypertrophy: Abnormal smooth cell hypertrophy within subcutaneous tissue compresses superficial lymphatic vessels, leading to impaired lymphatic reflux and ultimately resulting in LE[12].

The main treatment for TSC-PLE patients is rapamycin, which can alleviate both TSC-related symptoms and lymphatic vessel abnormality-related symptoms (*e.g*., LE)[9]. Liposuction and volume reduction surgery can also be performed to reduce lower limb oedema and improve the appearance of the affected limb. In this case, antiepileptic drugs were used to suppress seizures. In addition, when TSC-PLE is combined with other critical signs, such as osteofascial compartment syndrome caused by severe LE, aortic aneurysm caused by severe vascular malformations, erysipelas and systemic infections caused by LE, and pulmonary embolism caused by deep vein thrombosis, timely symptomatic treatment should be administered[13-15].

CONCLUSION

TSC-PLE is a rare, congenital and systemic disease closely related to a variety of gene mutations and is most common among young women, with an overall incidence rate of approximately 0.7%. The clinical manifestations of TSC-PLE are

Table 1 Summary of cases of tuberous sclerosis complex with primary lymphedema from 1986 to 2023

No	Ref.	Year	Number	Gender	Age (yr)	Edemasite	Gene	Treatment
1	Cottafava *et al*[16]	1986	1	Female	7	Left lower limb	Unknown	Anti convulsive drugs + anti ACTH drugs
2	Hirsch *et al*[17]	1999	1	Female	28	Left lower limb	Unknown	Subcutaneous lymphangiectomy + diuretic + elastic socks
3	Voudris *et al*[18]	2003	1	Female	5	Left lower limb	Unknown	Unknown
4	Lucas and Andrade[19]	2011	1	Female	1	Right lower limb	*TSC1*	Unknown
5	Sukulal and Namboodiri[12]	2012	1	Female	0	Left lower limb	Unknown	Unknown
6	Navarre and Poitras[13]	2014	1	Male	5	Left lower limb	*TSC2*	Fasectomy + toe amputation + antibiotics + enoxaparin + warfarin
7	Prato *et al*[20]	2014	1	Female	4	Left upper limb	*TSC2*	Carbamazepine + topiramate + everolimus + amoxicillin-clavulanate potassium
8	Geffrey *et al*[9]	2014	2	Female/Female	8/15	Left lower limb/Left lower limb	*TSC2*/*TSC2*	Rapamycin + lymphedema therapy
9	Hoshiai *et al*[21]	2015	2	Female/Female	2/0	Right lower limb/Right upper limb	Unknown	Unknown
10	Saffari *et al*[22]	2019	1	Male	6	lower limb but unknown left and right	*TSC2*	Everolimus
11	Wiemer-Kruel *et al*[14]	2020	1	Male	7	Left lower limb	*TSC2*	Levetiracetam + repair of aortic aneurysm + everolimus
12	Kaneshi *et al*[15]	2020	1	Male	0	lower limb but unknown left and right	Unknown	Ileostomy decompression + antibiotics + lymphedema therapy
13	Lin *et al*[11]	2020	1	Male	3	Left lower limb	*TSC1*	Albumin + diuretics
14	Klinner *et al*[23]	2020	1	Female	0	Right lower limb	*TSC1*	Aminohexenoic acid + lymphatic drainage + bandage compression
15	This case	2023	1	Male	16	Right lower limb	*TSC2*	Sirolimus + oxcarbazepine + liposuction

TSC: Tuberous sclerosis complex.

diverse and include epilepsy, memory loss, intellectual disability, lower limb swelling, *etc*. Multiple imaging methods can detect systemic organ and tissue lesions, which are important for clinical diagnosis and treatment. Rapamycin-targeted therapy is the main treatment method for this disease and can simultaneously treat the symptoms of both TSC and PLE. Liposuction can effectively improve limb swelling in patients However, the specific pathophysiological mechanism of TSC-PLE is still unclear and requires further research.

FOOTNOTES

Author contributions: Li XP and Wang RG were the major contributor in writing the manuscript and reviewing the literatures; Li XP, Wen Z and Jiang LH created figures and tables; Fu Y and Wen Z provided patient images information; Yue YL, Sun XL and Wang RG provided valuable comments; Liu X was the chief physician of the patient. All authors revised the manuscript and approved the final version.

Supported by National Natural Science Foundation of China, No. 61876216.

Informed consent statement: All study participants, or their legal guardian, provided informed written consent prior to study.

Conflict-of-interest statement: All the authors report no relevant conflicts of interest for this article.

CARE Checklist (2016) statement: The authors have read the CARE Checklist (2016), and the manuscript was prepared and revised according to the CARE Checklist (2016).

Country/Territory of origin: China

ORCID number: Yun-Long Yue 0000-0002-9768-8192; Ren-Gui Wang 0009-0000-5690-1658.

S-Editor: Zheng XM
L-Editor: A
P-Editor: Yu HG

REFERENCES

1 **Randle SC**. Tuberous Sclerosis Complex: A Review. *Pediatr Ann* 2017; **46**: e166-e171 [PMID: 28414398 DOI: 10.3928/19382359-20170320-01]
2 **Volpi A**, Sala G, Lesma E, Labriola F, Righetti M, Alfano RM, Cozzolino M. Tuberous sclerosis complex: new insights into clinical and therapeutic approach. *J Nephrol* 2019; **32**: 355-363 [PMID: 30406604 DOI: 10.1007/s40620-018-0547-6]
3 **Gupta S**, Kang HC, Faria SC, Choyke PL, Kundra V. Tuberous Sclerosis Complex (TSC): Renal and Extrarenal Imaging. *Acad Radiol* 2022; **29**: 439-449 [PMID: 33487538 DOI: 10.1016/j.acra.2020.12.019]
4 **Warren AG**, Brorson H, Borud LJ, Slavin SA. Lymphedema: a comprehensive review. *Ann Plast Surg* 2007; **59**: 464-472 [PMID: 17901744 DOI: 10.1097/01.sap.0000257149.42922.7e]
5 **Grada AA**, Phillips TJ. Lymphedema: Pathophysiology and clinical manifestations. *J Am Acad Dermatol* 2017; **77**: 1009-1020 [PMID: 29132848 DOI: 10.1016/j.jaad.2017.03.022]
6 **Ho B**, Gordon K, Mortimer PS. A Genetic Approach to the Classification of Primary Lymphoedema and Lymphatic Malformations. *Eur J Vasc Endovasc Surg* 2018; **56**: 465-466 [PMID: 30055909 DOI: 10.1016/j.ejvs.2018.07.001]
7 **Liu M**, Zhang Y, Li X, Hao Q, Li B, Wang R. MRI-based volume measurement methods for staging primary lower extremity lymphedema: a single-center study of asymmetric volume difference-a diagnostic study. *BMC Musculoskelet Disord* 2023; **24**: 810 [PMID: 37828475 DOI: 10.1186/s12891-023-06912-x]
8 **Wen Z**, Tong G, Liu Y. Potential Utilization of Lymphoscintigraphy in Patients With Klippel-Trenaunay Syndrome. *Clin Nucl Med* 2021; **46**: 25-30 [PMID: 33156055 DOI: 10.1097/RLU.0000000000003361]
9 **Geffrey AL**, Shinnick JE, Staley BA, Boronat S, Thiele EA. Lymphedema in tuberous sclerosis complex. *Am J Med Genet A* 2014; **164A**: 1438-1442 [PMID: 24668795 DOI: 10.1002/ajmg.a.36469]
10 **Pollack SF**, Geffrey AL, Thiele EA, Shah U. Primary intestinal lymphangiectasia treated with rapamycin in a child with tuberous sclerosis complex (TSC). *Am J Med Genet A* 2015; **167A**: 2209-2212 [PMID: 25943403 DOI: 10.1002/ajmg.a.37148]
11 **Lin WH**, Zhang ZH, Wang HL, Ren L, Geng LL. Tuberous sclerosis complex presenting as primary intestinal lymphangiectasia: A case report. *World J Clin Cases* 2020; **8**: 1995-2000 [PMID: 32518792 DOI: 10.12998/wjcc.v8.i10.1995]
12 **Sukulal K**, Namboodiri N. Congenital lymphedema: another unique and gender specific stigmata of tuberous sclerosis? *Indian Pediatr* 2012; **49**: 845 [PMID: 23144114 DOI: 10.1007/s13312-012-0178-2]
13 **Navarre P**, Poitras B. Lymphoedema in tuberous sclerosis: case report and review of the literature. *J Pediatr Orthop* 2014; **34**: e27-e32 [PMID: 24992349 DOI: 10.1097/BPO.0000000000000240]
14 **Wiemer-Kruel A**, Mayer H, Ewert P, Martinoff S, Eckstein HH, Kriebel T, Bissler J, Franz D, Bast T. Congenital Lymphatic Malformation and Aortic Aneurysm in a Patient with TSC2 Mutation. *Neuropediatrics* 2020; **51**: 57-61 [PMID: 31505689 DOI: 10.1055/s-0039-1694985]
15 **Kaneshi Y**, Shibasaki J, Aida N, Shimokaze T, Toyoshima K. Indocyanine green lymphography for congenital lymphatic dysplasia with tuberous sclerosis complex: A case report. *Pediatr Int* 2020; **62**: 234-236 [PMID: 31970872 DOI: 10.1111/ped.14071]
16 **Cottafava F**, Cosso D, Brida di Priò S, Grossi-Bianchi ML, Fedi M, Fontana F, Racugno A, Tosca P. [A case of Bourneville's tuberous sclerosis with elephantiasis (caused by lymphedema) of the left leg]. *Minerva Pediatr* 1986; **38**: 49-52 [PMID: 3702837]
17 **Hirsch RJ**, Silverberg NB, Laude T, Weinberg JM. Tuberous sclerosis associated with congenital lymphedema. *Pediatr Dermatol* 1999; **16**: 407-408 [PMID: 10627220 DOI: 10.1046/j.1525-1470.1999.016005406.2.x]
18 **Voudris KA**, Skardoutsou A, Vagiakou EA. Tuberous sclerosis and congenital lymphedema. *Pediatr Dermatol* 2003; **20**: 371-373 [PMID: 12869168 DOI: 10.1046/j.1525-1470.2003.20326_3.x]
19 **Lucas M**, Andrade Y. Congenital lymphedema with tuberous sclerosis and clinical Hirschsprung disease. *Pediatr Dermatol* 2011; **28**: 194-195 [PMID: 20738790 DOI: 10.1111/j.1525-1470.2010.01231.x]
20 **Prato G**, Mancardi MM, Baglietto MG, Janis S, Vercellino N, Rossi A, Consales A, Raso A, Garrè ML. Congenital segmental lymphedema in tuberous sclerosis complex with associated subependymal giant cell astrocytomas treated with Mammalian target of rapamycin inhibitors. *J Child Neurol* 2014; **29**: NP54-NP57 [PMID: 24056156 DOI: 10.1177/0883073813499969]
21 **Hoshiai S**, Oguma E, Sato Y, Konishi T, Minami M. Congenital focal lymphedema as a diagnostic clue to tuberous sclerosis complex: report of two cases diagnosed by ultrasound. *Skeletal Radiol* 2015; **44**: 1165-1168 [PMID: 25616615 DOI: 10.1007/s00256-015-2094-8]
22 **Saffari A**, Brösse I, Wiemer-Kruel A, Wilken B, Kreuzaler P, Hahn A, Bernhard MK, van Tilburg CM, Hoffmann GF, Gorenflo M, Hethey S, Kaiser O, Kölker S, Wagner R, Witt O, Merkenschlager A, Möckel A, Roser T, Schlump JU, Serfling A, Spiegler J, Milde T, Ziegler A, Syrbe S. Safety and efficacy of mTOR inhibitor treatment in patients with tuberous sclerosis complex under 2 years of age - a multicenter retrospective study. *Orphanet J Rare Dis* 2019; **14**: 96 [PMID: 31053163 DOI: 10.1186/s13023-019-1077-6]
23 **Klinner J**, Krüger M, Brunet T, Makowski C, Riedhammer KM, Mollweide A, Wagner M, Hoefele J. Congenital lymphedema as a rare and first symptom of tuberous sclerosis complex. *Gene* 2020; **753**: 144815 [PMID: 32479982 DOI: 10.1016/j.gene.2020.144815]

World Journal of Clinical Cases

Submit a Manuscript: https://www.f6publishing.com

World J Clin Cases 2024 May 26; 12(15): 2649-2654

DOI: 10.12998/wjcc.v12.i15.2649

ISSN 2307-8960 (online)

CASE REPORT

Cetuximab combined with chemotherapy for simultaneous esophageal squamous cell carcinoma and colon adenocarcinoma: A case report

Xin-Xin Luo, Yu-Xuan Du, Qi-Qing Zhang, Lin Zhang, Shu-Ying Zeng, Zhi-Hong Yu, Peng Shen, Zheng-Quan Feng

Specialty type: Medicine, research and experimental

Provenance and peer review: Unsolicited article; Externally peer reviewed.

Peer-review model: Single blind

Peer-review report's classification

Scientific Quality: Grade C, Grade D

Novelty: Grade C, Grade C

Creativity or Innovation: Grade C, Grade C

Scientific Significance: Grade C, Grade C

P-Reviewer: Adam CA, Romania

Received: February 16, 2024

Revised: March 15, 2024

Accepted: April 9, 2024

Published online: May 26, 2024

Xin-Xin Luo, Lin Zhang, Shu-Ying Zeng, The Second School of Clinical Medicine, Zhejiang Chinese Medical University, Hangzhou, 310053, Zhejiang Province, China

Yu-Xuan Du, Qi-Qing Zhang, Zhi-Hong Yu, Zheng-Quan Feng, Department of Oncology, Tongde Hospital of Zhejiang Province, Hangzhou 310012, Zhejiang Province, China

Peng Shen, Department of Medical Oncology, The First Affiliated Hospital, Medical College of Zhejiang University, Hangzhou 310003, Zhejiang Province, China

Corresponding author: Zheng-Quan Feng, MD, PhD, Chief Physician, Director, Department of Oncology, Tongde Hospital of Zhejiang Province, No. 234 Gucui Road, Xihu District, Hangzhou 310012, Zhejiang Province, China. fzhq213@aliyun.com

Abstract

BACKGROUND

Multiple primary carcinomas (MPCs) are defined as two or more independent primary cancers that occur simultaneously or sequentially in the same individual. Synchronous MPCs are rarer than solitary cancers or metachronous MPCs. Accurate diagnoses of synchronous MPCs and the choice of treatment are critical for successful outcomes in these cases.

CASE SUMMARY

A 64-year-old patient presented with dysphagia, without obvious cause. A diagnosis of synchronous esophageal squamous cell carcinoma and colon adenocarcinoma with liver metastasis was confirmed based on examination and laboratory results. After multi-disciplinary consultations, combination chemotherapy (a 3-wk cycle with oxaliplatin 212 mg administered on day 1 and capecitabine 1.5 g twice daily on days 1-14) and esophageal cancer radiotherapy were initiated. Based on the results of genetic testing, we switched to a regimen of leucovorin + fluorouracil + oxaliplatin and cetuximab regimen for 8 cycles. Subsequently, capecitabine and bevacizumab were administered until the most recent follow-up, at which the tumor remained stable.

CONCLUSION

Successful cetuximab chemotherapy treatment provides a reference for the non-operative and homogeneous treatment of different pathological types of

synchronous MCPs.

Key Words: Synchronous multiple primary carcinoma; Esophageal squamous cell carcinoma; Colon adenocarcinoma; Cetuximab; Chemotherapy; Case report

Core Tip: We report a case of a 64-year-old patient diagnosed with synchronous esophageal squamous cell carcinoma and colon adenocarcinoma with liver metastasis. After multi-disciplinary consultations, oxaliplatin + capecitabine chemotherapy and esophageal cancer radiotherapy were initiated. Based on genetic testing, treatment was switched to a regimen of leucovorin + fluorouracil + oxaliplatin and cetuximab for 8 cycles. Subsequently, capecitabine and bevacizumab were administered, and the tumor was stable at the most recent follow-up. This case demonstrates successful treatment of dual primary digestive tract tumors of differing pathological types using the same regimen, which supports non-surgical, simultaneous treatment for synchronous multiple primary cancers.

Citation: Luo XX, Du YX, Zhang QQ, Zhang L, Zeng SY, Yu ZH, Shen P, Feng ZQ. Cetuximab combined with chemotherapy for simultaneous esophageal squamous cell carcinoma and colon adenocarcinoma: A case report. *World J Clin Cases* 2024; 12(15): 2649-2654
URL: https://www.wjgnet.com/2307-8960/full/v12/i15/2649.htm
DOI: https://dx.doi.org/10.12998/wjcc.v12.i15.2649

INTRODUCTION

Multiple primary carcinomas (MPCs), also known as multiple carcinomas, refer to two or more independent primary carcinomas occurring simultaneously or sequentially in the same individual. According to the time interval between occurrences, MPCs can be divided into metachronous MPCs or synchronous MPCs. The overall reported frequency of MPCs varies between 2.4%-17%[1]. The occurrence of MPCs may be related to factors such as the patient's physical condition, lifestyle, environment, genetics, and treatment methods.

MPCs of the gastrointestinal tract have been treated by simultaneous surgical procedures[2]; however, few cases have been reported on the treatment of MPCs of different pathological types with non-operative regimens. Herein, we report a case of synchronous esophageal squamous cell carcinoma and colon adenocarcinoma with liver metastasis, successfully treated with a non-surgical regimen. This case may be used for guidance to improve the diagnosis and treatment of this disease.

CASE PRESENTATION

Chief complaints

A 64-year-old patient was admitted to the local gastroenterology department with a complaint of dysphagia, including difficulties with both eating and drinking.

History of present illness

In July 2022, the patient experienced worsening dysphagia, including difficulty swallowing food, and intermittent abdominal discomfort. These symptoms prompted the patient to seek medical attention.

History of past illness

In May 2022, the patient experienced dysphagia and mild difficulty defecating for approximately 1 month; he had no cough, intermittent abdominal discomfort, or diarrhea. These symptoms were found to have no obvious cause. The patient was not concerned and did not seek medical help.

Personal and family history

The patient had no relevant family history.

Physical examination

On physical examination, no obvious abdominal mass or superficial lymph node swelling was detectable.

Laboratory examinations

Prior to treatment, laboratory examinations revealed the following levels in peripheral blood samples: carcinoembryonic

antigen, 5.17 ng/mL; carbohydrate antigen 125, 5.9 U/mL; carbohydrate antigen 19-9, 19.45 IU/mL; white blood cells, 4.8 × 10^9/L; neutrophils, 3.3 × 10^9/L; red blood cells, 4.07 × 10^{12}/L; hemoglobin, 131 g/L. Routine urine, urine sediment, and routine fecal examinations, as well as occult blood testing, blood biochemistry, immune indicators, and infection indices showed no significant abnormalities.

Imaging examinations

Gastroscopy and colonoscopy examinations were performed. Gastroscopic pathology (Figure 1A) revealed chronic moderate superficial gastritis (active), *Helicobacter pylori* (+), and squamous cell carcinoma (esophageal mucosa). Colonoscopic pathology (Figure 1B) revealed adenocarcinoma in the sigmoid colon, 60 cm from the anus. Immunohistochemistry was performed on the colon samples, with the following results: succinate dehydrogenase complex iron sulfur subunit B (+), S-100 (-), smooth muscle actin (+), desmin (+), CD34 (+), CD117 (-), *Dog-1* (-), *P53* (wildtype), Ki-67 (+, 2%), and submucosal spindle cell tumor formation. These findings were consistent with leiomyoma. Liver biopsy (Figure 1C) revealed adenocarcinoma, and this was considered to be metastatic intestinal adenocarcinoma.

Esophageal meglumine diatrizoate angiography showed that the esophageal wall was locally thickened and stiffened in the anterior thoracic segment (Figure 2A). Positron emission tomography detected neoplasia in the anterior thoracic sigmoid colon 20 cm from the anus, occupying half of the intestinal cavity (Figure 2B). Multiple liver metastases were observed *via* magnetic resonance imaging (Figure 2C).

FINAL DIAGNOSIS

The patient was ultimately diagnosed with esophageal squamous cell carcinoma, colon adenocarcinoma with liver metastasis, and rectal leiomyoma.

TREATMENT

After multidisciplinary consultations, on July 23, 2022, the patient was started on a 3-wk chemotherapy cycle with 212 mg oxaliplatin on day 1 and 1.5 g capecitabine twice daily on days 1-14. While waiting for the genetic testing results from the intestinal biopsy, radiotherapy was administered for esophageal carcinoma on July 29, 2022.

Reference genetic testing indicated that the patient was wildtype for Kirsten *ras* oncogene homolog (*KRAS*), neuroblastoma *ras* oncogene homolog (*NRAS*), and *v-Raf* murine sarcoma viral oncogene homolog B (*BRAF*), with fibroblast growth factor receptor 1 gene amplification and microsatellite stability (MSS). Owing to the MSS, immunotherapy was not considered. However, based on these results, treatment was switched to leucovorin + fluorouracil + oxaliplatin (mFOLFOX) and cetuximab for 8 cycles, from August 12, 2022, to December 17, 2022. The patient developed hand-foot syndrome (grade III), bone marrow depression (grade I), and skin rash (grade I) during chemotherapy.

After 9 cycles of chemotherapy, the patient was administered a temporary anti-infective treatment for coronavirus 2019 pneumonia. For convenience during this time and considering the curative effect as well as patient preference, the chemotherapy regimen was suspended. Thereafter, the patient was switched to a capecitabine oral cycle; capecitabine + bevacizumab continues to be administered at this time.

OUTCOME AND FOLLOW-UP

In December 2023, chest computed tomography showed slight thickening of the esophageal wall in the thoracic segment, which was improved compared to the anterior segment. At the same follow-up, colonoscopy revealed that the sigmoid colon lesion was 20 cm from the anus and that the neoplasia occupied a quarter of the intestinal cavity, demonstrating a reduction in size from pre-treatment imaging. Liver magnetic resonance imaging revealed complete clinical response of the liver metastases. Overall outcome assessment indicated a partial response (PR). As of January 2024, the patient's condition remained stable.

DISCUSSION

Currently, the diagnosis of MPCs is based on the revised criteria of Warren and Gates[3]: (1) Malignancy must be confirmed pathologically for each tumor; (2) Each tumor must have its own unique pathological morphology, exist independently, and have no relationship to other tumors; (3) The tumors must occur in different sites or organs; and (4) Each tumor must be excluded as a metastatic focus from the other tumors. The interval between the occurrence of MPCs defines them as either synchronous (occurring within 6 months of each other) or metachronous (occurring more than 6 months apart).

The treatment of MPCs is similar to that of single primary carcinomas and significantly different from that of metastatic and recurrent carcinomas. In addition, the differences in pathological types and synchronicity influence the choice of treatment; therefore, accurate and timely diagnosis is crucial. Differential diagnosis of MPCs relies heavily on

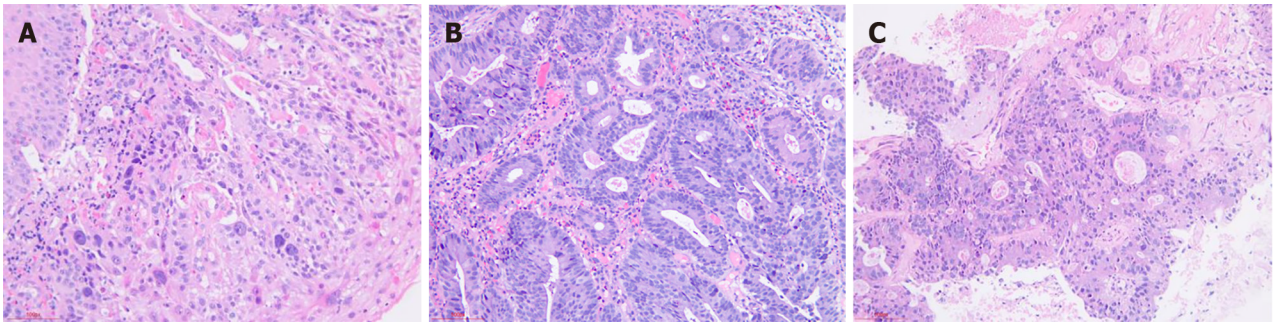

Figure 1 Pathological examinations. A: Squamous cell carcinoma of the esophagus (20 ×); B: Sigmoid adenocarcinoma (20 ×); C: Hepatic adenocarcinoma (20 ×).

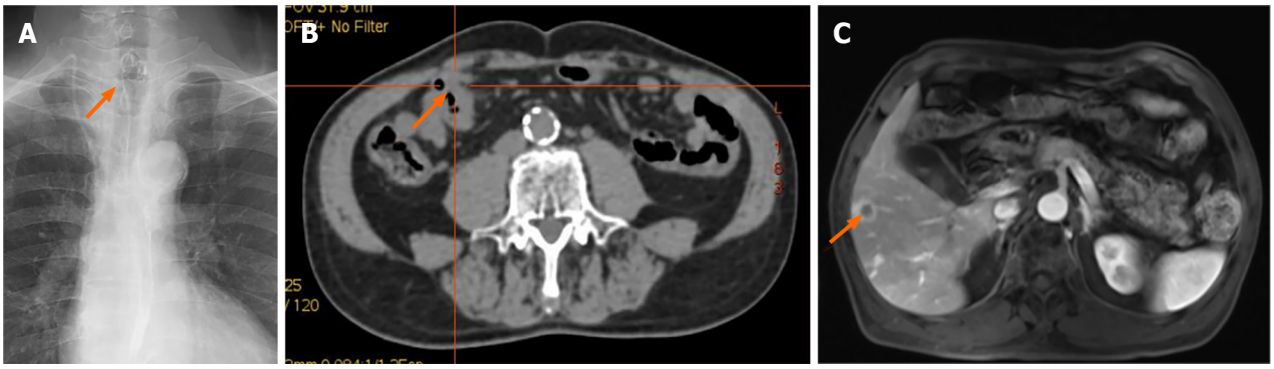

Figure 2 Imaging examinations. A: Esophageal meglumine diatrizoate angiography of esophageal lesions; B: Positron emission tomography of lesions in the sigmoid colon; C: Magnetic resonance imaging of multiple liver metastases.

histopathology screening. Our patient presented with squamous cell carcinoma of the esophagus and sigmoid colon adenocarcinoma with metastatic adenocarcinoma of the liver. The pathological types of the two tumors were significantly different; moreover, the different primary sites and the occurrence of metastasis made it challenging to choose a treatment plan for simultaneous treatment. Only a few cases of concurrent malignant tumors of different pathological types have been successfully treated.

Colon cancer with liver metastasis can be treated with mFOLFOX and cetuximab based on the pathological type and results of genetic testing. Guidelines also suggest that mFOLFOX can be used to treat esophageal cancer, with successful cases reported in the literature. Therefore, we treated this case with an mFOLFOX and cetuximab regimen. Reference genetic testing indicated the patient was KRAS/NRAS/BRAF wild-type. From August 12, 2022, to December 17, 2022, eight cycles of mFOLFOX + cetuximab were administered, with PR achieved; after eight cycles, PR was re-assessed. At follow-up in January 2024, the patient's condition remained stable.

MPCs of the first and second primary lesions are common in the digestive, respiratory, and urinary systems[4]. The digestive system is the most common, accounting for 48.7% of first and 44.0% of second primary lesions. Furthermore, the three most common sites for first and second primary lesions were found to be in the digestive system: the colorectum, stomach, and esophagus. Notably, studies[5-7] have suggested that patients with synchronous MPCs have a worse prognosis and lower overall survival than patients with metachronous MPCs. Therefore, to improve their prognosis, patients with MPCs should undergo an active treatment program promptly after diagnosis.

The primary treatments for MPCs are chemotherapy, radiotherapy, and surgery; however, a unified standard treatment strategy has not yet been established, and related research is insufficient. In the diagnosis and treatment of MPC, factors such as clinical stage and pathological type should be considered, and radical treatment should be adopted to the fullest extent, especially for localized tumors[8]. When a tumor cannot be resected, radiotherapy, chemotherapy, targeted therapy, and immunotherapy should be considered. Radiotherapy and chemotherapy, which have comprehensive anti-tumor activity, have the ability to concurrently control primary and metastatic lesions. Patients with locally advanced esophageal squamous cell carcinoma have been shown to be sensitive to chemoradiotherapy, with a high complete tumor regression rate and local tumor control[9].

The choice of drug therapy was based on the 2022 edition of the National Comprehensive Cancer Network (NCCN) guidelines[10], which recommends FOLFOX, CAPEOX, FOLFIRI or mFOLFIRINOX (leucovorin + fluorouracil + oxaliplatin, capecitabine + oxaliplatin, leucovorin + fluorouracil + irinotecan, and leucovorin + fluorouracil + irinotecan + oxaliplatin, respectively) as first-line treatment for metastatic colon cancer. If the patient is *KRAS*/*NRAS*/*BRAF* wildtype, they can be treated with chemotherapy + cetuximab. If mutations are found in the *KRAS*/*NRAS* genes, chemotherapy + bevacizumab can be administered. The first choice for patients with mismatch repair deficient tumors or high microsatellite instability is pembrolizumab.

The 2022 NCCN guidelines[10] recommend first-line treatment for locally advanced esophageal cancer, which is often selected because oxaliplatin is less toxic than cisplatin. Fluorouracil is also a commonly used drug for this cancer type. Chemotherapy + trastuzumab is recommended if the tumor is positive for human epidermal growth factor receptor 2 (HER2) overexpression and chemotherapy + immunotherapy if HER2 overexpression is negative.

For patients who have achieved PR after a certain number of cycles of chemotherapy, the existing maintenance treatment modes primarily include one of the following, based on the cumulative toxicity of the drugs: partial drug maintenance and dressing change maintenance, as in the original plan; chemotherapy termination; or targeted treatment.

The optimal radiotherapy dose for esophageal carcinoma remains controversial. In China, the conventional radiation dose for esophageal squamous cell carcinoma is 60 Gy, and its curative effect and long-term survival rate are consistent with relevant international studies[11]. The NCCN guidelines[10] consider 50.4 Gy as a safe and reliable dose for concurrent chemoradiotherapy. Recent studies[12] have demonstrated that an increased dose of radiotherapy combined with chemotherapy can improve the survival of patients with esophageal cancer. Therefore, 60 Gy was selected for treatment in this case.

CONCLUSION

In summary, imaging, endoscopic, and pathological examinations should be combined for the diagnosis of MPCs to differentiate primary malignant tumors from metastatic ones as accurately as possible. For multi-focal tumors, determining whether they are metastases is necessary. For the treatment of MPCs, the pathological characteristics of each tumor and the genetic status should be considered when choosing the individualized treatment scheme with the highest benefit for the patient. Surgery is the standard treatment for an early-stage tumor, with supplemental chemotherapy and biological therapy. The survival of patients with concurrent late metastasis of MPCs can be significantly prolonged by targeted chemotherapy or immunotherapy. This report describes the successful treatment of a case of simultaneous esophageal squamous cell carcinoma and colon adenocarcinoma with liver metastases. The characteristics and treatment plan of this case can be analyzed and used as a reference for the clinical treatment of similar MPCs.

FOOTNOTES

Author contributions: Luo XX, Zhang L and Zeng SY contributed to conceptualization, methodology, data curation and analysis, writing (original draft), and visualization; Luo XX, Du YX, Zhang QQ and Yu ZH contributed to data acquisition; Shen P and Feng ZQ contributed to writing (review and editing); Yu ZH, Shen P and Feng ZQ contributed to supervision. All authors have read and approved the final manuscript.

Informed consent statement: Informed written consent was obtained from the patient for publication of this report and any accompanying images.

Conflict-of-interest statement: All authors declare no relevant conflicts of interest for this article.

CARE Checklist (2016) statement: The authors have read the CARE Checklist (2016), and the manuscript was prepared and revised according to the CARE Checklist (2016).

Country/Territory of origin: China

ORCID number: Xin-Xin Luo 0009-0000-2479-3779; Yu-Xuan Du 0009-0000-5043-7049; Qi-Qing Zhang 0009-0009-2666-0182; Lin Zhang 0009-0003-1964-2142; Shu-Ying Zeng 0009-0009-7495-4994; Zhi-Hong Yu 0000-0001-8304-1833; Peng Shen 0000-0002-1123-9848; Zheng-Quan Feng 0009-0001-9060-8671.

S-Editor: Zheng XM
L-Editor: A
P-Editor: Yu HG

REFERENCES

1 **Copur MS**, Manapuram S. Multiple Primary Tumors Over a Lifetime. *Oncology (Williston Park)* 2019; **33**: 629384 [PMID: 31365752]
2 **Marano L**. Dual primary gastric and colorectal cancer: A complex challenge in surgical oncology. *World J Gastrointest Oncol* 2023; **15**: 2049-2052 [PMID: 38173432 DOI: 10.4251/wjgo.v15.i12.2049]
3 **Warren S**, Gates O. Multiple primary malignant tumors: A survey of the literature and statistical study. *Am J Cancer* 1932; **16**: 1358-1414

4 **Cai YL**. The clinical characteristics and prognosis of 234 multiple primary cancer patients. Ph.D. Dissertation, College of Medicine, Zhejiang University. 2018. Available from: https://kns.cnki.net/kcms2/article/abstract?v=Dl4MPbsAiWcWfY1btBpXwon0GWs-VxBEj_37ZWm1q_t3uH8sc0Wf3CRY5P8ml1XcPyCEDW2us9-bcEm85ynmrOOMQ8D7wZNipvgiEuAToM0SxI3-eDAiVH1yGarm0vZiTaoUWQn7XLQ=&uniplatform=NZKPT&flag=copy

5 **Natsugoe S**, Matsumoto M, Okumura H, Ishigami S, Uenosono Y, Owaki T, Takao S, Aikou T. Multiple primary carcinomas with esophageal squamous cell cancer: clinicopathologic outcome. *World J Surg* 2005; **29**: 46-49 [PMID: 15592914 DOI: 10.1007/s00268-004-7525-y]

6 **Baba Y**, Yoshida N, Kinoshita K, Iwatsuki M, Yamashita YI, Chikamoto A, Watanabe M, Baba H. Clinical and Prognostic Features of Patients With Esophageal Cancer and Multiple Primary Cancers: A Retrospective Single-institution Study. *Ann Surg* 2018; **267**: 478-483 [PMID: 28151796 DOI: 10.1097/SLA.0000000000002118]

7 **Su XY**, Yan Y, Jiang Q, Xia JH. [Overall survival analysis of double primary cancer patients with esophageal cancer as the first primary cancer]. *Zhonghua Xiaohuabing Yu Yingxiang Zazhi* 2021; **11**: 121-125

8 **Vogt A**, Schmid S, Heinimann K, Frick H, Herrmann C, Cerny T, Omlin A. Multiple primary tumours: challenges and approaches, a review. *ESMO Open* 2017; **2**: e000172 [PMID: 28761745 DOI: 10.1136/esmoopen-2017-000172]

9 **Kitagawa Y**, Uno T, Oyama T, Kato K, Kato H, Kawakubo H, Kawamura O, Kusano M, Kuwano H, Takeuchi H, Toh Y, Doki Y, Naomoto Y, Nemoto K, Booka E, Matsubara H, Miyazaki T, Muto M, Yanagisawa A, Yoshida M. Esophageal cancer practice guidelines 2017 edited by the Japan Esophageal Society: part 1. *Esophagus* 2019; **16**: 1-24 [PMID: 30171413 DOI: 10.1007/s10388-018-0641-9]

10 **National Comprehensive Cancer Network**. National Comprehensive Cancer Network guidelines: Colon cancer. Version 1. 2022

11 **Cheng G**, Jiang XD, Zhang HP, Yang P, Liu H, Gu KS. [Clinical observation of 54 cases of non-surgical esophageal cancer treated with capecitabine rhythm chemotherapy combined with concurrent dose modulated radiation therapy]. *Shandong Yiyao* 2017; **57**: 87-89

12 **Cheng XY**, Wu H, Zhang RR, Sun XM, Yan ZM, Liu X, Chen YS. [Prognostic analysis of 307 cases of stage II-III esophageal cancer treated with concurrent radiotherapy and chemotherapy]. *Zhonghua Fangshe Zhongliuxue Zazhi* 2018; **27**: 140-144

World Journal of Clinical Cases

Submit a Manuscript: https://www.f6publishing.com

World J Clin Cases 2024 May 26; 12(15): 2655-2663

DOI: 10.12998/wjcc.v12.i15.2655

ISSN 2307-8960 (online)

CASE REPORT

Transformation of marginal zone lymphoma into high-grade B-cell lymphoma expressing terminal deoxynucleotidyl transferase: A case report

Zhi-Min Fan, Dao-Lei Wu, Neng-Wen Xu, Li Ye, Li-Ping Yan, Lin-Jie Li, Jun-Yu Zhang

Specialty type: Medicine, research and experimental

Provenance and peer review: Unsolicited article; Externally peer reviewed.

Peer-review model: Single blind

Peer-review report's classification
Scientific Quality: Grade C
Novelty: Grade B
Creativity or Innovation: Grade B
Scientific Significance: Grade B

P-Reviewer: Kawabata H, Japan

Received: February 8, 2024
Revised: March 15, 2024
Accepted: April 9, 2024
Published online: May 26, 2024

Zhi-Min Fan, Neng-Wen Xu, Lin-Jie Li, Jun-Yu Zhang, Department of Hematology, Lishui Municipal Central Hospital, Lishui 323000, Zhejiang Province, China

Dao-Lei Wu, Department of Ophthalmology, Lishui Municipal Central Hospital, Lishui 323000, Zhejiang Province, China

Li Ye, Department of General Practice, Lishui Municipal Central Hospital, Lishui 323000, Zhejiang Province, China

Li-Ping Yan, Department of Pathology, Lishui Municipal Central Hospital, Lishui 323000, Zhejiang Province, China

Corresponding author: Dao-Lei Wu, MMed, Attending Doctor, Department of Ophthalmology, Lishui Municipal Central Hospital, No. 289 Kuocang Road, Lishui 323000, Zhejiang Province, China. zxnhh1967@163.com

Abstract

BACKGROUND

High-grade B-cell lymphoma (HGBL) is an unusual malignancy that includes myelocytomatosis viral oncogene (*MYC*), B-cell lymphoma-2 (*BCL-2*), and/or *BCL-6* rearrangements, termed double-hit or triple-hit lymphomas, and HGBL-not otherwise specific (HGBL-NOS), which are morphologically characteristic of HGBL but lack *MYC*, *BCL-2*, or *BCL-6* rearrangements. HGBL is partially transformed by follicular lymphoma and other indolent lymphoma, with few cases of marginal zone lymphoma (MZL) transformation. HGBL often has a poor prognosis and intensive therapy is currently mainly advocated, but there is no good treatment for these patients who cannot tolerate chemotherapy.

CASE SUMMARY

We reported a case of MZL transformed into HGBL-NOS with *TP53* mutation and terminal deoxynucleotidyl transferase expression. Gene analysis revealed the gene expression profile was identical in the pre- and post-transformed tissues, suggesting that the two diseases are homologous, not secondary tumors. The chemotherapy was ineffective and the side effect was severe, so we tried combination therapy including venetoclax and obinutuzumab. The patient tolerated treatment well, and reached partial response. The patient had recurrence of hepatocellular carcinoma and died of multifunctional organ failure. He

survived for 12 months after diagnosis.

CONCLUSION
Venetoclax combined with obinutuzumab might improve the survival in some HGBL patients, who are unsuitable for chemotherapy.

Key Words: Marginal zone lymphoma; High-grade B-cell lymphoma; Terminal deoxynucleotidyl transferase; Venetoclax; *TP53* mutation; Case report

Core Tip: Marginal zone lymphoma (MZL) are a group of B-cell malignant neoplastic diseases with the most common transformation to diffuse large B-cell lymphoma. Herein, we report one rare case of MZL converted to high-grade B-cell lymphoma, not otherwise specific (HGBL-NOS) and concomitant terminal deoxynucleotidyl transferase expression in a 63-year-old male for the first time. HGBL-NOS often has a poor prognosis. The current treatment advocates high-dose chemotherapy, but there is currently no effective treatment for patients who cannot tolerate chemotherapy. We have attempted targeted pharmacological combinations and achieved certain therapeutic effects, which may provide new treatment for these patients.

Citation: Fan ZM, Wu DL, Xu NW, Ye L, Yan LP, Li LJ, Zhang JY. Transformation of marginal zone lymphoma into high-grade B-cell lymphoma expressing terminal deoxynucleotidyl transferase: A case report. *World J Clin Cases* 2024; 12(15): 2655-2663
URL: https://www.wjgnet.com/2307-8960/full/v12/i15/2655.htm
DOI: https://dx.doi.org/10.12998/wjcc.v12.i15.2655

INTRODUCTION

Marginal zone lymphomas (MZLs) are a group of B-cell indolent malignant diseases with the possibility of transformation to aggressive lymphoma, often to diffuse large B-cell lymphomas (DLBCLs)[1]. *MYC* rearrangements have been detected in 5%-15% of DLBCLs, often with mutations in *BCL-2* and/or *BCL-6*, which is defined as high-grade B-cell lymphoma (HGBL) according to the 2016 World Health Organization classification[2,3]. In HGBL cases, the *MYC* rearrangement is termed a double attack when it is mutated with *BCL-2* or *BCL-6* and a triple attack when it is mutated with *BCL-2* and *BCL-6*, in addition to a specific subtype called HGBL-not otherwise specific (HGBL-NOS), which is morphologically characterized as a HGBL but lacks the genetic appearance of the *MYC*, *BCL-2*, or *BCL-6* rearrangement [1]. Terminal deoxynucleotidyl transferase (TDT) is often considered a marker for immature cells and is of importance in the diagnosis of B-lymphoblastoma/leukemia. However, in recent reports, a small proportion of HGBL cases were positive for TDT[4]. We recently identified a patient with MZL who converted to HGBL-NOS and concomitant TDT expression. To our knowledge, this is the first case of HGBL-NOS from MZL.

CASE PRESENTATION

Chief complaints

A 63-year-old man came to the hospital because of bilateral swollen lymph nodes.

History of present illness

In April 2020, the patient received a pathological examination performed on a right cervical lymph node biopsy and immunohistochemical examination revealed that the infiltrating cells were positive for cluster of differentiation 20 (CD20), paired box 5 (PAX5), BCL-2, CD21, CD23, and Ki-67 staining of 10%, and were negative for CD10, BCL-6, CyclinD1, sry-related HMG-box 11 (SOX-11), CD3, and CD5 (Figure 1). The involvement of bone marrow was not found. Positron emission tomography (PET)-computed tomography (CT) scan demonstrated mildly enlarged bilateral cervical lymph nodes (SUVmax: 5.4), and cirrhosis.The patient was diagnosed with MZL (Ann Arbor stage IIA, IPI 1 score). The patient refused radiation therapy, so we gave him 2 cycles of rituximab, cyclophosphamide, doxorubicin, vindesine and prednisone (R-CHOP). The enlarged lymph nodes disappeared after 2 cycles; however, the toxicity of chemotherapy was severe, so we reduced the dose of the drug (R-minCHOP). The patient reached complete response after 2 cycles, then he stopped chemotherapy, and the disease was stable during the follow-up period.

In April 2022, new lesions appeared, with notably enlarged lymph nodes on the right side of the neck. The patient then received a lymph node biopsy again. The lymph node was replaced by diffuse medium-to small tumor cells, with multifocal, and massive necrosis. Immunohistochemical examination showed that the cells were positive for CD20, BCL-2, CD10, and CD5, partially expressing TDT, but negative for BCL-6, CyclinD1, SOX-11, CD3, PAX5, CD21, and Ki-67

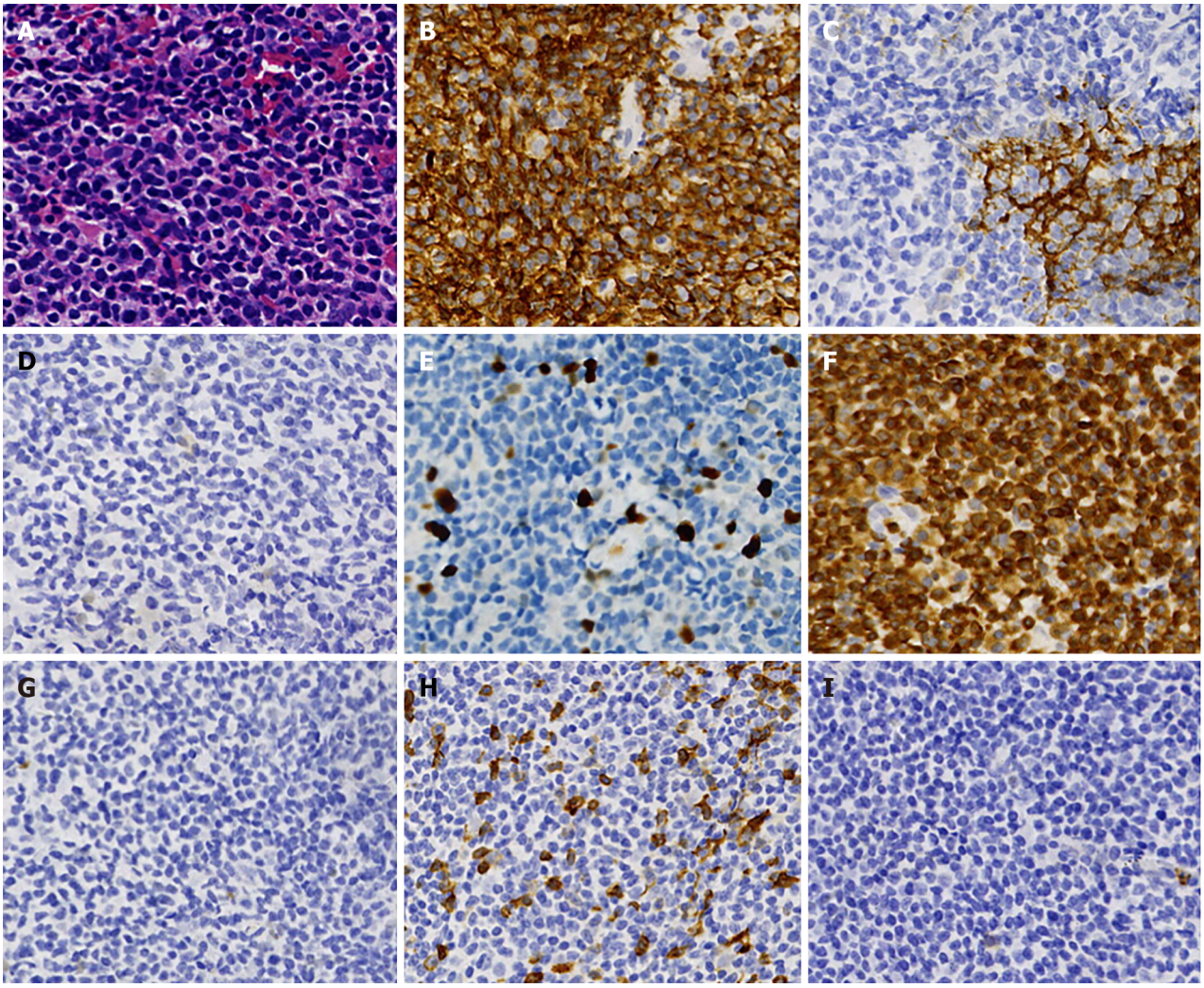

Figure 1 Immunohistochemistry and cellular morphology of the first lymph node biopsy. A: Tumor cells are diffuse, small to medium in size, with a slightly irregular nucleus. The lymphocytic hyperplasia shows partial cytoplasmic empty and a fuzzy nodular distribution (hematoxylin and eosin, 400 ×); B-I: The majority of the infiltrating cells were positive for CD20 (B), PAX5, B-cell lymphoma-2 (BCL-2) (F), CD21, CD23 (C), and negative for CD10 (I), CD5 (H), BCL-6 (G), and CyclinD1 (D). Their Ki-67 (E) showed approximately 10% (EnVision, 400 ×).

staining of approximately 30% (Figure 2). Therefore, the pathologic diagnosis of MZL with the possibility of transformation into HGBL was given. The PET-CT scans demonstrated that partial necrosis and multiple enlarged lymph nodes were observed on the right side of the cervix, with a large diameter of 2.2 cm (SUVmax: 7.6), and an enlarged lymph node in the right anterior aspect of the new ascending aorta, with a diameter of 0.9 cm (SUVmax: 7.2). Moreover, there was a new nodule in the liver measuring 2.9 cm × 2.0 cm (SUVmax 2.4), which was considered a recurrence of liver cancer. After the patient underwent hepatic artery chemoembolization and radiofrequency ablation of hepatocellular carcinoma, he received ultrasound-guided coarse-needle aspiration in the right cervical mass. Immunohistochemical staining showed that the neoplastic cells were positive for CD20, PAX5, CD5, TDT, BCL-2 (approximately 90%), CD10, C-MYC, CD7, CD43, MUM1, CD99 and Ki-67 staining of approximately 80% but negative for BCL-6, myeloperoxidase, CD34, CyclinD1, CD21, and CD3 (Figure 3). The CT scan showed the mass on the right side of the neck, measuring 6.4 cm × 4.0 cm.

History of past illness

The patient had a history of liver cancer and underwent surgical treatment in 2010.

Personal and family history

The patient had no remarkable personal or family history.

Physical examination

Physical examination showed bilateral mildly enlarged lymph nodes in the neck.

Laboratory examinations

The involvement of bone marrow was not found. Routine laboratory tests, including peripheral blood cells, lactic

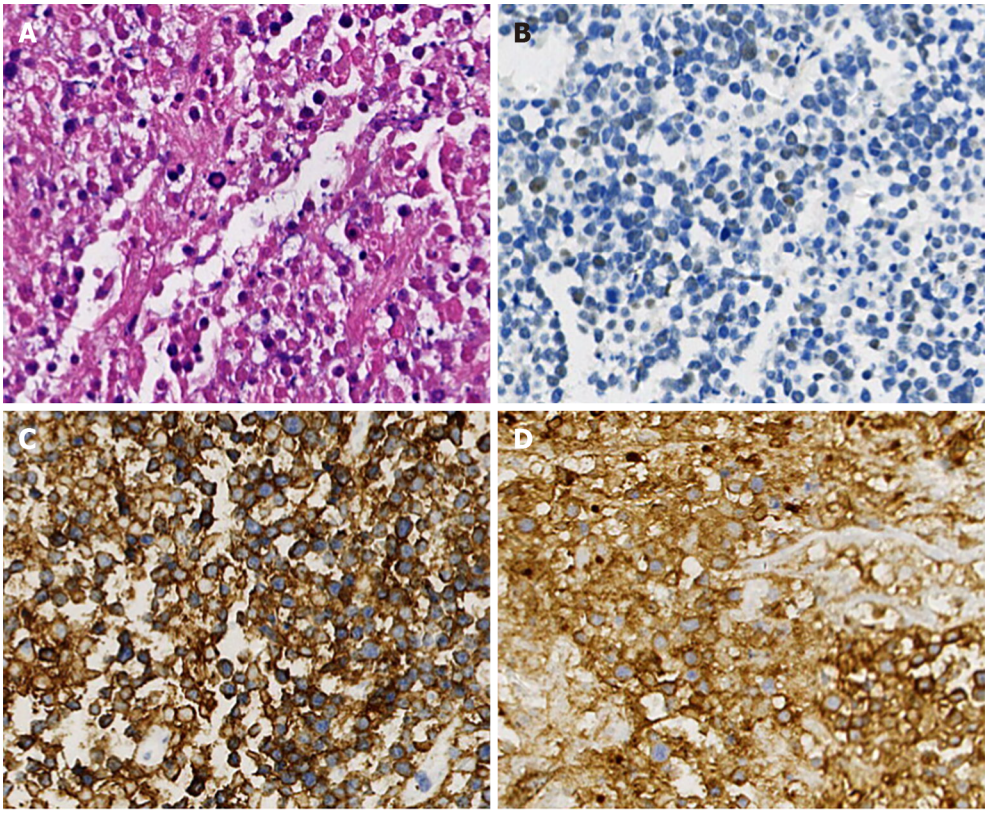

Figure 2 Immunohistochemistry and histopathology of the second lymph node biopsy. A: The lymph node was replaced by diffuse medium to small tumor cells, with multifocal and massive necrosis (hematoxylin and eosin, 400 ×); B-D: Immunohistochemistry showed the positives of CD20 (C), CD10 (D), and CD5, partially positive of terminal deoxynucleotidyl transferase (B) for tumor cells (EnVision, 400 ×).

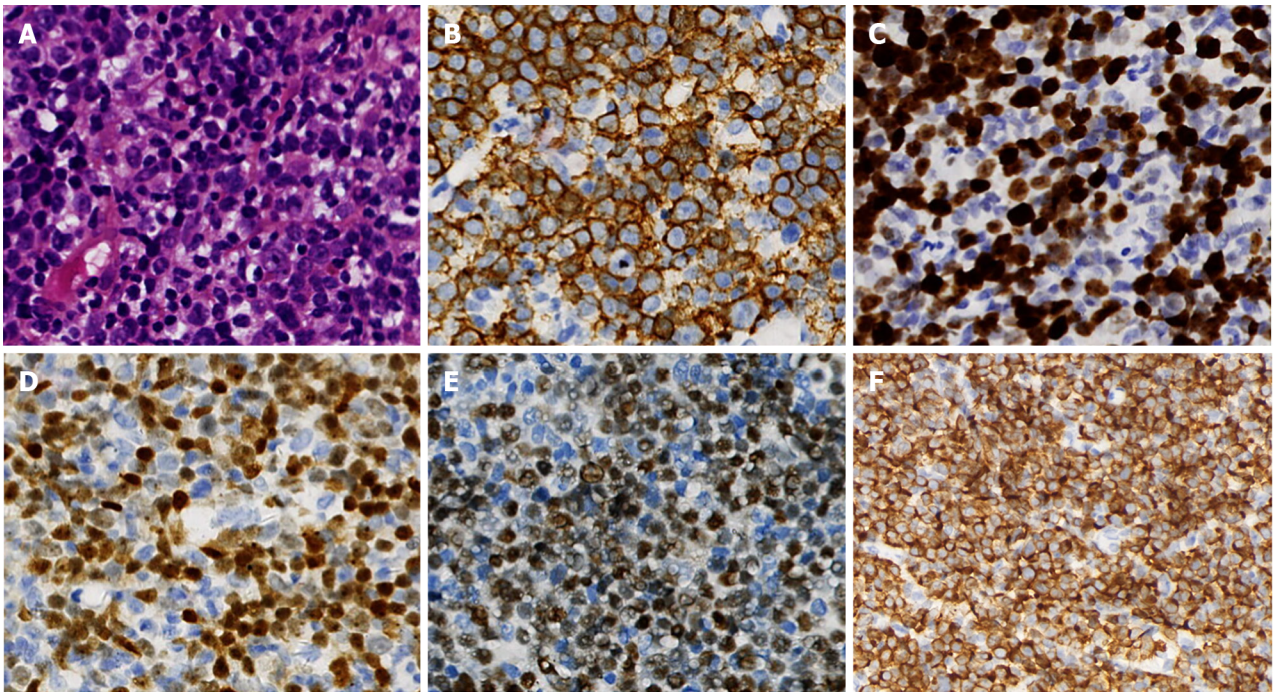

Figure 3 Immunohistochemistry and cellular morphology of the third lymph node biopsy. A: The lymph node was infiltrated diffusely by medium to moderately large tumor cells, which showed little to moderate cytoplasm, round oval or slightly depressed nuclei with slightly rough chromatin and nucleoli (hematoxylin and eosin, 400 ×); B-F: The neoplastic cells were positive for CD20 (B), terminal deoxynucleotidyl transferase (D), B-cell lymphoma-2 (F) (about 90%), C-myelocytomatosis viral oncogene (E) (about 70%), Ki-67 (C) (approximately 80%), immunohistchemically (EnVision, 400 ×).

dehydrogenase (168 U/L), liver, and renal function, were normal and the virus tests consisted of viral hepatitis B and epstein-barr virus were negative. The reexamination of bone marrow and routine laboratory tests were still normal, including lactate dehydrogenase (LDH) (195 U/L). Fluorescence in situ hybridization (FISH) analysis revealed positivity for the *MYC* gene but negativity for *BCL-2* and *BCL-6* (Figure 4). *MYC*/immunoglobulin heavy chain (*IGH*) rearrangement was confirmed by FISH examination. Retrospectively, we performed a next generation sequencing analysis of specimens of the mass before and after transformation. The mutational results before transformation showed that *TP53*, *PHF6*, *TPMT*, *HIST1H1C*, *KMT2D*, *SETD2*, *TNFAIP3* and *TRAF3* were positive, and after conversion, they still showed the same mutations, but the frequency of gene mutations decreased compared to before (Figure 5).

Imaging examinations

In April 2020, a PET-CT scan demonstrated mildly enlarged bilateral cervical lymph nodes (SUVmax: 5.4), and cirrhosis.

In April 2022, a follow-up PET-CT scan showed that partial necrosis and multiple enlarged lymph nodes were observed on the right side of the cervix, with a large diameter of 2.2 cm (SUVmax: 7.6), and an enlarged lymph node in the right anterior aspect of the new ascending aorta, with a diameter of 0.9 cm (SUVmax: 7.2). Moreover, there was a new nodule in the liver measuring 2.9 cm × 2.0 cm (SUVmax: 2.4), which was considered a recurrence of liver cancer. And 2 months later, the CT scan showed the mass on the right side of the neck, measuring 6.4 cm × 4.0 cm.

FINAL DIAGNOSIS

Based on histological, immunohistochemical, and consultation findings, a final diagnosis of *MYC*-rearranged HGBL, NOS, stage II, and IPI2 with TDT expression was made.

TREATMENT

We first diagnosed the patient as having B-lymphoblastic lymphoma because the atypical cells were positive for TDT and CD99. The tumor had been rapidly enlarging, so treatment was started immediately under a tentative diagnosis. The patient started on a combination of Gemox (oxaliplatin and gemcitabine) with lenalidomide, which was not effective. Then we changed it into BTK inhibitor (zanubrutinib), but the regimen was still ineffective. FISH analysis revealed positivity for the *MYC* gene but negativity for *BCL-2* and *BCL-6* (Figure 4). *MYC*/*IGH* rearrangement was confirmed by FISH examination. Due to the diagnostic dilemma, we undertook a pathology consultation with Gandi Li, Professor of Pathology at West China Hospital. Based on histological, immunohistochemical, and consultation findings, a final diagnosis of *MYC* rearranged HGBL, NOS, stage II, and IPI2 with TDT expression was made.

Subsequently, we given him a modified Hyper CVAD A regimen (cyclophosphamide, vincristine, mitoxantrone liposomal and dexamethasone) combined with obinutuzumab, when the diagnosis of HGBL-NOS was made. After two cycles of treatment, the cervical enhanced CT found the lesion was markedly reduced, measuring 1.7 cm × 3.3 cm. However, our patient developed myelosuppression followed severe infections and liver dysfunction. Depending on the previous response to therapy and drug-related toxicity we thought that conventional chemotherapy was inadequet. Therefore, we attempted to treat our patient with targeted combination therapies, and a new induction with obinutuzumab and venclexta was given.

OUTCOME AND FOLLOW-UP

Fortunately, the cervical mass disappeared after 2 cycles, and a partial response was achieved. The patient experienced no serious complications. Therefore, the treatment was continued, although the arch nodes of the ascending aorta were not reduced but were also in stable condition. However, the CT scan of the abdomen showed multiple lesions in the liver 6 months later. The patient also had fever, abdominal effusion, and pancytopenia, and we had to stop the therapy because of the severe situation. He was transferred to a local hospital for palliative care and died of multivisceral failure a few weeks later.

DISCUSSION

MZLs have the possibility of transformation to aggressive lymphoma, often to DLBCL. Conconi *et al*[5] retrospectively analyzed the clinical data of 373 patients with MZL, and the rate of pathological tissue transformation was 4%, of which 12 converted to DLBCL. Clinical characteristics at the time of initial MZL diagnosis that have been associated with the development of a transformation are elevated levels of LDH, advanced (III-IV) Ann Arbor stage, involvement of more than four nodal sites, a high follicular lymphoma international prognostic index score, history of cancer, and failure to achieve complete remission after first-line treatment[6]. The mechanism of transformation was still unclear. Some finds showed that *KMT2D*/*MLL2*, *TP53*, *NOTCH2*, and *TRAF3* mutations may be associated with an increased risk of transformation[7]. In our patient, liver cancer and a history of chemotherapy, *TP53* mutations, may confer a high transla-

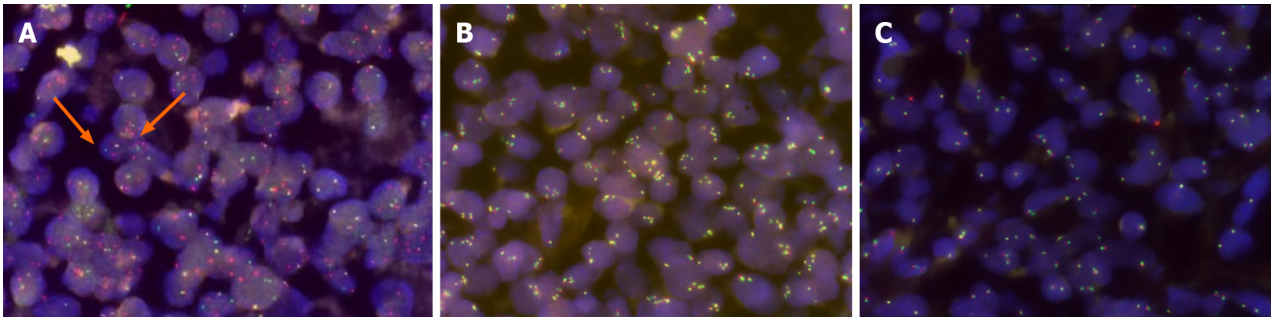

Figure 4 Fluorescence in situ hybridization of the third lymph node. A: The fluorescence in situ hybridization analysis was performed using probed from Vysis. 3'myelocytomatosis viral oncogene (MYC)-green spectrum, 5'MYC-red spectrum. White arrows indicate the signal of *MYC*-rearrangement; B and C: B-cell lymphoma-2 (*BCL-2*) (B) and *BCL-6* (C) rearrangements were negative.

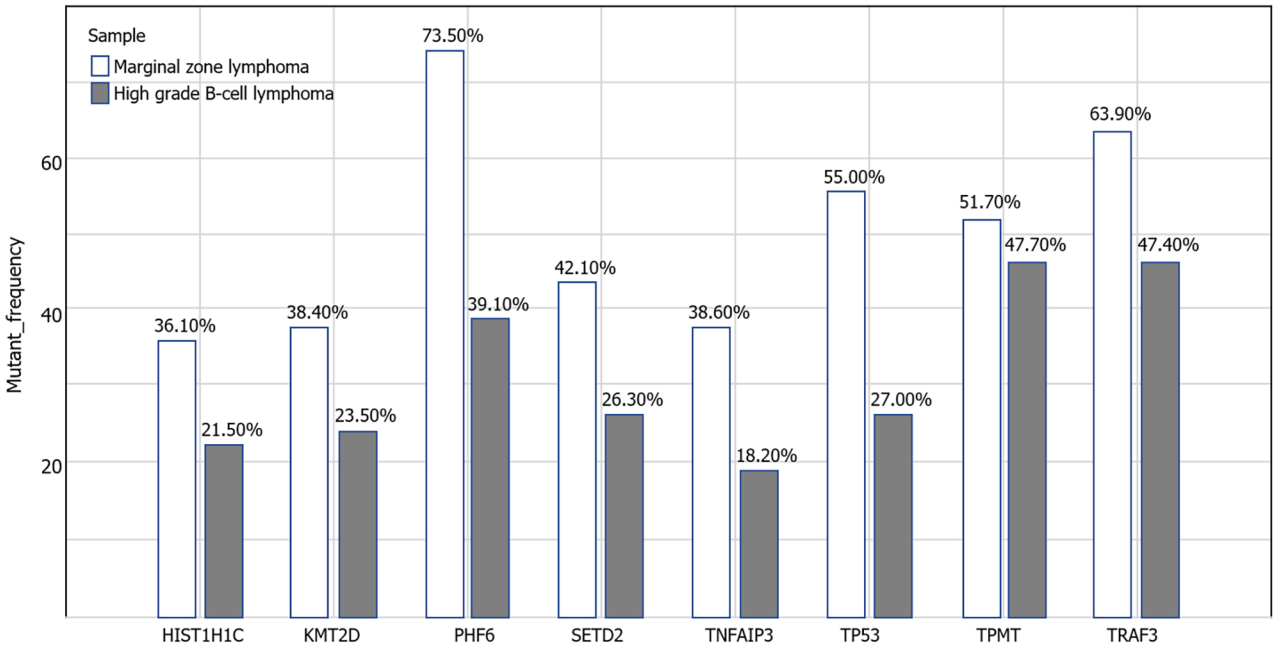

Figure 5 Next generation sequencing of tumor cells before and after transformation. Before transformation, *TP53*, *PHF6*, *TPMT*, *HIST1H1C*, *KMT2D*, *SETD2*, *TNFAIP3* and *TRAF3* were positive for tumor cells. Compared with before, they still had the same mutation but the mutation frequency was decreased.

tional risk and poor prognosis.

HGBL is an uncommonly aggressive B-cell malignancy that includes double-hit lymphoma (DHL), triple-hit lymphoma (THL) and HGBL-NOS[1]. HGBL-NOS are rare and heterogeneous, including tumors with Burkitt-like or blastoid morphology. However, there is some controversy regarding the diagnosis of this subtype, and the criteria for diagnosis are as follows: (1) Invasive mature B-cell lymphoma composed of medium-sized or blastocyte-like cells; and (2) Exclusion of other specific types of lymphoma[8]. Accurate classification requires evaluation by cytomorphology, immunohistochemistry, and FISH. In a pathologic study, they found that CD10, BCL-6 and BCL-2 were expressed in cases[9]. Another study described that among confirmed HGBLs, *MYC-R* was present in 46%, and the most common mutations involved *KMT2D* and *TP53*[10]. The Burkitt-like variant of HGBL-NOS was morphologically indistinguishable from BL but was negative for *MYC* rearrangement[9]. Blastoid HGBL, NOS, needs to be distinguished from B-lymphoblastic lymphoma, which always expresses TDT or CD34, whereas the emergence of *MYC* or *BCL-2* rearrangement is rare [11]. TDT is considered an immature marker that can be expressed in both T-cell and B-cell malignancies[12]. We first diagnosed our patient as having B-cell lymphoblastic lymphoma (B-LBL). However, B-LBL often occurs preferentially among young individuals under 18 years of age[13], and the expression of CD20 is negative in most cases[14]. Depending on the clinical features of our patient, we consider HGBL-NOS to be a more appropriate diagnosis for the patient. Reports that TDT is expressed in HGBL are not uncommon, often in the patients with DHL or THL[15]. Some cases were transformations from follicular lymphoma or other indolent B-cell lymphomas, but cases of HGBL-NOS with TDT expression have not been described.

The traditional view is that HGBL has a poor prognosis, particularly in patients with DHL or THL. Currently, there are no reliable data on prognostic factors specific to HGBL-NOS. A study of 2383 DLBCLs found no significant difference in outcomes between DLBCL with or without a single-hit *MYC-R*[16]. Some neoplasms were diagnosed as DLBCL having

striking biological similarities to HGBL, which are called molecular high-grade lymphomas. And the response to the R-CHOP regimen was poor, and the 3-year progression-free survival (PFS) was only 37% after treatment[17]. *TP53* alteration is always considered an independent adverse prognostic factor[18]. HGBL, NOS, with concurrent *MYC-R* and *TP53* alterations (deletion or mutation), often had complex karyotypes and dismal outcomes, which might further expand the molecular HGBL category[19].

As the first-line treatment, R-CHOP is still considered the preferred regimen for patients with early/limited-stage HGBL-NOS. The controversy of treatment in HGBL-NOS is whether intensified regimens are necessary. A study from Chinese cases showed that only 43% of patients achieved CR, and the disease relapsed soon after chemotherapy with R-CHOP. The median overall survival (OS) was 9 months, and there was no difference between DHL and *MYC-R* status [17]. These data suggest that R-CHOP may not be suitable for patients with advanced-stage HGBL, NOS, DHL or high-risk DLBCL, and we favor high-dose chemotherapy regimens. A study of patients with central nervous system involvement who received treatment with rituximab, cyclophosphamide, vincristine, doxorubicin, high-dose methotrexate/isocyclophosphamide, etoposide, and high-dose cytarabine showed that the 2-year PFS was 68%. However, toxicities were obvious, with grade 4 neutropenia in 88%[20]. Therefore, it is believed that high-dose chemotherapy may be appropriate for younger patients and in better general condition. However, in a recent retrospective analysis, only patients with advanced stage disease had significantly improved PFS with an intensified regimen, but the impact of a prolonged OS was small[21]. Therefore, further exploration of appropriate therapeutic options is still warranted. A trial of chimeric antigen receptor-T-cell therapy in high-risk DLBCLs, showed encouraging results (12-month OS 91%)[22]. Meanwhile, some researchers believe that combination therapy with targeted drugs can be attempted in these unfit patients[23]. A multicenter study of venetoclax in combination with bendamustine-rituximab in patients with relapsed/refractory non-Hodgkin's lymphoma showed that the regimen is superior in the treatment of aggressive lymphoma compared with indolent lymphoma, suggesting that the efficacy of venetoclax may be related to the expression of BCL-2 in different subtypes[24].

CONCLUSION

In the case reported here, the patient converted from MZL to HGBL after repeated chemotherapy and was unable to tolerate high-intensity chemotherapy and hematopoietic stem cell transplantation. There are no good treatments for these patients. In conjunction with the data from previous studies, we initiated treatment with venetoclax in combination with obinutuzumab based on pathological immunohistochemical BCL-2 overexpression and CD20 positivity. The patient achieved a partial response, and chemotherapy was tolerable. Although the patient eventually died, we still believed that venetoclax may have the opportunity to improve survival in some patients with HGBL, especially in those with high BCL-2 expression. However,additional data are needed to determine the safety and efficacy of combination therapy between targeted drugs.

ACKNOWLEDGEMENTS

The authors would like to thank the patient and families for their cooperation in this study.

FOOTNOTES

Author contributions: Fan ZM and Wu DL contributed equally to this work; Fan ZM and Wu DL wrote the first draft of the manuscript; Yan LP participation in pathological analysis; Xu NW, Ye L, Li LJ and Zhang JY revised the manuscript. All authors have read and approve the final manuscript.

Supported by The Lishui Science and Technology Planing Projects, No. 2020SJZC048.

Informed consent statement: The patient's daughter and wife provided written informed consent.

Conflict-of-interest statement: The authors declare that they have no conflict of interest.

CARE Checklist (2016) statement: The authors have read the CARE Checklist (2016), and the manuscript was prepared and revised according to the CARE Checklist (2016).

Country/Territory of origin: China

ORCID number: Zhi-Min Fan 0000-0002-2553-520X; Dao-Lei Wu 0009-0008-1152-8472; Lin-Jie Li 0000-0003-2674-2996; Jun-Yu Zhang 0000-

0002-1013-8172.

S-Editor: Zheng XM
L-Editor: A
P-Editor: Yu HG

REFERENCES

1 **Swerdlow SH**, Campo E, Pileri SA, Harris NL, Stein H, Siebert R, Advani R, Ghielmini M, Salles GA, Zelenetz AD, Jaffe ES. The 2016 revision of the World Health Organization classification of lymphoid neoplasms. *Blood* 2016; **127**: 2375-2390 [PMID: 26980727 DOI: 10.1182/blood-2016-01-643569]

2 **Niitsu N**, Okamoto M, Miura I, Hirano M. Clinical features and prognosis of de novo diffuse large B-cell lymphoma with t(14;18) and 8q24/c-MYC translocations. *Leukemia* 2009; **23**: 777-783 [PMID: 19151788 DOI: 10.1038/leu.2008.344]

3 **Snuderl M**, Kolman OK, Chen YB, Hsu JJ, Ackerman AM, Dal Cin P, Ferry JA, Harris NL, Hasserjian RP, Zukerberg LR, Abramson JS, Hochberg EP, Lee H, Lee AI, Toomey CE, Sohani AR. B-cell lymphomas with concurrent IGH-BCL2 and MYC rearrangements are aggressive neoplasms with clinical and pathologic features distinct from Burkitt lymphoma and diffuse large B-cell lymphoma. *Am J Surg Pathol* 2010; **34**: 327-340 [PMID: 20118770 DOI: 10.1097/PAS.0b013e3181cd3aeb]

4 **Moench L**, Sachs Z, Aasen G, Dolan M, Dayton V, Courville EL. Double- and triple-hit lymphomas can present with features suggestive of immaturity, including TdT expression, and create diagnostic challenges. *Leuk Lymphoma* 2016; **57**: 2626-2635 [PMID: 26892631 DOI: 10.3109/10428194.2016.1143939]

5 **Conconi A**, Franceschetti S, Aprile von Hohenstaufen K, Margiotta-Casaluci G, Stathis A, Moccia AA, Bertoni F, Ramponi A, Mazzucchelli L, Cavalli F, Gaidano G, Zucca E. Histologic transformation in marginal zone lymphomas†. *Ann Oncol* 2015; **26**: 2329-2335 [PMID: 26400898 DOI: 10.1093/annonc/mdv368]

6 **Alderuccio JP**, Zhao W, Desai A, Gallastegui N, Ramdial J, Kimble E, de la Fuente MI, Rosenblatt JD, Chapman JR, Vega F, Reis IM, Lossos IS. Risk Factors for Transformation to Higher-Grade Lymphoma and Its Impact on Survival in a Large Cohort of Patients With Marginal Zone Lymphoma From a Single Institution. *J Clin Oncol* 2018; JCO1800138 [PMID: 30312133 DOI: 10.1200/JCO.18.00138]

7 **Onaindia A**, Medeiros LJ, Patel KP. Clinical utility of recently identified diagnostic, prognostic, and predictive molecular biomarkers in mature B-cell neoplasms. *Mod Pathol* 2017; **30**: 1338-1366 [PMID: 28664939 DOI: 10.1038/modpathol.2017.58]

8 **Olszewski AJ**, Kurt H, Evens AM. Defining and treating high-grade B-cell lymphoma, NOS. *Blood* 2022; **140**: 943-954 [PMID: 34525177 DOI: 10.1182/blood.2020008374]

9 **Hüttl KS**, Staiger AM, Richter J, Ott MM, Kalmbach S, Klapper W, Biesdorf AS, Trümper L, Rosenwald A, Ziepert M, Horn H, Ott G. The "Burkitt-like" immunophenotype and genotype is rarely encountered in diffuse large B cell lymphoma and high-grade B cell lymphoma, NOS. *Virchows Arch* 2021; **479**: 575-583 [PMID: 33655392 DOI: 10.1007/s00428-021-03050-4]

10 **Collinge BJ**, Hilton LK, Wong J, Ben-Neriah S, Rushton CK, Slack GW, Farinha P, Cook JR, Ott G, Rosenwald A, Campo E, Amador C, Greiner TC, Raess PW, Song JY, Inghirami G, Jaffe ES, Weisenburger DD, Chan WC, Holte H, Beiske K, Fu K, Delabie J, Pittaluga S, Feldman AL, Savage KJ, Mungall AJ, Staudt LM, Steidl C, Rimsza LM, Morin RD, Scott DW. Characterization of the genetic landscape of high-grade B-cell lymphoma, NOS – an llmpp project. *Hematol Oncol* 2021; **39**: 157-159 [DOI: 10.1002/hon.13_2880]

11 **Moore EM**, Aggarwal N, Surti U, Swerdlow SH. Further Exploration of the Complexities of Large B-Cell Lymphomas With MYC Abnormalities and the Importance of a Blastoid Morphology. *Am J Surg Pathol* 2017; **41**: 1155-1166 [PMID: 28614202 DOI: 10.1097/PAS.0000000000000818]

12 **Jaffe ES**, Campo E, Harris NL, Pileri SA, Stein H, Swerdlow SH. Introduction and overview of the classification of lymphoid neoplasms. In: Swerdlow SH, Campo E, Harris NL, Jaffe ES, Pileri SA, Stein H, Thiele J, Arber DA, Hasserjian RP, Le Beau MM, Orazi A, Siebert R, editors. WHO Classification of Tumours of Haematopoietic and Lymphoid Tissues. Revised 4th ed. Lyon: IARC Press, 2017: 190-198

13 **Borowitz MJ**, Chan JKC, Downing JR, Le Beau MM, Arber DA. B-lymphoblastic leukemia/Lymphoma, not otherwise specified (NOS). In: Swerdlow SH, Campo E, Harris NL, Jaffe ES, Pileri SA, Stein H, Thiele J, Arber DA, Hasserjian RP, Le Beau MM, Orazi A, Siebert R, editors. WHO Classification of Tumours of Haematopoietic and Lymphoid Tissues. Revised 4th ed. Lyon: IARC Press, 2017: 200-202

14 **Bassan R**, Maino E, Cortelazzo S. Lymphoblastic lymphoma: an updated review on biology, diagnosis, and treatment. *Eur J Haematol* 2016; **96**: 447-460 [PMID: 26679753 DOI: 10.1111/ejh.12722]

15 **Ok CY**, Medeiros LJ, Thakral B, Tang G, Jain N, Jabbour E, Pierce SA, Konoplev S. High-grade B-cell lymphomas with TdT expression: a diagnostic and classification dilemma. *Mod Pathol* 2019; **32**: 48-58 [PMID: 30181564 DOI: 10.1038/s41379-018-0112-9]

16 **Rosenwald A**, Bens S, Advani R, Barrans S, Copie-Bergman C, Elsensohn MH, Natkunam Y, Calaminici M, Sander B, Baia M, Smith A, Painter D, Pham L, Zhao S, Ziepert M, Jordanova ES, Molina TJ, Kersten MJ, Kimby E, Klapper W, Raemaekers J, Schmitz N, Jardin F, Stevens WBC, Hoster E, Hagenbeek A, Gribben JG, Siebert R, Gascoyne RD, Scott DW, Gaulard P, Salles G, Burton C, de Jong D, Sehn LH, Maucort-Boulch D. Prognostic Significance of MYC Rearrangement and Translocation Partner in Diffuse Large B-Cell Lymphoma: A Study by the Lunenburg Lymphoma Biomarker Consortium. *J Clin Oncol* 2019; **37**: 3359-3368 [PMID: 31498031 DOI: 10.1200/JCO.19.00743]

17 **Li J**, Liu X, Yao Z, Zhang M. High-Grade B-Cell Lymphomas, Not Otherwise Specified: A Study of 41 Cases. *Cancer Manag Res* 2020; **12**: 1903-1912 [PMID: 32214848 DOI: 10.2147/CMAR.S243753]

18 **Song JY**, Perry AM, Herrera AF, Chen L, Skrabek P, Nasr MR, Ottesen RA, Nikowitz J, Bedell V, Murata-Collins J, Li Y, McCarthy C, Pillai R, Wang J, Wu X, Zain J, Popplewell L, Kwak LW, Nademanee AP, Niland JC, Scott DW, Gong Q, Chan WC, Weisenburger DD. Double-hit Signature with TP53 Abnormalities Predicts Poor Survival in Patients with Germinal Center Type Diffuse Large B-cell Lymphoma Treated with R-CHOP. *Clin Cancer Res* 2021; **27**: 1671-1680 [PMID: 33414134 DOI: 10.1158/1078-0432.CCR-20-2378]

19 **Deng M**, Xu-Monette ZY, Pham LV, Wang X, Tzankov A, Fang X, Zhu F, Visco C, Bhagat G, Dybkaer K, Chiu A, Tam W, Zu Y, Hsi ED, You H, Huh J, Ponzoni M, Ferreri AJM, Møller MB, Parsons BM, Hagemeister F, van Krieken JH, Piris MA, Winter JN, Li Y, Xu B, Liu P, Young KH. Aggressive B-cell Lymphoma with MYC/TP53 Dual Alterations Displays Distinct Clinicopathobiological Features and Response to Novel Targeted Agents. *Mol Cancer Res* 2021; **19**: 249-260 [PMID: 33154093 DOI: 10.1158/1541-7786.MCR-20-0466]

20 **McMillan AK**, Phillips EH, Kirkwood AA, Barrans S, Burton C, Rule S, Patmore R, Pettengell R, Ardeshna KM, Lawrie A, Montoto S,

Paneesha S, Clifton-Hadley L, Linch DC. Favourable outcomes for high-risk diffuse large B-cell lymphoma (IPI 3-5) treated with front-line R-CODOX-M/R-IVAC chemotherapy: results of a phase 2 UK NCRI trial. *Ann Oncol* 2020; **31**: 1251-1259 [PMID: 32464282 DOI: 10.1016/j.annonc.2020.05.016]

21 **Zeremski V**, McPhail ED, Habermann TM, Schieppati F, Gebauer N, Vassilakopoulos TP, Mougiakakos D. Treatment intensification might not improve survival in high-grade B-cell lymphoma with a concurrent MYC and BCL2 and/or BCL6 rearrangement: A retrospective, multicenter, pooled analysis. *Hematol Oncol* 2023; **41**: 776-780 [PMID: 36945194 DOI: 10.1002/hon.3130]

22 **Neelapu SS**, Dickinson M, Munoz J, Ulrickson ML, Thieblemont C, Oluwole OO, Herrera AF, Ujjani CS, Lin Y, Riedell PA, Kekre N, de Vos S, Lui C, Milletti F, Dong J, Xu H, Chavez JC. Axicabtagene ciloleucel as first-line therapy in high-risk large B-cell lymphoma: the phase 2 ZUMA-12 trial. *Nat Med* 2022; **28**: 735-742 [PMID: 35314842 DOI: 10.1038/s41591-022-01731-4]

23 **Hamadani M**, Radford J, Carlo-Stella C, Caimi PF, Reid E, O'Connor OA, Feingold JM, Ardeshna KM, Townsend W, Solh M, Heffner LT, Ungar D, Wang L, Boni J, Havenith K, Qin Y, Kahl BS. Final results of a phase 1 study of loncastuximab tesirine in relapsed/refractory B-cell non-Hodgkin lymphoma. *Blood* 2021; **137**: 2634-2645 [PMID: 33211842 DOI: 10.1182/blood.2020007512]

24 **de Vos S**, Swinnen LJ, Wang D, Reid E, Fowler N, Cordero J, Dunbar M, Enschede SH, Nolan C, Petrich AM, Ross JA, Salem AH, Verdugo M, Agarwal S, Zhou L, Kozloff M, Nastoupil LJ, Flowers CR. Venetoclax, bendamustine, and rituximab in patients with relapsed or refractory NHL: a phase Ib dose-finding study. *Ann Oncol* 2018; **29**: 1932-1938 [PMID: 30060083 DOI: 10.1093/annonc/mdy256]

World Journal of Clinical Cases

Submit a Manuscript: https://www.f6publishing.com

World J Clin Cases 2024 May 26; 12(15): 2664-2671

DOI: 10.12998/wjcc.v12.i15.2664

ISSN 2307-8960 (online)

CASE REPORT

Imaging characteristics and treatment strategies for carotid artery occlusion caused by skull base fracture: Three case reports

Pei-Xin Shangguan, Ke-Chun Zhou

Specialty type: Medicine, research and experimental

Provenance and peer review: Unsolicited article; Externally peer reviewed.

Peer-review model: Single blind

Peer-review report's classification

Scientific Quality: Grade A

Novelty: Grade A

Creativity or Innovation: Grade A

Scientific Significance: Grade A

P-Reviewer: Zhou Y, United States

Received: February 15, 2024

Revised: March 14, 2024

Accepted: April 9, 2024

Published online: May 26, 2024

Pei-Xin Shangguan, Ke-Chun Zhou, Department of Emergency, Lishui Municipal Central Hospital, Lishui 323000, Zhejiang Province, China

Corresponding author: Ke-Chun Zhou, Doctor, Surgeon, Department of Emergency, Lishui Municipal Central Hospital, No. 298 Kuocang Road, Lishui 323000, Zhejiang Province, China. 247025921@qq.com

Abstract

BACKGROUND

Traumatic internal carotid artery (ICA) occlusion is a rare complication of skull base fractures, characterized by high mortality and disability rates, and poor prognosis. Therefore, timely discovery and correct management are crucial for saving the lives of such patients and improving their prognosis. This article retrospectively analyzed the imaging and clinical data of three patients, to explore the imaging characteristics and treatment strategies for carotid artery occlusion, combined with severe skull base fractures.

CASE SUMMARY

This case included three patients, all male, aged 21, 63, and 16 years. They underwent plain film skull computed tomography (CT) examination at the onset of their illnesses, which revealed fractures at the bases of their skulls. Ultimately, these cases were definitively diagnosed through CT angiography (CTA) examinations. The first patient did not receive surgical treatment, only anticoagulation therapy, and recovered smoothly with no residual limb dysfunction (Case 1). The other two patients both developed intracranial hypertension and underwent decompressive craniectomy. One of these patients had high intracranial pressure and significant brain swelling postoperatively, leading the family to choose to take him home (Case 2). The other patient also underwent decompressive craniectomy and recovered well postoperatively with only mild limb motor dysfunction (Case 3). We retrieved literature from PubMed on skull base fractures causing ICA occlusion to determine the imaging characteristics and treatment strategies for this type of disease.

CONCLUSION

For patients with cranial trauma combined with skull base fractures, it is essential to complete a CTA examination as soon as possible, to screen for blunt cerebrovascular injury.

Key Words: Skull base fracture; Traumatic internal carotid artery occlusion; Blunt cerebrovascular injury; Imaging; Case report

Core Tip: This article emphasizes the importance of rapid computed tomography angiography examination for patients with skull base fractures, to detect potential carotid artery occlusions. This condition significantly complicates the prognosis due to its rarity, high mortality, and severe disability rates. Through the analysis of three distinct cases, this study showcases varied imaging characteristics and underscores the critical role of early diagnosis and tailored treatment strategies, including anticoagulation and decompressive surgery, in managing this severe complication effectively.

Citation: Shangguan PX, Zhou KC. Imaging characteristics and treatment strategies for carotid artery occlusion caused by skull base fracture: Three case reports. *World J Clin Cases* 2024; 12(15): 2664-2671
URL: https://www.wjgnet.com/2307-8960/full/v12/i15/2664.htm
DOI: https://dx.doi.org/10.12998/wjcc.v12.i15.2664

INTRODUCTION

The carotid canal is an important structure through which the internal carotid artery (ICA) enters the skull base. Located at the base of the skull within the temporal bone, it begins in the petrous part of the temporal bone and serves as the primary passage for the ICA to enter the cranial cavity. Once inside the skull, the artery extends upwards along the sphenoid bone's sinus part. While damage to the carotid canal and sphenoid bone is relatively common in skull base fractures, the progression to ICA occlusion is quite rare. ICA occlusion can lead to severe cerebrovascular ischemic injuries with high mortality and disability rates, and poor prognosis[1]. Therefore, early diagnosis and treatment are crucial for improving outcomes. Typically, patients with cranial injuries only undergo head computed tomography (CT) scans, which often result in a delayed assessment of the damage to the ICA. Therefore, conducting a comprehensive CT angiography (CTA) examination early on is particularly important. This paper reviews the cases of three patients hospitalized between January 2013 and December 2023 and analyzes their imaging characteristics and treatment strategies.

This study retrospectively collected data from three cases of skull base fractures combined with traumatic ICA occlusion, that were treated in Lishui Municipal Central Hospital from January 2013 to December 2023. The clinical research and the publication of this paper and its related images were approved by the Clinical Research Ethics Committee of Lishui Municipal Central Hospital. The retrospective analysis included clinical information from hospital records, such as age, sex, causative factors, symptoms, disease progression, imaging examinations, related injuries, and diagnoses. Detailed information about these three cases is presented in Table 1.

CASE PRESENTATION

Chief complaints

Case 1: A 21-year-old male was admitted to the hospital due to decreased movement in the left limbs 1 d, occurring 7 d post liver rupture surgery.

Case 2: The patient was brought to our hospital with a change in the level of consciousness 6 h after being struck on the head with a heavy object.

Case 3: This patient was admitted to our hospital 6 h after a vehicular accident which caused a change in consciousness.

History of present illness

Case 1: Following a high fall, the patient had experienced transient consciousness disturbances and was taken to a local hospital, where he was intubated and placed on mechanical ventilation. After thorough examination, he was diagnosed with liver rupture, cranial trauma, and a skull fracture. Therefore, he underwent surgery for liver laceration repair. On day 7 post-surgery, decreased movement in his left limbs was observed, and a head CT scan indicated a brain infarction, leading to his transfer to our intensive care unit.

Case 2: Approximately 6 h prior to admission, the patient suffered a head injury from a heavy object, leading to a transient disturbance in consciousness and nasal bleeding. En route to our hospital, the patient experienced another episode of loss of consciousness. Upon arrival, emergency tracheal intubation and mechanical ventilation were administered.

Case 3: The patient experienced a change in consciousness and bleeding from the nose and mouth 6 h prior, following a motorcycle accident. Upon arrival at the hospital, emergency tracheal intubation and mechanical ventilation were

Table 1 Clinical characteristics of patients

Characteristics	Case 1	Case 2	Case 3
Gender	Male	Male	Male
Age (yr)	21	63	16
Cause of injury	Fall from height	Struck by heavy object	Traffic accident
Admission GCS score	15	5	7
Time to detection of arterial occlusion	7 d	6 h	6 d
Skull base fracture location	Sphenoid bone	Petrous part of the temporal bone	Sphenoid bone
Treatment	Anticoagulation	Surgery	Surgery
Hospital stay (d)	46	10	76
MRS score	0	6	2

GCS: Glasgow coma scale; MRS: Modified rankin scale.

administered.

History of past illness

Case 1: The patient was previously healthy until he had sustained injuries from a high fall 7 d prior. This resulted in liver rupture, cranial trauma, and a skull fracture.

Case 2: The patient was previously healthy.

Case 3: The patient was previously healthy.

Personal and family history

The patients and their family denied any history of cerebrovascular diseases.

Physical examination

Case 1: Upon admission, the patient had a Glasgow Coma Scale (GCS) score of 15, was intubated and receiving mechanical ventilation support. He had a body temperature of 39.3 °C, a respiratory rate of 29 breaths per minute (on mechanical ventilation), a heart rate of 145 beats per minute, and a blood pressure of 107/68 mmHg. The left pupil was 3 mm in diameter with sensitivity to light. The right pupil was 5 mm in diameter with no light reflex observed. Cardiopulmonary auscultation was generally normal, the abdomen was soft, and there was no shifting dullness detected.

Case 2: Upon admission, the patient's GCS score was 5, body temperature was 37.4 °C, respiratory rate was 10 breaths per minute, heart rate was 91 beats per minute, and blood pressure was 115/70 mmHg. The right pupil was 4.0 mm with no light reflex; the left pupil was approximately 2.5 mm with sluggish light reflex. Cardiopulmonary auscultation was largely normal, and the abdomen was soft.

Case 3: Upon admission, the patient's GCS score was 7, body temperature was 37.9 °C, respiratory rate was 15 breaths per minute, heart rate was 91 beats per minute, and blood pressure was 134/73 mmHg. The right pupil was 2.0 mm with no light reflex; the left pupil was approximately 3.0 mm, also with no light reflex. Cardiopulmonary auscultation was generally normal, and the abdomen was soft.

Laboratory examinations

Case 1: Hemoglobin was 86 g/L, white blood cell count was 20.7 × 10^9/L, and platelet count was 268 × 10^9/L. Coagulation profile showed a prothrombin time of 13.4 s, and the international normalized ratio (INR) was 1.24.

Case 2: The patient's hemoglobin was 146 g/L; white blood cell count 15.1 × 10^9/L; platelet count 167 × 10^9/L; prothrombin time 13.1 s; INR 1.21; and D-dimer, 34.70 mg/L.

Case 3: Blood tests showed a hemoglobin level of 137 g/L, white blood cell count was 5.5 × 10^9/L, and platelet count was 213 × 10^9/L. Coagulation tests indicated a prothrombin time of 20.6 s, INR of 1.03, and a D-dimer of 9.57 mg/L.

Imaging examinations

Case 1: Head CTA showed: (1) Brain contusion with brain swelling (predominantly on the right side), and occlusion of the right ICA; and (2) Multiple skull base fractures with sinus fluid accumulation, bilateral frontal soft tissue contusion (Figure 1A-C). After 46 d of treatment, a follow-up cranial CT scan revealed: Partial cerebral gyral atrophy in the right frontal and temporal lobes (Figure 1D).

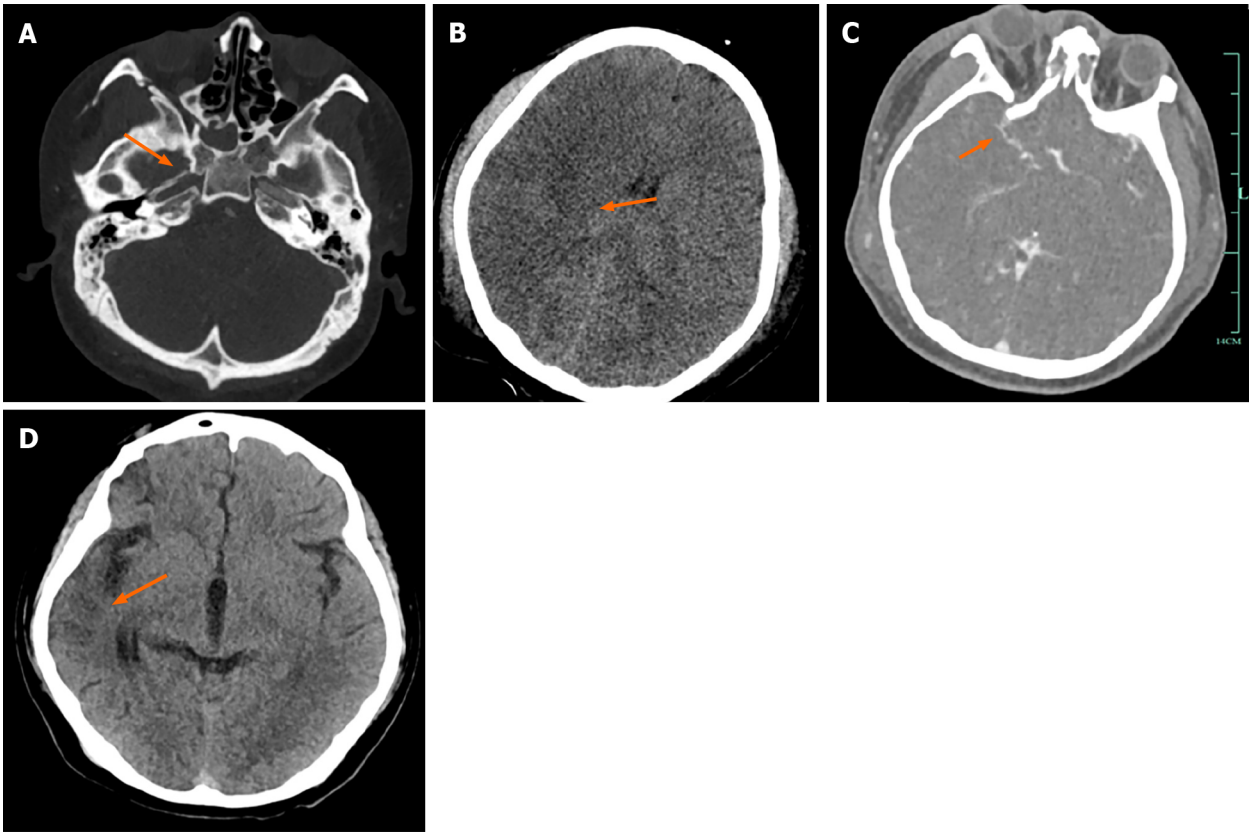

Figure 1 Cranial imaging scans of Case 1. A: A sphenoid bone fracture and non-opacification of the right internal carotid artery (indicated by an arrow); B: Ischemia in the right cerebral hemisphere (arrow), with no midline shift; C: Compensation by intracranial vascular collateral circulation (arrow); D: Demonstrates a reduction in the right-sided ischemic area after treatment and recovery (arrow).

Case 2: A head CT scan showed low-density lesions in the right cerebral hemisphere, fractures of the right maxillary sinus wall, zygomatic arch, walls of the orbit, right ethmoid sinus, walls of both sphenoid sinuses, and nasal septum, with sinus fluid accumulation (Figure 2A and B). An emergency head and neck arterial CTA showed occlusion of the right ICA (Figure 2C). On the second day of admission, a cranial CTA revealed a large area of cerebral infarction in the right hemisphere and brain herniation (Figure 2D), with poor compensatory collateral circulation in the right intracranial vessels (Figure 2E). On the 10th day of admission, a cranial CT scan indicated: Post-craniotomy changes due to right hemisphere infarction, increased cerebral tissue swelling compared to before, and an expanded infarction area (Figure 2F).

Case 3: Head and skull base CT scan revealed: (1) A right side frontal-temporal-parietal subdural hematoma, intraventricular hemorrhage, and pneumocephalus, widespread contusions in the facial and scalp soft tissues; and (2) Bilateral fractures of the frontal and temporal bones, top of the orbit, lateral wall of the sphenoid sinus, base of the middle cranial fossa, left side of the hard palate, with sinus and right mastoid effusion/blood accumulation (Figure 3A). On day 7 of hospitalization, the patient showed dilatation of the right pupil, and a CT scan indicated a large area of cerebral infarction and brain herniation on the right side (Figure 3B). The next day, a head CTA post-decompressive craniectomy showed right cerebral infarction and occlusion of the right ICA. Left side frontal-temporal subdural hematoma, intraventricular hemorrhage, and pneumocephalus; bilateral fractures of the frontal and temporal bones, top of the orbit, lateral wall of the sphenoid sinus, base of the middle cranial fossa, left side of the hard palate, with sinus and right mastoid effusion/blood accumulation were also confirmed (Figure 3C and D). After 76 d of treatment, a follow-up cranial CT scan indicated: Post-traumatic surgical changes, with a reduced lesion area in the right frontal, parietal, and temporal lobes compared to before (Figure 3E).

FINAL DIAGNOSIS

Case 1

The final diagnosis was skull base fracture, right cerebral infarction, occlusion of the right ICA, and liver laceration.

Case 2

The final diagnosis was skull base fracture, cerebral infarction, occlusion of the right ICA, and nasal bone fracture.

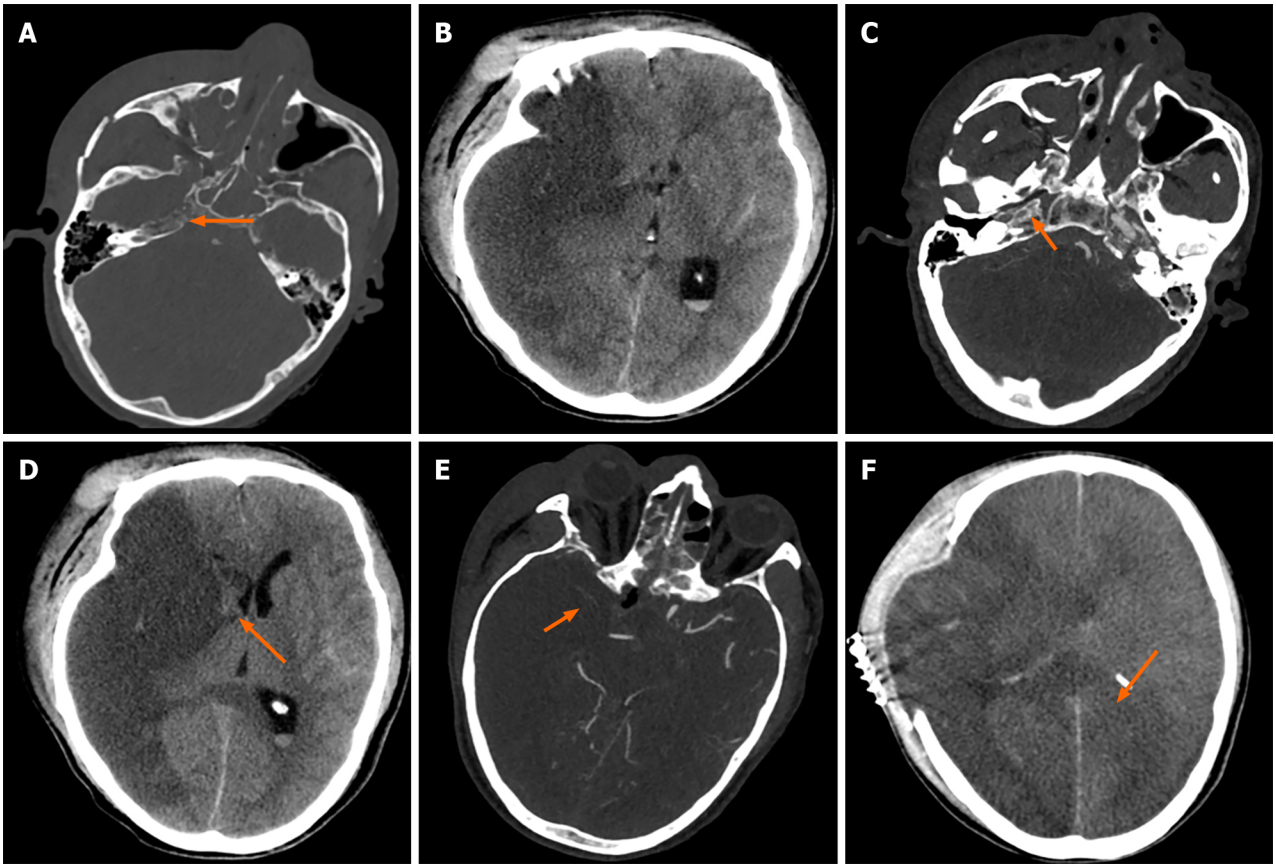

Figure 2 Cranial imaging scans of Case 2. A: A fracture of the right temporal bone's petrous part (arrow), with an incomplete structure of the carotid canal; B: Ischemic lesions in the right cerebral hemisphere; C: Occlusion of the right internal carotid artery (arrow); D: Ischemia in the right cerebral hemisphere (arrow), with midline shift and brain herniation; E: Poor compensation of intracranial vascular collateral circulation (arrow); F: The area of cerebral ischemia has increased following treatment (arrow), suggesting a poor prognosis.

Case 3

The final diagnosis was multiple skull base fractures, traumatic subarachnoid hemorrhage, occlusion of the right ICA, right cerebral infarction, subdural hematoma, and pulmonary contusion.

TREATMENT

Case 1

After multidisciplinary discussion, it was concluded that the patient's CTA showed abundant collateral circulation (Figure 1C) and no raised intracranial pressure, indicating no immediate need for emergency surgery. Considering the patient's recent abdominal surgery, multiple injuries, and fractures, along with a high risk of bleeding, it was decided to delay anticoagulation treatment. On the 7th day of hospital treatment, after fully assessing the bleeding risk, the patient received a low dose of low molecular weight heparin for anticoagulation (4000 U subcutaneous injection daily). During this period, coagulation factors were monitored, and no further bleeding was detected. On day 28 of hospitalization, the patient was switched to antiplatelet medication (aspirin 100 mg orally daily).

Case 2

After multidisciplinary discussion, considering the high risk and poor outcome of surgery due to the occlusion of the ICA caused by compression from fractured bone fragments, the patient's family opted to decline surgery. The following day, the patient's right pupil dilated significantly, and an emergency CT scan showed a large area of cerebral infarction in the right brain and brain herniation (Figure 2D). An emergency decompressive craniectomy was performed, followed by symptomatic supportive treatment. Due to insufficient compensatory circulation in the brain (Figure 2E), the area of cerebral infarction further increased (Figure 2F).

Case 3

The patient received routine mechanical ventilation, hypothermia to reduce brain swelling, and other symptomatic treatments after admission. On day 7, CT indicated cerebral infarction and brain herniation, prompting an emergency decompressive craniectomy. The next day, a head CTA confirmed right cerebral infarction and occlusion of the right ICA.

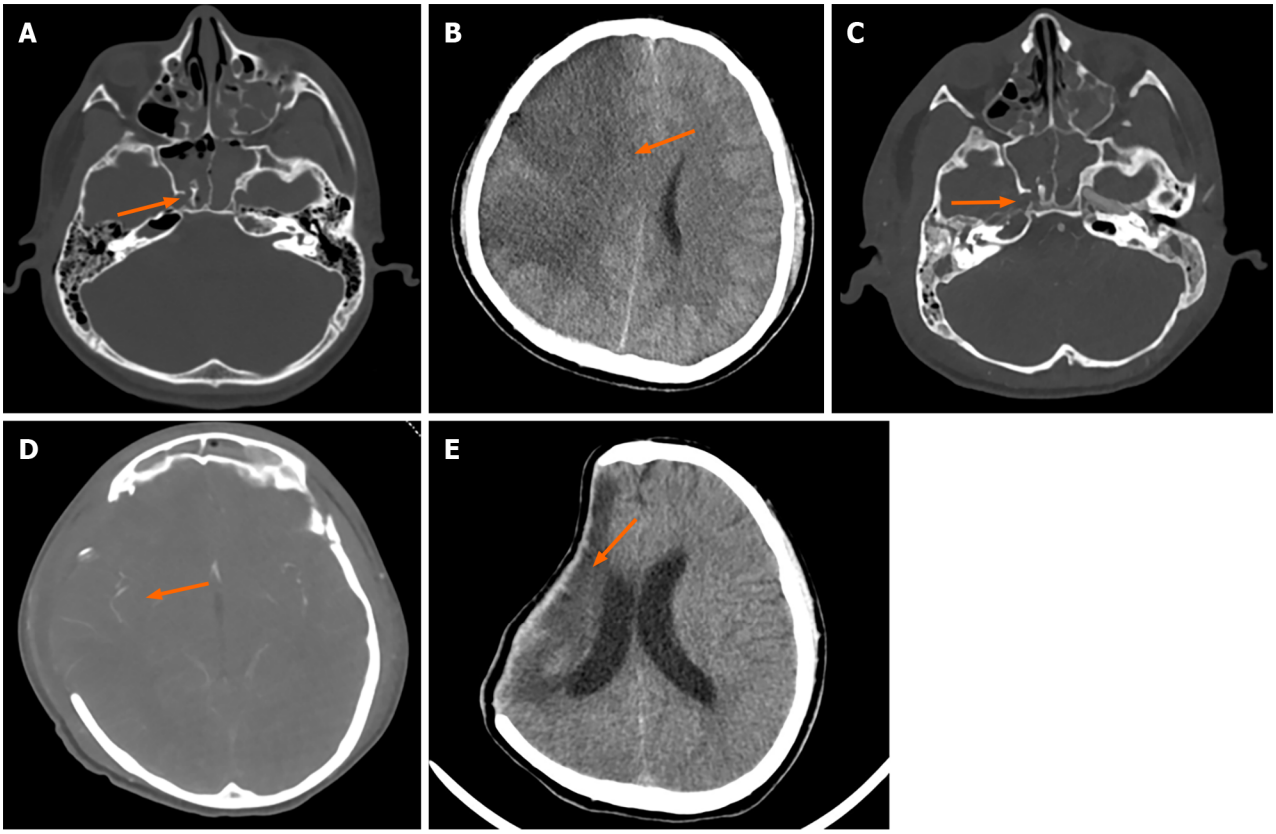

Figure 3 Cranial imaging scans of Case 3. A: A right sphenoid bone fracture (arrow), B: Right cerebral ischemia (arrow), midline shift, brain herniation; C: Right internal carotid artery occlusion (arrow); D: Compensation through collateral circulation in the right brain tissue (arrow); E: Post-treatment recovery with atrophy of the right ischemic area, slightly reduced in size.

After multidisciplinary discussion, it was concluded that, considering that the patient's collateral circulation was relatively functional (Figure 3D), emergency surgery was not immediately necessary. Therefore, a scheduled ICA bypass could be considered. Due to the high risk of bleeding and the family's refusal of anticoagulation therapy, no anticoagulants were administered until discharge.

OUTCOME AND FOLLOW-UP

Case 1

After 46 d of hospitalization, the patient improved and was discharged without any residual limb dysfunction. A follow-up head CT scan (Figure 1D) showed a significant reduction in the size of the cerebral infarction compared with that upon admission.

Case 2

The patient's family therefore, requested discharge to take him home, where he died on the same day.

Case 3

After 76 d of treatment, the patient was discharged in an improved condition: Muscle strength was Grade II in the left upper limb, Grade IV in the left lower limb, and Grade V in the right limbs. There was a slight decline in intelligence and speech. A follow-up head CT scan (Figure 3E) showed a reduction in the size of the right cerebral infarction lesion compared with previous images.

DISCUSSION

Falls from heights, traffic accidents, and crush injuries are common causes of fractures at the base of the skull, which can lead to blunt cerebrovascular injuries. These injuries have an incidence rate of less than 1%. They are often overlooked in clinical practice, eventually leading to severe traumatic ICA occlusion[2,3]. The mechanisms of these events are two-fold: Usually thrombotic, either due to thrombus formation at the site of intimal tear or by hemodynamic thrombus formation caused by arterial narrowing or obstruction, potentially leading to low-flow infarctions[4]. Due to their very low

occurrence rate, these conditions often result in late diagnosis or misdiagnosis, with serious consequences. In the assessment of complex injuries, early detection and treatment of traumatic ICA occlusion are critical for saving the patient's life.

In diagnosing patients with fractures at the base of the skull, vigilance is required in the following aspects: (1) Understanding the etiology of such diseases, particularly in patients with severe fractures at the base of the skull, there is a need to be alert to the possibility of ICA injury. The study by Li *et al*[3] found that the incidence of ICA injury in patients with carotid canal fractures was more than four times higher than that in those without carotid canal fractures. All three patients mentioned in this study had carotid canal fractures; (2) Attention to clinical presentation: Patients with severe craniofacial trauma often exhibit varying degrees of altered consciousness. Clinical manifestations caused by traumatic occlusion of the ICA can be masked by the primary injury, leading to missed or incorrect diagnoses; and (3) Imaging with cranial CT scans: Although a plain cranial CT scan cannot diagnose ICA injuries, patients with carotid canal fractures, an initial GCS score of less than 9, and a history of severe head injury as indicated by the Abbreviated Injury Scale should be considered for early screening with CTA[5]. These points highlight the importance of a comprehensive and cautious approach to diagnosing and managing patients with skull base fractures, particularly regarding the potential for vascular injuries.

The current treatment approaches for traumatic ICA occlusion are not yet standardized, as there are no specific guidelines. Available treatments include anticoagulation, antiplatelet therapy, and open surgery: (1) Use and selection of anticoagulants: Recent studies indicate that there often exists a latent, asymptomatic period between the development of traumatic hemorrhage and ischemic stroke, during which established antithrombotic or anticoagulant therapy can improve neurological outcomes and mortality[6]. However, systemic anticoagulation poses a significant bleeding risk in trauma patients, especially after traumatic brain injury. Anticoagulation should not be initiated within the first 3 d post-injury for patients with mild or high-risk intracranial hemorrhage, as even prophylactic doses of heparin may lead to brain hemorrhage, with intracranial bleeding rates of 8%-16%[7,8]. Eastham[9] suggest using antithrombotic agents, such as heparin or aspirin, for mild cases of blunt cerebrovascular injury, but no specific anticoagulation regimen for traumatic ICA occlusion was mentioned. Moreover, the timing of initiating anticoagulant or antiplatelet therapy remains controversial. The first patient used anticoagulants without severe adverse reactions, offering some reference for future treatments; (2) Assessment of collateral circulation: Studies have shown that rapid assessment of collateral circulation using CTA, for patients with complete ICA occlusion may help determine future treatment approaches and patient prognosis. For patients with poor collateral circulation, treatment should focus on maintaining an elevated mean arterial pressure to prevent watershed ischemia[10]. Strong collateral circulation can reduce the extent of brain ischemia associated with these injuries. However, the patient's survival rate and prognosis can be directly affected if there is insufficient compensatory collateral circulation. In the mentioned cases, the prognosis of the second patient was worse than the first and third due to inadequate intracranial collateral compensation and older age; and (3) Open surgery: Extracranial-intracranial bypass surgery has been proven to be a useful method of vascular reconstruction. Currently, the preferred method for treating ICA injuries is the precise excision of the damaged arterial segment and delicate reconstruction of the ICA. This process aims to ensure the continuity and stability of intracranial blood supply as much as possible, effectively preventing cerebral ischemia and related complications[11].

CONCLUSION

Traumatic ICA occlusion is a rare and serious complication resulting from skull base fractures. To address this: (1) Rapid cranial CTA: If a cranial CT scan suggests a fracture of the carotid canal, it is crucial to promptly perform a cranial CTA to ascertain the extent of the ICA injury; (2) Consider use of anticoagulants: Anticoagulant therapy may be beneficial for the patient, but this requires a thorough evaluation of the overall health status and careful consideration of bleeding risks; and (3) Collateral circulation evaluation: Assessing collateral circulation is crucial for deciding on cerebral vascular reconstruction and predicting patient outcomes. Strong collateral circulation often leads to better outcomes and lower ischemic risk. These steps are essential for effectively managing this complication.

FOOTNOTES

Author contributions: Zhou KC contributed to manuscript writing and editing, data collection and data analysis; Shangguan PX contributed to conceptualization and supervision. All authors have read and approved the final manuscript.

Informed consent statement: Informed written consent was obtained from the patient for publication of this report and any accompanying images.

Conflict-of-interest statement: Author(s) certify that there is no conflict of interest related to the manuscript. If any potential conflict-of-interest exists, author(s) certify that it is fully disclosed.

CARE Checklist (2016) statement: The authors have read the CARE Checklist (2016), and the manuscript was prepared and revised according to the CARE Checklist (2016).

Open-Access: This article is an open-access article that was selected by an in-house editor and fully peer-reviewed by external reviewers.

Country/Territory of origin: China

ORCID number: Ke-Chun Zhou 0009-0002-1908-7209.

S-Editor: Zheng XM
L-Editor: A
P-Editor: Yu HG

REFERENCES

1 **Nunnink L**. Blunt carotid artery injury. *Emerg Med (Fremantle)* 2002; **14**: 412-421 [PMID: 12534485 DOI: 10.1046/j.1442-2026.2002.00348.x]
2 **Franz RW**, Willette PA, Wood MJ, Wright ML, Hartman JF. A systematic review and meta-analysis of diagnostic screening criteria for blunt cerebrovascular injuries. *J Am Coll Surg* 2012; **214**: 313-327 [PMID: 22244206 DOI: 10.1016/j.jamcollsurg.2011.11.012]
3 **Li C**, Green L, Wang J, Tully D, Woliansky J, Gumm K, Iseli C, Martin K, Read D. Factors associated with blunt internal carotid artery injury in petrous temporal bone fractures. *Injury* 2022; **53**: 2023-2027 [PMID: 35346507 DOI: 10.1016/j.injury.2022.03.031]
4 **Debette S**, Leys D. Cervical-artery dissections: predisposing factors, diagnosis, and outcome. *Lancet Neurol* 2009; **8**: 668-678 [PMID: 19539238 DOI: 10.1016/S1474-4422(09)70084-5]
5 **Venkataraman SS**, Herbert JP, Ravindra VM, Yu BN, Bollo RJ, Cox CS Jr, Gannon SR, Limbrick DD Jr, Naftel RP, Ugalde IT, Yorkgitis BK, Weiner HL, Shah MN. Multi-Center Validation of the McGovern Pediatric Blunt Cerebrovascular Injury Screening Score. *J Neurotrauma* 2023; **40**: 1451-1458 [PMID: 36517974 DOI: 10.1089/neu.2022.0336]
6 **Cothren CC**, Moore EE, Biffl WL, Ciesla DJ, Ray CE Jr, Johnson JL, Moore JB, Burch JM. Anticoagulation is the gold standard therapy for blunt carotid injuries to reduce stroke rate. *Arch Surg* 2004; **139**: 540-5; discussion 545 [PMID: 15136355 DOI: 10.1001/archsurg.139.5.540]
7 **Eachempati SR**, Vaslef SN, Sebastian MW, Reed RL 2nd. Blunt vascular injuries of the head and neck: is heparinization necessary? *J Trauma* 1998; **45**: 997-1004 [PMID: 9867039 DOI: 10.1097/00005373-199812000-00004]
8 **Miller PR**, Fabian TC, Bee TK, Timmons S, Chamsuddin A, Finkle R, Croce MA. Blunt cerebrovascular injuries: diagnosis and treatment. *J Trauma* 2001; **51**: 279-85; discussion 285 [PMID: 11493785 DOI: 10.1097/00005373-200108000-00009]
9 **Eastham S**. Blunt cerebrovascular injuries in trauma. *Int J Surg* 2016; **33**: 251-253 [PMID: 26497781 DOI: 10.1016/j.ijsu.2015.09.075]
10 **Morton RP**, Hanak BW, Levitt MR, Fink KR, Peterson EC, Vilela MD, Kim LJ, Chesnut RM. Blunt traumatic occlusion of the internal carotid and vertebral arteries. *J Neurosurg* 2014; **120**: 1446-1450 [PMID: 24678781 DOI: 10.3171/2014.2.JNS131658]
11 **Rostomily RC**, Newell DW, Grady MS, Wallace S, Nicholls S, Winn HR. Gunshot wounds of the internal carotid artery at the skull base: management with vein bypass grafts and a review of the literature. *J Trauma* 1997; **42**: 123-132 [PMID: 9003271 DOI: 10.1097/00005373-199701000-00023]

World Journal of Clinical Cases

Submit a Manuscript: https://www.f6publishing.com

World J Clin Cases 2024 May 26; 12(15): 2672-2677

DOI: 10.12998/wjcc.v12.i15.2672

ISSN 2307-8960 (online)

CASE REPORT

Subclinical paraganglioma of the retroperitoneum: A case report

Li-Min Kang, Fa-Kun Yu, Fu-Wei Zhang, Lei Xu

Specialty type: Medicine, research and experimental

Provenance and peer review: Unsolicited article; Externally peer reviewed.

Peer-review model: Single blind

Peer-review report's scientific quality classification

Grade A (Excellent): 0
Grade B (Very good): 0
Grade C (Good): C, C
Grade D (Fair): 0
Grade E (Poor): 0

P-Reviewer: Abuhijla F, Jordan

Received: February 22, 2024
Revised: March 15, 2024
Accepted: April 3, 2024
Published online: May 26, 2024

Li-Min Kang, Fa-Kun Yu, Fu-Wei Zhang, Lei Xu, Department of Hepatobiliary and Pancreatic Surgery, Puer People's Hospital, Puer 665000, Yunnan Province, China

Corresponding author: Li-Min Kang, MD, PhD, Deputy Chief Physician, Department of Hepatobiliary and Pancreatic Surgery, Puer People's Hospital, No. 44 Zhenxing Street, Puer 665000, Yunnan Province, China. kanglimin2010@163.com

Abstract

BACKGROUND

Paraganglioma (PGL) located in the retroperitoneum presents challenges in diagnosis and treatment due to its hidden location, lack of specific symptoms in the early stages, and absence of distinctive manifestations on imaging.

CASE SUMMARY

A 56-year-old woman presented with a left upper abdominal mass discovered 1 wk ago during a physical examination. She did not have a history of smoking, alcohol consumption, or other harmful habits, no surgical procedures or infectious diseases, and had a 4-year history of hypertension. Upon admission, she did not exhibit fever, vomiting, or abdominal distension. Physical examination indicated mild percussion pain in the left upper abdomen, with no palpable enlargement of the liver or spleen. Laboratory tests and tumor markers showed no significant abnormalities. Enhanced computed tomography and magnetic resonance imaging of the upper abdomen revealed a cystic solid mass in the left epigastrium measuring approximately 6.5 cm × 4.5 cm, with inhomogeneous enhancement in the arterial phase, closely associated with the lesser curvature of the stomach and the pancreas. The patient underwent laparoscopic resection of the retroperitoneal mass, which was successfully removed without tumor rupture. A 12-month postoperative follow-up period showed good recovery.

CONCLUSION

This case report details the successful laparoscopic resection of a retroperitoneal subclinical PGL, resulting in a good recovery observed at the 12-month follow-up. Interestingly, the patient also experienced unexpected cure of hypertensive disease.

Key Words: Paraganglioma; Retroperitoneal anatomy; Subclinical; Pheochromocytoma; Laparoscopy; Case report

Core Tip: Retroperitoneal subclinical paragangliomas (PGLs) are exceptionally uncommon. In this report, we present a case of PGL that was effectively managed by laparoscopic retroperitoneal lumpectomy. The patient showed excellent recovery at the 12-month postoperative follow-up and notably experienced resolution of her hypertensive condition. The management of this case serves as a valuable reference for addressing retroperitoneal PGLs.

Citation: Kang LM, Yu FK, Zhang FW, Xu L. Subclinical paraganglioma of the retroperitoneum: A case report. *World J Clin Cases* 2024; 12(15): 2672-2677
URL: https://www.wjgnet.com/2307-8960/full/v12/i15/2672.htm
DOI: https://dx.doi.org/10.12998/wjcc.v12.i15.2672

INTRODUCTION

Paraganglioma (PGL), also known as extra-adrenal pheochromocytoma, is a rare tumor that develops in the paraganglia, specialized cells along the sympathetic or parasympathetic nervous system[1]. These tumors can be found in various locations such as the carotid body, aortic body, and other parasympathetic ganglia[2]. They can also occur in uncommon areas such as the skull base, mediastinum, and pelvis[3]. Retroperitoneal PGLs are particularly challenging to diagnose due to their asymptomatic nature and lack of specific imaging features[4]. We present a case of subclinical PGL in the left retroperitoneum that was successfully treated with surgery and confirmed by histopathological examination.

CASE PRESENTATION

Chief complaints

Before admission in January 2023, a 56-year-old woman attended the clinic due to a left upper abdominal mass found on physical examination 1 wk previously.

History of present illness

The patient was admitted to hospital with a 6.5 cm × 3.5 cm cystic solid mass in the left upper abdomen, as shown on abdominal ultrasound conducted 1 wk previously. The patient did not report any abdominal pain, distension, or discomfort.

History of past illness

The patient did not have a history of smoking, drinking, or other harmful habits, no known drug allergies or family history of genetic diseases, and no previous history of hepatitis, infectious diseases, or surgeries. She had been diagnosed with hypertension for 4 years and was currently taking oral amlodipine 2.5 mg and irbesartan 150 mg once daily.

Physical examination

No fever, vomiting, abdominal pain or distension were observed on admission. Physical examination revealed mild tenderness in the left upper abdomen, but no palpable abdominal mass.

Laboratory examinations

Laboratory tests revealed no blood, coagulation, liver function, renal function, or tumor marker abnormalities, including carcinoembryonic antigen and glycan antigen 199. Blood dopamine level was 11.0 pg/mL, epinephrine was 31.60 pg/mL, and norepinephrine was 269.50 pg/mL. Her 24-h urine sample showed a dopamine level of 204.39 μg/24 h, epinephrine 17.47 μg/24 h, and norepinephrine 57.96 μg/24 h. Both plasma and urine catecholamine test results were normal. In addition, electrocardiogram, chest X-ray, and 24-h ambulatory blood pressure monitoring were within the normal range.

Imaging examinations

Computed tomography (CT) and magnetic resonance imaging (MRI) scans of the upper abdomen revealed a cystic solid mass measuring approximately 6.5 cm × 4.5 cm in the left upper abdomen. The mass exhibited inhomogeneous enhancement during the arterial phase and was closely associated with the lesser curvature of the stomach and pancreas, as well as with the celiac trunk arteries and splenic arteries (Figure 1).

FINAL DIAGNOSIS

Based on intraoperative blood pressure fluctuations and postoperative pathologic findings, the final diagnosis in this patient was a retroperitoneal subclinical PGL.

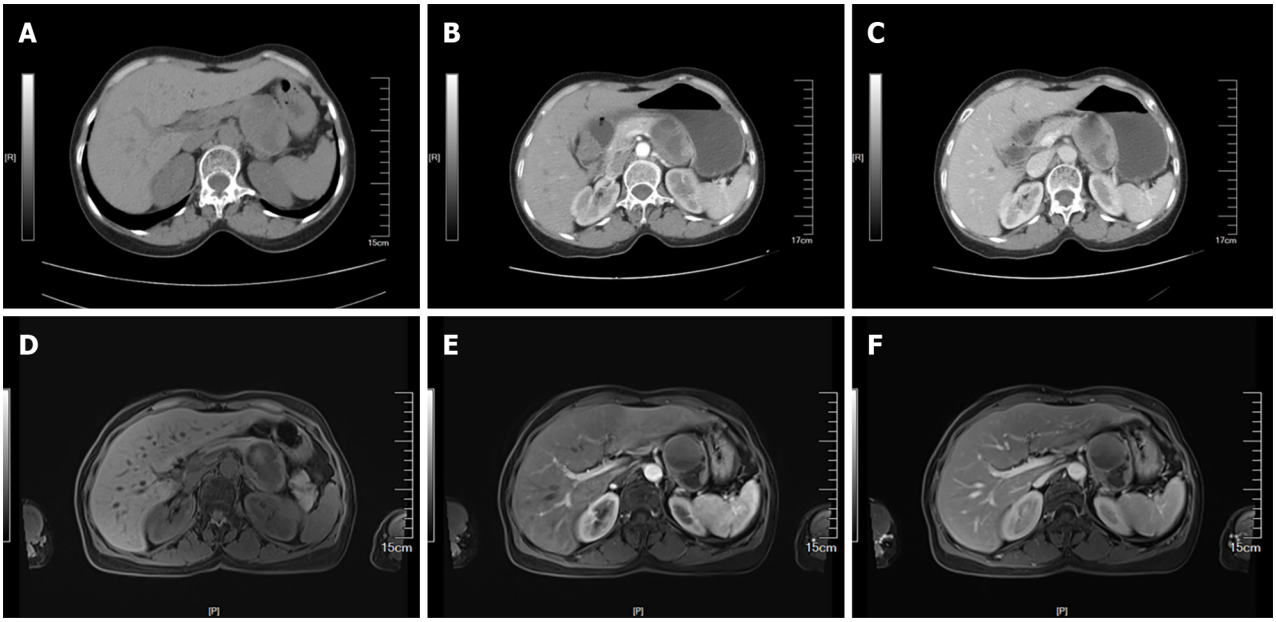

Figure 1 Abdominal computed tomography and magnetic resonance imaging show a 6.5 cm × 4.5 cm cystic solid mass in the left upper abdomen with heterogeneous density and mild enhancement in the arterial phase. A: Computed tomography (CT) plain scan period; B: CT arterial phase; C: CT venous phase; D: Magnetic resonance imaging (MRI) plain scan period; E: MRI arterial phase; F: MRI venous phase.

TREATMENT

Following standardized preoperative preparation and perioperative management, the patient underwent laparoscopic exploration of the abdominal cavity in January 2023. Intraoperatively, our exploratory findings were consistent with the preoperative imaging findings, which revealed a mass clearly originating from the retroperitoneum and closely related to the lesser curvature of the stomach, the pancreas and the celiac trunk and splenic artery, leading to a successful retroperitoneal mass resection without tumor rupture. Postoperatively, examination revealed that the mass weighed 350 g and measured 6.5 cm × 40 cm × 3 cm, displaying a cystic solid appearance with a thickened cyst wall. Examination of the mass confirmed cystic solidity with dark red fluid inside the capsule (Figure 2).

OUTCOME AND FOLLOW-UP

Intraoperative blood pressure fluctuated between 100-220/70-180 mmHg, prompting the anesthesiologist to administer active treatment to stabilize blood pressure post-surgery. Subsequent immunohistochemistry revealed positive markers for cluster of differentiation 56 (CD56), chromogranin (CgA), synaptophysin (Syn), soluble protein-100 (S-100), insulinoma-associated protein 1 (INSM1), succinate dehydrogenase type B (SDHB), and negative markers for melanin-A antibody, cytokeratin-P, and delay of germination 1, leading to a pathological diagnosis of retroperitoneal PGL. Following surgery, the patient's blood pressure normalized and oral antihypertensive medications were gradually tapered. Follow-up appointments at 1, 3, 6, and 12 months showed normal results for blood pressure, physical examination, and repeat abdominal ultrasound.

DISCUSSION

PGLs are neuroendocrine tumors that originate from neural crest cells and are classified into non-functional, subclinical, and functional types based on the presence or absence of typical clinical symptoms caused by the secretion of catecholamines into the bloodstream[5]. Non-functional retroperitoneal PGLs do not exhibit typical clinical symptoms; patients may experience abdominal discomfort or physical examination findings due to tumor growth compressing adjacent organs[6]. The subclinical type involves catecholamine secretion, but in small amounts that do not induce typical symptoms, leading to blood pressure fluctuations during surgery. Functional PGLs are characterized by periodic catecholamine release, resulting in symptoms such as hypertension, palpitations, and headaches[7]. Our patient showed no symptoms prior to surgery, but experienced a significant increase in blood pressure during the procedure, suggesting the diagnosis of subclinical PGL.

The incidence of PGL is low, making diagnosis relatively challenging due to the lack of specific clinical manifestations. Functional PGLs typically present with symptoms such as headache, palpitations, and hyperhidrosis (triad sign), but these neuroendocrine tumors often progress slowly, leading to delayed diagnosis. Patients may only seek medical

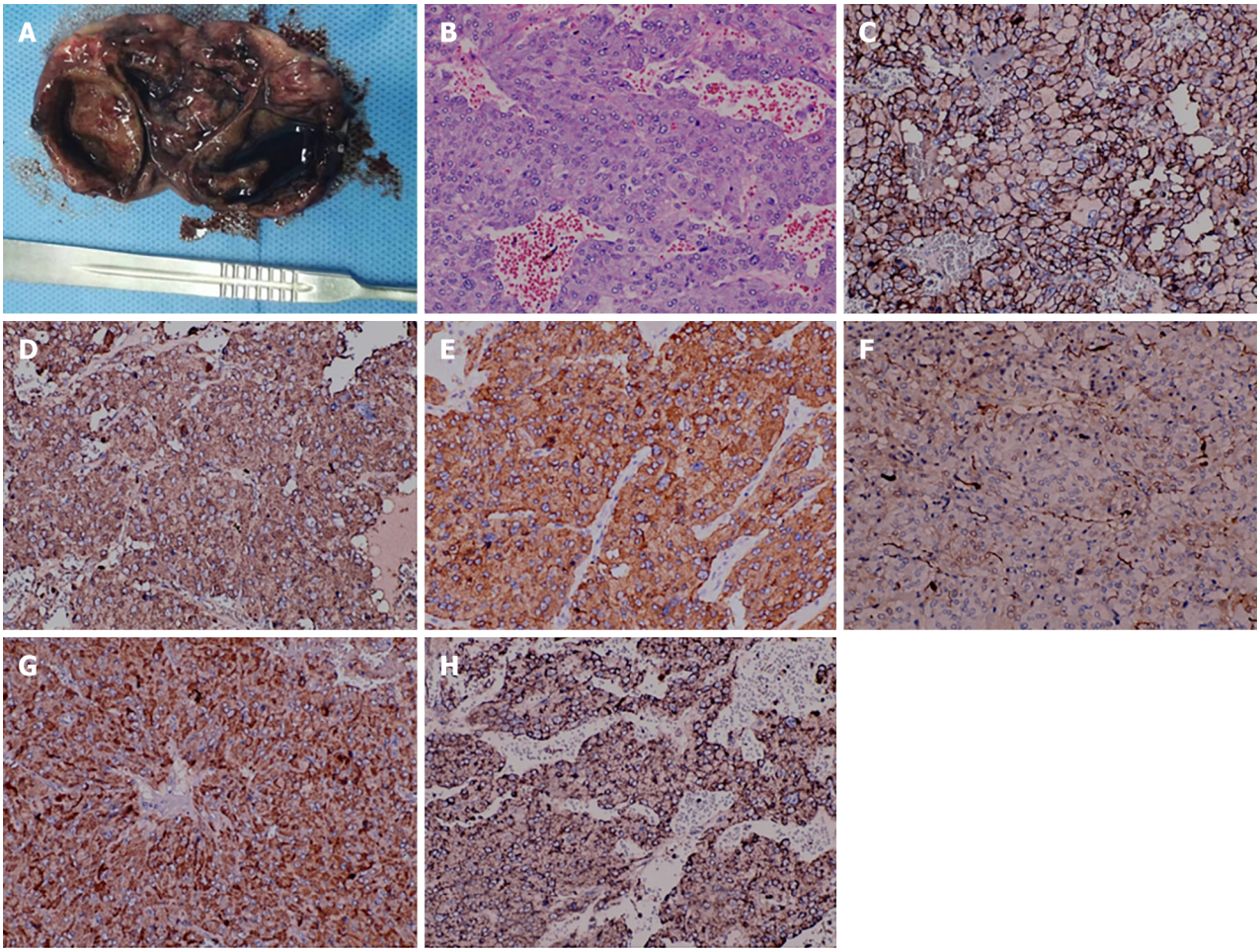

Figure 2 Gross features and pathologic characteristics of the resected tumor. A: Gross features of the tumor; B: Tumor hematoxylin and eosin staining (× 400); C: Cluster of differentiation 56 positive (× 400); D: Chromogranin positive (× 400); E: Synaptophysin positive (× 400); F: Soluble protein-100 positive (× 400); G: Insulinoma-associated protein 1 positive (× 400); H: Succinate dehydrogenase type B positive (× 400).

attention when they experience extremely high blood pressure or symptoms of tumor compression, increasing the risk of complications[8]. Nonfunctional or subclinical PGLs primarily cause discomfort due to tumor compression. According to expert consensus[9], liquid chromatography/tandem mass spectrometry is recommended for diagnosing pheochromocytoma and PGL by measuring plasma free catecholamine or urinary catecholamine concentrations. In this patient who was suspected of having pheochromocytoma, tests for plasma and urinary concentrations of dopamine, epinephrine, and norepinephrine, were all within the normal range. However, the patient experienced significant blood pressure fluctuations during surgery, posing challenges for preoperative diagnosis and increasing intraoperative risks. Laparoscopic exploration of retroperitoneal space occupation has a magnifying effect, which facilitates the dissection of blood vessels and other fine structures, and has the advantages of less trauma and quicker recovery, but at the same time, there are also the risks of bleeding that are not easy to control, rupture of the tumour, and the need to be prepared for open surgery.

Imaging techniques such as color ultrasound, CT, and MRI lack specificity in distinguishing PGLs from other conditions such as giant lymph node hyperplasia, nerve sheath tumors, ganglion cell neuroma, and solid pseudopapillary tumors of the pancreas[10]. Therefore, a combination of clinical manifestations, imaging, and laboratory examinations is typically needed to further clarify the nature of the mass. In this particular case, although ultrasound, CT, and MRI showed a cystic solid mass in the left upper abdomen, the origin of the mass and whether it was benign or malignant could not be determined. PGLs exhibit similar morphology regardless of their location and can be indistinguishable from adrenal gland pheochromocytomas. Microscopically, the tumor cells appear ovoid, cuboidal, or polygonal, larger than normal paragangliocytes, with granular basophilic cytoplasm, occasional melanin-like pigmentation, mild nuclear pleomorphism, and rare nuclear atypia. Tumor cells are organized in nests, cords, or adenoidal vesicles, with abundant blood sinuses between them that may be significantly dilated and hemorrhagic, sometimes showing vascular infiltration. The interstitium may exhibit sclerosis with fibroplasia, vitrification, or ossification[11]. Immunohistochemistry reveals that tumor cells express neuroendocrine markers such as neurospecific enolase, CgA, Syn, as well as calcitonin and vasoactive peptides. Support cells S-100 and glial fibrillary acidic protein are typically observed at the periphery of the cell clusters[12]. In this case, a PGL was not initially considered, but histological examination combined with immunohistochemistry for CD56, CgA, Syn, S-100, INSM1, and SDHB positivity ultimately led to the diagnosis of PGL.

PGLs can be categorized as either benign or malignant, with the majority being benign. Malignant PGLs represent a smaller percentage, ranging from 1% to 10%[13]. Distinguishing between benign and malignant forms based on morpho-

logical criteria is challenging. However, in cases of malignancy, certain characteristics such as tumor diameter exceeding 5 cm, presence of SDHB mutation, MYC associated factor X gene mutation, Ki67 index greater than 3%, noticeable cellular heterogeneity, atypical nuclear features, and localized necrosis are considered risk factors. Malignant PGLs have the potential to metastasize to various organs such as lymph nodes, bones, lungs, and liver, with metastasis serving as a key indicator of malignancy[14]. In the specific case discussed, the patient experienced normalization of blood pressure post-surgery, leading to the discontinuation of antihypertensive medication. Subsequent follow-up over 12 months showed a positive recovery outcome. Integrating intraoperative and pathological findings, the patient was diagnosed with a subclinical PGL. This case study provides valuable insights for the management of retroperitoneal PGLs.

CONCLUSION

A case of retroperitoneal subclinical PGL was successfully cured following surgical resection. This case serves as a valuable example of the management of retroperitoneal PGLs.

FOOTNOTES

Author contributions: Kang LM, Yu FK and Zhang FW collected the clinical data; Kang LM and Xu L analyzed the data and wrote the paper.

Informed consent statement: Informed written consent was obtained from the patient for publication of this report and any accompanying images.

Conflict-of-interest statement: The authors declare that they have no conflict of interest.

CARE Checklist (2016) statement: The authors have read the CARE Checklist (2016), and the manuscript was prepared and revised according to the CARE Checklist (2016).

Country/Territory of origin: China

ORCID number: Li-Min Kang 0000-0002-3062-897X; Fa-Kun Yu 0009-0007-1331-2432; Fu-Wei zhang 0009-0002-3737-0112; Lei Xu 0009-0002-7732-7856.

S-Editor: Zheng XM
L-Editor: A
P-Editor: Yu HG

REFERENCES

1 **Karray O**, Saadi A, Chakroun M, Ayed H, Cherif M, Bouzouita A, Slama MRB, Derouiche A, Chebil M. Retro-peritoneal paraganglioma, diagnosis and management. *Prog Urol* 2018; **28**: 488-494 [PMID: 29983333 DOI: 10.1016/j.purol.2018.06.003]
2 **Jain A**, Baracco R, Kapur G. Pheochromocytoma and paraganglioma-an update on diagnosis, evaluation, and management. *Pediatr Nephrol* 2020; **35**: 581-594 [PMID: 30603807 DOI: 10.1007/s00467-018-4181-2]
3 **Mete O**, Asa SL, Gill AJ, Kimura N, de Krijger RR, Tischler A. Overview of the 2022 WHO Classification of Paragangliomas and Pheochromocytomas. *Endocr Pathol* 2022; **33**: 90-114 [PMID: 35285002 DOI: 10.1007/s12022-022-09704-6]
4 **Kawanabe S**, Katabami T, Oshima R, Yanagisawa N, Sone M, Kimura N. A rare case of multiple paragangliomas in the head and neck, retroperitoneum and duodenum: A case report and review of the literature. *Front Endocrinol (Lausanne)* 2022; **13**: 1054468 [PMID: 36704041 DOI: 10.3389/fendo.2022.1054468]
5 **Lima JV Júnior**, Kater CE. The Pheochromocytoma/Paraganglioma syndrome: an overview on mechanisms, diagnosis and management. *Int Braz J Urol* 2023; **49**: 307-319 [PMID: 37115176 DOI: 10.1590/S1677-5538.IBJU.2023.0038]
6 **Liu Z**, Zhang Y, Zhang X, Kong L. Nonfunctional paraganglioma: A case report. *Exp Ther Med* 2024; **27**: 16 [PMID: 38125363 DOI: 10.3892/etm.2023.12304]
7 **Tevosian SG**, Ghayee HK. Pheochromocytoma/Paraganglioma: A Poster Child for Cancer Metabolism. *J Clin Endocrinol Metab* 2018; **103**: 1779-1789 [PMID: 29409060 DOI: 10.1210/jc.2017-01991]
8 **Meijs AC**, Snel M, Corssmit EPM. Pheochromocytoma/paraganglioma crisis: case series from a tertiary referral center for pheochromocytomas and paragangliomas. *Hormones (Athens)* 2021; **20**: 395-403 [PMID: 33575936 DOI: 10.1007/s42000-021-00274-6]
9 **Lenders JWM**, Kerstens MN, Amar L, Prejbisz A, Robledo M, Taieb D, Pacak K, Crona J, Zelinka T, Mannelli M, Deutschbein T, Timmers HJLM, Castinetti F, Dralle H, Widimský J, Gimenez-Roqueplo AP, Eisenhofer G. Genetics, diagnosis, management and future directions of

research of phaeochromocytoma and paraganglioma: a position statement and consensus of the Working Group on Endocrine Hypertension of the European Society of Hypertension. *J Hypertens* 2020; **38**: 1443-1456 [PMID: 32412940 DOI: 10.1097/HJH.0000000000002438]

10 **Rusyn L**, Kohn B. Succinate-Dehydrogenase Deficient Paragangliomas/Pheochromocytomas: Genetics, Clinical Aspects and Mini- Review. *Pediatr Endocrinol Rev* 2017; **14**: 312-325 [PMID: 28508602 DOI: 10.17458/per.vol14.2017.RK.succinatedehydrogenase]

11 **Lei J**, Qu T, Cha L, Tian L, Qiu F, Guo W, Cao J, Sun C, Zhou B. Clinicopathological characteristics of pheochromocytoma/paraganglioma and screening of prognostic markers. *J Surg Oncol* 2023; **128**: 510-518 [PMID: 37272486 DOI: 10.1002/jso.27358]

12 **Juhlin CC**. Challenges in Paragangliomas and Pheochromocytomas: from Histology to Molecular Immunohistochemistry. *Endocr Pathol* 2021; **32**: 228-244 [PMID: 33768452 DOI: 10.1007/s12022-021-09675-0]

13 **Hamidi O**. Metastatic pheochromocytoma and paraganglioma: recent advances in prognosis and management. *Curr Opin Endocrinol Diabetes Obes* 2019; **26**: 146-154 [PMID: 30893083 DOI: 10.1097/MED.0000000000000476]

14 **Jimenez C**, Fazeli S, Román-Gonzalez A. Antiangiogenic therapies for pheochromocytoma and paraganglioma. *Endocr Relat Cancer* 2020; **27**: R239-R254 [PMID: 32369773 DOI: 10.1530/ERC-20-0043]

World Journal of Clinical Cases

Submit a Manuscript: https://www.f6publishing.com

World J Clin Cases 2024 May 26; 12(15): 2678-2681

DOI: 10.12998/wjcc.v12.i15.2678

ISSN 2307-8960 (online)

LETTER TO THE EDITOR

Imaging features of malignant *vs* stone-induced biliary obstruction: Aspects to consider

Cristian Lindner

Specialty type: Medicine, research and experimental

Provenance and peer review: Invited article; Externally peer reviewed.

Peer-review model: Single blind

Peer-review report's classification

Scientific Quality: Grade C
Novelty: Grade C
Creativity or Innovation: Grade C
Scientific Significance: Grade C

P-Reviewer: Bai H, China

Received: February 8, 2024
Revised: April 3, 2024
Accepted: April 10, 2024
Published online: May 26, 2024

Cristian Lindner, Department of Radiology, Faculty of Medicine, University of Concepción, Concepción 4030000, Chile

Corresponding author: Cristian Lindner, Doctor, MD, Department of Radiology, Faculty of Medicine, University of Concepción, No. 1290 Victor Lamas, Concepción 4030000, Chile. Clindner@udec.cl

Abstract

Radiological studies play a crucial role in the evaluation of patients with biliary duct obstruction, allowing for the guidance of clinical diagnosis towards a malignant or stone-induced etiology through the recognition of relevant imaging features, which must be continuously revisited given their prognostic significance. This article aims to emphasize the importance of recognizing crucial imaging aspects of malignant and stone-induced biliary obstruction.

Key Words: Malignant biliary obstruction; Choledocholithiasis; Dilated bile ducts; Magnetic resonance; Multidetector computed tomography

Core Tip: Recognizing the radiological aspects of biliary obstruction is crucial for distinguishing between lithiasis and malignant origins, thereby facilitating the diagnosis and management of this pathology.

Citation: Lindner C. Imaging features of malignant *vs* stone-induced biliary obstruction: Aspects to consider. *World J Clin Cases* 2024; 12(15): 2678-2681
URL: https://www.wjgnet.com/2307-8960/full/v12/i15/2678.htm
DOI: https://dx.doi.org/10.12998/wjcc.v12.i15.2678

TO THE EDITOR

I read with great interest the letter written by Aydin and Irgul[1]. In their article, they aim to highlight some imaging findings for distinguishing between malignant biliary obstruction and common stone biliary obstruction.

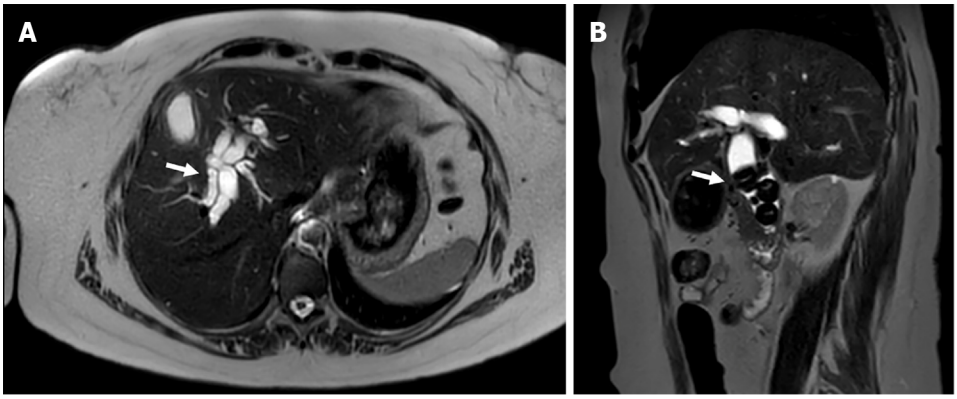

Figure 1 Distal choledocholithiasis in a 53-year-old man with acute secondary cholangitis. A: Axial magnetic resonance T2-weighted images depicts intra- and extrahepatic biliary ductal dilatation; B: Multiple void signal images within the lumen of the common bile duct.

I agree with Aydin and Irgul[1] that imaging studies play an invaluable role in the evaluation of patients with biliary tract obstruction. In the same line, I intend to contribute to the article highlighting some crucial imaging features of biliary obstruction that we should consider.

Obstruction of the biliary tree can occur as a result of gallstones disease[2] (Figure 1), as well as multiple types of cancers, including primary tumors originated from bile duct cells as well as those originating from adjacent organs that could cause extrinsic compression of the common bile duct (CBD), such as cholangiocarcinoma and pancreatic cancer respectively[3].

As expected, patients with biliary obstruction of malignant origin have a significantly worse clinical course compared to those with lithiasic obstruction of the bile duct, present a higher incidence of severe acute cholangitis, greater admission to critical care units, and 30-d mortality, as recently reported by Tsou *et al*[4], which underscores the importance of being able to differentiate the origin of biliary obstruction during the imaging study.

For instance, initial imaging evaluation of patients with biliary obstruction may depict dilatation of the CBD and common hepatic duct associated with heterogeneous sizeable non-encapsulated heterogeneous mass of irregular contour, accompanied by hepatic capsular retraction and dilated peripheral bile ducts, with progressive enhancement in delayed phases and slight-to high signal intensity on T2-weighted images (T2WI), and low signal intensity on T1-weighted images (T1WI), which is highly suggestive of primary bile duct carcinomas[3,5] (Figure 2).

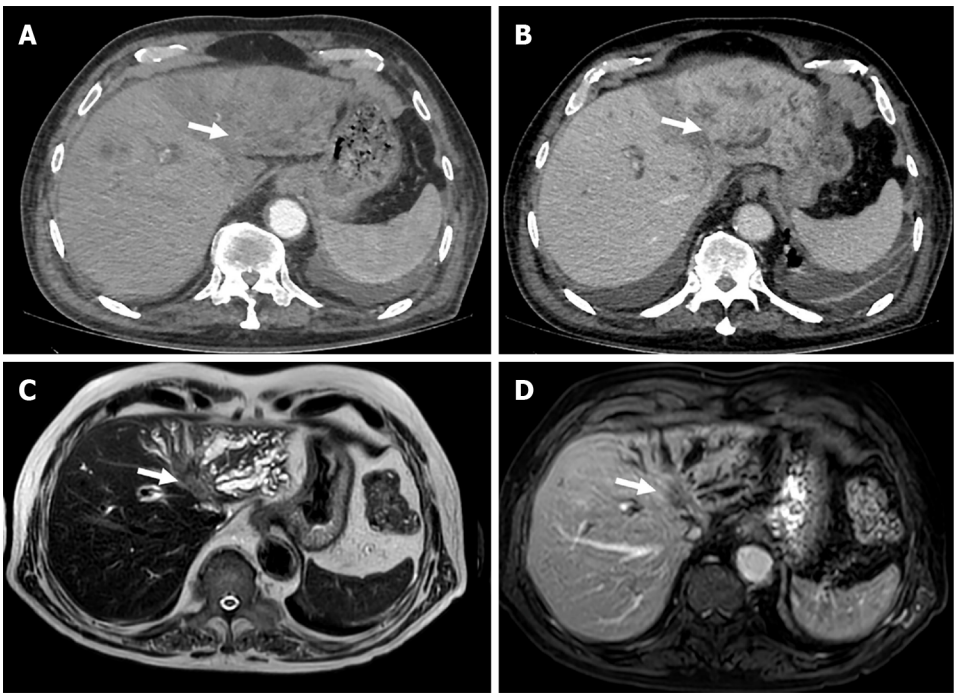

Figure 2 69-years-old woman with biliary obstruction secondary to intrahepatic mass-forming type cholangiocarcinoma with tumoral involvement of the biliary ducts confluence. A: Axial late computed tomography arterial phase depicts a soft-tissue mass in left hepatic lobe, with delayed phase enhancement; B: Dilatation of intrahepatic ducts; C: Axial magnetic resonance images demonstrate a T2-weighted images slightly hyperintense; D: T1-

weighted images hypointense heterogeneous mass occluding the confluence of the hepatic ducts with moderate dilatation of left lobar intrahepatic bile ducts, and tumoral involvement of the left intrahepatic biliary branches.

In addition, CBD dilation may also be associated with the presence of a heterogeneous enhancing mass dependent on the pancreatic head, with iso- to slightly hyperintense signal on T2WI, and hypointense signal on T1WI, which generates extrinsic compression of the CBD, which may produce secondary cholangitis[6] (Figure 3).

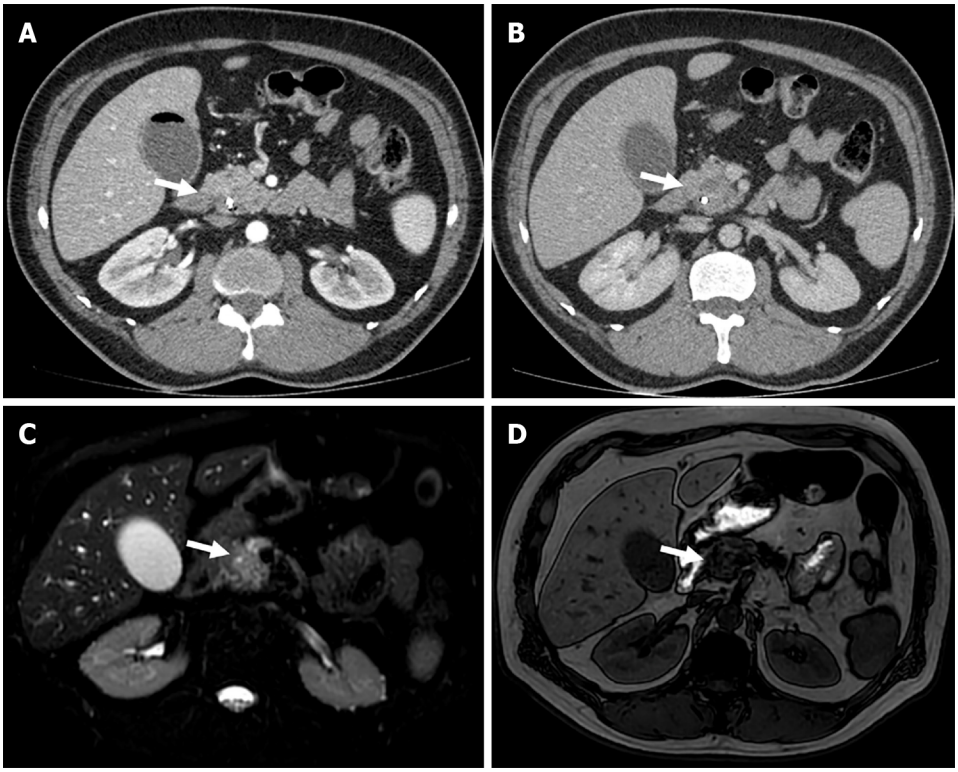

Figure 3 Pancreatic ductal adenocarcinoma in a 72-years-old man with obstructive jaundice. A: Axial contrast-enhanced computed tomography image shows a well-circumscribed exophytic tumor in the pancreatic head with heterogeneuos enhancement in delayed arterial; B: Portovenous phase; C: Axial magnetic resonance fat suppression T2-weighted images image showing a mildly hyperdense irregular mass in the head of the pancreas; D: T1-weighted images with hypointense signal.

In both cases, the additional finding of focal hypovascular liver lesions with a peripheral halo and perihilar and retroperitoneal lymphadenopathy further support the diagnosis of biliary obstruction towards a malignant origin[7,8].

In summary, when conducting radiological evaluations of patients with bile duct obstruction, comprehensive consideration should be given to various imaging findings, with a focus on analyzing important imaging information. Considering the clinical implication of these diseases, I hope the discussion on the interesting articles by Tsou *et al*[4]. and Aydin and Irgul[1] will promote the permanent ongoing review of the imaging features of malignant and stone-induced bile duct obstruction to further improve the early recognition and appropriate management of these patients.

FOOTNOTES

Author contributions: Lindner C wrote this article.

Conflict-of-interest statement: All the authors report no relevant conflicts of interest for this article.

Country/Territory of origin: Chile

ORCID number: Cristian Lindner 0000-0002-2642-4288.

S-Editor: Liu H
L-Editor: A
P-Editor: Yu HG

REFERENCES

1 **Aydin S**, Irgul B. Response letter to "Acute cholangitis: Does malignant biliary obstruction vs choledocholithiasis etiology change the outcomes?" with imaging aspects. *World J Clin Cases* 2024; **12**: 1029-1032 [PMID: 38414614 DOI: 10.12998/wjcc.v12.i5.1029]
2 **Duhancioglu G**, Arif-Tiwari H, Natali S, Reynolds C, Lalwani N, Fulcher A. Traveling gallstones: review of MR imaging and surgical pathology features of gallstone disease and its complications in the gallbladder and beyond. *Abdom Radiol (NY)* 2024; **49**: 722-737 [PMID: 38044336 DOI: 10.1007/s00261-023-04107-5]
3 **Katabathina VS**, Dasyam AK, Dasyam N, Hosseinzadeh K. Adult bile duct strictures: role of MR imaging and MR cholangiopancreatography in characterization. *Radiographics* 2014; **34**: 565-586 [PMID: 24819781 DOI: 10.1148/rg.343125211]
4 **Tsou YK**, Su YT, Lin CH, Liu NJ. Acute cholangitis: Does malignant biliary obstruction vs choledocholithiasis etiology change the clinical presentation and outcomes? *World J Clin Cases* 2023; **11**: 6984-6994 [PMID: 37946763 DOI: 10.12998/wjcc.v11.i29.6984]
5 **Joo I**, Lee JM, Yoon JH. Imaging Diagnosis of Intrahepatic and Perihilar Cholangiocarcinoma: Recent Advances and Challenges. *Radiology* 2018; **288**: 7-13 [PMID: 29869969 DOI: 10.1148/radiol.2018171187]
6 **Schawkat K**, Manning MA, Glickman JN, Mortele KJ. Pancreatic Ductal Adenocarcinoma and Its Variants: Pearls and Perils. *Radiographics* 2020; **40**: 1219-1239 [PMID: 32678699 DOI: 10.1148/rg.2020190184]
7 **Costello JR**, Kalb B, Chundru S, Arif H, Petkovska I, Martin DR. MR imaging of benign and malignant biliary conditions. *Magn Reson Imaging Clin N Am* 2014; **22**: 467-488 [PMID: 25086940 DOI: 10.1016/j.mric.2014.05.002]
8 **Kim DW**, Kim SY, Yoo C, Hwang DW. Update on Biliary Cancer Imaging. *Radiol Clin North Am* 2022; **60**: 825-842 [PMID: 35989047 DOI: 10.1016/j.rcl.2022.05.001]

World Journal of Clinical Cases

Submit a Manuscript: https://www.f6publishing.com

World J Clin Cases 2024 May 26; 12(15): 2682-2685

DOI: 10.12998/wjcc.v12.i15.2682

ISSN 2307-8960 (online)

LETTER TO THE EDITOR

Differences between the healthcare systems of Quebec and France for the treatment of pain due to spinal disorders

Lea Evangeline Boyer, Mathieu Boudier-Revéret, Min Cheol Chang

Specialty type: Medicine, research and experimental

Provenance and peer review: Unsolicited article; Externally peer reviewed.

Peer-review model: Single blind

Peer-review report's classification
Scientific Quality: Grade B
Novelty: Grade B
Creativity or Innovation: Grade B
Scientific Significance: Grade B

P-Reviewer: Majhi S, India

Received: February 14, 2024
Revised: April 8, 2024
Accepted: April 15, 2024
Published online: May 26, 2024

Lea Evangeline Boyer, Department of Physical Medicine and Rehabilitation, CHU de la Réunion, Reunion Island CIC 1410, France

Mathieu Boudier-Revéret, Department of Rehabilitation Medicine, University of Montreal Health Center, Montreal, QC H2X 3E4, Canada

Min Cheol Chang, Department of Physical Medicine and Rehabilitation, College of Medicine, Yeungnam University, Daegu 705-717, South Korea

Corresponding author: Min Cheol Chang, MD, Department of Physical Medicine and Rehabilitation, College of Medicine, Yeungnam University, 317-1, Daemyungdong, Namku, Daegu 705-717, South Korea. wheel633@gmail.com

Abstract

In Quebec, Canada, the public healthcare system offers free medical services. However, patients with spinal pain often encounter long waiting times for specialist appointments and limited physiotherapy coverage. In contrast, private clinics provide expedited care but are relatively scarce and entail out-of-pocket expenses. Once a patient with pain caused by a spinal disorder meets a pain medicine specialist, spinal intervention is quickly performed when indicated, and patients are provided lifestyle advice. Transforaminal epidural steroid injections are frequently administered to patients with radicular pain, and steroid injections are administered on a facet joint to control low back or neck pain. Additionally, medial branch blocks are performed prior to thermocoagulation. France's universal healthcare system ensures accessibility at controlled costs. It emphasizes physical activity and provides free physical therapy services. However, certain interventions, such as transforaminal and interlaminar epidural injections, are not routinely used in France owing to limited therapeutic efficacy and safety concerns. This underutilization may be a potential cause of chronic pain for many patients. By examining the differences, strengths, and weaknesses of these two systems, valuable insights can be gained for the enhancement of global spinal pain management strategies, ultimately leading to improved patient outcomes and satisfaction.

Key Words: Spinal pain; Healthcare system; France; Quebec; Pain treatment

Core Tip: The public healthcare system in Quebec, Canada, provides free services; however, patients with spinal pain face long waiting times for specialist appointments and limited physiotherapy coverage. Spinal interventions, including transforaminal epidural steroid injections for radicular pain, are performed quickly upon consultation with a pain specialist. In contrast, France's universal healthcare system emphasizes physical activity and offers free physiotherapy; however, certain interventions, such as epidural injections, are underutilized, potentially contributing to chronic pain. Each system has advantages and disadvantages. Understanding these differences can inform global spinal pain management strategies and enhance patient satisfaction and outcomes.

Citation: Boyer LE, Boudier-Revéret M, Chang MC. Differences between the healthcare systems of Quebec and France for the treatment of pain due to spinal disorders. *World J Clin Cases* 2024; 12(15): 2682-2685
URL: https://www.wjgnet.com/2307-8960/full/v12/i15/2682.htm
DOI: https://dx.doi.org/10.12998/wjcc.v12.i15.2682

TO THE EDITOR

We read the article by Wang *et al*[1] with great interest, in which the authors proposed a protocol for physicians to administer ultrasound-guided injections as treatment for spinal pain. Spinal pain is highly prevalent in the general population and often causes substantial suffering, many lost workdays, and high medical costs[2]. The healthcare system in every country has its preferred treatment strategy for spinal pain. Here, we provide our personal perspectives, aiming to introduce the strategies of the healthcare systems in Quebec and France, compare them, highlight their shortcomings, and provide potential solutions.

The first author is a resident in the Department of Physical Medicine and Rehabilitation at a university hospital in France and has been enrolled in an overseas resident training program in Montreal, Canada, since December 2023. In Montreal, we observed substantial differences between the healthcare systems' preferred strategies, especially regarding pain caused by spinal disorders, each with their own advantages and disadvantages. The functioning of healthcare systems is very complicated and is influenced by social, economic, and political factors[3,4].

In Quebec, Canada, medical institutions (hospitals and clinics) are categorized as public and private institutions[5]. Public institutions ensure that citizens receive medical services without incurring fees for visits and treatments. On the other hand, patients who receive care from private clinics cover the costs of treatment and procedures by themselves and are rarely reimbursed by insurance companies. Although the number of private clinics is increasing in Canada, Quebec has few.

Although the public healthcare system in Quebec offers free services, patients often wait several months or even years for an appointment with a physician. Private clinics provide an alternative for patients who are unwilling to endure long waiting times by offering fast access to medical care. However, the availability of private clinics and range of medical services offered are limited. Despite the option to expedite care by paying privately, this remains a less common choice because of the scarcity of such facilities and the associated costs.

Once patients with pain caused by spinal disorders meet a specialist in pain medicine, they are quickly referred for spinal intervention, if necessary, and given lifestyle advice. Spinal interventions are performed using nonparticulate corticosteroids. Transforaminal epidural steroid injections are frequently administered to patients with radicular pain, and steroid injections are administered on a facet joint to control low back or neck pain. Medial branch blocks are also performed. If patients experience pain reduction *via* medial branch blocks, pain physicians normally recommend thermocoagulation.

Physiotherapy is not covered by the public healthcare system and is mainly conducted in private clinics, for which patients must pay out of pocket. Only a small proportion of outpatients have access to free physiotherapy, mainly in public health institutions. Therefore, education regarding physiotherapy and exercise for the treatment of spinal pain is not well implemented in Quebec.

In France, medical institutions are divided into public sector (public hospitals) and private sector (clinics or independent practices) institutions[6,7]. Few nonprofit private healthcare providers exist. The public healthcare system is based on health insurance schemes-a universal healthcare system that ensures that patients receive care, consultations, and treatments with controlled, fixed costs. The system covers 70% of medical consultation costs, with a one-euro fee per consultation, and is complemented by other insurance systems. Hospitalization costs are split, with health insurance covering 80% and supplementary plans covering 20%. The solidarity health insurance or State aid can exempt those who cannot pay these fees. Private health insurance schemes can handle upfront costs.

In terms of healthcare access, patients with spinal pain follow a care pathway guided by general practitioners for optimal management[8]. Accessing public or private specialized care has become more difficult owing to a shortage of medical professionals, leading to waiting times of 2 d for general practitioners and 52 d for specialists, excluding urgent cases.

When a patient with spinal pain is referred to a pain specialist, the diagnosis is first revisited, and the likely cause is identified based on the patient's history[8]. Thereafter, the patient is provided counsel regarding physical activity, posture, lifestyle adjustments, muscle strengthening, and stabilization-exercise programs. Patients can receive physiotherapy at a physical therapist's office, which is covered by health insurance, private assurance, or county assurance. In

most cases, patients receive physiotherapy at no cost.

If the patient continues to experience severe pain or pain that does not improve during follow-up appointments, spinal intervention may be considered, with the specific type of treatment chosen according to patient-specific clinical factors. Caudal epidural injections are recommended for patients with radicular pain. However, in France, transforaminal and interlaminar epidural injections are not routinely administered because of their limited therapeutic efficacy and safety concerns. Pain specialists often use facet-joint infiltration to treat low back pain.

For chronic or recurrent spinal pain, comprehensive care may involve a rehabilitative stay at a day hospital for 3-6 wk, covered under standard hospitalization packages[8]. Such a program entails re-evaluation of various factors contributing to pain, addressing of the patient's beliefs and lifestyle, and provision of nutritional and psychological support and daily physiotherapy sessions.

In Quebec, the public healthcare system provides free access to medical services, and the conventional pathway for spinal interventions tends to depend on the interventionist. However, long waiting times for specialist appointments, which lead to delayed treatment, and limited coverage of physiotherapy are significant drawbacks. Few private clinics offer expedited care, largely owing to the associated costs, making them an uncommon choice. To improve this situation, Quebec should consider improving the system's efficiency or increasing funding to reduce waiting times and expand physiotherapy coverage.

France's universal healthcare system ensures affordable access to care and follows a thorough care pathway for spinal pain management. It minimizes costs by reducing the frequency of early interventions and offers easy and free access to physiotherapy. However, the use of certain interventions is limited and a passive approach to acute low back pain can predispose patients to chronic pain. To enhance the functioning of the system in France, considering therapeutic efficacy and potential side effects of different spinal interventions, the indications for spinal interventions should be expanded for patients who experience severe pain.

The health systems in Quebec and France have their strengths and weaknesses in terms of spinal pain management. The system in Quebec is more focused on chronic patient care, whereas the system in France emphasizes physical activity based on spontaneous remission of acute cases. Considering the strengths and weaknesses of the systems in Quebec and France may assist other countries in determining their treatment strategies for spinal pain to enhance patient outcomes and satisfaction.

FOOTNOTES

Author contributions: Boyer LE, Boudier-Revéret M and Chang MC designed the study, performed the study, analyzed the data and wrote the manuscript. All authors have read and approved the final manuscript.

Supported by National Research Foundation of Korea Grant, No. 00219725.

Conflict-of-interest statement: The authors report no relevant conflicts of interest.

Country of origin: South Korea

ORCID number: Lea Evangeline Boyer 0009-0005-5008-4227; Mathieu Boudier-Revéret 0000-0003-0259-8520; Min Cheol Chang 0000-0002-7629-7213.

S-Editor: Zheng XM
L-Editor: A
P-Editor: Zheng XM

REFERENCES

1 **Wang Y**, Wang AZ, Wu BS, Zheng YJ, Zhao DQ, Liu H, Xu H, Fang HW, Zhang JY, Cheng ZX, Wang XR. Chinese Association for the Study of Pain: Experts consensus on ultrasound-guided injections for the treatment of spinal pain in China (2020 edition). *World J Clin Cases* 2021; **9**: 2047-2057 [PMID: 33850924 DOI: 10.12998/wjcc.v9.i9.2047]

2 **Shin DA**, Choo YJ, Chang MC. Spinal Injections: A Narrative Review from a Surgeon's Perspective. *Healthcare (Basel)* 2023; **11**: 2355 [PMID: 37628553 DOI: 10.3390/healthcare11162355]

3 **National Academies of Sciences, Engineering, and Medicine**; Health and Medicine Division; Board on Health Care Services; Committee on Health Care Utilization and Adults with Disabilities. Health-Care Utilization as a Proxy in Disability Determination. Washington (DC): National Academies Press (US), 2018

4 **Osypuk TL**, Joshi P, Geronimo K, Acevedo-Garcia D. Do Social and Economic Policies Influence Health? A Review. *Curr Epidemiol Rep* 2014; **1**: 149-164 [PMID: 25984439 DOI: 10.1007/s40471-014-0013-5]

5 **Marchildon GP**. Canada, Health System of. In: Quah SR, Cockerham W, editors. International Encyclopedia of Public Health. 2nd ed.

Oxford: Academic Press, 2017: 320-327

6 **Honda A**, Cartailler J, Cailhol J, Noda S, Or Z. Factors for Consideration When Setting Prices for Private Healthcare Providers Operating in Public Systems: A Comparison of France and Japan. *Health Serv Insights* 2023; **16**: 11786329231173484 [PMID: 37228260 DOI: 10.1177/11786329231173484]

7 **Simonet D**. French Idiosyncratic Health-Care Reforms, Performance Management and Its Political Repercussions. *Risk Manag Healthc Policy* 2021; **14**: 2971-2981 [PMID: 34285611 DOI: 10.2147/RMHP.S306381]

8 **Haute Autorité de Santé**. Prise en charge du patient présentant une lombalgie commune. 2019. Available from: https://www.has-sante.fr/jcms/c_2961499/fr/prise-en-charge-du-patient-presentant-une-lombalgie-commune

Published by **Baishideng Publishing Group Inc**
7041 Koll Center Parkway, Suite 160, Pleasanton, CA 94566, USA
Telephone: +1-925-3991568
E-mail: office@baishideng.com
Help Desk: https://www.f6publishing.com/helpdesk
https://www.wjgnet.com